UNIVERSITÉ DE STRASBOURG

ÉCOLE DOCTORALE DES SCIENCES CHIMIQUES (ED222)

Institut de chimie - UMR 7177

THÈSE

présentée par :

Christophe WERLÉ

Soutenance le : **17 septembre 2014 à 14h**

pour obtenir le grade de : **Docteur de l'université de Strasbourg**

Discipline/ Spécialité : CHIMIE

Experimental and theoretical study of non-covalent interactions in organometallic chemistry

The concept of Hemichelation

THÈSE dirigée par :

[Dr. DJUKIC Jean-Pierre]	Directeur de recherche au CNRS, Université de Strasbourg

RAPPORTRICES :

[Pr. MARTIN-VACA Blanca]	Professeur des universités, Université de Toulouse
[Dr. COSTUAS Karine]	Chargée de recherche au CNRS, Université de Rennes

AUTRES MEMBRES DU JURY :

[Pr. ELSEVIER Cornelius J.]	Professeur des universités, Université de Amsterdam
[Dr. BARLOY Laurent]	Chargé de recherche au CNRS, Université de Strasbourg

Your time is limited, so don’t waste it living someone else’s life. Don’t be trapped by dogma – which is living with the results of other people’s thinking. Don’t let the noise of others’ opinions drown out your own inner voice. And most important, have the courage to follow your heart and intuition. They somehow already know what you truly want to become. Everything else, is secondary.

Steve Jobs.

À mon grand-père

Jean-Pierre KRUTH (1931-2005)

L'ensemble des travaux présentés dans ce manuscrit ont été réalisés à l'institut de chimie de Strasbourg au sein du laboratoire de chimie et systémique organo-métalliques (LCSOM) dont le Dr. Jean-Pierre DJUKIC est le directeur. Ce projet a été financé par l'agence nationale de la recherche (ANR projet WEAKINTERMET-2DA), ainsi que par un financement LABEX (Laboratoires d'excellence "Chimie des systèmes complexes").

Un travail de thèse n'est jamais le fruit d'une seule et unique personne mais la contribution d'un nombre important de personnes qui ont rendues chacune, à leur manière, cette histoire possible. En ce sens, je me permets d'adresser mes plus sincères remerciements à tous ceux qui y ont participé de près ou de loin.

J'aimerais en premier lieu exprimer ma profonde gratitude et admiration à mon directeur de thèse le Dr. Jean-Pierre DJUKIC, qui a été présent pour moi tout au long de ces trois années, me soutenant à force de patience et d'encouragements tout en m'offrant la possibilité de m'exprimer librement tant intellectuellement que devant la paillasse. Merci de m'avoir permis de grandir scientifiquement.

Je remercie également très vivement Pr. Blanca MARTIN-VACA (Toulouse), Dr. Karine COSTUAS (Rennes), Dr. Laurent BARLOY (Strasbourg) et le Pr. Cornelius J. (Kees) ELSEVIER (Amsterdam) de m'avoir fait l'honneur d'accepter de prendre part à ce jury de thèse et d'évaluer ce travail.

Je tiens également à remercier chaleureusement le Dr. Michel PFEFFER pour toutes ces discussions intéressantes que nous avons pu avoir et la bienveillance dont il a fait preuve à mon égard. Votre expertise dans la chimie du palladium, à laquelle j'ai eu accès pendant ces trois années, a énormément contribué à l'avancée de ce projet.

Je souhaite maintenant assurer le témoignage de ma reconnaissance à l'ensemble des personnes avec lesquelles j'ai eu la chance de partager tant et tant d'heures pour les aspects analytiques liés aux composés décrits dans cette thèse: Dr. Lydia BRELOT, Corinne BAILLY, Dr. Louis RICARD, Dr. Xavier-Frédéric LE GOFF à la cristallographie. Dr. Lionel ALLOUCHE, Dr. Bruno VINCENT, Jean-Daniel SAUER et Maurice COPPE à la RMN. Dr. Hélène NIERENGARTEN, Mélanie LEBRETON à la spectroscopie de masse. Dr. Martine HEINRICH, Claire GENOIS et Laurent LEVÊQUE aux analyses élémentaires. Dr. Sylvie CHOUA à la RPE. Un grand merci à vous tous!

Je ne saurais oublier de remercier mes camarades de laboratoire pour leur aimable collaboration et leur sympathique amitié. Tout spécialement Predrag PETROVIC, Mustapha HAMDAOUI, Frédéric LA PAGLIA, Noel Angel ESPINOSA JALAPA qui ont travaillé avec moi sur ce projet et sur d'autres.

Il m'est agréable d'exprimer ma profonde gratitude pour leur aide si importante sur tous les plans administratifs, ainsi que pour leur amitié: Geneviève STOLL, Jacques KLEIN.

Un merci tout particulier également à Nicolas RENARD pour toute son assistance technique pendant ces trois années, facilitant considérablement le quotidien au laboratoire.

Je voudrais maintenant adresser un grand merci à mes parents: Elisabeth et Adrien WERLÉ qui m'ont soutenu tout au long de ce chemin, qui ont été là pour moi dans les bons moments comme les moins bons. L'aboutissement de cette thèse c'est aussi grâce à vous!

Une pensée également à ma grand-mère Lucie KRUTH, à mon Papa Raul, à ma Mama Carmen, à mes frères Pablo et Diego TORRES dont le soutient inconditionnel compte énormément pour moi.

Et enfin je voudrais remercier ma femme, Maria, avec qui j'ai la chance de partager ma vie et dont l'amour me permet d'avancer au quotidien.

Abstract (Français)

Malgré l'omniprésence des interactions non-covalentes dans la nature, leur description exacte reste toutefois encore un défi majeur pour les chimistes. Pour des raisons qui tiennent à la directionnalité de ces interactions et en dépit de la difficulté à prédire leur manifestation, ces interactions non-covalentes sont communément utilisées pour l'élaboration rationnelle d'assemblages supramoléculaires. Il s'agit alors pour les expérimentateurs et les théoriciens de comprendre et d'analyser la nature de ces interactions afin de pouvoir au mieux anticiper et controler leur effet. Les interactions non-covalentes sont réputées centrales dans des processus cruciaux comme la reconnaissance moléculaire et chirale ou encore les phénomènes d'amplification chirale. Toutefois de nombreux efforts sont encore consentis afin d'améliorer leur description fondamentale, étant donné qu'il n'existait jusqu'alors, pas de méthodes théoriques rationnelles capables de les traiter sans faire intervenir d'importantes simplifications lorsqu'il fallait traiter des systèmes moléculaires de grande taille. En chimie de coordination, la règle de Langmuir (1921) - Sidgwick (1934), véritable extension de la règle empirique de l'octet de Lewis (1915), impose aux métaux de transition d'atteindre le nombre de 18 électrons dans leur couche de valence pour former des complexes stables. En réalité, pour une bonne partie des métaux des seconde et troisième lignes de la classification périodique, il est courant de rencontrer des situations où des complexes de métaux à « couche de valence » à 16 électrons sont stables. Les métaux tels que Ir, Rh, Pd et Pt en fournissent les meilleurs exemples. C'est précisément cette règle, qui n'est plus suffisante pour attester de la stabilité d'un système chimique, que nous avons battue en brèche. Tous les résultats obtenus et retranscrits dans cette thèse mettent en avant le rôle fondamental et moteur des interactions non-covalentes dans la stabilisation d'espèces électro-insaturées, spécialement dans le domaine de la chimie organométallique. Le concept d'hémichélation est une manière de rationnaliser leur effet et de décrire au mieux cette relation étroite existante entre le centre métallique électrodéficient et le ligand hétéroditopique formant l'hémichélate. Ces travaux ouvrent de nouvelles perspectives dans la compréhension des interactions non-covalentes, mais également de la chimie de coordination en générale.

Abstract (English)

According to the Langmuir(1921)-Sidgwick(1934) rule, which is a true extension of the empiric Lewis octet rule (1915), the stability of a transition metal complex is conditioned by its ability to reach an ideal 18 valence electron configuration at the metal. Of course many exceptions to this rule are known, particularly among precious metal complexes, which can very commonly accommodate 16 valence electron configurations in coordination complexes. Recently, the number of such heterodox complexes violating the 18-electron rules became more and more prevalent, forcing the field of organometallic chemistry to start moving toward a new paradigm where non-covalent interactions play a decisive role in the stabilisation of electron-deficient metal centres discrediting completely the mythic 18-electron rule. The purpose of this PhD thesis is to unveil the origin of the persistence of electron-deficient intermolecular aggregates and intramolecular bimetallic species and to understand the physical roots that make these species stable. The present manuscript will present a rational method of synthesis and characterization, determination of the electronic structure and dynamic behaviour of solution-persistent, and formally unsaturated binuclear Cr(0)-M complexes (with M= Pd(II), Pt(II) or Rh(I)). This new class of complexes constitutes rare examples of persistent coordinatively unsaturated 14-electrons complexes, whose cohesion stems essentially from a compensation of insufficient donor/acceptor Cr-Pd bonding by non-covalent interactions of preponderant attractive Coulombic nature. DFT investigations combined with a number of theoretical analyses of the bond framework suggested that the polar intermetallic interaction possesses no major covalent character. Through this study, we will reveal that by taking advantage of the ambiphilic character of an heteroditopic ligand (i.e. tricarbonyl(η^6-arene)chromium anion) capable of chelating a metal centre through covalent and noncovalent bonds (thus preserving its valence shell bonding), truly coordination-unsaturated complexes can be synthesized in a manageable form. Finally, we propose to name the half-covalent/half noncovalent bonding-relationship between the ambiphilic heteroditopic ligand and the electron-unsaturated metallic centre Hemichelation.

Scientific Productions

List of Publications:

1. Werlé, C.; Bailly, C.; Karmazin-Brelot, L.; Le Goff, X.-F.; Pfeffer, M.; Djukic, J.-P. Angew. Chem. Int. Ed. Engl. **2014**, 53, 9827.

2. Werlé, C.; Le Goff, X. F.; Djukic, J. P. *J. Organomet. Chem.* **2014**, *751*, 754.

3. Werlé, C.; Bailly, C.; Karmazin-Brelot, L.; Le Goff, X. F.; Ricard, L.; Djukic, J. P. *J. Am. Chem. Soc.* **2013**, *135*, 17839.

4. Werlé, C.; Hamdaoui, M.; Bailly, C.; Le Goff, X. F.; Brelot, L.; Djukic, J. P. *J. Am. Chem. Soc.* **2013**, *135*, 1715.

List of Conferences:

1. Oral communication (20 min): “Journées Scientifiques de l'Institut de Chimie de Strasbourg”, January 10th and 11th 2013 - Complexes bimétalliques électro-déficients de Cr(0)-Pd(II) à base indénique stabilisés par des interactions non-covalentes de type fluxionnelles).

2. Oral communication (20 min): “20th EuCheMS Conference on Organometallic Chemistry”, St-Andrews (SCOTLAND), June 30th-July 4th 2013 - Non-covalent chelation for the stabilization of electron-deficient metal centres

3. Oral communication (20 min): “Journée des doctorants, November 19th 2013 - Stabilization of Electron-deficient Metal Centres: The New Concept of Hemichelation.

4. Oral communication (10 min): “International Symposium of Metal-Mediated Chemistry”, November 22nd 2013, Université de Strasbourg (FRANCE) - Stabilization of Electron-deficient Metal Centres: The New Concept of Hemichelation.

5. Oral communication (20 min): “GECOM-CONCOORD 2014”, Vers (Lot, FRANCE), Mai 18th-23rd 2014 - Stabilization of Electron-deficient Metal Centres: The New Concept of Hemichelation.

Table of Contents

Acetic acid	(AA)
All-electron	(AE)
Basis set superposition error	BSSE
Becke-Johnson	(BJ)
Bond critical point	(BCP)
Cahn-Ingold-Prelog rules	(CIP)
Circular Dichroism	(CD)
Coupled cluster method covering single, double, and triple excitations iteratively	(CCSDT)
Donor−acceptor	(DA)
Density functional theory	(DFT)
Enantiomeric excess	(ee)
Energy decomposition analysis	(EDA)
Electron localization function	(ELF)
Extended transition state-natural orbitals for chemical valence	(ETS-NOCV)
Hartree-Fock	(HF)
Hydrogen bond	(H-bond)
Indenyl effect	(IndE)
Infrared	(IR)
Isotope effect	(IE)
Local density approximation	(LDA)
Metal nanoparticles	(M-NPs)
Microwave spectroscopy	(MW)
Natural Atomic Orbital	(NAO)
Natural Bond Orbital	(NBO)
Nitric oxide	(NO)
Non-covalent interactions	(NCIs)
Parts per million	(ppm)
Perdew−Burke−Ernzerhof	(PBE)

p-toluenesulfonic acid	(PTSA)
Potential-energy surface	(PES)
Quantum Monte Carlo	(QCM)
Quantum Theory of Atoms in Molecule	(QTAIM)
Silica gel	(SiO_2)
Single Chain Magnet	(SCM)
Single Molecule Magnet	(SMM)
Symmetry-adapted perturbation theory	(SAPT)
Tao-Perdew-Staroverov-Scuseria	(TPSS)
Tetrahydrofuran	(THF)
Tkatchenko-Scheffler	(TS)
Van der Waals	(vdW)
Vibration-rotation-tunnelling spectroscopy	(VRT)
Wiberg bond indices	(WBI)
Zero-point energies	(ZPEs)
Zero electron kinetic energy	(ZEKE)
Zeroth Order Regular Approximation	(ZORA)

I

An excursion into non-covalence

General Introduction

The first chapter introduces the non-covalent interactions and highlights the motivations of the research conducted during this PhD.

Chapter I - General Introduction.

1 - Forewords.

In 1962, through his masterpiece "The Structure of Scientific Revolution",[1] Thomas S. Kuhn fathered, defined and popularized the concept of "paradigm shift". The author argues that advancement in science is not evolutionary, but rather the succession of series of "peaceful interludes", the so-called "normal science", punctuated by intellectually violent revolutions. Those breakthrough moments disrupt accepted thinking and offer unanticipated ideas. During such revolutions, a new conceptual worldview replaces our previous vision of the universe. Thus, according to Kuhn, a scientific revolution occurs mainly after the discovery of "anomalies" which cannot be reasonably explained by the universally accepted paradigm within which scientific progress has thereto been made. When enough significant anomalies have occurred against a current paradigm, the scientific discipline is thrown into an intermediate state, the "state of crisis", during which new ideas, conceptions, dogmas (perhaps ones previously discarded) are tried; leading progressively to a new paradigm with its own new followers, starting an intellectual "battle" between the followers and the hold-outs of the old paradigm until the "crisis state" leads to a "revolution", establishing the new paradigm.

Figure 1: "Kaninchen und Ente" ("Rabbit and Duck"), the earliest known version of the duck–rabbit illusion, from the 23 October 1892 issue of Fliegende Blätter.[2] Author: Unknown; Public domain via Wikimedia Commons.

[1] [N°1] Kuhn, T. S. *The structure of scientific revolutions*; Fourth edition, **2012**.

[2] [N°2] *Fliegende Blätter* Universitätsbibliothek Heidelberg, **1892**; Vol. 2465, 147.

To explain his words, Kuhn often used the duck-rabbit optical illusion (Figure 1) which demonstrates how when such a shift occurs one is suddenly capable to see and understand a phenomenon, a set of data, differently, despite the fact that the person is still looking at exactly the same thing as before.

To some extension, the recent admission (during the past 15 to 20 years) of researchers in the area of molecular sciences of the key position of non-covalent interactions (NCIs) in a huge number of phenomena related to the whole realm of molecular and macroscopic science, somehow constitute one of those Kuhn's "breakthrough moments" disrupting accepted thinking. A good example of this is the so-called negligible role of "weak interactions", which up till now have been almost (completely) ignored. This "revolution", in a sense, supports the emergence and development of a rather new "paradigm shift" where those interactions appear to be essential in the understanding and description of complex molecular systems, especially in the transition metals chemistry. The core focus of this PhD thesis is to provide experimental and theoretical tools for advocacy in favour of this "new paradigm" in this disciplinary field.

2 - A Historical interlude.

Everything began in 1857 when Johannes Diderik van der Waals (Figure 2) after his university studies, learned of a treatise by Clausius on the nature of motion.[3] In his treatise, Clausius showed how Boyle's law could readily be derived on the assumption that a gas consists of material points which move at high velocity and that this velocity is of the order of that of sound, increasing in proportion to the square root of the absolute temperature. Clausius treatise was a revelation for Johannes D. van der Waals who realized, at the same time, that if a gas in the extremely dilute state (which volume is so large that the molecules can be regarded as points) consists of small moving particles, this will obviously remain the same when the volume is reduced; concluding that the reasons why a nondilute aggregate of moving particles fail to comply with Boyle's law are firstly, the **attraction** between the particles and secondly, their proper volume.

[3] [N°3] van der Waals, J. D. In *Nobel Lecture: The Equation of State for Gases and Liquids*; Nobelprize.org, Nobel Media AB 2013: Web. 26 Jun 2014: nobelprize.org/nobel_prizes/physics/laureates/1910/waals-lecture.html, 1910.

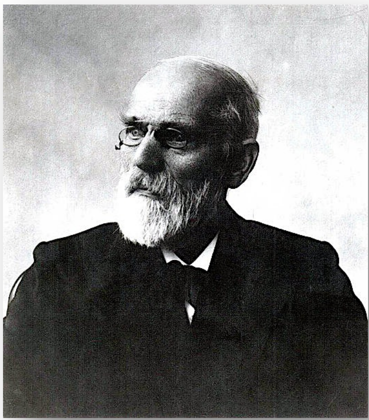

Figure 2: Johannes Diderik van der Waals (11/23/1837 – 3/08/1923); Nationality: Netherlands; Nobel Prize in Physics (1910)[4]: For his work on the equation of state for gases and liquids. Photographer: unknown; Public domain via Wikimedia Commons.

Based on these considerations Van der Waals discovered that the contradictions observed between the state function of a real gas and the ideal gas law could be explained by the attracting forces between molecules or either rare gas atoms and brought him to the following formula:

$$p = \frac{RT}{v - b} - \frac{a}{v^2}$$

Where p is the pressure, T is the temperature, R the ideal gas constant, and v the molar volume. a and b are the parameters that are determined empirically for each gas, but can also be estimated from their critical temperature and critical pressure. This equation of state, which is now universally known, suitable for describing the behaviour of real (in contrast to ideal) gases was part of the work which brought him in December 12th, 1910 to Stockholm for the Nobel Prize in Physics. Although this law is not the most accurate functional description for a real gas, it nevertheless has the merit of being a major breakthrough in their understanding, by making explicitly obvious that significant

[4] [N°4] van der Waals, J. D. In *"Johannes Diderik van der Waals - Facts"*; Nobelprize.org, Nobel Media AB 2013: Web. 26 Jun 2014: nobelprize.org/nobel_prizes/physics/laureates/1910/waals-facts.html.

attracting forces exist between gas molecules (or atoms for monoatomic gases), exhibiting a previously unknown tendency to form a new type of bond.

Another important breakthrough moment in the discovery and understanding of these attracting forces was the discovery of the liquefaction of helium in 1908 by Kamerlingh-Omnes (Figure 3).[5]

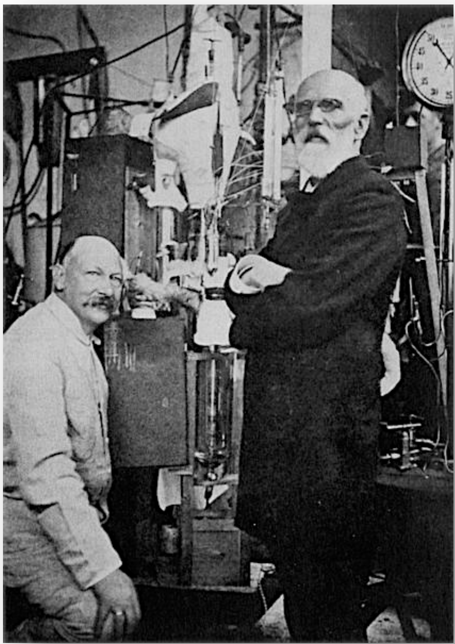

Figure 3: Heike Kamerlingh Onnes (left) and Johannes Diderik van der Waals (right) in front of the helium-'liquefactor', Leiden 1908. Photographer unknown Public domain via Wikimedia Commons.

The discovery of liquid helium, besides of providing Kamerlingh Omnes the Nobel Prize of Physic in 1913, was a decisive argument in favour of the existence of attractive intermolecular forces[6] acting even an between very small spherical rare gas, which does not bear any kind of charge or permanent dipolar moment. Heike Kamerlingh Omnes self words[7] for his Nobel lecture were: "It is true that Faraday's problem as to whether all gases can be liquefied has been solved step by step in the sense of Van der

[5] [N°5] Kamerlingh Onnes, H. *Proc. R. Netherlands Acad. Arts Sci. (KNAW) 11* **1909**, 168.

[6] [N°6] Page, C. H. *Phys. Rev.* **1938**, *53*, 426.

[7] [N°7] Kamerlingh Onnes, H. In *Nobel Lecture: Investigations into the Properties of Substances at Low Temperatures, which Have Led, amongst Other Things, to the Preparation of Liquid Helium*; Nobelprize.org, Nobel Media AB 2013: Web. 27 Jun 2014: nobelprize.org/nobel_prizes/physics/laureates/1913/onnes-lecture.html, 1913.

Waals' words, **matter will always show attraction**, and thus a fundamental problem has been removed". This somewhat supports van der Waal's early discoveries.

Many years later in 1930, Fritz London[8-10] (Figure 4) and soon after Hans Hellmann,[11] also took part in the understanding, description and interpretation of those forces.

Figure 4: Fritz London, Munich 1928 at the Bunsen congress. Author: GFHund; Public domain via Wikimedia Commons.

London provided the formulation of the very first explanation of the attraction between noble gas atoms by using a quantum-mechanical theory based on second-order perturbation theory, where the perturbation is the Coulomb interaction V between the electrons and nuclei of the two monomers (atoms or molecules) that constitute the dimer. All of these new considerations have been made possible mostly by the recently born quantum mechanics. Though several contributions can be interpreted by the so called "classical physics", the most important ones that consider the attraction and repulsion processes between systems having quantum origins, could only properly be made by using theoretical tools of quantum mechanics. The contribution of the different scientists previously mentioned regarding the discovery, description and understanding of these non-covalent interactions was clearly groundbreaking. Some

[8] [N°8] London, F. *Trans. Faraday Soc.* **1937**, *33*, 8b.

[9] [N°9] London, F. *Z. Physik* **1930**, *63*, 245.

[10] [N°10] Eisenschitz, R.; London, F. *Z. Physik* **1930**, *60*, 491.

[11] [N°11] Hellmann, H. *Acta Physicochim.* **1935**, 273.

other works of these pioneers can be found and are outlined in the classic book on intermolecular interactions, and in some reviews.[12-16]

3 - Why are non-covalent interactions essential?

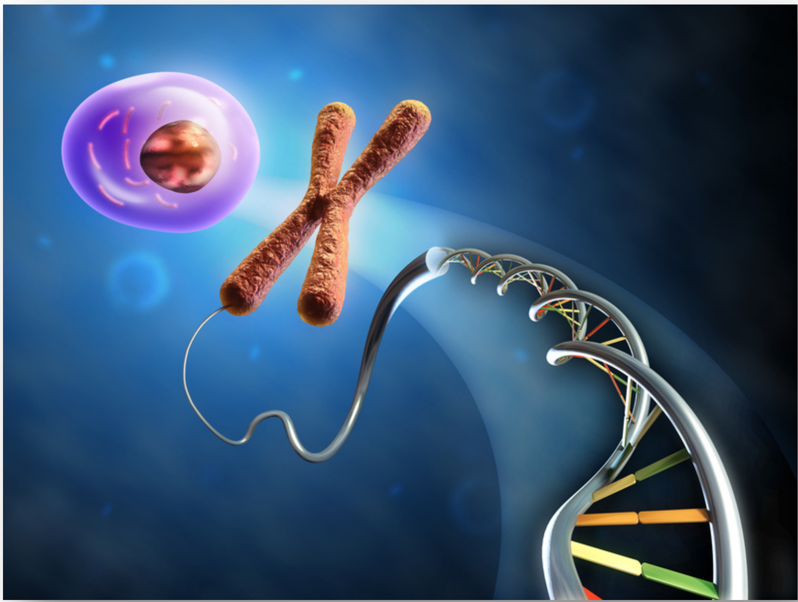

Figure 5: From the DNA to the cell, non-covalent interactions are essential for life, © Andrea Danti - Fotolia.com

In the perspective of understanding the evolution of life on Earth, it was essential to account for these special van der Waals (vdW) interactions: a class of much weaker bonding, besides the stronger covalent bonds. Indeed, van der Waals bonds (which are not energetically depending at all) can very easily be formed and not less easily split. Something that can be perceived at first as a weakness appears in fact to be a strength in the context, for instance, of supramolecular chemistry (defined by Lehn[17] as the "chemistry beyond the molecule"), of macromolecules or "supermolecules" which

[12] [N°12] Hobza, P.; Zahradnik, R.; Muller-Dethlefs, K. *Collect Czech Chem C* **2006**, *71*, 443.

[13] [N°13] Kaplan, I. G. *Intermolecular Interactions; Physical Picture, Computational Methods and Model Potentials*; Wiley, Chichester, **2006**.

[14] [N°14] Stone, A. J. *The Theory of Intermolecular Forces,* ; Oxford University Press; Oxford, **2002**.

[15] [N°15] Müller-Dethlefs, K.; Hobza, P. *Chem. Rev.* **2000**, *100*, 143.

[16] [N°16] Hirschfelder, J. O.; Curtiss, C. F.; Bird, R. B. *Molecular Theory of Gases and Liquids*; Wiley, New York, **1954**.

[17] [N°17] Lehn, J.-M. *Angew. Chem. Int. Ed. Engl.* **1988**, *27*, 89.

should be capable of repeating opening and closing without changing any important structure feature.[18]

4 - What about nomenclature?

Atoms, as well as molecules, can interact together leading to the formation of either a new "classical" molecule (reactive channel) or a molecular "cluster" (nonreactive channel).[19] In the first case, a covalent interaction is clearly involved. In the second one, where a covalent bond is neither formed nor broken, non-covalent interactions are at the origin of the cluster's formation. From a theoretical standpoint, molecular clusters can be studied by using the so called *ab initio* quantum-chemical methods, by treating the cluster as a "supermolecule" constituted of several moieties hold together trough non-covalent bonds (solely by electric multipole–electric multipole interactions, not only permanent, but also inductive and time-dependent multipoles), which constitute a significant feature of such complexes. Nevertheless, a very often-unclear issue in the literature remains the definition of non-covalently bound complexes as well as the use of the term vdW interactions, which is sometimes used only for a certain class of non-covalent interactions, mostly dispersion. When possible, it would be highly recommendable to use another kind of formalism for non-covalent bonds in contrast to the representation of covalent bonds, *i.e.* for covalent bond, a short full line (-) and for non-covalent bonds, three dots (. . .). Thus, for example, a proper representation of the hydrogen molecule would be H-H, while for the Helium (vdW) molecule He . . . He, or alternatively H_2 and $(He)_2$.[20] Nevertheless, the type of bonds that represent the He . . . He molecule still does not have a definite name. There is no doubt that it is possible to name it a non-covalent bond, but even if it really is non-covalent, this non-specific name does not represent a proper description of its true nature. Another label, which can be found in the literature as a derivation of the term weak interactions is "weak bonds". This has definitively to be considered as a misnomer because it is derived from a designation that has been used for a long time for a completely different context.

---

[18] [N°18] Hobza, P.; Muller-Dethlefs, K. In *Non-Covalent Interactions: Theory and Experiment*; The Royal Society of Chemistry: **2009**.

[19] [N°15] Müller-Dethlefs, K.; Hobza, P. *Chem. Rev.* **2000**, *100*, 143.

[20] [N°18] Hobza, P.; Muller-Dethlefs, K. In *Non-Covalent Interactions: Theory and Experiment*; The Royal Society of Chemistry: **2009**.

For years, the designation "van der Waals" was favoured for the specific case of vdW interactions, forces and bonds. Nevertheless, it has to be admitted that this nomenclature has also been corrupted, sometimes as a poorly defined use for a component of the empirical force field where the combination of dispersion and exchange-repulsion forces is often called under the "van der Waals" term.[21] Other authors in the literature, namely Hobza *et al.*[22] have proposed to name and use under the term "non-covalent" everything that remains *not covalent,* for instance: *electrostatic interactions* between permanent multipodes (charge-charge, charge dipole, charge-multipole, etc.), *induction and/or polarisation interactions* between instantaneous and induced multipoles, *dispersion interactions* between instantaneous and induced multipoles, but also: charge-transfer; formation of hydrogen, halogen or lithium bonding; and thus, metallic interactions, which is again not totally straightforward without ambiguity, but nevertheless remains so far one of the most accurate descriptions of the nature and origin of these interactions.

5 - Covalent bonds vs. non-covalent interactions.

Covalent and non-covalent interactions (NCIs) differ considerably due to their totally different origin.

5.1 - Characteristics of the covalent bonds.

The concept of covalent bonding, first described in 1916 by Lewis[23] (well before the birth of the quantum theory of the chemical bonds), is now, after more than 90 years of intense study, well established and understood. The description of the formation and breaking of these specific bonds can be performed at different theoretical levels (*e.g.*, beyond *ab initio* Hartree-Fock and Density Functional Theory, the so called DFT). The covalent interaction is the result of the distribution and delocalization of electrons over the entire considered molecule. This description is fully accurate when the molecule is

[21] [N°19] Ponder, J. W.; Case, D. A. *Advances in protein chemistry* **2003**, *66*, 27.
[22] [N°15] Müller-Dethlefs, K.; Hobza, P. *Chem. Rev.* **2000**, *100*, 143.
[23] [N°20] Lewis, G. N. *J. Am. Chem. Soc.* **1916**, *38*, 762.

considered in free space, isolated from all its surroundings.[24] Concerning the description of the electronic structure of isolated molecules, modern theoretical quantum chemistry methods, the so called *ab initio* method, have been extremely successful regarding precision, reaching some times the level of high-resolution spectroscopic results with no fundamental disagreements between state-of-art theory and experiment. From a theoretical standpoint, a covalent bond is formed when two subsystems bearing unfilled electronic shells start to overlap, increasing the electron density in the bonding region, which consequently is reflected by the formation and strengthening of the bond (more familiarly, it consists of a pair of electrons shared by two atoms). The opposite applies when the increase of the electron density occurs in the antibonding region, which entails the weakening of the bond. The most efficient overlap arises when the interatomic distances are found to be below 2 Å and becomes negligible at distances larger than about 4 Å.[25] From an experimental standpoint, we can find a great variety of spectroscopic methods that provide a look at a molecule in the gas phase in conditions chosen as such that, it can be considered unperturbed from collisions or other external forces (*e.g.* in molecular beams from supersonic jet expansions).[26] These high-resolution spectroscopy methods based on molecular quantum mechanics, group theory, and phenomenological Hamiltonians with well-defined matrix elements, offer very powerful and well-defined understood algorithms of interpretation.[27,28]

5.2 - Characteristics of the non-covalent interactions.

The basic principles of NCIs were formulated first by Linus Pauling[29] in 1931 for the case of the hydrogen bond (H-bond). In contrast with the covalent bonds, while it is possible to ascribe the stability of a complex to non-covalent interaction in nature, it is not always easy to localise such interactions in space. Moreover, the understanding of

[24] [N°15] Müller-Dethlefs, K.; Hobza, P. *Chem. Rev.* **2000**, *100*, 143.
[25] [N°18] Hobza, P.; Muller-Dethlefs, K. In *Non-Covalent Interactions: Theory and Experiment*; The Royal Society of Chemistry: **2009**.
[26] [N°21] Campargue, R. *J. Phys. Chem.* **1984**, *88*, 4466.
[27] [N°22] Herzberg, G. *Molecular Spectra and Molecular Structure: Electronic Spectra and Electronic Structure of Polyatomic Molecules*.
[28] [N°23] In *Molecular Symmetry and Spectroscopy*; Bunker, P. R., Ed.; Academic Press: **1979**.
[29] [N°24] Pauling, L. *J. Am. Chem. Soc.* **1931**, *53*, 1367.

the nature of NCIs is far less clear, calculations yielding frequently to results being in conflict with experimental data. Even if tremendous improvements have been made in theory as well as in experimental techniques during the last decades, we are still far away from a complete description and understanding of non-covalent systems without any unambiguity. Experiments, for instance, do not yet provide, for a defined molecular system, a complete description of all fundamental aspects related to non-covalent interactions, or require the combination of various techniques, inducing some ambiguities. Theory, on the other hand, can provide an accurate description of a non-covalent complex (*e.g.* reveal some information of the molecular structure, stabilization energy or any kind of other properties through the wavefunction). Despite the difficulties above-mentioned, it is well-established that NCIs can act at much greater distances than covalent bonds, sometimes at more than 10 Å and, in the case of biomacromolecules, even at more than 100 Å because an overlap is unnecessary (in fact overlap between occupied orbitals would only lead to repulsion). The reason of the attractions between interacting subsystems must be found elsewhere. It lies in fact purely in the electrical properties displayed by the subsystems and to a lesser extend, their magnetic properties. Consequently, non-covalent interactions originate from interaction between: permanent multipoles, permanent multipole and an induced multipole, or finally, an instantaneous time variable multipole and an induced multipole; which are all possible sources of attraction (or oppositely, repulsion) occurring between systems of different types. All of the various types of non-covalent interactions will be disclosed after a brief summary of related fundamental aspects of Quantum Mechanics.

5.2.1 - Quantum Mechanics considerations.

Quantum Mechanics strongly emphasizes the constant movement of electrons in an atom through the Schrödinger Equation[30] and the Heisenberg's Uncertainty Principle.[31] According to the latter, the energy of an electron is never zero; therefore, electrons are constantly moving around the orbitals. The square of the Schrödinger Equation for a

[30] [N°25] Schrödinger, E. *Phys. Rev.* **1926**, *28*, 1049.

[31] [N°26] Heisenberg, W. *Z. Physik* **1927**, *43*, 172.

particle in a box suggests that it is probable to find the electron (particle) anywhere in the orbital of the atom (box).[32] These two important aspects of Quantum Mechanics strongly suggest that because of the constant movement of the electrons of an atom, there is a high probability of dipole formation. When a group of electrons start to move from one to the other end of the atom, it creates an instantaneous dipole.[33]

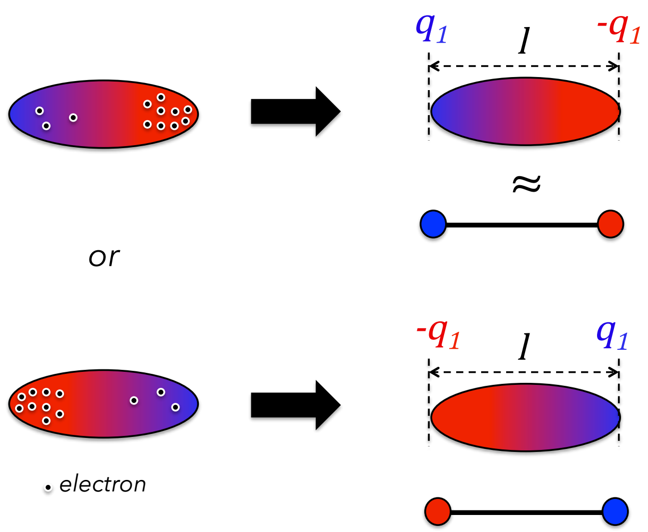

Figure 6: Illustration of the formation of dipoles through the movement of group of electrons.

Because these groups of electrons are in constant movement, they travel from one end of the atom to the other and back again continuously. Therefore, the opposite state is as probable of occurring as shown in (Figure 6). Therein NCIs will be classified under two different terminologies: *i.e.* the first-order NCIs and the second-order NCIs, where the former exist in all kind of systems independently of their intrinsic specificity, while the latest are rather depend on it (*e.g.* Hydrogen bonds interactions which require some specific structural conditions to be formed). Furthermore, second-order interactions can generally be identified as being a combination of first-order NCIs (with various degree of importance), for which a specific name has been associated to simplify (oversimplify?) their description (*e.g.* π-π stacking).

[32] [N°27] Than, J. Web. UC Davis Chemwiki an Open Access textbook environment.

[33] [N°28] Atkins, P.; de Paula, J. *Physical Chemistry for the Life Sciences*; Oxford, UK: Oxford University Press. 2006. 95.

5.2.2 - First order non-covalent interactions.

5.2.2.1 - Permanent multipole/permanent multipole.

The first type of first-order non-covalent interaction that will be disclosed occurs between two permanent multipoles applying in a subsystem. The usual terminology ascribed for their designation is the ***Electrostatic interaction***, which in terms of energy predominates in most cases over other energy terms.

Generally, a permanent dipole moment is defined as *molecules or atoms with equal and opposite electrical charges separated by a small distance.* This occurs when two atoms have a substantially different electronegativity: One atom in a molecule attracts electrons more than the other, becoming more negative, while the other atom becomes more positive. A molecule with a permanent dipole moment is called a polar molecule.

The major part of the following discussion will be based on the Coulombic potential energy of the interaction between two charges, given to the relative ease to adapt this expression to determine the potential energy of a point charge and a dipole and to some extension, to the interaction occurring between two dipoles. The so-called Coulomb's Law,[34-36] describing the force exerted on a charged object due to the presence of another charged object, provides an access to the electrostatic interaction energy.[37] Thus, when two charges q_1 and q_2 are separated by a distance r in a vacuum, the potential energy of their interaction is:

$$V = \frac{q_1 q_2}{4\pi\varepsilon_0 r}$$

[34] [N°29] Coulomb, C. A. *Premier mémoire sur l'électricité et le magnétisme*; Histoire de l'Académie Royale des Sciences, Imprimerie Royale, **1785**, 569-577.

[35] [N°30] Coulomb, C. A. *Second mémoire sur l'électricité et le magnétisme*; Histoire de l'Académie Royale des Sciences, Imprimerie Royale, **1785**, 578-611.

[36] [N°31] Jackson, J. D. *Classical Electrodynamics*; John Wiley & Sons Ltd., **1962**.

[37] [N°28] Atkins, P.; de Paula, J. *Physical Chemistry for the Life Sciences*; Oxford, UK: Oxford University Press. 2006. 95.

If we consider now the same two charges but immersed in a medium (such as air or a liquid), their potential energy is reduced to:

$$V = \frac{q_1 q_2}{4\pi\varepsilon r}$$

Where ε is the permittivity of the medium.

Considering the situation described bellow (Figure 7):

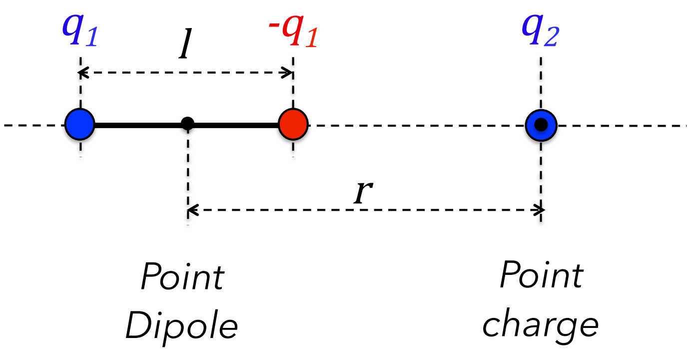

A point dipole is a dipole in which the separation between the charges is much smaller than the distance at which the dipole is been observed, l << r.

Figure 7: Consideration of an interaction between a point dipole and a point charge.

The sum of the potential energies between similar charges and attraction between opposite ones is:

$$V = \frac{1}{4\pi\varepsilon_0}\left(-\frac{q_1 q_2}{r - \frac{1}{2}l} + \frac{q_1 q_2}{r + \frac{1}{2}l}\right) = \frac{q_1 q_2}{4\pi\varepsilon_0}\left(-\frac{1}{1-x} + \frac{1}{1+x}\right)$$

$$Where: x = \frac{l}{2r}$$

Because, $l \ll r$ for a point dipole, we can simplify by expanding the terms in x, while retaining the other term:

$$V = \frac{q_1 q_2}{4\pi\varepsilon_0}\{-(1 + x + \cdots) + (1 - x + \cdots)\} \approx -\frac{2x q_1 q_2}{4\pi\varepsilon_0 r} = -\frac{q_1 q_2 l}{4\pi\varepsilon_0 r^2}$$

And finally:

$$V = -\frac{\mu_1 q_2}{4\pi\varepsilon_0 r^2}$$

With $\mu_1 = q_1 l$, μ in coulomb metres, q_2 in coulombs, and r in metres, V in joules.

The potential energy rises towards zero (the value at infinite separation of the charge and the dipole) more rapidly (as $1/r^2$) than between two point charges (which varies as $1/r$) because, from the viewpoint of the point charge, the partial charges of the dipole seem to merge and cancel as the distance r increases.

If we now consider the interaction between two dipoles in the following arrangement: (Figure 8),

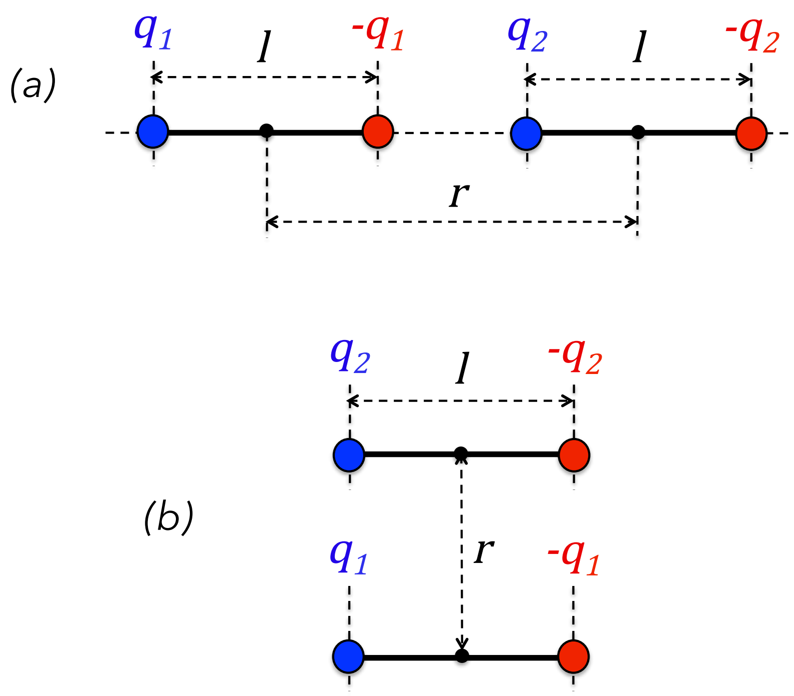

Figure 8: Consideration of the easiest manner of interaction between two dipoles.

By proceeding in the same way as before (Figure 7), the interaction energy for (Figure 8, case a) is now the sum of four pairwise terms: two terms relating the attractions between opposite charges (which contribute as negative terms to the potential energy) and two terms describing the repulsions between like charges (which contribute as positive terms) leading to the following equation:

$$V = \frac{1}{4\pi\varepsilon_0}\left(-\frac{q_1 q_2}{r+l} + \frac{q_1 q_2}{r} + \frac{q_1 q_2}{r} - \frac{q_1 q_2}{r-l}\right) = -\frac{q_1 q_2}{4\pi\varepsilon_0 r}\left(\frac{1}{1+x} - 2 + \frac{1}{1-x}\right)$$

With $x = l/r$. As before, provided $l << r$, we can expand the two terms in x and retain only the first surviving term, which is equal to $2x^2$, which leads to the simplified equation:

$$V = -\frac{2x^2 q_1 q_2}{4\pi\varepsilon_0 r}$$

Thus, because $\mu_1 = q_1 l$ and $\mu_2 = q_2 l$, the potential energy of the interaction associated is:

$$V = -\frac{\mu_1 \mu_2}{2\pi\varepsilon_0 r^3}$$

The potential energy rises towards zero (the value at infinite separation between the two dipoles) even faster (as $^1/_{r^3}$) than the case related in (Figure 7), with both interacting entities appearing neutral to each other at large separations. Very similarly for, (Figure 8, case b) the expression for the potential energy is:

$$V = \frac{\mu_1 \mu_2}{4\pi\varepsilon_0 r^3}$$

The most important thing to be notice for the above-mentioned cases is that the higher the order of the multipole is, the fastest the interaction energy falls off.

If we consider now more general cases, the potential energy of interaction between two dipoles (or polar molecules) is more complex due to their relative orientation, which has to be taken in consideration. When two dipoles are in a fixed parallel orientation (Figure 9), as it can be the case in a solid state, it remains relatively easy to determine the potential energy of interaction.

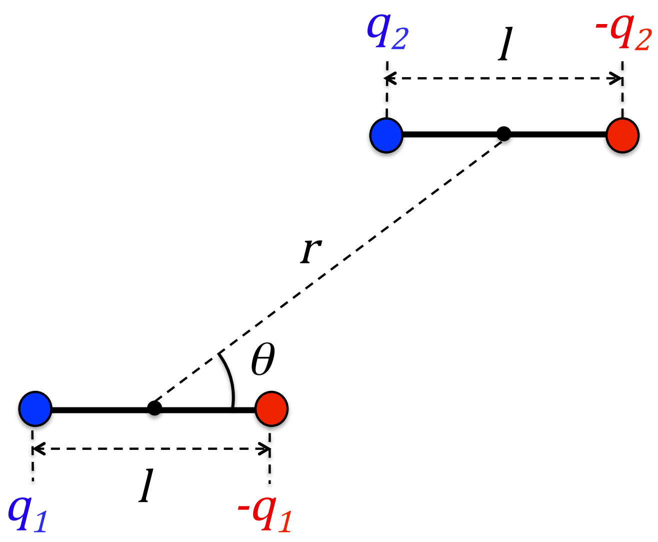

Figure 9: Consideration of the interaction between two parallel dipoles.

The associated potential energy of interaction is given by the following equation:

$$V = \frac{\mu_1 \mu_2 f(\theta)}{4\pi\varepsilon_0 r^3}$$

$$\textit{With: } f(\theta) = 1 - 3\cos^2\theta$$

In contrast, if we consider the situation in a fluid where two molecules can freely rotate, the interaction between dipoles will average zero due to the sign change of $f(\theta)$ as their orientation changes. The physical reason behind this is that the "like partial charges" of two molecules which freely rotates are close together as much as the two opposite charges, and the repulsion of the former is cancelled by the attraction of the latter. Therefore, the interaction energy of two freely rotating dipoles is zero. Nevertheless, due to the dependence of their mutual potential energy to their relative orientation, the molecules do not really rotate completely freely and this is true even in the gas phase.

Because the lower energy orientations are always favoured, there is a nonzero average interaction between polar molecules, which can be ascribed through the following equation:

$$\langle V \rangle = -\frac{C}{r^6}$$

$$C = \frac{2\mu_1^2\mu_2^2}{3(4\pi\varepsilon_0)^2 kT}$$

This equation describes the **Keesom interaction** (named after Willem Hendrik Keesom), which constitutes the first of the contributions to the so-called van der Waals interaction.

It is important to underline: the negative sign means that the average interaction energy is attractive; the dependence of the energy on the inverse sixth power of the separation (r) confirms the non-covalent nature of the interaction and the inverse dependence on the temperature, reflects the fact that the greater thermal motion overcomes the mutual orientating effects of the dipole at higher temperature. The inverse sixth power of the separation takes its origin in the inverse third power of the interaction potential energy, which is weighted by the energy in the Boltzmann term, being also proportional to the inverse third power of the separation.

It has to be mentioned that even if we have considered here the case of the interaction between dipoles, it remains quite easy to extend the expression given above for the energy of interaction to higher multipoles or arrays of point charges. Moreover, an ***n-pole*** is an array of point charges with an *n-pole* moment but no lower moment as shown in (Figure 10).

Monopole (n=1): A point charge for which the monopole moment is normally called the overall charge.

Dipole (n=2): Array of charges bearing no monopole moment (no net charge).

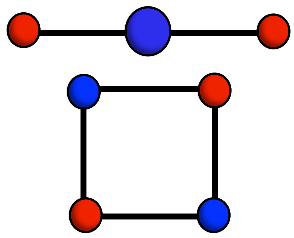

Quadrupole (n=3): Array of point charges bearing neither net charge nor dipole moment (*e.g.* CO_2).

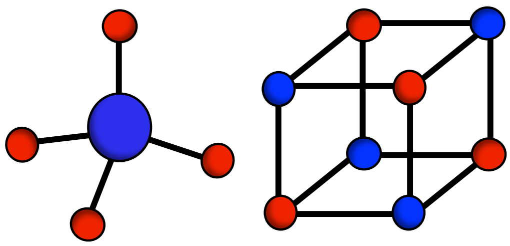

Octupole (n=4): Array of point charges that sum zero bearing neither a dipole moment nor a quadrupole moment (*e.g.* CH_4).

Figure 10: Illustration of typical charge arrays corresponding to electric multipoles.

5.2.2.2 - Permanent multipole/induced multipoles.

A second type of non-covalent interaction is the so-called ***Induction (polarisation) interaction***, which represents the interaction occurring between permanent and induced multipoles. For instance, if one subsystem has no permanent multipole moments, *i.e.* it is neutral and spherically symmetric (*i.e.* an atom), the electrostatic interaction term is zero and induction is responsible for attraction. Therefore, an induced dipole moment is a temporary condition during which a neutral nonpolar atom (*e.g.* Helium) undergoes a separation of charges due to the environment, *i.e.* when a polar molecule with a dipole moment μ_1 approaches a neighbouring polarizable molecule it can cause that molecule to also generate a dipole μ_2*.[38] The neighbouring molecule is then considered to have an induced dipole moment (Figure 11). The induced dipole interacts with the permanent dipole of the first molecule and both are attracted together.

[38] [N°28] ibid.

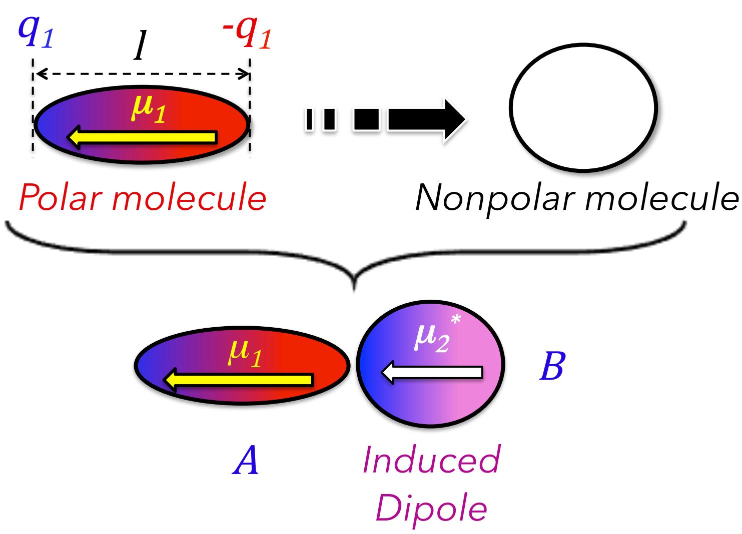

Figure 11: Illustration of the formation of an induced dipole by a polar molecule.

The average interaction energy when the separation of the molecules is *r* is given by the following equation:

$$V = -\frac{C}{r^6}$$

$$C = \frac{\mu_1^2 \alpha_2'}{4\pi\varepsilon_0}$$

Where α_2' is the polarizability volume of molecule B and μ_1 is the permanent dipole moment of molecule A. This equation describes the **Debye force**, (named after Peter J.W. Debye), which constitutes the second of the contributions to the, so-called, van der Waals interactions.

By contrast with dipole-dipole interaction, the dipole-induced dipole interaction energy is independent of the temperature because thermal motion has no influence on the averaging process. Moreover, similarly to the dipole-dipole interaction, the potential energy depends on $^1/_{r^6}$ stemming from the $^1/_{r^3}$ dependence of the field (and hence the magnitude of the induced dipole) and the $^1/_{r^3}$ dependence of the potential energy of interaction between the permanent and the induced dipoles.

5.2.2.3 - Instantaneous multipole/Induced multipole interaction.

Systems with vanishing permanent dipole moments, for instance, two nonpolar molecules (including closed-shell atoms, such as argon), exhibit attraction as well. This experimental finding manifested by the formation of condensed phases of non-polar substances, for instance, the condensation of hydrogen; [39] the discovery of the liquefaction of noble gases in the early 20th century;[40] or the fact that benzene is liquid at room temperature,[41] was at that time very surprising. It was only possible on the basis of quantum mechanics to theoretically derive the attraction between noble-gas atoms in terms of the so-called ***London dispersion energy***. At that time this explanation represented an important argument in favour of the importance of the recently born quantum mechanics. London's theory took into account the oscillations of electron clouds and nuclei, which are responsible of the generation of instantaneous multipoles, which vanish when integrated over time. To have a better perception of the origin of these interactions, it is supposed that the electrons of a molecule flicker into an arrangement then, a so-called *instantaneous dipole* μ_1^* (in contrast of a permanent dipole) moment is formed, generating an electric field that will polarize another molecule, and induce in that molecule an instantaneous dipole moment μ_2^* (Figure 12).

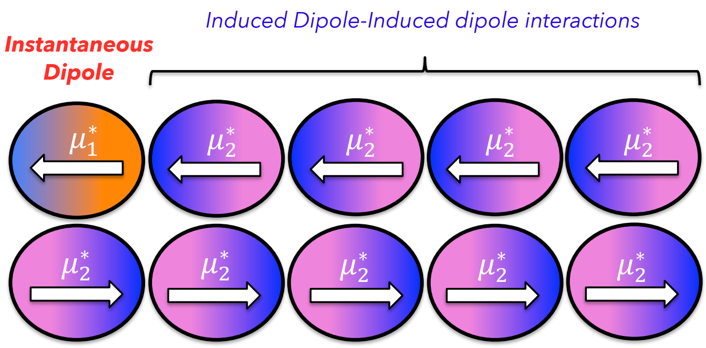

Figure 12: An instantaneous dipole on one molecule induces a dipole on another molecule, and then both dipoles interact to lower the energy.

[39] [N°32] Leachman, J. W.; Jacobsen, R. T.; Penoncello, S. G.; Lemmon, E. W. *J. Phys. Chem.* **2009**, *38*.

[40] [N°7] Kamerlingh Onnes, H. In *Nobel Lecture: Investigations into the Properties of Substances at Low Temperatures, which Have Led, amongst Other Things, to the Preparation of Liquid Helium*; Nobelprize.org, Nobel Media AB 2013: Web. 27 Jun 2014: nobelprize.org/nobel_prizes/physics/laureates/1913/onnes-lecture.html, 1913.

[41] [N°33] Benmore, C. J.; Tomberli, B.; Egelstaff, P. A.; Neuefeind, J. *Mol. Phys.* **2001**, *99*, 787.

The two dipoles will display a mutual attraction, resulting in the lowering of the potential energy of the pair. Moreover, if the first molecule undergoes a change of the size and direction of its instantaneous dipole, the electron distribution of the second molecule will follow meaning that the two molecules are also correlated in direction (Figure 13).

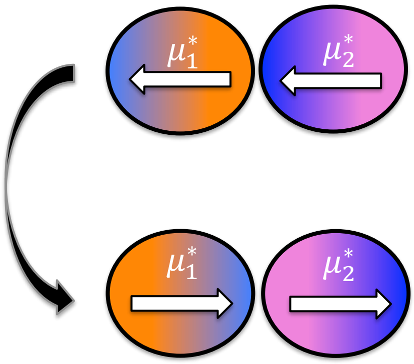

Figure 13: The two instantaneous dipoles are correlated, although they occur in different orientations at different instants.

Due to this correlation, the attraction between the two instantaneous dipoles does not average to zero and gives therefore rise to an induced-dipole-induced-dipole interaction. Several names can be found in the literature to ascribe this interaction, for instance, **the dispersion interaction**, **London interaction** (named after Fritz London[42,43]), or finally the **London dispersion interaction**.

The dispersion interaction is directly dependent on several key parameters such as the polarizability of the first molecule as the instantaneous dipole moment μ_1^* depends on the "looseness" of the control that the nuclear charge exercises over the outer electrons. Moreover, the strength of the interaction also depends on the polarizability of the second molecule, which constitutes a determining factor on how readily a dipole can be induced by another molecule.

[42] [N°8] London, F. *Trans. Faraday Soc.* **1937**, *33*, 8b.

[43] [N°9] London, F. *Z. Physik* **1930**, *63*, 245.

Actual theoretical calculation of the dispersion energy is quite sophisticated, but a reasonable approximation to the interaction energy can be found in the London formula where:

$$V = -\frac{C}{r^6}$$

$$C = \frac{3}{2}\alpha_1'\alpha_2'\frac{I_1 I_2}{I_1+I_2}$$

I_1 and I_2 correspond to the ionization energies of the two molecules.

As asset by the above-mentioned equation, the dispersion energy is proportional to the inverse sixth power of the separation of the molecules, which identifies this interaction as the third part of the van der Waals interaction. It was believed for a long time that dispersion energy was always smaller than the two previously mentioned energy contributions (*i.g*. Keesom interaction and Debye interaction) and was mainly involved in the stabilization of noble gas atoms. It has now been shown that dispersion energy between aromatic systems with delocalised electrons is important, and is comparable to other interactions such as, for example, hydrogen-bonded structures. This finding changed considerably our vision on the nature of the stabilisation of bio macromolecules such as DNA and proteins.

All three above-mentioned contributions to the van der Waals interaction energy[44-47] (Keesom, Debye, and London) are attractive by nature, and as such should be balanced by some repulsive force. The so-called exchange-repulsive energy[48] is of quantum-chemical nature too and becomes important when two subsystems overlap.

---

[44] [N°34] Béguin, L.; Vernier, A.; Chicireanu, R.; Lahaye, T.; Browaeys, A. *Phys. Rev. Lett.* **2013**, *110*, 263201.
[45] [N°35] Tadmor, R. *J. Phys. Condens. Mat.* **2001**, *13*, L195.
[46] [N°36] de Boer, J. H. *Trans. Faraday Soc.* **1936**, *32*, 10.
[47] [N°37] Bradley, R. S. *Phil. Mag. Ser. 7* **1932**, *13*, 853.
[48] [N°38] Brdarski, S.; Karlström, G. *J. Phys. Chem. A* **1998**, *102*, 8182.

5.2.2.4 - Repulsive interaction.

The repulsive interaction directly arises from two very important aspects of quantum theory[49-52]:

- According to the Heisenberg uncertainty principle, the electrons, which are located within the confines of an atom, possess kinetic energy that would exert an outward pressure were it not for the compensating attractive force of the positively charged nucleus. But even the very slight decrease in volume that would result from squeezing the atom into a smaller space will raise this pressure so as to effectively resist this change in volume. This is the basic reason that condensed states of matter have extremely small compressibility's.[53]
- The Pauli exclusion principle: Each electron must have a different set of quantum numbers. When two same spin electrons intersect in space, their orthogonalized orbitals take on larger slopes to keep their overlap zero. The increase in slope causes an increase in kinetic energy, which causes a large portion of the Pauli repulsion.

Thus, when the distance between two atoms decreases, their electron clouds approach each other and their charge distributions gradually overlap. The Pauli exclusion principle (named after Wolfgang Ernst Pauli[54]) prohibits all the electrons from occupying the overlap region and so reduces the electron density in this region. The positively charged nucleis of the atoms are then incompletely shielded from each other and therefore exert a repulsive force on each other. Thus, the electron overlap increases the total energy of the system and gives a repulsive contribution to the interaction. The repulsions increase steeply with decreasing separation in a way that can be deduced only by very extensive and complicated molecular structure

[49] [N°39] Pavarini, E.; Koch, E.; Anders, F. In *Correlated electrons: From Models to Materials* **2012**.

[50] [N°40] Weisskopf, V. F. *Science* **1975**, *187*, 605.

[51] [N°41] Andersen, H. C.; Chandler, D.; Weeks, J. D. *J. Chem. Phys.* **1972**, *56*, 3812.

[52] [N°42] Dirac, P. A. M. *Proc. royal. soc. Lond. S. A* **1926**, *112*, 661.

[53] [N°27] Than, J. Web. UC Davis Chemwiki an Open Access textbook environment.

[54] [N°43] Pauli, W. In *Nobel Lecture: Exclusion Principle and Quantum Mechanics*; Nobelprize.org, Nobel Media AB 2013: Web. 8 Jul 2014: nobelprize.org/nobel_prizes/physics/laureates/1945/pauli-lecture.html.

calculations. Nevertheless, it is possible in certain cases to evaluate the repulsion by using greatly simplified representations of the potential energy, where the details are almost ignored, and where the general features are expressed through a few adjustable parameters. One of such approximations is the hard-sphere potential.

In contrast to the above-mentioned interactions, the so-called ***hydrogen bond***, ***hydrophobic effect*** and the ***π–π stacking***, which are also of attractive nature, will be separated herein as being systemic second-order NCIs, where the first-order NCIs described intervene in various degree of importance.

5.2.3 - Second-order non-covalent interactions.

5.2.3.1 - Hydrogen bonds.

As mentioned in **5.2.1**, hydrogen bonds[55] are not inherent to all molecules, but apply under specific conditions when two species establish a link of the form A–**H**•••B, where A and B are highly electronegative elements, and B possesses a lone pair of electrons (Figure 14).

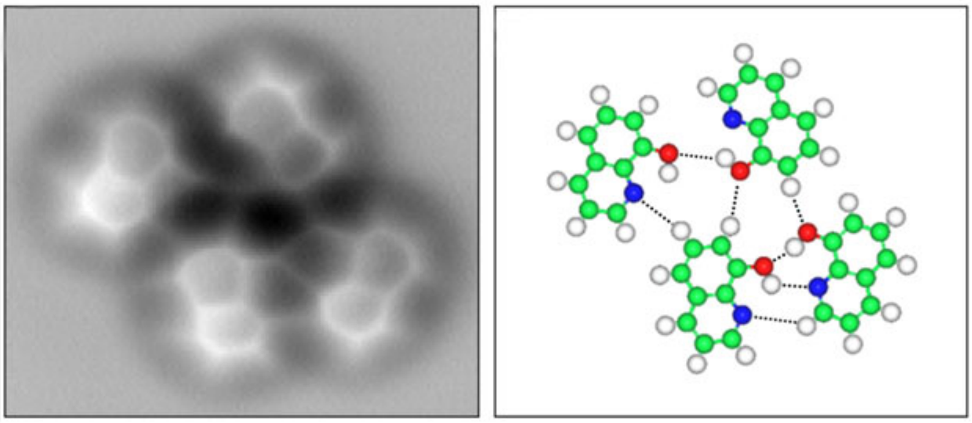

Figure 14: Hydrogen bonding visualized in 8-hydroxyquinoline using a non-contact AFM microscope at the National Centre for Nanoscience and Technology, China. Author: Royal Society of Chemistry (rsc.org), Public domain via Wikimedia Commons.

[55] [N°44] In *IUPAC. Compendium of Chemical Terminology*, Version 2.3.3 - 2014-02-24 - the "Gold Book". ed. XML on-line corrected version: Web. 24 Jul 2014: goldbook.iupac.org.

Generally a hydrogen bond is regarded as being limited to atoms such as N, O, and F. Nevertheless, if for instance B is an anionic species (such as Cl^-), it may also participate in hydrogen bonding. There is no strict rule saying that an atom can participate or not in hydrogen bonding, but N, O or F are indeed the most often concerned. The Hydrogen bonds formation can be considered in two ways:

a) As the approach between a partial positive charge of H and a partial negative charge of B. This consist on the treatment of the A–**H**•••B system as an array of point charges (partial negative charges on A and on B, partial positive charge on H). This suggests that the lowest energy is achieved when the bond is linear, situation in which the negative charges are furthest apart (X-ray studies often support a linear or near-linear arrangement).

b) As a particular example of delocalized molecular orbital formation in which A, H, and B each supply one atomic orbital from which three new molecular orbitals are built as shown in Figure 15.[56]

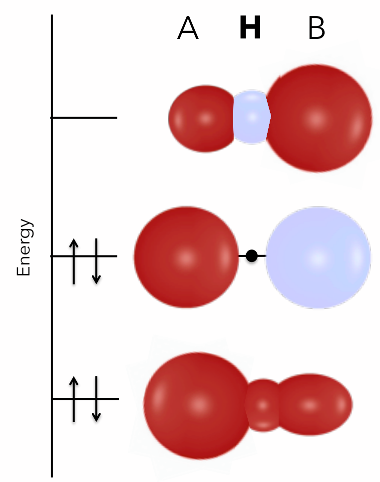

Figure 15: Molecular orbital interpretation of the formation of **A–**H···**B**. By starting from the three A, H, B orbitals, three new molecular orbitals can be formed. Only the two lower energetically orbitals are occupied, which may lead to a net diminution in energy compared with the separate AH and B species.

[56] [N°28] Atkins, P.; de Paula, J. *Physical Chemistry for the Life Sciences*; Oxford, UK: Oxford University Press. 2006. 95.

If we consider now the situation related in case b). The A-H bond is formed from the overlapping process of an orbital on A (ψ_A) with a hydrogen *1s* orbital (ψ_H), and the lone pair on B occupies an orbital on B (ψ_B). We can then build three molecular orbitals from the three basis orbitals (assuming that the two molecules are close enough), thus:

$$\psi = c_1\psi_1 + c_2\psi_2 + c_3\psi_3$$

Where one of the molecular orbitals is bonding, another almost nonbonding and the third one anti-bonding. These three orbitals need to accommodate four electrons (two from the original A-H bond and two coming from the B lone pair). As displayed in Figure 15, two electrons will be placed in the bonding orbital and two in the non-bonding one. Therefore, as the antibonding orbital remains empty, the formation of the H-bond should result, depending on the precise location of the almost nonbonding orbital, in a lowering of energy of the system. In practice, because of the direct dependence of the bonding formation with the possibility that the orbital overlaps, the H-Bond is virtually a contact-like interaction, which is possible when, A-H touches B and is zero as soon as the contact is broken. Generally, when hydrogen bonding is present in a molecular system it will dominate the other intermolecular interactions. Structural evidences for hydrogen bonding can be found when the internuclear distance between formally non-bonded atoms is less than their van der Waals contact distance, suggesting that a dominating attractive interaction is occurring. Finally, it has to be mentioned that hydrogen bonds can be symmetric or unsymmetric. Indeed, it is possible to find the atoms lying midway between the two other atoms in a symmetrical arrangement (*e.g.* for the F–**H**•••F^- hydrogen bond, [57,58] where both bond lengths are 120 pm), or either an unsymmetrical arrangement, where the A-**H** bond is found to be shorter than the **H**•••B bond, which represents the most common case.

[57] [N°45] Nieckarz, R. J.; Oldridge, N.; Fridgen, T. D.; Li, G. P.; Hamilton, I. P.; McMahon, T. B. *J. Phys. Chem. A* **2009**, *113*, 644.

[58] [N°46] Emsley, J.; Parker, R. J.; Overill, R. E. *J. Chem. Soc., Farad. T. 2* **1983**, *79*, 1347.

Typically, when we consider the stabilization of non-covalent complexes we take into account the favourable energetically effect of non-covalent interactions on the system. Thus, the energy of the complex is lower than the sum of the energies of its separated subsystem, which occurs systematically if the complex is formed *in vacuo*. These considerations are different in another environment and mainly in the water phase. This is principally due to the fact that the equilibrium of any non-covalent (but also covalent) process is not determined by the change of energy (enthalpy), but rather by the change of the Gibbs energy ($\Delta G = \Delta H - T\Delta S$). Therefore, the binding can be now realised not only due to favourable energy (enthalpy) but also because of favourable entropy ($\Delta S > 0$). In this specific case, the enthalpy (energy) can be even unfavourable ($\Delta H > 0$). This is the so-called hydrophobic interaction and will be now disclosed.

5.2.3.2 - The hydrophobic effect.

It is well known that nonpolar molecules only dissolve very slightly in polar solvents. Moreover strong interactions between solute and solvent are not possible, resulting in individual solute molecules surrounded by a solvent cage (the so-called clathrates). The Hydrophobic interactions[59,60] describe the specific relation occurring between water and hydrophobes (non polar molecules, which are low water-soluble). For instance, mixing oil with water represents a good example of how this particular interaction works. Walter Kauzmann[61] discovered that nonpolar substances like fat molecules tend to clump up together rather than distributing itself in a water medium, because this will minimize the contact with water as shown in Figure 16.[62]

[59] [N°47] Chandler, D. *Nature* **2005**, *437*, 640.

[60] [N°48] Tanford, C. *Prot. Sci.* **1997**, *6*, 1358.

[61] [N°49] Kauzmann, W. In *Advances in Protein Chemistry*; C.B. Anfinsen, M. L. A. K. B., John, T. E., Eds.; Academic Press: **1959**; Vol. Volume 14, p 1.

[62] [N°27] Than, J. Web. UC Davis Chemwiki an Open Access textbook environment.

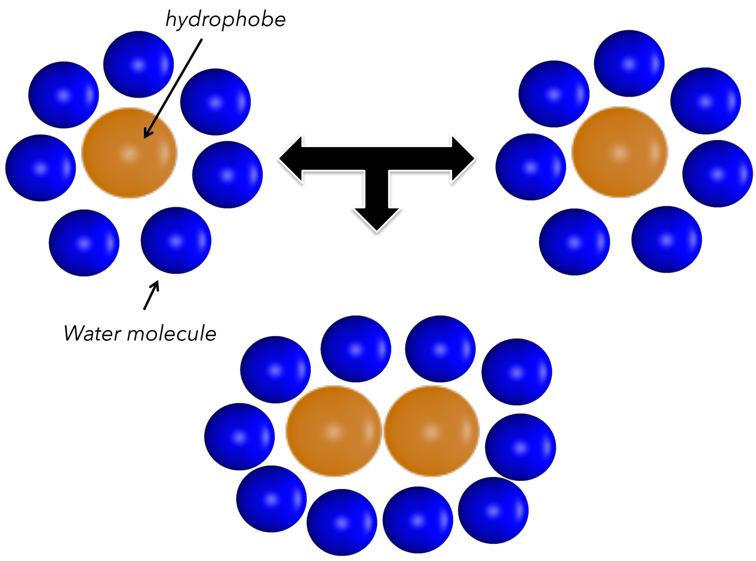

Figure 16: Illustration showing that when hydrophobes come together they will have less contact with the water molecules.

Before forming hydrophobic interactions, the hydrophobe dropped in an aqueous medium will first break hydrogen bonds between water molecules in order to get some space in the polar medium, without any reaction occurring between water molecules and the hydrophobes. Water molecules that are distorted by the presence of the hydrophobe will then have to create new hydrogen bonds, forming an ice-like cage structure around the hydrophobe. This result in a system (hydrophobe) being more structured with a decrease of the total entropy ($\Delta S < 0$).

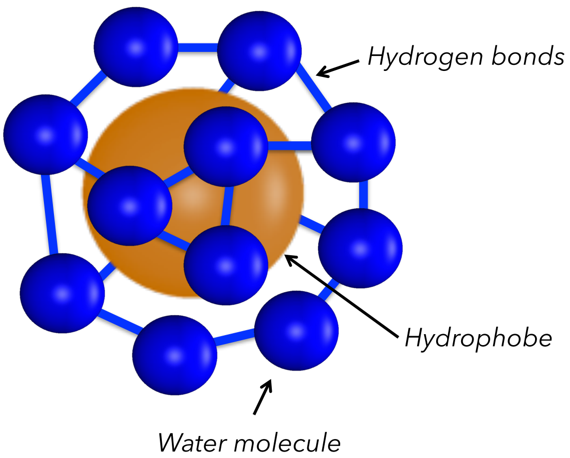

Figure 17: Illustration of water clathrates forming around the hydrophobe.

The variation in enthalpy (ΔH) of the system does not matter here in the determination of the spontaneity of the reaction because the variation of enthalpy is insignificant compared to the variation of entropy (ΔS), which is much higher. According to the Gibbs free energy equation:

$$\Delta G = \Delta H - T\Delta S$$

With: a small-unknown value of ΔH and a large negative value of ΔS.

This results in a positive value of ΔG, meaning that the inclusion of the hydrophobe among water molecules is not a spontaneous process. In contrast, hydrophobic interactions between hydrophobes are spontaneous (Figure 18). Indeed, when hydrophobes come together and interact, enthalpy increases ($\Delta H > 0$) because some of the hydrogen bonds that form the clathrate cage will break. The deformation of the clathrate cage (tearing down a portion) will induce an increase of the entropy ($\Delta S > 0$). Again, according to the Gibbs free energy equation, and with ΔH = small positive value, ΔS = large positive value, this results in a value of ΔG which is negative and hence hydrophobic interactions are spontaneous.

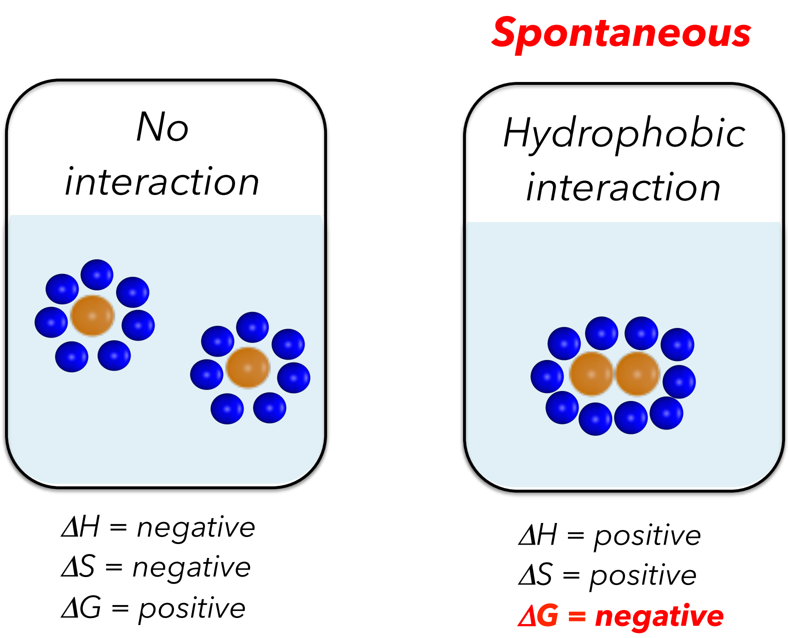

Figure 18: Illustration of the spontaneous process of the hydrophobic interaction.

Hydrophobic interactions are relatively stronger than other non-covalent interactions[63] (*i.e.*, van der Waals interactions or Hydrogen bonds). They are significantly influenced by some key parameters such as:

- The temperature: As temperature increases, the strength of hydrophobic interactions increases too. Nevertheless, very high temperature will denature the hydrophobic interactions.
- The number of carbons constituting the hydrophobes: Molecules with greater numbers of carbons will have stronger hydrophobic interactions.
- The shape of the hydrophobes: Aliphatic organic molecules have stronger interactions than aromatic compounds. Branches on a carbon chain will reduce the hydrophobic effect, whereas linear carbon chains will increase the interaction. This is due to the fact that carbon branches negatively produce some steric hindrance, which prevent two hydrophobes to interact with each other minimalizing their contact with water molecules.

Hydrophobic interactions have many biological interests,[64] especially for the folding of proteins, which is important for keeping a protein alive and biologically active as it allows the protein to subsequently decrease its surface and thus, decrease undesirable contacts with water.

5.2.3.3 - The so-called π-π stacking.

When unsaturated organic groups are involved in noncovalent interactions, the terms "π–π stacking", or more generally "π-π interactions" are often used'' in number of chemical, biological areas, especially the supramolecular field.[65-71] However both

[63] [N°47] Chandler, D. *Nature* **2005**, *437*, 640.
[64] [N°50] Dyson, H. J.; Wright, P. E.; Scheraga, H. A. *Proc. Natl. Acad. Sci. USA* **2006**, *103*, 13057.
[65] [N°51] Cerny, J.; Hobza, P. *Phys. Chem. Chem. Phys.* **2007**, *9*, 5291.
[66] [N°52] Meyer, E. A.; Castellano, R. K.; Diederich, F. *Angew. Chem. Int. Ed. Engl.* **2003**, *42*, 1210.
[67] [N°53] Kannan, N.; Vishveshwara, S. *Ptrotein Eng.* **2000**, *13*, 753.
[68] [N°54] Kim, K. S.; Tarakeshwar, P.; Lee, J. Y. *Chem. Rev.* **2000**, *100*, 4145.
[69] [N°15] Müller-Dethlefs, K.; Hobza, P. *Chem. Rev.* **2000**, *100*, 143.
[70] [N°55] Hobza, P.; Šponer, J. *Chem. Rev.* **1999**, *99*, 3247.

appellations do not accurately describe the forces that drive association between aromatic molecules, according to several groups.[72-75] This classification has a quite mysterious flavour.[76] Moreover, for larger structures the so-called *π–π* stacking is not well understood theoretically, although some progress has been made.[77,78] Nevertheless, it can be concluded for sure, based on many studies, especially of the benzene dimer[79-81] and other complexes involving phenyl rings,[82,83] that the *p* orbitals do not function as in conventional overlap driven by covalent bonding. Thus, number of recent studied have claimed that this term is misleading and should no longer be used.[84,85] For almost two decades Hunter and Sanders[86] had a quite remarkable approach for the understanding of this particular interaction by considering the *π*-system polarization. This provided a qualitative starting point for predicting the observed T-shaped or offset-stacked geometries, which have been almost exclusively observed for most aromatics. Again, the same Hunter and Sanders model was able to correctly predict that a face-centred stacking between aromatic units will dominate when electron-rich aromatics (donors) interact with electron-deficient aromatics (acceptors). These unique situations can, according to Iverson *et al.*,[87] most accurately be referred as aromatic donor–acceptor interactions in order to capture the special circumstances that lead to face-centred stacking. Referring to such systems as involving ''*π*-stacking'' or ''*π–π* interactions'' is a move toward far less informative and descriptive terms. Dominant notions of complementary electrostatic interactions between

---

[71] [N°56] Lehn, J.-M. In *Supramolecular Chemistry*; Wiley-VCH Verlag GmbH & Co. KGaA: **1995**.

[72] [N°57] Djukic, J.-P.; Sortais, J.-B.; Barloy, L.; Pannetier, N.; Sirlin, C.; Pfeffer, M. *Organometallics* **2012**, *31*, 2821.

[73] [N°58] Martinez, C. R.; Iverson, B. L. *Chem. Sci.* **2012**, *3*, 2191.

[74] [N°59] Grimme, S. *Angew. Chem. Int. Ed. Engl.* **2008**, *47*, 3430.

[75] [N°60] Swart, M.; van der Wijst, T.; Fonseca Guerra, C.; Bickelhaupt, F. M. *J. Mol. Model.* **2007**, *13*, 1245.

[76] [N°61] Sinnokrot, M. O.; Sherrill, C. D. *J. Phys. Chem. A* **2006**, *110*, 10656.

[77] [N°62] Grimme, S.; Mück-Lichtenfeld, C.; Antony, J. *J. Phys. Chem. C* **2007**, *111*, 11199.

[78] [N°63] Rapacioli, M.; Calvo, F.; Spiegelman, F.; Joblin, C.; Wales, D. J. *J. Phys. Chem. A* **2005**, *109*, 2487.

[79] [N°64] Podeszwa, R.; Bukowski, R.; Szalewicz, K. *J. Phys. Chem. A* **2006**, *110*, 10345.

[80] [N°65] Grant Hill, J.; Platts, J. A.; Werner, H.-J. *Phys. Chem. Chem. Phys.* **2006**, *8*, 4072.

[81] [N°64] Podeszwa, R.; Bukowski, R.; Szalewicz, K. *J. Phys. Chem. A* **2006**, *110*, 10345.

[82] [N°61] Sinnokrot, M. O.; Sherrill, C. D. *J. Phys. Chem. A* **2006**, *110*, 10656.

[83] [N°66] Tsuzuki, S. In *Intermolecular Forces and Clusters I*; Wales, D. J., Ed.; Springer Berlin Heidelberg: **2005**; Vol. 115, p 149.

[84] [N°58] Martinez, C. R.; Iverson, B. L. *Chem. Sci.* **2012**, *3*, 2191.

[85] [N°59] Grimme, S. *Angew. Chem. Int. Ed. Engl.* **2008**, *47*, 3430.

[86] [N°67] Hunter, C. A.; Sanders, J. K. M. *J. Am. Chem. Soc.* **1990**, *112*, 5525.

[87] [N°58] Martinez, C. R.; Iverson, B. L. *Chem. Sci.* **2012**, *3*, 2191.

polarized π-systems[88,89] are being refined or even supplanted by considering the importance of solvation effects in strongly interacting solvents,[90,91] as well as the direct interactions between ring substituents.[92-94] Finally, according to Grimme,[95] the term "π-π stacking" should be used exclusively as a geometrical descriptor of the interaction mode in unsaturated molecules and π–π interactions should be understood as a special type of electron correlation (dispersion) effect that can only act in large unsaturated systems when they are spatially close, which is only possible in the stacked orientation.

Figure 19: Schemes describing the electrostatic view of aromatic interactions reported by Iverson *et al.*[96] the various modes of stacking are presented, emphasizing locations of electrostatic attraction or repulsion. © Royal Society of Chemistry. *(Figure removed because subjected to copyright).*

[88] [N°68] Cozzi, F.; Ponzini, F.; Annunziata, R.; Cinquini, M.; Siegel, J. S. *Angew. Chem. Int. Ed. Engl.* **1995**, *34*, 1019.

[89] [N°67] Hunter, C. A.; Sanders, J. K. M. *J. Am. Chem. Soc.* **1990**, *112*, 5525.

[90] [N°69] Cubberley, M. S.; Iverson, B. L. *J. Am. Chem. Soc.* **2001**, *123*, 7560.

[91] [N°52] Meyer, E. A.; Castellano, R. K.; Diederich, F. *Angew. Chem. Int. Ed. Engl.* **2003**, *42*, 1210.

[92] [N°70] Rashkin, M. J.; Waters, M. L. *J. Am. Chem. Soc.* **2002**, *124*, 1860.

[93] [N°71] Wheeler, S. E. *J. Am. Chem. Soc.* **2011**, *133*, 10262.

[94] [N°72] Wheeler, S. E.; Houk, K. N. *J. Am. Chem. Soc.* **2008**, *130*, 10854.

[95] [N°59] Grimme, S. *Angew. Chem. Int. Ed. Engl.* **2008**, *47*, 3430.

[96] [N°58] Martinez, C. R.; Iverson, B. L. *Chem. Sci.* **2012**, *3*, 2191.

Now that the different types of non-covalent interactions have so far been discussed, the question, which can legitimately be asked, is: Is it possible to experimentally visualize non-covalent interactions?

5.3 - Can non-covalent interactions be experimentally observed?

5.3.1 - Experimental Methods.

To answer this question, we have to figure out which specific properties of the non-covalent interactions (and specially of the non-covalent complexes) can be observed. Unfortunately, there are not many of them. As the structure of non-covalent complexes cannot be directly observed other alternatives have to be considered.

In that quest, molecular clusters constitute ideal systems[97] for experimentally studying non-covalent interactions and have therefore been widely investigated over the last decades.[98,99] The interest for molecular clusters is principally due to the facility with which they can be prepared under isolated, unperturbed conditions in supersonic jet expansions. Indeed, when a compound seeded in helium, neon, or argon is expanded in a jet, noncovalent interactions will generally lead to the formation of non-covalently bound clusters. Important parameters such as the expansion conditions and concentration of the seed molecule will determine the distribution of clusters in the jet. The last 20 years have been the subject of important work to devise and employ experimental tools, providing accurate information and description of the structure and dynamics of molecular clusters. In that quest, spectroscopic analysis or mass selective detection have been extensively used.

A very important property related to any non-covalent complex is not just its "equilibrium structure" but rather its potential-energy surface (PES)[100] with its stationary points. Thus, if local minima of similar energy of the global minimum are present on the

---

[97] [N°15] Müller-Dethlefs, K.; Hobza, P. *Chem. Rev.* **2000**, *100*, 143.

[98] [N°73] Hobza, P.; Selzle, H. L.; Schlag, E. W. *Chem. Rev.* **1994**, *94*, 1767.

[99] [N°74] Hobza, P.; Zahradnik, R. *Chem. Rev.* **1988**, *88*, 871.

[100] [N°18] Hobza, P.; Muller-Dethlefs, K. In *Non-Covalent Interactions: Theory and Experiment*; The Royal Society of Chemistry: **2009**.

PES, the last being separated by high barriers, the formation of different cluster structures is possible, which are isolable in the jet expansion. Therefore, the use of analytical methods such as vibration rotation spectroscopy, UV and IR hole burning,[101] REMPI, and ZEKE spectroscopy will provide tools to identify isomers and to study the structural changes occurring upon electronic excitation and ionization. Thus:

- Vibrational frequencies can be obtained trough infrared (IR) absorption or the Raman effect. Even if significant work has been devoted to the development of stimulated Raman population transfer as a method of vibrationally resolved spectroscopy,[102-105] this method has not yet known a huge success. Indeed, most of the studies of vibrational spectroscopy for the determination of vibrational energy levels are based on ionisation detection.[106-110] The determination of vibrational frequencies is often straightforward and provides information on the structure and strength of a non-covalent complex.[111-115]
- Rotational constants can be obtained giving access to the three principal moments of inertia of a molecule, which are obtained from high-resolution spectroscopy with rotational level resolution, for instance: the microwave spectroscopy (MW) presenting the highest resolving power, [116-124] The vibration-

[101] [N°75] Riehn, C.; Lahmann, C.; Wassermann, B.; Brutschy, B. *Chem. Phys. Lett.* **1992**, *197*, 443.
[102] [N°76] Tanner, C.; Henseler, D.; Leutwyler, S.; Connell, L. L.; Felker, P. M. *J. Chem. Phys.* **2003**, *118*, 9157.
[103] [N°77] Lee, S.; Romascan, J.; Felker, P. M.; Pedersen, T. B.; Fernandez, B.; Koch, H. *J. Chem. Phys.* **2003**, *118*, 1230.
[104] [N°78] Lee, S.; Chung, J. S.; Felker, P. M.; Cacheiro, J. L.; Fernandez, B.; Pedersen, T. B.; Koch, H. *J. Chem. Phys.* **2003**, *119*, 12956.
[105] [N°79] Kim, W.; Schaeffer, M. W.; Lee, S.; Chung, J. S.; Felker, P. M. *J. Chem. Phys.* **1999**, *110*, 11264.
[106] [N°80] Garrett, B. C.; Dixon, D. A.; Camaioni, D. M.; Chipman, D. M.; Johnson, M. A.; Jonah, C. D., . . . Zwier, T. S. *Chem. Rev.* **2005**, *105*, 355.
[107] [N°81] Abou El-Nasr, A. B. E. H.; Fujii, A.; Ebata, T.; Mikami, N. *Mol. Phys.* **2005**, *103*, 1561.
[108] [N°82] El-Hakam, E. A.; Ei-Nasr, A.; Fujii, A.; Yahagi, T.; Ebata, T.; Mikami, N. *J. Phys. Chem. A* **2005**, *109*, 2498.
[109] [N°83] Imhof, P.; Krugler, D.; Brause, R.; Kleinermanns, K. *J. Chem. Phys.* **2004**, *121*, 2598.
[110] [N°84] Wu, R. H.; Brutschy, B. *J. Phys. Chem. A* **2004**, *108*, 9715.
[111] [N°85] Schmitt, M.; Ratzer, C.; Meerts, W. L. *J. Chem. Phys.* **2004**, *120*, 2752.
[112] [N°86] Westphal, A.; Jacoby, C.; Ratzer, C.; Reichelt, A.; Schmitt, M. *Phys. Chem. Chem. Phys.* **2003**, *5*, 4114.
[113] [N°87] Schmitt, M.; Jacoby, C.; Gerhards, M.; Unterberg, C.; Roth, W.; Kleinermanns, K. *J. Chem. Phys.* **2000**, *113*, 2995.
[114] [N°88] Jacoby, C.; Roth, W.; Schmitt, M.; Janzen, C.; Spangenberg, D.; Kleinermanns, K. *J. Phys. Chem. A* **1998**, *102*, 4471.
[115] [N°89] Roth, W.; Schmitt, M.; Jacoby, C.; Spangenberg, D.; Janzen, C.; Kleinermanns, K. *Chem. Phys.* **1998**, *239*, 1.
[116] [N°90] Giuliano, B. M.; Ottaviani, P.; Caminati, W.; Schnell, M.; Banser, D.; Grabow, J. U. *Chem. Phys.* **2005**, *312*, 111.
[117] [N°91] Sanchez, R.; Blanco, S.; Lesarri, A.; Lopez, J. C.; Alonso, J. L. *Chem. Phys. Lett.* **2005**, *401*, 259.
[118] [N°92] Blanco, S.; Lopez, J. C.; Lesarri, A.; Caminati, W.; Alonso, J. L. *Mol. Phys.* **2005**, *103*, 1473.
[119] [N°93] Giuliano, B. M.; Caminati, W. *Angew. Chem. Int. Ed. Engl.* **2005**, *44*, 603.
[120] [N°94] Caminati, W.; Lopez, J. C.; Alonso, J. L.; Grabow, J. U. *Angew. Chem. Int. Ed. Engl.* **2005**, *44*, 3840.

rotation-tunnelling spectroscopy (VRT),[125 - 127] the rotational electronic spectroscopy[128 - 132] and deconvolution of only partially resolved rotational structure.[133-136]

- Zero electron kinetic energy (ZEKE) provides directly measurable high accuracy information on stabilisation energies.[137-141]
- Resonance-enhanced multiphoton ionisation (REMPI) provides spectroscopic information on the excited states of neutral systems.[142-144]

The most suitable methods are based on mass spectrometry, particularly time-offlight methods incorporating a mass signature,[145, 146] which is particularly useful for the identification of molecular clusters[147] and, in addition, provide singlemolecule detection efficiency.

[121] [N°95] Lesarri, A.; Cocinero, E. J.; Lopez, J. C.; Alonso, J. L. *Angew. Chem. Int. Ed. Engl.* **2004**, *43*, 605.
[122] [N°96] Alonso, J. L.; Antolinez, S.; Blanco, S.; Lesarri, A.; Lopez, J. C.; Caminati, W. *J. Am. Chem. Soc.* **2004**, *126*, 3244.
[123] [N°97] Cole, G. C.; Legon, A. C. *J. Chem. Phys.* **2004**, *121*, 10467.
[124] [N°98] Fowler, P. W.; Legon, A. C.; Thumwood, J. M. A.; Waclawik, E. R. *Coord. Chem. Rev.* **2000**, *197*, 231.
[125] [N°99] Goldman, N.; Leforestier, C.; Saykally, R. J. *Philos. Trans. Roy .Soc. A* **2005**, *363*, 493.
[126] [N°100] Keutsch, F. N.; Cruzan, J. D.; Saykally, R. J. *Chem. Rev.* **2003**, *103*, 2533.
[127] [N°101] Cruzan, J. D.; Braly, L. B.; Liu, K.; Brown, M. G.; Loeser, J. G.; Saykally, R. J. *Science* **1996**, *271*, 59.
[128] [N°102] Chervenkov, S.; Wang, P. Q.; Braun, J. E.; Georgiev, S.; Neusser, H. J.; Nandi, C. K.; Chakraborty, T. *J. Chem. Phys.* **2005**, *122*.
[129] [N°103] Nguyen, T. V.; Korter, T. M.; Pratt, D. W. *Mol. Phys.* **2005**, *103*, 2453.
[130] [N°104] Georgiev, S.; Neusser, H. J. *J. Electron Spect.* **2005**, *142*, 207.
[131] [N°105] Kang, C.; Pratt, D. W. *Int. Rev. Phys. Chem.* **2005**, *24*, 1.
[132] [N°106] Pratt, D. W. *Science* **2002**, *296*, 2347.
[133] [N°107] Ford, M. S.; Muller-Dethlefs, K. *Phys. Chem. Chem. Phys.* **2004**, *6*, 23.
[134] [N°108] Lee, Y. H.; Jung, J. W.; Kim, B.; Butz, P.; Snoek, L. C.; Kroemer, R. T.; Simons, J. P. *J. Phys. Chem. A* **2004**, *108*, 69.
[135] [N°109] Tong, X.; Ford, M. S.; Dessent, C. E. H.; Muller-Dethlefs, K. *J. Chem. Phys.* **2003**, *119*, 12908.
[136] [N°110] Ford, M. S.; Tong, X.; Dessent, C. E. H.; Muller-Dethlefs, K. *J. Chem. Phys.* **2003**, *119*, 12914.
[137] [N°111] Dessent, C. E. H.; Muller-Dethlefs, K. *Chem. Rev.* **2000**, *100*, 3999.
[138] [N°112] Muller-dethlefs, K. *J. Chem. Phys.* **1991**, *95*, 4821.
[139] [N°113] Mullerdethlefs, K.; Sander, M.; Schlag, E. W. *Z. Naturforsch. A* **1984**, *39*, 1089.
[140] [N°114] Mullerdethlefs, K.; Sander, M.; Schlag, E. W. *Chem. Phys. Lett.* **1984**, *112*, 291.
[141] [N°115] Habenicht, W.; Reiser, G.; Mullerdethlefs, K. *J. Chem. Phys.* **1991**, *95*, 4809.
[142] [N°116] Beattie, D. A.; Donovan, R. J. *Prog. React. Kinet. Mec.* **1998**, *23*, 281.
[143] [N°117] Leutwyler, S.; Bosiger, J. *Chem. Rev.* **1990**, *90*, 489.
[144] [N°118] Bernstein, R. B. *J. Phys. Chem.* **1982**, *86*, 1178.
[145] [N°119] Krause, H.; Neusser, H. J. *J. Chem. Phys.* **1993**, *99*, 6278.
[146] [N°120] Zhu, L.; Johnson, P. *J. Chem. Phys.* **1991**, *94*, 5769.
[147] [N°121] Chapman, D. M.; Müller-Dethlefs, K.; Peel, J. B. *J. Chem. Phys.* **1999**, *111*, 1955.

5.3.2 - Limitations.

Even though very sophisticated, all of these methods do not systematically provide unambiguous answers regarding the structure and geometry of the molecule. This point can be illustrated by the study of the intramolecular hydrogen atom dynamics of acetylacetone where, a hydrogen-shifting keto–enol tautomerisation and an interconversion of the enol in two indistinguishable enolone structures occurs. [148,149] Ultrafast electron-diffraction experiments [150, 151] on acetylacetone by Zewail and coworkers[152,153] have shown that of the two tautomeric forms in dynamic equilibrium the C_s-enolic structure is the dominant one. The observation of a C_s structure seems to contradict results from microwave spectra of acetylacetone that are compatible with a C_{2v} structure.[154] It can be easily understood that the microwave experiment will show an averaged C_{2v} structure provided that the interconversion barrier between the two enolones is sufficiently low. The same difficulties can be experienced in the determination of *stabilisation energies*; of the various experimental techniques available, only zero-electron kinetic energy (ZEKE) spectroscopy provides high-accuracy information on stabilisation energies. Other directly observable characteristics of a noncovalent complex are *vibrational frequencies*, not all of which may be seen due to Franck–Condon factors[155,156] or symmetry selection rules.

While *experimental data* cannot always provide an easy access to the structure and geometry of a non-covalent complex, *theoretical quantum-chemical methods* using gradient optimisation techniques, yield reliable structural and geometrical information even for extended complexes. Therefore, contemporary research of molecular interactions aims at converging the best part of both disciplines, giving access to very

---

[148] [N°122] Dannenberg, J. J.; Rios, R. *J. Phys. Chem.* **1994**, *98*, 6714.
[149] [N°123] vBuemi, G.; Gandolfo, C. *J. Chem. Soc., Faraday Trans. 2* **1989**, *85*, 215.
[150] [N°124] Cao, J.; Ihee, H.; Zewail, A. H. *Proc. Natl. Acad. Sci. USA* **1999**, *96*, 338.
[151] [N°125] Dantus, M.; Kim, S. B.; Williamson, J. C.; Zewail, A. H. *J. Phys. Chem.* **1994**, *98*, 2782.
[152] [N°126] Srinivasan, R.; Feenstra, J. S.; Park, S. T.; Xu, S.; Zewail, A. H. *J. Am. Chem. Soc.* **2004**, *126*, 2266.
[153] [N°127] Xu, S. J.; Park, S. T.; Feenstra, J. S.; Srinivasan, R.; Zewail, A. H. *J. Phys. Chem. A* **2004**, *108*, 6650.
[154] [N°128] Caminati, W.; Grabow, J.-U. *J. Am. Chem. Soc.* **2005**, *128*, 854.
[155] [N°44] In *IUPAC. Compendium of Chemical Terminology*; Version 2.3.3 - 2014-02-24 - the "Gold Book". ed. XML on-line corrected version: Web. 24 Jul 2014: goldbook.iupac.org.
[156] [N°129] Condon, E. *Phys. Rev.* **1926**, *28*, 1182.

precise and reliable data obtained through a number of experimental methods coupled with well-developed theoretical calculations for the most accurate description of molecular systems. Thus, the quote "Facts without theory is chaos, but theory without facts is fantasy" (Charles O. Whitman 1894), takes all its legitimacy in the field of non-covalent interactions.

5.4 - Theoretical methods.

Over the last decade, the huge improvement in terms of computer technology (always faster and more efficient) as well as software's development has provided a continuous enhancement of the accuracy with which calculations, especially heavy *ab initio* calculation methods, can be applied for solving chemical problems. In contrast with earlier years when most calculations were limited to the Hartree-Fock[157] level, it becomes more and more frequent to add electron correlation to systems of even moderate size. Nonetheless, the ability consisting of performing calculations incorporating all possible configurations is not normally possible. Therefore various methods have been developed in order to incorporate as much electron as possible and in an efficient manner.

Non-covalent interactions can be studied pretty similarly to covalent interactions by the mean of *standard methods* of quantum chemistry based either on perturbation or variation theory.[158 - 159] While the perturbation approach separates the overall stabilisation energy into various physically well-defined contributions (*i.e.* electrostatic, induction, dispersion and exchange-repulsion energies), the variation method consist in the determination of the stabilization energy indirectly as the difference between the energy of the molecular cluster (supersystem) and the energies of the isolated subsystems. As always, both approaches have their advantages as well as a number of inconveniencies. Because the stabilization energy in the case of the *perturbation method* is directly calculated and not the result of an energy difference, it can be

[157] [N°130] Froese Fischer, C. *Comp. Phys. Comm.* **1987**, *43*, 355.

[158] [N°18] Hobza, P.; Muller-Dethlefs, K. In *Non-Covalent Interactions: Theory and Experiment*; The Royal Society of Chemistry: **2009**.

[159] [N°15] Müller-Dethlefs, K.; Hobza, P. *Chem. Rev.* **2000**, *100*, 143.

considered free of any inconsistency originating from different descriptions of "supersystems" and subsystems which are typical of variational treatments. Furthermore, the various energy terms obtained have a clear physical meaning. A major disadvantage of *perturbational* calculations is the fact that they are more demanding than variational ones. This constitutes a non-negligible limit in the treatment of large molecular systems, or systems for which many intramolecular and intermolecular degrees of freedom have to be optimized simultaneously. Nevertheless, *perturbational methods* remain well suited for the determination of interactions between rigid systems in the form of symmetry-adapted perturbation theory (SAPT),[160] providing highly accurate calculations of rigid systems, and a benchmark for supermolecular calculations. Extensive studies in the past years have given good stabilization energies of various molecular complexes of either: Helium based: *e.g.* $(He)_2$,[161] He…CO[162] and He…HF;[163] Argon based: Ar…HF,[164] $(Ar)_2$…HF,[165] Ar…CH_4 ,[166] $(Ar)_3$;[167] Water and depth water: $(H_2O)_2$;[168169] Other Hydrogen derivatives: H_2…CO and D_2…CO,[170] $(CO_2)_2$.[171] In contrast, the variation method is almost exclusively used[172] for the evaluation of stabilization energies of larger systems where the total energy is determined as the sum of *Hartree-Fock (HF)* and *correlation energy (COR)*.[173] Moreover, methods such as the *full configuration interaction (FCI)* method and *coupled cluster method* covering single, double, and triple excitations iteratively *(CCSDT)* are considered as methods of choice[174] but are impractical for larger molecular clusters.

[160] [N°131] Jeziorski, B.; Moszynski, R.; Szalewicz, K. *Chem. Rev.* **1994**, *94*, 1887.
[161] [N°132] Bukowski, R.; Jeziorski, B.; Szalewicz, K. *J. Chem. Phys.* **1996**, *104*, 3306.
[162] [N°133] Moszynski, R.; Korona, T.; Wormer, P. E. S.; van der Avoird, A. *J. Chem. Phys.* **1995**, *103*, 321.
[163] [N°134] Moszynski, R.; Wormer, P. E. S.; Jeziorski, B.; van der Avoird, A. *J. Chem. Phys.* **1994**, *101*, 2811.
[164] [N°135] Lotrich, V. F.; Williams, H. L.; Szalewicz, K.; Jeziorski, B.; Moszynski, R.; Wormer, P. E. S.; van der Avoird, A. *J. Chem. Phys.* **1995**, *103*, 6076.
[165] [N°136] Lotrich, V. F.; Jankowski, P.; Szalewicz, K. *J. Chem. Phys.* **1998**, *108*, 4725.
[166] [N°137] Heijman, T. G. A.; Korona, T.; Moszynski, R.; Wormer, P. E. S.; vanderAvoird, A. *J. Chem. Phys.* **1997**, *107*, 902.
[167] [N°138] Lotrich, V. F.; Szalewicz, K. *J. Chem. Phys.* **1997**, *106*, 9688.
[168] [N°139] Mas, E. M.; Szalewicz, K.; Bukowski, R.; Jeziorski, B. *J. Chem. Phys.* **1997**, *107*, 4207.
[169] [N°140] Mas, E. M.; Szalewicz, K. *J. Chem. Phys.* **1996**, *104*, 7606.
[170] [N°141] Jankowski, P.; Szalewicz, K. *J. Chem. Phys.* **1998**, *108*, 3554.
[171] [N°142] Bukowski, R.; Sadlej, J.; Jeziorski, B.; Jankowski, P.; Szalewicz, K.; Kucharski, S. A., . . . Rice, B. M. *J. Chem. Phys.* **1999**, *110*, 3785.
[172] [N°143] Scheiner, S. *Hydrogen Bonding. A Theoretical Perspective;*; Oxford University Press: New York, **1997**.
[173] [N°144] Bartlett, R. J.; Stanton, J. F. In *Reviews in Computational Chemistry*; John Wiley & Sons, Inc.: **2007**, p 65.
[174] [N°145] Hobza, P. *Acc. Chem. Res.* **2012**, *45*, 663.

Therefore, a good compromise between both economy and accuracy is the coupled cluster method covering single and double excitations iteratively and triple excitations in a noniterative way, *also known as CCSD(T),* [175] which represent one of the most robust methods for the evaluation of correlation energy of molecular clusters and should preferentially be used over other coupled cluster levels as well as over higher levels of *Møller-Plesset perturbation theory (MP3, MP4SDQ, MP4SDTQ).*[176] The most economical and widely used second-order *MP theory (MP2)* constitutes a method applicable to extended complexes providing good estimations of the correlation energy. Furthermore, highly accurate evaluations of interaction energies of very large molecular clusters with hundreds of atoms can be obtained from local models of electron correlation.[177] The scaling of the *local MP2 method* with the number of atomic orbitals is similar to that of the *HF method*. It has also to be mentioned the famous so-called *density functional theory* (DFT), for the development of which, Walter Kohn[178] (Figure 20) was awarded with the Nobel Prize in Chemistry in 1998.

Figure 20: Walter Kohn at the 62nd Lindau Nobel Laureate Meeting on July 3rd, 2012; Nationality: American; Nobel Prize in Physics (1998): For his work on the Electronic Structure of Matter – Wave Functions and Density Functionals. Photographer: Markus Pössel; Public domain via Wikimedia Commons.

[175] [N°146] Raghavachari, K.; Trucks, G. W.; Pople, J. A.; Head-Gordon, M. *Chem. Phys. Lett.* **1989**, *157*, 479.

[176] [N°147] Bartlett, R. J. *An. Rev. Phys. Chem.* **1981**, *32*, 359.

[177] [N°148] Saebo/, S.; Pulay, P. *J. Chem. Phys.* **1987**, *86*, 914.

[178] [N°149] Kohn, W. In *Nobel Lecture: Electronic Structure of Matter Wave Functions and Density Functionals*; Nobelprize.org, Nobel Media AB 2013: Web. 11 Jul 2014: nobelprize.org/nobel_prizes/chemistry/laureates/1998/kohn-lecture.html, 1999.

The initial work on DFT was reported in two major publications, *i.e.* one of Kohn with Pierre Hohenberg in 1964[179], and another one with Lu J. Sham in 1965,[180] almost 40 years after E. Schrödinger published the first paper stating the beginning of wave-mechanics.[181] Since that time, DFT has been gaining ground, especially over the past years, as the method is much less computationally demanding than, for instance, *Hartree-Fock methods*. Indeed, while WFT methods, are strongly dependent on the quality of the basis set, DFT remains much less dependent, thus, reliable results can be obtained with a medium basis set. In DFT, the energy is determined by using exchange and correlation functionals showing remarkable good results on properties of isolated systems like geometry, vibration frequencies, etc. (the same being true for non-covalent complexes). As few examples: highly accurate data are obtained in the determination of geometry and energetics of H-bonded complexes,[182,183] geometry and spectral features of classic charge-transfer complexes,[184] the magnetic exchange coupling between transition-metal ions in binuclear complexes[185] and metal–ligand aromatic cation–π interactions (important for metalloproteins).[186] However, the application of DFT methods to noncovalent complexes with density functionals (based on local density, its gradient, and the local kinetic-energy density) was for a long time limited as the method fails to describe the (nonlocal) dispersion energy. The fact that this dispersion energy was not included in the local DFT energy has not been readily accepted by the DFT community, although the first papers showing this drawback were published in the mid 1990s.[187,188] Despite the lack of dispersion consideration, as surprising as it may be, it appeared that DFT was able to reproduce results in very good agreement with reference data (experimental and WFT-based) in the case of hydrogen-bond complexes (where dispersion appears to play an important role). The reason being an

[179] [N°150] Hohenberg, P.; Kohn, W. *Phys. Rev.* **1964**, *136*, B864.
[180] [N°151] Kohn, W.; Sham, L. J. *Phys. Rev.* **1965**, *140*, A1133.
[181] [N°152] Schrödinger, E. *Annalen der Physik* **1926**, *79*, 361.
[182] [N°153] Sirois, S.; Proynov, E. I.; Nguyen, D. T.; Salahub, D. R. *J. Chem. Phys.* **1997**, *107*, 6770.
[183] [N°154] Sim, F.; St. Amant, A.; Papai, I.; Salahub, D. R. *J. Am. Chem. Soc.* **1992**, *114*, 4391.
[184] [N°155] Liao, M. S.; Lu, Y.; Parker, V. D.; Scheiner, S. *J. Phys. Chem. A* **2003**, *107*, 8939.
[185] [N°156] Desplanches, C.; Ruiz, E.; Rodríguez-Fortea, A.; Alvarez, S. *J. Am. Chem. Soc.* **2002**, *124*, 5197.
[186] [N°157] Zaric, S. D. *Eur. J. Inorg. Chem.* **2003**, 2197.
[187] [N°158] Hobza, P.; Sponer, J.; Reschel, T. *J. Comput. Chem.* **1995**, *16*, 1315.
[188] [N°159] Kristyan, S.; Pulay, P. *Chem. Phys. Lett.* **1994**, *229*, 175.

error cancellation, where the dispersion is partially "compensated" in some density functionals by the (erroneous) attraction part of the so-called exchange functional,[189] or compensated in many DFT calculations by the basis set superposition error (BSSE), which amounts to several kcal/mol for the medium-sized dimers and double-zeta quality basis sets (The BSSE in DFT methods is in general smaller than that in WFT methods).[190-193] The same occurs for single molecules of the size in the range or larger than the sums of the vdW radii of their substituent atom, for which, we cannot rely on the BSSE compensation (even more if the molecule is composed of highly polarisable groups such as peptide bonds or phenyl rings). The reason behind that being that the error compensation (which for its part is not reliable and even less acceptable) produces sufficient non-physical attraction for the description of H-bonded complexes, but when the systems taken into account are dispersion-bonded complexes the results accuracy is meaningless. Consequently, the results obtained have to be exploited carefully. Thus, the perspective of using DFT methods for the study of non-covalent complexes (*i.e.* for most biological applications), where dispersion energy is of a determining importance was for a long time prohibited. Since then, it became of first necessity to find a way to include dispersion interaction into DFT and correct this major drawback. Therefore, successive attempts were made, by following three main directions:

I. Theoretically based approaches by avoiding as much as possible the empiricism (non-empirical approaches).
II. Attempts to reparametrise the existing density functionals so that they describe dispersion properly or cover the dispersion energy, at least qualitatively.
III. Empirical approaches, based on the force-field-like terms, where the empirical expression for dispersion energy is simply applied and the total energy is constructed as a sum of DFT and dispersion energies.

---

[189] [N°160] Zhang, Y. K.; Pan, W.; Yang, W. T. *J. Chem. Phys.* **1997**, *107*, 7921.

[190] [N°18] Hobza, P.; Muller-Dethlefs, K. In *Non-Covalent Interactions: Theory and Experiment*; The Royal Society of Chemistry: **2009**.

[191] [N°161] Balabin, R. M. *J. Chem. Phys.* **2008**, *129*.

[192] [N°162] Paizs, B.; Suhai, S. *J. Comput. Chem.* **1998**, *19*, 575.

[193] [N°73] Hobza, P.; Selzle, H. L.; Schlag, E. W. *Chem. Rev.* **1994**, *94*, 1767.

Hobza *et al.,*[194] but also other groups[195,196] (especially Grimme[197,198]), developed empirical corrections for DFT, which was found to provide very successful results for the much bigger systems that represent biomacromolecules. Hobza *et al.* conclusions can be summarized in six different points:

1. The presence of a simple empirical dispersion correction enhances significantly the description of intermolecular interactions.
2. There is a critical point, which is the dumping function of the empirical dispersion term, because it is related to the problem of double counting of the correlation energy and range of a given correlation functional.
3. The importance of extending the basis set. The more the basis set quality increases, the more the empirical correction becomes obvious and the results including the empirical dispersion term converge to the reference WFT data.
4. In the case of H-bonded systems, the BSSE for the basis sets of DZ quality is of the same direction and of almost the same size as the dispersion interaction.[199] BSSE uncorrected DFT calculations provide reasonable agreement with experiment, which in other terms reveal the precise role of dispersion energy which is often overlooked in these complexes.
5. Following the two previous points, it is highly recommended to add dispersion corrections only to sufficiently large basis sets (at least TZVP quality). In general, the more advanced functionnals (hybrid, meta GGA…) give better results when they are combined with empirical dispersion than other functionals (simple GGA…).
6. The accuracy of the results obtained are considerably limited by the quality of the XC functional used. Best results are said to be obtained by using TPSS functional (especially TPSS-meta-GGA).

---

[194] [N°163] Jurecka, P.; Cerny, J.; Hobza, P.; Salahub, D. R. *J. Comput. Chem.* **2007**, *28*, 555.
[195] [N°164] Civalleri, B.; Zicovich-Wilson, C. M.; Valenzano, L.; Ugliengo, P. *Crystengcomm* **2008**, *10*, 1693.
[196] [N°165] Elstner, M.; Hobza, P.; Frauenheim, T.; Suhai, S.; Kaxiras, E. *J. Chem. Phys.* **2001**, *114*, 5149.
[197] [N°166] Grimme, S. *J. Comput. Chem.* **2006**, *27*, 1787.
[198] [N°167] Grimme, S. *J. Comput. Chem.* **2004**, *25*, 1463.
[199] [N°168] Plumley, J. A.; Dannenberg, J. J. *J. Comput. Chem.* **2011**, *32*, 1519.

All of these experienced limits have had the positive effect to force us to find solutions to mitigate the impact of the lack of an accurate long-range description in the local[200] and semilocal functionals.[201] Since, a large variety of vdW correction schemes have been efficiently implemented[202-207] like the DFT-D2,[208] vdWDF, [209,210] and recently the Tkatchenko-Scheffler (TS) and the TS-self-consistent screening (TS-SCS) methods.[211,212] Number of groups around the world have provided their own results aiming to extend existing benchmarking[213-221] of vdW corrections in DFT, increasing its accuracy and reliability in widely fields. Thus, when the method properly includes the dispersion energy, its applicability increases considerably and the method has a chance to become an ''universal'' technique, suitable for the treatment of complex molecular systems (*i.e.* extended molecular complexes as well as extended isolated systems like peptides or proteins).

After the WFT or DFT schemes of theoretical investigations it has also to be mentioned that another completely different procedure exists in the determination of electronic structures, namely the Quantum Monte Carlo (QCM) method.[222-224] This method is also

[200] [N°169] Ceperley, D. M.; Alder, B. J. *Phys. Rev. Lett.* **1980**, *45*, 566.
[201] [N°170] Perdew, J. P.; Burke, K.; Ernzerhof, M. *Phys. Rev. Lett.* **1996**, *77*, 3865.
[202] [N°171] Thonhauser, T.; Cooper, V. R.; Li, S.; Puzder, A.; Hyldgaard, P.; Langreth, D. C. *Phys. Rev. B* **2007**, *76*, 125112.
[203] [N°172] Björkman, T.; Gulans, A.; Krasheninnikov, A. V.; Nieminen, R. M. *J. Phys. Condens. Mat.* **2012**, *24*, 424218.
[204] [N°173] Silvestrelli, P. L. *Phys. Rev. Lett.* **2008**, *100*, 053002.
[205] [N°174] Yanai, T.; Tew, D. P.; Handy, N. C. *Chem. Phys. Lett.* **2004**, *393*, 51.
[206] [N°175] Langreth, D. C.; Mehl, M. J. *Phys. Rev. B* **1983**, *28*, 1809.
[207] [N°176] Wu, X.; Vargas, M. C.; Nayak, S.; Lotrich, V.; Scoles, G. *J. Chem. Phys.* **2001**, *115*, 8748.
[208] [N°166] Grimme, S. *J. Comput. Chem.* **2006**, *27*, 1787.
[209] [N°177] Lee, K.; Murray, É. D.; Kong, L.; Lundqvist, B. I.; Langreth, D. C. *Phys. Rev. B* **2010**, *82*, 081101.
[210] [N°178] Dion, M.; Rydberg, H.; Schröder, E.; Langreth, D. C.; Lundqvist, B. I. *Phys. Rev. Lett.* **2004**, *92*, 246401.
[211] [N°179] Tkatchenko, A.; Ambrosetti, A.; DiStasio, R. A. *J. Chem. Phys.* **2013**, *138*.
[212] [N°180] Tkatchenko, A.; Scheffler, M. *Phys. Rev. Lett.* **2009**, *102*, 073005.
[213] [N°181] Lüder, J.; Sanyal, B.; Eriksson, O.; Puglia, C.; Brena, B. *Phys. Rev. B* **2014**, *89*, 045416.
[214] [N°182] DiLabio, G. A.; Johnson, E. R.; Otero-de-la-Roza, A. *Phys. Chem. Chem. Phys.* **2013**, *15*, 12821.
[215] [N°183] Marom, N.; Tkatchenko, A.; Rossi, M.; Gobre, V. V.; Hod, O.; Scheffler, M.; Kronik, L. *J. Chem. Theory Comput.* **2011**, *7*, 3944.
[216] [N°184] DiLabio, G.; Koleini, M.; Torres, E. *Theor. Chem. Acc.* **2013**, *132*, 1.
[217] [N°185] Grimme, S. *WIREs: Comput. Mol. Sci.* **2011**, *1*, 211.
[218] [N°186] Hujo, W.; Grimme, S. *Phys. Chem. Chem. Phys.* **2011**, *13*, 13942.
[219] [N°187] Grimme, S.; Ehrlich, S.; Goerigk, L. *J. Comput. Chem.* **2011**, *32*, 1456.
[220] [N°188] Grimme, S.; Steinmetz, M. *Phys. Chem. Chem. Phys.* **2013**, *15*, 16031.
[221] [N°189] Grimme, S.; Huenerbein, R.; Ehrlich, S. *ChemPhysChem* **2011**, *12*, 1258.
[222] [N°190] Rousseau, V. G. *Phys. Rev. E* **2008**, *77*, 056705.
[223] [N°191] Mella, M.; Anderson, J. B. *J. Chem. Phys.* **2003**, *119*, 8225.

very attractive as it includes the correlation energy explicitly in the multielectron wavefunction (it is not necessary to partition the total energy), thus, the effect of the finite basis set is very small or inexistent (as used only for the building of the guiding function). Moreover, QCM is size consistent and variational; current cubic scaling is found to be much more favourable than for WFT methods. Finally, the QCM algorithm being intrinsically parallel, it scales linearly with number of processors. Nevertheless a major drawback of this method is that only the energy can be obtained and there is no easy way to calculate the energy derivatives. In other terms, the chance, for instance, to optimise the geometry of the studied systems are very small. Furthermore, the quality of the nodal system used affects directly the quality of the results. Fortunately in the case of NCIs this error cancels out. The QCM method has been used successfully in the case of various small complexes.[225]

5.5 - Non-covalent interactions in nature.

For most people the term chemistry is associated to the formation or breaking of bonds (covalent bonds) between atoms, which leads, upon transformation, to the creation of a whole new molecule with new interesting properties. In other words, the chemistry world (and by extension, nature) is "covalently dependent." Other less-known interactions, especially the "weak" interactions, seem not to have a particular or fundamental importance in this "chemistry world". All of this remains perfectly accurate if we limit the molecule to be located in free space, isolated from any surroundings. For instance, in molecular beams from a supersonic jet expansion.[226] Nevertheless, it has to be admitted that this is not the most frequent situation... Molecules have more chances to be surrounded by other molecules (for instance in solution, in the bulk…) than to be totally isolated. The presence of other molecules will of course affect the covalent bonding, but also the electronic system of the molecule, which will be perturbed and modified. This perturbation will be a function of the strength and extent of the non-covalent interactions occurring (the most important changes are observed in ionic and

[224] [N°192] Foulkes, W. M. C.; Mitas, L.; Needs, R. J.; Rajagopal, G. *Rev. mod. Phys.* **2001**, *73*, 33.

[225] [N°193] Diedrich, C.; Luchow, A.; Grimme, S. *J. Chem. Phys.* **2005**, *123*, 184106.

[226] [N°194] Lubman, D. M.; Rettner, C. T.; Zare, R. N. *J. Phys. Chem.* **1982**, *86*, 1129.

H-bonded systems). This constitutes the first important point: NCIs can be found everywhere in nature.

If we now intend to perform a strength comparison between the non-covalent interactions and the covalent bonds, the former will be found to be considerably weaker by one to three orders of magnitudes (except in exceptional cases) than the later. Nevertheless, that is exactly the reason why NCIs play such a subtle and decisive key role in nature. For instance, the possible existence of liquid phases with all the associated effects (*e.g.* solvation phenomena…). The existence of a condensed phase is probably one of the most amazing expressions of the non-covalent interactions, which remains a major challenge to the theoretical community,[227-231] in particular the proper description of the role of solvents in general, and specifically water.[232]

If we stay a few moments with water, it has to be mentioned that the expression of NCIs toward the water molecule is tremendous. First, the physical properties of water such as its high boiling point (consequence of the high energy required to break the hydrogen bonds, *i.e.* NCIs) is the reason why water molecules exist principally in a liquid state in the range of environments where life flourishes. Other water molecular analogues, namely the hydrogen sulphide (H_2S), that are not capable to easily form hydrogen bonds behave as a gas at room temperature,[233] even if it has twice the molecular weight of water. The same H-bonds provide water an unusual behaviour when freezing. Similarly to other compounds, the water liquid state becomes denser by lowering the temperature. Nevertheless, there is one point where water remains unique compared to most materials: when the cooling process rises the freezing point, the presence of H-bonds and its capacity to form new ones allows the molecules to rearrange upon decreasing temperature in order to minimise the energy of the global system. The

[227] [N°195] Zhou, Y.; Pu, J. *J. Chem. Theory Comput.* **2014**.
[228] [N°196] Manby, F. R. *Accurate Condensed-Phase Quantum Chemistry (Computation in Chemistry)*; CRC Press, **2010**.
[229] [N°197] Knight, C.; Maupin, C. M.; Izvekov, S.; Voth, G. A. *J. Chem. Theory Comput.* **2010**, *6*, 3223.
[230] [N°198] Glover, W. J.; Larsen, R. E.; Schwartz, B. J. *J. Chem. Phys.* **2010**, *132*.
[231] [N°199] Politzer, P.; Murray, J. S.; Peralta-Inga, Z. *Int. J. Quantum Chem.* **2001**, *85*, 676.
[232] [N°200] Knight, C.; Voth, G. A. *Acc. Chem. Res.* **2011**, *45*, 101.
[233] [N°201] Haynes, W. M. *Handbook of Chemistry and Physics*; CRC Press, 95th ed., **2014**.

water molecules go further apart from each other (than if they were in the liquid state), resulting in the formation of a supramolecular assemblage that has actually a lower density than liquid water. Consequently, ice, which is nothing else that water in solid form, floats in water (similarly for icebergs in the ocean). Two other very important properties of water[234-238] have also to be mentioned because they are directly related to the establishment of NCIs, which appear to be biologically essential, *i.e.*:

> ***Water is a polar molecule.*** The reason associated to this polarity is that the molecule is bent, not linear, and so the distribution of charge is asymmetric. The oxygen nucleus draws back the electrons from the hydrogen atoms, which consequently leave the region around the hydrogen nuclei with a net positive charge.
>
> ***Water cohesion.*** By the mean of hydrogen bonds, water molecules strongly interact with each other. Networks of hydrogen bonds will be responsible for the structural cohesion of water, which, as above-mentioned, is apparent in the structure of ice. Similar interactions link molecules in liquid water, although in the liquid state some of the hydrogen bonds are broken. This high cohesion between water molecules will directly affect the behaviour of other molecules in aqueous solution.

Thus, as a consequence of its polarity and capacity of H-bonds formation, the water molecule is a highly interacting molecule (*i.e.* water is an excellent solvent for polar molecules). Indeed, water is capable to greatly weaken electrostatic forces and hydrogen bonding between other polar molecules by competing in the establishment of these interactions (Figure 21).

---

[234] [N°202] Moilanen, D. E.; Fenn, E. E.; Lin, Y.-S.; Skinner, J. L.; Bagchi, B.; Fayer, M. D. *Proc. Natl. Acad. Sci. USA* **2008**, *105*, 5295.

[235] [N°203] Smith, J. D.; Cappa, C. D.; Wilson, K. R.; Cohen, R. C.; Geissler, P. L.; Saykally, R. J. *Proc. Natl. Acad. Sci. USA* **2005**, *102*, 14171.

[236] [N°204] Berg, J. M.; Tymoczko, J. L.; Stryer, L. *Biochemistry*; W.H.Freeman & Co Ltd; 5th Revised edition - Internationnal edition, **2002**.

[237] [N°205] Sharp, K. A. In *eLS*; John Wiley & Sons, Ltd: **2001**.

[238] [N°206] Eisenberg, D.; Kauzmann, W. *The Structure and Properties of Water*; Oxford University Press, New York, **1969**; Vol. 166.

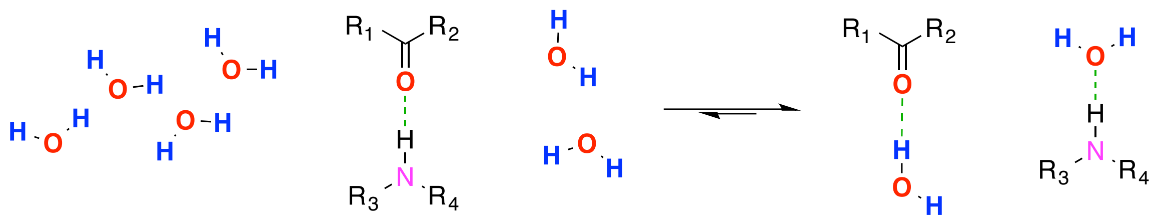

Figure 21: Competition of water molecules with other polar molecules in the establishment of non-covalent interactions.

Moreover, the high dielectric constant of water (near 80)[239] is directly related to its polarity and ability to self-organize, forming oriented solvent shells around ions. These shells will produce an electric field, which will be opposed to the fields produced by the ions, resulting in a significant decrease of the electrostatic interactions between ions. It is possible that life on Earth is directly dependent on the presence of water, especially on its capacity to dissolve a high number of polar molecules of biological importance such as fuels, building blocks, catalysts, and information carriers.[240,241] These polar molecules can coexist in water at relative high concentrations, while remaining free to diffuse and interact. However, the high capacity of water as a solvent has also its drawbacks. Indeed, as above-mentioned, it also weakens interactions between polar molecules. Fortunately, the presence of water-free microenvironments [242] within biological systems is the water response to mother nature to circumvent this problem. Many examples of these specially constructed environments can be found in biomacromolecules such as DNA, RNA, and proteins.[243-245] Moreover, the presence of water with its polar nature permits another kind of weak interaction to take place, namely the *hydrophobic effect*, which drives the folding of proteins. Indeed, several amino acids that make proteins have nonpolar groups. These nonpolar amino acids (~hydrophobes) behave strongly by associating together inside the interior of the folded protein. The increased entropy of water, resulting from the interaction of these

239 [N°207] Owen, B. B.; Miller, R. C.; Milner, C. E.; Cogan, H. L. *J. Phys. Chem.* **1961**, *65*, 2065.

240 [N°208] Denniston, K.; Topping, J.; Woodrum, K.; Caret, R. *General, Organic and Biochemistry* **2013**.

241 [N°204] Berg, J. M.; Tymoczko, J. L.; Stryer, L. *Biochemistry*; W.H.Freeman & Co Ltd; 5th Revised edition - Internationnal edition, **2002**.

242 [N°209] Karukstis, K. K.; Frazier, A. A.; Martula, D. S.; Whiles, J. A. *J. Phys. Chem.* **1996**, *100*, 11133.

243 [N°210] Pauling, L.; Corey, R. B.; Branson, H. R. *Proc. Natl. Acad. Sci. USA* **1951**, *37*, 205.

244 [N°211] Astbury, W. T. *Trans. Faraday Soc.* **1933**, *29*, 193.

245 [N°212] Strekowski, L.; Wilson, B. *Mut. Res.* **2007**, *623*, 3.

hydrophobes, helps to compensate the entropy lost as a result of the folding process. This folding process occurs favourably as a combination of the entropy (hydrophobic effect), and the enthalpy change (formation of hydrogen bonds[246] and van der Waals interactions) makes the overall free energy negative.[247] Moreover, the double-helical structure of DNA, which is of key importance for transfer of genetic information,[248] is directly related to NCIs[249-251] in which the interactions of nucleic acid bases play a dominant role. These polar aromatic heterocycles have several possibilities for interacting: *i.e.* via planar H-bonds or vertical π–π interactions, resulting in two structural motifs, planar H-bonding and π-stacking. Both are important not only in determining the architecture of nucleic acids but also in a much more general sense. It was for a long time thought that the energetically term associated to specific H-bonding (originating from electrostatic effects) was of much more importance than the non-specific stacking term (due to London dispersion effects). Only the most recent calculations[252 - 256] revealed that stacking interactions could bear surprisingly large stabilization energies of the same amount of strong H-bonding. Furthermore, NCIs play also a subtle but very important role in molecular recognition processes,[257-262] which are of high importance in many fundamental life processes. Indeed, they ensure an extremely high fidelity in the formation of the right protein, with the right properties, for the right purpose.

---

246 [N°213] Watson, J. D.; Crick, F. H. C. *Nature* **1953**, *171*, 737.

247 [N°214] Breiten, B.; Lockett, M. R.; Sherman, W.; Fujita, S.; Al-Sayah, M.; Lange, H., . . . Whitesides, G. M. *J. Am. Chem. Soc.* **2013**, *135*, 15579.

248 [N°215] Griffiths, A. J. F.; Miller, J. H.; Suzuki, D. T.; Lewontin, R. C.; Gelbart, W. M. *An Introduction to Genetic Analysis*; New York: W. H. Freeman, 7th edition, **2000**.

249 [N°216] Yurenko, Y. P.; Novotny, J.; Sklenar, V.; Marek, R. *Phys. Chem. Chem. Phys.* **2014**, *16*, 2072.

250 [N°217] Blanco, F.; Kelly, B.; Sánchez-Sanz, G.; Trujillo, C.; Alkorta, I.; Elguero, J.; Rozas, I. *J. Phys. Chem. B* **2013**, *117*, 11608.

251 [N°51] Cerny, J.; Hobza, P. *Phys. Chem. Chem. Phys.* **2007**, *9*, 5291.

252 [N°218] Kolar, M.; Hobza, P. *J. Phys. Chem. A* **2007**, *111*, 5851.

253 [N°219] Jurecka, P.; Hobza, P. *J. Am. Chem. Soc.* **2003**, *125*, 15608.

254 [N°220] Jurecka, P.; Hobza, P. *Chem. Phys. Lett.* **2002**, *365*, 89.

255 [N°221] Hobza, P.; Sponer, J. *J. Am. Chem. Soc.* **2002**, *124*, 11802.

256 [N°222] Hobza, P.; Riehn, C.; Weichert, A.; Brutschy, B. *Chem. Phys.* **2002**, *283*, 331.

257 [N°223] Baron, R.; McCammon, J. A. *An. Rev. Phys. Chem.* **2013**, *64*, 151.

258 [N°224] Bielawski, C.; Chen, Y.-S. *Chem. Commun.* **1998**, 1313.

259 [N°225] Grunenberg, J. *Phys. Chem. Chem. Phys.* **2011**, *13*, 10136.

260 [N°226] Cosic, I. *Biomed. Eng.* **1994**, *41*, 1101.

261 [N°227] Gellman, S. H. *Chem. Rev.* **1997**, *97*, 1231.

262 [N°228] Knox, J. R.; Pratt, R. F. *Antimicrob. Agents Chemother.* **1990**, *34*, 1342.

Finally, if we look at the macroscopic scale, non-covalent interactions are perfectly expressed by one of the most astonishing animal, a little nocturnal lizard, namely: the gecko[263] (Figure 22).

Figure 22: Picture of two Geckos © bridgendboy (left), swisshippo (right) - Fotolia.com

This little lizard can perfectly climb smooth vertical walls, trees, even glass. Whether the surface is rough or smooth, wet or dry, it is all the same to the gecko.[264, 265] Since Aristotle first recorded his observations: "run up and down a tree in any way, even with the head downwards",[266] this extraordinary ability of geckos has challenged number of people around the world for millennia. What is gecko's secret? The answer lies in the Gecko's toes (Figure 23).

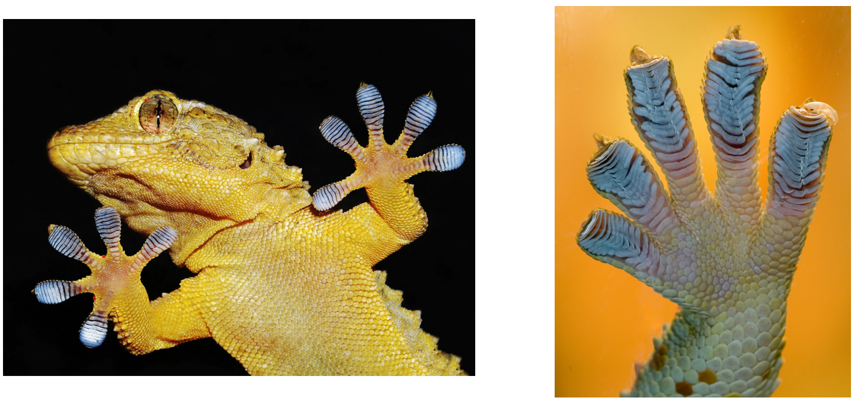

Figure 23: Picture of Gecko's toes © nico99 (left), Thomas Beitz (right) - Fotolia.com

[263] [N°229] Forbes, P. *The gecko's foot: How scientists are taking a leaf from nature's book*; Harper Perennial, **2006**.

[264] [N°230] Russell, A. P. *J. Zool.* **1975**, *176*, 437.

[265] [N°231] Maderson, P. F. A. *Nature* **1964**, *203*, 780.

[266] [N°232] Aristotle In *Historia Animalium*; Clarendon, Oxford ed. WEB: classics.mit.edu/Aristotle/historypanim.html, 1918.

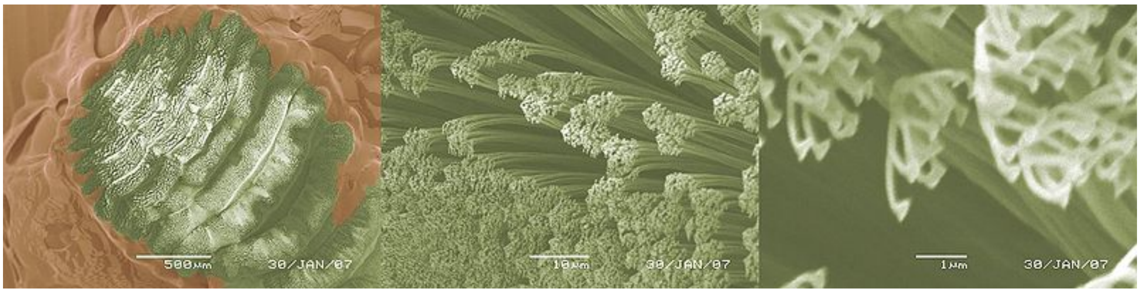

Figure 24: The foot of a Gecko, photograph taken by a scanning electron microscope - author: Oskar Gellerbrant; Public domain via Wikimedia Commons.

A gecko can fully support its substantial body weight by establishing non-covalent interactions (namely dispersion) between, millions of micro-fibrils, called setae, bearing billions of nano-sized branches, terminating in small plates called spatula and the surface (Figure 24).[267-276] Once the phenomenon was understood, an impressive variety of synthetic mimics[277-287] based on the adhesive qualities of the gecko system have been developed, showing that there is just a very small step from the "chemistry beyond the molecule"[288] to the macroscopic scale and how much these NCIs might one day impact our every day's life.

[267] [N°233] Hu, S.; Lopez, S.; Niewiarowski, P. H.; Xia, Z. *J. Royal Soc. Inter.* **2012**.
[268] [N°234] Kim, T. W.; Bhushan, B. *Journal of the Royal Society, Interface / the Royal Society* **2008**, *5*, 319.
[269] [N°235] Persson, B. N. J. *MRS Bulletin* **2007**, *32*, 486.
[270] [N°236] Autumn, K.; Sitti, M.; Liang, Y. A.; Peattie, A. M.; Hansen, W. R.; Sponberg, S., . . . Full, R. J. *Proc. Natl. Acad. Sci. USA* **2002**, *99*, 12252.
[271] [N°237] Autumn, K.; Peattie, A. M. *Intergr. Comp. Biol.* **2002**, *42*, 1081.
[272] [N°238] Autumn, K.; Liang, Y. A.; Hsieh, S. T.; Zesch, W.; Chan, W. P.; Kenny, T. W., . . . Full, R. J. *Nature* **2000**, *405*, 681.
[273] [N°239] Autumn, K.; Hsieh, T.; Zesch, W.; Chan, W. P.; Fearing, R.; Full, R. J. *Am. Zool.* **1999**, *39*, 105A.
[274] [N°240] Hiller, U. *Z. Morph. Tiere* **1968**, *62*, 307.
[275] [N°241] WILLIAMS, E. E.; PETERSON, J. A. *Science* **1982**, *215*, 1509.
[276] [N°242] Ruibal, R.; Ernst, V. *J. Morph.* **1965**, *117*, 271.
[277] [N°243] Murphy, M. P.; Aksak, B.; Sitti, M. *Small* **2009**, *5*, 170.
[278] [N°244] Jeong, H. E.; Lee, J.-K.; Kim, H. N.; Moon, S. H.; Suh, K. Y. *Proc. Natl. Acad. Sci. USA* **2009**, *106*, 5639.
[279] [N°245] Qu, L.; Dai, L.; Stone, M.; Xia, Z.; Wang, Z. L. *Science* **2008**, *322*, 238.
[280] [N°246] Autumn, K.; Gravish, N. *Phil. Trans. Royal Soc. A* **2008**, *366*, 1575.
[281] [N°247] Northen, M. T.; Greiner, C.; Arzt, E.; Turner, K. L. *Adv. Mater.* **2008**, *20*, 3905.
[282] [N°248] del Campo, A.; Greiner, C.; Álvarez, I.; Arzt, E. *Adv. Mater.* **2007**, *19*, 1973.
[283] [N°249] Ge, L.; Sethi, S.; Ci, L.; Ajayan, P. M.; Dhinojwala, A. *Proc. Natl. Acad. Sci. USA* **2007**, *104*, 10792.
[284] [N°250] Zhao, Y.; Tong, T.; Delzeit, L.; Kashani, A.; Meyyappan, M.; Majumdar, A. *J. Vac. Sci. Tech. B* **2006**, *24*, 331.
[285] [N°251] Michael, T. N.; Kimberly, L. T. *Nanotech.* **2005**, *16*, 1159.
[286] [N°252] Yurdumakan, B.; Raravikar, N. R.; Ajayan, P. M.; Dhinojwala, A. *Chem. Commun.* **2005**, 3799.
[287] [N°253] Geim, A. K.; Dubonos, S. V.; Grigorieva, I. V.; Novoselov, K. S.; Zhukov, A. A.; Shapoval, S. Y. *Nat. Mater.* **2003**, *2*, 461.
[288] [N°17] Lehn, J.-M. *Angew. Chem. Int. Ed. Engl.* **1988**, *27*, 89.

Now that the different kinds of non-covalent interactions have been introduced, and we have had some insights into non-covalency that showed their omnipresence and fundamental importance, lets focus more specifically in the source of our interests: *i.e.* the transition metals chemistry.

5.6 - Non-covalent interactions in inorganic, coordination and organometallic chemistry: An intimate relationship with metals.

5.6.1 - Stabilization of "naked" metals? NCIs can do it!

The possible stabilization of "naked" metals by NCIs provides an original manner to introduce the importance of NCIs in the field of transition metals.

The syntheses and applications of transition-metal nanoparticles have found broad interest in several areas of modern science,[289] where well-defined and stable metal nanoparticles (M-NPs) are of high importance. [290 - 296] For instance, W and Mo nanoparticles in olefin metathesis reactions.[297] Stable M-NPs (with M= Cr, Mo, W, Mn, Re, Fe, Ru, Os, Co, Rh or Ir) have been synthesized by means of microwave, thermal or photolytic decomposition from their metal carbonyl precursors $M_x(CO)_y$ in targeted ionic liquid medium. [298-301]

[289] [N°254] Pârvulescu, V. I.; Hardacre, C. *Chem. Rev.* **2007**, *107*, 2615.

[290] [N°255] Scariot, M.; Silva, D. O.; Scholten, J. D.; Machado, G.; Teixeira, S. R.; Novak, M. A., . . . Dupont, J. *Angew. Chem. Int. Ed. Engl.* **2008**, *47*, 9075.

[291] [N°256] Prechtl, M. H. G.; Scariot, M.; Scholten, J. D.; Machado, G.; Teixeira, S. R.; Dupont, J. *Inorg. Chem.* **2008**, *47*, 8995.

[292] [N°257] Lu, A.-H.; Salabas, E. L.; Schüth, F. *Angew. Chem. Int. Ed. Engl.* **2007**, *46*, 1222.

[293] [N°258] Migowski, P.; Dupont, J. *Chem. Eur. J.* **2007**, *13*, 32.

[294] [N°259] Park, J.; Joo, J.; Kwon, S. G.; Jang, Y.; Hyeon, T. *Angew. Chem. Int. Ed. Engl.* **2007**, *46*, 4630.

[295] [N°260] Mastai, Y.; Gedanken, A. *Chemistry of Nanomaterials*; ed. C. N. R. Rao, A. Müller and A. K. Cheetham, Wiley-VCH, Weinheim, **2004**.

[296] [N°261] Gedanken, A. *Ultrasonics Sonochemistry* **2004**, *11*, 47.

[297] [N°262] Braunstein, P.; Rosé, J. *Metal Clusters in Chemistry*; ed. Braunstein, P.; Oro; L. A. and Raithby, P. R. - Wiley-VCH, Weinheim, vol. 2, ch. 2, **2001**, 616–677.

[298] [N°263] Redel, E.; Thomann, R.; Janiak, C. *Chem. Commun.* **2008**, 1789.

[299] [N°264] Kramer, J.; Redel, E.; Thomann, R.; Janiak, C. *Organometallics* **2008**, *27*, 1976.

[300] [N°265] Redel, E.; Kramer, J.; Thomann, R.; Janiak, C. *J. Organomet. Chem.* **2009**, *694*, 1069.

[301] [N°266] Redel, E.; Thomann, R.; Janiak, C. *Inorg. Chem.* **2008**, *47*, 14.

Figure 25: Stabilization and surface capping (functionalization, derivatization) of Au nanoparticles . The original image was published by Janiak *et al.*[302] © John Wiley & Sons, Inc. *(Figure removed because subjected to copyright).*

The possible existence of “naked” transition metals has to be assigned to the high ionic charge, high polarity, high dielectric constant and ability to form supramolecular hydrogen bonding networks [303] of ionic liquids. This provides a very efficient electrostatic “protective shell” for MNPs (Figure 25), in the way that no extra stabilizing molecules are needed.[304-306]

5.6.2 - NCIs: a glue in the conception of non-covalent bonded supramolecular metallic assemblies.

The science of crystal engineering is based on the understanding of physical phenomena such as hydrogen bonding, electrostatic interactions, charge transfer, van der Waals interactions, and π–π stacking; in other terms NCIs.[307] The elaboration of supramolecular species (especially with transition metals) is a powerful technique to gain access to functionalized materials with optimized properties [308-321] which has been

[302] [N°267] Redel, E.; Walter, M.; Thomann, R.; Vollmer, C.; Hussein, L.; Scherer, H., . . . Janiak, C. *Chem. Eur. J.* **2009**, *15*, 10047.

[303] [N°268] Dupont, J. *J. Braz. Chem. Soc.* **2004**, *15*, 341.

[304] [N°269] Kaper, H.; Endres, F.; Djerdj, I.; Antonietti, M.; Smarsly, B. M.; Maier, J.; Hu, Y. S. *Small* **2007**, *3*, 1753.

[305] [N°270] Astruc, D.; Lu, F.; Aranzaes, J. R. *Angew. Chem. Int. Ed. Engl.* **2005**, *44*, 7852.

[306] [N°271] Antonietti, M.; Kuang, D. B.; Smarsly, B.; Yong, Z. *Angew. Chem. Int. Ed. Engl.* **2004**, *43*, 4988.

[307] [N°272] Taylor, R. *Crystengcomm* **2014**, *16*, 6852.

[308] [N°273] O’Keeffe, M.; Yaghi, O. M. *Chem. Rev.* **2011**, *112*, 675.

[309] [N°274] Lu, W.; Chan, M. C. W.; Zhu, N.; Che, C.-M.; He, Z.; Wong, K.-Y. *Chem. Eur. J.* **2003**, *9*, 6155.

[310] [N°275] Moulton, B.; Zaworotko, M. J. *Chem. Rev.* **2001**, *101*, 1629.

[311] [N°276] Ohba, S.; Hosomi, H.; Ito, Y. *J. Am. Chem. Soc.* **2001**, *123*, 6349.

applied to various organometallic compounds.[322-337] The flexible π-bonds between metal and ligands lead to highly variable organometallic structures (and packing modes), directly related to NCIs (intra- as well as intermolecular interactions).

5.6.3 - When NCIs contribute to long-range effects of supramolecular complexes.

The Single Molecule Magnet (SMM)[338 - 343] and Single Chain Magnet[344, 345] (SCM) paradigms led to large investigations in various areas of coordination magneto

[312] [N°277] Xu, Z.; Lee, S.; Kiang, Y. H.; Mallik, A. B.; Tsomaia, N.; Mueller, K. T. *Adv. Mater.* **2001**, *13*, 637.

[313] [N°278] Galan-Mascaros, J. R.; Dunbar, K. R. *Chem. Commun.* **2001**, 217.

[314] [N°279] Noro, S.-i.; Kitagawa, S.; Kondo, M.; Seki, K. *Angew. Chem. Int. Ed. Engl.* **2000**, *39*, 2081.

[315] [N°280] Tabares, L. C.; Navarro, J. A. R.; Salas, J. M. *J. Am. Chem. Soc.* **2000**, *123*, 383.

[316] [N°281] Seo, J. S.; Whang, D.; Lee, H.; Jun, S. I.; Oh, J.; Jeon, Y. J.; Kim, K. *Nature* **2000**, *404*, 982.

[317] [N°282] Miller, J. S. *Inorg. Chem.* **2000**, *39*, 4392.

[318] [N°283] Eddaoudi, M.; Li, H.; Yaghi, O. M. *J. Am. Chem. Soc.* **2000**, *122*, 1391.

[319] [N°284] R. Desiraju, G. *Chem. Commun.* **1997**, 1475.

[320] [N°285] Li, H.; Eddaoudi, M.; O'Keeffe, M.; Yaghi, O. M. *Nature* **1999**, *402*, 276.

[321] [N°286] Hollingsworth, M. D.; Werner-Zwanziger, U.; Brown, M. E.; Chaney, J. D.; Huffman, J. C.; Harris, K. D. M.; Smart, S. P. *J. Am. Chem. Soc.* **1999**, *121*, 9732.

[322] [N°287] Shin, Dong M.; Lee, In S.; Chung, Young K. *Eur. J. Inorg. Chem.* **2003**, *2003*, 2311.

[323] [N°288] Braga, D.; Maini, L.; Polito, M.; Scaccianoce, L.; Cojazzi, G.; Grepioni, F. *Coord. Chem. Rev.* **2001**, *216–217*, 225.

[324] [N°289] Braga, D.; Maini, L.; Grepioni, F.; Elschenbroich, C.; Paganelli, F.; Schiemann, O. *Organometallics* **2001**, *20*, 1875.

[325] [N°290] Aakeroy, C. B.; Beatty, A. M.; Leinen, D. S.; Lorimer, K. R. *Chem. Commun.* **2000**, 935.

[326] [N°291] Atencio, R.; Domasevitch, K. V.; Zaworotko, M. J. *Crystal Eng.* **2000**, *3*, 63.

[327] [N°292] Aakeröy, C. B.; Beatty, A. M.; Leinen, D. S. *Angew. Chem. Int. Ed. Engl.* **1999**, *38*, 1815.

[328] [N°293] B. Aakeroy, C.; M. Beatty, A.; A. Helfrich, B. *J. Chem. Soc., Dalton Trans.* **1998**, 1943.

[329] [N°294] Braga, D.; Maini, L.; Grepioni, F. *Angew. Chem. Int. Ed. Engl.* **1998**, *37*, 2240.

[330] [N°295] Braga, D.; Grepioni, F.; Desiraju, G. R. *Chem. Soc. Rev.* **1998**, *98*, 1375.

[331] [N°296] Chen, Z.-N.; Zhang, H.-X.; Yu, K.-B.; Zheng, K.-C.; Cai, H.; Kang, B.-S. *J. Chem. Soc., Dalton Trans.* **1998**, 1133.

[332] [N°297] Aakeröy, C. B.; Beatty, A. M.; Leinen, D. S. *J. Am. Chem. Soc.* **1998**, *120*, 7383.

[333] [N°298] Munakata, M.; Wu, L. P.; Kuroda-Sowa, T.; Maekawa, M.; Suenaga, Y.; Ning, G. L.; Kojima, T. *J. Am. Chem. Soc.* **1998**, *120*, 8610.

[334] [N°299] Braga, D.; Grepioni, F. *Acc. Chem. Res.* **1997**, *30*, 81.

[335] [N°300] Schauer, C. L.; Matwey, E.; Fowler, F. W.; Lauher, J. W. *J. Am. Chem. Soc.* **1997**, *119*, 10245.

[336] [N°301] Braga, D.; Grepioni, F. *Chem. Commun.* **1996**, 571.

[337] [N°302] Burrows, A. D.; Chan, C.-W.; Chowdhry, M. M.; McGrady, J. E.; Mingos, D. M. P. *Chem. Soc. Rev.* **1995**, *24*, 329.

[338] [N°303] Feltham, H. L. C.; Brooker, S. *Coord. Chem. Rev.* **2014**, *276*, 1.

[339] [N°304] Inglis, R.; Papaefstathiou, G. S.; Wernsdorfer, W.; Brechin, E. K. *Aust. J. Chem.* **2009**, 1108.

[340] [N°305] Aromi, G.; Brechin, E. K. *Struct. Bond* **2006**, *122*, 1.

[341] [N°306] Bircher, R.; Chaboussant, G.; Dobe, C.; Gudel, H. U.; Ochsenbein, S. T.; Sieber, A.; Waldmann, O. *Adv. Funct. Mater.* **2006**, *16*, 209.

[342] [N°307] Christou, G.; Gatteschi, D.; Hendrickson, D. N.; Sessoli, R. *MRS Bulletin* **2000**, *25*, 66.

[343] [N°308] Gatteschi, D.; Sessoli, R. *Angew. Chem. Int. Ed. Engl.* **2003**, *42*, 268.

[344] [N°309] Bogani, L.; Sangregorio, C.; Sessoli, R.; Gatteschi, D. *Angew. Chem. Int. Ed. Engl.* **2005**, *44*, 5817.

[345] [N°310] Bernot, K.; Bogani, L.; Caneschi, A.; Gatteschi, D.; Sessoli, R. *J. Am. Chem. Soc.* **2006**, *128*, 7947.

chemistry, synthetic, instrumental and theoretical chemistry, bringing into focus the issues of magnetic anisotropy. By extension, supramolecular SMMs, in which exchange coupling between the molecules results in quantum behaviour different from that of the individual molecule, constitutes very interesting systems in which the quantum properties of the original molecular SMMs can be finely tuned by considering the role/importance of the inter-cluster interactions.[346-349] Using SMMs as the building blocks in the supramolecular architectures (assembly of 1D–3D SMM) including both covalent and non-covalent interactions is thus an important field of study.[350,351] Unfortunately, most of the recently SMM characterization has focussed purely on the molecule itself and often excluded the influence of the molecular environment (*i.e.* the crystal lattice). Crystal packing effects including weak interactions (*i.e.* H-bonds, electrostatic interactions, π-π interaction etc.) may affect the properties of the individual molecules, which can translate to the magnetic response at (moderately) low temperatures.

Figure 26: Packing diagram emphasizing by space filled representation the hydrogen bonded dimeric units $[Er(NO_3)_4(H_2O)_2]^-$, while the $[Fe(bpca)_2]^+$ are represented as wireframe. Published by Ferbinteanu et *al.*[352]*© Elsevier B.V. (Figure removed because subjected to copyright).*

[346] [N°311] Miyasaka, H.; Yamashita, M. *Dalton Trans.* **2007**, 399.

[347] [N°312] Wittick, L. M.; Murray, K. S.; Moubaraki, B.; Batten, S. R.; Spiccia, L.; Berry, K. J. *Dalton Trans.* **2004**, 1003.

[348] [N°313] Yoo, J.; Wernsdorfer, W.; Yang, E.-C.; Nakano, M.; Rheingold, A. L.; Hendrickson, D. N. *Inorg. Chem.* **2005**, *44*, 3377.

[349] [N°314] Roubeau, O.; Clérac, R. *Eur. J. Inorg. Chem.* **2008**, *2008*, 4325.

[350] [N°315] Hill, S.; Edwards, R. S.; Aliaga-Alcalde, N.; Christou, G. *Science* **2003**, *302*, 1015.

[351] [N°316] Wernsdorfer, W.; Aliaga-Alcalde, N.; Hendrickson, D. N.; Christou, G. *Nature* **2002**, *416*, 406.

[352] [N°317] Ferbinteanu, M.; Cimpoesu, F.; Kajiwara, T.; Yamashita, M. *Solid State Sci* **2009**, *11*, 760.

Following these considerations, the lanthanide chemistry constitutes a challenging chapter of molecular magnetism.[353] The lanthanide complexes display a very large structural variety and possibilities[354-360] including peculiarities such as the occurrence of SMM effects at low nuclearities, *e.g.* d–f binuclears [361, 362] or even lanthanide mononuclears.[363,364] The challenging magnetic and structural problems of d–f systems attract considerable interest and once more can only be understood by considering both experimental and theoretical fields. [365-367]

5.6.4 - The isotope effect (IE): a powerful tool for the investigations of NCIs in host-guests complexes.

Another subtle concept worth noting is the Isotope effect (IE), which arises from differences in atomic mass. [368-370] On a chemical standpoint, molecules that differ only in their isotopic substitution, or isotopologues,[371] have identical electronic structure, but often display a difference in their chemical reactivity due to changes in the vibrational frequencies and zero-point energies (ZPEs) [372,373] of isotopically substituted bonds. Since the awareness that an isotopic substitution can perturb the

[353] [N°318] Tanase, S.; Reedijk, J. *Coord. Chem. Rev.* **2006**, *250*, 2501.
[354] [N°319] Ferbinteanu, M.; Zaharia, A.; Girtu, M. A.; Cimpoesu, F. *Cent. Eur. J. Chem.* **2010**, *8*, 519.
[355] [N°317] Ferbinteanu, M.; Cimpoesu, F.; Kajiwara, T.; Yamashita, M. *Solid State Sci* **2009**, *11*, 760.
[356] [N°320] Maretti, L.; Ferbinteanu, M.; Cimpoesu, F.; Islam, S. S.; Ohba, Y.; Kajiwara, T., . . . Yamauchi, S. *Inorg. Chem.* **2007**, *46*, 660.
[357] [N°321] Pointillart, F.; Bernot, K.; Sessoli, R.; Gatteschi, D. *Chem. Eur. J.* **2007**, *13*, 1602.
[358] [N°322] Mishra, A.; Wernsdorfer, W.; Abboud, K. A.; Christou, G. *J. Am. Chem. Soc.* **2004**, *126*, 15648.
[359] [N°323] Zaleski, C. M.; Depperman, E. C.; Kampf, J. W.; Kirk, M. L.; Pecoraro, V. L. *Angew. Chem. Int. Ed. Engl.* **2004**, *43*, 3912.
[360] [N°324] Costes, J.-P.; Dahan, F.; Donnadieu, B.; Fernandez-Garcia, M.-I.; Rodriguez-Douton, M.-J. *Dalton Trans.* **2003**, 3776.
[361] [N°325] Ferbinteanu, M.; Kajiwara, T.; Choi, K. Y.; Nojiri, H.; Nakamoto, A.; Kojima, N., . . . Yamashita, M. *J. Am. Chem. Soc.* **2006**, *128*, 9008.
[362] [N°326] Costes, J.-P.; Dahan, F.; Wernsdorfer, W. *Inorg. Chem.* **2005**, *45*, 5.
[363] [N°327] Ishikawa, N.; Sugita, M.; Wernsdorfer, W. *Angew. Chem. Int. Ed. Engl.* **2005**, *44*, 2931.
[364] [N°328] Ishikawa, N.; Sugita, M.; Wernsdorfer, W. *J. Am. Chem. Soc.* **2005**, *127*, 3650.
[365] [N°317] Ferbinteanu, M.; Cimpoesu, F.; Kajiwara, T.; Yamashita, M. *Solid State Sci* **2009**, *11*, 760.
[366] [N°325] Ferbinteanu, M.; Kajiwara, T.; Choi, K. Y.; Nojiri, H.; Nakamoto, A.; Kojima, N., . . . Yamashita, M. *J. Am. Chem. Soc.* **2006**, *128*, 9008.
[367] [N°329] Paulovič, J.; Cimpoesu, F.; Ferbinteanu, M.; Hirao, K. *J. Am. Chem. Soc.* **2004**, *126*, 3321.
[368] [N°330] Świderek, K.; Paneth, P. *Chem. Rev.* **2013**, *113*, 7851.
[369] [N°331] Wade, D. *Chem. Biol. Inter.* **1999**, *117*, 191.
[370] [N°332] Kohen, A.; Limbach, H. H. *Isotope Effects in Chemistry and Biology*; Taylor & Francis -CRC Press.
[371] [N°44] In *IUPAC. Compendium of Chemical Terminology*; Version 2.3.3 - 2014-02-24 - the "Gold Book". ed. XML on-line corrected version: Web. 24 Jul 2014: goldbook.iupac.org.
[372] [N°333] Liu, Y.; Warmuth, R. *Org. Lett. 9* **2007**, *9*, 2883.
[373] [N°334] Zhao, Y.-L.; Houk, K. N.; Rechavi, D.; Scarso, A.; Rebek, J. *J. Am. Chem. Soc.* **2004**, *126*, 11428.

thermodynamics and kinetics of chemical processes without altering the electronic energy surface of the involved molecular species, the IEs where rightly pointed as interesting tools toward the investigation of the fundamental intermolecular interactions operating during chemical reactions. Number of studies took the IEs approach to elucidate the mechanism of chemical reactions in biological as well as in chemical systems. [374 - 381] Indeed, noncovalent isotope effects have been widely experimentally observed for substrate–enzyme complexes. Isotopic substitution of a substrate will drastically alter its affinity towards an enzyme.[382] Furthermore, quite interesting is the difference between the behaviours of isotopic molecules, which have recently received particular attention in supramolecular host–guest complexes. Many researchers have used IEs to probe noncovalent intermolecular interactions in supramolecular host–guest systems; because the specific noncovalent interactions responsible for host–guest chemistry cannot be easily directly studied. The weak, reversible and dynamic nature of noncovalent interactions make their relative importance and contribution to the overall free energy of molecular recognition events difficult to dissect. There are many contributions to the overall free energy of binding,[383] including both enthalpic (Coulombic attractions, cation−π and CH−π interactions, heats of solvation/desolvation) and entropic (entropies of solvation/desolvation, translational entropy as well as modification in the conformational flexibility of both host/guest upon guest binding) terms. These interactions are often largely responsible for directing supramolecular self-assembly and host–guest recognition.[384-387]. Furthermore, it has been established that even a

[374] [N°335] Liu, M.; Girma, E.; Glicksman, M. A.; Stein, R. L. *Biochemistry* **2010**, *49*, 4921.
[375] [N°336] Wiley, K. L.; Tormos, J. R.; Quinn, D. M. *Chem. Biol. Inter.* **2010**, *187*, 124.
[376] [N°337] Gonzalez-James, O. M.; Singleton, D. A. *J. Am. Chem. Soc.* **2010**, *132*, 6896.
[377] [N°338] Abe, T.; Miyazawa, A.; Konno, H.; Kawanishi, Y. *Chem. Phys. Lett.* **2010**, *491*, 199.
[378] [N°339] Giagou, T.; Meyer, M. P. *Chem. Eur. J.* **2010**, *16*, 10616.
[379] [N°340] Stojković, V.; Kohen, A. *Israel J. Chem.* **2009**, *49*, 163.
[380] [N°341] de La Harpe, K.; Crespo-Hernández, C. E.; Kohler, B. *J. Am. Chem. Soc.* **2009**, *131*, 17557.
[381] [N°342] Zhang, H.; Wang, S.; Sun, Q.; Smith, S. C. *Phys. Chem. Chem. Phys.* **2009**, *11*, 8422.
[382] [N°331] Wade, D. *Chem. Biol. Inter.* **1999**, *117*, 191.
[383] [N°343] Leung, D. H.; Bergman, R. G.; Raymond, K. N. *J. Am. Chem. Soc.* **2008**, *130*, 2798.
[384] [N°344] Yoshizawa, M.; Klosterman, J. K.; Fujita, M. *Angew. Chem. Int. Ed. Engl.* **2009**, *48*, 3418.
[385] [N°345] Saalfrank, R. W.; Maid, H.; Scheurer, A. *Angew. Chem. Int. Ed. Engl.* **2008**, *47*, 8794.
[386] [N°346] Oshovsky, G. V.; Reinhoudt, D. N.; Verboom, W. *ChemInform.* **2007**, *38*, no.
[387] [N°347] Stang, P. J.; Olenyuk, B. *Acc. Chem. Res.* **1997**, *30*, 502.

small modification in the guest size and shape dramatically alter guest binding [388-391] and reactivity, [392-394] which precludes the use of structure–activity-type studies (*e.g.*, replacing hydrogen with fluorine atoms to alter guest electronics) to systematically investigate host–guest interactions. Thus, IEs constitute an ideal and powerful method to interrogate host–guest interactions as isotopic substitution only minimally affects the guest structure, but gives information about how specific, for instance, C–H/D bond vibrational frequencies change upon guest binding. The isotopic substitution and the resulting kinetic and equilibrium of IEs on noncovalent interactions have been successfully used to examine host–guest exchange[395,396] and binding[397-403]processes in a variety of supramolecular systems. Cyclodextrins (CDs) include a variety of guests that are complementary to their interiors in H_2O. The guest binding affinities increased in D_2O owing to a solvent isotope effect.[404] The replacement of a molecule of hydrogen with deuterium made it less polar or hydrophobic. Aoyama *et al.* reported the noncovalent isotope effect on the formation of host–guest complexes in aqueous media.[405] Furthermore, very interesting applications of host-guests have been reported by Nitschke *et al.*,[406] where white phosphorus is found air-stable within a self-assembled tetrahedral capsule, or by Haino *et al.,* [407] where rare examples of lanthanide mediated cage-like assemblies have been reported.

---

[388] [N°348] Pluth, M. D.; Fiedler, D.; Mugridge, J. S.; Bergman, R. G.; Raymond, K. N. *Proc. Natl. Acad. Sci. USA* **2009**, *106*, 10438.
[389] [N°349] Hastings, C. J.; Pluth, M. D.; Biros, S. M.; Bergman, R. G.; Raymond, K. N. *Tetrahedron* **2008**, *64*, 8362.
[390] [N°350] Davis, A. V.; Fiedler, D.; Seeber, G.; Zahl, A.; van Eldik, R.; Raymond, K. N. *J. Am. Chem. Soc.* **2006**, *128*, 1324.
[391] [N°351] Parac, T. N.; Scherer, M.; Raymond, K. N. *Angew. Chem. Int. Ed. Engl.* **2000**, *39*, 1239.
[392] [N°352] Pluth, M. D.; Bergman, R. G.; Raymond, K. N. *Angew. Chem. Int. Ed. Engl.* **2007**, *46*, 8587.
[393] [N°353] Leung, D. H.; Bergman, R. G.; Raymond, K. N. *J. Am. Chem. Soc.* **2006**, *128*, 9781.
[394] [N°354] Leung, D. H.; Fiedler, D.; Bergman, R. G.; Raymond, K. N. *Angew. Chem. Int. Ed. Engl.* **2004**, *43*, 963.
[395] [N°333] Liu, Y.; Warmuth, R. *Org. Lett. 9* **2007**, *9*, 2883.
[396] [N°355] Felder, T.; Schalley, C. A. *Angew. Chem. Int. Ed. Engl.* **2003**, *42*, 2258.
[397] [N°356] Mugridge, J. S.; Bergman, R. G.; Raymond, K. N. *J. Am. Chem. Soc.* **2011**, *134*, 2057.
[398] [N°357] Mugridge, J. S.; Bergman, R. G.; Raymond, K. N. *J. Am. Chem. Soc.* **2010**, *132*, 1182.
[399] [N°358] Haino, T.; Fukuta, K.; Iwamoto, H.; Iwata, S. *Chem. Eur. J.* **2009**, *15*, 13286.
[400] [N°359] Tran, C. D.; Mejac, I.; Rebek, J.; Hooley, R. J. *Anal. Chem.* **2008**, *81*, 1244.
[401] [N°360] Laughrey, Z. R.; Upton, T. G.; Gibb, B. C. *Chem. Commun.* **2006**, 970.
[402] [N°361] Liu, Y.; Warmuth, R. *Angew. Chem. Int. Ed. Engl.* **2005**, *44*, 7107.
[403] [N°334] Zhao, Y.-L.; Houk, K. N.; Rechavi, D.; Scarso, A.; Rebek, J. *J. Am. Chem. Soc.* **2004**, *126*, 11428.
[404] [N°362] Wang, A. S.; Matsui, Y. *Bull. Chem. Soc. Jpn.* **1994**, *67*, 2917.
[405] [N°363] Fujimoto, T.; Yanagihara, R.; Kobayashi, K.; Aoyama, Y. *Bull. Chem. Soc. Jpn.* **1995**, *68*, 2113.
[406] [N°364] Mal, P.; Breiner, B.; Rissanen, K.; Nitschke, J. R. *Science* **2009**, *324*, 1697.
[407] [N°365] El Aroussi, B.; Guénée, L.; Pal, P.; Hamacek, J. *Inorg. Chem.* **2011**, *50*, 8588.

Figure 27: Self-assembled tetrahedral capsule cage's conformation and the placement of the guest within the cage and stabilized through van der Waals interactions with the hydrophobic phenylene groups lining the cage's published by Nitschke et *al.*[408] © 2014 American Association for the Advancement of Science. *(Figure removed because subjected to copyright).*

5.6.5 - Metallopolymers, a subtle balance between covalency and non-covalency in transition metal complexes.

The development of methods targeting the control of self-organization of molecules to create polymers and homo- or heterometallic coordination aggregates (the so-called metallopolymers) is an important field of current scientific research.[409 - 420] The metallopolymers somehow perfectly illustrate how the subtle equilibrium between covalency and non-covalency is well suited for the emergence of new properties and applications to molecular systems. The linkages responsible for the binding of the metal centres can almost continuously vary between strong (essentially covalent bonds

[408] [N°364] Mal, P.; Breiner, B.; Rissanen, K.; Nitschke, J. R. *Science* **2009**, *324*, 1697.
[409] [N°366] Amo-Ochoa, P.; Zamora, F. *Coord. Chem. Rev.* **2014**, *276*, 34.
[410] [N°367] Zhang, J.; Chen, Y. P.; Miller, K. P.; Ganewatta, M. S.; Bam, M.; Yan, Y., . . . Tang, C. *J. Am. Chem. Soc.* **2014**, *136*, 4873.
[411] [N°368] Eloi, J.-C.; Chabanne, L.; Whittell, G. R.; Manners, I. *Materials Today* **2008**, *11*, 28.
[412] [N°369] Abd-El-Aziz, A. S.; Manners, I. In *Frontiers in Transition Metal-Containing Polymers*; John Wiley & Sons, Inc.: **2007**, p i.
[413] [N°370] Williams, K. A.; Boydston, A. J.; Bielawski, C. W. *Chem. Soc. Rev.* **2007**, *36*, 729.
[414] [N°371] Whittell, G. R.; Manners, I. *Adv. Mater.* **2007**, *19*, 3439.
[415] [N°372] Caseri, W. R.; Chanzy, H. D.; Feldman, K.; Fontana, M.; Smith, P.; Tervoort, T. A., . . . Stutzmann, N. *Adv. Mater.* **2003**, *15*, 125.
[416] [N°373] Leininger, S.; Olenyuk, B.; Stang, P. J. *Chem. Rev.* **2000**, *100*, 853.
[417] [N°374] Eddaoudi, M.; Moler, D. B.; Li, H.; Chen, B.; Reineke, T. M.; O'Keeffe, M.; Yaghi, O. M. *Acc. Chem. Res.* **2001**, *34*, 319.
[418] [N°375] Caulder, D. L.; Raymond, K. N. *Acc. Chem. Res.* **1999**, *32*, 975.
[419] [N°295] Braga, D.; Grepioni, F.; Desiraju, G. R. *Chem. Soc. Rev.* **1998**, *98*, 1375.
[420] [N°347] Stang, P. J.; Olenyuk, B. *Acc. Chem. Res.* **1997**, *30*, 502.

leading to the irreversible or "static" binding of the metal centre) and weak and labile (non-covalent coordination interactions that allow for reversible, "dynamic" or "metallosupramolecular") binding. As an illustration, the conjugated conducting metallopolymers [421] constitute a very exciting class of functional optoelectronic materials, which still has to be explored.[422-425] The singular properties of these hybrid-(inorganic/organic) materials take their origins directly in the interaction of transition metals with the organic scaffold, by the mean of electron/energy transfer between distal transition metals mediated by the π-conjugated polymer backbone. Such interactions ensure enhanced properties for a large panel of applications; for instance, photovoltaics, [426-430] electrocatalysis,[431,432] photocatalysis,[433,434] templated formation of ordered networks, [435-438] advanced electrode materials,[439] and conjugated coordination polymers;[440,441] as well as in the field of biological sensing; for instance, nitric oxide (NO) in the recently discovered water-soluble metallopolymers. [442-444] Eventhough,

[421] [N°376] Do, L.; Smith, R. C.; Tennyson, A. G.; Lippard, S. J. *Inorg. Chem.* **2006**, *45*, 8998.
[422] [N°377] Weder, C. *Chem. Commun.* **2005**, 5378.
[423] [N°378] Holliday, B. J.; Swager, T. M. *Chem. Commun.* **2005**, 23.
[424] [N°379] Cameron, C. G.; MacLean, B. J.; Pickup, P. G. *Macromol. Symp.* **2003**, *196*, 165.
[425] [N°380] G. Pickup, P. *J. Mat. Chem.* **1999**, *9*, 1641.
[426] [N°381] Chan, W. K.; Hui, C. S.; Man, K. Y. K.; Cheng, K. W.; Wong, H. L.; Zhu, N.; Djurišić, A. B. *Coord. Chem. Rev.* **2005**, *249*, 1351.
[427] [N°382] Man, K. Y. K.; Wong, H. L.; Chan, W. K.; Kwong, C. Y.; Djurišić, A. B. *Chem. Mater.* **2004**, *16*, 365.
[428] [N°383] Zhang, M.; Lu, P.; Wang, X.; He, L.; Xia, H.; Zhang, W., . . . Tamai, N. *J. Phys. Chem. B* **2004**, *108*, 13185.
[429] [N°384] Pron, A.; Rannou, P. *Prog. Polym. Sci.* **2002**, *27*, 135.
[430] [N°385] Ng, P. K.; Gong, X.; Chan, S. H.; Lam, L. S. M.; Chan, W. K. *Chem. Eur. J.* **2001**, *7*, 4358.
[431] [N°386] Dahm, C. E.; Peters, D. G. *Anal. Chem.* **1994**, *66*, 3117.
[432] [N°387] Kingsborough, R. P.; Swager, T. M. *Chem. Mater.* **2000**, *12*, 872.
[433] [N°388] Chan, W. K. *Metal Coordination Polymers; Macromolecules Containing Metal and Metal-Like Elements*; Vol. 5; Abd-El-Aziz, A. S., Carraher, C. E., Jr., Pittman, C. U., Jr., Zeldin, M., Eds.; Wiley: New York, **2005**.
[434] [N°389] Hayashida, N.; Yamamoto, T. *Bull. Chem. Soc. Jpn.* **1999**, *72*, 1153.
[435] [N°390] Kokil, A.; Yao, P.; Weder, C. *Macromolecules* **2005**, *38*, 3800.
[436] [N°391] Kokil, A.; Huber, C.; Caseri, W. R.; Weder, C. *Macromol. Chem. Phys.* **2003**, *204*, 40.
[437] [N°392] Kokil, A.; Shiyanovskaya, I.; Singer, K. D.; Weder, C. *J. Am. Chem. Soc.* **2002**, *124*, 9978.
[438] [N°393] Huber, C.; Bangerter, F.; Caseri, W. R.; Weder, C. *J. Am. Chem. Soc.* **2001**, *123*, 3857.
[439] [N°394] Roncali, J. *J. Mat. Chem.* **1999**, *9*, 1875.
[440] [N°395] Knapton, D.; Rowan, S. J.; Weder, C. *Macromolecules* **2005**, *39*, 651.
[441] [N°396] Iyer, P. K.; Beck, J. B.; Weder, C.; Rowan, S. J. *Chem. Commun.* **2005**, 319.
[442] [N°397] Serrano Ruiz, M.; Romerosa, A.; Sierra-Martin, B.; Fernandez-Barbero, A. *Angew. Chem. Int. Ed. Engl.* **2008**, *47*, 8665.
[443] [N°398] Lidrissi, C.; Romerosa, A.; Saoud, M.; Serrano-Ruiz, M.; Gonsalvi, L.; Peruzzini, M. *Angew. Chem. Int. Ed. Engl.* **2005**, *117*, 2624.
[444] [N°399] Wang, X.-S.; Winnik, M. A.; Manners, I. *Macromol. Rap. Comm.* **2002**, *23*, 210.

CMP-based sensors are in an earlier stage of evolution, notable resistivity[445] and fluorescence-based[446] sensors for nitric oxide (NO) have already been described.

5.6.6 - H-bonds in TM chemistry.

5.6.6.1 - H-bond new generation: The metal hydrides.

Over the last years, the H-bond concept has drastically evolved, not only in the sense of elucidation of the nature, but also in the extension of the range of bonding partners.[447] Thus, after the classical version of H-bond A–**H**•••B (limited to A atoms such as N, O, and F) the concept was broadened by the elements of periods III-IV (P, S, Cl, etc.). The same elements bearing lone electron pairs, as well as the π electrons of multiple bonds or arene rings, have been shown to be proton-accepting sites "B". More recently, the discovery of unconventional basic centres specific for organometallic complexes has opened a new page in the hydrogen-bond concept (*i.e.*, A–**H**•••M or A–**H**•••H-M, etc.), which is still under active investigation.[448-453] Their fundamental and practical (catalysis, new materials) importance elicited studies from several research groups. As a result, we are beginning to understand the organometallic HBs involved in protontransfer processes.[454-457]

---

[445] [N°400] Shioya, T.; Swager, T. M. *Chem. Commun.* **2002**, 1364.

[446] [N°401] Smith, R. C.; Tennyson, A. G.; Lim, M. H.; Lippard, S. J. *Org. Lett.* **2005**, *7*, 3573.

[447] [N°402] Crabtree, R. H.; Eisenstein, O.; Sini, G.; Peris, E. *J. Organomet. Chem.* **1998**, *567*, 7.

[448] [N°403] Belkova, N. V.; Besora, M.; Baya, M.; Dub, P. A.; Epstein, L. M.; Lledos, A., . . . Shubina, E. S. *Chem. Eur. J.* **2008**, *14*, 9921.

[449] [N°404] Belkova, N. V.; Gribanova, T. N.; Gutsul, E. I.; Minyaev, R. M.; Bianchini, C.; Peruzzini, M., . . . Epstein, L. M. *J. Mol. Struct.* **2007**, *844*, 115.

[450] [N°405] Belkova, N. V.; Dub, P. A.; Baya, M.; Houghton, J. *Inorg Chim Acta*
Inorg Chim Acta **2007**, *360*, 149.

[451] [N°406] Belkova, N. V.; Shubina, E. S.; Epstein, L. M. *Accounts of chemical research* **2005**, *38*, 624.

[452] [N°407] Belkova, N. V.; Collange, E.; Dub, P.; Epstein, L. M.; Lemenovskii, D. A.; Lledos, A., . . . Vorontsov, E. V. *Chemistry* **2005**, *11*, 873.

[453] [N°408] Shubina, E. S.; Belkova, N. V.; Epstein, L. M. *J. Organomet. Chem.* **1997**, *536*, 17.

[454] [N°409] Epstein, L. M.; Shubina, E. S. *Coord. Chem. Rev.* **2002**, *231*, 165.

[455] [N°410] Brammer, L. *Dalton Trans.* **2003**, 3145.

[456] [N°411] Alkorta, I.; Elguero, J. *Chem. Soc. Rev.* **1998**, *27*, 163.

[457] [N°412] Custelcean, R.; Jackson, J. E. *Chem. Rev.* **2001**, *101*, 1963.

5.6.6.2 - Transmission of NCIs: solvent···anion···cation interactions an amazing situation.

Since Kubas *et al.*[458] reported the first isolable transition-metal dihydrogen complex, this class of coordination compounds rapidly became an important field of investigation.[459] Mono- and polyhydride complexes, as well as dihydrogen complexes were all reported as playing a key role in number of catalytic processes.[460-462] The behaviour of the initially formed [M(η^2-H_2)] complex is strongly dependent on the electronic properties of the metal:

- It is stable when the metal centre bears suitable Lewis acidity and π back-bonding ability,
- It isomerises to a polyhydride structure if the metal centre is strongly back-donating.
- It releases H_2 when the metal centre is insufficiently back-donating.

When a neutral hydride complex is protonated, the nature of the solvent was suspected to affect the outcome through its polarity and/or the possible establishment of specific interactions (hydrogen bonding) with the neutral solutes (hydride complex, proton donor) or with the proton-transfer product.[463]

Few previous contributions have specifically addressed solvent effects on the protonation process of neutral hydride complexes.[464-468] More recently, Poli et *al.* [469-471]

---

[458] [N°413] Kubas, G. J.; Ryan, R. R.; Swanson, B. I.; Vergamini, P. J.; Wasserman, H. J. *J. Am. Chem. Soc.* **1984**, *106*, 451.

[459] [N°414] Kubas, G. J. *Metal Dihydrogen and σ-Bond Complexes*; Kluwer Academic/Plenum Press, New York, **2001**.

[460] [N°415] Szymczak, N. K.; Tyler, D. R. *Coord. Chem. Rev.* **2008**, *252*, 212.

[461] [N°416] Lau, C. P.; Ng, S. M.; Jia, G.; Lin, Z. *Coord. Chem. Rev.* **2007**, *251*, 2223.

[462] [N°417] Esteruelas, M. A.; Oro, L. A. *Chem. Rev.* **1998**, *98*, 577.

[463] [N°418] Besora, M.; Lledos, A.; Maseras, F. *Chem. Soc. Rev.* **2009**, *38*, 957.

[464] [N°404] Belkova, N. V.; Gribanova, T. N.; Gutsul, E. I.; Minyaev, R. M.; Bianchini, C.; Peruzzini, M., . . . Epstein, L. M. *J. Mol. Struct.* **2007**, *844*, 115.

[465] [N°419] Algarra, A. G.; Basallote, M. G.; Feliz, M.; Fernández-Trujillo, M. J.; Llusar, R.; Safont, V. S. *Chem. Eur. J.* **2006**, *12*, 1413.

[466] [N°420] Basallote, M. G.; Feliz, M.; Fernández-Trujillo, M. J.; Llusar, R.; Safont, V. S.; Uriel, S. *Chem. Eur. J.* **2004**, *10*, 1463.

[467] [N°421] Belkova, N. V.; Besora, M.; Epstein, L. M.; Lledós, A.; Maseras, F.; Shubina, E. S. *J. Am. Chem. Soc.* **2003**, *125*, 7715.

[468] [N°422] Gründemann, S.; Ulrich, S.; Limbach, H.-H.; Golubev, N. S.; Denisov, G. S.; Epstein, L. M., . . . Chaudret, B. *Inorg. Chem.* **1999**, *38*, 2550.

[469] [N°423] Dub, P. A.; Belkova, N. V.; Filippov, O. A.; Daran, J.-C.; Epstein, L. M.; Lledós, A., . . . Poli, R. *Chem. Eur. J.* **2010**, *16*, 189.

reported the very specific behaviour of Mo molecular analogues. The low-temperature protonation at 200 K of Mo complexes by $Et_2O{\bullet}HBF_4$ gives a different result subtlety dependant on the nature of the solvent used:

- A dihydrogen complex $[Mo(CO)(Cp^*)(\eta^2\text{-}H_2)(PMe_3)_2]^+$ is obtained in THF.
- A tautomeric dihydride $[Mo(CO)(Cp^*)(H)_2(PMe_3)_2]^+$ is the only observable product in dichloromethane.

Once the temperature raises up to 230 K, both Mo species lose H_2 (at approximately the same rate) leading to the formation of a rather new species $[Mo(CO)(Cp^*)(FBF_3)(PMe_3)_2]$, which in accordance with the two previous complexes, also decomposes at ambient temperature in a $[Mo(CO)(Cp^*)(FH{\cdots}FBF_3)(PMe_3)_2]$ derivative bearing a neutral HF ligand coordinated to the transition metal through the F atom and to the BF_4^- anion through a hydrogen bond. Through this particular case the authors addressed the key role of non-covalent anion–solvent interactions, capable to modulate the anion–cation interaction, ultimately altering the energetic balance between the two isomeric forms of Mo derivatives.

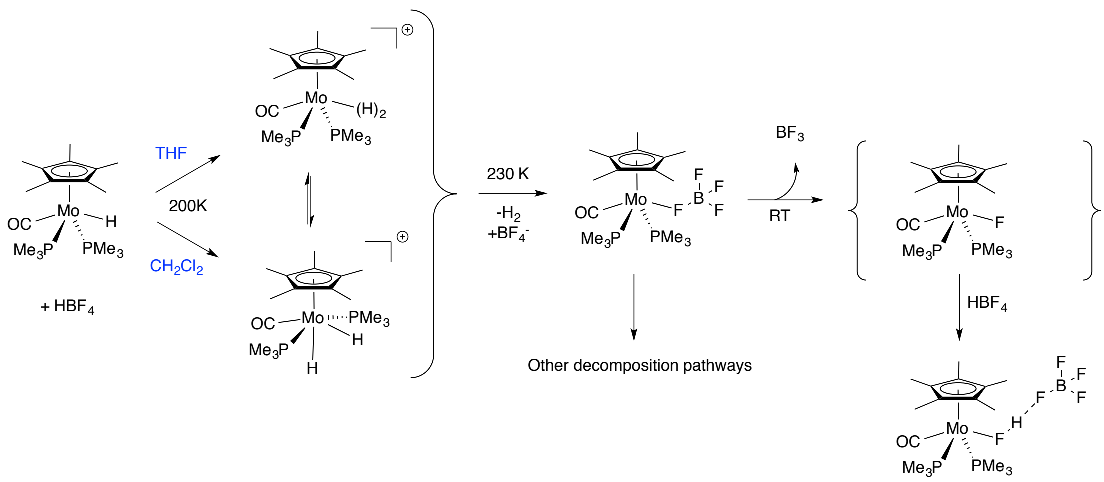

Figure 28: Overall reaction of Mo complex with HBF_4. Published by Poli et *al.*[472] © 2014 American Association for the Advancement of Science

[470] [N°424] Baya, M.; Dub, P. A.; Houghton, J.; Daran, J.-C.; Belkova, N. V.; Shubina, E. S., . . . Poli, R. *Inorg. Chem.* **2008**, *48*, 209.

[471] [N°425] Dub, P. A.; Baya, M.; Houghton, J.; Belkova, N. V.; Daran, J.-C.; Poli, R., . . . Shubina, E. S. *Eur. J. Inorg. Chem.* **2007**, *2007*, 2813.

[472] [N°423] Dub, P. A.; Belkova, N. V.; Filippov, O. A.; Daran, J.-C.; Epstein, L. M.; Lledós, A., . . . Poli, R. *Chem. Eur. J.* **2010**, *16*, 189.

5.6.7 - And what about Halogen-bonds correlated with transition metals? Another product of NCIs.

Halogen bonds A•••Hal (Hal= Cl, Br, or I; A= N, O, S, or π) is also a product of noncovalent interaction between a halogen atom and an electron-rich partner.[473]

Early observation that halogen atoms could form attractive directional interactions with Lewis bases comes from the structural work of Hassel.[474] Because of their prominent role in supramolecular architectures,[475-479] as well as in recognition process[480,481] and regarding biological systems,[482-485] Halogen-bonded interactions have been widely studied under experimental or theoretical standpoints. For a while, the reason why halogen-bonded complexes could be formed has been confusing because covalently bonded halogens are generally considered to be negative. Politzer *et al.*[486-488] helped shed light on this issue by studying the electrostatic potentials of halogen-containing molecules. Their results unveiled that the halogen atom bound to carbon often bears a region of positive potential along the direction of the C—Halogen bond and directed toward the electron donor, the so-called "σ-hole" region. Very similarly to H-bonding interaction, electrostatics and polarization constitute the two major driving forces in halogen bonding, as well as London dispersion contributions, which play an important role.[489] Recently, halogen bonds involving metals became a new topic with applications in crystal engineering and allied areas.[490-497] An illustrative example of the influence of

[473] [N°426] Brammer, L.; Minguez Espallargas, G.; Libri, S. *Crystengcomm* **2008**, *10*, 1712.
[474] [N°427] Hassel, O. *Science* **1970**, *170*, 497.
[475] [N°428] Legon, A. C. *Phys. Chem. Chem. Phys.* **2010**, *12*, 7736.
[476] [N°429] Metrangolo, P.; Meyer, F.; Pilati, T.; Resnati, G.; Terraneo, G. *Angew. Chem. Int. Ed. Engl.* **2008**, *47*, 6114.
[477] [N°430] Nguyen, H. L.; Horton, P. N.; Hursthouse, M. B.; Legon, A. C.; Bruce, D. W. *J. Am. Chem. Soc.* **2003**, *126*, 16.
[478] [N°431] Metrangolo, P.; Resnati, G. *Chem. Eur. J.* **2001**, *7*, 2511.
[479] [N°432] Corradi, E.; Meille, S. V.; Messina, M. T.; Metrangolo, P.; Resnati, G. *Angew. Chem. Int. Ed. Engl.* **2000**, *39*, 1782.
[480] [N°433] Cavallo, G.; Metrangolo, P.; Pilati, T.; Resnati, G.; Sansotera, M.; Terraneo, G. *Chem. Soc. Rev.* **2010**, *39*, 3772.
[481] [N°434] Metrangolo, P.; Neukirch, H.; Pilati, T.; Resnati, G. *Acc. Chem. Res.* **2005**, *38*, 386.
[482] [N°435] Parisini, E.; Metrangolo, P.; Pilati, T.; Resnati, G.; Terraneo, G. *Chem. Soc. Rev.* **2011**, *40*, 2267.
[483] [N°436] Lu, Y.; Wang, Y.; Zhu, W. *Phys. Chem. Chem. Phys.* **2010**, *12*, 4543.
[484] [N°437] Lu, Y.; Shi, T.; Wang, Y.; Yang, H.; Yan, X.; Luo, X., . . . Zhu, W. *J. Med. Chem.* **2009**, *52*, 2854.
[485] [N°438] Auffinger, P.; Hays, F. A.; Westhof, E.; Ho, P. S. *Proc. Natl. Acad. Sci. USA* **2004**, *101*, 16789.
[486] [N°439] Politzer, P.; Murray, J. S.; Clark, T. *Phys. Chem. Chem. Phys.* **2010**, *12*, 7748.
[487] [N°440] Clark, T.; Hennemann, M.; Murray, J.; Politzer, P. *J. Mol. Model.* **2007**, *13*, 291.
[488] [N°441] Politzer, P.; Lane, P.; Concha, M.; Ma, Y.; Murray, J. *J. Mol. Model.* **2007**, *13*, 305.
[489] [N°442] Politzer, P.; Riley, K. E.; Bulat, F. A.; Murray, J. S. *Comp. Theor. Chem.* **2012**, *998*, 2.
[490] [N°443] Clemente-Juan, J. M.; Coronado, E.; Minguez Espallargas, G.; Adams, H.; Brammer, L. *Crystengcomm* **2010**, *12*, 2339.

metal centres on halogen bonding is the case of C-X_1•••X_2-M halogen bonds,[498] where the metal-bound halogen (the ''inorganic halogen'') acts as the halogen bond acceptor (nucleophile) and the carbon-bound halogen (the ''organic halogen'') is the halogen bond donor (electrophile). The strength of the halogen bond is the uttermost important topic for researchers. Zhao *et al.* [499] as well as others, [500 - 502] have remarkably investigated, by the mean of quantum chemical methods, the nature of the halogen bonding interactions, especially when a transition metal is involved. Their results clearly argue that the introduction of transition metal atoms have an influence on both halogen bond donor and acceptor. Thus, a fine-tuning of the molecular structures and geometries of halogen-bonding complexes (by modulating the halogen atoms and/or metal centres) constitute a useful tool in the design and synthesis of new functional materials.[503]

5.6.8 - NCIs of π systems, touching transition metals.

5.6.8.1 - Stacking interactions.

The study of NCIs regarding π-systems has known great enthusiasm over the last years, due to the importance of these interactions for many molecular systems, going from molecular biology to crystal engineering. [504-526] NCIs involving metal centres have been

[491] [N°444] Mínguez Espallargas, G.; Zordan, F.; Arroyo Marín, L.; Adams, H.; Shankland, K.; van de Streek, J.; Brammer, L. *Chem. Eur. J.* **2009**, *15*, 7554.
[492] [N°445] Mínguez Espallargas, G.; Brammer, L.; Allan, D. R.; Pulham, C. R.; Robertson, N.; Warren, J. E. *J. Am. Chem. Soc.* **2008**, *130*, 9058.
[493] [N°446] Smart, P.; Espallargas, G. M.; Brammer, L. *Crystengcomm* **2008**, *10*, 1335.
[494] [N°426] Brammer, L.; Minguez Espallargas, G.; Libri, S. *Crystengcomm* **2008**, *10*, 1712.
[495] [N°447] Zordan, F.; Espallargas, G. M.; Brammer, L. *Crystengcomm* **2006**, *8*, 425.
[496] [N°448] Mínguez Espallargas, G.; Brammer, L.; Sherwood, P. *Angew. Chem. Int. Ed. Engl.* **2006**, *45*, 435.
[497] [N°449] Brammer, L.; Minguez Espallargas, G.; Adams, H. *Crystengcomm* **2003**, *5*, 343.
[498] [N°450] L. Brammer, F. Z., G. Mínguez Espallargas, S. L. Purver, L. Arroyo Marín, H. Adams *Trans. Am. Cryst. Assoc.* **2004**, *39*, 114.
[499] [N°451] Zhao, Q.; Feng, D. *J. Mol. Model.* **2013**, *19*, 1267.
[500] [N°452] Wu, W.; Lu, Y.; Liu, Y.; Peng, C.; Liu, H. *Comp. Theor. Chem.* **2014**, *1029*, 21.
[501] [N°453] Wang, Y.; Wu, W.; Liu, Y.; Lu, Y. *Chem. Phys. Lett.* **2013**, *578*, 38.
[502] [N°454] Xu, L.; Lv, J.; Sang, P.; Zou, J. W.; Yu, Q. S.; Xu, M. B. *Chem. Phys.* **2011**, *379*, 66.
[503] [N°455] Cheng, N.; Liu, Y.; Zhang, C.; Liu, C. *J. Mol. Model.* **2013**, *19*, 3821.
[504] [N°456] Ohno, K.; Sugaya, T.; Kato, M.; Matsumoto, N.; Fukano, R.; Ogino, Y., . . . Nagasawa, A. *Cryst. Growth Des.* **2014**.
[505] [N°457] Caracelli, I.; Haiduc, I.; Zukerman-Schpector, J.; Tiekink, E. R. T. *Coord. Chem. Rev.* **2013**, *257*, 2863.
[506] [N°458] Fiol, J. J.; Barceló-Oliver, M.; Tasada, A.; Frontera, A.; Terrón, À.; García-Raso, Á. *Coord. Chem. Rev.* **2013**, *257*, 2705.
[507] [N°459] Singh, N. J.; Min, S. K.; Kim, D. Y.; Kim, K. S. *J. Chem. Theory Comput.* **2009**, *5*, 515.

the source of specific attention, as it appeared that planar chelate rings with delocalized π-bonds can form stacking[527 - 538] interactions similar to those of aromatic organic molecules.[539-542] These observations could be connected with speculations of aromatic character in planar chelate rings with delocalized π-bonds.[543,544] Recent studies by Zarić et *al.* evidenced stacking interactions between chelate and C6-aromatic rings in crystal structures of square planar transition-metal complexes, bearing mutual slipped-parallel (offset face-to-face) orientations between chelate and C6-aryl rings (similar to the

508 [N°460] Schneider, H.-J. *Angew. Chem. Int. Ed. Engl.* **2009**, *48*, 3924.

509 [N°461] Nishio, M.; Umezawa, Y.; Honda, K.; Tsuboyama, S.; Suezawa, H. *Crystengcomm* **2009**, *11*, 1757.

510 [N°462] Gray, J. C.; Pagelot, A.; Collins, A.; Fabbiani, F. P. A.; Parsons, S.; Sadler, P. J. *Eur. J. Inorg. Chem.* **2009**, *2009*, 2673.

511 [N°463] Tiekink, E. R. T.; Zukerman-Schpector, J. *Crystengcomm* **2009**, *11*, 1176.

512 [N°464] Ringer, A. L.; Sherrill, C. D. *J. Am. Chem. Soc.* **2009**, *131*, 4574.

513 [N°465] Wheeler, S. E.; Houk, K. N. *Mol. Phys.* **2009**, *107*, 749.

514 [N°466] Yi, H.-B.; Lee, H. M.; Kim, K. S. *J. Chem. Theory Comput.* **2009**, *5*, 1709.

515 [N°467] Fernández-Botello, A.; Holý, A.; Moreno, V.; Operschall, B. P.; Sigel, H. *Inorg. Chim. Acta* **2009**, *362*, 799.

516 [N°468] Singh, M.; Butcher, R. J.; Singh, N. K. *Polyhedron* **2009**, *28*, 1197.

517 [N°72] Wheeler, S. E.; Houk, K. N. *J. Am. Chem. Soc.* **2008**, *130*, 10854.

518 [N°469] Yanagisawa, S.; Crowley, P. B.; Firbank, S. J.; Lawler, A. T.; Hunter, D. M.; McFarlane, W., . . . Dennison, C. *J. Am. Chem. Soc.* **2008**, *130*, 15420.

519 [N°470] Cherrier, M. V.; Cavazza, C.; Bochot, C.; Lemaire, D.; Fontecilla-Camps, J. C. *Biochemistry* **2008**, *47*, 9937.

520 [N°471] Dinadayalane, T. C.; Afanasiev, D.; Leszczynski, J. *J. Phys. Chem. A* **2008**, *112*, 7916.

521 [N°472] Qu, X.; Wang, X.; Zhu, D. *Environ. Sci. Technol.* **2007**, *41*, 8321.

522 [N°473] Terrón, A.; Fiol, J. J.; García-Raso, A.; Barceló-Oliver, M.; Moreno, V. *Coord. Chem. Rev.* **2007**, *251*, 1973.

523 [N°474] Novokmet, S.; Heinemann, F. W.; Zahl, A.; Alsfasser, R. *Inorg. Chem.* **2005**, *44*, 4796.

524 [N°475] Burghardt, T. P.; Juranić, N.; Macura, S.; Ajtai, K. *Biopolymers* **2002**, *63*, 261.

525 [N°476] Steiner, T. *Angew. Chem. Int. Ed. Engl.* **2002**, *41*, 48.

526 [N°477] Pletneva, E. V.; Laederach, A. T.; Fulton, D. B.; Kostić, N. M. *J. Am. Chem. Soc.* **2001**, *123*, 6232.

527 [N°478] Malenov, D. P.; Ninković, D. B.; Sredojević, D. N.; Zarić, S. D. **2014**, n/a.

528 [N°479] Jurca, T.; Korobkov, I.; Gorelsky, S. I.; Richeson, D. S. *Inorg. Chem.* **2013**, *52*, 5749.

529 [N°480] Mosae Selvakumar, P.; Suresh, E.; Subramanian, P. S. *Polyhedron* **2009**, *28*, 245.

530 [N°481] Wang, X.-J.; Jian, H.-X.; Liu, Z.-P.; Ni, Q.-L.; Gui, L.-C.; Tang, L.-H. *Polyhedron* **2008**, *27*, 2634.

531 [N°482] Sredojevic, D.; Bogdanovic, G. A.; Tomic, Z. D.; Zaric, S. D. *Crystengcomm* **2007**, *9*, 793.

532 [N°483] Sredojević, D.; Tomić, Z.; Zarić, S. *Cent. Eur. J. Chem.* **2007**, *5*, 20.

533 [N°484] Tomic, Z. D.; Sredojevic, D.; Zaric, S. D. *Cryst. Growth Des.* **2006**, *6*, 29.

534 [N°485] Pucci, D.; Albertini, V.; Bloise, R.; Bellusci, A.; Cataldi, A.; Catapano, C. V., . . . Crispini, A. *J. Inorg. Chem.* **2006**, *100*, 1575.

535 [N°486] Tomic, Z. D.; Novakovic, S. B.; Zaric, S. D. *Eur. J. Inorg. Chem.* **2004**, 2215.

536 [N°487] Mukhopadhyay, U.; Choquesillo-Lazarte, D.; Niclos-Gutierrez, J.; Bernal, I. *Crystengcomm* **2004**, *6*, 627.

537 [N°488] Craven, E.; Zhang, C.; Janiak, C.; Rheinwald, G.; Lang, H. *Z. Anorg. Allg. Chem.* **2003**, *629*, 2282.

538 [N°489] Castiñeiras, A.; Sicilia-Zafra, A. G.; González-Pérez, J. M.; Choquesillo-Lazarte, D.; Niclós-Gutiérrez, J. *Inorg. Chem.* **2002**, *41*, 6956.

539 [N°490] Pitoňák, M.; Neogrády, P.; Řezáč, J.; Jurečka, P.; Urban, M.; Hobza, P. *J. Chem. Theory Comput.* **2008**, *4*, 1829.

540 [N°491] Lee, E. C.; Kim, D.; Jurečka, P.; Tarakeshwar, P.; Hobza, P.; Kim, K. S. *J. Phys. Chem. A* **2007**, *111*, 3446.

541 [N°61] Sinnokrot, M. O.; Sherrill, C. D. *J. Phys. Chem. A* **2006**, *110*, 10656.

542 [N°64] Podeszwa, R.; Bukowski, R.; Szalewicz, K. *J. Phys. Chem. A* **2006**, *110*, 10345.

543 [N°492] Milcic, M. K.; Ostojic, B. D.; Zaric, S. D. *Inorg. Chem.* **2007**, *46*, 7109.

544 [N°493] Masui, H. *Coord. Chem. Rev.* **2001**, *219-221*, 957.

slipped-parallel orientation of two benzene rings). However, C6-aromatic rings can also form CH-π interactions with chelate rings, where the hydrogen atoms of the C6-aryl rings are perpendicular to the π-system of the chelate ring.[545,546] The analyses of the tendency for stacking *vs* CH-π interactions in crystal structures of square-planar transition-metal complexes showed that the number of stacking interactions is a few times larger than the number of CH-π interactions. Based on the fact that chelate rings with delocalized π-bonds can form a noncovalent interaction similar to those of aromatic organic molecules, it can be anticipated that two chelate rings could also undergo a mutual stacking interaction, and indeed Zarić *et al.*[547] have evidenced chelate−chelate-stacking interactions in the case of neutral square-planar complexes.

Figure 29: Calculated energies of stacking interactions between metal chelates and benzene, plotted as the function of offset value *r*. White dots are associated to [Ni($C_3H_3O_2$)-(HCO_2)], while the grey dots are associated to [Cu($C_3H_3O_2$)(HCO_2)]; published by Zarić *et al.*[548] © John Wiley & Sons, Inc. *(Figure removed because subjected to copyright).*

[545] [N°494] Milčić, M. K.; Medaković, V. B.; Zarić, S. D. *Inorg. Chim. Acta* **2006**, *359*, 4427.

[546] [N°495] Milcic, M. K.; Medakovic, V. B.; Sredojevic, D. N.; Juranic, N. O.; Zaric, S. D. *Inorg. Chem.* **2006**, *45*, 4755.

[547] [N°496] Sredojević, D. a. N.; Tomić, Z. D.; Zarić, S. a. D. *Cryst. Growth Des.* **2010**, *10*, 3901.

[548] [N°496] ibid.

5.6.8.2 - An extension? The NCIs between a coordinated water molecule and π-systems.

The interaction of a water molecule with aromatic systems is preponderant in many areas from biology to material science. [549-558]

Thus, important interactions of aromatic rings with water molecules in aquaporins,[559,560] nanotubes, [561,562] and nanoporous materials[563] have been unveiled. Consequently, the water–benzene complex has been the subject of extensive investigation. [564 - 570] Theoretical investigation, revealed a minimum energy for the structure of the water–benzene dimer, in the case where the water molecule is above the ring and oriented in such a way as to form a single hydrogen bond with the ring (*i.e.* an OH–π interaction), which was recently confirmed experimentally by the observation of a OH–π interaction between liquid water and benzene.[571] These results evidently argue in favour of the important role of water in biological binding, recognition, and signalling processes. Interactions of water molecules with ions, molecules and interfaces have been intensively studied,[572-575] revealing the influence of ions regarding water properties.[576]

---

549 [N°497] Raghavender, U. S.; Chatterjee, B.; Saha, I.; Rajagopal, A.; Shamala, N.; Balaram, P. *J. Phys. Chem. B* **2011**, *115*, 9236.
550 [N°498] Voloshina, E.; Usvyat, D.; Schutz, M.; Dedkov, Y.; Paulus, B. *Phys. Chem. Chem. Phys.* **2011**, *13*, 12041.
551 [N°499] Natarajan, R.; Charmant, J. P. H.; Orpen, A. G.; Davis, A. P. *Angew. Chem. Int. Ed. Engl.* **2010**, *49*, 5125.
552 [N°500] Kim, S.-J.; Seo, H.-I.; Boo, B. H. *Mol. Phys.* **2009**, *107*, 1261.
553 [N°501] Takaiwa, D.; Hatano, I.; Koga, K.; Tanaka, H. *Proc. Natl. Acad. Sci. USA* **2008**, *105*, 39.
554 [N°502] Agre, P. *Angew. Chem. Int. Ed. Engl.* **2004**, *43*, 4278.
555 [N°503] Kozono, D.; Yasui, M.; King, L. S.; Agre, P. *J. Clinical Invest.* **2002**, *109*, 1395.
556 [N°504] Hummer, G.; Rasaiah, J. C.; Noworyta, J. P. *Nature* **2001**, *414*, 188.
557 [N°505] Steiner, T.; Koellner, G. *J. Mol. Biol.* **2001**, *305*, 535.
558 [N°506] Zaric, S. D.; Popovic, D. M.; Knapp, E. W. *Chemistry* **2000**, *6*, 3935.
559 [N°502] Agre, P. *Angew. Chem. Int. Ed. Engl.* **2004**, *43*, 4278.
560 [N°503] Kozono, D.; Yasui, M.; King, L. S.; Agre, P. *J. Clinical Invest.* **2002**, *109*, 1395.
561 [N°501] Takaiwa, D.; Hatano, I.; Koga, K.; Tanaka, H. *Proc. Natl. Acad. Sci. USA* **2008**, *105*, 39.
562 [N°504] Hummer, G.; Rasaiah, J. C.; Noworyta, J. P. *Nature* **2001**, *414*, 188.
563 [N°499] Natarajan, R.; Charmant, J. P. H.; Orpen, A. G.; Davis, A. P. *Angew. Chem. Int. Ed. Engl.* **2010**, *49*, 5125.
564 [N°507] Veljkovic, D. Z.; Janjic, G. V.; Zaric, S. D. *Crystengcomm* **2011**, *13*, 5005.
565 [N°508] Slipchenko, L. V.; Gordon, M. S. *J. Phys. Chem. A* **2008**, *113*, 2092.
566 [N°509] Tarakeshwar, P.; Choi, H. S.; Lee, S. J.; Lee, J. Y.; Kim, K. S.; Ha, T.-K., . . . Lee, H. *J. Chem. Phys.* **1999**, *111*, 5838.
567 [N°510] Feller, D. *J. Phys. Chem. A* **1999**, *103*, 7558.
568 [N°511] Courty, A.; Mons, M.; Dimicoli, I.; Piuzzi, F.; Gaigeot, M.-P.; Brenner, V., . . . Millié, P. *J. Phys. Chem. A* **1998**, *102*, 6590.
569 [N°512] F. Malone, J.; M. Murray, C.; H. Charlton, M.; Docherty, R.; J. Lavery, A. *J. Chem. Soc., Faraday Trans.* **1997**, *93*, 3429.
570 [N°513] Suzuki, S.; Green, P. G.; Bumgarner, R. E.; Dasgupta, S.; Goddard, W. A.; Blake, G. A. *Science* **1992**, *257*, 942.
571 [N°514] Gierszal, K. P.; Davis, J. G.; Hands, M. D.; Wilcox, D. S.; Slipchenko, L. V.; Ben-Amotz, D. *J. Phys. Chem. Lett.* **2011**, *2*, 2930.
572 [N°514] ibid.
573 [N°515] Wang, J.; White, T. A.; Arachchige, S. M.; Brewer, K. J. *Chem. Commun.* **2011**, *47*, 4451.

Complementary, Zarić *et al.*[577] studied the influence of water molecules (non-coordinating and coordinating) and aromatic rings and showed an influence of water coordination on water–aromatic interactions. The interactions of coordinating water were found to be stronger even if the aqua complex was neutral (interaction energy of non-coordinating water: -3.36 kcal mol^{-1}; neutral aqua complexes: -6.5 kcal mol^{-1}). Positively charged complexes establish much stronger interactions (the strongest calculated interaction energy is -14.85 kcal mol^{-1}). Moreover, the authors argue that the stronger interaction energy of coordinating water in neutral complexes compared to non-coordinating water is due to larger partial positive charges of the water hydrogen atoms in the complexes and the larger size of aqua complexes compared to the water molecule. As above-mentioned OH–π interactions occur in hydrated biological interfaces[578] and this study makes us aware of the importance of NCIs, especially NCIs established with coordinating water since liquid water in biological systems contains many metal ions.

Figure 30: Geometric parameters used by Zarić *et al.*[579] describing OH–π water–aromatic interaction. © Royal Society of Chemistry. *(Figure removed because subjected to copyright).*

574 [N°516] Yamada, S.; Nojiri, Y. *Chem. Commun.* **2011**, *47*, 9143.

575 [N°517] Kleiner, C. M.; Schreiner, P. R. *Chem. Commun.* **2006**, 4315.

576 [N°518] Paschek, D.; Ludwig, R. *Angew. Chem. Int. Ed. Engl.* **2011**, *50*, 352.

577 [N°519] Vojislavljevic, D. Z.; Janjic, G. V.; Ninkovic, D. B.; Kapor, A.; Zaric, S. D. *Crystengcomm* **2013**, *15*, 2099.

578 [N°514] Gierszal, K. P.; Davis, J. G.; Hands, M. D.; Wilcox, D. S.; Slipchenko, L. V.; Ben-Amotz, D. *J. Phys. Chem. Lett.* **2011**, *2*, 2930.

579 [N°519] Vojislavljevic, D. Z.; Janjic, G. V.; Ninkovic, D. B.; Kapor, A.; Zaric, S. D. *Crystengcomm* **2013**, *15*, 2099.

5.6.9 - When NCIs immerses in Metal-ligand and Metal-Metal systems.

Since the first description of heterometallic complexes containing a metal-metal bond between a group 11 d^{10} ion and another transition metal by Coffey *et al.*[580] a considerable interest for this family of compounds has emerged. Thus, the existence of metal···metal contacts shorter than the sum of the van der Waals radii between linear d^{10} transition-metal complexes has been reported in recent years in a large number of crystal structures[581-583] (the closely related $d^{10}\cdots d^{8}$ interactions,[584-587] as-well as $d^{8}\cdots d^{8}$ have also been reported).[588-591]

This is especially true for Au(I) compounds, for which many contacts are found between 2.7 and 3.5 Å (the sum of the van der Waals radii for Au being 3.40 Å).[592-594] The overwhelming presence of such contacts in Au(I) compounds lead Schmidbaur to promote the term "aurophilicity".[595] By extension the term "metallophilicity" is now commonly used to denote such contacts between metals in general, or "numismophilicity" to refer to the coinage metals.[596] In some cases, such complexes display some interesting additional features, for instance, noncovalent d^{10}–d^{10} interactions between the metal centres, which are of current interest from an experimental and a theoretical point of view. Thus, Novoa *et al.*[597] investigated the

580 [N°520] Coffey, C. E.; Lewis, J.; Nyholm, R. S. *J. Chem. Phys.* **1964**, 1741.
581 [N°521] Tiekink, E. R. T. *Coord. Chem. Rev.* **2014**, *275*, 130.
582 [N°522] Pyykko, P. *Chem. Rev.* **1997**, *97*, 597.
583 [N°523] Jansen, M. *Angew. Chem. Int. Ed. Engl.* **1987**, *26*, 1098.
584 [N°524] Xia, B.-H.; Zhang, H.-X.; Che, C.-M.; Leung, K.-H.; Phillips, D. L.; Zhu, N.; Zhou, Z.-Y. *J. Am. Chem. Soc.* **2003**, *125*, 10362.
585 [N°525] Crespo, O.; Laguna, A.; Fernández, E. J.; López-de-Luzuriaga, J. M.; Jones, P. G.; Teichert, M., . . . Werner, H.-J. *Inorg. Chem.* **2000**, *39*, 4786.
586 [N°526] Yoon, K.; Parkin, G. *Polyhedron* **1995**, *14*, 811.
587 [N°527] Rundle, R. E. *J. Am. Chem. Soc.* **1954**, *76*, 3101.
588 [N°528] Weber, M.; Klein, J. E. M. N.; Miehlich, B.; Frey, W.; Peters, R. *Organometallics* **2013**, *32*, 5810.
589 [N°529] Nebra, N.; Ladeira, S.; Maron, L.; Martin-Vaca, B.; Bourissou, D. *Chem. Eur. J.* **2012**, *18*, 8474.
590 [N°530] Luo, J.; Khusnutdinova, J. R.; Rath, N. P.; Mirica, L. M. *Chem. Commun.* **2012**, *48*, 1532.
591 [N°531] Smith, D. C.; Gray, H. B. *Coord. Chem. Rev.* **1990**, *100*, 169.
592 [N°532] Mathieson, T.; Schier, A.; Schmidbaur, H. *J. Chem. Soc., Dalton Trans.* **2000**, 3881.
593 [N°533] Grohmann, A.; Schmidbaur, H. In *Comprehensive Organometallic Chemistry II*; Abel, E. W., Stone, F. G. A., Wilkinson, G., Eds.; Elsevier: Oxford, **1995**, p 1.
594 [N°534] Schmidbaur, H. *Gold Bull.* **1990**, *23*, 11.
595 [N°535] Scherbaum, F.; Grohmann, A.; Huber, B.; Krüger, C.; Schmidbaur, H. *Angew. Chem. Int. Ed. Engl.* **1988**, *27*, 1544.
596 [N°536] Vicente, J.; Chicote, M. T.; Lagunas, M. C. *Inorg. Chem.* **1993**, *32*, 3748.
597 [N°537] Carvajal, M. A.; Alvarez, S.; Novoa, J. J. *Chem. Eur. J.* **2004**, *10*, 2117.

nature of the intermolecular interactions between dicoordinate Cu(I) ions, which has been analysed by means of combined theoretical and structural database studies. The authors related that a perturbative evaluation of the components of the intermolecular interaction energies, by means of the IMPT scheme of Stone,[598] indicates that both the Coulombic and dispersion forces are important in determining the Cu(I)•••Cu(I) bonding interactions, because only a small part of that energy is attributable to Cu•••Cu interactions, while a large component results from Cu•••ligand interactions. Furthermore, heterometallic complexes, described by Braunstein *et al.,* [599, 600] for instance, a coordinatively unsaturated 14-electron Pd^0 centre bonded to an Fe-Hg-Fe chain, bear, according to the authors, a delicate energetic balance between metal–metal and metal–ligand interactions.

Figure 31: X-ray structure of the tetranuclear $\{Fe_2HgPd\}$ published by Braunstein et *al.*[601] © John Wiley & Sons, Inc. *(Figure removed because subjected to copyright).*

Truly comparable is the case related by Grimme et Djukic [602] of tetrakis(isonitrile)rhodium(I) cationic complexes which form cation-cation dimers in solution.

[598] [N°538] Hayes, I. C.; Stone, A. J. *Mol. Phys.* **1984**, *53*, 83.
[599] [N°539] Schuh, W.; Braunstein, P.; Benard, M.; Rohmer, M. M.; Welter, R. *J. Am. Chem. Soc.* **2005**, *127*, 10250.
[600] [N°540] Schuh, W.; Braunstein, P.; Benard, M.; Rohmer, M. M.; Welter, R. *Angew. Chem. Int. Ed. Engl.* **2003**, *42*, 2161.
[601] [N°540] ibid.
[602] [N°541] Grimme, S.; Djukic, J.-P. *Inorg. Chem.* **2011**, *50*, 2619.

Two reasons can justify such an unfavourable interaction between two clearly positive charges:

- The formation of a strong covalent bond, which at least in principle can easily pay off the Coulombic repulsion. Nevertheless, this is clearly not the case here.
- The action of the ubiquitous, entirely attractive London dispersion forces.

When the eight PhNC moieties arrange spatially in an optimal π-stacked fashion, the energy gain is of the order of the Coulomb repulsion. In the case treated here, dispersion is overwhelming, driving the formation of a stable complex in solution. The present findings nuances the role of the metal-metal d^8-d^8 interactions, which are present on a relatively small scale (about 10-15 % of the total dispersion contribution to the binding energy) compared to the effects of the ligands.

Figure 32: Tetrakis(isonitrile)rhodium(I) dimers where the Coulombic repulsion is overwhelmed by attractive dispersion, principally published by Djukic *et al.*[603] © American Chemical Society. *(Figure removed because subjected to copyright).*

Certainly, the literature contains number of other non-covalently bonded molecular aggregates for which the “binding mode” has never been thoroughly settled, and whose stability was simply labelled “M-M interactions”. The case unveiled by Djukic *et al.* perfectly illustrates that such considerations have to be nuanced, which was perfectly perceived by Peters *et al.*[604] for a similar subtle Pd(II)•••Pd(II) case (Figure 33), as well as by others, for many unsupported M•••M interactions.[605 - 620] For instance, Nd•••Fe

603 [N°541] ibid.

604 [N°528] Weber, M.; Klein, J. E. M. N.; Miehlich, B.; Frey, W.; Peters, R. *Organometallics* **2013**, *32*, 5810.

605 [N°542] Mandal, S.; Reber, A. C.; Qian, M.; Liu, R.; Saavedra, H. M.; Sen, S., . . . Sen, A. *Dalton Trans.* **2012**, *41*, 5454.

heterobimetallic complex for which DFT identified the M-M bond as principally of a ionic character (Figure 34).

Figure 33: Monomeric ferrocene bis-imidazoline bis-palladacycles monomeric species where a sublte interplay between d^8-d^8 coulombic repulsion and dispersion occurs, published by Peters et *al.*[621] © American Chemical Society. *(Figure removed because subjected to copyright).*

Figure 34: First complex with an unsupported 4f–3d metal–metal bond that was sufficiently stable to be isolated; the bond was identified as principally ionic in nature by DFT calculations published by Arnold *et al.*[622] © Royal Society of Chemistry. *(Figure removed because subjected to copyright).*

[606] [N°543] Laurila, E.; Tatikonda, R.; Oresmaa, L.; Hirva, P.; Haukka, M. *Crystengcomm* **2012**, *14*, 8401.

[607] [N°544] van der Eide, E. F.; Yang, P.; Walter, E. D.; Liu, T.; Bullock, R. M. *Angew. Chem. Int. Ed. Engl.* **2012**, *51*, 8361.

[608] [N°545] Liddle, S. T.; Mills, D. P.; Gardner, B. M.; McMaster, J.; Jones, C.; Woodul, W. D. *Inorg. Chem.* **2009**, *48*, 3520.

[609] [N°546] Niskanen, M.; Hirva, P.; Haukka, M. *J. Chem. Theory Comput.* **2009**, *5*, 1084.

[610] [N°547] Liddle, S. T.; McMaster, J.; Mills, D. P.; Blake, A. J.; Jones, C.; Woodul, W. D. *Angew. Chem. Int. Ed. Engl.* **2009**, *48*, 1077.

[611] [N°548] Hartl, F.; Renfrew, A. K.; Lafolet, F.; Mahabiersing, T.; Calhorda, M. J.; Chardon-Noblat, S., . . . Deronzier, A. *Inorg. Chem.* **2009**, *48*, 8233.

[612] [N°549] Minasian, S. G.; Krinsky, J. L.; Williams, V. A.; Arnold, J. *J. Am. Chem. Soc.* **2008**, *130*, 10086.

[613] [N°550] Katz, M. J.; Sakai, K.; Leznoff, D. B. *Chem. Soc. Rev.* **2008**, *37*, 1884.

[614] [N°551] Hirva, P.; Haukka, M.; Jakonen, M.; Pakkanen, T. A. *Inorg. Chim. Acta* **2006**, *359*, 853.

[615] [N°552] Villarroya, B. E.; Tejel, C.; Rohmer, M.-M.; Oro, L. A.; Ciriano, M. A.; Bénard, M. *Inorg. Chem.* **2005**, *44*, 6536.

[616] [N°553] Angurell, I.; Martinez-Ruiz, I.; Rossell, O.; Seco, M.; Gomez-Sal, P.; Martin, A. *Chem. Commun.* **2004**, 1712.

[617] [N°554] Fontana, M.; Chanzy, H.; Caseri, W. R.; Smith, P.; Schenning, A. P. H. J.; Meijer, E. W.; Gröhn, F. *Chem. Mater.* **2002**, *14*, 1730.

[618] [N°555] Masciocchi, N.; Moret, M.; Cairati, P.; Ragaini, F.; Sironi, A. *J. Chem. Soc., Dalton Trans.* **1993**, 471.

[619] [N°556] Porchia, M.; Casellato, U.; Ossola, F.; Rossetto, G.; Zanella, P.; Graziani, R. *J. Chem. Soc., Chem. Commun.* **1986**, 1034.

[620] [N°557] Underhill, A. E.; Watkins, D. M. *Chem. Soc. Rev.* **1980**, *9*, 429.

[621] [N°528] Weber, M.; Klein, J. E. M. N.; Miehlich, B.; Frey, W.; Peters, R. *Organometallics* **2013**, *32*, 5810.

5.6.10 - When NCIs induce "anomalies" in transition metal chemistry: on the way to a new paradigm.

5.6.10.1 - Stabilization of rare examples of air-stable unsaturated Mn(I) (16e) complexes by the mean of NCIs.

Weak metal-metal bonds between 3d transition metals in organometallic species have probably not yet got the attention they deserve. The few theoretical analyses that have addressed them so far have often understated the role of NCIs, especially intramolecular London dispersion (Van der Waals) forces, the focus being principally put on covalency as a prerequisite for stable metal-metal bonds. In a recent study Djukic *et al.*[623] studied, by means of DFT methods, the bonding features of *syn*-facial Cr-Mn benzylic complexes where the unsaturated *syn*-facial (16 electrons) arrangement predominates over the associated saturated *anti*-facial (18 electrons) one. The authors established the multifaceted nature of the intermetallic interaction where a somehow subtle interplay of steric and electronic effects leads to kinetically and thermodynamically viable structures by contributing to their structural cohesion, whereby the two metal centres interact through a combination of interactions, namely: London dispersion forces and donor acceptor bonding between the two metal centres; the latter being partitioned into a three-orbital four-electron Cr→Mn interaction and its Cr←Mn π back-bonding counterpart. Moreover, the evaluation of the interaction energy reveals a differential of about 9-15 kcal.mol^{-1}, a quite unexpected favourable bias for the *syn*-facial arrangement versus *anti*-facial. This study procured a new light into the treatment of metal-metal interactions, which are usually divided into three classes of bonding, *i.e.*, covalent, dative, and ionic, with not much room for long range NCIs. In light of these results, what was termed elusively in the past by Ceccon *et al.*[624] as a justification of the *syn*-facial stereoselectivity of their heterobimetallic compounds as a "heterodox, intermetallic linkage, which helps the metals to achieve a formal

[622] [N°558] Arnold, P. L.; McMaster, J.; Liddle, S. T. *Chem. Commun.* **2009**, 818.

[623] [N°559] Hyla-Kryspin, I.; Grimme, S.; Djukic, J. P. *Organometallics* **2009**, *28*, 1001.

[624] [N°560] Bonifaci, C.; Ceccon, A.; Santi, S.; Mealli, C.; Zoellner, R. W. *Inorg Chim Acta* **1995**, *240*, 541.

electronic saturation", might turn out to be the keystone stabilizing interaction in more cases than generally expected.[625]

Figure 35: Optimized structure of the singlet state of the *syn*-facial complexe and WBI for Cr-Mn interaction published by Djukic et *al.*[626] © American Chemical Society. *(Figure removed because subjected to copyright).*

5.6.10.2 - <u>When NCIs induce stereospecificity in bimetallic complexes: NCIs win over sterics.</u>

The nature of this "heterodox bond"[627] of Ceccon's bimetallic indene complexes has been investigated by Djukic *et al.*[628] by the mean of high-level *ab* initio electronic structure methods, with a special focus on the contribution of intramolecular London dispersion effects. Understanding the related electronic features occurring in such situations is highly relevant for the implementation of new stereoselective processes whereby weak interactions may contribute decisively to provide stereospecificity.[629-636] Thus, the *anti*- and *syn*-facial rhodium(I)[637 - 641] and iridium(I)[642] derivatives of

[625] [N°561] Pizzotti, M.; Ugo, R.; Dragonetti, C.; Annoni, E.; Demartin, F.; Mussini, P. *Organometallics* **2003**, *22*, 4001.
[626] [N°559] Hyla-Kryspin, I.; Grimme, S.; Djukic, J. P. *Organometallics* **2009**, *28*, 1001.
[627] [N°560] Bonifaci, C.; Ceccon, A.; Santi, S.; Mealli, C.; Zoellner, R. W. *Inorg Chim Acta* **1995**, *240*, 541.
[628] [N°562] Schwabe, T.; Grimme, S.; Djukic, J.-P. *J. Am. Chem. Soc.* **2009**, *131*, 14156.
[629] [N°563] Lattanzi, A.; De Fusco, C.; Russo, A.; Poater, A.; Cavallo, L. *Chem. Commun.* **2012**, *48*, 1650.
[630] [N°564] Grasso, G. I.; Bellia, F.; Arena, G.; Vecchio, G.; Rizzarelli, E. *Inorg. Chem.* **2011**, *50*, 4917.
[631] [N°565] Shinisha, C. B.; Sunoj, R. B. *Org. Biomol. Chem.* **2008**, *6*, 3921.
[632] [N°566] Sabo-Etienne, S.; Chaudret, B. In *Modern Coordination Chemistry: The Legacy of Joseph Chatt*; Leigh, G. J., Winterton, N., Eds.; The Royal Society of Chemistry: **2002**, p 45.
[633] [N°567] Knowles, J. R. *Nature* **1991**, *350*, 121.
[634] [N°568] Borghesani, G.; Pulidori, F.; Remelli, M.; Purrello, R.; Rizzarelli, E. *J. Chem. Soc., Dalton Trans.* **1990**, 2095.
[635] [N°569] Okawa, H.; Tokunaga, H.; Katsuki, T.; Koikawa, M.; Kida, S. *Inorg. Chem.* **1988**, *27*, 4373.
[636] [N°570] Ōkawa, H.; Nakamura, M.; Kida, S. *Inorg. Chim. Acta* **1986**, *120*, 185.
[637] [N°571] Mantovani, L.; Ceccon, A.; Gambaro, A.; Santi, S.; Ganis, P.; Venzo, A. *Organometallics* **1997**, *16*, 2682.

tricarbonyl(η^6-indene)chromium reported by Ceccon and coworkers constitute one relevant illustrative molecular system.[643] In these systems, Djukic *et al.* unveiled the occurrence of two separable nonlocal correlation (London dispersion) effects, ligand−metal and ligand−ligand (Figure 36), as well as a surprisingly strong metal−metal interaction (associated by the authors to an intermediate M−M distance and significant overlap density, the theoretical methods involved do not sufficiently account for the intramolecular ligand−ligand effects).

Figure 36: The nature of the "heterodox" metal−metal bond in bimetallic indenyl systems is revealed by a new high-level electronic structure analysis procedure based on perturbation theory within a localized molecular orbital basis. Differences in intrafragment (diagonalentries) and interfragment (off-diagonal entries) correlation energies (kcal.mol^{-1}) between *syn*-bimetallic and *anti*-bimetallic are given at the SCS-MP2 level, published by Djukic *et al.*[644] © American Chemical Society. *(Figure removed because subjected to copyright).*

Through this study the authors highlighted the importance of intramolecular van der Waals interactions even for quite small organometallic systems, suggesting that a deeper understanding of these so-called medium-range dispersion effects[645 - 647] (Occurring typically between 250 and 350 pm) can lead to more rational design principles in organometallic chemistry.

[638] [N°572] Bonifaci, C.; Carta, G.; Ceccon, A.; Gambaro, A.; Santi, S.; Venzo, A. *Organometallics* **1996**, *15*, 1630.
[639] [N°573] Bonifaci, C.; Ceccon, A.; Gambaro, A.; Ganis, P.; Santi, S.; Venzo, A. *Organometallics* **1995**, *14*, 2430.
[640] [N°574] Bonifaci, C.; Ceccon, A.; Gambaro, A.; Ganis, P.; Santi, S.; Valle, G.; Venzo, A. *Organometallics* **1993**, *12*, 4211.
[641] [N°575] Ceccon, A.; Gambaro, A.; Santi, S.; Valle, G.; Venzo, A. *J. Chem. Soc., Chem. Commun.* **1989**, 51.
[642] [N°576] Cecchetto, P.; Ceccon, A.; Gambaro, A.; Santi, S.; Ganis, P.; Gobetto, R., . . . Venzo, A. *Organometallics* **1998**, *17*, 752.
[643] [N°577] Bonifaci, C.; Ceccon, A.; Gambaro, A.; Manoli, F.; Mantovani, L.; Ganis, P., . . . Venzo, A. *J. Organomet. Chem.* **1998**, *557*, 97.
[644] [N°562] Schwabe, T.; Grimme, S.; Djukic, J.-P. *J. Am. Chem. Soc.* **2009**, *131*, 14156.
[645] [N°578] Sieffert, N.; Bühl, M. *Inorg. Chem.* **2009**, *48*, 4622.
[646] [N°579] Grimme, S. *Angew. Chem. Int. Ed. Engl.* **2006**, *45*, 4460.
[647] [N°580] Grimme, S. *Chem. Eur. J.* **2004**, *10*, 3423.

5.6.10.3 - When NCIs explain the formation of Lewis adducts: Archetype of a non-bridged "dative" M-M bond.

After the two above-mentioned cases arguing in favour of the involvement of dispersion forces in 3d transition-metal complexes containing weak intramolecular intermetallic interactions, the so-called "dative metal−metal bonds" have also to be considered as borderline cases because the metal−metal donor−acceptor (DA) interaction commonly associates a significant amount of covalent character.[648] Thus, for several cases the presence of a dative bond between an electron-deficient metal and a saturated metal was postulated and reported in the literature for quite a number of bridged binuclear species, [649 - 652] though with few thorough investigations of the metal−metal interaction.[653] Pomeroy *et al.* reported the synthesis and characterization of a series of archetypes of metal−metal DA Lewis adducts bearing an original nonbridged metal−metal dative bond. [654 - 656] Since then, a huge variety of other examples that proved the experimental validity of the concept of dative bonds between different closed-shell metal centres were further put in advance. [657-667] Recent studies of Djukic *et al.* aimed to study the bonding relationship existing in such Os−Cr and Os−W complexes by the mean of recently developed DFT-D and wavefunction-based

---

648 [N°581] Arndt, L. W.; Darensbourg, M. Y.; Delord, T.; Bancroft, B. T. *J. Am. Chem. Soc.* **1986**, *108*, 2617.
649 [N°574] Bonifaci, C.; Ceccon, A.; Gambaro, A.; Ganis, P.; Santi, S.; Valle, G.; Venzo, A. *Organometallics* **1993**, *12*, 4211.
650 [N°582] Kalinin, V. N.; Cherepanov, i. y. A.; Moiseev, S. K.; Batsanov, A. S.; Struchkov, Y. T. *Mendeleev Commun.* **1991**, *1*, 77.
651 [N°583] Edelmann, F.; Töfke, S.; Behrens, U. *J. Organomet. Chem.* **1986**, *308*, 27.
652 [N°584] Hock, A. A.; Mills, O. S. *Acta Cryst.* **1961**, *14*, 139.
653 [N°585] Barr, R. D.; Green, M.; Marsden, K.; Stone, F. G. A.; Woodward, P. *J. Chem. Soc., Dalton Trans.* **1983**, 507.
654 [N°586] Einstein, F. W. B.; Pomeroy, R. K.; Rushman, P.; Willis, A. C. *Organometallics* **1985**, *4*, 250.
655 [N°587] Einstein, F. W. B.; Jones, T.; Pomeroy, R. K.; Rushman, P. *J. Am. Chem. Soc.* **1984**, *106*, 2707.
656 [N°588] Fleming, M. M.; Pomeroy, R. K.; Rushman, P. *J. Organomet. Chem.* **1984**, *273*, C33.
657 [N°589] Jiang, F.; Jenkins, H. A.; Biradha, K.; Davis, H. B.; Pomeroy, R. K.; Zaworotko, M. J. *Organometallics* **2000**, *19*, 5049.
658 [N°590] Jiang, F.; Biradha, K.; Leong, W. K.; Pomeroy, R. K.; Zaworotko, M. J. *Can. J. Chem.* **1999**, *77*, 1327.
659 [N°591] Poblet, J.-M.; Benard, M. *Chem. Commun.* **1998**, 1179.
660 [N°592] Jiang, F.; Male, J. L.; Biradha, K.; Leong, W. K.; Pomeroy, R. K.; Zaworotko, M. J. *Organometallics* **1998**, *17*, 5810.
661 [N°593] Shipley, J. A.; Batchelor, R. J.; Einstein, F. W. B.; Pomeroy, R. K. *Organometallics* **1991**, *10*, 3620.
662 [N°594] Batchelor, R. J.; Davis, H. B.; Einstein, F. W. B.; Pomeroy, R. K. *J. Am. Chem. Soc.* **1990**, *112*, 2036.
663 [N°595] Davis, H. B.; Einstein, F. W. B.; Glavina, P. G.; Jones, T.; Pomeroy, R. K.; Rushman, P. *Organometallics* **1989**, *8*, 1030.
664 [N°596] Einstein, F. W. B.; Jennings, M. C.; Krentz, R.; Pomeroy, R. K.; Rushman, P.; Willis, A. C. *Inorg. Chem.* **1987**, *26*, 1341.
665 [N°586] Einstein, F. W. B.; Pomeroy, R. K.; Rushman, P.; Willis, A. C. *Organometallics* **1985**, *4*, 250.
666 [N°597] Einstein, F. W. B.; Martin, L. R.; Pomeroy, R. K.; Rushman, P. *J. Chem. Soc., Chem. Commun.* **1985**, 345.
667 [N°598] Martin, L. R.; Einstein, F. W. B.; Pomeroy, R. K. *Inorg. Chem.* **1985**, *24*, 2777.

methods.[668] This work, complemented Nakatsuji *et al.*'s early investigations and highlighted the conspicuous evidence on the crucial role of dispersion forces in the stabilization of nonbridged dative metal−metal bonds.[669]

Figure 37: Os→Cr and Os→W compounds classified as a "dispersion-driven donor−acceptor bond with a small covalent contribution" in contrast with the previously asserted "dative metal−metal bond", thus outlining the role of long-range dispersion-type interactions published by Djukic and Grimme[670] © American Chemical Society. *(Figure removed because subjected to copyright).*

Through this study, Djukic and Grimme clearly demonstrated that even for small transition-metal complexes with sterically non-demanding substituents, long-range dispersion-type interactions are of the utmost importance for a quantitative understanding of bonding. The metal−metal interaction in these complexes can be classified as a dispersion-driven DA bond with only a small amount of truly covalent contribution. In the light of these results, our earlier conception of dative-bonds in the case of unsaturated species has to be modulated.

6 - Final introduction's words...

For sure, the literature conceals much more of such "heterodox"[671] and atypical species[672-675] that, according to Kuhn,[676] the "normal science" was not able to explain,

[668] [N°599] Grimme, S.; Djukic, J.-P. *Inorg. Chem.* **2010**, *49*, 2911.

[669] [N°600] Nakatsuji, H.; Hada, M.; Kawashima, A. *Inorg. Chem.* **1992**, *31*, 1740.

[670] [N°599] Grimme, S.; Djukic, J.-P. *Inorg. Chem.* **2010**, *49*, 2911.

[671] [N°560] Bonifaci, C.; Ceccon, A.; Santi, S.; Mealli, C.; Zoellner, R. W. *Inorg Chim Acta* **1995**, *240*, 541.

[672] [N°601] Cullen, W. R.; Rettig, S. J.; Zhang, H. *Organometallics* **1993**, *12*, 1964.

maybe because scientists lacked the accurate experimental or theoretical tools that could provide the right answer to the right question at the right moment. Or, maybe because it was simpler to stay in a conservative reality? This PhD thesis clearly aims to highlight, understand and describe such specific "anomalies" that the organometallic chemistry carries and which cannot be reasonably explained by the universally accepted paradigm, hoping that it can contribute to a breakthrough moment in transition metal chemistry by unveiling the fundamental role of non-covalent interactions in this field.

[673] [N°602] Töfke, S.; Behrens, U. *J. Organomet. Chem.* **1980**, *338*, 29.

[674] [N°603] Lindley, P. F.; Mills, O. S. *J. Chem. Soc. A* **1969**, 1286.

[675] [N°584] Hock, A. A.; Mills, O. S. *Acta Cryst.* **1961**, *14*, 139.

[676] [N°1] Kuhn, T. S. *The structure of scientific revolutions*; Fourth edition, **2012**.

II

An excursion into non-covalence

GROUP 7 TRANSITION METALS

This chapter describes our first approach in the investigation of non-covalent interactions in organometallic chemistry by the study of Mn/Re metallospiralenes derivatives.

Chapter II - The Metallospiralenes.

1 - Introduction.

In the late 90's Djukic *et al.*[677-680] reported the formation of new classes of self-arranged helical chelated complexes: the metallospiralenes (Figure 38).

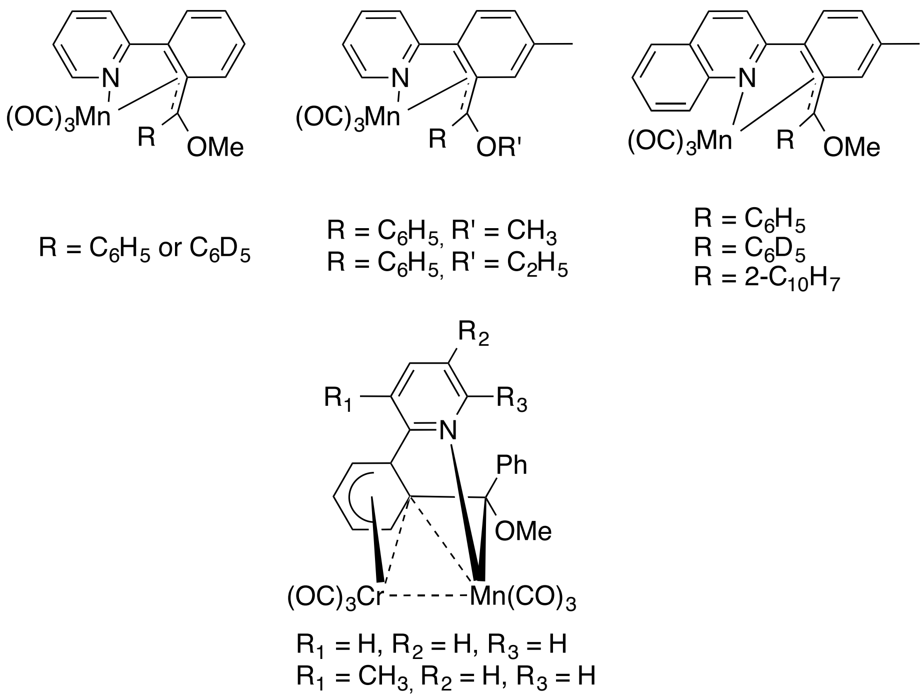

Figure 38: New classes of self-arranged helical chelated complexes.

The "helical shape" displayed by either the monometallic or the bimetallic product is the reason why the authors used this terminology[681]. They considered that this novel class of organometallic helical complexes could be accounted as "spiralenes", because their structures remind a spiral staircase in which the metallic core plays the role of a scaffold sustaining an organic "spiral"[682] (Figure 39).

[677] [N°604] Djukic, J. P.; Pfeffer, M.; Dotz, K. H. *C.R. Acad. Sci. Paris, Ser. IIc* **1999**, *2*, 403.
[678] [N°605] Djukic, J. P.; Maisse, A.; Pfeffer, M.; Dotz, K. H.; Nieger, M. *Eur. J. Inorg. Chem.* **1998**, 1781.
[679] [N°606] Djukic, J. P.; Maisse, A.; Pfeffer, M. *J. Organomet. Chem.* **1998**, *567*, 65.
[680] [N°607] Djukic, J. P.; Dotz, K. H.; Pfeffer, M.; DeCian, A.; Fischer, J. *Organometallics* **1997**, *16*, 5171.
[681] [N°608] Djukic, J. P.; Maisse-Francois, A.; Pfeffer, M.; Dotz, K. H.; De Cian, A.; Fischer, J. *Organometallics* **2000**, *19*, 5484.
[682] [N°609] Djukic, J. P.; Michon, C.; Maisse-Francois, A.; Allagapen, R.; Pfeffer, M.; Dotz, K. H., . . . Fischer, J. *Chem. Eur. J.* **2000**, *6*, 1064.

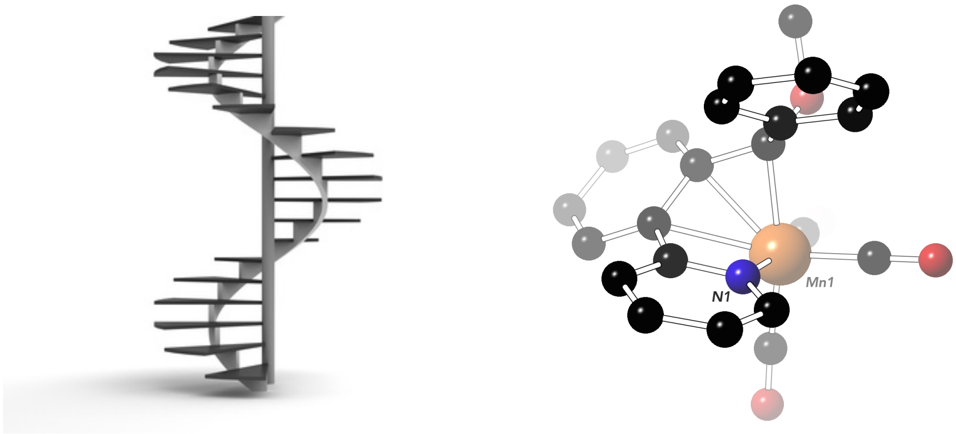

Figure 39: The geometrical analogy between a "spiralene" (right) and a "spiral staircase" (left). The manganese (I) centre sustains the helical molecular arrangement in a fashion similar to that of a pillar (in light grey) in a spiral staircase.

This class of compounds can be obtained through two different pathways[683] (Figure 40):

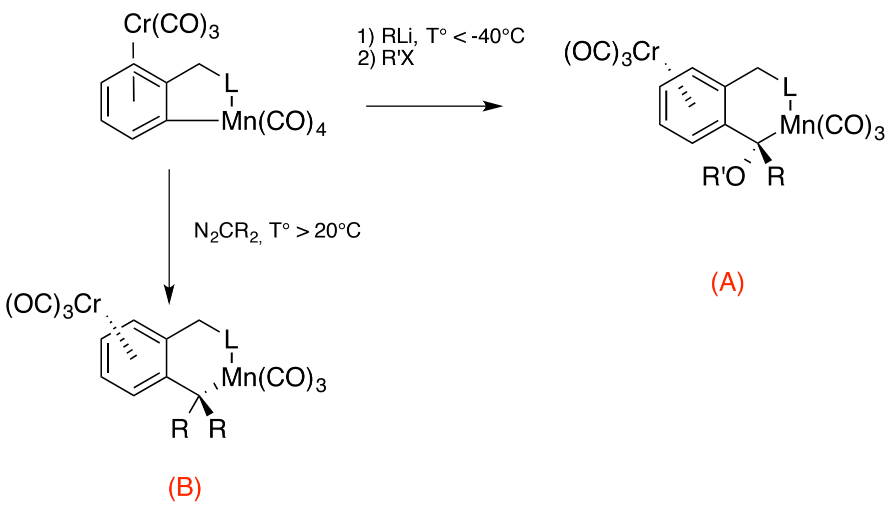

Figure 40: Two pathways for the synthesis of the metallospiralenes complexes.

A) A sequential treatment of cyclomanganated aromatics of the type cis-(L∧C, *κL,κC*)Mn(CO)$_4$ (L∧C = chelating aromatic ligand with L = endogenous two-electron ligand and C = aromatic carbon one-electron ligand) with an aryl-

[683] [N°608] Djukic, J. P.; Maisse-Francois, A.; Pfeffer, M.; Dotz, K. H.; De Cian, A.; Fischer, J. *Organometallics* **2000**, *19*, 5484.

lithium reagent and MeOTf (namely: "E. O. Fischer method") at subambient temperatures (Figure 41).

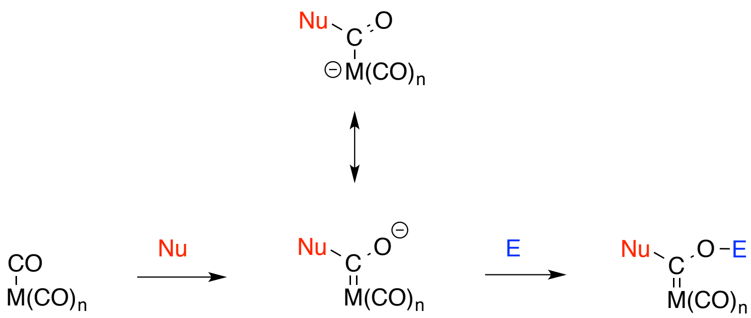

Figure 41: Fischer-type carbine intermediate mechanism.

Or:

B) A thermolytic reaction of the cyclomanganated substrate with diazoalkane derivates.

Concerning these two methods, Djukic *et al.*[684] describe the second method to be softer and more reliable than the first one because of one major limitation.

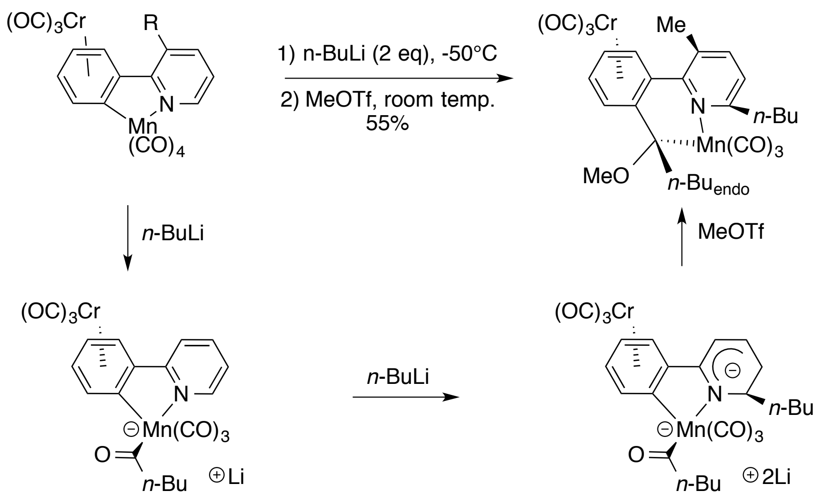

Figure 42: Helical shape of the bimetallic species.

Indeed the stereoselective formation of *syn*-facial Cr, Mn benzyl complexes by the sequential reaction of organolithium reagents and hard electrophiles requires, because of the high reactivity of RLi reagents towards heterocycles, a strict 1:1 ratio between RLi

[684] [N°610] Djukic, J. P.; Michon, C.; Berger, A.; Pfeffer, M.; de Cian, A.; Kyritsakas-Gruber, N. *J. Organomet. Chem.* **2006**, *691*, 846.

and the manganese substrate in order to avoid the double addition of RLi to the substrate[685] as shown in (Figure 42). Furthermore, the nature of the substitution pattern at the carbene carbon atom is shown to play a determining role in the stereoselectivity of spiralene formation.[686,687] The authors demonstrated that the nucleophilic attack of a carbonyl ligand attached to a Manganese (abbr. Mn) or a Rhenium (abbr. Re) atom by RLi was found to be very sensitive to steric hindrance and a stereoselective addition of the lithiated agent at a Mn attached carbonyl ligand located *exo* with respect to the sterically hindered $Cr(CO)_3$ fragment will occur (Figure 43).

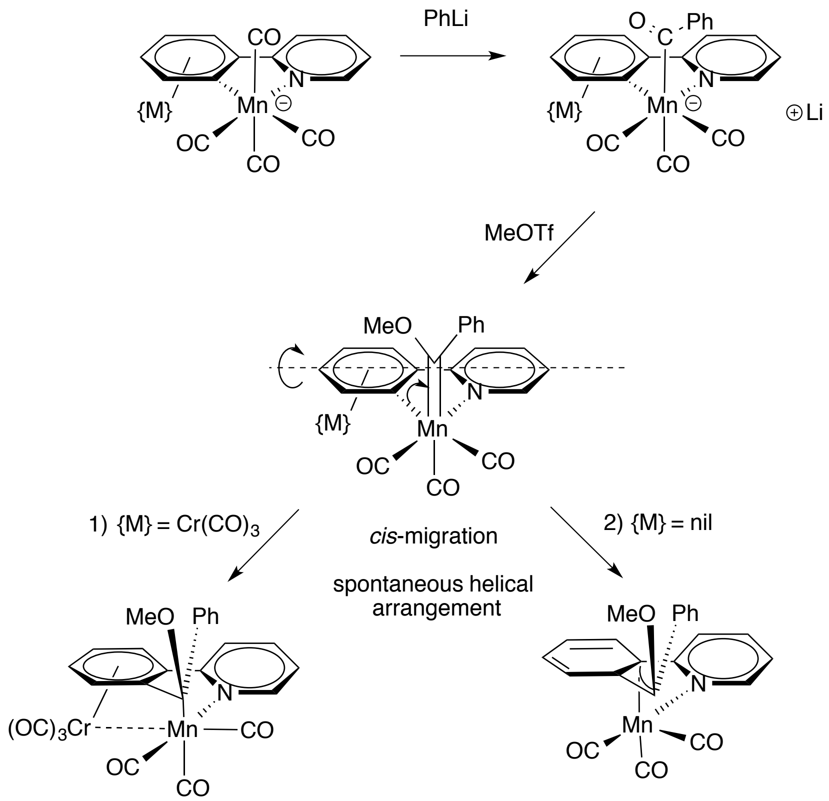

Figure 43: Synthesis of helical *syn*-facial heterobimetallic (η^6-aryl)benzyl and mononuclear η^3-benzylic complexes.

The insertion results, formally, in the loss of 2 electrons in the valence shell of the metal where the "vacancy" can be filled (if sterics are favourable) by a direct interaction with a vicinal aryl, thus establishing a η^3-interaction conferring the helical shape to the molecule. When sterics are unavoidable due to the presence of a π-bonded $Cr(CO)_3$

[685] [N°608] Djukic, J. P.; Maisse-Francois, A.; Pfeffer, M.; Dotz, K. H.; De Cian, A.; Fischer, J. *Organometallics* **2000**, *19*, 5484.

[686] [N°609] Djukic, J. P.; Michon, C.; Maisse-Francois, A.; Allagapen, R.; Pfeffer, M.; Dotz, K. H., . . . Fischer, J. *Chem. Eur. J.* **2000**, *6*, 1064.

[687] [N°611] Djukic, J. P.; Maisse, A.; Pfeffer, M.; Dotz, K. H.; Nieger, M. *Organometallics* **1999**, *18*, 2786.

moiety for example, the system preferably adopts the folded conformation that brings the two metals in a *syn*-facial arrangement, the chelated metal facing the Cr centre. This class of Mn-group complexes represent rare cases of 16-electron complexes of Mn(I) and Re(I) carbonyls that are persistent in solution as well as in the solid state and that display air and water-stability comparable to that of coordinatively saturated congeners.

Most intriguing were cases of Mn(I) 6-member metallacycles derivatives of the 2-phenylpyridine, where the sequential addition of alkyllithium reagents and MeOTf to such derivatives afforded mixtures of two isomeric spiralenes (Figure 44).

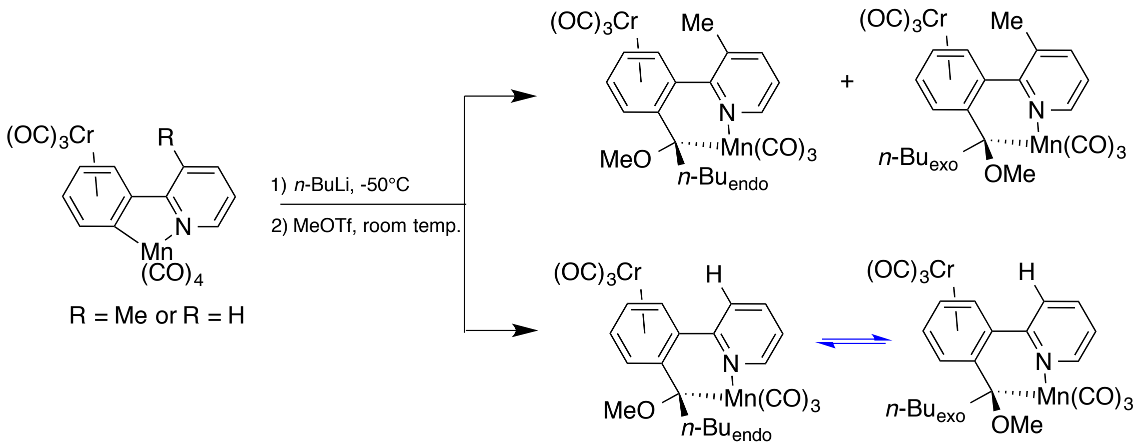

Figure 44: Formation of two isomeric spiralenes with a possible interconversion in the case of the more structurally flexible phenylpyridines.

In the case of the more structurally flexible hetero-bimetallic isomers (with R = H) the authors demonstrated the possibility of interconversion between the two isomers while the same remains impossible in the case of constrained species (R = Me). After following the interconversion of the two isomers by ^{1}H NMR spectroscopy it appeared that dissolving an enriched mixture of either one or the other isomer leads, after 48 h, to a rough 1:1 mixture. This interconversion was found to occur with the probable mediation of biradical species formed after homolytic disruption of the benzylic C-Mn bond as described in (Figure 45).

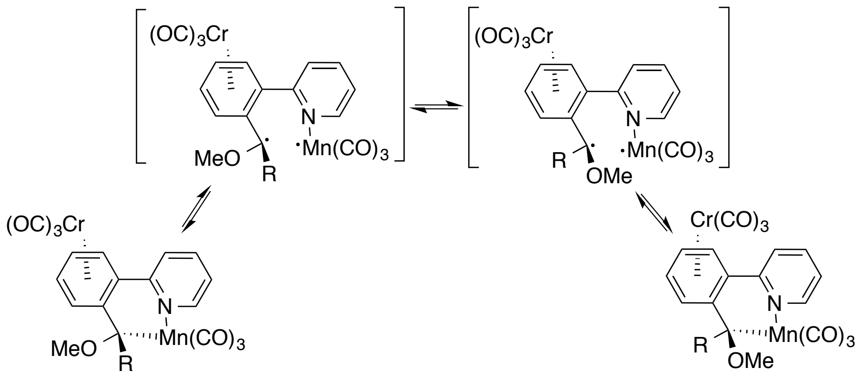

Figure 45: Interconversion between the two isomers with the probable mediation of biradical species.

The case of 2-oxazolinyl derivatives unveiled the origin of the diastereoselective formation of spiralenes. Indeed after sequential addition of PhLi and MeOTf to a cyclomanganated oxazoline derivative (Figure 46), the authors observed the formation of a mixture of two products, both resulting from the insertion of a Ph(MeO)C: moiety into the C_{Ar}-Mn bond (Figure 46).

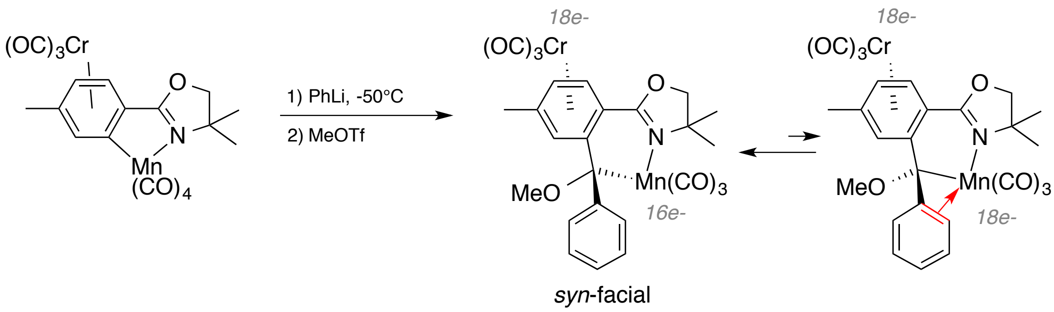

Figure 46: Formation of a mixture of two "pseudoconformers". A *syn*-facial unsaturated 18-16 electrons isomer and a saturated 18-18 electrons isomer.

By the means of X-ray diffraction analyses it appeared that the two compounds are "pseudoconformers" which differs from the position of the Mn moiety: in one case, the $Mn(CO)_3$ fragment was found to be located close to the $Cr(CO)_3$ group in a *syn*-facial manner, while in the other case, it is part of a nearly planar six-membered manganacyclic ring coplanar with the π-coordinated arene. In the crystalline state the authors mentioned a ratio of 15:1 in favour of the *syn*-facial isomer. Due to the occurrence of radical species in solution, the interconversion between the two isomers could not, in this case, be properly followed by ^{1}H NMR spectroscopy. Nevertheless these results gave some outputs concerning the helical and spiral-type arrangements in "spiralenes" type molecules, which are stereoselectively produced if at least one substituent of the transient carbene complex is an aromatic ring capable of electronic interaction with the Mn(I) centre during the *cis*-migration process. A reasonable explanation given by the authors for the observed stereoselectivity was the intervention of a late transition state that prefigures an intermediate with a structure similar to that displayed in (Figure 47) In such a case, the Mn atom would be able to circumvent the "loss" of two valence electrons occurring during the *cis*-migration step by a stabilizing interaction with an adjacent two-electron ligand such as the phenyl group attached to the former carbene carbon.

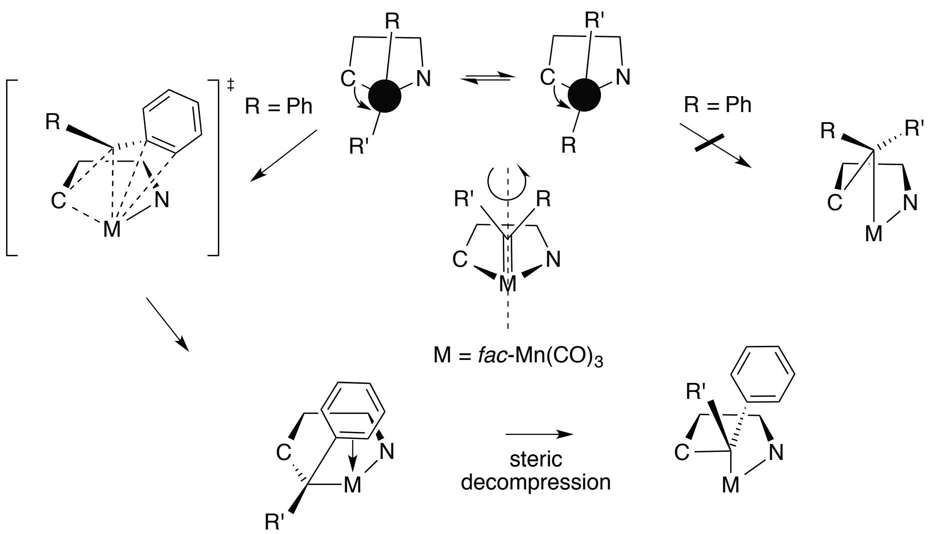

Figure 47: Origin of stereoselective formation of metallospiralenes species.

This would allow a discrimination between the two carbene conformers by favouring the one in which the donating two-electron ligand is located at an accessible position in relation to the Mn centre in order to establish an effective interaction with it. The authors thought that the formation of the C_{Ar}-C_{benzyl} bond affords a strained and tense planar six-membered manganacyclic product which conformationally may stabilize itself by tilting the $Mn(CO)_3$ group toward the $Cr(CO)_3$ tripod. These considerations entail that the intermetallic interactions between the Cr and Mn atoms as well as the intramolecular π-π and CH/π interactions are not essential in the process of formation of *syn*-facial heterobimetallic complexes.

A few years later, by the mean of Density functional theory (DFT), Djukic *et al.*[688] performed a statistical study of a series of metallospiralenes molecules (Figure 48) and concluded that the Cr-to-Mn distance is in fact rather independent of the nature and steric size of the substituents present at the benzylic carbon as well as at a remote position such as the donor ligand. The M-M distance which amounts to an average value of *ca.* 3.04 Å, was found to be related to weak but attractive bonding interaction where London dispersion prevails over covalency and donor-acceptor interactions.

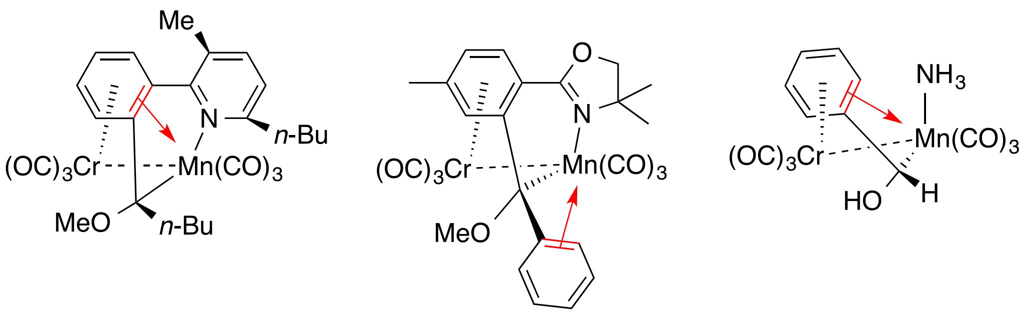

Figure 48: Some metallospiralenes molecules used in the theoretical study.

An examination of the molecular orbitals in *syn*-facial Cr-Mn benzylic complexes indicates low Wiberg bond indices (bellow 0,04) for the Cr-Mn segment, meaning that the intermetallic interaction is only weakly related to covalency. A subtle interplay of steric and electronic effects results in kinetically and thermodynamically viable structures, whereby the two metal centres happen to interact through a multifaceted interaction. For the authors, the best description of this interaction is a sterically favourable combination of dispersion bonding to a weak donor-acceptor interaction between the two metal centres, the latter being partitioned into a three-orbital four-electron Cr-Mn interaction and its Cr-Mn π back-bonding counterpart.

A way proposed by the authors to evaluate the interaction energy was to compare the intrinsic interaction energies of *syn*-facial and *anti*-facial systems; a differential of about 9 to 15 kcal.mol^{-1} seems to translate the unexpected favourable bias for a *syn*-facial arrangement versus *anti*-facial. This means that the stabilization from a "chemist's

[688] [N°559] Hyla-Kryspin, I.; Grimme, S.; Djukic, J. P. *Organometallics* **2009**, *28*, 1001.

standpoint" of the chemically susceptible 16 electron Mn (I) centre is largely the result of favourable London dispersion forces contributing, cooperatively with steric effects, to structural cohesion of the bimetallic entities (Figure 49).

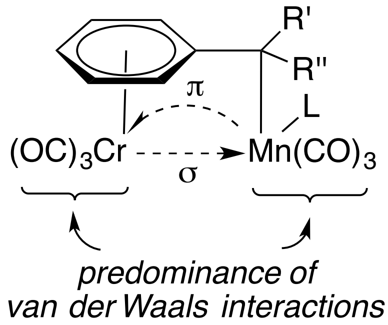

Figure 49: Lewis-type structure displaying the bonding interaction between the two metal centres.

2 - Purpose.

Our attempt to synthesize Re analogues[689] of those formally electron-unsaturated 6-membered cyclomanganated 2-oxazoline derivatives (Figure 50) studied by Djukic *et al*.[690] is the focus of the present chapter. Indeed, at this point of the research we estimated that two crucial issues remained to be further addressed to achieve a comprehensive understanding of this specific molecular system. Consequently, we decided to, first, properly evaluate the interconversion in solution of the heterobimetallic isomers by the use of ^{1}H NMR spectroscopy, which remained impossible in the case of the cyclomanganated derivatives due to the recurrence of radical species. We reasonably expected that the replacement of a Mn by Re atom, which would increase the binding energy of the C-M bond[691], will reduce the proportion of radicalar side-products, found to be responsible of the low resolution and quality of the ^{1}H NMR spectra.

[689] [N°612] Werlé, C.; Le Goff, X. F.; Djukic, J. P. *J. Organomet. Chem.* **2014**, *751*, 754.

[690] [N°608] Djukic, J. P.; Maisse-Francois, A.; Pfeffer, M.; Dotz, K. H.; De Cian, A.; Fischer, J. *Organometallics* **2000**, *19*, 5484.

[691] [N°613] Cobar, E. A.; Khaliullin, R. Z.; Bergman, R. G.; Head-Gordon, M. *Proc. Natl. Acad. Sci. USA* **2007**, *104*, 6963.

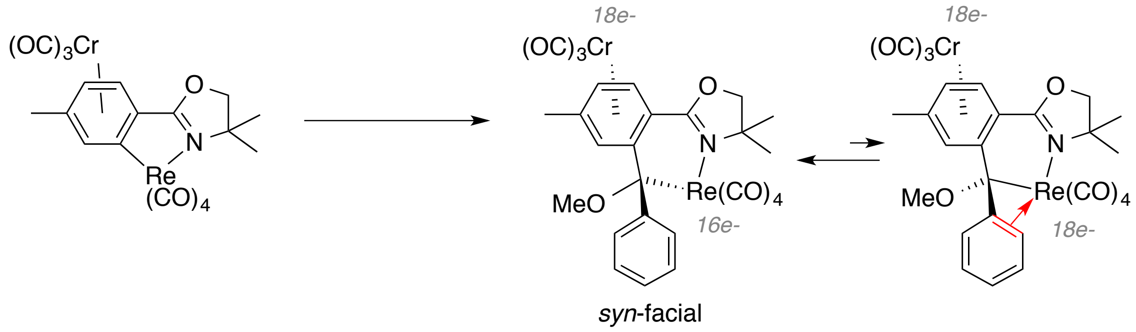

Figure 50: Expected formation of two "pseudoconformers". A *syn*-facial electron-unsaturated 18-16 electrons isomer and an electron-saturated 18-18 electrons isomer.

Second, by the means of DFT, we planned to evaluate the contribution of non-covalent interactions in the molecular cohesion of the electron-unsaturated complexes by an expected attractive steric occlusion of the 6th vacant Re coordination site that faces the Cr centre.

3 - Results and discussion.

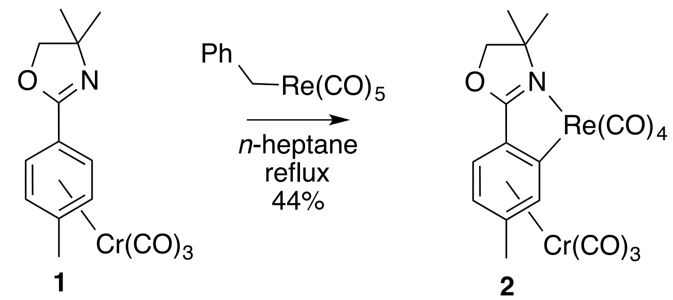

Figure 51: Formation of the cyclometallated 5-membered ring rhenium compound.

First, starting compound **2** was readily synthesized in 44 % isolated yield by the thermolytic treatment of ligand **1**[692] with $PhCH_2Re(CO)_5$ in refluxing heptane[693] (Figure 51). This compound was fully characterized analytically, spectroscopically and structurally by X-ray diffraction analysis (Figure 52). The cyclometallated rhenium is shown to be part of a planar 5-membered ring, almost equidistant to C_3 and N_1 (*ca.* Re-C_3 ≈ Re-N_1 ≈ 2.19 Å).

[692] [N°614] Lai, C. C.; Own, Z. Y.; Unruh, L. E.; Chou, M. W. *J. Chin. Chem. Soc.* **1991**, *38*, 207.

[693] [N°615] Djukic, J. P.; Dotz, K. H.; Pfeffer, M.; De Cian, A.; Fischer, J. *Inorg. Chem.* **1998**, *37*, 3649.

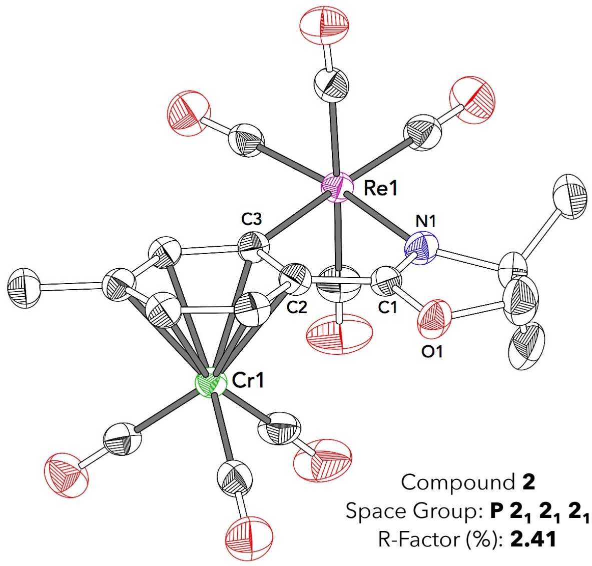

N°	*A*	*B*	*C*	*D*	*Lengths (Å)*	*Torsion Angles (°)*
1	Re_1	N_1	-	-	2.187(3)	-
2	Re_1	C_3	-	-	2.190(3)	-
3	Re_1	C_3	C_2	C_1	-	-12.1(4)
4	Re_1	N_1	C_1	C_2	-	1.8(4)

Figure 52: X-ray structure and selected interatomic distances of compound **2.**

It is worthy to note that its IR spectrum displays the typical signature of chelated tetracarbonylmetal compounds of the *cis*-$L_2M(CO)_4$ configuration with three out of four C-O stretching modes (2095, 1971, 1881 cm^{-1}) superimposed with the A_1 – E modes arising from the *facial*-$Cr(CO)_3$ moiety (1927, 1860 cm^{-1}), the A_1 vibration mode of the carbonyls of the $Re(CO)_4$ fragment showing up at 2095 cm^{-1}.

It is now well established that labile and electron-deficient transition metal complexes may react with diazoalkane reagents[694] (Figure 53) to form new metal carbene complexes with concomitant release of dinitrogen.[695-699]

[694] [N°609] Djukic, J. P.; Michon, C.; Maisse-Francois, A.; Allagapen, R.; Pfeffer, M.; Dotz, K. H., . . . Fischer, J. *Chem. Eur. J.* **2000**, *6*, 1064.
[695] [N°616] Schwab, P.; Grubbs, R. H.; Ziller, J. W. *J. Am. Chem. Soc.* **1996**, *118*, 100.
[696] [N°617] Schwab, P.; Mahr, N.; Wolf, J.; Werner, H. *Angew. Chem. Int. Ed. Engl.* **1993**, *32*, 1480.
[697] [N°618] Herrmann, W. A.; Weidenhammer, K.; Ziegler, M. L. *Z. Anorg. Allg. Chem.* **1980**, *460*, 200.
[698] [N°619] Herrmann, W. A. *Angew. Chem. Int. Ed. Engl.* **1978**, *17*, 800.
[699] [N°620] Herrmann, W. A. *Chem. Ber.* **1975**, *108*, 486.

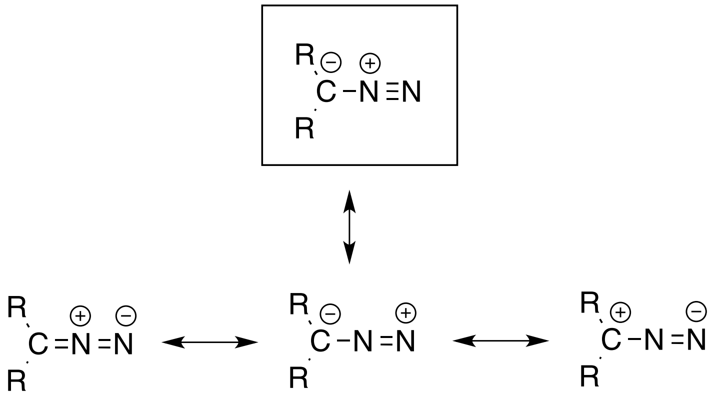

Figure 53: Charge delocalisation and mesomeric diazoalkane forms.

This is a common route well used for the synthesis of d-block transition metal carbene complexes and in systems devised for the metal-mediated cyclopropanation of olefins.[700,701] From our standpoint, the introduction of a carbene species starting from a diazoalkane, would offer the advantage of requiring absolutely neutral conditions softer and more reliable[702] than the "E. O. Fischer method". This approach consists of a reaction between a transition metal complex possessing at least one available coordination site and an alkylidene precursor, namely the diazoalkane. The creation of this necessary vacant coordination site on $Mn(CO)_4$ or $Re(CO)_4$ moieties can be performed mainly by three methods: a photolytic decarbonylation,[703] an oxidative decarbonylation by reaction with tertiary amine oxides[704,705] or a thermally promoted decarbonylation.[706] However, the first two aforementioned methods are not suitable for the class of bimetallic substrates that we studied since they are not selective and may have initiated an unpredictable amount of decomposition as a result of undiscriminated decarbonylations at the Cr or Re metal centres. The last of these three methods, namely thermal decarbonylation, happen in fact to be the more promising one in regard to the limitations aforementioned and has already proven its efficacy in previous Mn cases.[707,708]

[700] [N°621] Doyle, M. P. *Chem. Rev.* **1986**, *86*, 919.

[701] [N°622] Pfeiffer, J.; Nieger, M.; Dotz, K. H. *Eur. J. Org. Chem.* **1998**, 1011.

[702] [N°623] Michon, C.; Djukic, J. P.; Ratkovic, Z.; Collin, J. P.; Pfeffer, M.; de Cian, A., . . . Nieger, M. *Organometallics* **2002**, *21*, 3519.

[703] [N°624] Grigsby, W. J.; Main, L.; Nicholson, B. K. *Organometallics* **1993**, *12*, 397.

[704] [N°625] Liebeskind, L. S.; Gasdaska, J. R.; Mccallum, J. S.; Tremont, S. J. *J. Org. Chem.* **1989**, *54*, 669.

[705] [N°626] Cambie, R. C.; Metzler, M. R.; Rutledge, P. S.; Woodgate, P. D. *J. Organomet. Chem.* **1990**, *381*, C26.

[706] [N°627] Cambie, R. C.; Metzler, M. R.; Rutledge, P. S.; Woodgate, P. D. *J. Organomet. Chem.* **1992**, *429*, 41.

[707] [N°623] Michon, C.; Djukic, J. P.; Ratkovic, Z.; Collin, J. P.; Pfeffer, M.; de Cian, A., . . . Nieger, M. *Organometallics* **2002**, *21*, 3519.

However, the treatment of complex **2** with an excess of diphenyldiazomethane and *t*-butylphenyldiazomethane under these well-established thermolytic conditions, consisting of the slow addition of diazoalkane to a refluxing solution of rhenacycle in apolar solvents, did not produce any of the expected *syn*-facial electrodeficient monoinsertion products **3a** or **4a** (Figure 54).

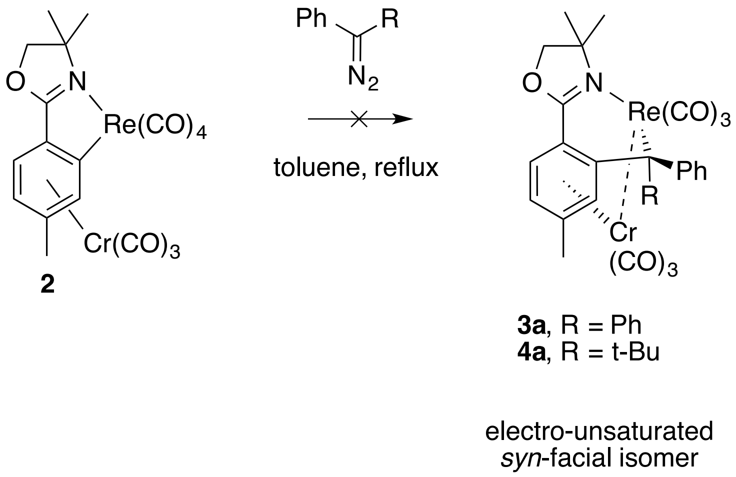

Figure 54: Expected formation of electron unsaturated heterobimetallic species.

In the case of the reaction with Ph_2CN_2 (Figure 55), which proved to be accompanied with major signs of decomposition, the main product was readily identified as the electron-saturated 18-18 electrons complex **3b** resulting from a mono-insertion of a Ph_2C: carbene into the Re-C_{Ar} bond of a decarbonylated derivative of **2**. A side product obtained in trace amounts, *i.e.* **3c**, was identified as the product of the reaction of **3b** with dissolved CO resulting from decomposition.

[708] [N°609] Djukic, J. P.; Michon, C.; Maisse-Francois, A.; Allagapen, R.; Pfeffer, M.; Dotz, K. H., . . . Fischer, J. *Chem. Eur. J.* **2000**, *6*, 1064.

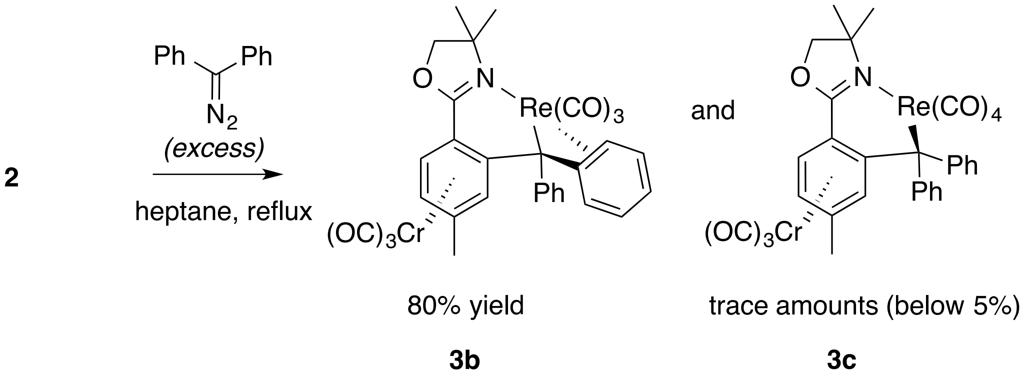

Figure 55: Reaction of **2** with Ph_2CN_2.

In complex **3b**, one of the two phenyl rings interacts with the Re centre to establish a characteristic trihaptobenzylic bonding interaction implicating the former carbene's carbon atom (Figure 56).

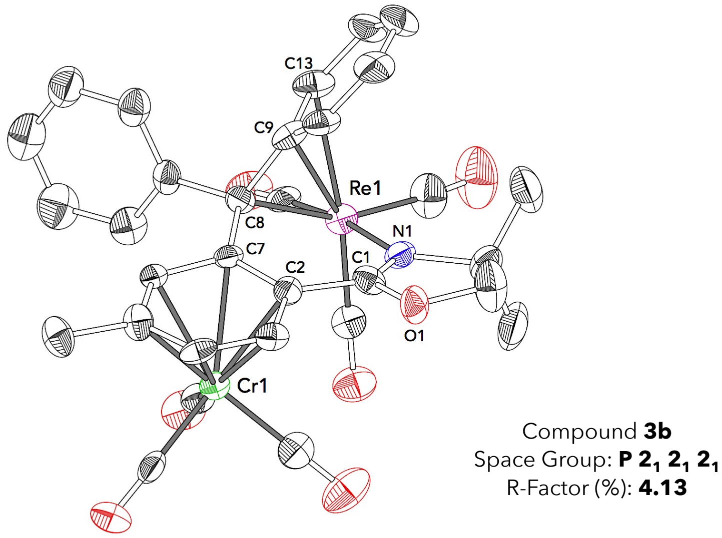

N°	A	B	C	D	Lengths (Å)	Angles (°)	Torsion Angles (°)
1	Re_1	C_8	-	-	2.290(8)	-	-
2	Re_1	C_9	-	-	2.445(7)	-	-
3	Re_1	N_1	-	-	2.180(6)	-	-
4	Re_1	C_8	C_7	-	-	116.4(5)	-
5	C_9	C_8	C_7	-	-	116.0(6)	-
6	Re_1	C_8	C_7	C_2	-	-	38.1(8)
7	Re_1	N_1	C_1	C_2	-	-	-2(1)

Figure 56: X-ray structure and selected interatomic distances of compound **3b.**

This bonding interaction is characterized by increasing Re-C distances following the order Re-C_{13}= 2.535(8) > Re-C_9= 2.445(7) > Re-C_8= 2.290(8), which is, at this stage, not surprising since it has already been observed in the case of a $Cr(CO)_3$-devoid manganese analogue.[709] The significant conformational flexibility of oxazolyl-based chelates is responsible for this propensity to stabilize the chelated metal by a side trihaptobenzylic interaction, in the absence of major steric strains. Consequently, the system expresses in its ^{1}H NMR spectrum marked signs of fluxionality related to the restrained rotation of the η^2-bonded phenyl group. In the case of **3b**, partial decoalescence of the η^2-bonded phenyl group could be achieved at *ca.* 227 K in deuterated toluene (Figure 57).

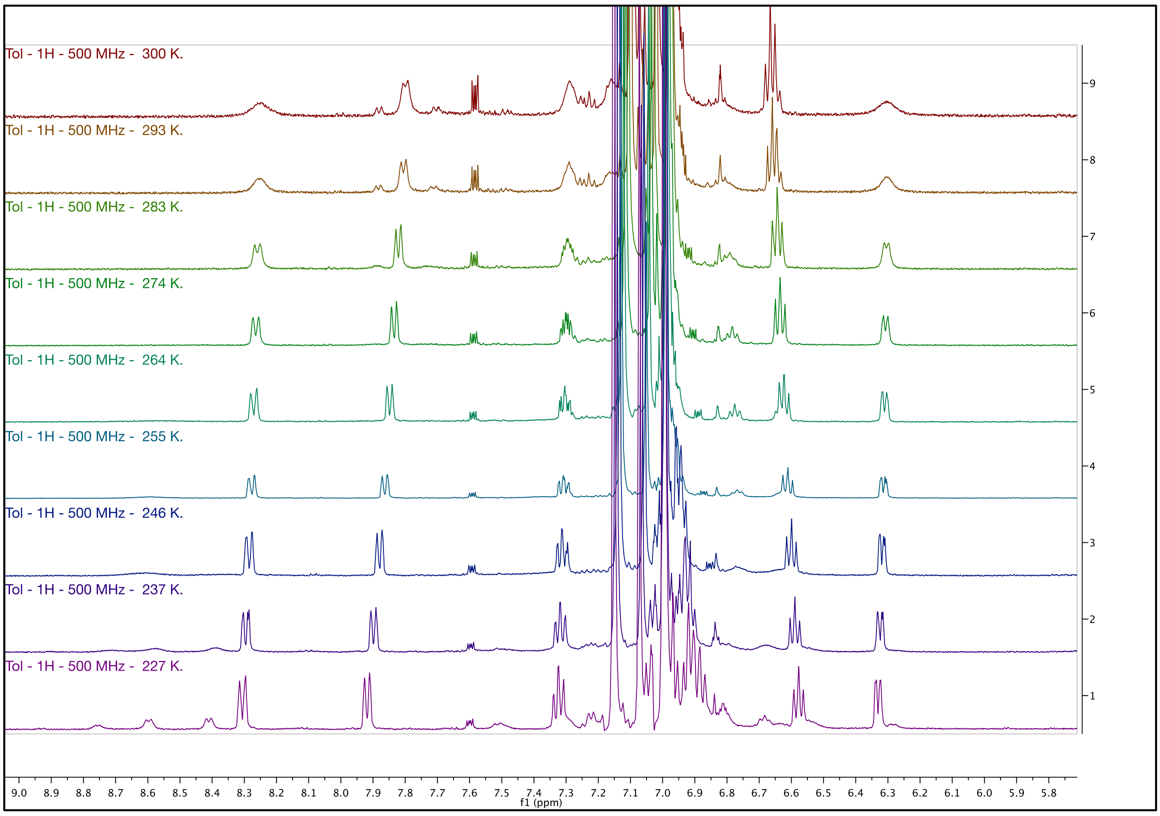

Figure 57: Variable temperature in deuterated toluene showing the partial decoalescence of the 2-bonded phenyl group.

In complex **3c** the trihaptobenzylic bonding interaction is broken due to the coordination of a residual carbonyl group leading to a saturated 18 electron metal centre geometrically located in a *antara*-facial manner by regards to the $Cr(CO)_3$ moiety (Figure 58).

[709] [N°628] Michon, C.; Djukic, J. P.; Pfeffer, M.; Gruber-Kyritsakas, N.; de Cian, A. *J. Organomet. Chem.* **2007**, *692*, 1092.

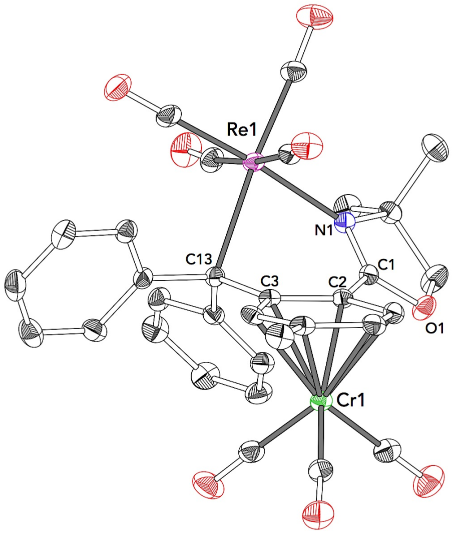

Compound **3c**
Space Group: **P -1**
R-Factor (%): **2.86**

N°	A	B	C	D	Lengths (Å)	Angles (°)	Torsion Angles (°)
1	Re_1	C_{13}	-	-	2.398(3)	-	-
2	Re_1	N_1	-	-	2.200(3)	-	-
3	N_1	Re_1	C_{13}	-	-	80.4(1)	-
5	Re_1	C_{13}	C_3	C_2	-	-	56.3(3)
6	Re_1	N_1	C_1	C_2	-	-	4.7(4)
7	N_1	C_1	C_2	C_3	-	-	-39.8(4)
8	C_{13}	C_3	C_2	C_1	-	-	-2.3(4)

Figure 58: X-ray structure and selected interatomic distances of compound **3c.**

In the case of the reaction of **2** with *t*-buthylphenyldiazomethane, the main product was identified as compound **4c** (Figure 59).

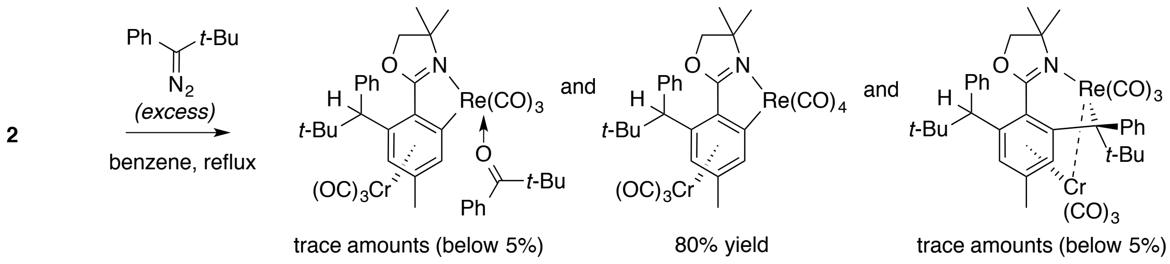

4b **4c** **4d**

Figure 59: Reaction of **2** with (*t*-Bu)(Ph)CN_2.

Two other side products, *i.e.* **4b** and **4d**, were also isolated in amounts insufficient to perform analytical characterizations but nonetheless sufficient to perform complete structural X-ray diffraction analyses (Figure 60 and Figure 61).

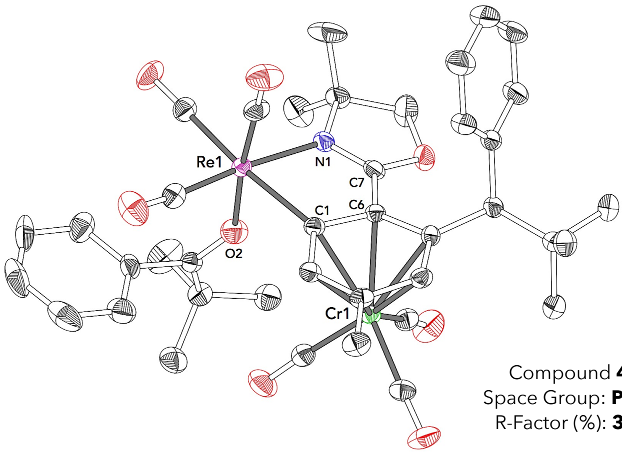

Compound **4b**
Space Group: **P 2$_1$/c**
R-Factor (%): **3.58**

N°	*A*	*B*	*C*	*D*	*Lengths (Å)*	*Angles (°)*	*Torsion Angles (°)*
1	Re$_1$	C$_1$	-	-	2.194(3)	-	-
2	Re$_1$	N$_1$	-	-	2.173(3)	-	-
3	Re$_1$	O$_2$	-	-	2.188(3)	-	-
4	N$_1$	Re$_1$	O$_2$	-	-	87.7(1)	-
5	C$_1$	Re$_1$	O$_2$	-	-	80.5(1)	-
6	C$_1$	Re$_1$	N$_1$	-	-	75.1(1)	-
7	Re$_1$	C$_1$	C$_6$	C$_7$	-	-	-11.6(3)
8	Re$_1$	N$_1$	C$_7$	C$_6$	-	-	-4.6(4)

Figure 60: X-ray structure and selected interatomic distances of compound **4b.**

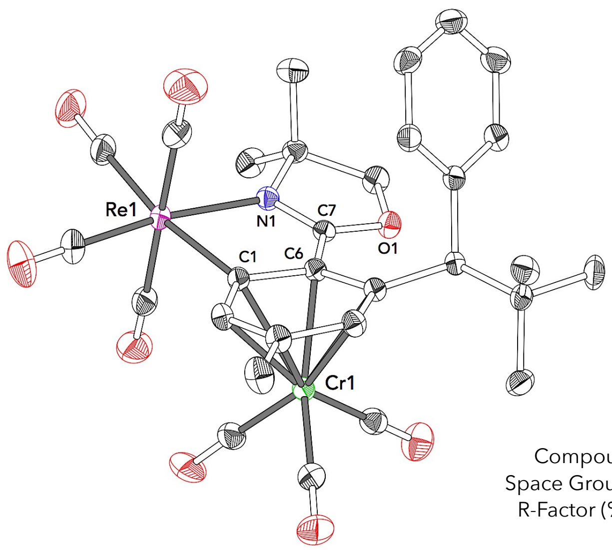

Compound **4c**
Space Group: **P 2$_1$/c**
R-Factor (%): **2.43**

N°	*A*	*B*	*C*	*D*	*Lengths (Å)*	*Angles (°)*	*Torsion Angles (°)*
1	Re$_1$	C$_1$	-	-	2.190(2)	-	-
2	Re$_1$	N$_1$	-	-	2.157(2)	-	-
4	N$_1$	Re$_1$	C$_1$	-	-	75.08(8)	-
7	Re$_1$	C$_1$	C$_6$	C$_7$	-	-	-10.1(2)
8	Re$_1$	N$_1$	C$_7$	C$_6$	-	-	-8.4(3)

Figure 61: X-ray structure and selected interatomic distances of compound **4c.**

From the structure of **4b** and **4c**, it is speculated that the former might be a precursor of the latter. This implies that **4b** (which is a rare example of a solvato-complex of a tricarbonyl rhenium(I) complex containing 2,2,2- trimethylacetophenone, a common minor pollutant of (t-Bu)(Ph)CN_2) resulted from a complex transformation involving the transient formation of **4a** and its conversion by an intra- or intermolecular C-H bond activation process into this precursor of stable **4c**.

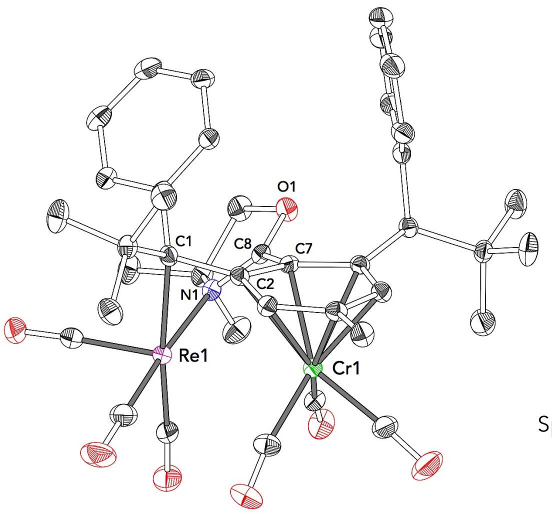

Compound **4d**
Space Group: **P 2_1/c**
R-Factor (%): **2.61**

N°	*A*	*B*	*C*	*D*	*Lengths (Å)*	*Angles (°)*	*Torsion Angles (°)*
1	Re_1	Cr_1	-	-	3.1519(2)	-	-
2	Re_1	C_1	-	-	2.333(2)	-	-
3	Re_1	N_1	-	-	2.185(2)	-	-
4	N_1	Re_1	C_1	-	-	80.44(8)	-
5	Re_1	C_1	C_2	-	-	82.5(1)	-
7	Re_1	C_1	C_2	C_7	-	-	80.1(2)
8	Re_1	N_1	C_8	C_7	-	-	9.1(3)

Figure 62: X-ray structure and selected interatomic distances of compound **4d**.

Quite logically, compound **4d**, which displays the typical structure of 18-16 electron *syn*-facial Cr-Re complexes, stems from a reaction of **4c** or **4b** with a second equivalent of (*t*-Bu)(Ph)CN_2 (Figure 62).

Figure 63 proposes a mechanism rationalizing the double condensation of (*t*-Bu)(Ph)CN_2 with the formation of a radical intermediate after an assumed homolytic disruption of the benzylic C-Re bond leading, after transposition of the metal centre and a C-H activation, to the heterobimetallic **4d**.

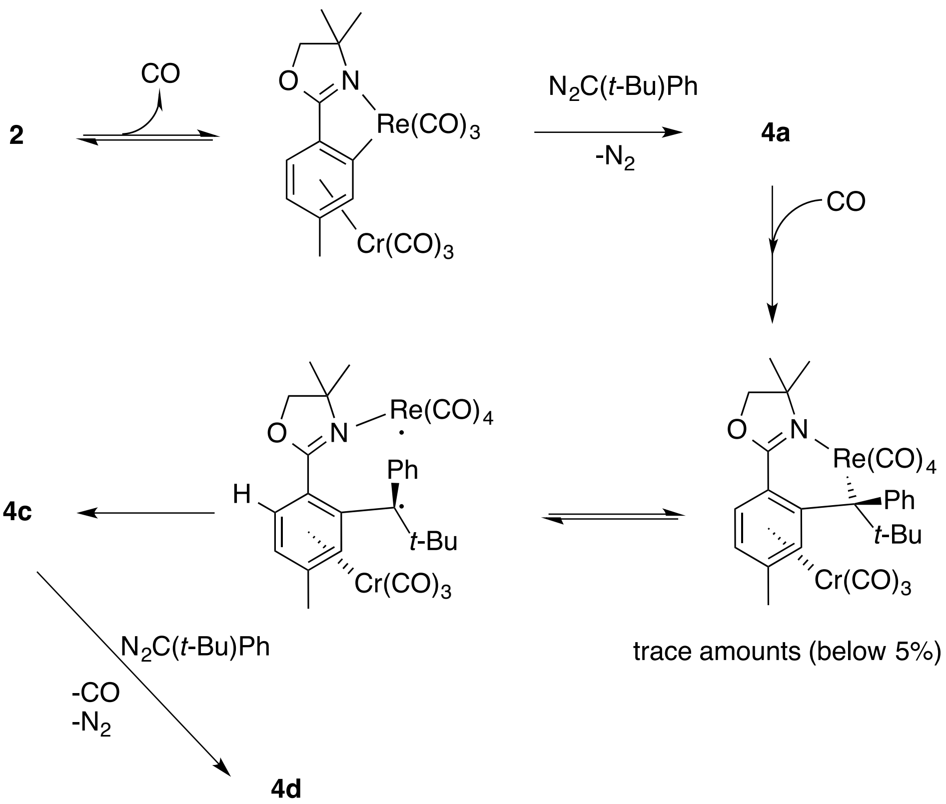

Figure 63: Mechanism rationalizing the double condensation of (*t*-Bu)(Ph)CN_2.

The key step here is the degradation of putative intermediate **4a** which plays the role of a metallation agent similarly to $PhCH_2Re(CO)_5$. This reaction is most probably intermolecular and very much dependent on the conditions used to perform the reaction and particularly, on the amount of available CO which is necessary for the formation of stable **4c**.

In compound **4d** the intermetallic Cr-Re distance amounts 3.152(2) Å, which is about 0.1 Å longer than the average Cr-M (M = Mn, Re) distance measured in other analogues derived from 2-phenylpyridines.[710] In line with previous studies, preliminary theoretical analyses of the intermetallic interaction using Yang's[711,712] electron density topology-based analysis of non-covalent interactions (NCI) regions, a typical bonded non-covalent interaction between the Re and the Cr centre (Figure 64).

[710] [N°559] Hyla-Kryspin, I.; Grimme, S.; Djukic, J. P. *Organometallics* **2009**, *28*, 1001.

[711] [N°629] Contreras-García, J.; Johnson, E. R.; Keinan, S.; Chaudret, R.; Piquemal, J.-P.; Beratan, D. N.; Yang, W. *J. Chem. Theory Comput.* **2011**, *7*, 625.

[712] [N°630] Johnson, E. R.; Keinan, S.; Mori-Sánchez, P.; Contreras-García, J.; Cohen, A. J.; Yang, W. *J. Am. Chem. Soc.* **2010**, *132*, 6498.

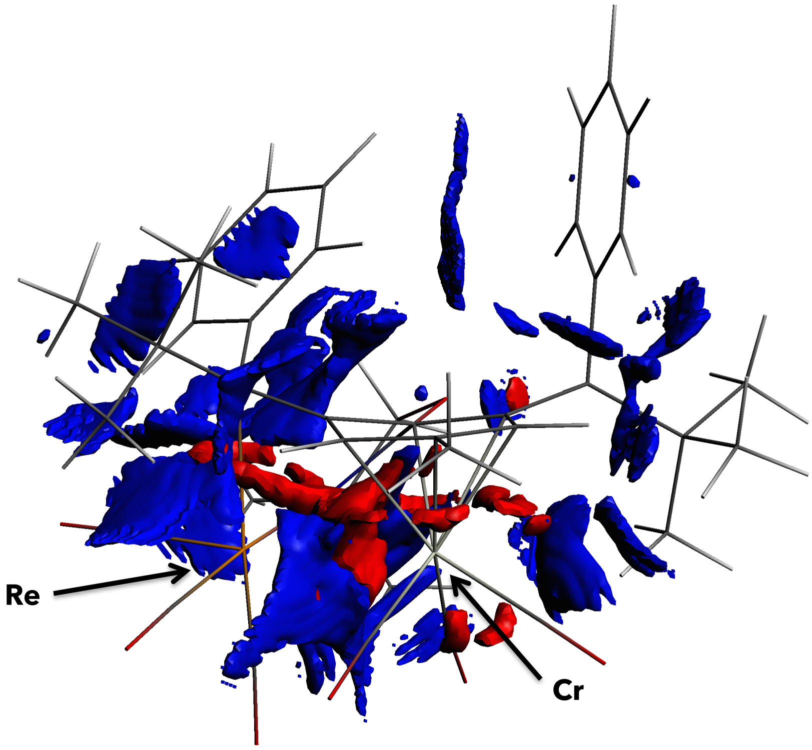

Figure 64: ADFview 2013 plot of NCI regions materialized by reduced density gradients isosurfaces (cutoff value s= 0.02 au, ρ= 0.05) coloured according to the signed density $\lambda_2\rho$ (red and blue colours are assigned to negative and positive signs respectively) for the gas-phase singlet ground state geometry of 4d computed at the ZORA-PBE-D3(BJ)/all electron TZP level).

Bader's AIM analysis stressing the absence of any bond critical point in the Cr-Re segment. Figure 64 displays the NCI regions where red-coloured isosurfaces depict regions of bonded non-covalent interactions and blue ones, regions of non-bonded or repulsive NCIs on a minimum energy singlet ground state geometry optimized by a method of the density functional theory. Overall computed geometric features are in good accord with the experimental geometry obtained by X-ray diffraction analysis.

4 - Conclusion.

This study shows that the reactivity of complex **2** towards diazomethanes is in no way straightforward. The planned carbene mono-insertion products **3a** and **4a** were not isolated and it is very much probable that if they intervene as transients their intrinsic reactivity would be responsible for the unexpected outcome reported herein, particularly for the reaction involving (*t*-Bu)(Ph)CN_2. It must be pointed out at this stage that all our efforts to lower the reaction temperature down to *ca.* 60 °C using hexanes instead of toluene as solvent only provided **3b** and **4c** in much lower yields, not changing anything to the overall trend. To the best of our knowledge **4c** is seemingly the first example of a product resulting from the successive insertion of a carbene ligand and metal transposition via a probable C-H activation route, a complex process that warrants further mechanistic investigations.

III

An excursion into non-covalence

Group 10 Transition Metals

After the difficulties experienced in chapter II, we decided to change our approach in the investigation of non-covalent interactions: a new class of metals as well as another kind of bridging ligands, the "indenyl derivatives", were chosen to be studied. This chapter describes the results obtained in the case of Cr/Pd, Cr/Pt bimetallic species, leading to formulate a new concept of coordination chemistry: **THE HEMICHELATION**.

Chapter III - Emergence of Hemichelation: The case of Pd and Pt hemichelates.

1 - Introduction.

Hemilability is an important property of transition metal ligands. It enables, upon appropriate chemical solicitation, the creation of a vacant coordination site and extension of the coordination environment of the considered metal. To some extent, the so-called "indenyl effect" (IndE) can also be considered as a form of intrinsic hemilability. Moreover, the indenyl effect correlated with the unique properties induced by the presence of a benzo-ring bound $Cr(CO)_3$ opens new perspectives in the stabilisation of coordinative unsaturated transition metal complexes.

1.1 - The "indenyl effect".

Following the initial studies on CO insertion reactions in molybdenum complexes by Mawby[713], Basolo[714, 715] studied, in the early 1980s, the kinetics of phosphine substitution on Rh and Mn carbonyl complexes.

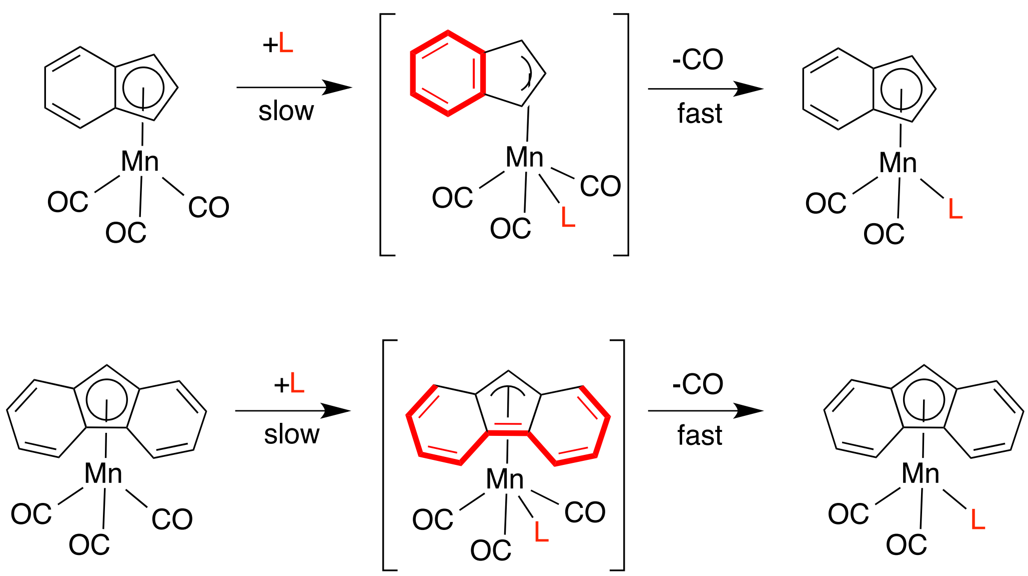

Figure 65: Substitution reactions on indenyl and fluorenyl Mn carbonyl complexes.

[713] [N°631] Hart-Davis, A. J.; Mawby, R. J. *J. Chem. Soc. A* **1969**, 2403.

[714] [N°632] Rerek, M. E.; Ji, L. N.; Basolo, F. *J. Chem. Soc., Chem. Commun.* **1983**, 1208.

[715] [N°633] Rerek, M. E.; Basolo, F. *J. Am. Chem. Soc.* **1984**, *106*, 5908.

It appeared that the rate of carbonyl substitution by triphenylphosphine (PPh_3) in the indenyl complexes Rh(η-C_9H_7)$(CO)_2$ and Mn(η-C_9H_7)$(CO)_3$ is, in both cases, much faster than cyclopentadienyl analogues.[716] For rhodium, a rate enhancement of 10^8 was found for the indenyl compound over the corresponding cyclopentadienyl compound. Basolo assessed "the indenyl effect" to explain the enhanced ligand substitution rates. The rate enhancement increases with the ligand's π system extension (Figure 65 in red), as shown by studies[717] with fluorenyl complexes (X = Flu = $C_{13}H_9^-$), being directly related with the stability of the lower hapticity intermediates, normally η^3-X species. Furthermore, by means of molecular orbital calculations, Veiros[718] studied the addition of PH_3 to [(η^5-X)$Mn(CO)_3$], with X = cyclopentadienyl (Cp = $C_5H_5^-$), indenyl (Ind = $C_9H_7^-$), fluorenyl (Flu = $C_{13}H_9^-$), cyclohexadienyl (Chd = $C_6H_7^-$), and 1-hydronaphthalene (Hnaph = $C_{10}H_9^-$). The obtained activation energies indicate the following order for the reaction rates: Cp <<< Ind ≈ Chd < Flu < Hnaph, which correlates with the (η^5-X)-Mn bond strength in the reactants (Figure 66). Thus, further enhancement by a factor of 10^6 can be achieved when the indenyl ligand is replaced by a hydronaphthalenyl ligand.

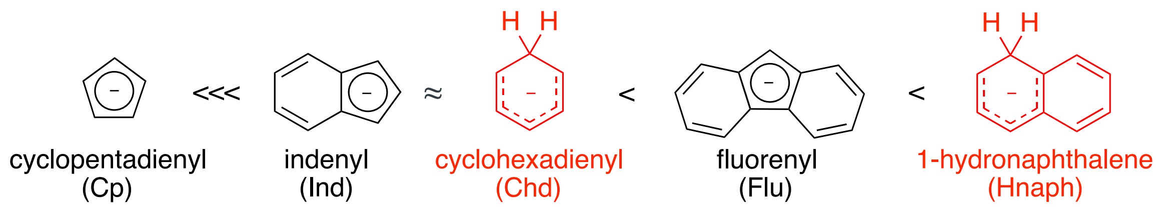

Figure 66: Ligand dependency of the reaction rates.

The indenyl ligand can relatively easily switch between a perturbed η^5-coordination mode and η^3-allyl-type coordination, which is even easier for the Flu or Hnaph ligands (Figure 67).

[716] [N°634] Angelici, R. J.; Loewen, W. *Inorg. Chem.* **1967**, *6*, 682.

[717] [N°635] Ji, L. N.; Rerek, M. E.; Basolo, F. *Organometallics* **1984**, *3*, 740.

[718] [N°636] Veiros, L. F. *Organometallics* **2000**, *19*, 3127.

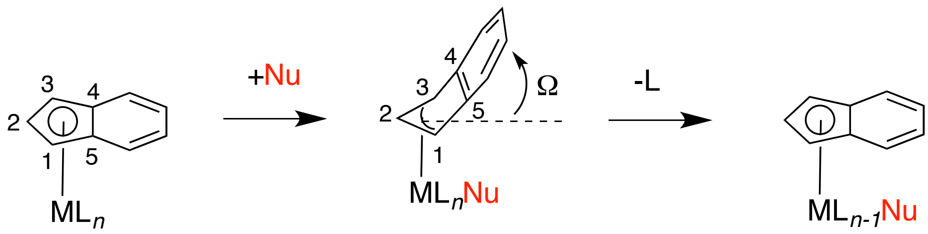

Figure 67: η^3-η^1-indenyl ligand switch.

This process leads to a reduced electron count of two at the metal centre thus providing the possibility for an associative ligand substitution pathway. The origin of the indenyl effect is clearly a result of the rearomatization of the annulated benzene ring upon hapticity interconversion.[719, 720] Recent theoretical studies also suggest that the higher stability of the (η^5-Cp)−M bond versus the (η^5-Ind)−M bond and the reversed order for the η^3- bound intermediates play a crucial role; thereby, the activation of an η^5−η^3 rearrangement requires less energy for indenyl complexes, resulting in higher reaction rates.[721,722]

This indenyl effect, which has now been well documented for a host of metal complexes,[723 - 726] has more recently be extended to the pentadienyl ("open Cp") chemistry by Tamm *et al.*[727,728] with the formation of ruthenium and iron complexes bearing a phenylmethallyl ligand, oInd^{Me} (Figure 68).

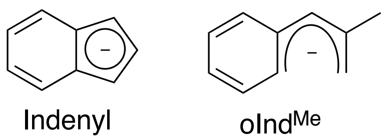

Figure 68: The indenyl and the open indenyl, oInd^{Me}, ligands.

719 [N°637] Calhorda, M. J.; Veiros, L. s. F. *Coord. Chem. Rev.* **1999**, *185-186*, 37.

720 [N°638] Cadierno, V.; Díez, J. n.; Pilar Gamasa, M.; Gimeno, J.; Lastra, E. *Coord. Chem. Rev.* **1999**, *193–195*, 147.

721 [N°639] Calhorda, M. J.; Romao, C. C.; Veiros, L. F. *Chemistry* **2002**, *8*, 868.

722 [N°640] Veiros, L. F.; Calhorda, M. J. *Dalton Trans.* **2011**, *40*, 11138.

723 [N°641] Anderson, S.; Hill, A. F.; Nasir, B. A. *Organometallics* **1995**, *14*, 2987.

724 [N°642] Okuda, J.; König, P.; Rushkin, I. L.; Kang, H.-C.; Massa, W. *J. Organomet. Chem.* **1995**, *501*, 37.

725 [N°643] Bitterwolf, T. E.; Lukmanova, D.; Gallagher, S.; Rheingold, A. L.; Guzei, I. A.; Liable-Sands, L. *J. Organomet. Chem.* **2000**, *605*, 168.

726 [N°644] Groux, L. F.; Belanger-Gariepy, F.; Zargarian, D. *Can. J. Chem.* **2005**, *83*, 634.

727 [N°645] Glockner, A.; Arias, O.; Bannenberg, T.; Daniliuc, C. G.; Jones, P. G.; Tamm, M. *Dalton Trans.* **2011**, *40*, 11511.

728 [N°646] Glöckner, A.; Bannenberg, T.; Ibrom, K.; Daniliuc, C. G.; Freytag, M.; Jones, P. G., . . . Tamm, M. *Organometallics* **2012**, *31*, 4480.

This specific ligand can be considered as an "open indenyl ligand", which showed the possible hapticity switch upon addition of a ligand L, very similar to what is observed for the indenyl derivatives (Figure 69).

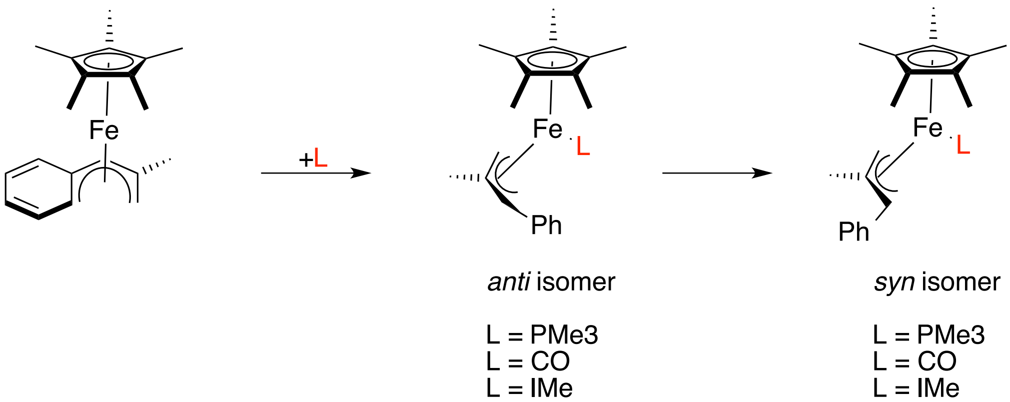

Figure 69: Hapticity switch of open indenyl ligand upon addition of a ligand L.

However the opposite effect has also been found (the so-called "reverse indenyl effect") for ligand substitution on 19-electron centres, illustrated with the reduction of $[(\eta^5$-$X)Fe(CO)_3]^+$ (X = Cp and Ind).[729] Since Basolo's early studies, the indenyl effect was proved to play an important role in the reactivity of d-block metals and in stoichiometric reactions as well as in metal-mediated catalytic transformations.[730-738] Although a wide variety of η-indenyl complexes of group 10 metals have been reported,[739-742] both η^3 and η^1 coordination modes have been depicted as stable and persistent in solution (Figure 70).[743,744]

[729] [N°647] Pevear, K. A.; Holl, M. M. B.; Carpenter, G. B.; Rieger, A. L.; Rieger, P. H.; Sweigart, D. A. *Organometallics* **1995**, *14*, 512.
[730] [N°640] Veiros, L. F.; Calhorda, M. J. *Dalton Trans.* **2011**, *40*, 11138.
[731] [N°648] Casey, C. P.; Vos, T. E.; Brady, J. T.; Hayashi, R. K. *Organometallics* **2003**, *22*, 1183.
[732] [N°649] Garrett, C. E.; Fu, G. C. *J. Org. Chem.* **1998**, *63*, 1370.
[733] [N°650] Schmid, M. A.; Alt, H. G.; Milius, W. *J. Organomet. Chem.* **1996**, *514*, 45.
[734] [N°651] Llinas, G. H.; Day, R. O.; Rausch, M. D.; Chien, J. C. W. *Organometallics* **1993**, *12*, 1283.
[735] [N°652] Foo, T.; Bergman, R. G. *Organometallics* **1992**, *11*, 1801.
[736] [N°653] Marder, T. B.; Roe, D. C.; Milstein, D. *Organometallics* **1988**, *7*, 1451.
[737] [N°654] Borrini, A.; Diviersi, P.; Ingrosso, G.; Lucherini, A.; Serra, G. *J. Mol. Catal.* **1985**, *30*, 181.
[738] [N°655] Bönnemann, H. *Angew. Chem. Int. Ed. Engl.* **1985**, *24*, 248.
[739] [N°656] Huber, T. A.; Bayrakdarian, M.; Dion, S.; Dubuc, I.; Bélanger-Gariépy, F.; Zargarian, D. *Organometallics* **1997**, *16*, 5811.
[740] [N°657] Stradiotto, M.; McGlinchey, M. J. *Coord. Chem. Rev.* **2001**, *219-221*, 311.
[741] [N°658] O'Hare, D. *Organometallics* **1987**, *6*, 1766.
[742] [N°659] Alías, F. M.; Belderraín, T. R.; Paneque, M.; Poveda, M. L.; Carmona, E.; Valerga, P. *Organometallics* **1998**, *17*, 5620.
[743] [N°660] Sui-Seng, C.; Enright, G. D.; Zargarian, D. *Organometallics* **2004**, *23*, 1236.
[744] [N°661] Sui-Seng, C.; Enright, G. D.; Zargarian, D. *J. Am. Chem. Soc.* **2006**, *128*, 6508.

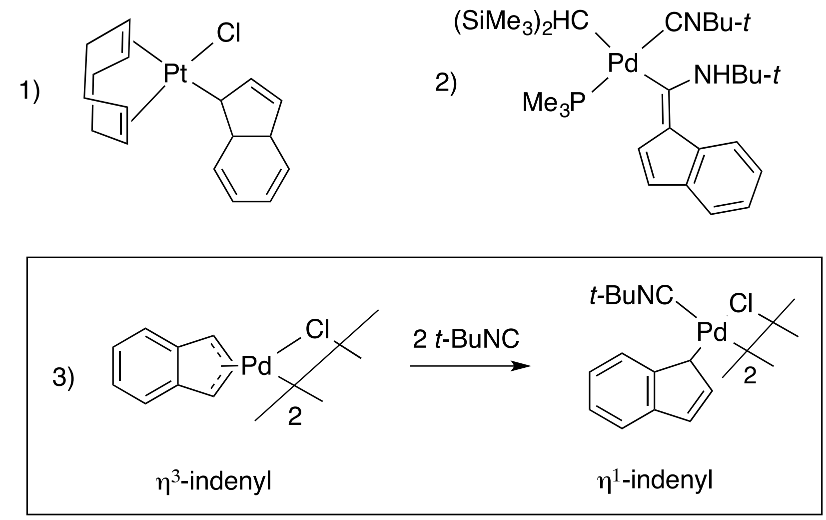

Figure 70: η-indenyl complexes of group 10 metals.

1.2 - The (indenyl) chromium arenes.

Since 1957, when Fischer and Öfele reported the first preparation of an arene tricarbonylchromium complex[745], namely the "tricarbonyl(η^6-benzene)chromium", a wide range of transition-metal (Cr, Mo, W, Fe, Ru, Os, Mn) arenes complexes have been synthesised and described in the literature.[746-752] However, among this multitude, the tricarbonyl(η^6-arene)chromium derivatives remain the most used, especially in organic synthesis.[753-755] This preference for chromium derivatives is mostly due to their relative stability[756,757] (stable to air, only sensitive to oxidizing reagents and to light), often crystalline and the ease to remove the chromium fragment upon transformations

[745] [N°662] Fischer, E. O.; Öfele, K. *Chem. Ber.* **1957**, *90*, 2532.
[746] [N°663] Kündig, E. P.; Fabritius, C.-H.; Grossheimann, G.; Romanens, P.; Butenschön, H.; Wey, H. G. *Organometallics* **2004**, *23*, 3741.
[747] [N°664] Auffrant, A.; Prim, D.; Rose-Munch, F.; Rose, E.; Schouteeten, S.; Vaissermann, J. *Organometallics* **2003**, *22*, 1898.
[748] [N°665] Kamikawa, K.; Norimura, K.; Furusyo, M.; Uno, T.; Sato, Y.; Konoo, A., . . . Uemura, M. *Organometallics* **2003**, *22*, 1038.
[749] [N°666] Kundig, E. P.; Fabritius, C. H.; Grossheimann, G.; Robvieux, F.; Romanens, P.; Bernardinelli, G. *Angew. Chem. Int. Ed. Engl.* **2002**, *41*, 4577.
[750] [N°667] Abd-El-Aziz, A. S.; Bernardin, S. *Coord. Chem. Rev.* **2000**, *203*, 219.
[751] [N°668] Mills, R. C.; Abboud, K. A.; Boncella, J. M. *Organometallics* **2000**, *19*, 2953.
[752] [N°669] Harman, W. D. *Chem. Rev.* **1997**, *97*, 1953.
[753] [N°670] Davies, S. G. *Organotransition Metal Chemistry: applications to Organic Synthesis*; Pergamon Press: Oxford, U.K., **1992**.
[754] [N°671] Beller, M.; Bolm, C. *Transition Metals for Organic Synthesis*; Wiley-VCH: Weinheim, Germany, **1998**.
[755] [N°672] Kündig, E. P. *Transition Metal Arene π-Complexes in Organic Synthesis and Catalysts; Topics in Organometallic Chemistry*, **2004**; Vol. 7.
[756] [N°673] Rosillo, M.; Dominguez, G.; Perez-Castells, J. *Chem. Soc. Rev.* **2007**, *36*, 1589.
[757] [N°674] Ziegler, T.; Heber, U. *Beilstein J. Org. Chem.* **2012**, *8*, 1059.

releasing the modified organic ligand. Indeed, the complexation of an arene to a transition metal changes drastically the chemical behaviour of the organic ligand, giving rise to unprecedented transformations and properties (Figure 71). For example, the electron-withdrawing effect[758] (which can be compared with that of nitrogroup) of the chromium unit; it increases the acidity of the aromatic protons[759] and the electrophilicity of the aromatic ring,[760] allowing efficient nucleophilic attack (SN_{Ar} and dearomatization reactions).[761] Similarly, the benzylic and homo-benzylic positions are found to be more acidic, more prone to deprotonation, nucleophilic substitution[762] or solvolysis,[763] due to the stabilization of both benzylic and homo-benzylic carbanions and even carbenium ions[764,765] by the tricarbonylchromium unit.

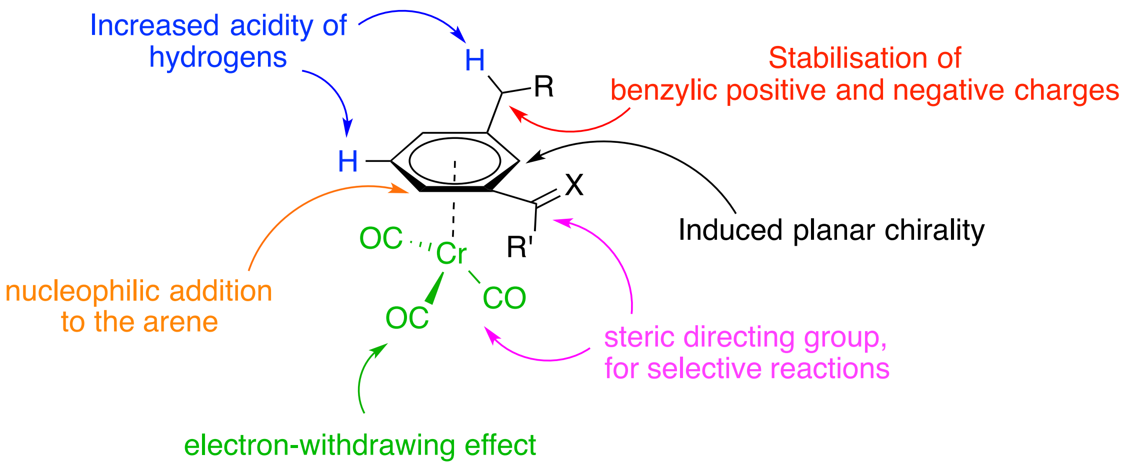

Figure 71: Summary of the main properties induced by the coordination of a $Cr(CO)_3$ unit to an arene ligand.

Because of its ability to stabilize both benzylic cations,[766-768] anions[769] and even radicals,[770,771] the $Cr(CO)_3$ moiety has been described as "hermaphroditic".[772] In spite of

[758] [N°675] Holmes, J. D.; Jones, D. A. K.; Pettit, R. *J. Organomet. Chem.* **1965**, *4*, 324.
[759] [N°676] Solladié-Cavallo, A. *Polyhedron* **1985**, *4*, 901.
[760] [N°677] Merlic, C. A.; Miller, M. M.; Hietbrink, B. N.; Houk, K. N. *J. Am. Chem. Soc.* **2001**, *123*, 4904.
[761] [N°678] Pape, A. R.; Kaliappan, K. P.; Kündig, E. P. *Chem. Rev.* **2000**, *100*, 2917.
[762] [N°679] Semmelhack, M. F.; Hall, H. T.; Farina, R.; Yoshifuji, M.; Clark, G.; Bargar, T., . . . Clardy, J. *J. Am. Chem. Soc.* **1979**, *101*, 3535.
[763] [N°675] Holmes, J. D.; Jones, D. A. K.; Pettit, R. *J. Organomet. Chem.* **1965**, *4*, 324.
[764] [N°673] Rosillo, M.; Dominguez, G.; Perez-Castells, J. *Chem. Soc. Rev.* **2007**, *36*, 1589.
[765] [N°680] Semmelhack, M. F.; Clark, G. R.; Garcia, J. L.; Harrison, J. J.; Thebtaranonth, Y.; Wulff, W.; Yamashita, A. *Tetrahedron* **1981**, *37*, 3957.
[766] [N°681] Vasen, D.; Salzer, A.; Gerhards, F.; Gais, H.-J.; Stürmer, R.; Bieler, N. H.; Togni, A. *Organometallics* **2000**, *19*, 539.
[767] [N°682] Netz, A.; Polborn, K.; Nöth, H.; Müller, T. J. J. *Eur. J. Org. Chem.* **2005**, *2005*, 1823.
[768] [N°683] Netz, A.; Drees, M.; Strassner, T.; Muller, T. J. J. *Eur. J. Org. Chem.* **2007**, 540.

the withdrawing effect, a way to explain the ability to strongly stabilize positive charges in the benzylic position is the "neighbour's group effect" arising from an overlap of occupied *d* orbitals of the metal and the empty orbital of the carbenium centre. Furthermore, if a non-symmetrically 1,2- or 1,3-disubstituted arene ring is complexed to chromium, the resulting molecule lacks symmetry elements resulting in a chiral compound (Figure 72) with a plane as the origin of chirality and a steric bulk (the $Cr(CO)_3$ moiety) exerting great facial control by shielding one face of the arene,[773] which, in turn, makes these chiral complexes attractive asymmetric catalysts for enantioselective reactions.[774-782] Moreover, because of the planar chirality, compound **A** cannot be superimposed to its mirror image (**ent-A**).

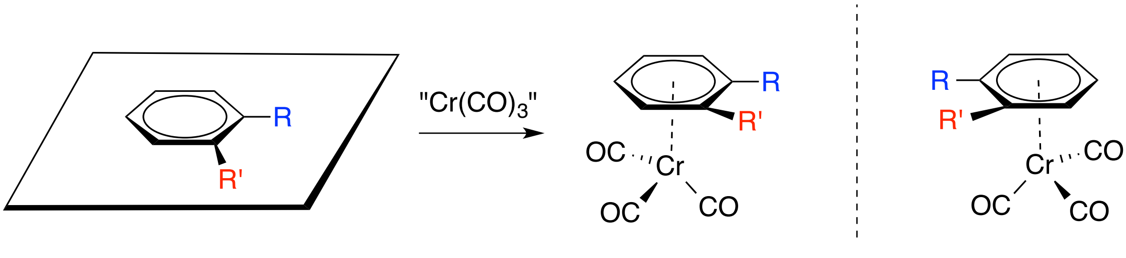

Figure 72: The coordination of a $Cr(CO)_3$ moiety to an arene results in a chiral compound.

Concerning the stereochemical assignment of such chiral compounds, two different approaches have been described in the literature, namely the rules introduced by Schlögl[783,784] and the extended Cahn-Ingold-Prelog rules (CIP),[785,786] the latter having

769 [N°684] Koide, H.; Hata, T.; Uemura, M. *J. Org. Chem.* **2002**, *67*, 1929.

770 [N°685] Merlic, C. A.; Hietbrink, B. N.; Houk, K. N. *J. Org. Chem.* **2001**, *66*, 6738.

771 [N°686] Merlic, C. A.; Walsh, J. C. *J. Org. Chem.* **2001**, *66*, 2265.

772 [N°687] Merlic, C. A.; Walsh, J. C.; Tantillo, D. J.; Houk, K. N. *J. Am. Chem. Soc.* **1999**, *121*, 3596.

773 [N°688] Xie, L.; Jones, G. B. *Tetrahedron Lett.* **2005**, *46*, 3579.

774 [N°673] Rosillo, M.; Dominguez, G.; Perez-Castells, J. *Chem. Soc. Rev.* **2007**, *36*, 1589.

775 [N°678] Pape, A. R.; Kaliappan, K. P.; Kündig, E. P. *Chem. Rev.* **2000**, *100*, 2917.

776 [N°689] Gibson, S. E.; Ibrahim, H. *Chem. Commun.* **2002**, 2465.

777 [N°690] Rose-Munch, F.; Rose, E. *Eur. J. Inorg. Chem.* **2002**, *2002*, 1269.

778 [N°691] Kamikawa, K.; Watanabe, T.; Uemura, M. *J. Synth. Org. Chem. Jpn.* **2001**, *59*, 1078.

779 [N°692] Nelson, S. G.; Hilfiker, M. A. *Org. Lett. 9* **1999**, *1*, 1379.

780 [N°693] Bolm, C.; Muniz, K. *Chem. Soc. Rev.* **1999**, *28*, 51.

781 [N°694] Butenschon, H. *Synlett* **1999**, 680.

782 [N°695] Son, S. U.; Jang, H. Y.; Lee, I. S.; Chung, Y. K. *Organometallics* **1998**, *17*, 3236.

783 [N°696] Schlogl, K. *J. Organomet. Chem.* **1986**, *300*, 219.

found more acceptance.[787] Following this approach with the example shown in (Figure 73), all the carbons of the coordinated arene ring are considered to be pseudo-tetrahedral with the metal centre occupying the fourth corner of the tetrahedron. The priorities are assessed according to the CIP rules. The tetrahedron is then rotated in such a way that the position having the lowest priority is the furthest away from the observer. Finally, the application of all of these results in a clockwise screw correlate to a (1*R*) centre.

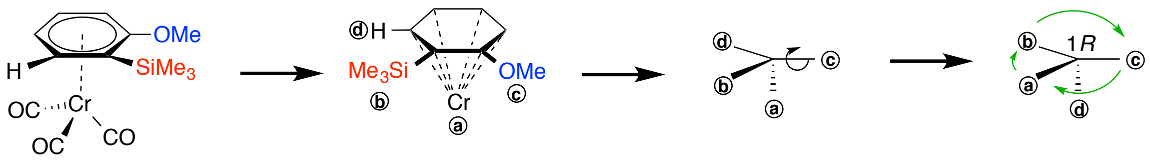

with : a = Cr > b = Si > c = C, Cr, O > d = C, Cr, H

(1*pR*)-B

Figure 73: Example of stereochemical assignment of the chirality of a chromium arene complex.

To specify the element of chirality an italic *"p"* letter (for planar) is used and put in front, or after, the assignment attributed to the planar chirality. Worthy to note that it is in most cases sufficient to classify only the stereogenic centre bearing the highest priority substituent.

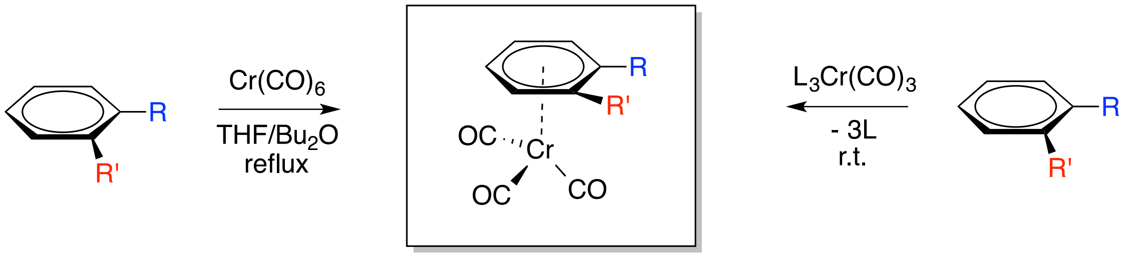

Figure 74: Pathways for the preparation of chromium arene complexes.

As shown in Figure 74 chromium arene complexes are ideally synthesized by thermolytic reaction of $Cr(CO)_6$ under an inert atmosphere in a highboiling THF/dibuthyl ether mixture of solvents over a long period (up to 4 days)[788] or by using

[784] [N°697] Schlögl, K. *Top. Stereochem.* **1967**, *1*, 39.

[785] [N°698] Cahn, R. S.; Ingold, C.; Prelog, V. *Angew. Chem. Int. Ed. Engl.* **1966**, *5*, 385.

[786] [N°699] Solladié-Cavallo, A. *Advances in Metal Organic Chemistry*; ed. L. S. Liebeskind, JAI, London, **1989**; Vol. 2, p. 99.

[787] [N°673] Rosillo, M.; Dominguez, G.; Perez-Castells, J. *Chem. Soc. Rev.* **2007**, *36*, 1589.

[788] [N°700] Mahaffy, C. A. L.; Pauson, P. L. *Inorg. Synth.* **1990**, *28*, 136.

microwaves.[789] Alternatively, they can also be obtained by arene exchange from naphthalene chromium tricarbonyl[790] or with $Cr(CO)_3L_3$ (with L = two electrons ligands, typically: acetonitrile, pyridine…).

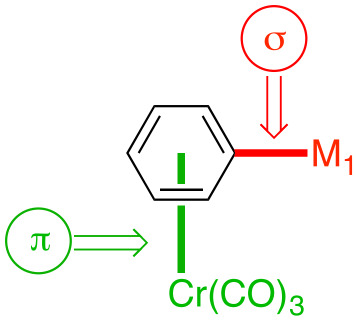

Figure 75: σ-π-bridged heterobimetallic complex.

Furthermore the preparation of σ-π-bridged heterobimetallic complexes derived from (η^6-arene)tricarbonylchromium complexes (Figure 75) is well documented in the literature.[791,792] At least eight different methods can be used for their synthesis on a preparative scale. Figure 76 summarizes these synthetic routes, which range from the classical reactions of deprotonation–lithiation ***(Path I)***, transmetalation ***(Path II)***, ligand exchange ***(Path III)***, the aromatic nucleophilic ***(Path IV)*** and electrophilic ***(Path V)*** additions of anionic and cationic metal complexes, respectively. Less frequently used but rather possible are the routes involving an interaction between a metal and an aromatic C-Halogen bond (oxidative addition in cross-coupling reactions, Grignard-like procedures) ***(Path VI)*** and the extrusion of CO ligand from acylmetal-substituted (η^6-arene)$Cr(CO)_3$ complexes ***(Path VII)*** or the cleavage, in neutral conditions, of a C_{Ar}-H bond (*ortho*-manganation and 1,2-polymetalation) ***(Path VIII)***.

[789] [N°701] Lee, Y. T.; Choi, S. Y.; Lee, S. I.; Chung, Y. K.; Kang, T. J. *Tetrahedron Lett.* **2006**, *47*, 6569.

[790] [N°702] Kündig, E. P.; Perret, C.; Spichiger, S.; Bernardinelli, G. *J. Organomet. Chem.* **1985**, *286*, 183.

[791] [N°703] Prim, D.; Andrioletti, B.; Rose-Munch, F.; Rose, E.; Couty, F. *Tetrahedron* **2004**, *60*, 3325.

[792] [N°704] Berger, A.; Djukic, J. P.; Michon, C. *Coord. Chem. Rev.* **2002**, *225*, 215.

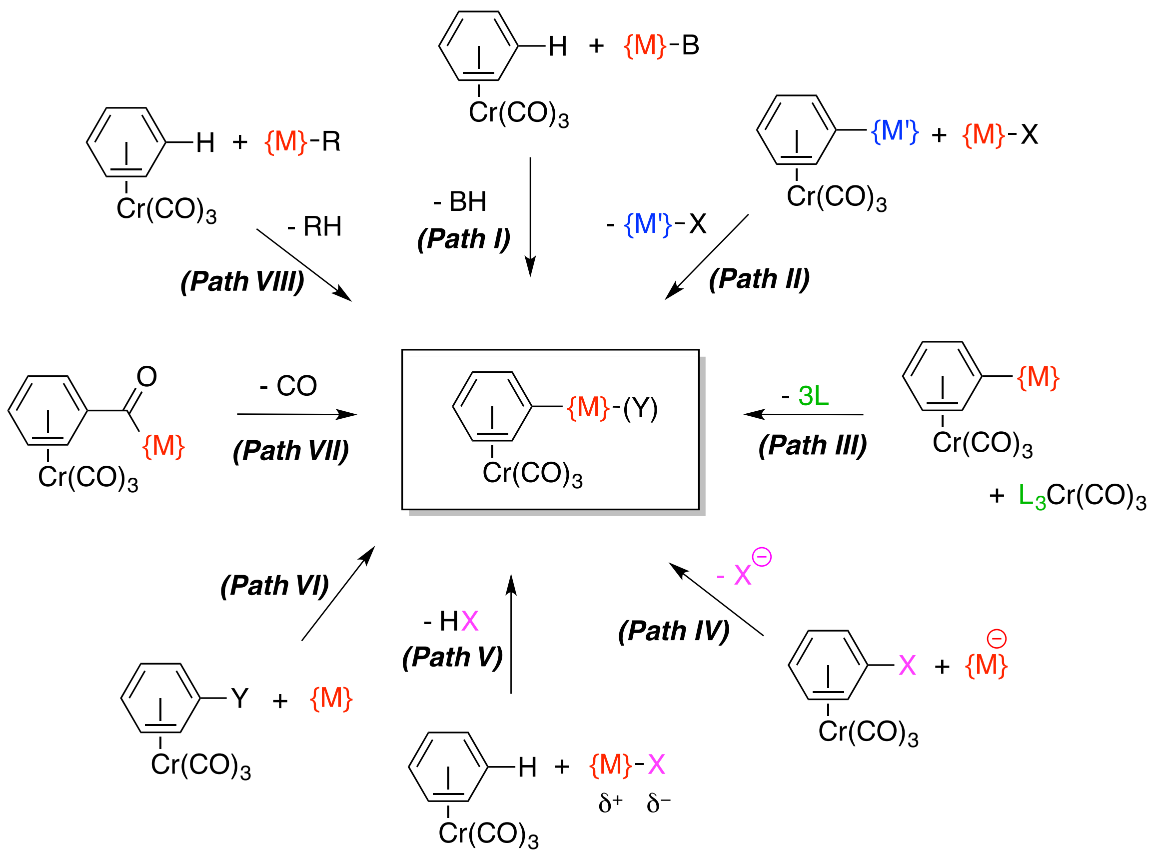

Figure 76: Summary of the different routes to prepare σ-π-bridged heterobimetallic complexes bearing a $Cr(CO)_3$ unit.

2 - General Purpose.

Coordinatively unsaturated transition metal complexes are thought to take part in a number of catalytic processes as pivotal intermediates.[793-795] Stabilizing such kinetically unstable species that are electron-unsaturated from the standpoint of the so-called Sidwick-Langmuir 18 valence electrons rule [796 - 798] represents a great challenge. Persistence can be achieved by using steric occlusion or by promoting labile weak interactions between the metal centre and proximal groups of atoms. In that way, Hofmann[799] and others[800-805] showed that labile C-H … M agostic interactions allow the

793 [N°705] Faza, R. Á. O. N.; de Lera, A. R.; Cárdenas, D. J. *Adv. Synth. Catal.* **2007**, *349*, 887.

794 [N°706] Sergeev, A. G.; Spannenberg, A.; Beller, M. *J. Am. Chem. Soc.* **2008**, *130*, 15549.

795 [N°707] Marrone, A.; Re, N.; Romeo, R. *Organometallics* **2008**, *27*, 2215.

796 [N°708] Jensen, W. B. *J. Chem. Educ.* **2005**, *82*, 28.

797 [N°709] Langmuir, I. *Science* **1921**, *54*, 59.

798 [N°710] Pyykkö, P. *J. Organomet. Chem.* **2006**, *691*, 4336.

799 [N°711] Urtel, H.; Meier, C.; Eisenträger, F.; Rominger, F.; Joschek, J. P.; Hofmann, P. *Angew. Chem. Int. Ed. Engl.* **2001**, *40*, 781.

800 [N°712] Walter, M. D.; White, P. S.; Brookhart, M. *New J. Chem.* **2013**, *37*, 1128.

stabilization of unusual d^8-metal complexes. Along this line numerous stable models of T-shaped complexes of Pd[806-810] and Pt[811-814] have been reported. Figueroa's use of bulky alkylisonitriles as ligands of d-transition metals is a good example of how well steric occlusion and cluttering can force the electron-unsaturated metal centre into unusual coordination geometries.[815-819] Serendipity has offered a host of unusual 16 electron Mn(I) and Re(I) complexes, the structural cohesion of which is thought to stem from a combination of steric cluttering and attractive noncovalent local and nonlocal interactions.[820] In our continued efforts to analyse the non-covalent interactions, the present chapter will present a rational method of synthesis and characterization, determination of the electronic structure, and dynamic behaviour of, neutral 14-electron Pd(II) and Pt(II) complexes.[821,822] The results presented exemplifies the directing and stabilizing virtues of non-covalent interactions like Coulombic attraction and electron correlation between two metal centres taking advantage of the ambiphilic character of the tricarbonyl(η^6-indenyl)chromium anion, the main property of which is to behave as a conventional heteroditopic ligand capable of chelating a metal centre through covalent and noncovalent bonding (as shown by Figure 77 and the map of

801 [N°713] Rivada-Wheelaghan, O.; Ortuño, M. A.; Díez, J.; Lledós, A.; Conejero, S. *Angew. Chem. Int. Ed. Engl.* **2012**, *51*, 3936.
802 [N°714] Braunschweig, H.; Gruss, K.; Radacki, K. *Angew. Chem. Int. Ed. Engl.* **2007**, *46*, 7782.
803 [N°715] Crosby, S. H.; Clarkson, G. J.; Rourke, J. P. *J. Am. Chem. Soc.* **2009**, *131*, 14142.
804 [N°716] Baratta, W.; Stoccoro, S.; Doppiu, A.; Herdtweck, E.; Zucca, A.; Rigo, P. *Angew. Chem. Int. Ed. Engl.* **2003**, *42*, 105.
805 [N°717] Ara, I.; Forniés, J.; García, A.; Gómez, J.; Lalinde, E.; Moreno, M. T. *Chem. Eur. J.* **2002**, *8*, 3698.
806 [N°718] Gerber, R.; Blacque, O.; Frech, C. M. *Dalton Trans.* **2011**, *40*, 8996.
807 [N°719] Pérez-Rodríguez, M. n.; Braga, A. A. C.; de Lera, A. R.; Maseras, F.; Álvarez, R.; Espinet, P. *Organometallics* **2010**, *29*, 4983.
808 [N°720] Yandulov, D. V.; Tran, N. T. *J. Am. Chem. Soc.* **2007**, *129*, 1342.
809 [N°721] Stambuli, J. P.; Weng, Z.; Incarvito, C. D.; Hartwig, J. F. *Angew. Chem. Int. Ed. Engl.* **2007**, *46*, 7674.
810 [N°722] Stambuli, J. P.; Incarvito, C. D.; Bühl, M.; Hartwig, J. F. *J. Am. Chem. Soc.* **2004**, *126*, 1184.
811 [N°723] Kefalidis, C. E.; Tsipis, C. A. *J. Comput. Chem.* **2012**, *33*, 1689.
812 [N°724] Braunschweig, H.; Radacki, K.; Rais, D.; Scheschkewitz, D. *Angew. Chem. Int. Ed. Engl.* **2005**, *44*, 5651.
813 [N°725] Ingleson, M. J.; Mahon, M. F.; Weller, A. S. *Chem. Commun.* **2004**, 2398.
814 [N°726] Clegg, W.; Eastham, G. R.; Elsegood, M. R. J.; Heaton, B. T.; Iggo, J. A.; Tooze, R. P., . . . Zacchini, S. *Organometallics* **2002**, *21*, 1832.
815 [N°727] Lewis, R. A.; George, S. P.; Chapovetsky, A.; Wu, G.; Figueroa, J. S.; Hayton, T. W. *Chem. Commun.* **2013**, *49*, 2888.
816 [N°728] Emerich, B. M.; Moore, C. E.; Fox, B. J.; Rheingold, A. L.; Figueroa, J. S. *Organometallics* **2011**, *30*, 2598.
817 [N°729] Margulieux, G. W.; Weidemann, N.; Lacy, D. C.; Moore, C. E.; Rheingold, A. L.; Figueroa, J. S. *J. Am. Chem. Soc.* **2010**, *132*, 5033.
818 [N°730] Labios, L. A.; Millard, M. D.; Rheingold, A. L.; Figueroa, J. S. *J. Am. Chem. Soc.* **2009**, *131*, 11318.
819 [N°731] Fox, B. J.; Sun, Q. Y.; DiPasquale, A. G.; Fox, A. R.; Rheingold, A. L.; Figueroa, J. S. *Inorg. Chem.* **2008**, *47*, 9010.
820 [N°559] Hyla-Kryspin, I.; Grimme, S.; Djukic, J. P. *Organometallics* **2009**, *28*, 1001.
821 [N°732] Werlé, C.; Bailly, C.; Karmazin-Brelot, L.; Le Goff, X. F.; Ricard, L.; Djukic, J. P. *J. Am. Chem. Soc.* **2013**, *135*, 17839.
822 [N°733] Werlé, C.; Hamdaoui, M.; Bailly, C.; Le Goff, X. F.; Brelot, L.; Djukic, J. P. *J. Am. Chem. Soc.* **2013**, *135*, 1715.

Coulombic potential, Figure 78) thus preserving its unsaturated valence shell. This chapter will further document this peculiar type of chelation.

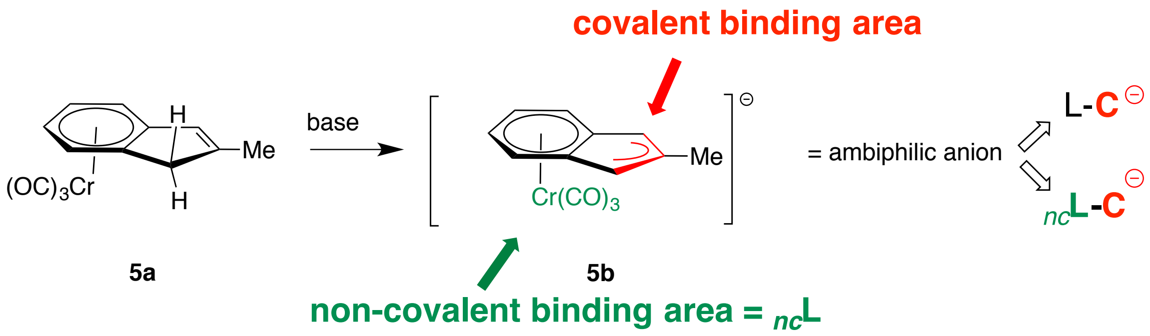

Figure 77: Ambiphilic character of anion **5b**.

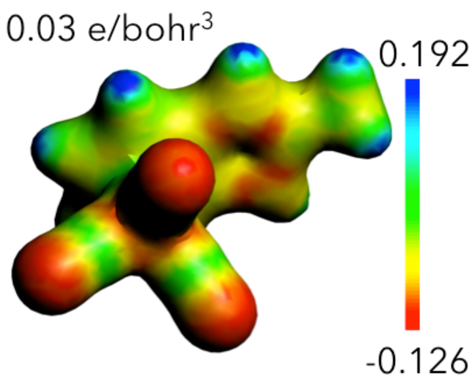

Figure 78: Map of Coulombic Potential of anion **5b** showing the buildup of charge density at the double bond of the indenyl ligand and at the Cr(CO)$_3$ moiety.

3 - The case of (η^3-allyl)-Pd(II) complexes.

3.1 - Experimental aspects.

Indene complexes like **5a** can readily be deprotonated to afford the corresponding anion **5b**, whose stability stems from a major delocalization of charge density all over the complex down to the Cr and O atoms of the Cr(CO)$_3$ moiety, best illustrated by three limiting forms in Figure 79.

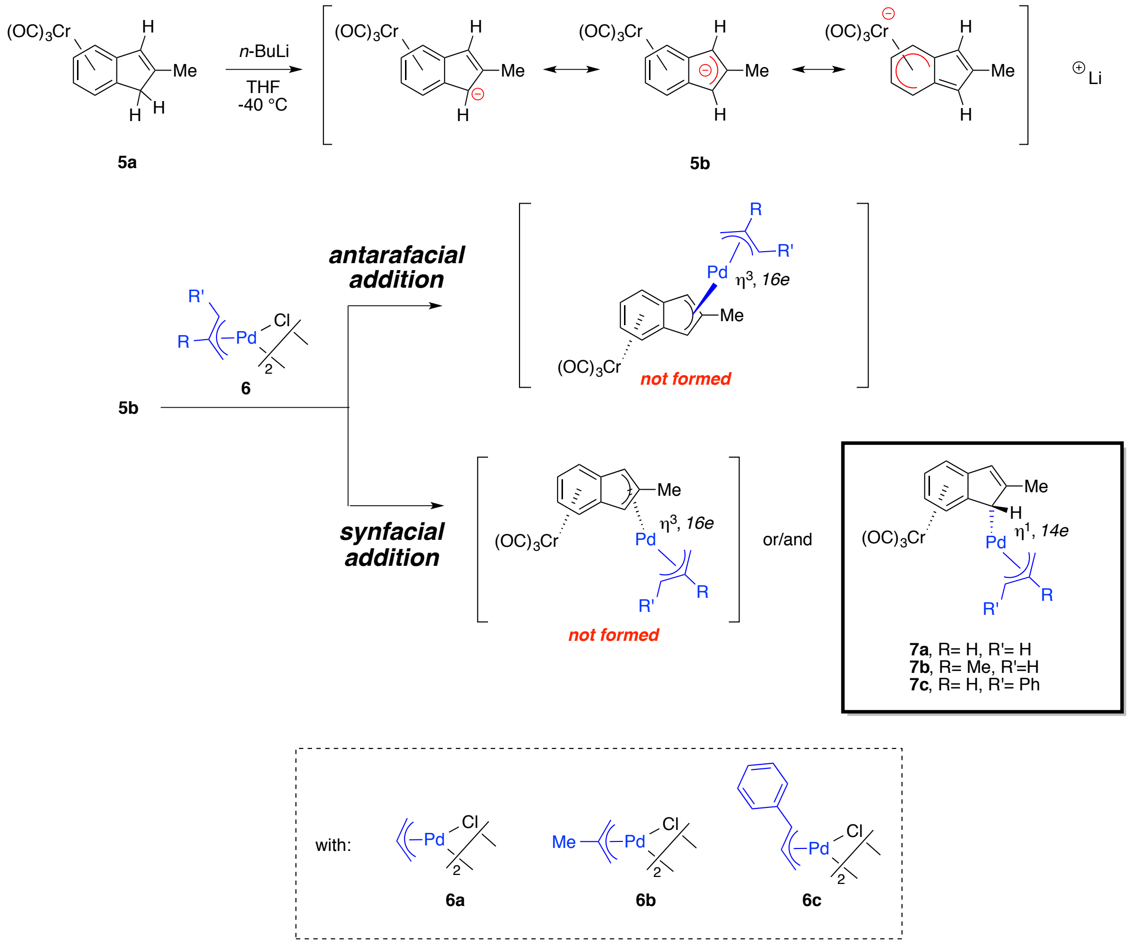

Figure 79: Synthesis of complexes **7a-c** derived from 2-Methyl-1*H*-indene.

Several μ-chloro-bridged (η^3-allyl)palladium dimers **6** were probed for their reactivity toward anion **5b** anticipating the possible formation of a mixture of *syn*- and *antara*-facial products (Figure 79). Nevertheless, treating **5b** with a stoichiometric amount (or slight excess) of bis[(η^3-allyl)palladium chloride], bis[(η^3-2-methylallyl)palladium chloride], or bis[(η^3-1-phenylallyl)palladium chloride] led, after ≈1 h, to the quantitative formation of **7a-c** according to ^{1}H NMR analyses of the reaction medium. Solutions of **7a-c** were persistent for few days at low temperature (*i.e.* below -20 °C) allowing isolation and subsequent analytical characterizations. Suitable crystals for structural X-ray diffraction analyses were obtained under anaerobic conditions by slowly diffusing solutions containing a majority of toluene into dry-*n*-heptane and subsequently handled wet under a cold argon stream to prevent decomposition.

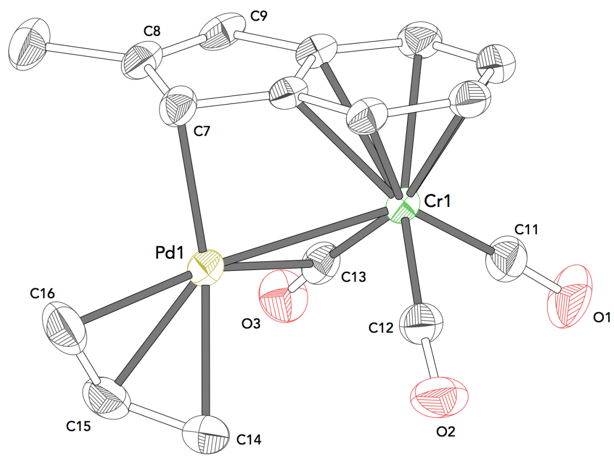

Compound **7a**
Space Group: **P 2_1/c**
R-Factor (%): **4.07**

N°	*A*	*B*	*C*	*Lengths (Å)*	*Angles (°)*
1	Pd_1	Cr_1	-	2.7542(5)	-
2	Pd_1	C_{13}	-	2.428(4)	-
3	Cr_1	C_{13}	-	1.873(4)	-
4	Cr_1	C_{12}	-	1.840(5)	-
5	Cr_1	C_{11}	-	1.832(4)	-
6	Pd_1	C_7	-	2.175(5)	-
7	Pd_1	C_8	-	2.950(5)	-
8	Pd_1	C_{16}	-	2.147(4)	-
9	Pd_1	C_{15}	-	2.133(3)	-
10	Pd_1	C_{14}	-	2.174(5)	-
11	Cr_1	C_{13}	O_3	-	169.2(4)
12	Cr_1	C_{12}	O_2	-	175.7(4)
13	Cr_1	C_{11}	O_1	-	177.2(4)

Figure 80: X-ray structure and selected interatomic distances of compound **7a.**

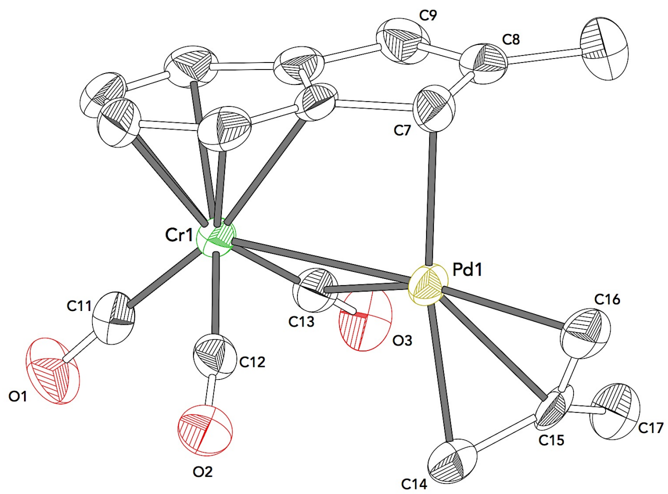

Compound **7b**
Space Group: **P -1**
R-Factor (%): **3.87**

N°	*A*	*B*	*C*	*Lengths (Å)*	*Angles (°)*
1	Pd_1	Cr_1	-	2.7465(6)	-
2	Pd_1	C_{13}	-	2.443(4)	-
3	Cr_1	C_{13}	-	1.862(4)	-
4	Cr_1	C_{12}	-	1.846(3)	-
5	Cr_1	C_{11}	-	1.853(4)	-
6	Pd_1	C_7	-	2.184(4)	-
7	Pd_1	C_8	-	2.868(5)	-
8	Pd_1	C_{16}	-	2.152(3)	-
9	Pd_1	C_{15}	-	2.146(3)	-
10	Pd_1	C_{14}	-	2.168(4)	-
11	Cr_1	C_{13}	O_3	-	169.5(3)
12	Cr_1	C_{12}	O_2	-	174.4(3)
13	Cr_1	C_{11}	O_1	-	177.5(3)

Figure 81: X-ray structure and selected interatomic distances of compound **7b.**

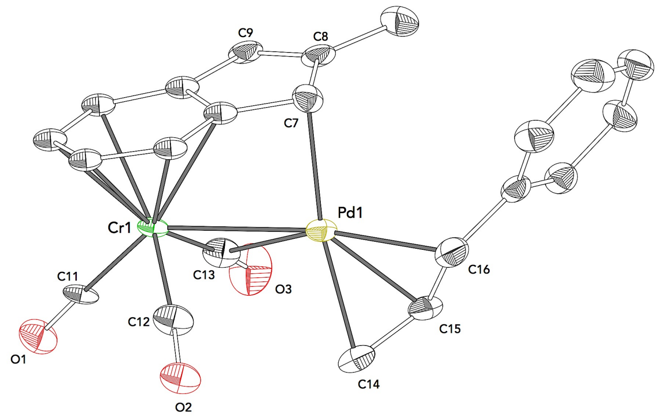

Compound **7c**
Space Group: **P 2$_1$/c**
R-Factor (%): **8.2**

N°	*A*	*B*	*C*	*Lengths (Å)*	*Angles (°)*
1	Pd_1	Cr_1	-	2.737(2)	-
2	Pd_1	C_{13}	-	2.340(1)	-
3	Cr_1	C_{13}	-	1.860(1)	-
4	Cr_1	C_{12}	-	1.850(1)	-
5	Cr_1	C_{11}	-	1.845(9)	-
6	Pd_1	C_7	-	2.193(9)	-
7	Pd_1	C_8	-	2.932(9)	-
8	Pd_1	C_{16}	-	2.218(9)	-
9	Pd_1	C_{15}	-	2.139(9)	-
10	Pd_1	C_{14}	-	2.160(1)	-
11	Cr_1	C_{13}	O_3	-	167.2(9)
12	Cr_1	C_{12}	O_2	-	175.5(9)
13	Cr_1	C_{11}	O_1	-	178.1(8)

Figure 82: X-ray structure and selected interatomic distances of compound **7c.**

Figure 80 to Figure 82 display the X-ray structure of **7a-c** which reveal that the Pd(II) centre is η^1-bonded to the indenyl's five membered ring but also apparently engaged in a delocalized interaction with a proximal carbonyl ligand and with the Cr atom. The Pd-Cr distance of ~2.75 Å lies in the range of those reported by Kalinin *et al.*[823-825] for two [(η^6: η^1- benzyl)-tricarbonylchromium] [(η^3-allyl)palladium] complexes (Figure 83).

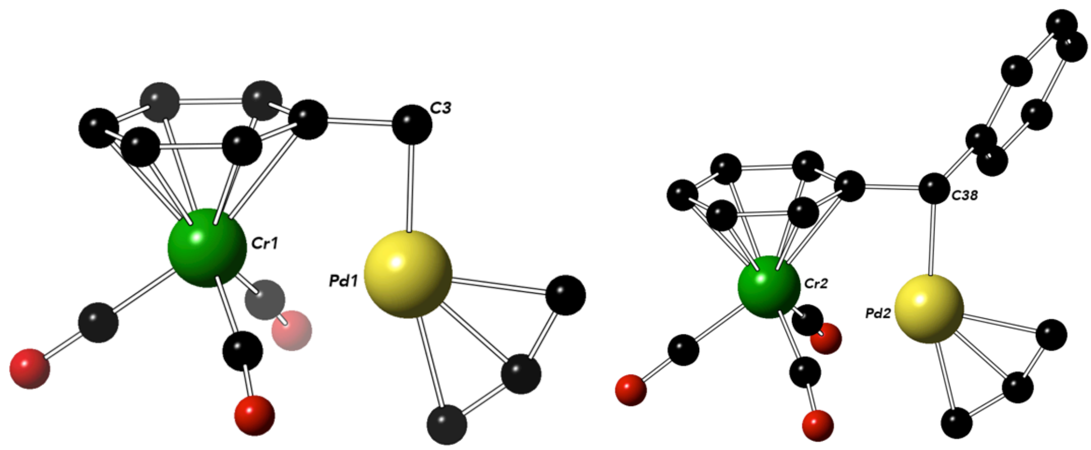

Figure 83: X-Ray structures of molecular analogues of **7a-c** reported by Kalinin *et al.*

[823] [N°734] Moiseev, S. K.; Cherepanov, I. A.; Petrovskii, P. V.; Ezernitskaya, M. G.; Butenschön, H.; Strotmann, M.; Kalinin, V. N. *Inorg. Chim. Acta* **1998**, *280*, 71.

[824] [N°735] Kalinin, V. N.; Cherepanov, I. A.; Moiseev, S. K.; Dolgushin, F. M.; Yanovsky, A. I.; Struchkov, Y. T. *Acta Cryst. Sect. C* **1993**, *49*, 805.

[825] [N°582] Kalinin, V. N.; Cherepanov, i. y. A.; Moiseev, S. K.; Batsanov, A. S.; Struchkov, Y. T. *Mendeleev Commun.* **1991**, *1*, 77.

The C_{13}-Pd distance of ~2.44 Å that materializes the interaction between a CO ligand and the Pd centre is slightly shorter than in Kalinin's cases. The slight bending of the related Cr-C_{13}-O_3 angle of ~170° and the slightly elongated Cr-C_{13} distance, as compared to Cr-C_{12}, suggests a weak bridging interaction. However, the ATR-FTIR spectra of amorphous powders of **7a**, **b** did not reveal any of the typical CO stretching mode expected for a bridging CO ligand but rather stretching modes of a *fac*-$L_3Cr(CO)_3$ moiety consisting of a strong narrow band at 1930 cm^{-1} and a strong and broad band centred at 1840 cm^{-1}. Complex **7c** is characterized by the lifted degeneracy of the carbonyl C-O stretching E band (the A band appears at *ca.* 1941 cm^{-1}) that gives rise to two distinct bands at *ca.* 1864 (s), and 1821 (s) cm^{-1}. This spectroscopic peculiarity characterizes the lack of local C_{3v} symmetry[826,827] at the $Cr(CO)_3$ moiety in the solid state.

3.2 - Theoretical aspects.

Given the possible role of nonlocal interactions (dispersion) in stabilizing bimetallics like **7a-c**,[828-830] state-of-the-art DFT-D3[831] methods as well as other dispersion-corrected functionals, *e.g.*, PBE0-dDsC,[832,833] M06-L, and M06-2X,[834,835] were considered to address the issues of bonding and electronic structure (Figure 84).

[826] [N°736] van Meurs, F.; Baas, J. M. A.; van Bekkum, H. *J. Organomet. Chem.* **1977**, *129*, 347.
[827] [N°737] van Meurs, F.; Baas, J. M. A.; van Bekkum, H. *J. Organomet. Chem.* **1976**, *113*, 353.
[828] [N°599] Grimme, S.; Djukic, J.-P. *Inorg. Chem.* **2010**, *49*, 2911.
[829] [N°559] Hyla-Kryspin, I.; Grimme, S.; Djukic, J. P. *Organometallics* **2009**, *28*, 1001.
[830] [N°562] Schwabe, T.; Grimme, S.; Djukic, J.-P. *J. Am. Chem. Soc.* **2009**, *131*, 14156.
[831] [N°738] Grimme, S.; Antony, J.; Ehrlich, S.; Krieg, H. *J. Chem. Phys.* **2010**, *132*, 154104.
[832] [N°739] Steinmann, S. N.; Piemontesi, C.; Delachat, A.; Corminboeuf, C. *J. Chem. Theory Comput.* **2012**, *8*, 1629.
[833] [N°740] Steinmann, S. N.; Corminboeuf, C. *J. Chem. Theory Comput.* **2011**, *7*, 3567.
[834] [N°741] Zhao, Y.; Truhlar, D. *Theor. Chem. Acc.* **2008**, *120*, 215.
[835] [N°742] Zhao, Y.; Truhlar, D. G. *J. Chem. Phys.* **2006**, *125*.

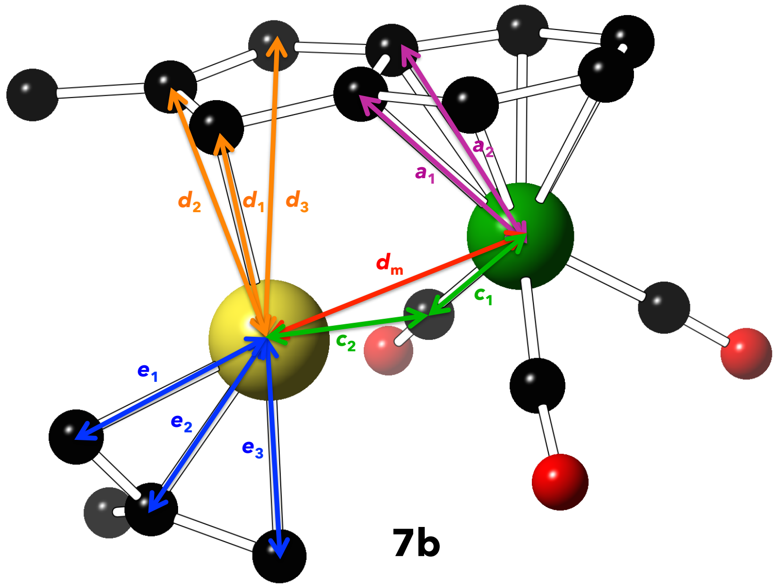

	expt	PBE-D3(BJ)	PBE	M06-L	M06-2X	TPSS-D3(BJ)	B3LYP	B3LYP-D3	PBE0	PBE0-DdSc
a_1	*2.275*	2.275	2.283	2.252	2.306	2.272	2.316	2.299	2.264	2.251
a_2	*2.344*	2.378	2.396	2.341	2.359	2.36	2.413	2.38	2.42	2.317
d_m	*2.747*	2.728	2.759	2.788	2.839	2.722	2.832	2.782	2.751	2.724
d_1	*2.184*	2.212	2.225	2.23	2.269	2.21	2.237	2.216	2.196	2.181
d_2	*2.868*	2.935	2.977	2.941	2.901	2.919	2.998	2.938	2.938	2.888
d_3	*3.419*	3.476	3.514	3.545	3.451	3.447	3.566	3.505	3.482	3.434
c_1	*1.862*	1.867	1.831	1.86	1.847	1.878	1.868	1.863	1.849	1.843
c_2	*2.444*	2.445	2.444	2.462	2.741	2.444	2.567	2.529	2.495	2.462
e_1	*2.152*	2.179	2.185	2.166	2.186	2.176	2.194	2.189	2.156	2.15
e_2	*2.146*	2.155	2.166	2.187	2.175	2.153	2.196	2.18	2.154	2.141
e_3	*2.168*	2.201	2.208	2.218	2.209	2.194	2.228	2.218	2.181	2.173
Δd_m	-	**-0.009**	**0.012**	**0.041**	**0.092**	**-0.025**	**0.085**	**0.035**	**0.004**	**-0.023**
Δa_1	-	**0.008**	**-0.023**	**0.031**	**-0.003**	**0.041**	**0.024**	**-0.011**	**0.012**	**0.008**
Δd_1	-	**0.028**	**0.041**	**0.046**	**0.085**	**0.026**	**0.053**	**0.032**	**0.012**	**-0.003**
Δe_2	-	**0.009**	**0.02**	**0.041**	**0.029**	**0.007**	**0.05**	**0.034**	**0.008**	**-0.005**

Figure 84: List of interatomic distances in models **7b** computed with various functionals ((ZORA) GGA, meta-GGA, hybrid (all-electron TZP basis set). Interatomic distance shifts are given relative to the experimental (X-ray diffraction analysis) value and defined for example as: $\Delta d_x = d_x^{calcd} - d_x^{exptl}$.

Grimme's DFT-D3 methods with the so-called Becke-Johnson (BJ)[836] damping function, *e.g.*, TPSS[837]-D3(BJ)[838,839] or PBE[840]-D3(BJ)[841,842] and Corminboeuf's density-dependent dispersion-corrected functional PBE0[843, 844]-dDsC[845] reproduced well the singlet ground-state geometry of **7b**, particularly in the vicinity of the two metal atoms, a critical area where non-covalent interactions obviously dominate. Notably, M06-2X and B3LYP[846] equally produced long and non-realistic interatomic distances for Cr-arene and Pd-allyl bonds. The largest deviation from experiment, *i.e.*, ~0.1 Å, was noticed for the Cr-Pd distance. Therefore, further investigations were carried out with PBE-D3(BJ), TPSSD3(BJ), or PBE0-dDsC functionals associated with all-electron triple-ζ Slater-type basis sets for all elements within the ZORA[847] formalism.

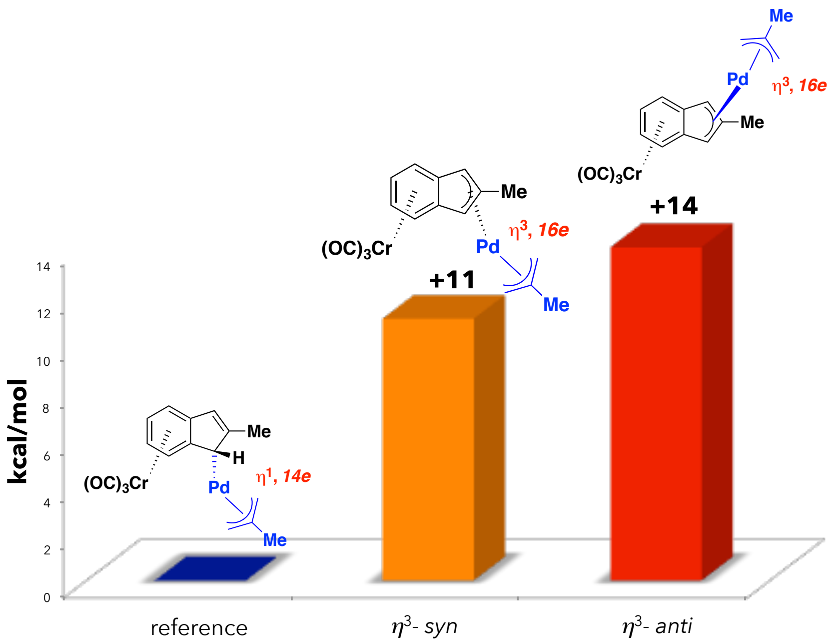

Figure 85: Energetic bias in favor of the η^1 mode in the *syn*-facial arrangement.

836 [N°187] Grimme, S.; Ehrlich, S.; Goerigk, L. *J. Comput. Chem.* **2011**, *32*, 1456.
837 [N°743] Tao, J.; Perdew, J. P.; Staroverov, V. N.; Scuseria, G. E. *Phys. Rev. Lett.* **2003**, *91*, 146401.
838 [N°738] Grimme, S.; Antony, J.; Ehrlich, S.; Krieg, H. *J. Chem. Phys.* **2010**, *132*, 154104.
839 [N°187] Grimme, S.; Ehrlich, S.; Goerigk, L. *J. Comput. Chem.* **2011**, *32*, 1456.
840 [N°170] Perdew, J. P.; Burke, K.; Ernzerhof, M. *Phys. Rev. Lett.* **1996**, *77*, 3865.
841 [N°738] Grimme, S.; Antony, J.; Ehrlich, S.; Krieg, H. *J. Chem. Phys.* **2010**, *132*, 154104.
842 [N°187] Grimme, S.; Ehrlich, S.; Goerigk, L. *J. Comput. Chem.* **2011**, *32*, 1456.
843 [N°744] Ernzerhof, M.; Scuseria, G. E. *J. Chem. Phys.* **1999**, *110*, 5029.
844 [N°745] Adamo, C.; Barone, V. *J. Chem. Phys.* **1999**, *110*, 6158.
845 [N°740] Steinmann, S. N.; Corminboeuf, C. *J. Chem. Theory Comput.* **2011**, *7*, 3567.
846 [N°746] Stephens, P. J.; Devlin, F. J.; Chabalowski, C. F.; Frisch, M. J. *J. Phys. Chem.* **1994**, *98*, 11623.
847 [N°747] van Lenthe, E.; van Leeuwen, R.; Baerends, E. J.; Snijders, J. G. *Int. J. Quantum Chem.* **1996**, *57*, 281.

Calculations performed on models of **7a,b** (Figure 85) confirmed that the η^1 coordination mode of the cyclopentadienylic part of the indenyl ligand to Pd surpassed in stability the η^3 one by ~11 kcal/mol (including zero point energy, ZPE) in the *syn*-facial bimetallic arrangement, where the Cr-Pd distance amounts to ~2.7 Å. The η^3 mode entails a Cr-Pd distance of ~3.1 Å, with an *anti*-eclipsed conformation of the $Cr(CO)_3$ tripod. Furthermore, the η^1 *syn*-facial arrangement was more favourable by ~13 kcal/mol (ZPE included) than the *antara*-facial alternative, which favours η^3 coordination of the indenyl to the Pd(II) centre, in good agreement with early conclusions of Nakamura *et al.* on monometallic indenyl analogues.[848]

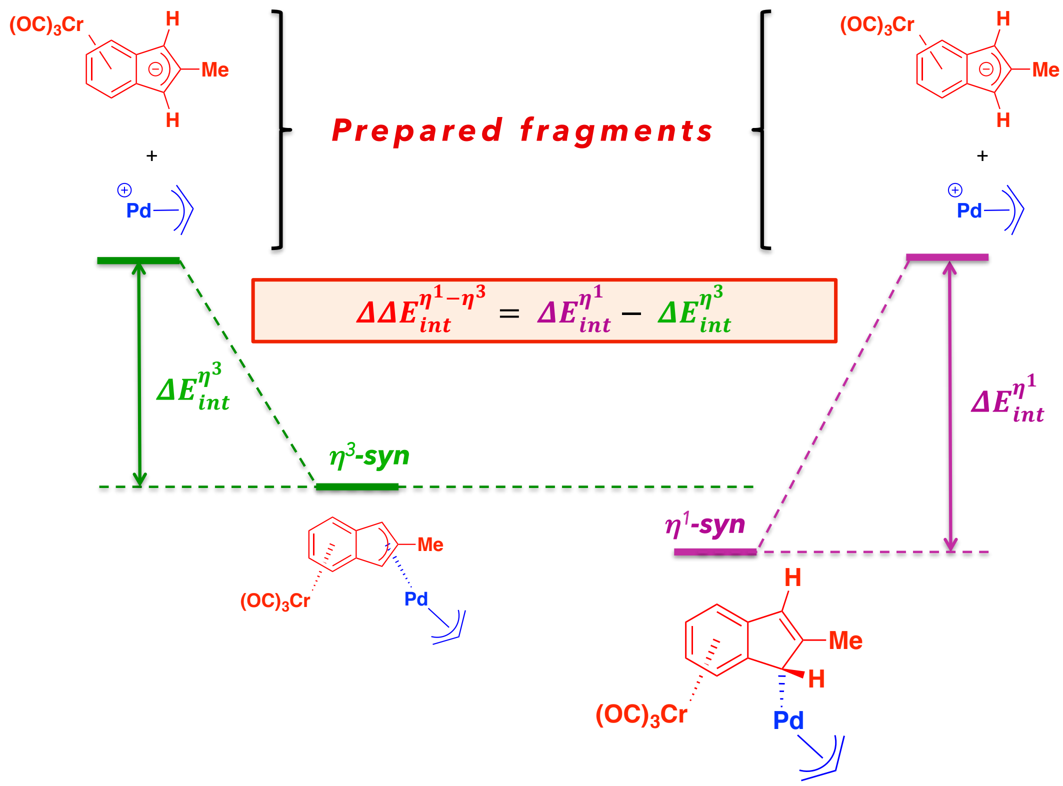

Figure 86: Considered fragments for the energy decomposition analysis.

This energetic bias in favour of the η^1 mode in the *syn*-facial arrangement was investigated by a comparative energy decomposition analysis[849] with η^1-**7a** and η^3-**7a**, which allowed a detailed dichotomy of the intrinsic interaction energy ΔE_{int} into

848 [N°748] Nakasuji, K.; Yamaguchi, M.; Murata, I.; Tatsumi, K.; Nakamura, A. *Organometallics* **1984**, *3*, 1257.

849 [N°749] Ziegler, T.; Rauk, A. *Inorg. Chem.* **1979**, *18*, 1755.

repulsive (Pauli, ΔE_{Pauli}) and attractive (electrostatic ΔE_{elec}, orbital ΔE_{orb}, and dispersion ΔE_{disp}) interaction energy terms for the interactions of prepared anion **5b** with prepared $[(\eta^3\text{-allyl})\text{palladium}]^+$ (Figure 86).

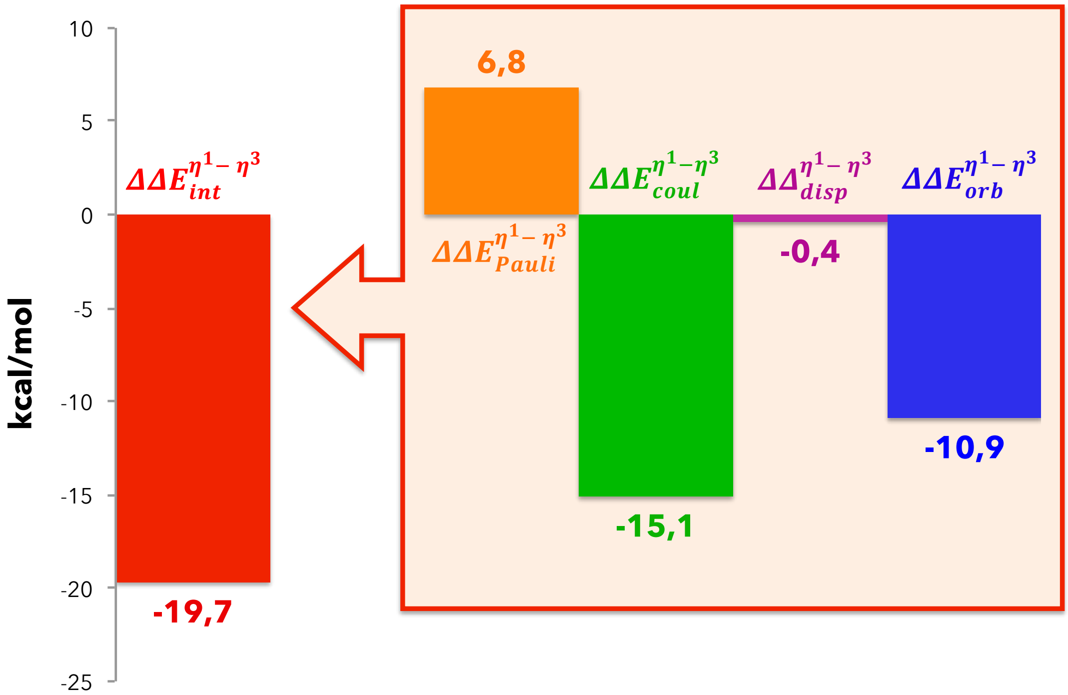

$$\Delta\Delta E^{\eta^1-\eta^3}_{int} = \Delta\Delta E^{\eta^1-\eta^3}_{Pauli} + \Delta\Delta E^{\eta^1-\eta^3}_{coul} + \Delta\Delta^{\eta^1-\eta^3}_{disp} + \Delta\Delta E^{\eta^1-\eta^3}_{orb}$$

Figure 87: Contribution of each term in the stabilization of the η^1 coordination mode.

The preference for the η^1 mode (Figure 87) stems from larger orbital and electrostatic interaction energy terms, as suggested by the energy difference: $\Delta\Delta E^{\eta^1-\eta^3}_{int} = \Delta E^{\eta^1}_{int} - \Delta E^{\eta^3}_{int}$: $\Delta\Delta E^{\eta^1-\eta^3}_{int} = -19.7$ kcal/mol, $\Delta\Delta E^{\eta^1-\eta^3}_{Pauli} = +6.8$ kcal/mol, $\Delta\Delta E^{\eta^1-\eta^3}_{coul} = -15.1$ kcal/mol, $\Delta\Delta^{\eta^1-\eta^3}_{disp} = -0.4$ kcal/mol, $\Delta\Delta E^{\eta^1-\eta^3}_{orb} = -10.9$ kcal/mol.

The larger Coulombic term in η^1-**7a** is associated with a marked polarization of the molecule and an imbalance in the charge density distribution around the Pd (natural charge q_{NPA} = +0.598) and Cr (q_{NPA} = −0.815) atoms. Analysis of the Wiberg bond indices (WBI) outlined the low covalent character of the interaction between the Pd centre and the arenechromiumtricarbonyl moiety. In η^1-**7a**, $WBI_{Pd\text{-}Cr}$, $WBI_{Pd\text{-}C(7)}$, and $WBI_{Pd\text{-}C(13)}$ amount to 0.14, 0.26, and 0.20, respectively, and the weak covalent Pd-C_{13}

interaction does not affect $WBI_{C(13)-O(3)}$ (2.01), which is similar to $WBI_{C(12)-O(2)}$ (2.07). NOCV-ETS analyses[850,851] provided a picture of the direction of electron density transfer in the orbital interaction between the closed-shell prepared anionic and cationic fragments, *i.e.*, **5b** and [(η^3-allyl)palladium]$^+$, respectively, in η^1-**7a**. (Figure 88) displays the density-deformation plots of the first four NOCVs of highest orbital interaction energies.

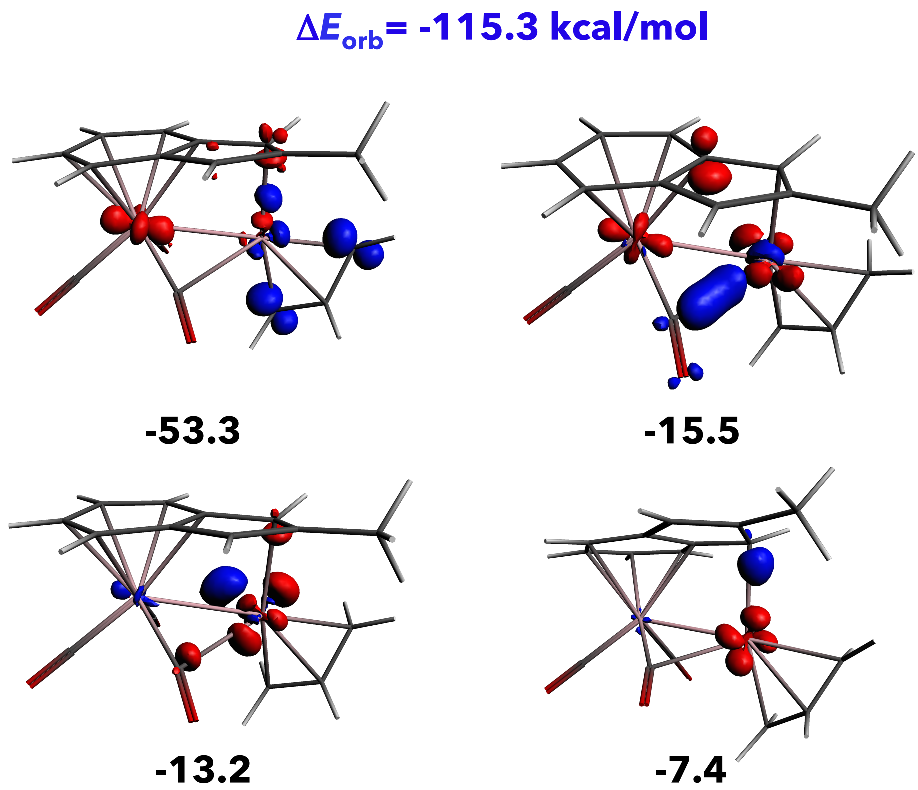

Figure 88: NOCV-ETS $\Delta\rho^{orb}$ deformation densities computed at the (ZORA) PBE[-D3(BJ)]/all-electron TZP level for the interaction between closed-shell prepared fragments **5b** and [(η^3-allyl)Pd]$^+$ in η^1-**7a** with the associated orbital interaction energies (kcal/mol) with isosurfaces of 0.01 and 0.005 e/bohr^3 for the plots of highest orbital interaction energy and for the remaining three plots respectively. Blue and red colours are respectively associated with areas of electron density build-up and depletion upon interaction.

The strongest contribution (Figure 88, −53.3 kcal/mol) corresponds to a transfer of electron density from the Cr and benzylic position toward the allyl ligand π system, the Pd centre and the Pd-C_7 σ bond. This contribution of Cr is complemented with a donation of electron density to the C_7-Pd σ bond from the Pd centre in the

[850] [N°750] Mitoraj, M. P.; Michalak, A.; Ziegler, T. *J. Chem. Theory Comput.* **2009**, *5*, 962.

[851] [N°751] Mitoraj, M. P.; Michalak, A.; Ziegler, T. *Organometallics* **2009**, *28*, 3727.

representation of lowest energy (−7.4 kcal/mol). The Pd-C_{13} σ bond (−15.5 kcal/mol) results from density donation of the two metal centres and the arene's π system. As for a possible Cr-Pd interaction (Figure 88, −13.2 kcal/mol), the analysis suggested some density transfer from Pd to the Cr centre and toward a volume of space located within the Pd-C_6-Cr triangle.

Analysis of the electron pairing in a geometrically correct model of **7b** (Figure 89) by the electron localization function[852,853] (ELF) revealed a weak disynaptic domain in the Cr-Pd segment (0.2 < ELF < 0.3) and no sensible disynaptic domain for the Pd-C_{13} interaction.

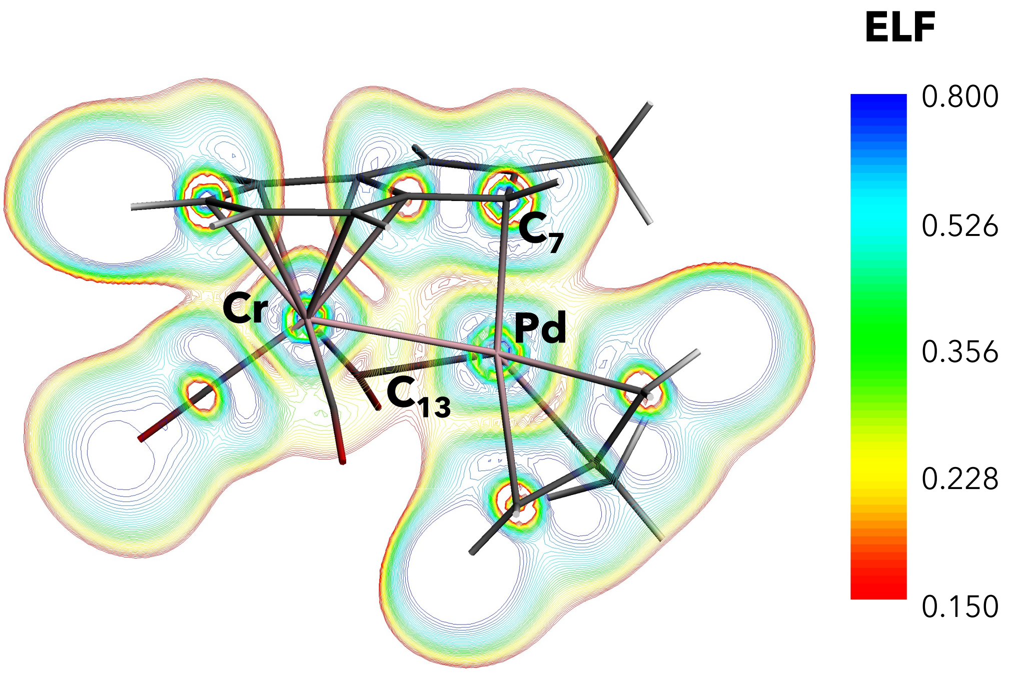

Figure 89: Contour plot of the ELF in **7b** from a (ZORA) PBE0 (-dDsC)/all-electron-TZP gas phase minimum in the plane defined by Cr, Pd, and C_7.

In slight contrast, the so-called atom-in-molecules[854,855] analysis (Figure 90) of the electron density topology revealed no bond critical point (BCP) within or in the vicinity

[852] [N°752] Savin, A.; Jepsen, O.; Flad, J.; Andersen, O. K.; Preuss, H.; von Schnering, H. G. *Angew. Chem. Int. Ed. Engl.* **1992**, *31*, 187.

[853] [N°753] Becke, A. D.; Edgecombe, K. E. *J. Chem. Phys.* **1990**, *92*, 5397.

[854] [N°754] Popelier, P. *Atoms in Molecules, An Introduction*; Prentice Hall, Harlow, England, **2000**.

[855] [N°755] Bader, R. F. W. In *Atoms in Molecules: A Quantum Theory*; Clarendon: Oxford, **1990**.

of the Cr-Pd segment. Nonetheless, a BCP displaying features typical of a weak closed-shell interaction was found within the Pd-C_{13} segment (BCP#60, Figure 90).

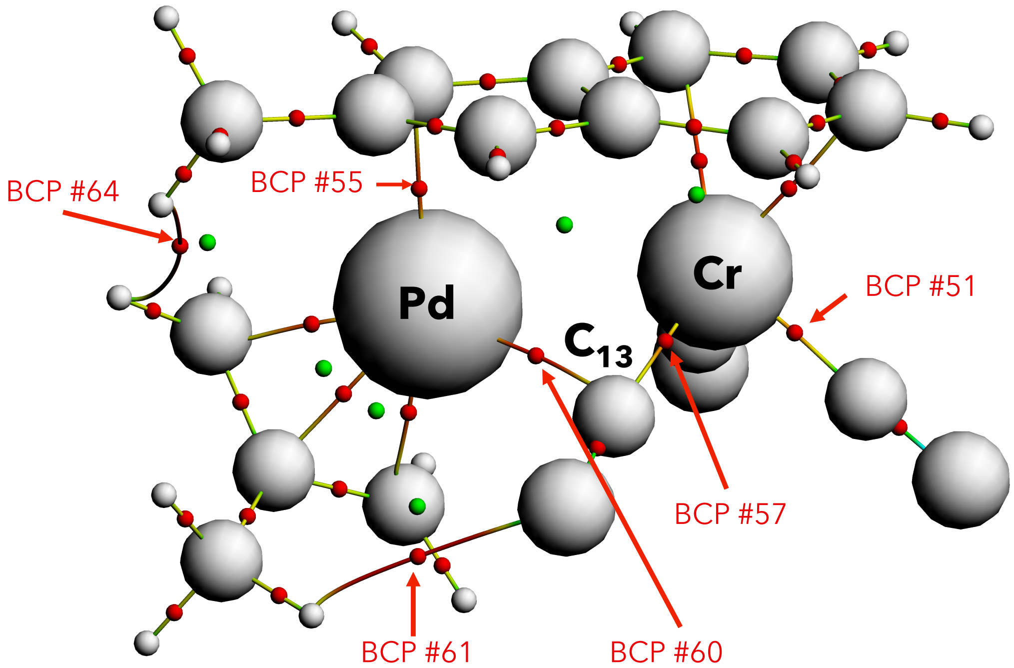

Figure 90: Atom-in-molecules analysis of the electron density topology for **7b**. Red and green dots are associated to Bond (BCP) and Ring (RCP) Critical Points respectively. Grey spheres materialize the atomic critical points scaled by the associated density. Selected BCPs: #51, r= 0.1394 Lb= 0.1338; #55, r= 0.0856 Lb= -0.0444; #57, r=0.1335 Lb= -0.1193; #60, r=0.0493 Lb= -0.0290; #61, r= 0.00516 Lb= -0.00532; #64, r= 0.0407 Lb= - 0.00348. BCPs 55 and 60 correspond to the same type of closed shell interactions according to Popelier. BCP 61 does not fully fulfil the criteria for H bonding due to long interatomic distance. Worthy to note, there is no BCP in the Cr-Pd segment or in its immediate vicinity.

In summary, all analyses concurred in establishing the nature of the interaction between the Pd centre and the $Cr(CO)_3$ moiety as mostly non-covalent.

3.3 - A Fluxional behaviour.

In solution, **7a-c** displayed fluxional behaviour on the time scale of ^{1}H (600 MHz) and ^{13}C (150 and 125 MHz) NMR spectroscopy. At room temperature, the ^{13}C NMR spectra of the three complexes displayed multiple large signals for the carbonyls of the $Cr(CO)_3$ moiety (Figure 91): a set of two signals in a 1:2 ratio at ~239 and 235 ppm for **7a,b** and a set of three signals in a 1:1:1 ratio at δ 238, 236, and 235 ppm for **7c**.

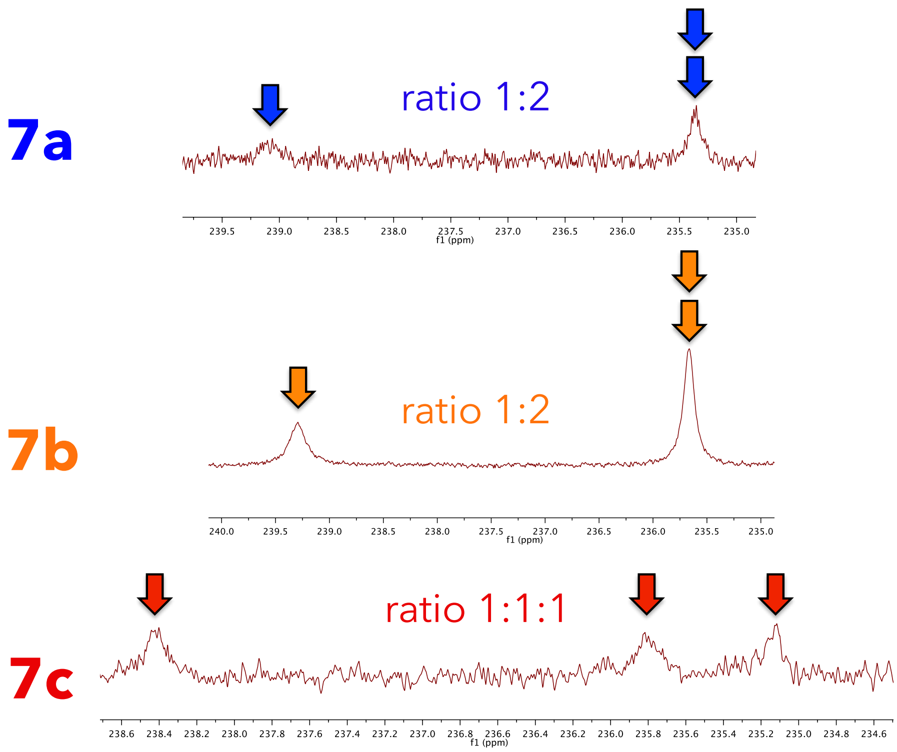

Figure 91: Multiple large ^{13}C NMR signals at room temperature for the carbonyls of the $Cr(CO)_3$ moiety in the case of complexes **7a-c**.

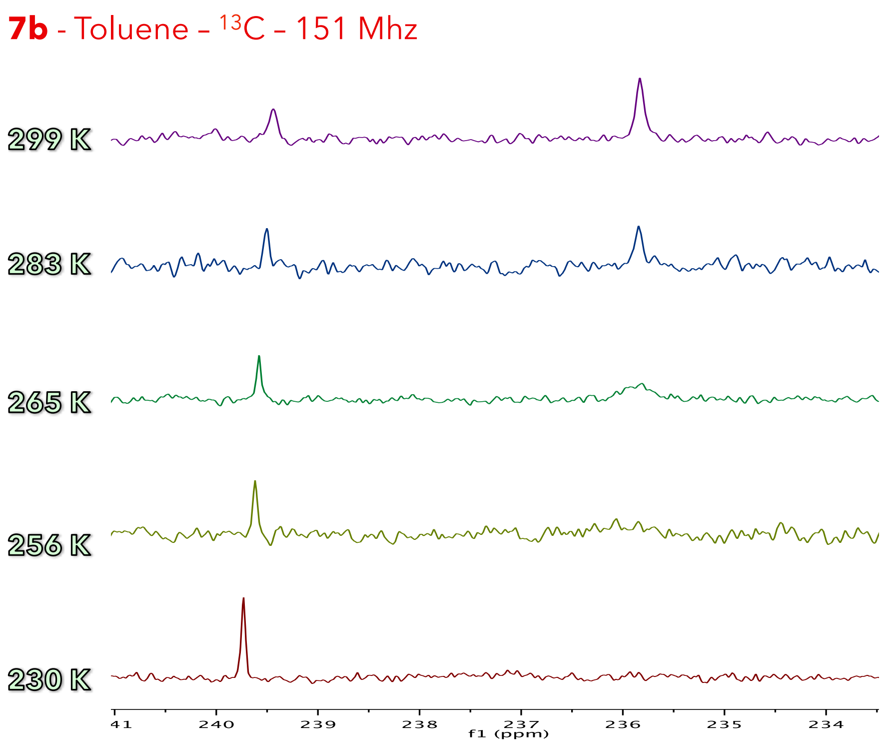

Figure 92: ^{13}C NMR variable temperature experiment displaying the evolution of the carbonyl signals of the $Cr(CO)_3$ moiety.

Low temperature ^{13}C NMR experiments on **7b** (Figure 92) further revealed the temperature dependence of the line width and of the apparent intensity ratio of the signals arising from $Cr(CO)_3$. These symptoms of significant hindrance to rotation operated over the $Cr(CO)_3$ rotor were accompanied by other signs of fluxionality for the indenyl ^{13}C and ^{1}H signals.

The ^{1}H NMR spectra of **7a,b** at 298(1) K displayed patterns of apparently symmetric molecules very much in agreement with a putative symmetric η^3-**7a, b** static model in which the Pd would be η^3-bound to the indenyl (Figure 93).

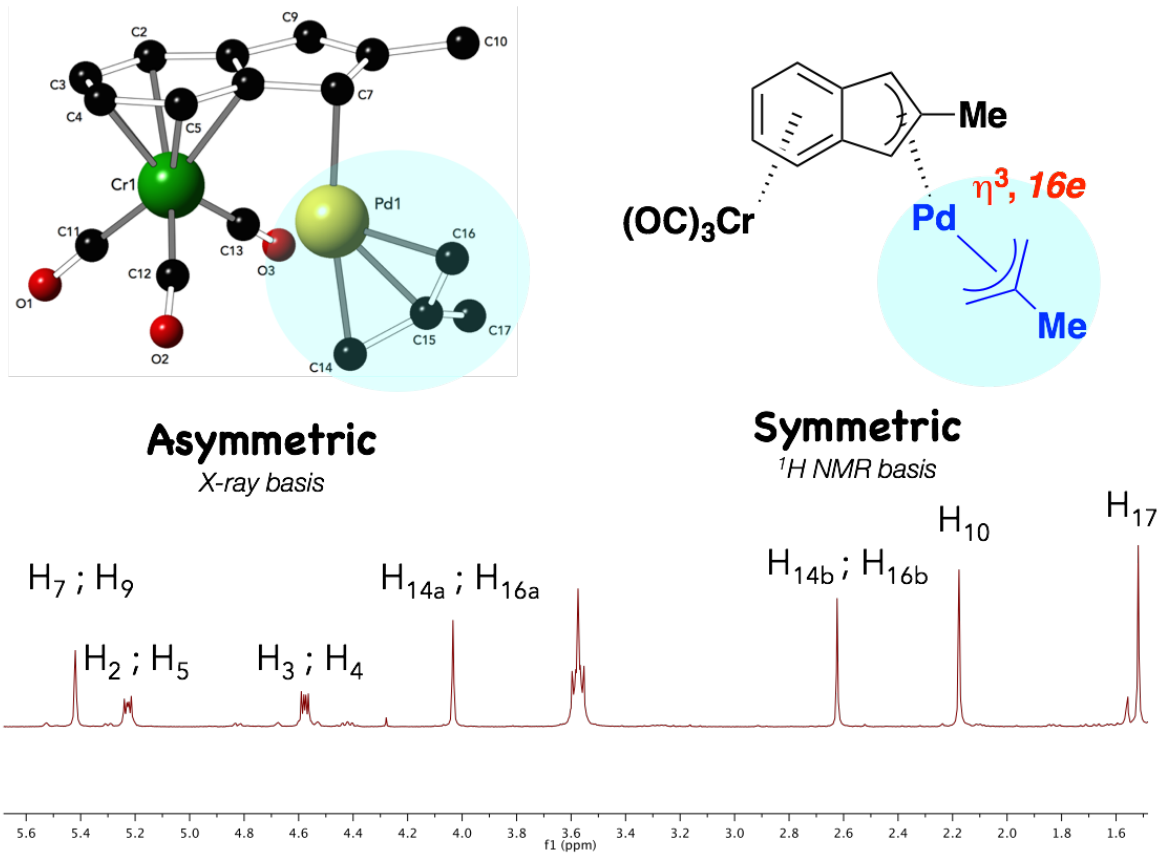

Figure 93: Contradictions between the ^{1}H NMR spectrum of an apparently symmetric molecule and the X-ray structure showing an asymmetric complex.

However, at room temperature, the indenyl protons attached to C_7 and C_9, *i.e.*, H_7 and H_9, showed up as a single broad singlet in the ^{1}H NMR spectra (600 MHz) that would broaden significantly upon decreasing the temperature to 223(1) K (Figure 94).

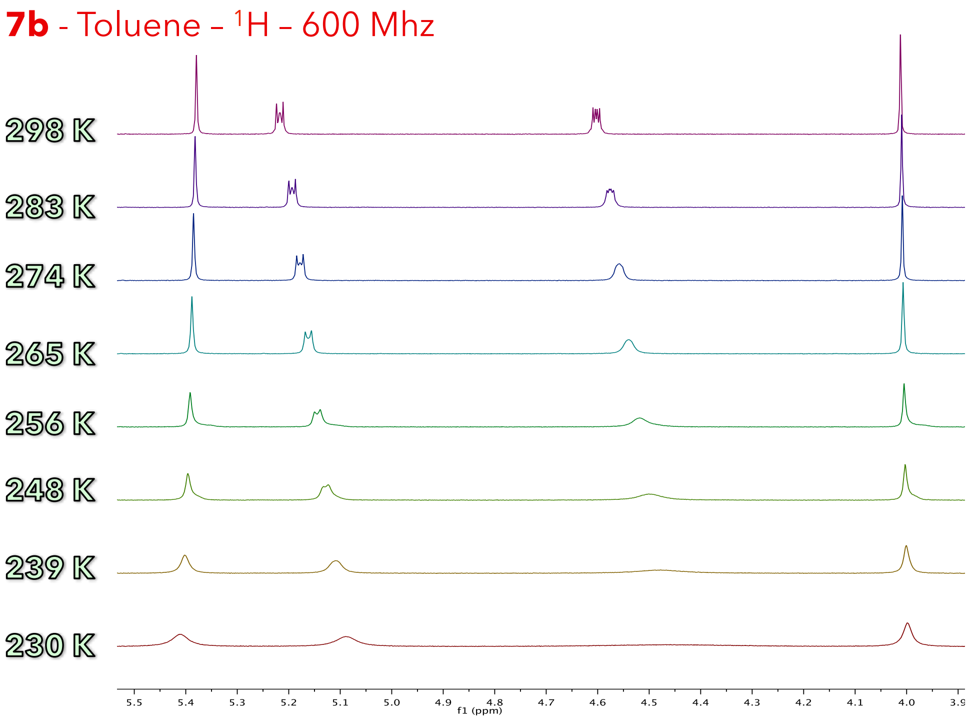

Figure 94: ^{1}H NMR variable temperature displaying the signal broadening upon decreasing the temperature.

A full line-shape analysis[856] was undertaken (all details in experimental) with **7b** assuming that the temperature dependence of the line width of the indenyl-related protons was the result of fluxionality via haptotropy, *i.e.*, reversible migration of the Pd centre from C_7 to C_9 in a typical η^1-η^3-η^1 sequence, where the η^3 state is a metastable intermediate (Figure 95).

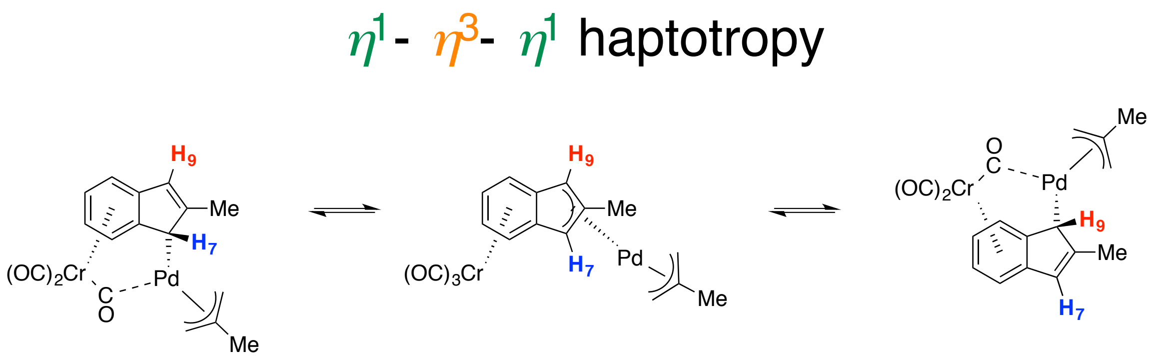

η^1-**7b** η^3-**7b** η^1-**7b**

Figure 95: Supposed fluxional behavior of the Pd centre.

[856] [N°756] Sandstrom, J. *Dynamic NMR Spectroscopy*; Academic Press: New York, **1982**.

Similar cases of fluxional behavior were evidenced with η^1-bound Cu(I) and Hg(II) indenyl complexes[857,858] (Figure 96).

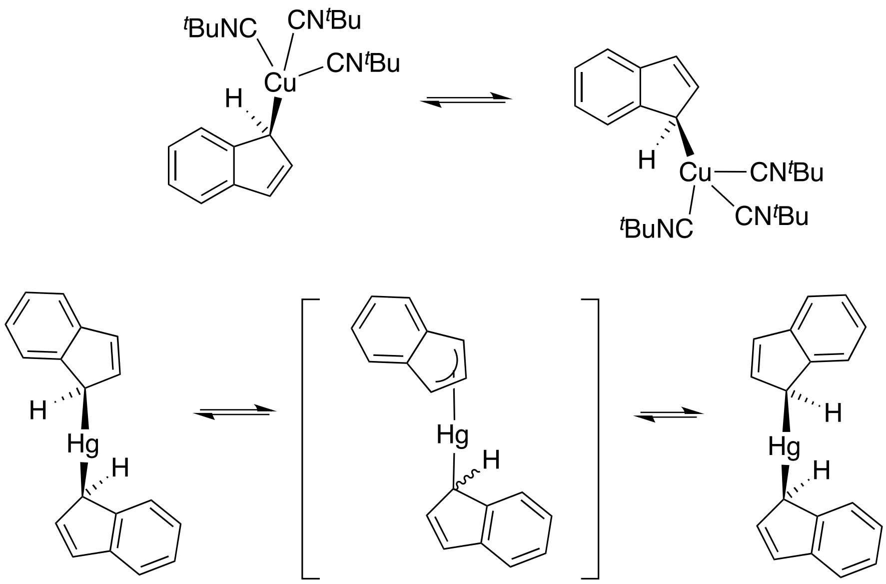

Figure 96: Fluxional behaviour of Cu(I) and Hg(II) derivatives.

Convergent DFT calculations of the theoretical ^{1}H NMR spectrum of η^1-**3b** solvated by toluene (COSMO[859] model) at two different levels of theory (ZORA/PBE- D3(BJ)/AE-TZP and ZORA-SAOP[860]/AE-TZP) provided the low-exchange-rate peak separation for uncoupled H_7 and H_9 ($\Delta\delta$ = 0.270 ppm), a key parameter that could not be determined by experiment (Figure 97).

857 [N°657] Stradiotto, M.; McGlinchey, M. J. *Coord. Chem. Rev.* **2001**, *219-221*, 311.

858 [N°757] Cotton, F. A.; Marks, T. J. *J. Am. Chem. Soc.* **1969**, *91*, 3178.

859 [N°758] Klamt, A.; Schuurmann, G. *J. Chem. Soc., Perkin Trans. 2* **1993**, 799.

860 [N°759] Gritsenko, O. V.; Schipper, P. R. T.; Baerends, E. J. *Chem. Phys. Lett.* **1999**, *302*, 199.

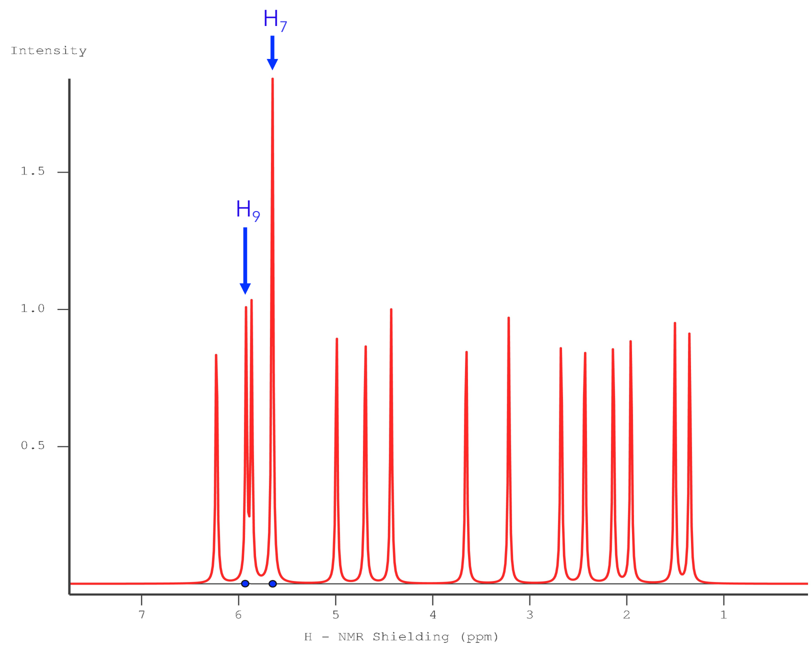

Figure 97: Theoretical ^{1}H NMR spectrum (ADFview 2012) calculated for η^1-**7b** at the COSMO(toluene)(ZORA)-SAOP/AE-TZP level from a ground state singlet geometry calculated at the COSMO (toluene) (ZORA)-PBE-D3(BJ)/AE-TZP. The two blue dots point the peaks arising from H_9 (left hand side peak) and H_7 (right hand side peak). The numbering is that of the experimental structure of **3b**, H_7 is connected to C_7, the carbon atom vicinal to the Pd centre.

The DNMR3 Binsch-Kleier algorithm[861] applied to a set of spectra recorded at 223(1)–273(1) K provided exchange rates *k* spanning 2−23.5 kHz (Figure 98 and Figure 99).

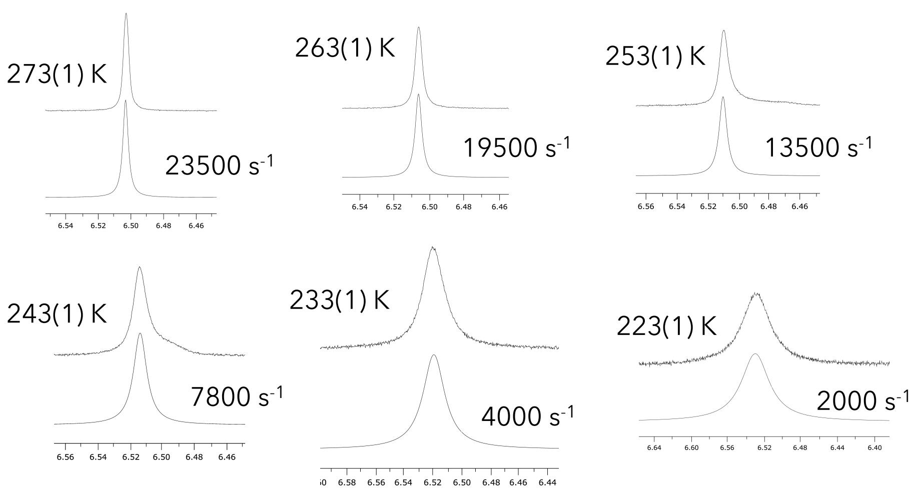

Figure 98: Line shape analysis of the mutual exchange between H_7 and H_9. Upper and lower plots correspond to the experimental and simulated lorentzian spectra respectively.

[861] [N°760] Binsch, G.; Kleier, D. A. *QCPE No. 165*; Indiana University, **1970**.

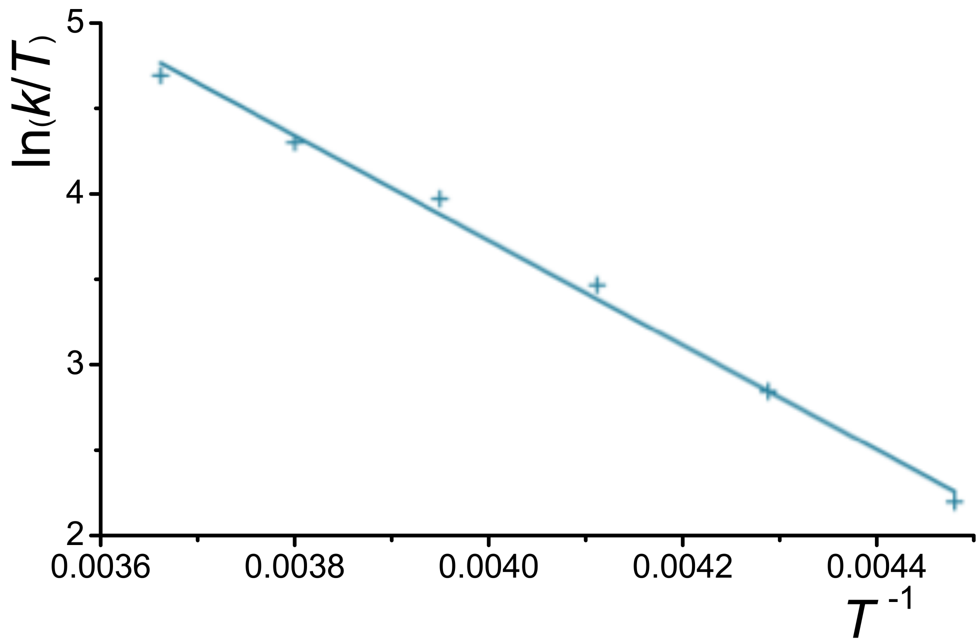

Figure 99: Eyring plot of ln(*k/T*) vs T^{-1} (K^{-1}) for exchange rate constants (equipopulated mutual exchange, T_2 = 0.5 s) determined from ^{1}H NMR (600 MHz) line-shape analysis of the H_7 and H_9 signals of **7b** between 213(1) and 263(1) K in ~10:1 d_8-toluene/THF.

Treatment of the associated Eyring curve (Figure 99) produced the enthalpy and entropy of activation, $\Delta H^{\ddagger} = +6.0(2)\ kcal/mol$ and $\Delta S^{\ddagger} = -15.5(9) cal/mol \cdot K$ which were reasonably approached theoretically (toluene COSMO ZORA-PBE-D3(BJ)/AE TZP, rigid rotor harmonic oscillator approximation), assuming the $\eta^3 \rightarrow \eta^1$ barrier to be negligible (Figure 100): $\Delta H_c^{\ddagger} = +9.9(2)\ kcal/mol$ and $\Delta S_c^{\ddagger} = -0.7(9) cal/mol \cdot K$.

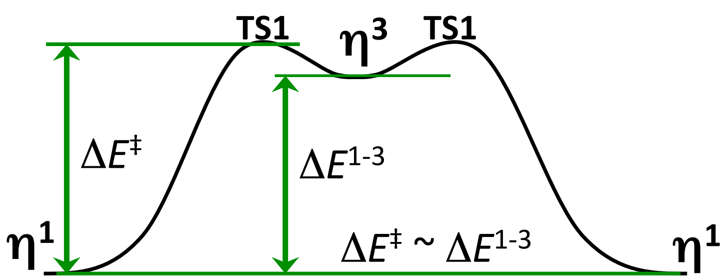

Figure 100: Diagram describing the mutual exchange between the indenyl benzylic positions assuming the $\eta^3 \rightarrow \eta^1$ barrier to be negligible.

With **7c**, similar dynamic features were observed in the NMR spectra. However, due to the compound's asymmetry and the near impossibility of measuring the slow exchange ^{1}H NMR spectrum, information from VT NMR data was not sought. The possible contribution of the allyl ligand's η^1-η^3 isomerization[862] (Figure 101) to the observed fluxionality was ruled out based on theory and experiment.

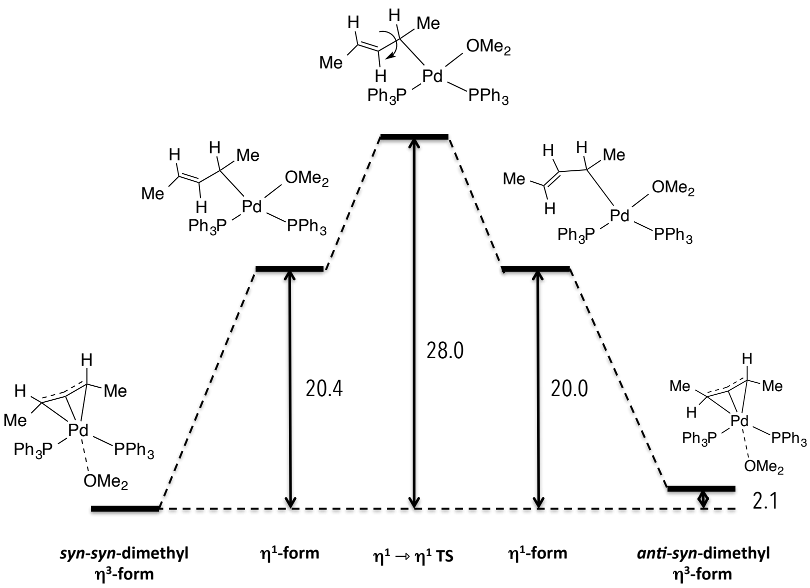

Figure 101: Diagram reproducing the $\eta^3 \rightarrow \eta^1 \rightarrow \eta^3$ isomerization process of (η^3-allyl)palladium complexes have been studied by Solin *et al.*[863] by applying density functional theory at the B3PW91(DZ+P) level.

The energies of the related η^1-allyl intermediates were systematically higher than that of the putative η^3 metastable intermediate, whether or not an explicit THF molecule was introduced to promote η^1-η^3 allyl isomerization. ^{1}H NMR signals associated with the terminal CH_2 position of the allyls were insensitive to temperature change in all cases, supporting a passive role of the allyl ligand in the abovementioned fluxionality.

Complexes **7a-c** proved to be stable for hours in benzene or toluene solutions under anaerobic conditions. Exposure to air or to a slight excess of PPh_3 led to rapid decomposition by loss of Pd(0), affording a variety of products of heterocoupling between the tricarbonyl(η^6-2-methylindenyl)chromium moiety and the allyl ligand, *i.e.*, **8a-c** (Figure 102). Compounds **7a,b** were generally unstable in the solid state under vacuum, turning swiftly to a black powder containing Pd-black and **8a,b**. Compound **7c** was stable in the solid state and displayed sluggish reactivity to air or to PPh_3: its

[862] [N°761] Solin, N.; Szabó, K. J. *Organometallics* **2001**, *20*, 5464.
[863] [N°761] ibid.

decomposition favoured indenyl's homocoupling to give **8d**, yielding **8c** and **8d** in a 2:3 ratio.

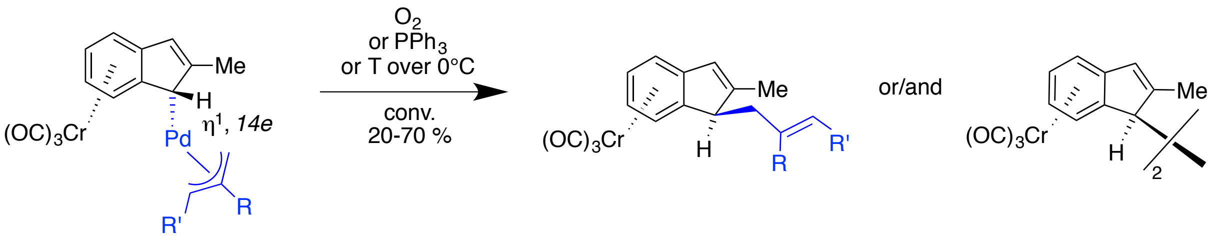

7a, R= H, R'= H
7b, R= Me, R'=H
7c, R= H, R'= Ph

8a, R= H, R'= H
8b, R= Me, R'= H
8c, R= H, R'= Ph

8d

Figure 102: Decomposition pathway of **7a-c** leading to the tricarbonyl(η^6-2-methylindenyl)chromium moiety and the allyl ligand.

The *anti* position of the allyl group in **8a,b** and **8d** with respect to the $Cr(CO)_3$ moiety suggests that the decomposition does not follow a typical reductive *cis*-elimination mechanism (Figure 103).

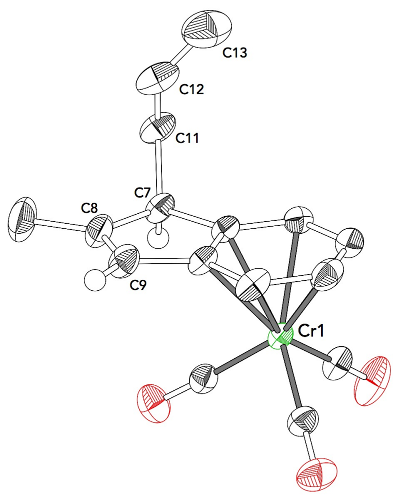

Compound **8a**
Space Group: **P 2_1/c**
R-Factor (%): **2.83**

N°	*A*	*B*	*Lengths (Å)*
1	C_7	C_{11}	1.542(2)
2	C_{11}	C_{12}	1.497(2)
3	C_{12}	C_{13}	1.316(3)
4	C_7	C_8	1.517(2)
5	C_8	C_9	1.344(1)

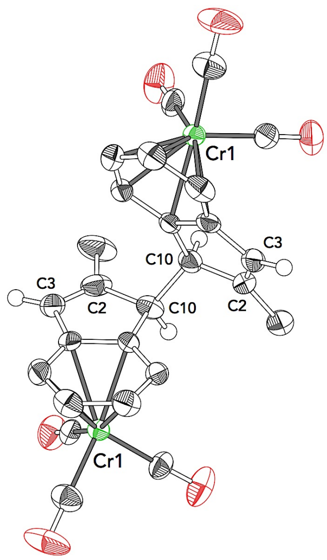

Compound **8d**
Space Group: **C 2/c**
R-Factor (%): **4.62**

N°	*A*	*B*	*Lengths (Å)*
1	C_{10}	C_{10}	1.534(5)
2	C_{10}	C_2	1.534(5)
3	C_2	C_3	1.336(6)

Figure 103: X-ray structure and selected interatomic distances of compounds **8a** and **8d.**

During the process of purification of **8a-d**, it was noticed that basic activated alumina promoted irreversible quantitative isomerization of **8a-d** into the thermodynamically favoured isomers **9a-d** (Figure 104 to Figure 106).

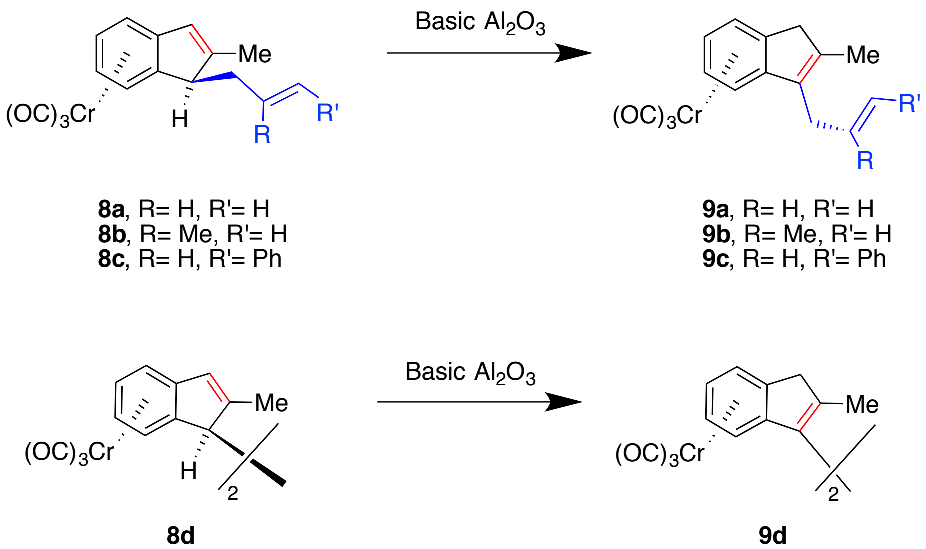

Figure 104: Basic activated alumina promotes the isomerization of **8a-d** into the thermodynamically favoured isomers **9a-d.**

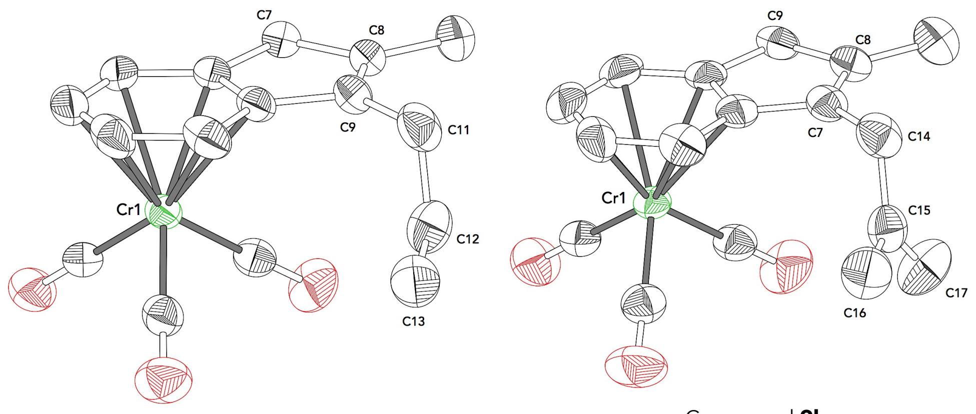

Compound **9a**
Space Group: **P 2_1/c**
R-Factor (%): **4.04**

N°	*A*	*B*	*Lengths (Å)*
1	C_7	C_8	1.508(2)
2	C_8	C_9	1.344(3)
3	C_{11}	C_{12}	1.508(4)
4	C_{12}	C_{13}	1.308(4)

Compound **9b**
Space Group: **P 2_1/c**
R-Factor (%): **3.65**

N°	*A*	*B*	*Lengths (Å)*
1	C_9	C_8	1.507(3)
2	C_8	C_7	1.346(3)
3	C_{14}	C_{15}	1.514(4)
4	C_{15}	C_{16}	1.317(4)
5	C_{15}	C_{17}	1.495(4)

Figure 105: X-ray structure and selected interatomic distances of compounds **9a** and **9b.**

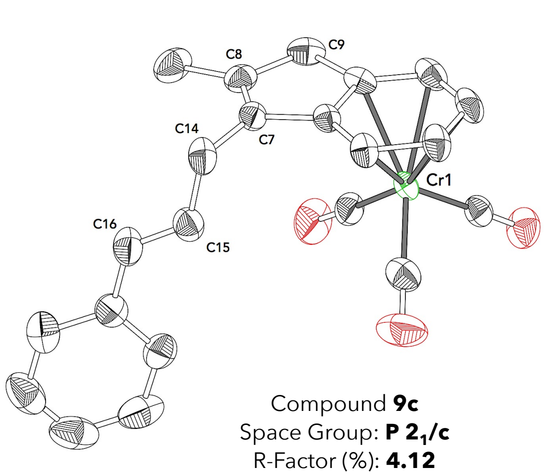

Compound **9c**
Space Group: **P 2_1/c**
R-Factor (%): **4.12**

N°	*A*	*B*	*Lengths (Å)*
1	C_9	C_8	1.511(2)
2	C_8	C_7	1.341(3)
3	C_{14}	C_{15}	1.513(3)
4	C_{15}	C_{16}	1.318(2)

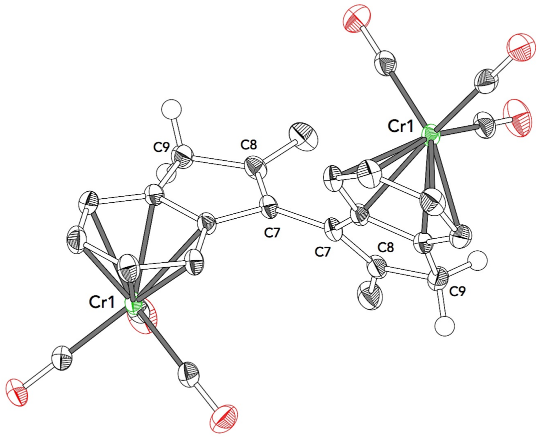

Compound **9d**
Space Group: **C 2/c**
R-Factor (%): **3.67**

N°	*A*	*B*	*Lengths (Å)*
1	C_9	C_8	1.510(2)
2	C_8	C_7	1.347(2)

Figure 106: X-ray structure and selected interatomic distances of compounds **9c** and **9d.**

3.4 - Conclusion.

The new complexes **7a-c** reported here are rare examples of persistent coordinatively unsaturated Pd(II) complexes, whose cohesion stems from a compensation of insufficient donor/acceptor Cr-Pd bonding by non-covalent interactions of preponderant attractive Coulombic nature. Even though this bonding situation is not sufficient to ensure permanent anchorage of the Pd centre to the $Cr(CO)_3$ moiety, the *syn*-facial η^1 coordination of the indenyl ligand to Pd is thermodynamically preferred over the *syn*-facial and *antara*-facial η^3 modes. The observed fluxionality is a direct consequence of the evanescence of the polar intermetallic interaction.[864,865] These results lay the ground for further investigations of what could be considered a new concept of hemilability based on the cohesive role of non-covalent interactions (electron correlation, London force, and Coulombic attraction) in loose but manageable donor/acceptor metal-based Lewis pairs. Due to the major disadvantage of these complexes, being air sensitive and kinetically unstable at room temperature, a new

[864] [N°559] Hyla-Kryspin, I.; Grimme, S.; Djukic, J. P. *Organometallics* **2009**, *28*, 1001.

[865] [N°562] Schwabe, T.; Grimme, S.; Djukic, J.-P. *J. Am. Chem. Soc.* **2009**, *131*, 14156.

strategy had to be considered to increase the thermal stability of those compounds while preserving the *syn*-facial η^1 coordination selectivity. In that way the replacement of the (η^3-allyl)palladium moiety by a cyclometallated palladium fragment seemed to be a good compromise, expecting to take advantage of the associated intrinsic properties of palladacycles.

4 - The case of (T-shaped)-Pd(II) complexes.

4.1 - Introduction: The palladacycles.

Palladacycles are generally defined as palladium compounds containing one palladium-carbon bond intramolecularly stabilized by one or two neutral donor atom (Y).[866] They can be divided into two different classes based on the organic fragment: 1) type (**CY**) when the organic fragment acts as a C-anionic four-electron donor ligand or 2) type (**YCY**) when it acts as a C-anionic six-electron donor ligand (Figure 108).

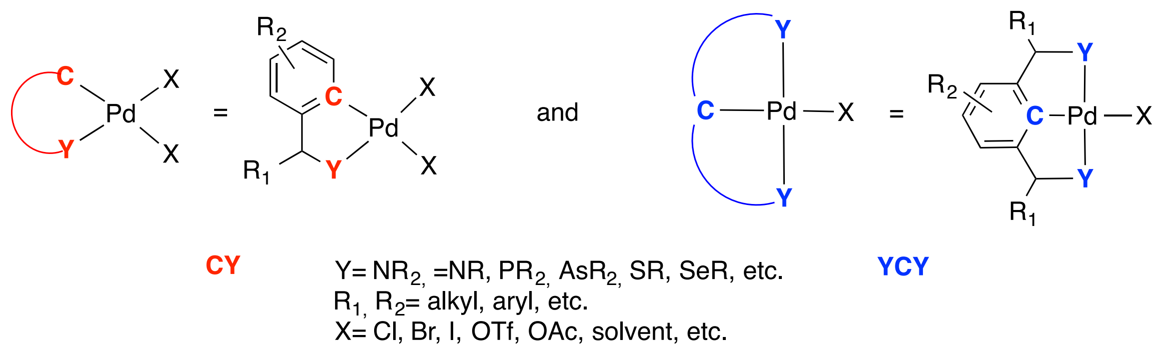

Figure 107: Structural definition of the palladacycles.

Usually palladacycles of the **CY** type exist under the shape of halogen or acetate bridged dimers[867, 868] as two geometric isomers, *cisoid* and *transoid* conformations (Figure 108).

[866] [N°762] Morales-Morales, D. In *Palladacycles*; Wiley-VCH Verlag GmbH & Co. KGaA: **2008**.

[867] [N°763] Dupont, J.; Consorti, C. S.; Spencer, J. *Chem. Rev.* **2005**, *105*, 2527.

[868] [N°764] Dehand, J.; Pfeffer, M. *Coord. Chem. Rev.* **1976**, *18*, 327.

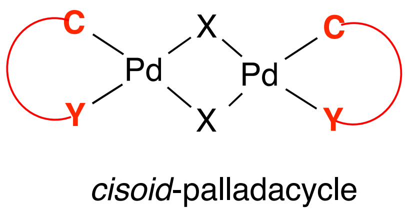

Figure 108: Geometric isomers of the **CY** type Palladacycles.

Additionally, **CY** species can exist under neutral, cationic[869] or anionic form,[870] where the neutral species can be found as monomers, dimers or bis-cyclopalladated complexes, depending on the nature of the other ligands "X" (Figure 109).

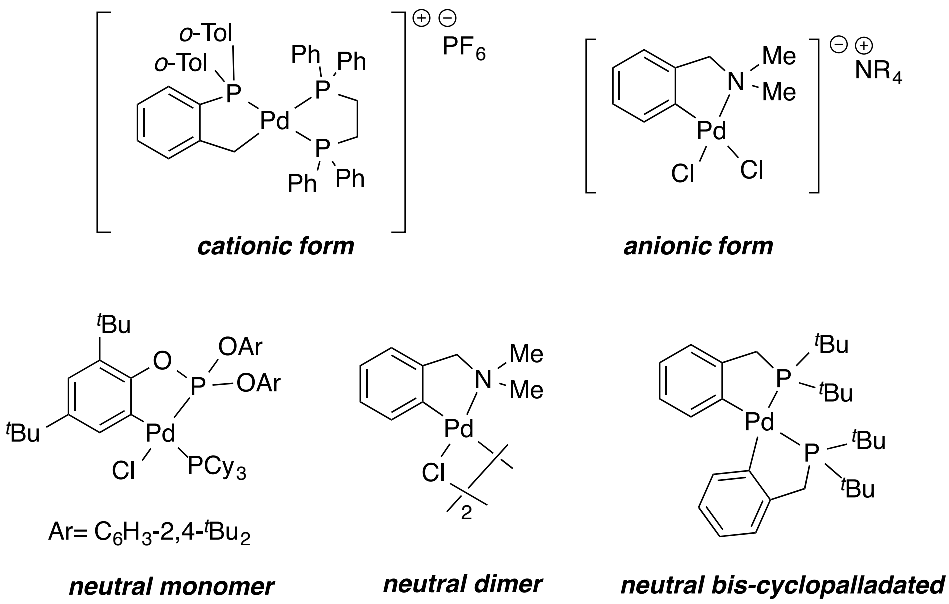

Figure 109: Different kind of **CY** species.

Concerning their synthesis,[871] these compounds can be very easily obtained (by C-H activation, oxidative addition, transmetalation, or nucleophilic addition onto an unsaturated bond) and often, a five- or six- membered chelate is formed as a result of the formation of a stable Pd-C bond, assisted by coordination of the two-electron donor group (Figure 110).

[869] [N°765] Schwarz, J.; Herdtweck, E.; Herrmann, W. A.; Gardiner, M. G. *Organometallics* **2000**, *19*, 3154.

[870] [N°766] Braunstein, P.; Dehand, J.; Pfeffer, M. *J. Inorg. Nucl. Chem.* **1974**, *10*, 581.

[871] [N°763] Dupont, J.; Consorti, C. S.; Spencer, J. *Chem. Rev.* **2005**, *105*, 2527.

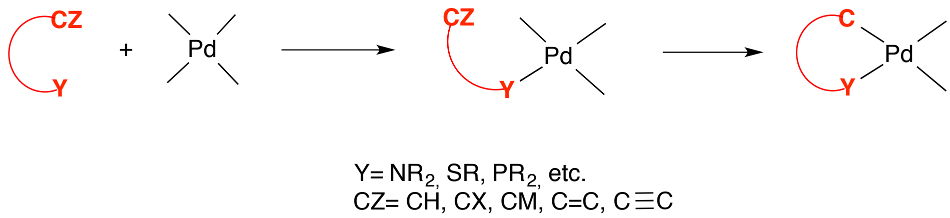

Figure 110: Methods for the generation of palladacycles.

From a historical perspective, three different events have defined the development of the palladacycles chemistry. The first major event was the discovery of the cyclometallation reaction in 1963 by Kleinmann and Dubeck[872] when they reacted azobenzene with $NiCp_2$ to obtain a five-membered metallacycle, which was found to be monomeric, soluble in organic solvents and stable to air (Figure 111).

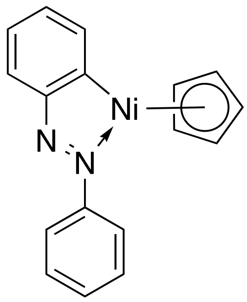

Figure 111: First metallacycle described by Kleinmann and Dubeck in 1963.

The second major event was the extension of this chemistry in the mid-1960 to other group-10 transition metals by Cope *et al.* with the first synthesis of Palladium and Platinum metallacycles of azobenzene [873] and their N,N-dimethylbenzylamine analogues[874] (Figure 112).

[872] [N°767] Kleiman, J. P.; Dubeck, M. *J. Am. Chem. Soc.* **1963**, *85*, 1544.

[873] [N°768] Cope, A. C.; Siekman, R. W. *J. Am. Chem. Soc.* **1965**, *87*, 3272.

[874] [N°769] Cope, A. C.; Friedrich, E. C. *J. Am. Chem. Soc.* **1968**, *90*, 909.

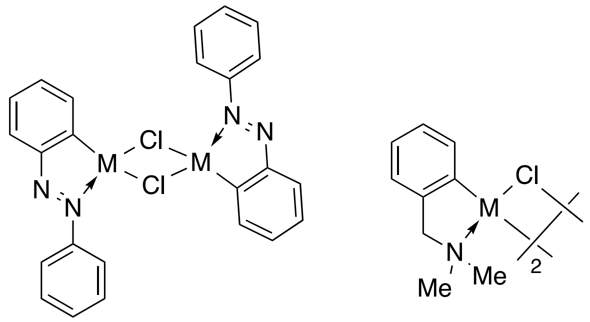

Figure 112: First palladium and platinum metallacycles described by Cope *et al*.

Finally, the physical properties of these compounds, in particular the high thermal stability in the solid state, led to the third and probably most important discovery which was the introduction, by Herrmann *et al.,* of the cyclopalladated tri-*o*-tolyl-phosphine complex (Figure 113) as a catalyst precursor for palladium-catalysed cross-coupling reactions in 1995.[875]

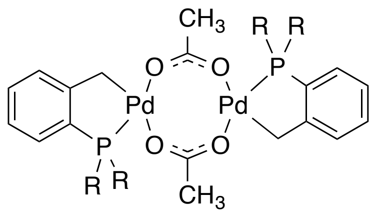

Figure 113: The first cyclopalladated catalyst precursor namely the tri-*o*-tolyl-phosphine complex.

This raised high expectations for this class of compounds, as these species are able to activate more economic substrates than those applied thus far (aryl iodides or aryl triflates), such as poorly reactive aryl chlorides, increasing the interest of these palladacycle catalysts for potential industrial applications. Hence, palladacycle compounds have undergone a growing success and have become a widely investigated topic of research,[876-896] which is well shown by the evolution of the number

[875] [N°770] Herrmann, W. A.; Brossmer, C.; Ofele, K.; Reisinger, C. P.; Priermeier, T.; Beller, M.; Fischer, H. *Angew. Chem. Int. Ed. Engl.* **1995**, *34*, 1844.

[876] [N°771] Szabó, K. J. *Synlett* **2006**, *2006*, 811.

[877] [N°772] Dunina, V. V.; Gorunova, O. N. *Rus. Chem. Rev.* **2005**, *74*, 871.

[878] [N°773] Dunina, V. V.; Gorunova, O. N. *Rus. Chem. Rev.* **2004**, *73*, 309.

[879] [N°774] Beletskaya, I. P.; Cheprakov, A. V. *J. Organomet. Chem.* **2004**, *689*, 4055.

[880] [N°775] Omae, I. *Coord. Chem. Rev.* **2004**, *248*, 995.

of published articles (Figure 114) and citations related to those compounds over the past years (Figure 115). Indeed, they act as important intermediates in palladium mediated organic synthesis[897-899] and homogeneous catalysis.[900-904]

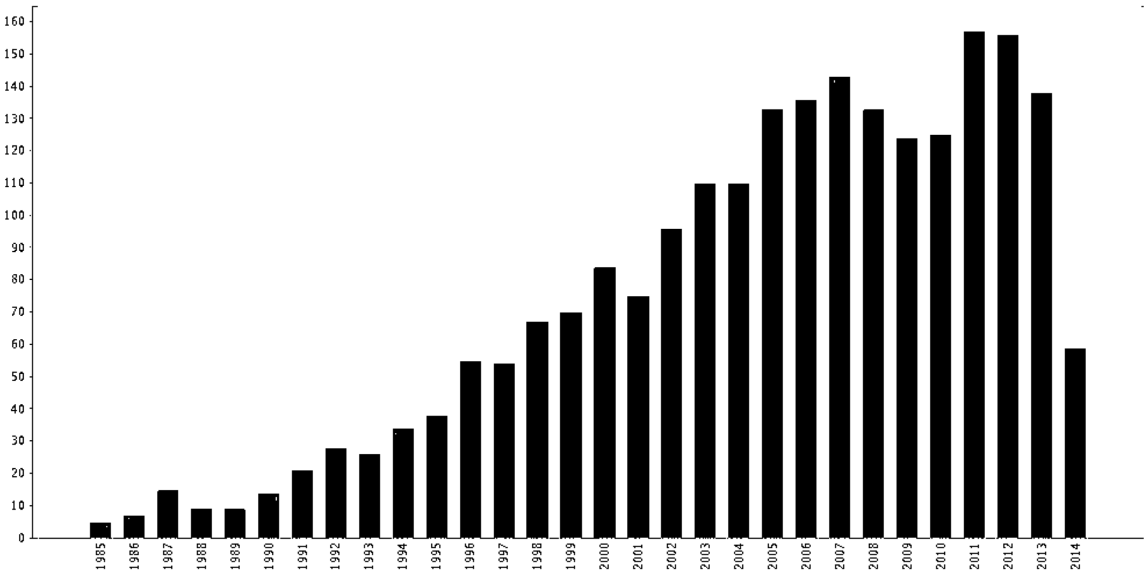

Figure 114: Evolution of the number of publications including palladacycles over the last 20 years. *(Source: web of science, Thomson Reuters).*

---

881 [N°776] Singleton, J. T. *Tetrahedron* **2003**, *59*, 1837.

882 [N°777] van der Boom, M. E.; Milstein, D. *Chem. Rev.* **2003**, *103*, 1759.

883 [N°778] Bedford, R. B. *Chem. Commun.* **2003**, 1787.

884 [N°779] Dupont, J.; Pfeffer, M.; Spencer, J. *Eur. J. Inorg. Chem.* **2001**, *2001*, 1917.

885 [N°780] Albrecht, M.; van Koten, G. *Angew. Chem. Int. Ed. Engl.* **2001**, *40*, 3750.

886 [N°781] Steenwinkel, P.; Gossage, R. A.; van Koten, G. *Chem. Eur. J.* **1998**, *4*, 759.

887 [N°782] Pfeffer, M. *Pure Appl. Chem.* **1992**, *64*, 335.

888 [N°783] Ryabov, A. D. *Chem. Rev.* **1990**, *90*, 403.

889 [N°784] Newkome, G. R.; Puckett, W. E.; Gupta, V. K.; Kiefer, G. E. *Chem. Rev.* **1986**, *86*, 451.

890 [N°785] Rothwell, I. P. *Polyhedron* **1985**, *4*, 177.

891 [N°786] Ryabov, A. D. *Synthesis* **1985**, 233.

892 [N°787] Constable, E. C. *Polyhedron* **1984**, *3*, 1037.

893 [N°788] Omae, I. *Coord. Chem. Rev.* **1982**, *42*, 245.

894 [N°789] Omae, I. *Coord. Chem. Rev.* **1980**, *32*, 235.

895 [N°790] Omae, I. *Coord. Chem. Rev.* **1979**, *28*, 97.

896 [N°791] Bruce, M. I. *Angew. Chem. Int. Ed. Engl.* **1977**, *16*, 73.

897 [N°792] Catellani, M. *Synlett* **2003**, 298.

898 [N°793] Dyker, G. *Chem. Ber.* **1997**, *130*, 1567.

899 [N°794] Dyker, G.; Korning, J.; Nerenz, F.; Siemsen, P.; Sostmann, S.; Wiegand, A., . . . Bubenitschek, P. *Pure Appl. Chem.* **1996**, *68*, 323.

900 [N°795] Alacid, E.; Alonso, D. A.; Botella, L.; Najera, C.; Pacheco, M. C. *Chem. Rec.* **2006**, *6*, 117.

901 [N°796] Bellina, F.; Carpita, A.; Rossi, R. *Synthesis* **2004**, 2419.

902 [N°797] Bedford, R. B.; Cazin, C. S. J.; Holder, D. *Coord. Chem. Rev.* **2004**, *248*, 2283.

903 [N°798] Herrmann, W. A.; Ofele, K.; Von Preysing, D.; Schneider, S. K. *J. Organomet. Chem.* **2003**, *687*, 229.

904 [N°799] Herrmann, W. A.; Bohm, V. P. W.; Reisinger, C. P. *J. Organomet. Chem.* **1999**, *576*, 23.

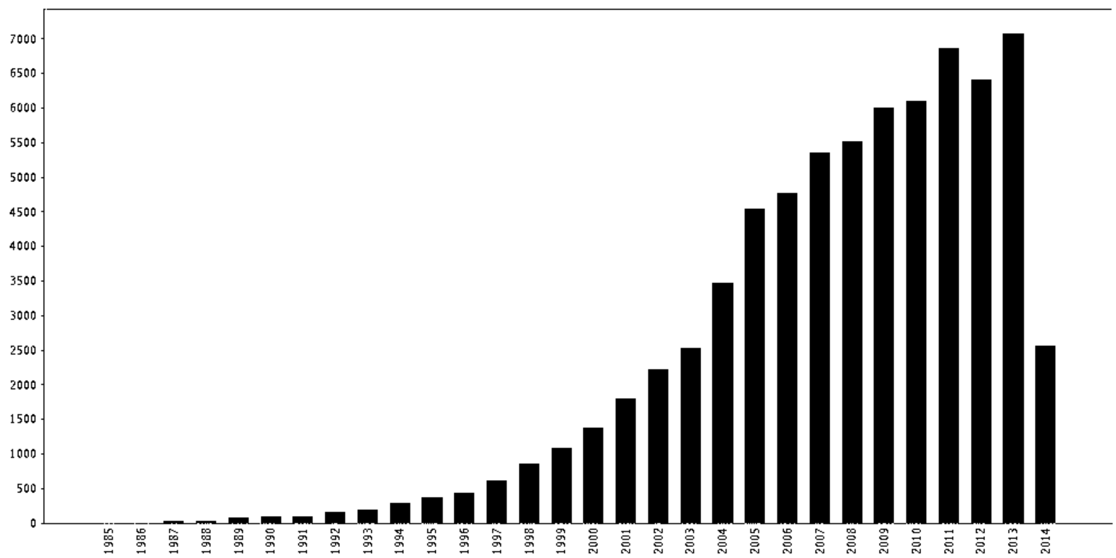

Figure 115: Evolution of the number of citations of the related articles over the last 20 years. *(Source: web of science, Thomson Reuters).*

4.2 - Purpose.

In our continued efforts to analyse the modes of stabilization of electron-deficient centres by noncovalent interactions, it was found that the three previous examples of highly fluxional 14 electron Pd(II) complexes had the disadvantage of being air sensitive and kinetically unstable at room temperature. The present section of the chapter will disclose new cases of air/moisture-stable, solid state and solution-persistent 14 electron neutral T-shaped Pd(II) and Pt(II) bimetallic complexes. A rational method of synthesis is proposed. This method takes again advantage of the ambiphilic character of the tricarbonyl(η^6-indenyl)chromium anion, the main property of which is to behave, as previously mentioned (see Figure 77), as a nonconventional heteroditopic ligand capable of chelating a metal centre through covalent and non-covalent bonding, thus preserving its unsaturated valence shell. This part of the manuscript will further document this peculiar type of chelation that will be named herein *hemichelation*, where the prefix hemi (from the Greek ημι meaning *half*) suggests the half-covalent/half noncovalent nature of chelation. Theoretical and experimental investigations carried out to establish the physical nature of the intramolecular interactions highlight the stabilizing role of noncovalent interactions.

4.3 - Experimental aspects.

Several μ-chloro-bridged palladacycles **10a-h** and **11a** (Figure 116) were probed for their reactivity toward anion **5b**, anticipating here also, the possible formation of a mixture of *syn*- and *antara*-facial products **12-13** and **14**, respectively (Figure 117).

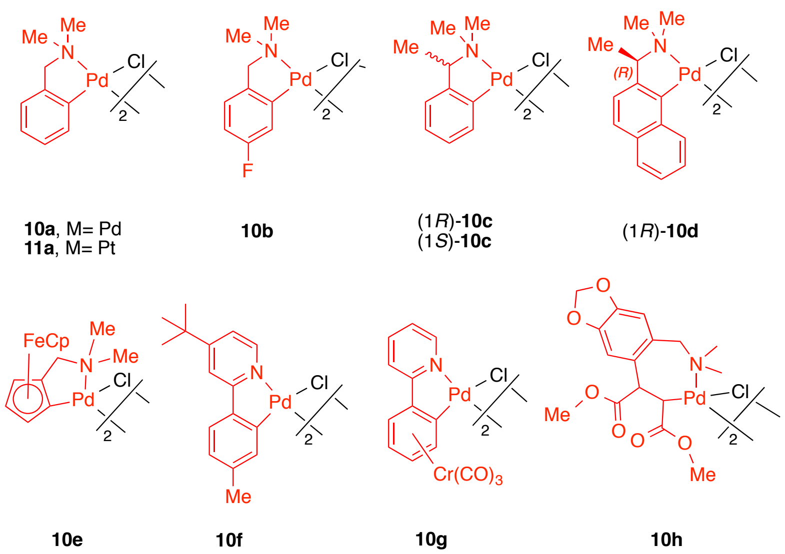

Figure 116: μ-chloro-bridged palladacycles which were probed for their reactivity toward anion **5b**.

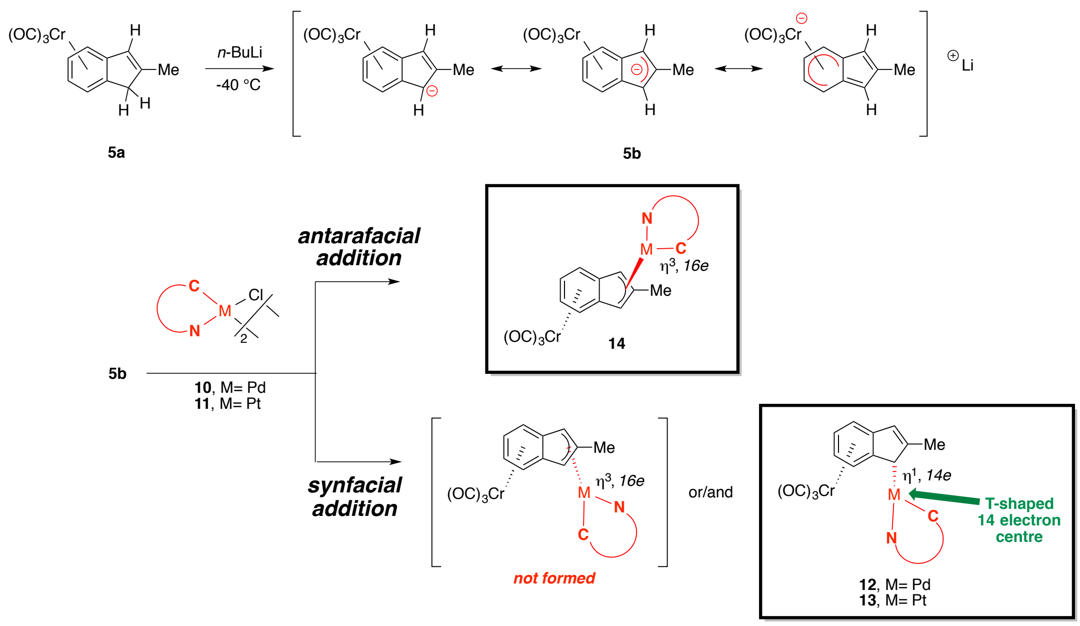

Figure 117: The ambiphilic character of anion **5b** allows two facial interactions with Pd and Pt metallacycles **10** or **11**, that is, either the *antara*-facial leading to the (η^3-indenyl)M complexes **14** or the *syn*-facial leading exclusively to (η^1-indenyl)M complexes **12** and **13**, a new class of electron-unsaturated T-shaped η^1-indenyl Pd/Pt complexes.

Optimal conversions were achieved when palladacycles **10**[905-909] reacted with anion **5b** in a dry mixture of ether and toluene at −40 °C. The corresponding *syn*-facial complexes **12a–h** were isolated mostly by recrystallization with yields spanning 46–86 %. In the case of the reaction of **5b** with **10b**, the *antara*-facial isomer **14b** precipitated out during the course of the reaction, which eased its separation from the *syn*-facial isomer **12b**. However, complex **14b**, which formed in about the same amounts as **12b**, displayed low kinetic stability in solution and generally decomposed within an hour into **5a** and other untraceable products. This peculiar instability in solution might explain why no other examples of similar electron-saturated complexes arising from **10a** of **10c–g** were isolated or detected in reaction mixtures, which always displayed typical signs of decomposition (Pd black). The only other case where the *antara*-facial isomer could be detected and isolated was for palladacycle **10h** where the steric hindrance induced by the organic cyclometallated ligand left no chance to the system to accommodate any *syn*-facial arrangement. Owing to the poor reactivity of platinacycle **11a**[910] in organic solvents, slightly forced conditions consisting of a prolonged reaction time with **5b** at room temperature had to be applied to produce **13a** in small amounts in *ca.* 4 % yield. Preliminary conversion of **11a** into a more reactive intermediary thioether adduct (Me_2S•**11a**),[911] which was not isolated, slightly improved the yield in **13a** (12 %). Complexes **12a-g** and **13a** were air-stable in the solid state and displayed far better kinetic stability in solution in moderately polar solvents than complexes **7a, 7b** and even **7c**, reported previously. Acidic treatment in organic solvents would, in all cases, regenerate **5a** and lead to the decomposition of the palladacycle.

---

905 [N°800] Berger, A.; de Cian, A.; Djukic, J.-P.; Fischer, J.; Pfeffer, M. *Organometallics* **2001**, *20*, 3230.

906 [N°801] Ryabov, A. D.; Van Eldik, R.; Le Borgne, G.; Pfeffer, M. *Organometallics* **1993**, *12*, 1386.

907 [N°802] Gaunt, J. C.; Shaw, B. L. *J. Organomet. Chem.* **1975**, *102*, 511.

908 [N°803] Otsuka, S.; Nakamura, A.; Kano, T.; Tani, K. *J. Am. Chem. Soc.* **1971**, *93*, 4301.

909 [N°769] Cope, A. C.; Friedrich, E. C. *J. Am. Chem. Soc.* **1968**, *90*, 909.

910 [N°804] Schmulling, M.; Ryabov, A. D.; van Eldik, R. *J. Chem. Soc., Chem. Commun.* **1992**, 1609.

911 [N°805] Thomas, S. W.; Venkatesan, K.; Müller, P.; Swager, T. M. *J. Am. Chem. Soc.* **2006**, *128*, 16641.

Structural characterization by means of X-ray diffraction analysis was successful with palladium complexes **12a–e**, **12g**, **14c** and **14h** as well as with platinum complex **13a** (Figure 118 to Figure 127). Being rather insoluble, **12f** failed to yield suitable crystals.

Figure 118, Figure 119, Figure 121-Figure 125, display the structures of the *syn*-facial Cr(0)–Pd(II)/Pt(II) complexes. The Cr–Pd distances are all in the range of 2.84–2.93 Å which is in the approximate range of the sum of empirical van der Waals radii[912] for Cr (1.4 Å)/Pd (1.4 Å) and Cr/Pt (1.4 Å). The Cr–Pt distance of *ca.* 2.88 Å in **13a** (Figure 126) is shorter by 0.04 Å than the Cr–Pd distance in **12a** (Figure 118).

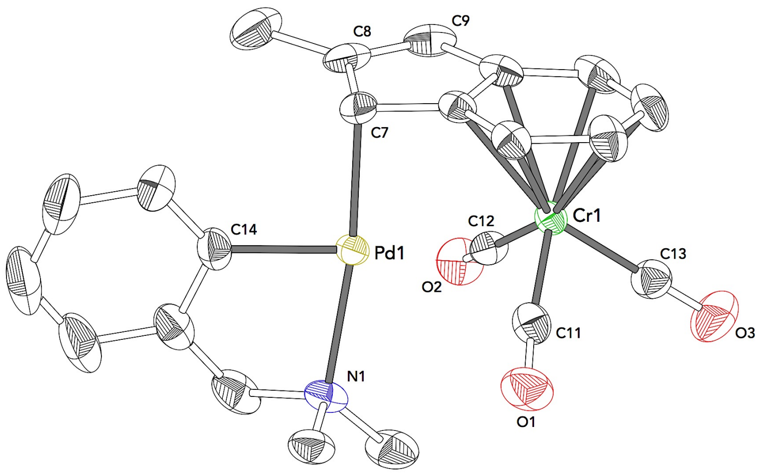

Compound **12a**
Space Group: **P 2_1/c**
R-Factor (%): **2.28**

N°	A	B	C	Lengths (Å)	Angles (°)
1	Pd_1	Cr_1	-	2.9290(3)	-
2	Pd_1	C_7	-	2.108(2)	-
3	Pd_1	C_8	-	2.913(2)	-
4	Pd_1	C_{14}	-	2.016(2)	-
5	Pd_1	N_1	-	2.206(2)	-
6	Pd_1	C_{11}	-	2.962(2)	-
7	Pd_1	C_{12}	-	2.572(2)	-
8	Cr_1	C_{11}	-	1.835(2)	-
9	Cr_1	C_{12}	-	1.856(2)	-
10	Cr_1	C_{13}	-	1.850(1)	-
11	C_{11}	O_1	-	1.158(2)	-
12	C_{12}	O_2	-	1.157(2)	-
13	C_{13}	O_3	-	1.143(2)	-
14	Cr_1	C_{11}	O_1	-	174.0(2)
15	Cr_1	C_{12}	O_2	-	170.8(2)
16	Cr_1	C_{13}	O_3	-	178.7(2)

Figure 118: X-ray structure and selected interatomic distances of compound **12a.**

[912] [N°806] Slater, J. C. *J. Chem. Phys.* **1964**, *41*, 3199.

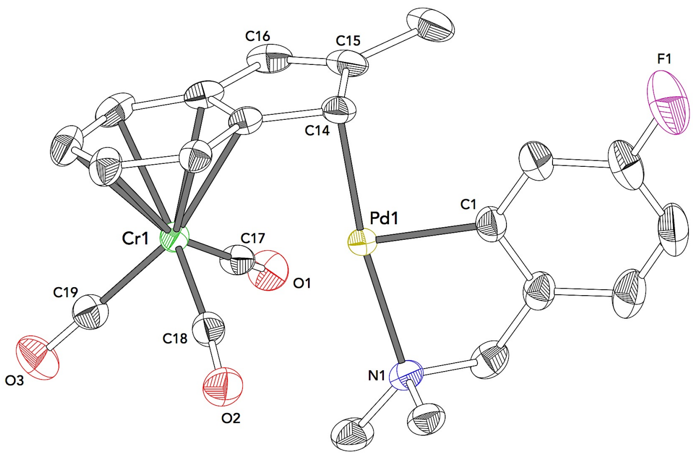

Compound **12b**
Space Group: **P 2_1/c**
R-Factor (%): **2.75**

N°	*A*	*B*	*C*	*Lengths (Å)*	*Angles (°)*
1	Pd_1	Cr_1	-	2.9125(5)	-
2	Pd_1	C_{14}	-	2.111(3)	-
3	Pd_1	C_{15}	-	2.908(3)	-
4	Pd_1	C_1	-	2.017(2)	-
5	Pd_1	N_1	-	2.203(2)	-
6	Pd_1	C_{17}	-	2.604(2)	-
7	Pd_1	C_{18}	-	2.867(2)	-
8	Cr_1	C_{17}	-	1.854(3)	-
9	Cr_1	C_{18}	-	1.840(3)	-
10	Cr_1	C_{19}	-	1.855(2)	-
11	C_{17}	O_1	-	1.160(3)	-
12	C_{18}	O_2	-	1.153(3)	-
13	C_{19}	O_3	-	1.142(3)	-
14	Cr_1	C_{17}	O_1	-	171.7(2)
15	Cr_1	C_{18}	O_2	-	174.1(2)
16	Cr_1	C_{19}	O_3	-	178.6(2)

Figure 119: X-ray structure and selected interatomic distances of compound **12b.**

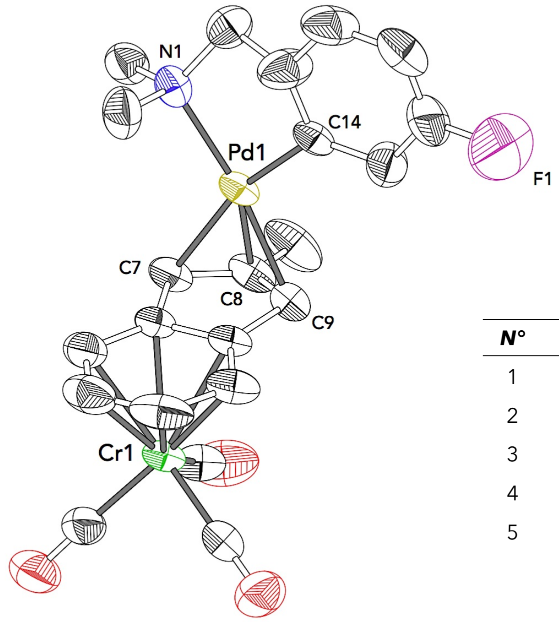

Compound **14b**
Space Group: **P 2_1/c**
R-Factor (%): **3.61**

N°	*A*	*B*	*C*	*Lengths (Å)*	*Angles (°)*
1	Pd_1	C_7	-	2.351(3)	-
2	Pd_1	C_8	-	2.189(3)	-
3	Pd_1	C_9	-	2.161(2)	-
4	Pd_1	C_{14}	-	2.010(4)	-
5	Pd_1	N_1	-	2.109(2)	-

Figure 120: X-ray structure and selected interatomic distances of compound **14b.**

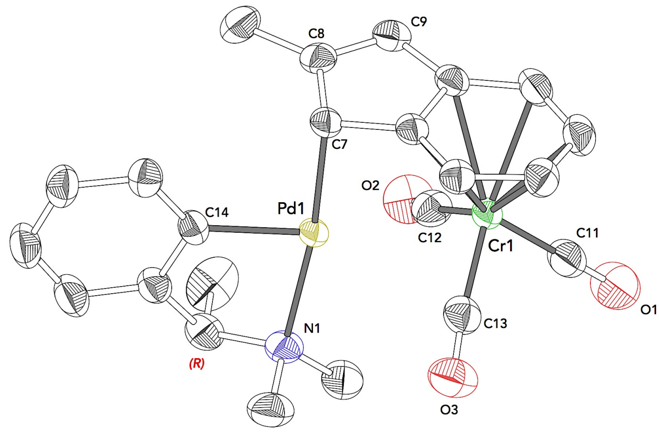

Compound (1*R*)-**12c**
Space Group: **P 2$_1$**
R-Factor (%): **1.41**
Flack' s parameter x = **0.018(10)**

N°	A	B	C	Lengths (Å)	Angles (°)
1	Pd_1	Cr_1	-	2.921(2)	-
2	Pd_1	C_7	-	2.113(2)	-
3	Pd_1	C_8	-	2.919(2)	-
4	Pd_1	C_{14}	-	2.018(1)	-
5	Pd_1	N_1	-	2.198(2)	-
6	Pd_1	C_{12}	-	2.548(1)	-
7	Pd_1	C_{13}	-	2.917(1)	-
8	Cr_1	C_{11}	-	1.847(2)	-
9	Cr_1	C_{12}	-	2.857(1)	-
10	Cr_1	C_{13}	-	2.847(2)	-
11	C_{11}	O_1	-	1.148(3)	-
12	C_{12}	O_2	-	1.161(2)	-
13	C_{13}	O_3	-	1.151(2)	-
14	Cr_1	C_{11}	O_1	-	178.2(2)
15	Cr_1	C_{12}	O_2	-	168.8(1)
16	Cr_1	C_{13}	O_3	-	173.4(1)

Figure 121: X-ray structure and selected interatomic distances of compound (1-*R*)-**12c.**

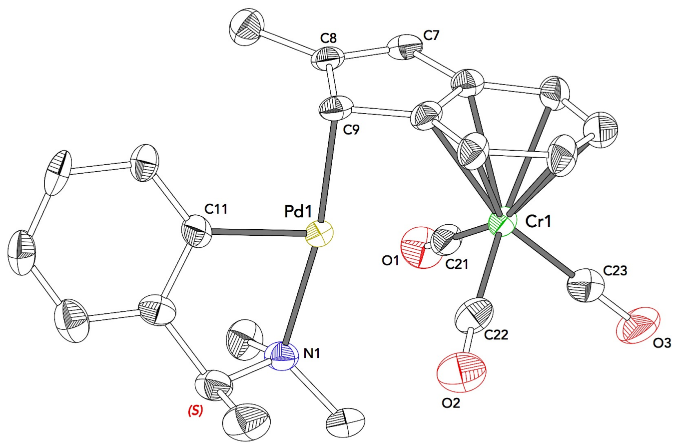

Compound (1*S*)-**12c**
Space Group: **P 2$_1$**
R-Factor (%): **4.04**
Flack' s parameter x = **0.02(3)**

N°	A	B	C	Lengths (Å)	Angles (°)
1	Pd_1	Cr_1	-	2.932(1)	-
2	Pd_1	C_9	-	2.107(5)	-
3	Pd_1	C_8	-	2.859(5)	-
4	Pd_1	C_{11}	-	2.001(6)	-
5	Pd_1	N_1	-	2.185(5)	-
6	Pd_1	C_{21}	-	2.572(7)	-
7	Pd_1	C_{22}	-	2.971(6)	-
8	Cr_1	C_{21}	-	1.844(6)	-
9	Cr_1	C_{22}	-	1.858(7)	-
10	Cr_1	C_{23}	-	1.834(7)	-
11	C_{21}	O_1	-	1.175(8)	-
12	C_{22}	O_2	-	1.147(8)	-
13	C_{23}	O_3	-	1.161(8)	-
14	Cr_1	C_{21}	O_1	-	169.4(6)
15	Cr_1	C_{22}	O_2	-	174.8(6)
16	Cr_1	C_{23}	O_3	-	179.4(6)

Figure 122: X-ray structure and selected interatomic distances of compound (1-*S*)-**12c.**

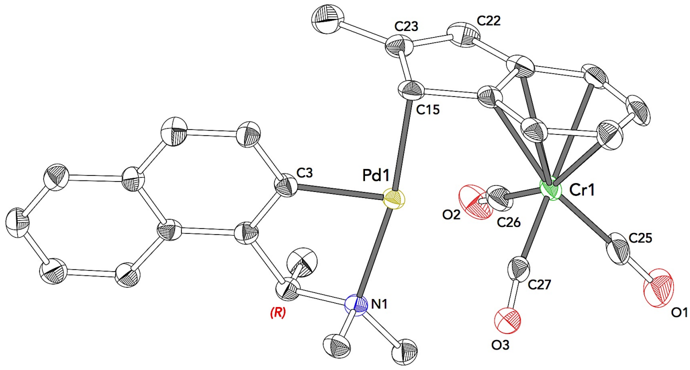

Compound (1*R*)-**12d**
Space Group: **P 2_1**
R-Factor (%): **2.92**
Flack' s parameter x = **0.02(3)**

N°	A	B	C	Lengths (Å)	Angles (°)
1	Pd_1	Cr_1	-	2.9294(5)	-
2	Pd_1	C_{15}	-	2.117(3)	-
3	Pd_1	C_{23}	-	2.886(3)	-
4	Pd_1	C_3	-	2.017(2)	-
5	Pd_1	N_1	-	2.170(2)	-
6	Pd_1	C_{26}	-	2.700(5)	-
7	Pd_1	C_{27}	-	2.737(5)	-
8	Cr_1	C_{25}	-	1.838(3)	-
9	Cr_1	C_{26}	-	1.861(5)	-
10	Cr_1	C_{27}	-	1.849(5)	-
11	C_{25}	O_1	-	1.148(4)	-
12	C_{26}	O_2	-	1.149(6)	-
13	C_{27}	O_3	-	1.156(6)	-
14	Cr_1	C_{25}	O_1	-	178.4(4)
15	Cr_1	C_{26}	O_2	-	171.3(4)
16	Cr_1	C_{27}	O_3	-	171.3(4)

Figure 123: X-ray structure and selected interatomic distances of compound (1-*R*)-**12d.**

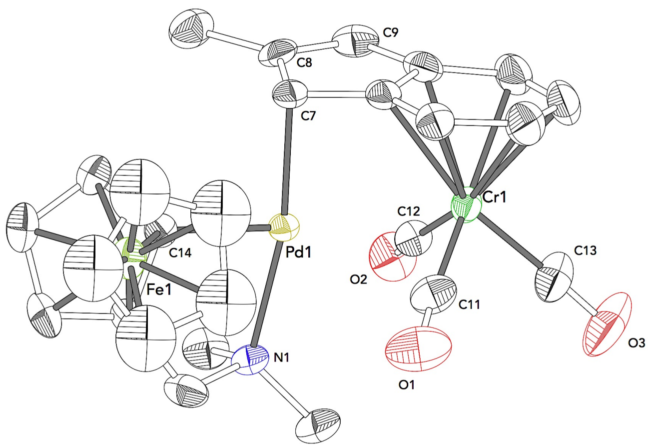

Compound **12e**
Space Group: **P 2_1/c**
R-Factor (%): **4.12**

N°	A	B	C	Lengths (Å)	Angles (°)
1	Pd_1	Cr_1	-	2.8505(7)	-
2	Pd_1	C_7	-	2.111(3)	-
3	Pd_1	C_8	-	2.835(3)	-
4	Pd_1	C_{14}	-	2.004(3)	-
5	Pd_1	N_1	-	2.212(3)	-
6	Pd_1	C_{11}	-	2.763(4)	-
7	Pd_1	C_{12}	-	2.567(3)	-
8	Cr_1	C_{11}	-	1.839(3)	-
9	Cr_1	C_{12}	-	1.857(4)	-
10	Cr_1	C_{13}	-	1.841(3)	-
11	C_{11}	O_1	-	1.152(4)	-
12	C_{12}	O_2	-	1.157(5)	-
13	C_{13}	O_3	-	1.146(4)	-
14	Cr_1	C_{11}	O_1	-	174.3(3)
15	Cr_1	C_{12}	O_2	-	169.3(3)
16	Cr_1	C_{13}	O_3	-	177.8(4)

Figure 124: X-ray structure and selected interatomic distances of compound **12e.**

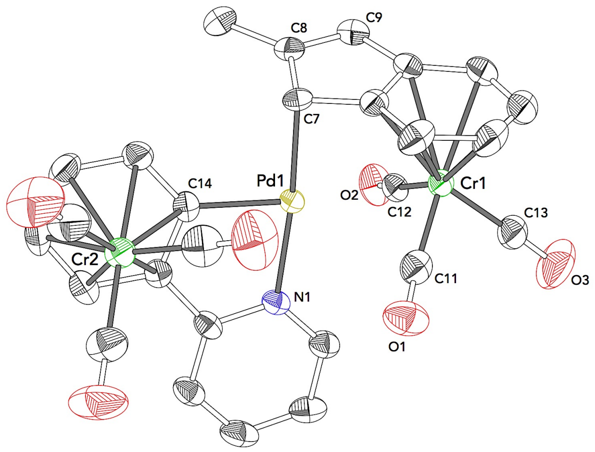

Compound **12g**
Space Group: **P b c a**
R-Factor (%): **4.71**

N°	*A*	*B*	*C*	*Lengths (Å)*	*Angles (°)*
1	Pd_1	Cr_1	-	2.8392(5)	-
2	Pd_1	C_7	-	2.112(3)	-
3	Pd_1	C_8	-	2.888(3)	-
4	Pd_1	C_{14}	-	2.013(3)	-
5	Pd_1	N_1	-	2.111(3)	-
6	Pd_1	C_{11}	-	2.806(3)	-
7	Pd_1	C_{12}	-	2.515(3)	-
8	Cr_1	C_{11}	-	1.850(3)	-
9	Cr_1	C_{12}	-	1.849(3)	-
10	Cr_1	C_{13}	-	1.843(4)	-
11	C_{11}	O_1	-	1.153(5)	-
12	C_{12}	O_2	-	1.159(4)	-
13	C_{13}	O_3	-	1.148(5)	-
14	Cr_1	C_{11}	O_1	-	173.3(3)
15	Cr_1	C_{12}	O_2	-	169.4(3)
16	Cr_1	C_{13}	O_3	-	178.1(3)

Figure 125: X-ray structure and selected interatomic distances of compound **12g.**

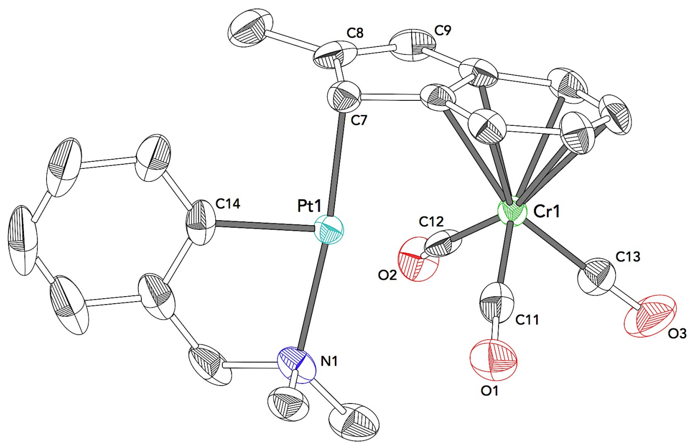

Compound **13a**
Space Group: **P 2_1/c**
R-Factor (%): **4.01**

N°	*A*	*B*	*C*	*Lengths (Å)*	*Angles (°)*
1	Pd_1	Cr_1	-	2.8834(6)	-
2	Pd_1	C_7	-	2.099(5)	-
3	Pd_1	C_8	-	2.929(5)	-
4	Pd_1	C_{14}	-	2.017(3)	-
5	Pd_1	N_1	-	2.183(4)	-
6	Pd_1	C_{11}	-	3.024(4)	-
7	Pd_1	C_{12}	-	2.408(4)	-
8	Cr_1	C_{11}	-	1.841(5)	-
9	Cr_1	C_{12}	-	1.876(5)	-
10	Cr_1	C_{13}	-	1.844(3)	-
11	C_{11}	O_1	-	1.155(6)	-
12	C_{12}	O_2	-	1.161(6)	-
13	C_{13}	O_3	-	1.144(4)	-
14	Cr_1	C_{11}	O_1	-	174.8(4)
15	Cr_1	C_{12}	O_2	-	163.2(4)
16	Cr_1	C_{13}	O_3	-	178.4(4)

Figure 126: X-ray structure and selected interatomic distances of compound **13a.**

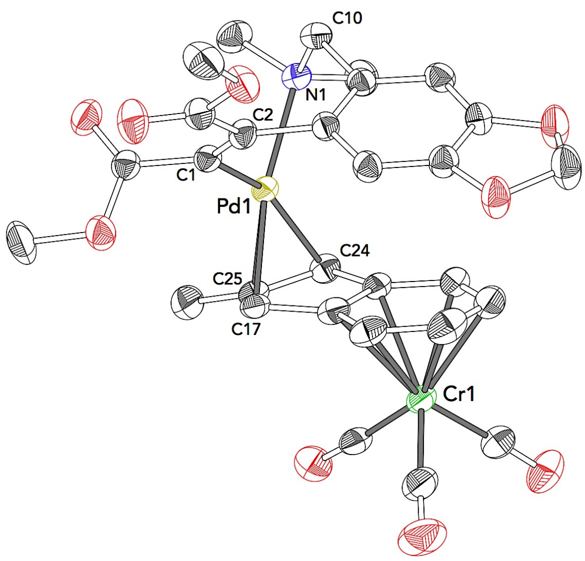

Compound **14h**
Space Group: **P -1**
R-Factor (%): **3.62**

N°	A	B	C	Lengths (Å)	Angles (°)
1	Pd_1	C_{17}	-	2.132(2)	-
2	Pd_1	C_{24}	-	2.319(2)	-
3	Pd_1	C_{25}	-	2.177(2)	-
4	Pd_1	C_1	-	2.011(2)	-
5	Pd_1	N_1	-	2.142(2)	-

Figure 127: X-ray structure and selected interatomic distances of compound **14h.**

In all structures of *syn*-facial complexes the chelated Pd or Pt centres are in short contact with one of the vicinal Cr-bound CO ligands and are bonded in a η^1-fashion to the indenyl ligand. For the sake of clarity, the η^1-prefix of complexes **12** and **13** (Figure 117) will be omitted in further discussions unless justified for comparison purposes. It is worth noting that for complexes **12e** and **12g** the planar chiral palladacycles adopt the same orientation in the crystal lattice, the bulky π-bonded metal fragment being placed in the *exo* position, *i.e.*, away from the indenyl ligand. Structural X-ray diffraction analyses showed in two distinct experiments (acquisition of structure displayed in Figure 128 performed in Paris, while the acquisition of structure displayed in Figure 129 was performed in Strasbourg), that crystals of compound (1*S*)-**12c** (space group $P2_1$, Flack's absolute structure parameter x = -0.02(3)) contained the two *endo*-(p*S*,1*S*) and *exo*-(p*R*,1*S*)-**12c** diastereoisomers in a 1:1 ratio within the unit cell (Figure 128, Figure 129).

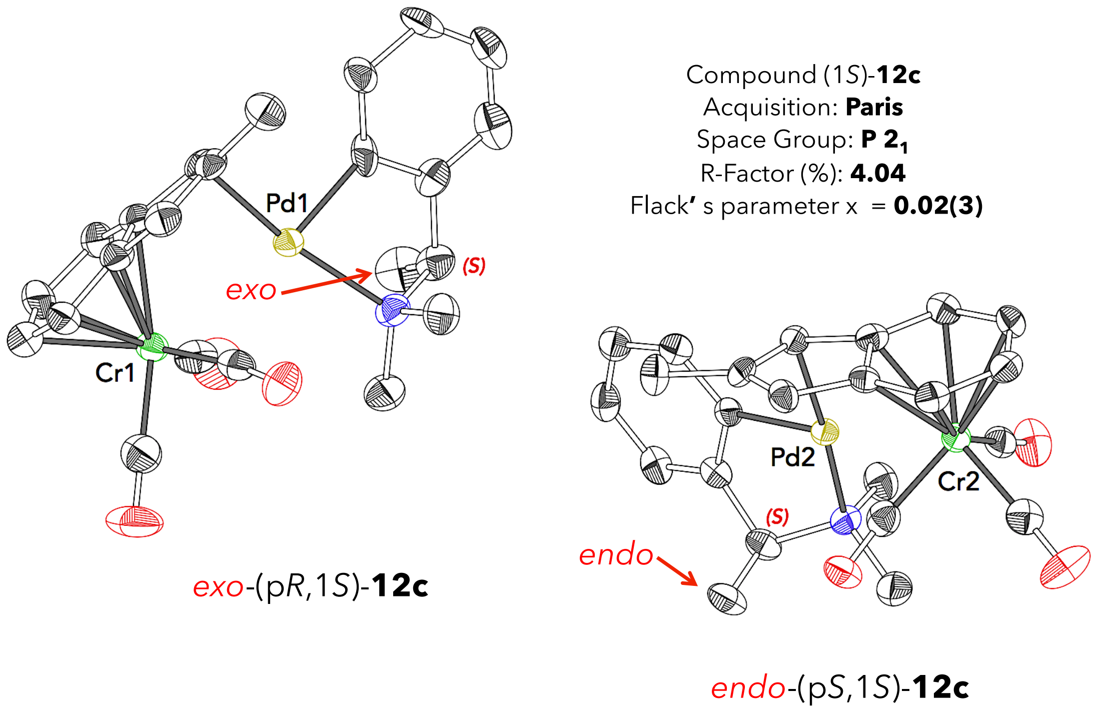

Figure 128: X-ray structure of compound (1-*S*)-**12c** (acquisition performed in Paris).

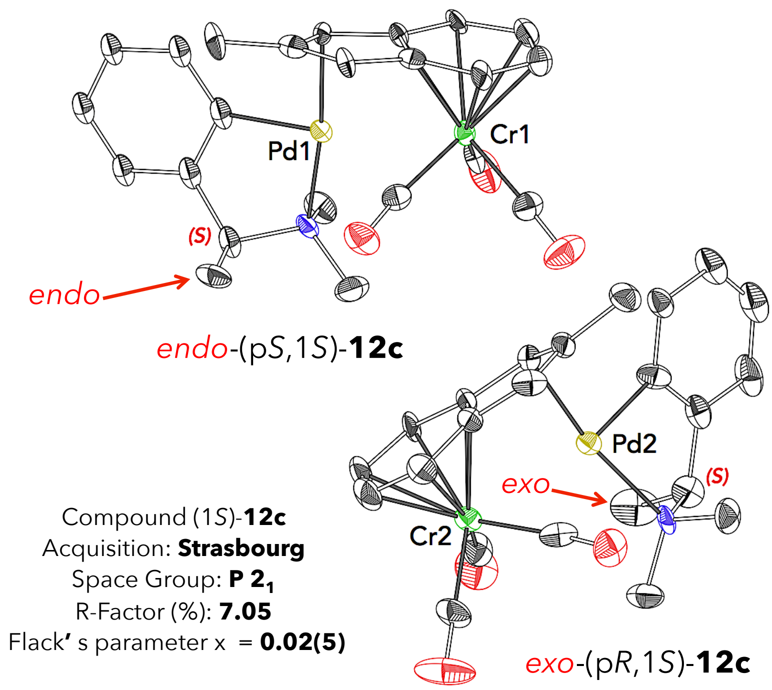

Figure 129: X-ray structure of compound (1-*S*)-**12c** (acquisition performed in Strasbourg).

Compounds (1*R*)-**12c** and (1*R*)-**12d**, which crystallized in the same space group $P2_1$ (x = 0.018(10) and x= 0.02(3) respectively) yielded, in both cases, a crystal containing only the *endo* diastereomer with the absolute configuration (p*R*, 1*R*) (Figure 130, Figure 131).

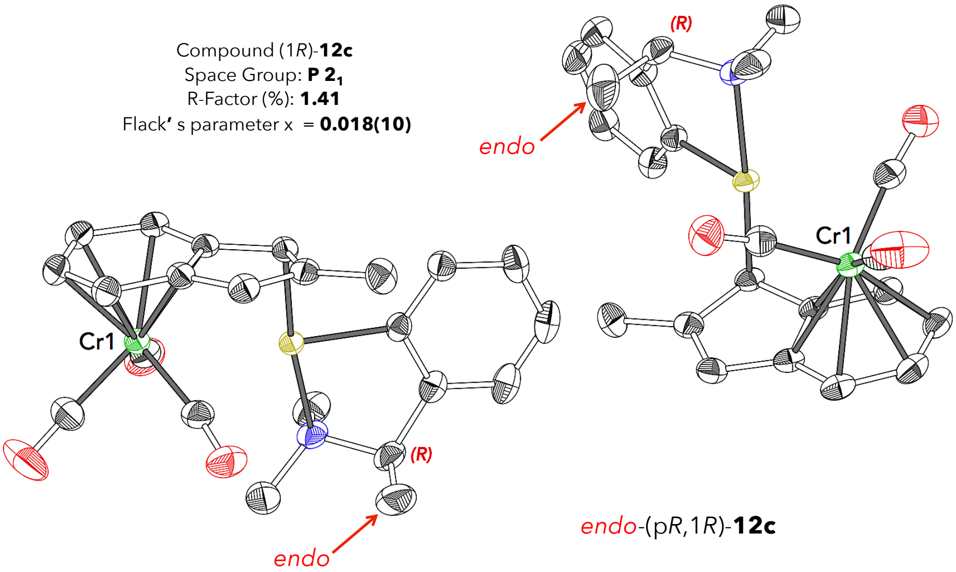

Figure 130: X-ray structure of compound (1*R*)-**12c** containing only the *endo* diastereomer.

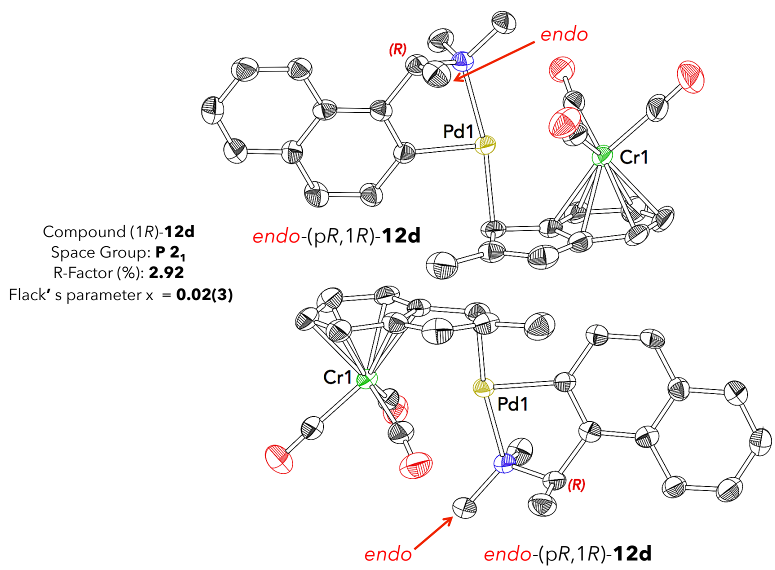

Figure 131: X-ray structure of compound (1*R*)-**12d** containing only the *endo* diastereomer.

The structure of **14b** as well as **14h** (Figure 120, Figure 127), presents an unusual dissymmetry of the η^3-indenyl-Pd bonding which seemingly results from the unbalanced trans influence of the Pd-bound heterochelate *via* C_{14} and N_1 for **14b** (C_1 and N_1 for **14h**). The distance C_7–Pd_1 was found to be longer than distance C_9–Pd_1 by *ca.* 0.2 Å in the case of **14b** (similarly the distance C_{24}−Pd_1 was also found to be longer than distance C_{17}−Pd_1 by *ca.* 0.2 Å for **14h**).

Solution (CH_2Cl_2, CaF_2 cell) and solid state attenuated total reflectance (ATR)-FT-IR spectra of the *syn*-facial complexes are characterized by the lifted degeneracy of the carbonyl C−O stretching E band (the A band appears at *ca.* 1956−1940 cm^{-1}) that gives rise to two distinct bands at *ca.* 1880 (s) and 1840 (vs) cm^{-1}. This spectroscopic peculiarity characterizes the lack of local C_{3v} symmetry[913-916] at the $Cr(CO)_3$ moiety in solution as well as in the solid state. According to DFT calculations of the vibrational modes within the rigid rotor harmonic oscillator (RRHO) approximation for models of η^1-**12** computed in the gas phase singlet ground state, the band of highest frequency is associated with the "symmetric" elongations of the three C−O bonds of the $Cr(CO)_3$ moiety. The band of lowest frequency is associated with the "anti-symmetric" elongations of the pseudobridging CO ligand and the CO ligand distant from M (M = Pd, Pt). The midband corresponds to the antisymmetric elongations of the nonbridging CO ligand proximal to M and the CO ligand distant from M. IR spectroscopy suggests that the pseudo-bridging situation observed in the X-ray diffraction structures has a minor electronic influence on the interaction of the M centre with the $Cr(CO)_3$ moiety; in other terms it has no major electronic effect upon the force constants of the considered C−O bonds, the vibrational modes of which remain overall in the spectral region of conventional (η^6-arene)tricarbonylchromium complexes. The average relative shift $\Delta(\nu)_{\text{aver } \mathbf{12\text{-}5a}}$ to higher reciprocal wavelengths of the considered vibrational bands of **12** with respect to reference compound **5a** (A, 1934 cm^{-1}; E, 1839 cm^{-1}; $\nu_{\text{aver } \mathbf{5a}}$= 1870 cm^{-1}) spans +11 to +26 cm^{-1}. For complexes **14b** and **14h**, the local C_{3v} symmetry of the $Cr(CO)_3$ rotor is preserved: A and E bands of the pseudo-C_{3v} *fac*-tricarbonylmetal moiety appear at 1933 (s) and 1843 (broad and vs) cm^{-1} in the case of **14b**; 1942(s), 1851(broad and vs) cm^{-1} for **14h**. As far as complex **12c** is concerned, the solid state IR spectrum of either crystalline or amorphous solid obtained by freeze-drying a benzene

913 [N°736] van Meurs, F.; Baas, J. M. A.; van Bekkum, H. *J. Organomet. Chem.* **1977**, *129*, 347.

914 [N°737] van Meurs, F.; Baas, J. M. A.; van Bekkum, H. *J. Organomet. Chem.* **1976**, *113*, 353.

915 [N°807] W. Neuse, E. *J. Organomet. Chem.* **1975**, *99*, 287.

916 [N°808] Adams, D. M.; Squire, A. *J. Chem. Soc., Dalton Trans.* **1974**, 558.

solution has proved inconclusive as to the possible coexistence of *endo* and *exo* diastereomers in solution; a single set of three vibrational bands being observed.

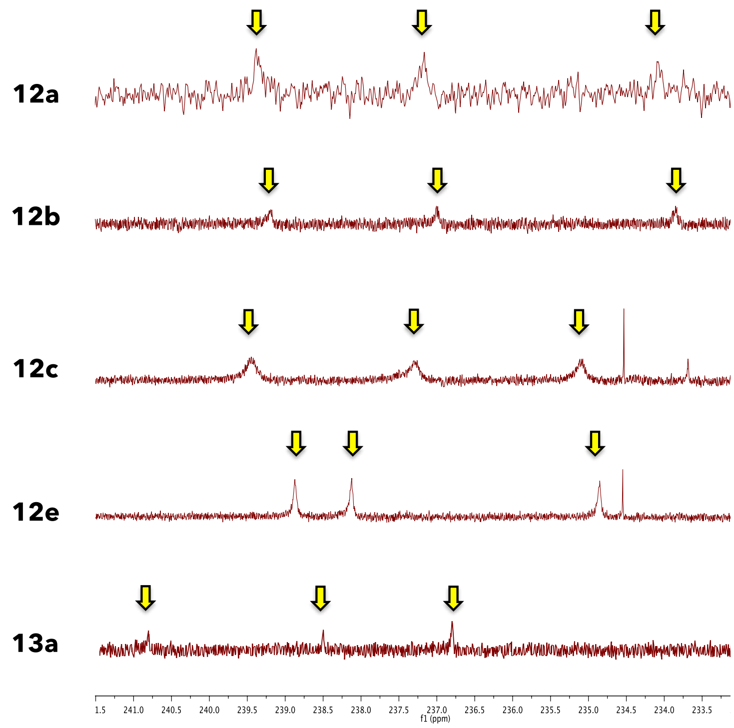

Figure 132: The ^{13}C NMR spectra of complexes **12** in d_6-benzene present the typical signature of a rotation-hindered $Cr(CO)_3$ moiety in an asymmetric local environment that is materialized by three broad signals at around δ 239, 237, and 235 ppm.

The room temperature ^{13}C NMR spectra of **12a–g** and **13a** in d_6-benzene present the typical signature of a rotation-hindered $Cr(CO)_3$ moiety in an asymmetric local environment[917-919] that is materialized by three broad signals at around δ 239, 237, and 235 ppm (Figure 132). All the remaining signals pertaining to the indenyl ligand and the palladacycle are sharp and well resolved. Given that fluxionality was inherent to complexes **7a, 7b**, compounds **12** were investigated by conventional dynamic NMR techniques.[920] The method based on peak separation for the determination of exchange rates in two-state systems was not considered. Unfortunately, the conventional band shape analysis, Deverell-Morgan-Strange method,[921] EXSY, and

[917] [N°609] Djukic, J. P.; Michon, C.; Maisse-Francois, A.; Allagapen, R.; Pfeffer, M.; Dotz, K. H., . . . Fischer, J. *Chem. Eur. J.* **2000**, *6*, 1064.

[918] [N°608] Djukic, J. P.; Maisse-Francois, A.; Pfeffer, M.; Dotz, K. H.; De Cian, A.; Fischer, J. *Organometallics* **2000**, *19*, 5484.

[919] [N°604] Djukic, J. P.; Pfeffer, M.; Dotz, K. H. *C.R. Acad. Sci. Paris, Ser. IIc* **1999**, *2*, 403.

[920] [N°756] Sandstrom, J. *Dynamic NMR Spectroscopy*; Academic Press: New York, **1982**.

[921] [N°809] Deverell, C.; Morgan, R. E.; Strange, J. H. *Mol. Phys.* **1970**, *18*, 553.

polarization transfer experiments proved inconclusive as to the fluxional nature of the new complexes **12**. Indeed, the band shape analysis of the temperature-dependent ^{1}H NMR spectrum with the equipopulated mutual exchange model was found to be inappropriate for two reasons. First, the asymmetry introduced by the metallacycle entails the magnetic inequivalence of protons H_1 and H_3 ($\Delta\delta(^{H_1}/_{H_3})$ ~ 1 ppm) in the 203 K - 298 K domain and at higher temperatures (Figure 133). This precludes any oversimplification of the exchange mechanism by assimilating at all temperature the η^3 transients to transition states and by reducing the system to a simple mutual exchange between two η^1 forms. Second, bandwidth variations on the basis of a 10 K temperature step over a 80 K temperature range were not found sufficiently significant ($\Delta\omega$ < 10 Hz for $^{H_1}/_{H_3}$ in **12a** and **13a** as well as in **14g** at the lowest temperatures) to prevent large systematic errors from occurring on the determination of the exchange rate *k*. Further attempts to alternatively determine the exchange constant from a study of the relaxation time $T_{1\rho}$ by the Deverell-Morgan-Strange method with a d_8.toluene solution of **12a** faced the major obstacle of the first order scalar coupling relaxation caused by the quadrupolar ^{105}Pd nucleus, which putatively produced a complex dependence of $T_{1\rho}$ towards spin-echo pulse frequency. Nonetheless, theory suggested that the energetic barrier to a possible $\eta^1 - \eta^3 - \eta^1$ transposition in complexes **12** (Figure 133) might be of the same amplitude as that estimated for **7b** in d_8-toluene (see Figure 95, Figure 100).

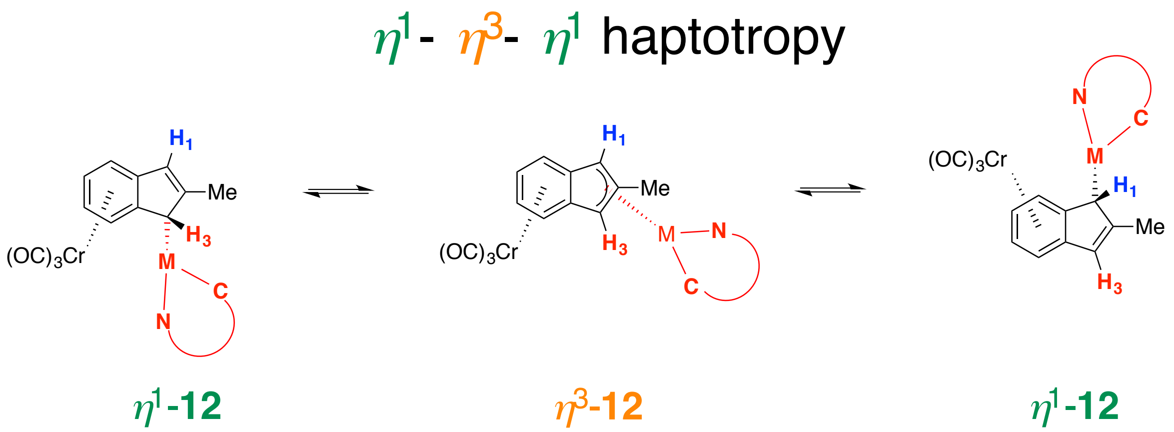

Figure 133: Assumed fluxional behavior of the Pd centre.

In **12a** and **13a** the differences in Gibbs enthalpy ΔG between the singlet ground states of the respective η^1 states and the η^3 transients amount to, according to DFT calculations, 8.9 and 11.3 kcal/mol (conductor-like screening model (COSMO) toluene, zero order regular approximation (ZORA)-PBE-D3(BJ)/all electron TZP), suggests that all the new disclosed complexes might well be fluxional in solution. A few examples are particularly remarkable by their typical ^{1}H NMR signature. For instance, complex **12g**, which contains a planar-chiral palladacycle, produces a single set of signals in ^{1}H NMR spectroscopy, whereas theory suggests that the *exo* and *endo*-**12g** isomers corresponding to the two possible positions of the $Cr(CO)_3$ moiety in the 2-phenylpyridine ligand should be nearly equally populated (Figure 134). Theory predicts an *endo* to *exo* Gibbs enthalpy of activation difference of ~10 kcal/mol for **12g** in the gas phase at 298.15 K.

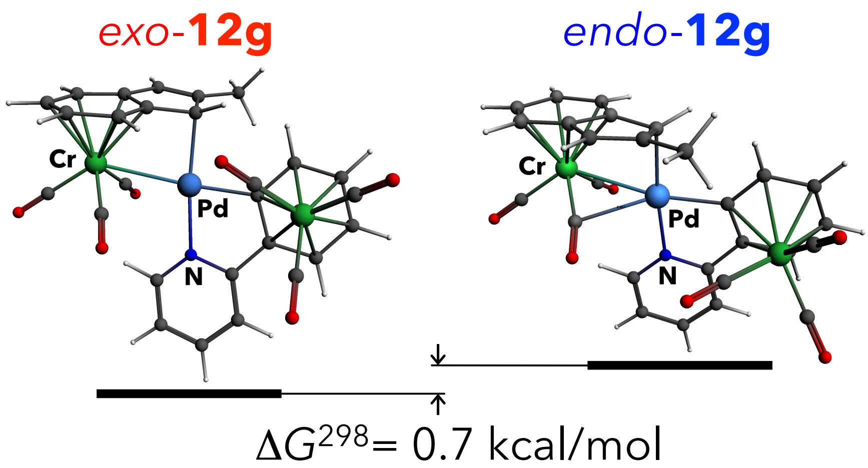

Figure 134: Gas-phase singlet ground-state geometries of the isoenergetic *exo* and *endo*-**12g** diastereomers (ZORA-PBE-D3(BJ)/all electron TZP, T = 298.15 K).

In this respect, also particularly significant is the case of (1*S*)-**12c** which contains a chiral moiety, that is, the palladated (1*S*)-*N*,*N*-dimethyl,1-phenylethylamine (ee ≈ 98 %) ligand. The room temperature ^{1}H NMR spectrum of this compound in d_8- toluene reveals also a single set of signals, a rather ambiguous situation that apparently contradicts the results of structural X-ray diffraction analyses.

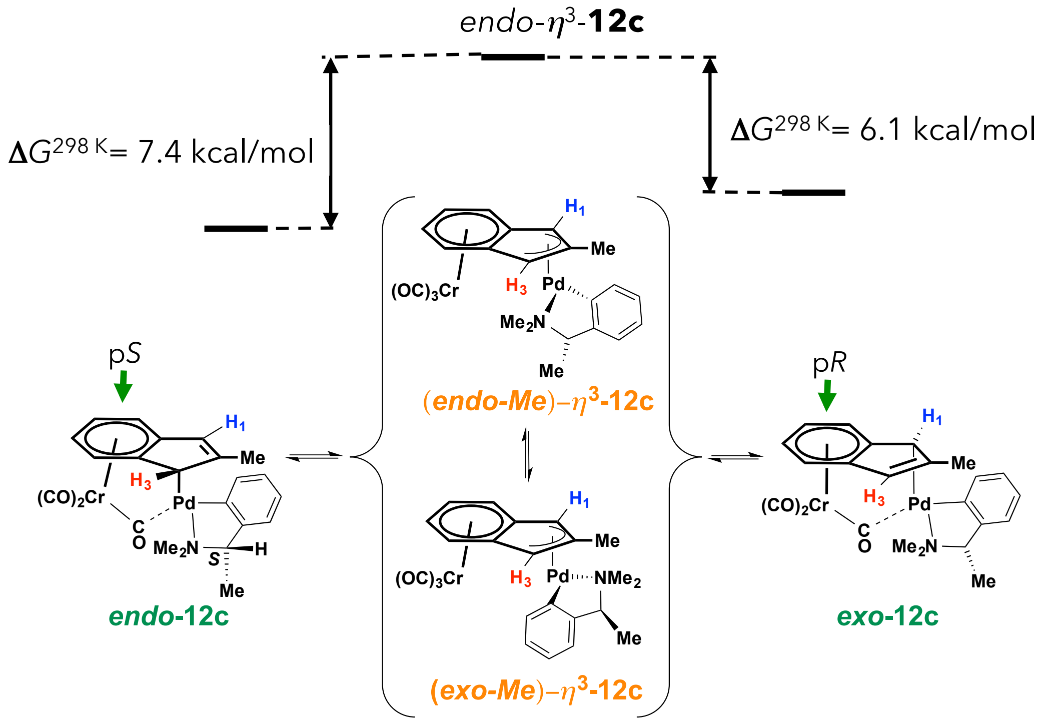

Figure 135: Putative mechanism of transposition of the palladacyclic unit in (1*S*)-**12c** modeled by DFT (COSMO toluene). Planar chiral configurations are assigned according to Schlögl's convention[922] giving priority n°1 to the Pd-substituted carbon position.

The ^{1}H NMR spectrum of **12c** in d_8-toluene at room temperature displays the signals of protons H_1 and H_3 (Figure 135) as two distinct singlets at δ 5.6 and 4.4 ppm ($\Delta\delta$ (ppm) = 1.2 ppm). Variable temperature ^{1}H NMR investigations of the same d_8-toluene solution of (1*S*)-**12c** at subambiant temperatures (213(1) < T (K) < 298(1)) did not reveal any significant line-broadening of the signals of H_1 and H_3 upon cooling, which precluded further extraction of thermodynamic parameters from dynamic NMR band shape analysis (Figure 136).

[922] [N°697] Schlögl, K. *Top. Stereochem.* **1967**, *1*, 39.

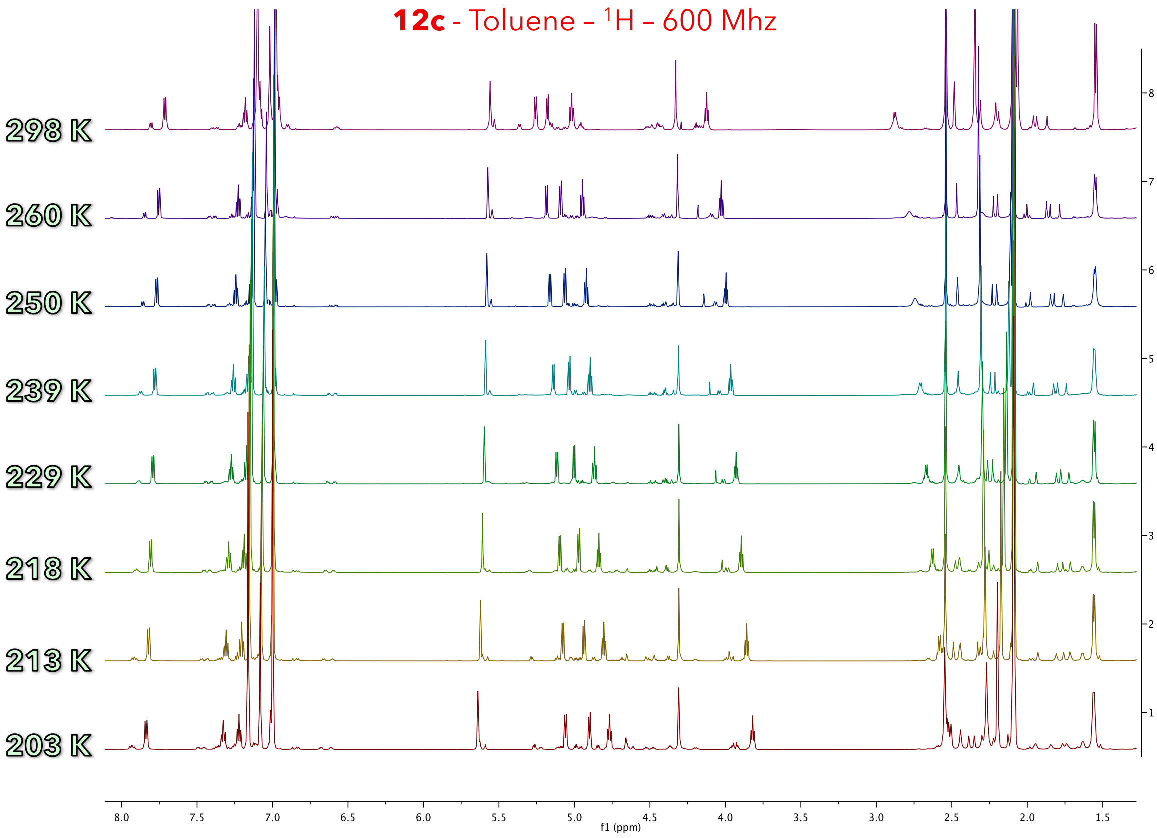

Figure 136: ^{1}H NMR variable temperature investigations of (1*S*)-**12c** at subambiant temperatures did not reveal any significant line broadening of the signals of H_1 and H_3 upon cooling.

Nonetheless, modelling the transposition process by means of the DFT with an ad hoc treatment of solvation in toluene (COSMO ZORA[923]-PBE[924]-D3(BJ)/TZP), revealed a Gibbs enthalpy variation ΔG^{298}_{theor} (*endo*-η^1-**12c**-to-*endo*-η^3-**12c**) of +7.4 kcal/mol at 298.15 K, that is, by *ca.* 3−4 kcal/mol lower than the one estimated for **7b**; diastereomers *endo* and *exo*-**12c** being practically isoenergetic (Figure 135). In this simplified transposition mechanism, the $\eta^1 - \eta^3 - \eta^1$ excursion of the palladium centre at the indenyl ligand (Figure 135) entails two nearly isoenergetic metastable η^3-**12c** transients in which one side of the palladacycle faces the $Cr(CO)_3$ tripod, with the α-Me group pointing either toward (*endo* orientation) or outward the latter tripod (*exo* orientation).

923 [N°810] Van Lenthe, E.; Baerends, E. J. *J. Comput. Chem.* **2003**, *24*, 1142.

924 [N°170] Perdew, J. P.; Burke, K.; Ernzerhof, M. *Phys. Rev. Lett.* **1996**, *77*, 3865.

The ^{1}H NMR of **13a** (Figure 137) is characterized by the typical satellite signals arising from the coupling of ^{1}H nuclei with the ^{195}Pt isotope (33.8 % natural abundance, experimental $\delta^{195}Pt = -2524$ ppm, ZORA-PBE-D3(BJ)/all electron TZP $\delta^{195}Pt = -2139$ ppm).

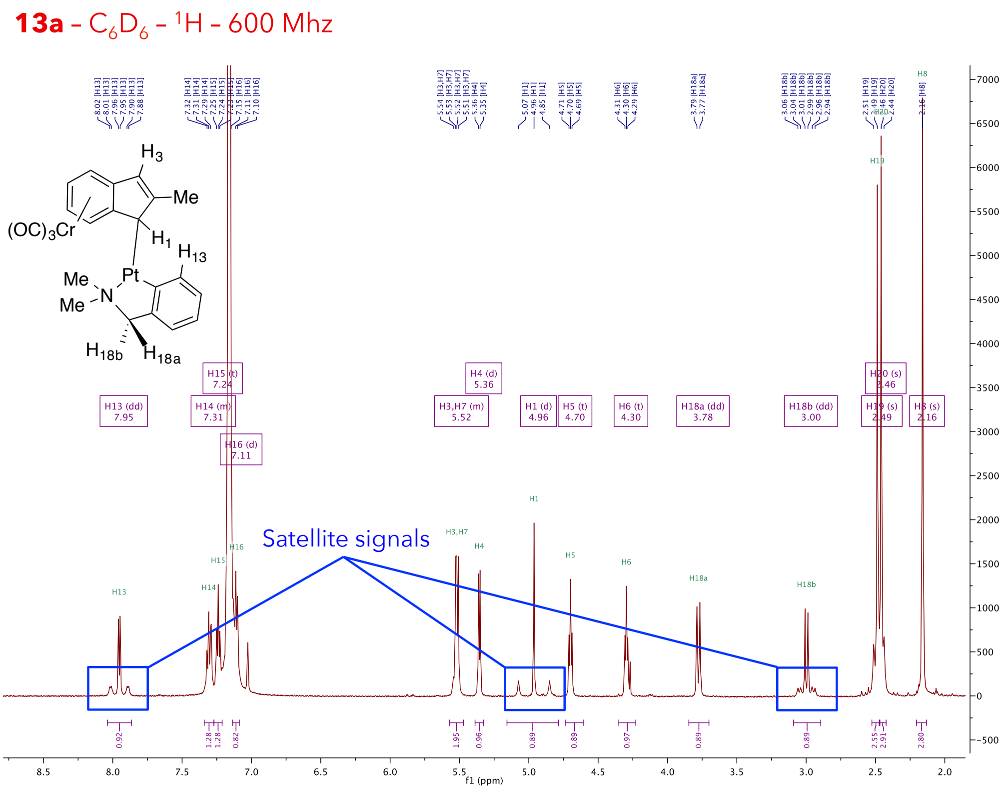

Figure 137: Typical satellite signals arising from the coupling of ^{1}H nuclei with the ^{195}Pt isotope in complex **13a**.

On the basis of the computed ^{195}Pt-coupled NMR spectrum (COSMO, ZORA-PBE-D3(BJ)/all electron TZP) it was established that signals that bear the strongest $^{1}H-^{195}Pt$ scalar coupling constants in absolute value are those of H_1 ($|J_{exp}|$ = 134.7 Hz, $|J_{theor}|$ = 116.8 Hz), H_{13} ($|J_{exp}|$= 74.7 Hz, $|J_{theor}|$ = 65.6 Hz), H_{18a} ($|J_{exp}|$ = 61.9 Hz, $|J_{theor}|$ = 86.8 Hz), H_3 ($|J_{exp}|$ = 19.6 Hz, $|J_{theor}|$ = 15.6 Hz) and the methyl groups ($|J_{exp}|$ = 31.8 and 24.0 Hz). Owing to an approximate 90 deg H_{18a}–C–N–Pt dihedral angle, proton H_{18a} displays no measurable coupling with the ^{195}Pt nucleus in the experimental spectrum ($|J_{theor}|$ = 2.3 Hz). It is worth noting that the satellite signals progressively broaden upon lowering the temperature of the NMR probe to eventually vanish at 213 K (Figure 138).

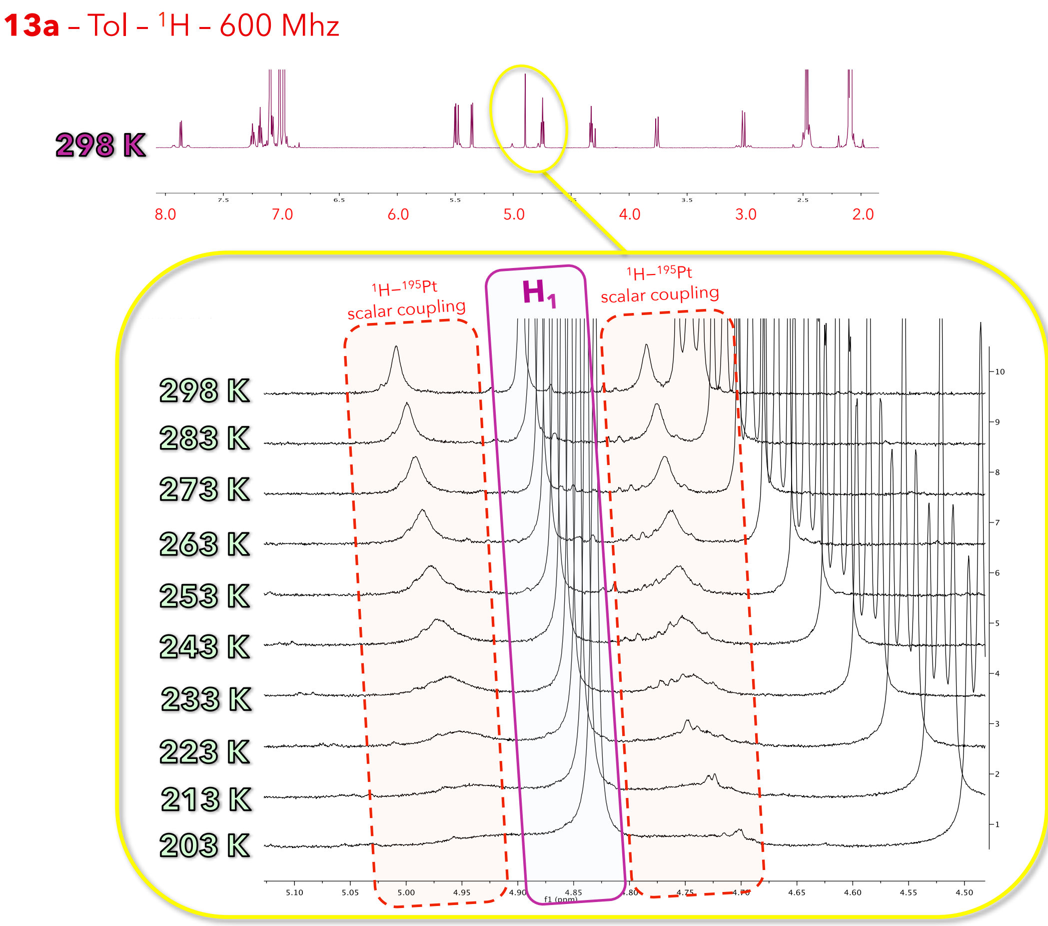

Figure 138: ^{1}H NMR variable temperature of **13a** revelling the satellite signals broadening upon lowering the temperature of the NMR probe to eventually vanish at 213 K.

4.4 - Theoretical aspects.

All experimental geometries of **12** were reproduced acceptably with DFT-D3 methods,[925, 926] that is, the dispersion-corrected PBE[927]-D3(BJ) and TPSS[928]-D3(BJ) functionals, and with the hybrid PBE0-dDsC[929] functional. The methods expectedly (similarly to **7a-c**) all gave slightly shorter Cr–M distances as compared to that of crystal state structures (Figure 139), leading to an apparent slight mutual tightening of metal centres and overbinding of the latter with their ligands.

925 [N°187] Grimme, S.; Ehrlich, S.; Goerigk, L. *J. Comput. Chem.* **2011**, *32*, 1456.

926 [N°738] Grimme, S.; Antony, J.; Ehrlich, S.; Krieg, H. *J. Chem. Phys.* **2010**, *132*, 154104.

927 [N°170] Perdew, J. P.; Burke, K.; Ernzerhof, M. *Phys. Rev. Lett.* **1996**, *77*, 3865.

928 [N°811] Staroverov, V. N.; Scuseria, G. E.; Tao, J.; Perdew, J. P. *J. Chem. Phys.* **2003**, *119*, 12129.

929 [N°739] Steinmann, S. N.; Piemontesi, C.; Delachat, A.; Corminboeuf, C. *J. Chem. Theory Comput.* **2012**, *8*, 1629.

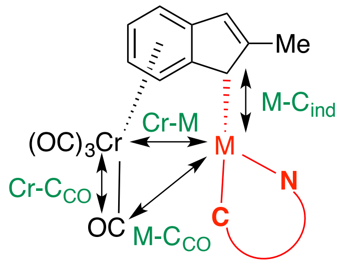

Cmpd/method[a]	***Cr-M***	***M-C$_{ind}$***	***M-C$_{CO}$***	***Cr-C$_{CO}$***
		12a (M= Pd)		
X-ray diffr.[b]	2.9290(3)	2.1080(15)	2.5720(16)	1.8564(16)
PBE-D3(BJ)[c]	2.852	2.141	2.434	1.863
PBE0-dDsC[c]	2.792	2.123	2.437	1.846
		13a (M= Pt)		
X-ray diffr.	2.8834(6)	2.099(4)	2.408(4)	1.876(4)
PBE-D3(BJ)[c]	2.823	2.122	2.212	1.910
TPSS-D3(BJ)[c]	2.807	2.125	2.231	1.914
PBE0-dDsC[c]	2.830	2.095	2.343	1.860
		12b (M= Pd)		
X-ray diffr.	2.9125(4)	2.110(2)	2.605(2)	1.854(2)
PBE-D3(BJ)[c]	2.844	2.143	2.434	1.863
TPSS-D3(BJ)[c]	2.801	2.141	2.420	1.876
PBE0-dDsC[c]	2.790	2.119	2.435	1.845
		endo-(p*S*,1*S*)-**12c** (M= Pd)		
X-ray diffr.	2.9130(16)	2.114(8)	2.517(10)	1.858(10)
PBE-D3(BJ)[c]	2.894	2.135	2.504	1.859
		exo-(p*R*,1*S*)-**12c** (M= Pd)		
X-ray diffr.	2.9392(17)	2.115(8)	2.572(11)	1.845(12)
PBE-D3(BJ)[c]	2.905	2.135	2.550	1.855
		12e (M= Pd)		
X-ray diffr.	2.8505(6)	2.111(3)	2.567(3)	1.857(3)
PBE-D3(BJ)[c]	2.815	2.145	2.508	1.857
TPSS-D3(BJ)[c]	2.774	2.146	2.516	1.864
PBE0-dDsC[d]	2.833	2.142	2.494	1.814
		12f (M= Pd)		
PBE-D3(BJ)[c]	2.830	2.146	2.473	1.864
		12g (M= Pd)		
X-ray diffr.	2.8392(6)	2.111(3)	2.515(3)	1.849(3)
PBE-D3(BJ)[c]	2.816	2.138	2.444	1.864

[a] all-electron triple-Slater-ζ type orbital basis sets with one polarization function (TZP) were used throughout this studyunless otherwise stated. [b] Based on the obtained Xray distances. [c] *ad-hoc* all electron TZP basis set associated to the scalar relativistic ZORA[930] treatment. [d] all electron TZP basis set (C,H,N,O, Cr, Fe), frozen core up to 11e level for Pd.

Figure 139: Selected distances (in Å) taken from Structural X-ray Diffraction Analysis and DFT Calculations at Different Levels of Theory.

930 [N°810] Van Lenthe, E.; Baerends, E. J. *J. Comput. Chem.* **2003**, *24*, 1142.

The computed geometries of **12** were subsequently analysed by an array of methods in order to identify the nature of the interactions exiting between the $Cr(CO)_3$ moiety and the M centre (M = Pd, Pt) at its fourth vacant coordination site. Analysis by the Natural Bond Orbital (NBO)[931] method established clearly the η^1 mode of coordination of M (M = Pd, Pt) to the indenyl ligand. The $C_{indenyl}$–M bonds in models of **12a** and **13a** bear Wiberg indexes (abbreviation, wbi) of 0.36 and 0.48, respectively, that are relatively lower than those of metallacyclic C_{Ar}–M bonds, which amount to 0.53 and 0.60, respectively. According to the NBO analysis of **13a**, the hybrid natural orbital at the carbon contributing to the Pt–$C_{indenyl}$ bond (Pt–C_1 according to atom numbering in (Figure 140), natural bonding orbital population 1.73 e) possesses an overwelming p character (sp^5) that confines the interaction with the Pt centre to a typical σ coordinative bond.[932] In the case of **13a**, the NBO analysis, which relies on Lewis structures computed with a bond electron population threshold of 1.5 electron, did not produce any information on the Pd–$C_{indenyl}$ interaction due to its formal low electron population.

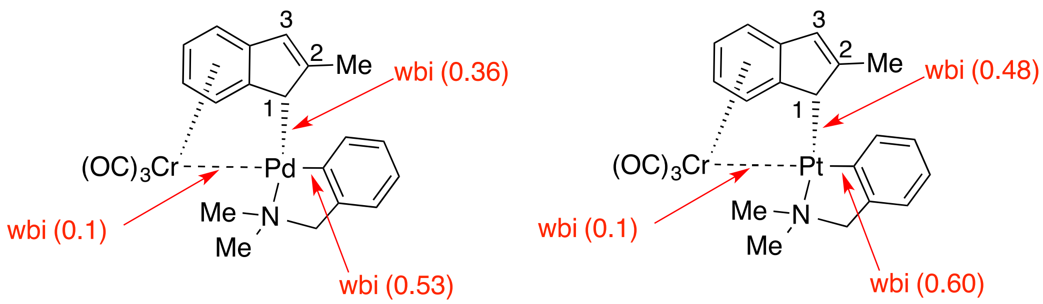

12a **13a**

Figure 140: Inspection of the Wiberg bond indices for **12a** and **13a**.

Nonetheless, the neighbouring C_1–C_2 and C_2–C_3 bonds (cf. numbering in (Figure 140)) at the indenyl ligand in **12a** and **13a** were found to have a single (wbi ~1.0) and a double (wbi ~1.6) bond character, respectively. In **13a**, ^1H–^{13}C coupling constants for the nuclei at position 1 (J_{C-H} = 158 Hz) and 3 (J_{C-H} = 169 Hz) displayed values similar to those observed in **5a** for the CH_2 (J_{C-H} = 157 Hz) and CH (J_{C-H} = 167 Hz) position,

[931] [N°812] Weinhold, F. In *Encyclopedia of Computational Chemistry*; Schleyer, P. v. R., Allinger, N. L., Clark, T., Gasteiger, J., Kollman, P. A., III, H. F. S., Schreiner, P. R., Eds.; John Wiley & Sons, Chichester, UK: **1998**; Vol. 3, p 1792.

[932] [N°813] Weinhold, F.; Landis, C. R. *Valency and Bonding, a Natural Bond Orbital Donor-Acceptor Perspective*; University Press: Cambridge, UK, **2005**.

respectively, at the five-membered ring, which suggests that C_1 has a quasi-sp^3 hybridization. Inspection of the Wiberg bond indices for the Cr−M (M = Pd, Pt) segment indicated, in all addressed cases, values close to 0.1, which suggested a very low covalent character for the metal−metal interaction (Figure 141).

	5a	**12a**	**13a**	**7a**	η^1-**12b**	η^3-**12b**	**14b**
q(Cr)	-0.86	-0.84	-0.82	-0.82	-0.84	-0.81	-0.82
q(C_{CO}-Pd)	+0.60 [a]	+0.59	+0.53	+0.59	+0.59	+0.63 [b]	+0.65 [a]
q($Cr(CO)_3$)	-0.27	-0.39	-0.46	-0.34	-0.39	-0.34	-0.27
Δq[$Cr(CO)_3$] [c]		-0.12	-0.19	-0.07	-0.12	-0.07	0.00
q(M)		+0.59 [d]	+0.59 [e]	+0.60 [d]	+0.60 [d]	+0.68 [d]	+0.64 [d]
Δq(M) [f]		+0.03	+0.13	-0.03	+0.04	+0.02	-0.01
wbi(Cr-M)		0.1 [d]	0.1 [e]	0.1 [d]	0.1 [d]	0.0 [d]	0.0 [d]

[a] Averaged value. [b] Calculated for the shortest C_{CO}−Pd distance (3.20 Å). [c] Δq[complex, $Cr(CO)_3$] = *q*[compound, $Cr(CO)_3$] − *q*[**5a**, $Cr(CO)_3$]. [d] M = Pd. [e] M = Pt. [f] $\Delta q(M) = q(M)_{compound} - q(M)_{prepared\ fragment}$, where the prepared fragment is the metalated indenyl ligand in its prepared geometry prior to interaction with the prepared $Cr(CO)_3$ moiety.

Figure 141: Wiberg Indices for the Cr-M Segment (wbi(Cr-M) M = Pd, Pt) and Natural Charges (*q*, Natural Population Analysis) at the $Cr(CO)_3$ Moiety in a Series of Gas-Phase Singlet Ground State Models.

Further the extended transition state-natural orbitals for chemical valence (ETSNOCV) analysis,[933,934] which provides symmetry-ordered information on the orbital interaction between two closed shell intramolecular fragments, were carried out with a model of **12a**. The mutual interaction of the $Cr(CO)_3$ moiety with the palladated indenyl ligand was considered and orbital interactions that could be involved in a possible M−$Cr(CO)_3$ interaction were identified.

Figure 142, displays a selection of four-density deformation $\Delta\rho$ plots ordered by decreasing orbital interaction energy for the considered interfragment interaction. One can clearly notice that $\Delta\rho_1$ contains a significant component of electron density donation mostly from the chromium toward the intermetallic space and the palladacycle. $\Delta\rho_3$ contains partly an indirect Pd-to-Cr back-donation component. Most of the orbital interaction in both cases is focused on the build-up of Cr−arene bonds.

933 [N°750] Mitoraj, M. P.; Michalak, A.; Ziegler, T. *J. Chem. Theory Comput.* **2009**, *5*, 962.
934 [N°751] Mitoraj, M. P.; Michalak, A.; Ziegler, T. *Organometallics* **2009**, *28*, 3727.

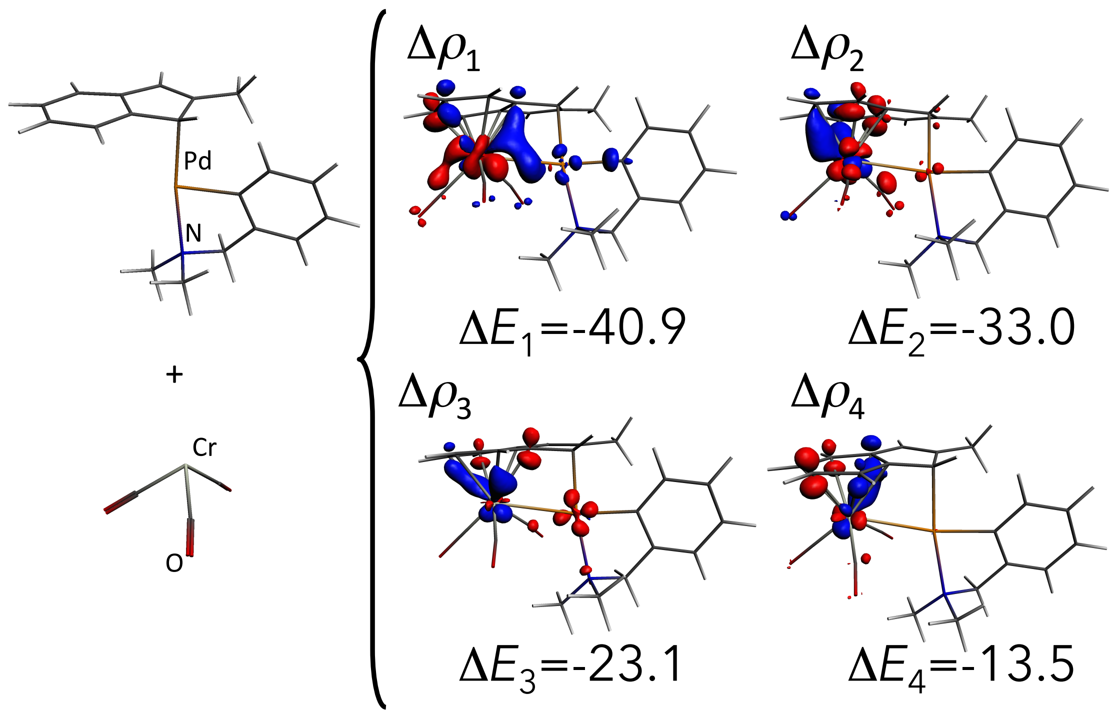

Figure 142: ETS-NOCV deformation densities $\Delta\rho$ and their stabilization energy ΔE_{orb} (in kcal/mol) for the interaction of prepared $Cr(CO)_3$ and palladated indenyl fragments of **12a**. Red and blue-colored isosurfaces materialize regions where charge density depletion and build up occur, respectively: electron density transfer operates from red-coloured areas to blue ones upon bonding. Deformation density isosurface contour was set to 0.005 e/bohr^3.

These two interactions represent less than 50 % of the total orbital interaction energy, which amounts to −155.3 kcal/mol. Similar observations can be made for **13a**. Qualitative information on the electronic influence of the metallacycle onto the $Cr(CO)_3$ moiety was gained by an inspection of the sum of natural charges[935] at the $Cr(CO)_3$ tripod of **12a**, **13a**, and **12b**, *i.e.* $q[Cr(CO)_3]$. Worthy to note, the Cr and the M (M = Pd, Pt) centres display marked negative and positive natural charges (Figure 141). Natural charges reflect, in an atom-wise manner, the molecular distribution of charge densities and may provide basic information on the redistribution of electron density. For instance, the electronic effect of the Pd/Pt centre bound to the indenyl ligand was evaluated by the deviation $\Delta q[Cr(CO)_3]$ of the sum of charges born by the $Cr(CO)_3$ moiety in a given complex by comparison to a reference compound, that is, **5a**, where the benzylic position is occupied by two hydrogen atoms. The negative charge increase

[935] [N°812] Weinhold, F. In *Encyclopedia of Computational Chemistry*; Schleyer, P. v. R., Allinger, N. L., Clark, T., Gasteiger, J., Kollman, P. A., III, H. F. S., Schreiner, P. R., Eds.; John Wiley & Sons, Chichester, UK: **1998**; Vol. 3, p 1792.

apparent from (Figure 141) for all complexes **12** ($\Delta q[Cr(CO)_3] \approx -0.15$) is accompanied with a slight increase of the positive natural charge at M (M = Pd, Pt). It is speculated that this relative overall electron density enrichment at the tripod of **5a** is slightly compensated by the $(CO)_3Cr{\rightarrow}Pd$ donor−acceptor interaction embodied by $\Delta\rho_1$ (Figure 142), which may explain the slight shift to a higher frequency relative to **5a**, observed for the IR signature of the carbonyl stretching bands of **12** (
Figure 143).

Cmpd	***Reciprocal wavelengths in cm^{-1}***		
5a	1935	-	1839
12a	1954	1877	1841
13a	1953	1872	1818
12b	1956	1886	1847
14b	1933	-	1843
12c	1941	1891	1832
12d	1935	1865	1843
12e	1941	1872	1843
12f	1948	1887	1843
12g	1974 (s) 1940 (s) 1911 (s) 1876 (vs) 1851 (vs)		
14h	1942	-	1851

Figure 143: IR vibrations of carbonyl groups.

Given the low Wiberg indices of the M−Cr segment, further analyses with Bader's *Quantum Theory of Atoms in Molecule* (QTAIM)[936, 937] were carried out with a selected group of models in order to clarify the weight of covalence in the $M{-}Cr(CO)_3$ interaction. Several cases displaying rather different computed Cr−M distances were considered. These are namely **12a**, **13a**, **12b**, and **12e**, the geometries of which were optimized with the hybrid PBE0[938, 939] functional to which a dDsC[940] density-dependent correction for mid-to-long-range dispersion is appended (Figure 139). The absence of electron density topological *bond critical point* (BCP) and bond path in the Cr−M segment, that is, two sufficient conditions to rule out the existence of a covalent

[936] [N°754] Popelier, P. *Atoms in Molecules, An Introduction*; Prentice Hall, Harlow, England, **2000**.
[937] [N°755] Bader, R. F. W. In *Atoms in Molecules: A Quantum Theory*; Clarendon: Oxford, **1990**.
[938] [N°744] Ernzerhof, M.; Scuseria, G. E. *J. Chem. Phys.* **1999**, *110*, 5029.
[939] [N°745] Adamo, C.; Barone, V. *J. Chem. Phys.* **1999**, *110*, 6158.
[940] [N°740] Steinmann, S. N.; Corminboeuf, C. *J. Chem. Theory Comput.* **2011**, *7*, 3567.

Cr−metal bond according to Bader's QTAIM criteria, was established in all cases. The only feature related to some direct interaction of M with the $Cr(CO)_3$ fragment was a recurrent BCP(3,-1) located in between the M (M = Pd, Pt) centre and the vicinal pseudobridging carbon atom of the carbonyl ligand for models of **12b** and **12e** (Figure 144).

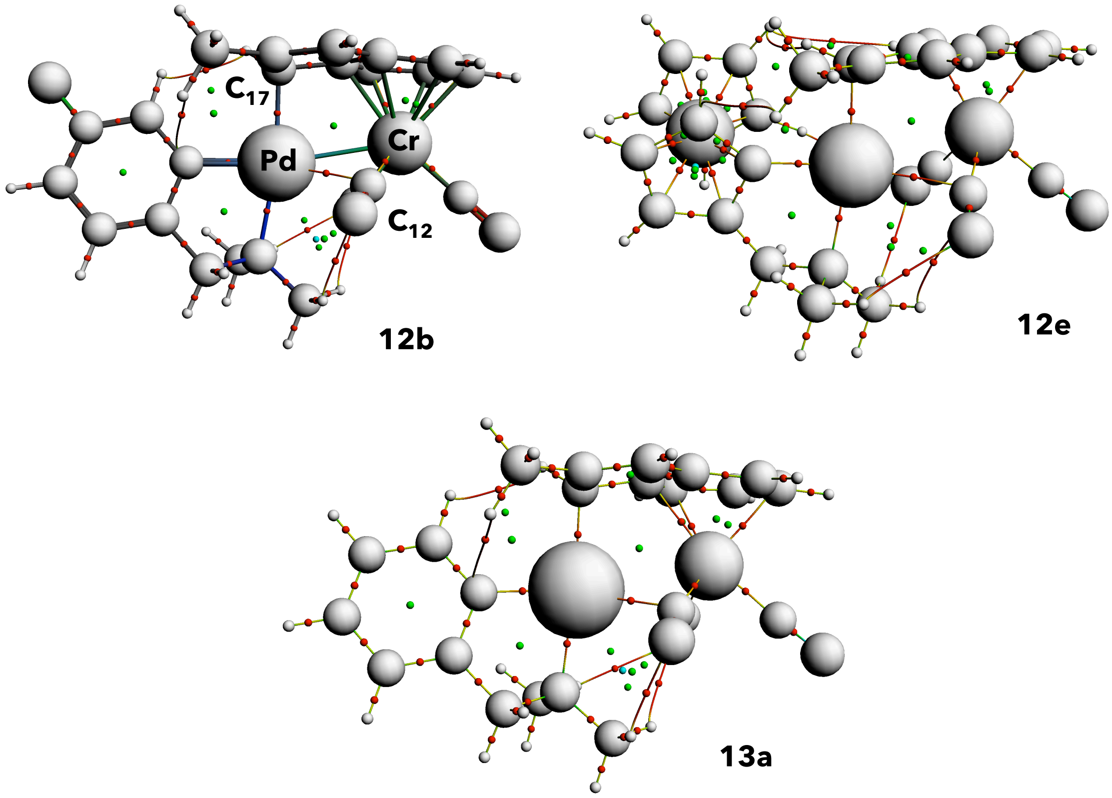

Figure 144: Atoms-in-molecule analysis of the electron density topology for **12b**, **12e** and **13a**. Red and green dots are associated to Bond (BCP) and Ring (RCP) Critical Points, respectively. Grey spheres materialize the atomic positions scaled by their associated density.

In both cases, this BCP (ρ = 0.050 au, L= −0.0297 au, and ρ = 0.044 au, L= −0.0268 au respectively) localized in the Pd_1−C_{17} and the Pd_1−C_{12} bond paths (Figure 144) fulfils the criteria of a weak closed-shell van der Waals interaction (Wiberg indice ≈ 0.2) according to Popelier.[941] Compared to other cases where carbonyl bridges are characterized by at least 5-to-10-fold larger values of electron density population ρ at

[941] [N°754] Popelier, P. *Atoms in Molecules, An Introduction*; Prentice Hall, Harlow, England, **2000**.

the BCP, as in tetracobalt clusters[942] (Figure 145, left) and nonacarbonyldiiron[943] (Figure 145, top-right) complexes, the CO bridge described here is incipient from a bonding point of view and much weaker than in the typical semibridging situations described by Bénard for a carbonyl dirhodium complex.[944] (Figure 145, bottom-right)

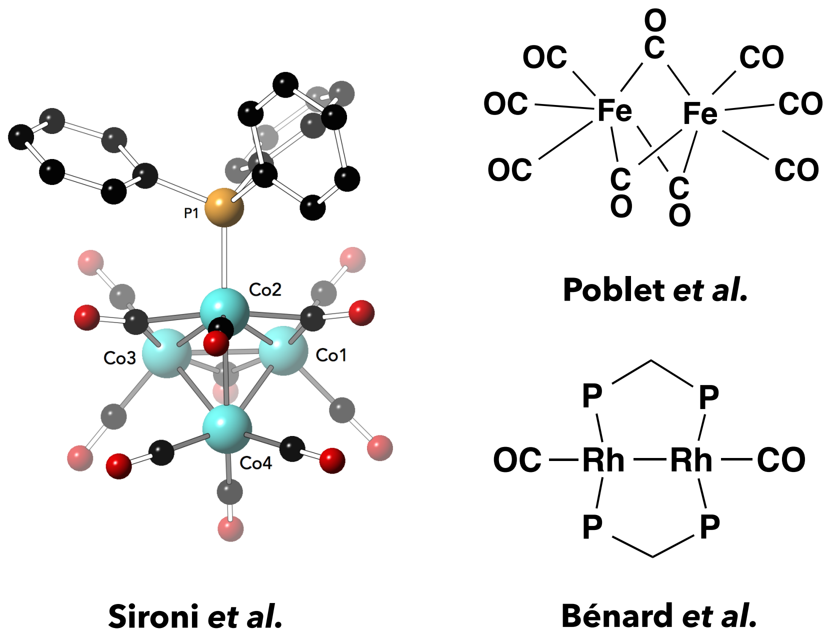

Figure 145: Other examples of carbonyl complexes.

Yang and co-workers[945] proposed recently a new method of detection and visualization of noncovalent interactions in the real space based on electron density ρ and its derivatives. Highly complementary to analyses based on the QTAIM theory, Yang's Non-Covalent Interaction (NCI) region analysis provides an intuitive 3-D isosurfaces representation[946] of local Pauli repulsion, van der Waals interactions, and other local attractive noncovalent interactions like H-bonds.[947] This method is based on the strong dependence of the so-called reduced density gradient s on the signed value of the density $\lambda_2\rho$, which allows, by the choice of an appropriate cut-off value for s, to separate

942 [N°814] Macchi, P.; Garlaschelli, L.; Martinengo, S.; Sironi, A. *J. Am. Chem. Soc.* **1999**, *121*, 10428.

943 [N°815] Bo, C.; Sarasa, J. P.; Poblet, J. M. *J. Phys. Chem.* **1993**, *97*, 6362.

944 [N°816] Bo, C.; Costas, M.; Poblet, J. M.; Rohmer, M.-M.; Benard, M. *Inorg. Chem.* **1996**, *35*, 3298.

945 [N°630] Johnson, E. R.; Keinan, S.; Mori-Sánchez, P.; Contreras-García, J.; Cohen, A. J.; Yang, W. *J. Am. Chem. Soc.* **2010**, *132*, 6498.

946 [N°629] Contreras-García, J.; Johnson, E. R.; Keinan, S.; Chaudret, R.; Piquemal, J.-P.; Beratan, D. N.; Yang, W. *J. Chem. Theory Comput.* **2011**, *7*, 625.

947 [N°817] Johansson, M. P.; Swart, M. *Phys. Chem. Chem. Phys.* **2013**, *15*, 11543.

noncovalent from covalent interactions, the former being further sorted into either attractive or nonbonded (van der Waals) and repulsive (Pauli) classes depending on the sign of the second electron-density Hessian eigenvalue λ_2. The sign of the latter is purportedly positive for nonbonded and repulsive interactions, and negative for a range of attractive noncovalent interactions such as H-bonds and the so-called "halogen bonds".

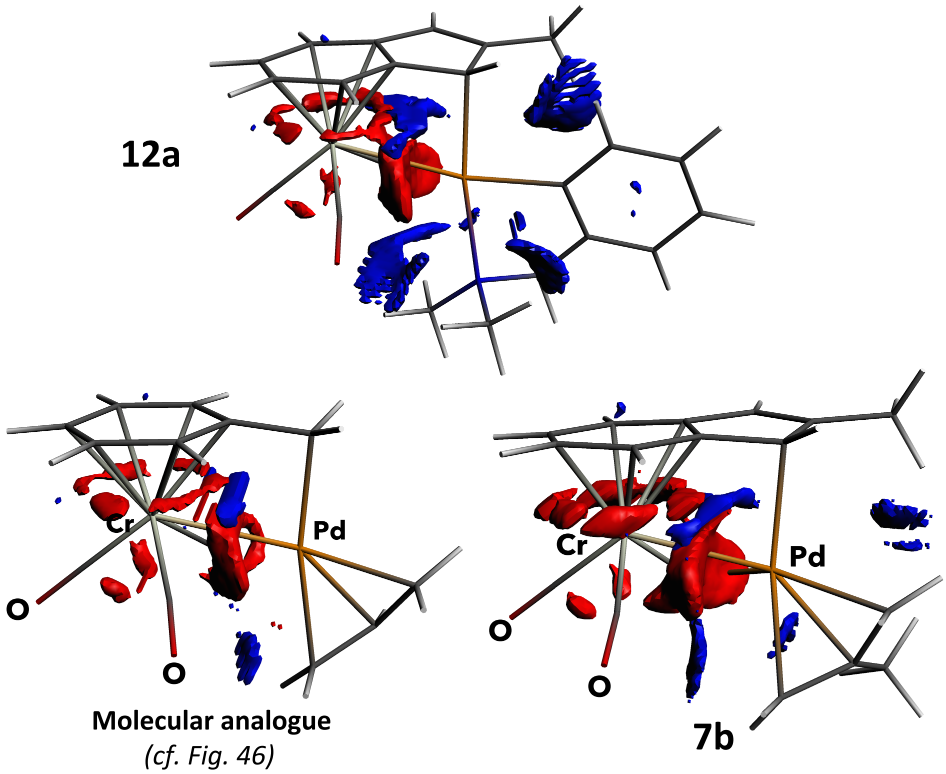

Figure 146: ADFview2013 plots of noncovalent interaction (NCI) regions materialized by *reduced density gradient isosurfaces* (cut-off value s = 0.02 au, ρ = 0.05 au) coloured according to the sign of the signed density $\lambda_2\rho$ (red and blue colours are associated to negatively and positively signed terms) for gas-phase relaxed singlet ground state models of Pd-containing complexes **12a**, **7b**, and the **molecular analogue** reported by Kalinin *et al.* (cf. **Figure 145** and CSDB refcode SOSTID). All calculations were performed with gas phase singlet ground state optimized geometries at the ZORA-PBE0-dDsC/all electron TZP level. Selected distances (in Å) for 7: Cr−Pd, 2.698 (SOSTID 2.764); Pd−C_{benzyl}, 2.119 (SOSTID 2.103); Pd−$_{CCO}$, 2.370 (SOSTID 2.639).

To the best of our knowledge, there is no report in the literature on the use of Yang's NCI analysis for organometallic systems. Figure 146 displays NCI region plots for models of **12a**, **7b** and a **molecular analogue** first reported by Kalinin *et al* [948-950] The

[948] [N°734] Moiseev, S. K.; Cherepanov, I. A.; Petrovskii, P. V.; Ezernitskaya, M. G.; Butenschön, H.; Strotmann, M.; Kalinin, V. N. *Inorg. Chim. Acta* **1998**, *280*, 71.

[949] [N°735] Kalinin, V. N.; Cherepanov, I. A.; Moiseev, S. K.; Dolgushin, F. M.; Yanovsky, A. I.; Struchkov, Y. T. *Acta Cryst. Sect. C* **1993**, *49*, 805.

red coloured isosurfaces are associated with attractive interactions and blue isosurfaces are associated with van der Waals and repulsive interactions for a cut-off value of *s* of 0.02 au.

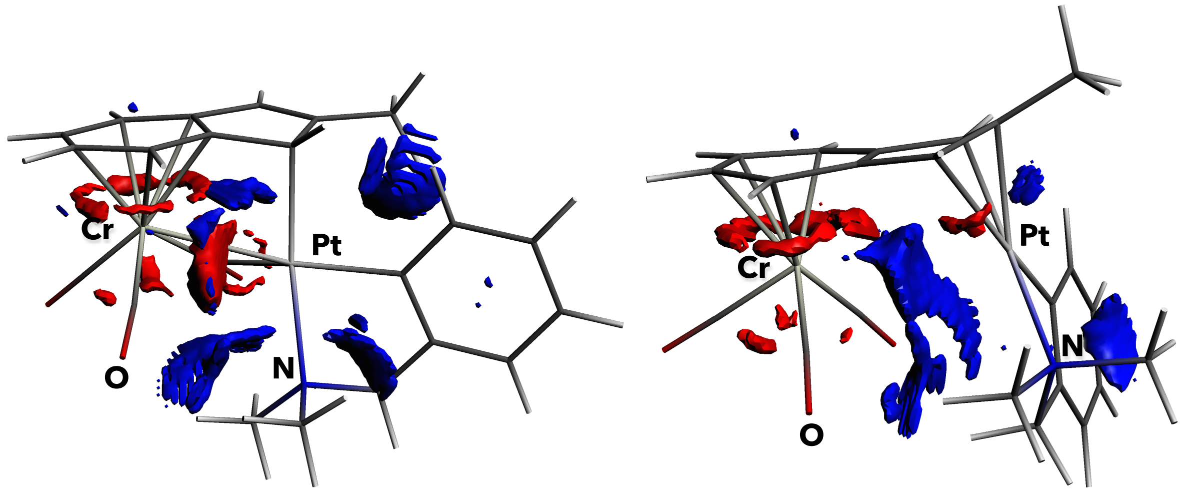

η^1-**13a** η^3-**13a**

$$E_{\eta^3-\mathbf{13a}} - E_{\eta^1-\mathbf{13a}} = 15\ kcal/mol \qquad \text{(PBE0-dDsC)}$$

Figure 147: ADFview2013 NCI plots of reduced density gradient isosurfaces (cut-off value s = 0.02 au, ρ = 0.05 au) coloured according to the sign of the signed density $\lambda_2\rho$ (red and blue colours are associated to negatively and positively signed terms) for models of η^1-**13a** and η^3-**13a**. Calculations were performed at the ZORA-PBE0-dDsC/all electron TZP level with gas phase singlet ground state optimized geometries.

The red isosurfaces are for the largest part located in the Cr−M segment, while remaining residues materialize attractive NCI regions between the η^6-arene ligand and the $Cr(CO)_3$ moiety. Figure 147 displays a confrontation of the (η^1-indenyl)platinum isomer **13a**, written here as η^1-**13a**, and its parent high-energy (η^3-indenyl)platinum singlet ground state fictitious isomer η^3-**13a**. It must be noted here that η^3-**13a** is by *ca.* 12 to 15 kcal/mol of total energy (difference of ZPVE, *i.e.*, zero point vibrational energy, ≈ 0.6 kcal/mol) less stable than η^1-**13a** (PBE-D3(BJ) and PBE0-dDsC). The large blue-colored NCI region between the Pt centre and the $Cr(CO)_3$ (Cr−Pt: 3.548 Å) moiety formally denotes a nonbonded interaction ($\lambda_2 > 0$).

[950] [N°582] Kalinin, V. N.; Cherepanov, i. y. A.; Moiseev, S. K.; Batsanov, A. S.; Struchkov, Y. T. *Mendeleev Commun.* **1991**, *1*, 77.

Early literature on related $Cr(CO)_3$ devoid (indenyl)Pd(II)XL complexes tends to suggest a preference for the η^3 bonding mode of coordination to reach valence saturation at Pd.[951-955] The previously outlined importance of noncovalent interactions in the isolated *syn*-facial isomers raises further the question of the nature of the forces that drive the chemical system into such an unusual formally electron-unsaturated situation. The information on the so-called interaction energy ΔE_{int} obtained by a Ziegler–Rauk energy decomposition analysis (EDA)[956, 957] was used to evaluate the benefits gained from a η^1-*syn*-facial arrangement compared to the η^3-*antara*-facial option. Deformation energies ΔE_{def} were therefore not considered here. According to the general EDA method, the related interaction energies ΔE_{int} were computed for so-called prepared fragments, that is for $Cr(CO)_3$ and 2-methylindenyls substituted with various pertinent metallacycles taken in their geometry in the bonded molecule (Figure 148).

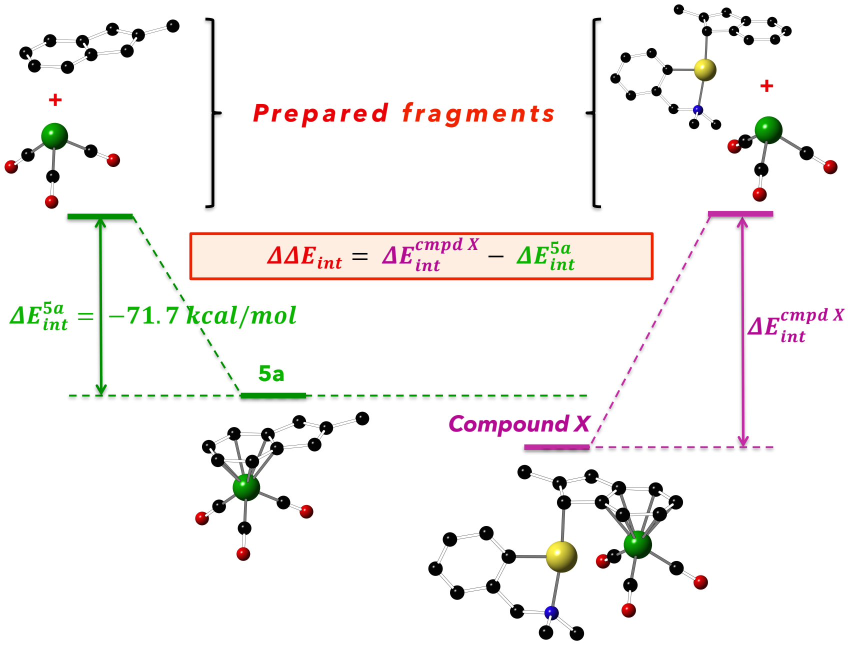

Figure 148: Considered fragments for the energy decomposition analysis.

[951] [N°818] Bielinski, E. A.; Dai, W.; Guard, L. M.; Hazari, N.; Takase, M. K. *Organometallics* **2013**, *32*, 4025.

[952] [N°819] Chalkley, M. J.; Guard, L. M.; Hazari, N.; Hofmann, P.; Hruszkewycz, D. P.; Schmeier, T. J.; Takase, M. K. *Organometallics* **2013**, *32*, 4223.

[953] [N°661] Sui-Seng, C.; Enright, G. D.; Zargarian, D. *J. Am. Chem. Soc.* **2006**, *128*, 6508.

[954] [N°660] Sui-Seng, C.; Enright, G. D.; Zargarian, D. *Organometallics* **2004**, *23*, 1236.

[955] [N°659] Alías, F. M.; Belderraín, T. R.; Paneque, M.; Poveda, M. L.; Carmona, E.; Valerga, P. *Organometallics* **1998**, *17*, 5620.

[956] [N°820] Bickelhaupt, F. M.; Baerends, E. J.; Lipkowitz, K. B.; Boyd, D. B.; Eds.; Wiley: New-York, **2000**, pp 1-86.

[957] [N°749] Ziegler, T.; Rauk, A. *Inorg. Chem.* **1979**, *18*, 1755.

The complexes considered thereof are listed in (Figure 149).

Complex	***ΔΔE$_{int}$***	***ΔΔE$_{Pauli}$***	***ΔΔE$_{coul}$***	***ΔΔE$_{disp}$***	***ΔΔE$_{orb}$***
12a	-29	64	-59	-6	-29
13a	-38	137	-106	-6	-63
12b	-29	66	-60	-6	-30
endo-**12c**	-28	50	-49	-6	-24
exo-**12c**	-40	45	-43	-6	-37
12e	-30	62	-59	-6	-27
12g	-29	58	-54	-6	-29
14b	0	-14	+6	0	+7
7a	-32	58	-56	-4	-30

$$\Delta\Delta E_{int} = \Delta E_{int}^{compound} - \Delta E_{int}^{\boldsymbol{5a}} \text{ with } \Delta E_{int}^{\boldsymbol{5a}} = -71.7\ kcal/mol.$$

$$\Delta\Delta E_{int} = \Delta\Delta E_{Pauli} + \Delta\Delta E_{coul} + \Delta\Delta E_{disp} + \Delta\Delta E_{orb}$$

Figure 149: Energy decomposition analysis for the interaction of prepared fragments of $Cr(CO)_3$ and substituted 2-methylindenes giving rise to compounds **12a**, **13a**, **12b**, **12c**, **12e**, **12g**, **14b** and **7a** (Energies are expressed in kcal/mol).

The interaction energy difference $\Delta\Delta E_{int}$ is introduced here as an evaluation tool of the binding capability of the considered fragments for a given complex relative to a reference case, for example, here compound **5a**. For instance, for **12a**: $\Delta\Delta E_{int}^{\boldsymbol{12a}} = \Delta E_{int}^{\boldsymbol{12a}} - \Delta E_{int}^{\boldsymbol{5a}}$. (Figure 149) lists the corresponding differential EDA subsets of Pauli repulsion ($\Delta\Delta E_{Pauli}$), attractive Coulombic ($\Delta\Delta E_{coul}$), attractive dispersion ($\Delta\Delta E_{disp}$), and orbital ($\Delta\Delta E_{orb}$) contributions to the interaction energy for optimized singlet ground state models and their associated interacting fragments as treated by ADF's specific fragment-analysis routine.[958] The η^1-*syn*-facial bonding interaction is largely favourable with $\Delta\Delta E_{int}$ = −30 kcal/mol (Figure 149) in Pd-containing complexes. The situation is similar in **13a** where $\Delta\Delta E_{int}$ = −38 kcal/mol. Worthy to note, **14b** displays a value of $\Delta\Delta E_{int}$ close to zero, which suggests that the presence of the η^3-bonded metallacycle does not influence much the bonding capability of the indenyl ligand ($\Delta\Delta E_{int}^{\boldsymbol{14b}} \approx$ 0 kcal/mol) toward the $Cr(CO)_3$ moiety. This analysis also shows that for all η^1-*syn*-facial heterobimetallics, Pauli repulsion is largely compensated by attractive electrostatic and orbital interactions, dispersion offering a modest contribution at this level of theory.

[958] [N°821] te Velde, G.; Bickelhaupt, F. M.; Baerends, E. J.; Fonseca Guerra, C.; van Gisbergen, S. J. A.; Snijders, J. G.; Ziegler, T. *J. Comp. Chem.* **2001**, *22*, 931.

DFT calculations show, in all the cases treated thereof, that the *syn*-facial η^1 bonding of the indenyl ligand to the M (M = Pd, Pt) centre is largely favoured thermodynamically over any *syn*-facial or *antara*-facial η^3 mode. For instance, **12b** is more stable than complex **14b** by 13.5 kcal/mol of total energy (ZPVE variation ≈ 0.6 kcal/mol). If one performs an EDA analysis by considering now the interaction between prepared anion **5b** and the corresponding prepared cationic fluorinated palladacycle, the energetic bias in favour of **12b** (Figure 149) appears to result from a major contribution of the Coulombic (electrostatic) attractive energy component of the interaction energy. This electrostatic term [$\Delta\Delta E_{elec}^{12b-14b} = -20.5\ kcal/mol$] combined to minor dispersion and orbital terms [$\Delta\Delta E_{disp}^{12b-14b} = -6.0\ kcal/mol$], [$\Delta\Delta E_{orb}^{12b-14b} = -6.2\ kcal/mol$] largely compensates the Pauli repulsion term [$\Delta\Delta E_{Pauli}^{12b-14b} = +8.8\ kcal/mol$] that expectedly rises with increased cluttering. Coulombic attraction appears to be the kernel of the stabilization of those *syn*-facial complexes.

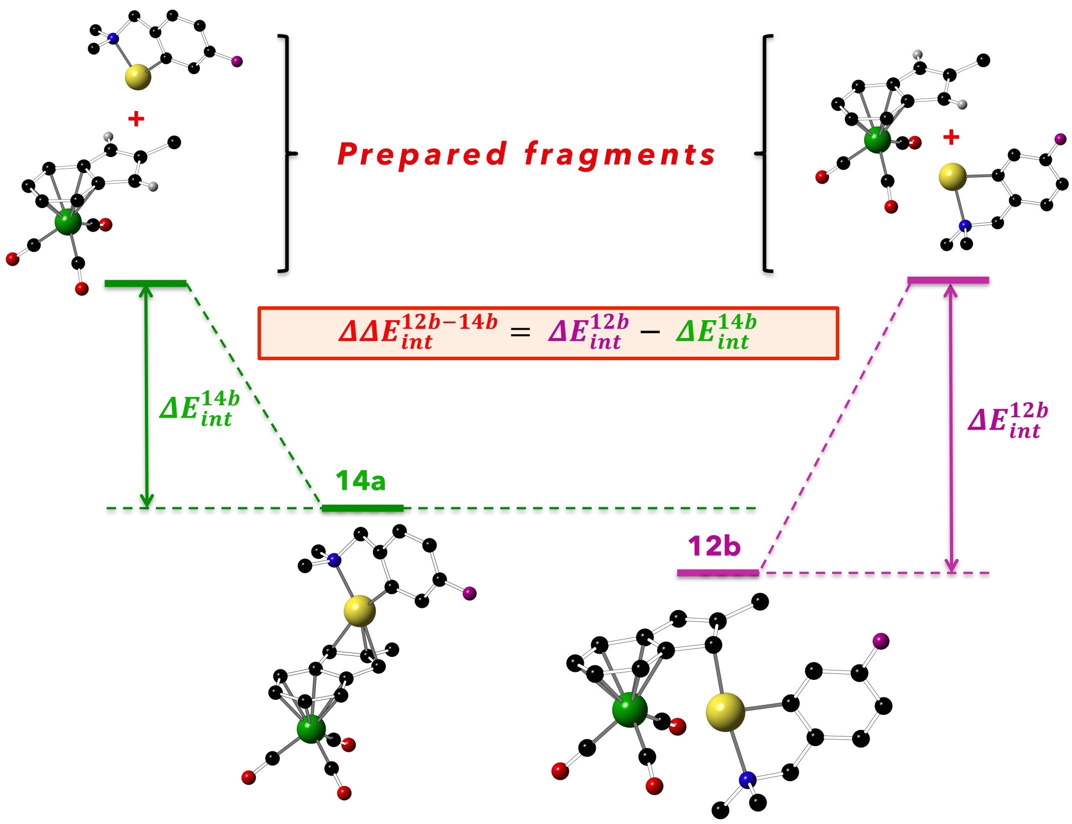

Figure 150: Considered fragments for the energy decomposition analysis.

4.5 - Metallotropy.

The presumed fast equilibrium between the *endo* and *exo* diastereomers of **12c** was perceived as a promising property that could be applied to the production of enantioenriched planar-chiral complex **5a** by way of a kinetic chemical quench of the Pd-related transposition process. The latter quench was probed at various temperatures by submitting (1*S*) and (1*R*)-**12c** to an acidic treatment with the goal of protodepalladation of the indenyl ligand and the release of scalemic compound **5a**. A temperature-dependent enantiomeric excess (*ee*) of the latter might express, according to the *Curtin-Hammett* principle, the temperature-dependence of the Boltzmann distribution of *endo*-**12c** and *exo*-**12c** isomers (Figure 151) in solution.

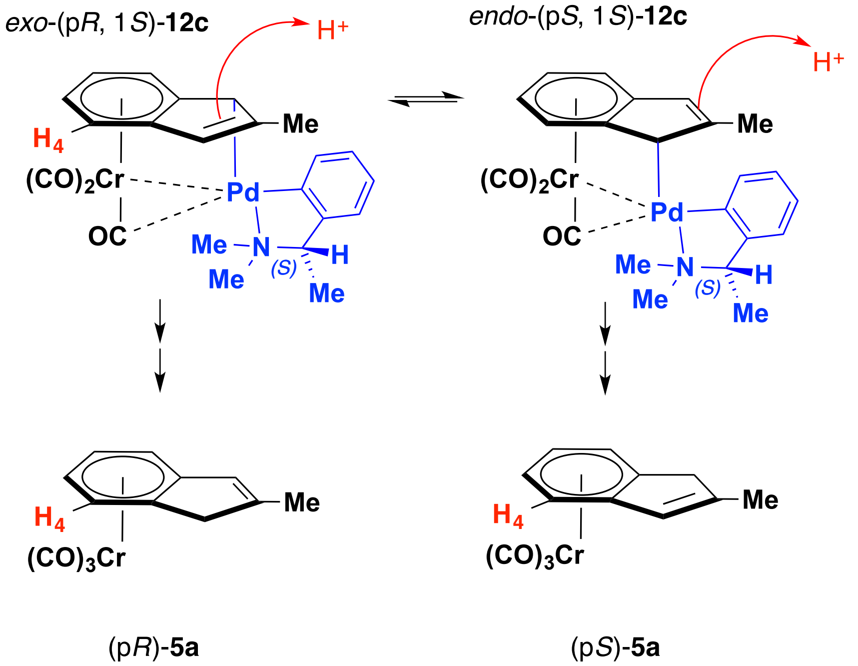

Figure 151: Kinetic quench of the putative *endo-exo* isomerization by proto-depalladation results from an *exo*-attack of H^+ at the indenyl, a pathway established by a reaction of **12a** with CD_3CO_2D, which resulted into the predominant formation of *exo* deuterated *rac*-**5a** at position 1.

Proto-depalladation experiments were carried out by treating (1*S*)- and (1*R*)-**12c** with various sources of protons such as acetic acid (AA), *p*-toluenesulfonic acid (PTSA), or even silica gel (SiO_2) at different temperatures, scalemic **5a** being subsequently isolated and purified and its ee determined by the most direct way as described below. In a first stage, the determination of the respective absolute configuration of the main enantiomers of **5a** produced from (1*S*)- and (1*R*)-**12c**, respectively, by treatment with acetic acid in CH_2Cl_2 at 20 °C was sought. The method suggested by Flack and co workers was used.[959, 960] It is based on the combined use of structural X-ray diffraction analyses and spectropolarimetric data (namely absorption UV–visible circular dichroism). The solution CD spectra of freshly prepared batches of scalemic **5a** were compared with the CD signatures of solutions obtained by dissolving the enantiopure crystals from which absolute structures were firmly established by structural X-ray diffraction analyses (Figure 152 to Figure 155).

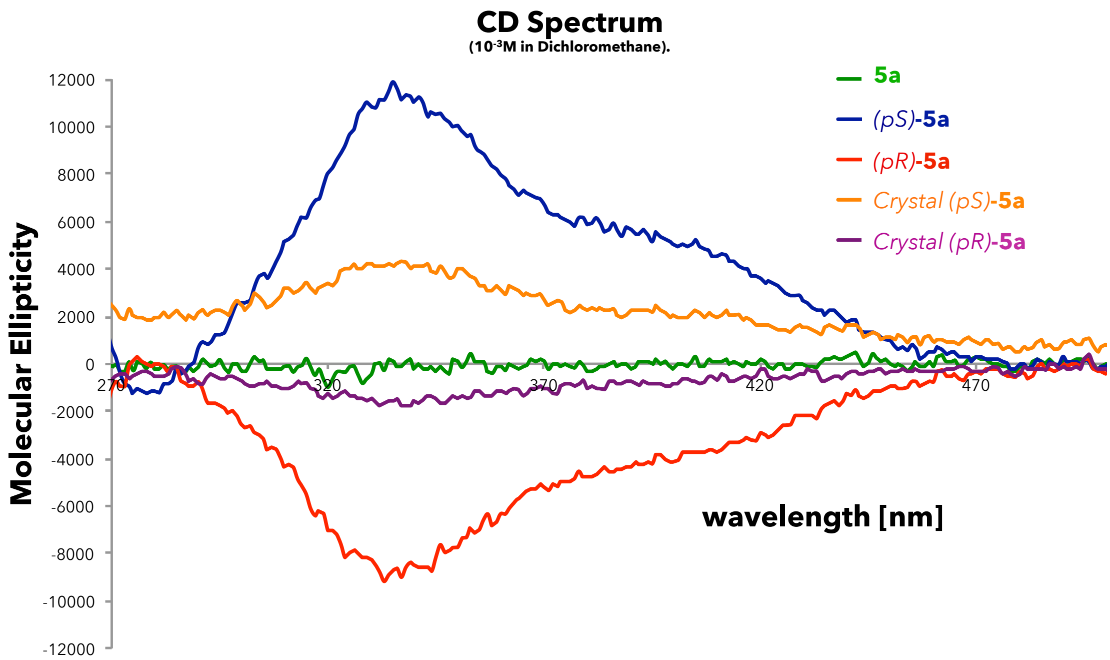

Figure 152:Circular dichroism (CD) spectra (molecular ellipticity vs wavelength in nm, 10^{-3} M solutions in degassed CH_2Cl_2) of the isolated batches of scalemic compounds overlaid with the raw CD signatures (+ and Δ, ordinates are in mdeg) of CH_2Cl_2 solutions of the enantiomorphic crystals (crystals) preliminarily submitted to X-ray diffraction analyses. The flat CD spectrum of the racemic rac-**5a** is given as a control reference.

959 [N°822] Djukic, J.-P.; Hijazi, A.; Flack, H. D.; Bernardinelli, G. *Chem. Soc. Rev.* **2008**, *37*, 406.

960 [N°823] Flack, H. D.; Bernardinelli, G. *Acta Cryst. Sect. A* **1999**, *55*, 908.

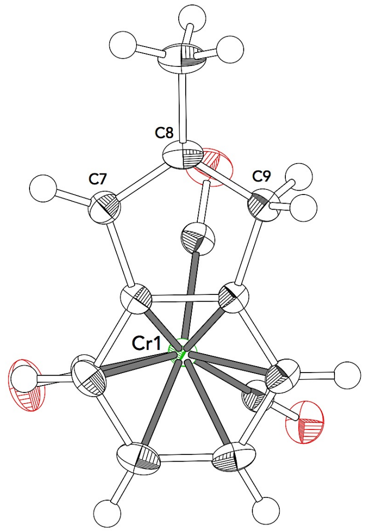

Compound (p*R*)-**5a**
Space Group: **P 2_1 2_1 2_1**
R-Factor (%): **2.47**
Flack' s parameter x = **0.001(16)**

N°	***A***	***B***	***Lengths (Å)***
1	C_7	C_8	1.415(2)
2	C_8	C_9	1.436(2)

Figure 153: X-ray structure and selected interatomic distances of compound (p*R*)-**5a**.

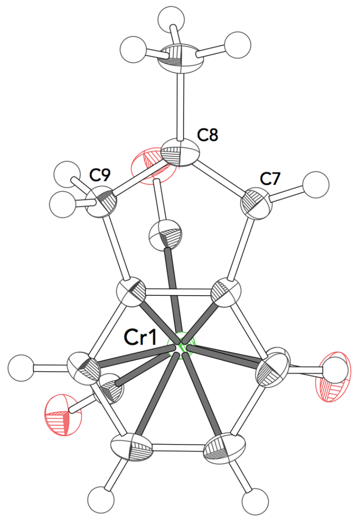

Compound (p*S*)-**5a**
Space Group: **P 2_1 2_1 2_1**
R-Factor (%): **2.29**
Flack' s parameter x = -**0.005(14)**

N°	***A***	***B***	***Lengths (Å)***
1	C_7	C_8	1.408(2)
2	C_8	C_9	1.444(2)

Figure 154: X-ray structure and selected interatomic distances of compound (p*S*)-**5a**.

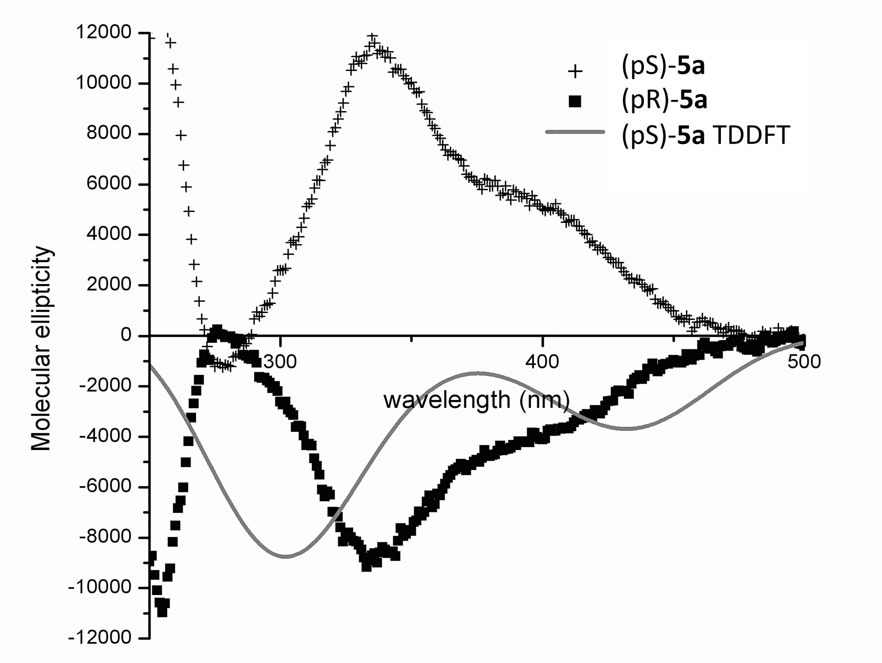

Figure 155: Experimental CD in CH_2Cl_2 vs TDDFT CD of (p*R*)-**5a** in gas phase (ZORA SAOP/all electron QZ4P, Gaussian fixed height, linewidth 70, scaling 1.1, vide infra).

This procedure that ensures the proper determination of absolute configurations[961] was further backed[962] by comparison of the experimental and TDDFT-computed CD spectra of (p*R*)-**5a** (ZORA SAOP/all electron QZ4P), which gave a reasonable good match (Figure 155). It was first concluded that proto-depalladations of (1*S*)-**12c** and (1*R*)-**12c** at room temperature mainly yielded (p*S*)-**5a** and (p*R*)-**5a**, respectively. The enantiomeric excesses of samples of scalemic **5a** produced at different temperatures were assessed in all cases by ^{1}H NMR spectroscopy in the presence of Lacour's Λ-TRISPHAT salt,[963-965] which was used here as a chiral shift reagent. Careful integration of the 2-fold split signal of proton H_7 (Figure 151) gave access to the *ee* with a reasonable accuracy of ±5 %. Under the conditions of chiral shift, proton H_7 shows up as a set of two doublets cantered at δ 5.10 ppm ($\Delta\delta$(Hz) = 15, T = 298 K, 400 or 600 MHz) when compound **5a** is dissolved in a 1:5 mixture of d_6-acetone and d_6-benzene saturated with $\mathbf{\Lambda}$-[NBu_3H][TRISPHAT] ($[\alpha]_D^{20}$= +299, EtOH).

[961] [N°822] Djukic, J.-P.; Hijazi, A.; Flack, H. D.; Bernardinelli, G. *Chem. Soc. Rev.* **2008**, *37*, 406.
[962] [N°824] Pescitelli, G.; Kurtan, T.; Florke, U.; Krohn, K. *Chirality* **2009**, *21*, E181.
[963] [N°825] Lacour, J. *C.R. Chimie* **2010**, *13*, 985.
[964] [N°826] Favarger, F.; Goujon-Ginglinger, C.; Monchaud, D.; Lacour, J. *J. Org. Chem.* **2004**, *69*, 8521.
[965] [N°827] Lacour, J. *Chimia* **2002**, *56*, 672.

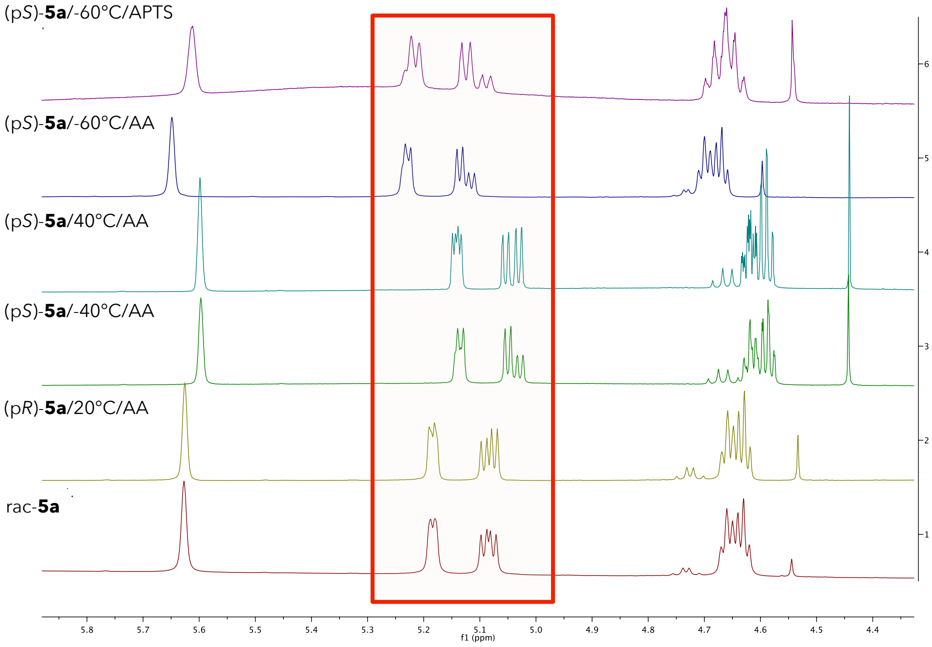

[1]H NMR spectra (20 °C, 600 MHz, 1:6 d_6-acetone in C_6D_6) of the two enantiomers of **5a** (0.03 mmol) in the presence of [*n*-Bu_3NH][**Λ**-TRISPHAT] (0.11 mmol): the signals appearing at *ca.* 5.10 ppm as two doublets were intergrated for the determination of the *ee*.

Figure 156: TRISPHAT titration of the enantiomeric excess of **5a**.

Substrate/ °C[a] /acid[b]	***Prod.***	***yield (%)***	$[\alpha]_D^{20}$ ***[c]***		***ee (%)[d]***	***CD[e] 340 nm (Mol. Ellip.)***		***CD[e] 400 nm (Mol. Ellip.)***	
			C_6H_6	**CH_2Cl_2**		**C_6H_6**	**CH_2Cl_2**	**C_6H_6**	**CH_2Cl_2**
(1*S*)-**12c**/SiO_2 [f]	(p*S*)-**5a**	72	+269.2	+292.3	20	9105	9321	4414	4243
(1*S*)-**12c**/-60°C/AA [g]	(p*S*)-**5a**	83	*	*	34	*	*	*	*
(1*S*)-**12c**/-60°C/APTS [h]	(p*S*)-**5a**	45	+907.7	*	55	30693	*	13647	*
(1*S*)-**12c**/-40°C/AA [g]	(p*S*)-**5a**	68	*	+573.1	32	*	19053	*	8584
(1*S*)-**12c**/20°C/AA [g]	(p*S*)-**5a**	32	*	+346.2	13	*	11045	*	5014
(1*S*)-**12c**/40°C/AA [g]	(p*R*)-**5a**	63	*	-80.8	-7	*	-3250	*	-1493
(1*R*)-**12c**/-60°C/APTS [h]	(p*R*)-**5a**	35	-819.2	*	49	- 29839	*	-13740	*
(1*R*)-**12c**/20°C/AA [g]	(p*R*)-**5a**	48	-269.2	-226.9	11	-9022	-8473	-3720	-4114

[a] Temperature of the reaction. [b] acid used to promote the reaction. [c] (*c* 0.026). [d] determined by [1]H NMR in the presence of *Λ*–TRISPHAT anion. [e] Circular dichroism (CD). [f] silica gel. [g] acetic acid. [h] *p*-tolylsulfonic acid.

Figure 157: List of enantiomeric excesses, specific rotations and chiroptic data (CD UV-vis.)

On the basis of the absolute configuration of the major product of the reaction and on the structures of diastereomers *endo* and *exo*-**12c**, it is now speculated that the predominant reaction path that leads to (p*S*)-**5a** from (1*S*)-**12c** consists of the *exo* protonation of the indenyl's double bond of *endo*(p*S*,1*S*)-**12c** (Figure 151), which might be the main component of the diastereomeric mixture in solution according to the theoretical analysis of the CD spectrum of (1*S*)-**12c** (Figure 155). Additional indication of a facial-selectivity of the initial protonation was collected from deuterium-labeling experiments (Figure 158). The deuteriolysis of (1*R*)-**12c** by CD_3CO_2D produced the *exo* deuterated isomer *exo*-D-**5a**, which was isolated in 39 % yield. This result has to be compared with the lack of selectivity of the quench of **5b** by D_2O that yields *exo* and *endo*-D-**5a** nearly in a 1:1 ratio (54 % isolated yield).

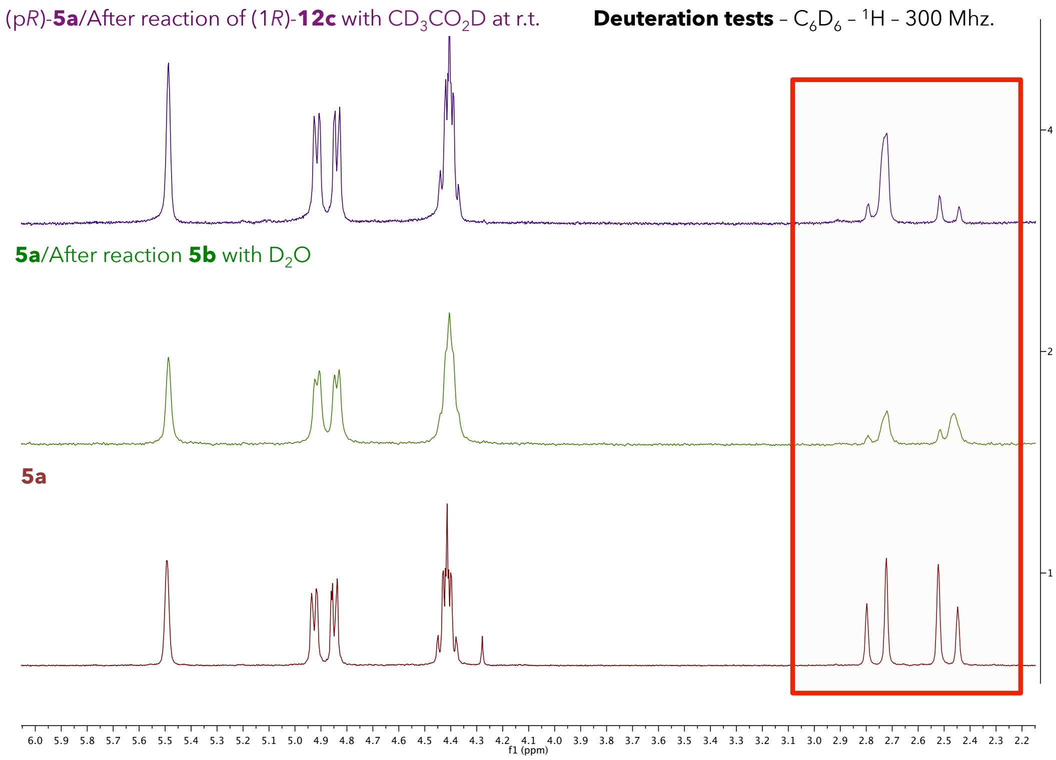

The upper ^{1}H NMR spectrum indicates clearly that the deutero-depalladation occurred rather selectively by deuteration of a single site at the benzylic position of **5a** that is assumed to be the methylenic *exo* position of the indene with respect to the $Cr(CO)_3$ moiety. The green-coloured spectrum suggests that a simple deuteration of anion **5b** is not selective and leads to deuteration at the *exo* and *endo* positions.

Figure 158: Benzylic deuteration of 5a and deutero-depalladation of (1*R*)-12c

Even though the nature of the acid influences slightly the enantioselectivity, the obvious temperature-dependence of the ee (Figure 157), which varies by a factor of about 5 from +20 °C to −60 °C (11−13 % < ee < 50− 55 %, Figure 159), supports the hypothesis of the fluxional nature of **12c** in solution. Another plausible alternative could be a temperature-dependent proto-depalladation that could target different sites depending on the temperature at which the reaction is carried out. At the present stage, it was not possible to rule out any of the latter proposals.

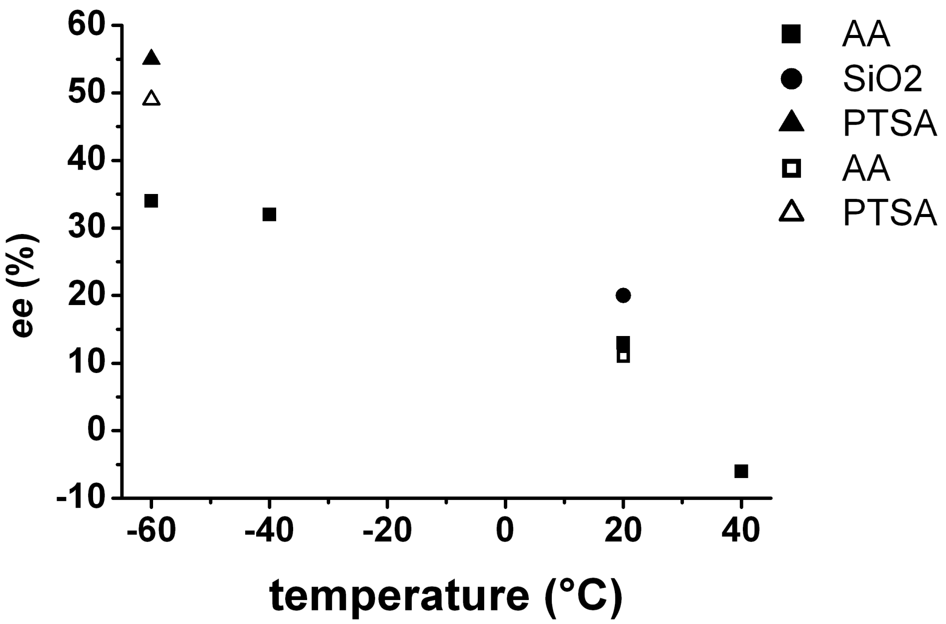

Figure 159: *ee* vs temperature (isolated yields span from 30 to 60 %), the negative value corresponds to a reversed enantioselectivity; filled and unfilled symbols are for reactions carried out with (1*S*) and (1*R*)-**12c**, respectively. (Enantiomeric excess *ee* was calculated for reactions with (1*S*)-**12c** as follows: ee = 100 × {[p*S*-**5a**] − [p*R*-**5a**]/([p*R*-**5a**] + [p*S*-**5a**])} where brackets express concentrations. For reactions with (1*R*)-**12c** the numerator becomes [pR-**5a**] − [pS-**5a]**).

4.6 - Conclusion.

Unprecedented cases of air-stable and solution-persistent neutral T-shaped 14 electron complexes of palladium and platinum have been prepared by a reliable method and extensively structurally characterized.

In all cases, a *syn*-facial heterobimetallic complex is the major product, the structure of which is characterized by a Cr−M (M = Pd, Pt) distance of *ca.* 2.88 Å. The *syn*-facial arrangement in the isolated η^1-**12** complexes (14 + 18 valence electrons) is by more than 10 kcal/mol of total energy preferred over the electron-saturated (16 + 18 valence electrons) *antara*-facial arrangement in **14** (Figure 117) and the fictitious *syn*-facial η^3-**12** geometries. This report establishes the feasibility of a permanent stabilization of a coordinatively unsaturated metal centre M by noncovalent interactions with vicinal groups. Even though the propensity of arenetricarbonylchromium complexes to form donor−acceptor adducts with Lewis acids is long known,[966-968] in the cases treated here, the donor−acceptor component of the $(CO)_3Cr{-}M$ interaction revealed by ETS-NOCV analyses is not predominant according to QTAIM. We propose to name the subtle bonding balance between steric repulsion and electrostatic attraction observed in compounds **12** an *attractive Coulombic occlusion* of a free coordination site (Figure 160).

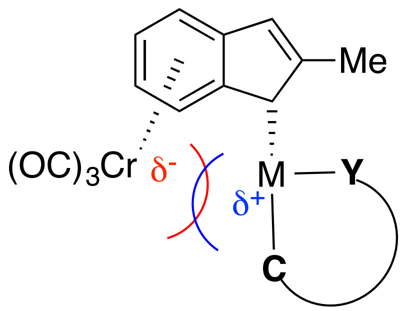

Figure 160: Reductionist representation of the stabilization by attractive Coulombic occlusion of the electron-unsaturated M centre (M = Pd, Pt) with a proximal large moiety (here $Cr(CO)_3$) on which charge density concentrates.

The term "chelation" introduced by Morgan and Drew[969] entails the covalent bonding of a ditopic ligand to a metal centre. We propose to name "*hemi*chelation" any half-covalent/half noncovalent bonding-relationship similar to that existing between the ambiphilic heteroditopic tricarbonyl(η^6-indenyl) chromium ligand and the electron-unsaturated Pd(II) or Pt(II) centres (Figure 161).

---

[966] [N°828] Lokshin, B. V.; Rusach, E. B.; Kolobova, N. E.; Makarov, Y. V.; Ustynyuk, N. A.; Zdanovich, V. I., . . . Setkina, V. N. *J. Organomet. Chem.* **1976**, *108*, 353.

[967] [N°829] Magomedov, G. K. I.; Syrkin, V. G.; Frenkel, A. S.; Zakharchenko, O. A. *Zh. Obshch. Khim.* **1975**, *45*, 2530.

[968] [N°830] Edgar, K.; Johnson, B. F. G.; Lewis, J.; Wild, S. B. *J. Chem. Soc. A* **1968**, 2851.

[969] [N°831] Morgan, G. T.; Drew, H. D. K. *J. Chem. Soc., Trans.* **1920**, *117*, 1456.

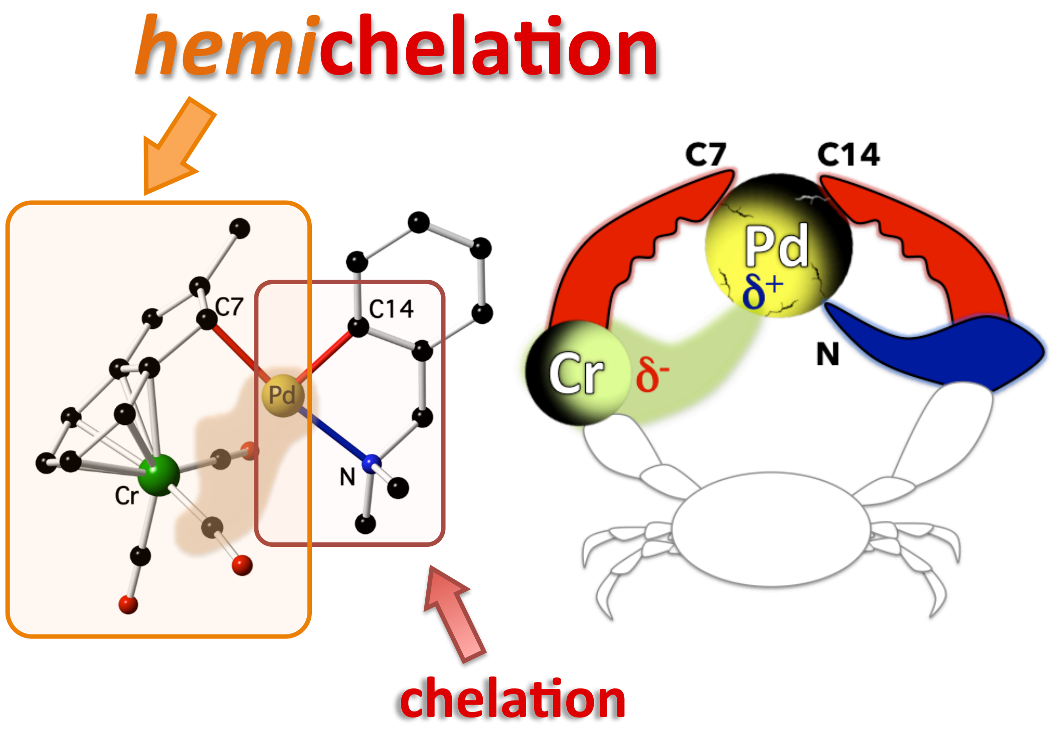

Figure 161: Illustration of the concept of *hemichelation*.

In line with the observations made for complexes **12** and **7a-c**, the compound synthesized by Kalinin,[970-972] (Figure 83), obviously displays the characteristics of a (η^6-benzyl)tricarbonylchromium hemichelate. Our results also suggest that all situations where similar hemichelation might be playing a relevant stabilizing role should warrant extensive investigations.

It must be stressed here that the absence of a BCP and bond path between metals and, incidentally, the absence of a net metal−metal bond has been pointed out for a number of homometallic bridged transition metal carbonyl dimers and clusters. [973, 974]

970 [N°734] Moiseev, S. K.; Cherepanov, I. A.; Petrovskii, P. V.; Ezernitskaya, M. G.; Butenschön, H.; Strotmann, M.; Kalinin, V. N. *Inorg. Chim. Acta* **1998**, *280*, 71.

971 [N°735] Kalinin, V. N.; Cherepanov, I. A.; Moiseev, S. K.; Dolgushin, F. M.; Yanovsky, A. I.; Struchkov, Y. T. *Acta Cryst. Sect. C* **1993**, *49*, 805.

972 [N°582] Kalinin, V. N.; Cherepanov, i. y. A.; Moiseev, S. K.; Batsanov, A. S.; Struchkov, Y. T. *Mendeleev Commun.* **1991**, *1*, 77.

973 [N°832] Farrugia, L. J.; Senn, H. M. *J. Phys. Chem. A* **2010**, *114*, 13418.

974 [N°833] Farrugia, L. J. *Chem. Phys. Lett.* **2005**, *414*, 122.

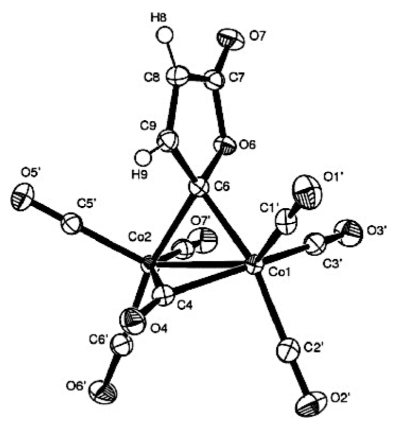

Farrugia, L. J.

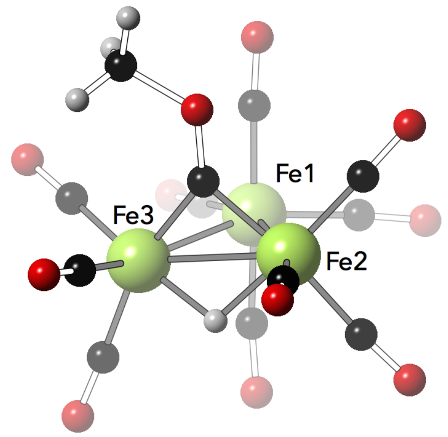

Farrugia, L. J. *et al.*

Figure 162: Examples of homometallic bridged transition metal carbonyl dimers described by Farrugia *et al*.

This issue has been the subject of a host of reports,[975] which focused on the relative limitations of QTAIM and on the need for complementary analytical tools,[232, 976] such as the Source Function,[977] the Electron Localizability Indicator[978] and the Delocalization Indice[979] to deepen the analysis of such elusory metal–metal bonding. There is no doubt that the cases reported therein pose a very similar challenge that could be addressed by acquisition of accurate experimental information on the electron density by multipole refinement high resolution structural X-ray diffraction analysis and subsequent quantum chemical treatment,[980] which was not at reach for the present study. Nonetheless, DFT provides a reasonable insight into the origin of the preference given to the *syn*-facial η^1-indenyl bonding. Theory outlines the stabilizing nature of the noncovalent interactions existing between chelated M (M = Pd, Pt) and the $Cr(CO)_3$ moiety and the minor role of direct intermetallic donor–acceptor interactions. The formation of the *syn*-facial arrangement is thermodynamically mostly driven by electrostatic attractive interactions between the M centre and the $Cr(CO)_3$ moiety, which contributes to structural cohesion.

---

975 [N°834] Gervasio, G.; Bianchi, R.; Marabello, D. *Chem. Phys. Lett.* **2005**, *407*, 18.

976 [N°835] Overgaard, J.; Clausen, H. F.; Platts, J. A.; Iversen, B. B. *J. Am. Chem. Soc.* **2008**, *130*, 3834.

977 [N°836] Bader, R. F. W.; Gatti, C. *Chem. Phys. Lett.* **1998**, *287*, 233.

978 [N°837] Kohout, M. *Int. J. Quantum Chem.* **2004**, *97*, 651.

979 [N°838] Fradera, X.; Austen, M. A.; Bader, R. F. W. *J. Phys. Chem. A* **1999**, *103*, 304.

980 [N°839] Gatti, C. In *Zeitschrift für Kristallographie* 2005; Vol. 220, p 399.

5 - Extension of the concept of hemichelation to the fluorene unit.

5.1 - Purpose.

The present section will disclose the first extension of the concept of hemichelation to another arene unit, namely: the fluorene. The synthesis of new cases of air/moisture-stable, solid state and solution-persistent 14 electron neutral T-shaped Pd(II) bimetallic complexes has been achieved by using the tricarbonyl(η^6-fluorenyl)chromium anion. Because of its ambiphilic character, the fluorene anion, can reasonably be considered as a good candidate for the formation of new palladium hemichelates. Furthermore, the use of a fluorene will assess if hemichelation remains possible while the Metallotropy of the Pd unit is prevented. Indeed, the depletion of charge density at the aromatic carbons in the 2,3 position, like shown in Figure 163 by the analysis of the partial natural charges (Natural Population Analysis) [981] of singlet ground state geometries of **5a** and **15a** (throughout these computed models were optimized at the ZORA-TPSS[982]-D3(BJ)[983] / all electron TZP level), may considerably limit an eventual η^3 coordination of the metal centre, and thus fluxionality.

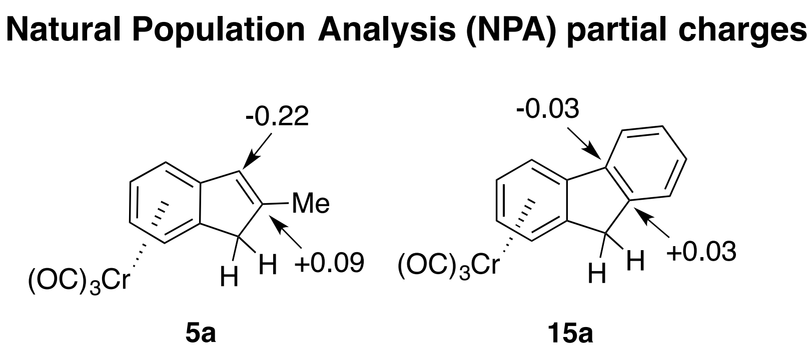

Figure 163: Natural partial charges (NPA) at C_2 and C_3 positions in **5a** and **15a** computed from gas phase singlet ground state geometries optimized at the ZORA-TPSS-D3(BJ)/all electron TZP level.

[981] [N°813] Weinhold, F.; Landis, C. R. *Valency and Bonding, a Natural Bond Orbital Donor-Acceptor Perspective*; University Press: Cambridge, UK, **2005**.

[982] [N°743] Tao, J.; Perdew, J. P.; Staroverov, V. N.; Scuseria, G. E. *Phys. Rev. Lett.* **2003**, *91*, 146401.

[983] [N°187] Grimme, S.; Ehrlich, S.; Goerigk, L. *J. Comput. Chem.* **2011**, *32*, 1456.

Therefore, several μ-chloro-bridged palladacycles **10** (Figure 164) were probed for their reactivity toward anion **15b** leading under the ascribed conditions to the formation of new Pd hemichelates (Figure 165).

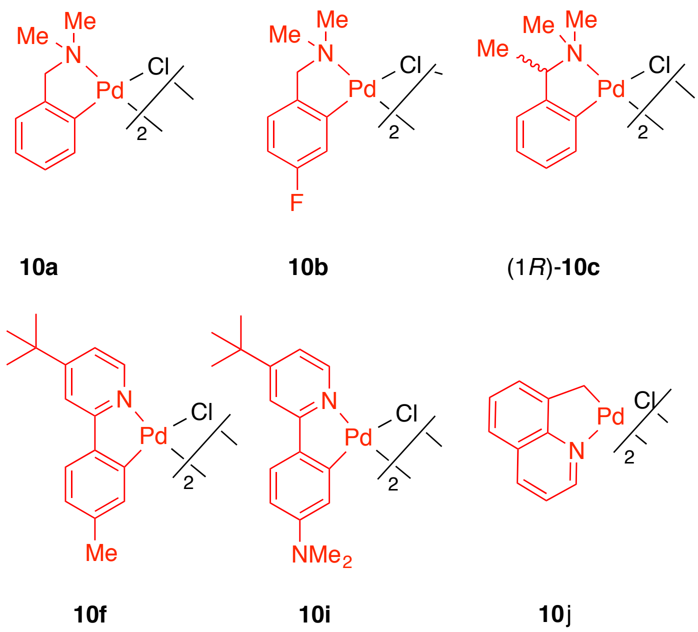

Figure 164: μ-chloro-bridged palladacycles which were probed for their reactivity toward anion **15b**.

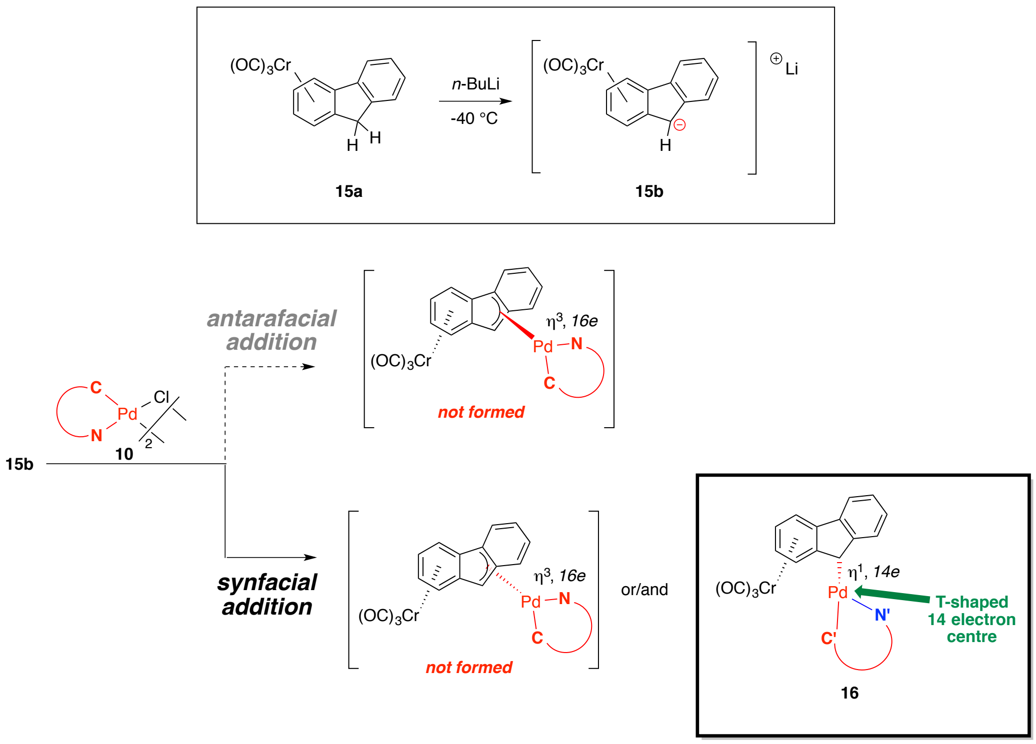

Figure 165: The ambiphilic character of anion **15b** allows only one facial interaction with Pd metallacycles **10**, that is the *syn*-facial, leading exclusively to (η^1-fluorenyl)M complexes, a new class of electron-unsaturated T-shaped η^1-fluorenyl Pd complexes.

Optimal conversions were achieved when palladacycles **10** were reacted with anion **15b** in a dry mixture of ether at −40 °C. The corresponding *syn*-facial complexes **16a, 16b, 16f** and **16i** were isolated mostly by recrystallization, with yields spanning 30−60 %. Worthy to note that the reaction of **15b** with **10c** and **10j** didn't produce the expected compounds **16c** and **16j** (only residues of **15a** were observed).

Structural characterization by means of X-ray diffraction analysis was successful with palladium complexes **16a**, **16f,** and **16i**; complex **16b** failing to yield suitable crystals. Figure 166 to Figure 168 display new cases of *syn*-facial hemichelates of palladium, where the metal centres are found to be in short contact with one of the vicinal Cr-bound CO ligands and are bonded in a η^1-fashion to the fluorene ligand (similarly to bimetallics **12**, **13**). Worthy to note is the quite unexpected orientation of the cyclometallated fragment for which the carbon of the [NC]chelate (Figure 166) is found to be in a *trans* position regarding the benzylic carbon of the fluorene unit. This orientation is quite different of what was previously observed in the case of bimetallics **12** and **13**, where the carbon of the [NC]chelate was systematically in a *cis* position.

Thus, compounds **16** constitute rare examples of antisymbiotic[984-985] compounds, which seem to find their origin in hemichelation. The Cr−Pd distances are all in the range of 2.68−2.71 Å (0.1 Å shorter than those of bimetallics **12**), which is consistent with the sum of empirical van der Waals radii[986] for Cr (1.4 Å)/Pd (1.4 Å).

[984] [N°840] Burmeister, J. L.; DeStefano, N. J. *J. Chem. Soc., Chem. Commun.* **1970**, 1698.
[985] [N°841] Jennings, M. A.; Wojcicki, A. *J. Organomet. Chem.* **1968**, *14*, 231.
[986] [N°806] Slater, J. C. *J. Chem. Phys.* **1964**, *41*, 3199.

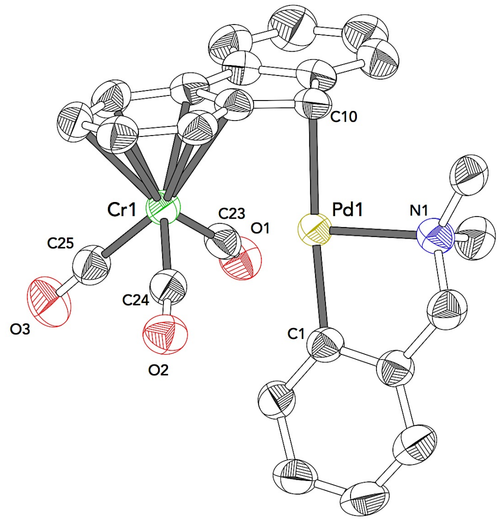

Compound **16a**
Space Group: **C 2/c**
R-Factor (%): **4.66**

N°	*A*	*B*	*C*	*Lengths (Å)*	*Angles (°)*
1	Cr_1	Pd_1	-	2.7123(9)	-
2	Cr_1	C_{23}	-	1.898(6)	-
3	Cr_1	C_{24}	-	1.851(4)	-
4	Cr_1	C_{25}	-	1.843(4)	-
5	C_{23}	O_1	-	1.163(7)	-
6	C_{24}	O_2	-	1.151(5)	-
7	C_{25}	O_3	-	1.145(5)	-
8	Pd_1	C_{10}	-	2.230(4)	-
9	Pd_1	N_1	-	2.169(4)	-
10	Pd_1	C_1	-	2.045(4)	-
11	Pd_1	C_{23}	-	2.204(4)	-
12	Pd_1	C_{24}	-	3.033(6)	-
13	Cr_1	C_{23}	O_1	-	160.8(4)
14	Cr_1	C_{24}	O_2	-	173.8(4)
15	Cr_1	C_{25}	O_3	-	177.4(4)
16	C_{23}	Cr_1	C_{24}	-	103.4(2)

Figure 166: X-ray structure and selected interatomic distances of compound **16a**.

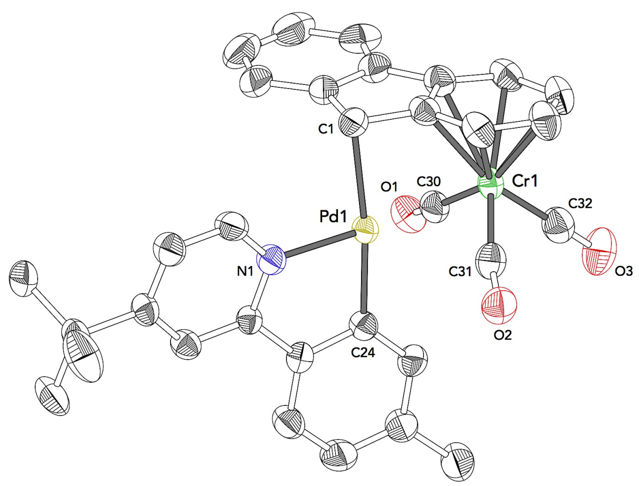

Compound **16f**
Space Group: **P c a 2$_1$**
R-Factor (%): **3.95**

N°	*A*	*B*	*C*	*Lengths (Å)*	*Angles (°)*
1	Cr_1	Pd_1	-	2.698(1)	-
2	Cr_1	C_{30}	-	1.880(4)	-
3	Cr_1	C_{31}	-	1.866(6)	-
4	Cr_1	C_{32}	-	1.846(6)	-
5	C_{30}	O_1	-	1.153(6)	-
6	C_{31}	O_2	-	1.151(7)	-
7	C_{32}	O_3	-	1.148(8)	-
8	Pd_1	C_1	-	2.254(5)	-
9	Pd_1	N_1	-	2.079(5)	-
10	Pd_1	C_{24}	-	2.040(5)	-
11	Pd_1	C_{30}	-	2.425(6)	-
12	Pd_1	C_{31}	-	2.626(5)	-
13	Cr_1	C_{30}	O_1	-	167.0(5)
14	Cr_1	C_{31}	O_2	-	170.8(5)
15	Cr_1	C_{32}	O_3	-	178.9(6)
16	C_{30}	Cr_1	C_{31}	-	103.6(2)

Figure 167: X-ray structure and selected interatomic distances of compound **16f**.

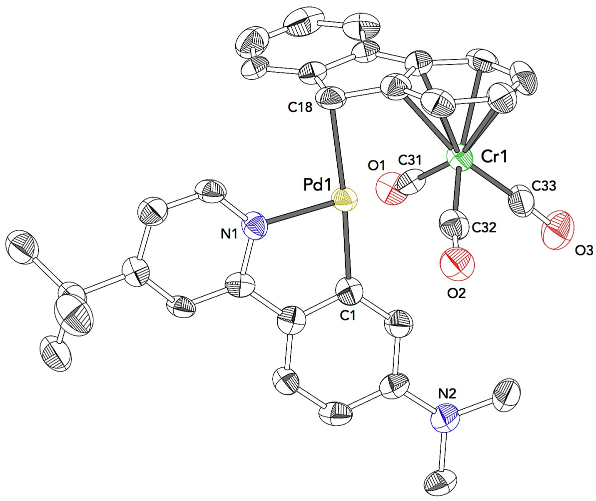

Compound **16i**
Space Group: **P -1**
R-Factor (%): **4.6**

N°	*A*	*B*	*C*	*Lengths (Å)*	*Angles (°)*
1	Cr_1	Pd_1	-	2.6776(9)	-
2	Cr_1	C_{31}	-	1.896(7)	-
3	Cr_1	C_{32}	-	1.856(7)	-
4	Cr_1	C_{33}	-	1.843(5)	-
5	C_{31}	O_1	-	1.153(8)	-
6	C_{32}	O_2	-	1.154(8)	-
7	C_{33}	O_3	-	1.152(6)	-
8	Pd_1	C_{18}	-	2.269(5)	-
9	Pd_1	N_1	-	2.092(4)	-
10	Pd_1	C_1	-	2.057(5)	-
11	Pd_1	C_{31}	-	2.289(5)	-
12	Pd_1	C_{32}	-	2.610(7)	-
13	Cr_1	C_{31}	O_1	-	163.8(5)
14	Cr_1	C_{32}	O_2	-	171.6(5)
15	Cr_1	C_{33}	O_3	-	177.0(5)
16	C_{31}	Cr_1	C_{32}	-	103.1(3)

Figure 168: X-ray structure and selected interatomic distances of compound **16i**.

Quite remarkable and unexpected is the behaviour of these species in solution (*i.e.* Toluene, or benzene) at temperatures above 0°C: the carbon of the [NC]chelate initially in a *trans* position, undergoes an isomerization process leading to a *cis* arrangement between the two carbons (the reverse process was not observed, Figure 169). An interpretation of this phenomenon could be that the kinetic compound **16**, which is exclusively formed under the reaction conditions, is progressively converted in the thermodynamically most stable species **17** at temperatures over 0°C (Figure 169).

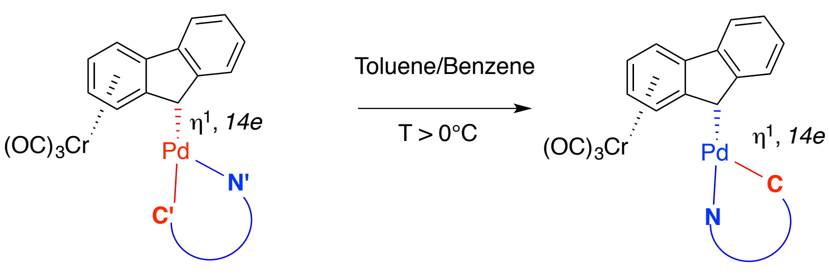

16 **17**

Figure 169: Isomerization process of **16** into **17** occurring in solution at temperatures over 0°C.

First theoretical results support an isomerization mechanism as represented in Figure 170, which occurs through an increase of the distance M…M, followed by a rotation of the metallacycle leading to a pseudo η^3 coordination mode of the Pd centre, and finally to the hemichelates **17**. More studies related to this mechanism are being carried out at the moment this thesis is being written.

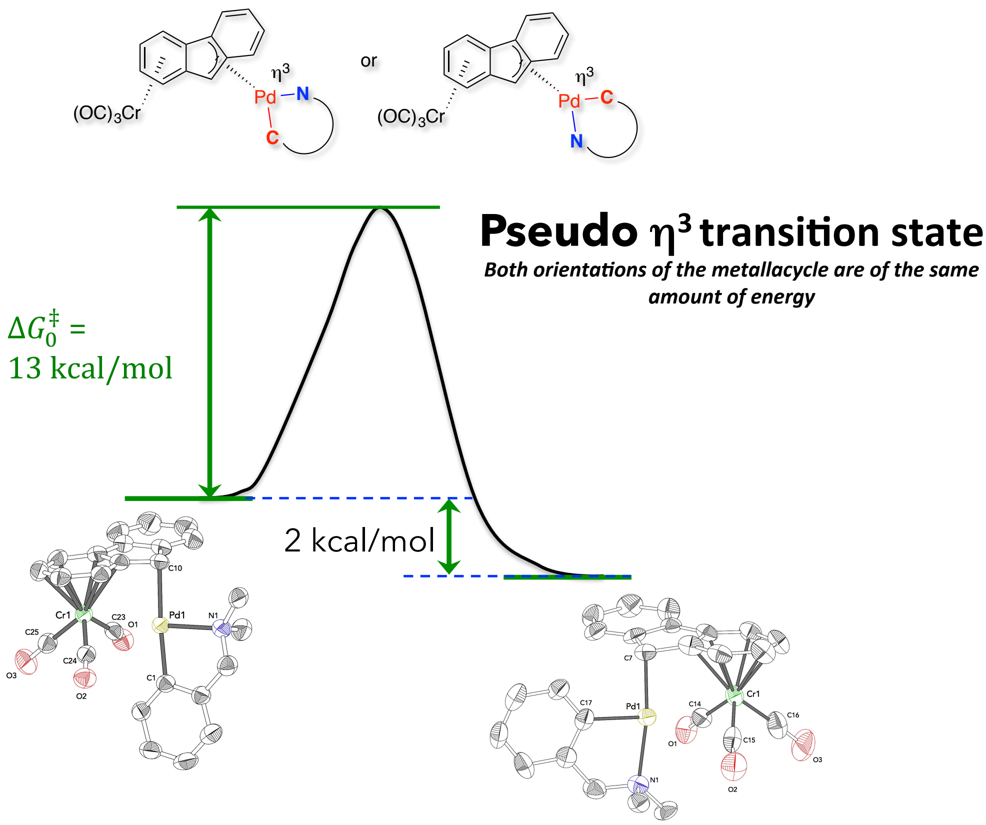

Figure 170: Illustration of the isomerization mechanism of **16a** into **17a**.

In order to determine the thermodynamic parameters associated to the isomerization process, a kinetic study has been performed by the mean of ^{1}H NMR spectroscopy (Figure 171). The conversion of **16a** and **16b**, respectively into **17a** and **17b**, was studied at 5 different temperatures (*i.e.* between 275 and 298K*) N.B.:* **16f** and **16i** failed to convert in the associated **17** isomers within a reasonable time (even at room temperature) and were thus not considered. Moreover, the possible decomposition into **15a** and untraceable subproducts at higher temperatures would have altered the accuracy of the kinetic data.

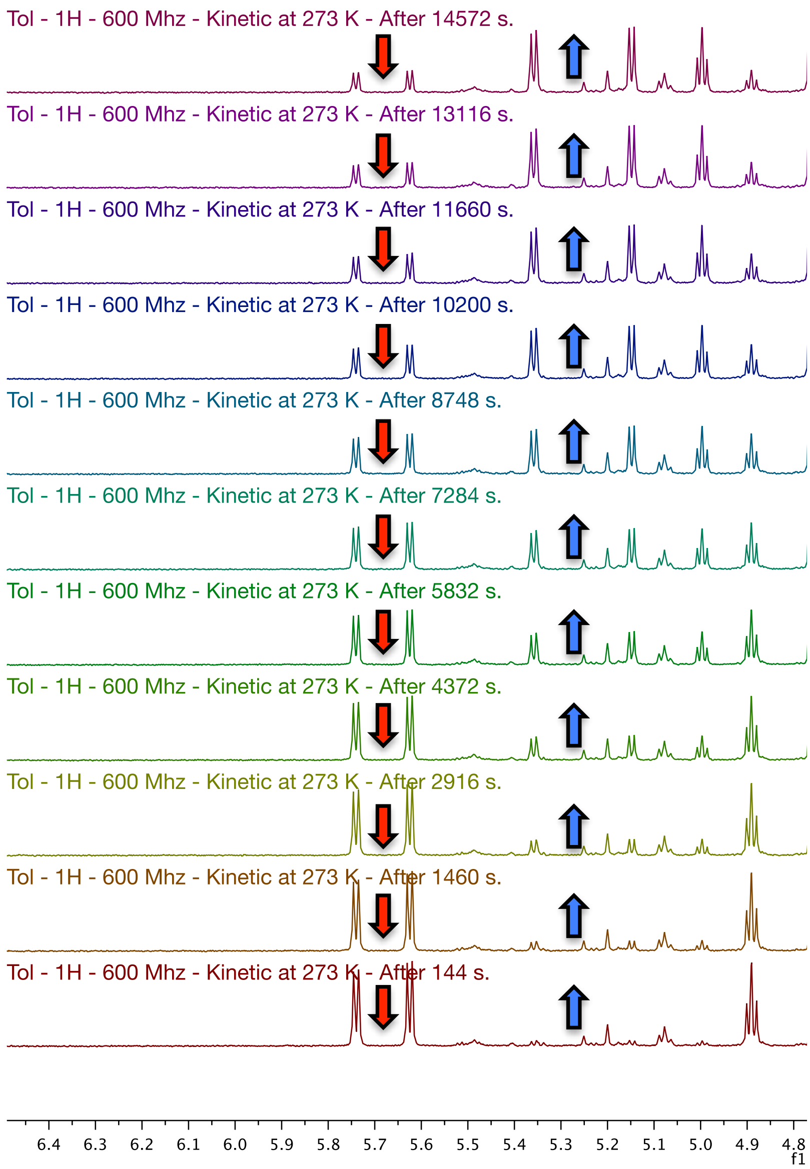

Figure 171: ^{1}H-NMR spectra in toluene at 273 K, showing the progressive disappearance of the signals associated to bimetallic **16a** (red arrows) and the apparition of the signal of **17a** (blue arrows).

The thermodynamic parameters associated to the isomerization process (considered as a first order kinetic reaction) were obtained after analysis of the respective Eyring curves (Figure 172, Figure 173). It was found for the isomerization of **16a** into **17a**: $\Delta G_{exp}^{298K} = 20.7\ kcal/mol$ and for **16b** into **17b**: $\Delta G_{exp}^{298} = 19.4\ kcal/mol$. Worthy to note is the relatively close value obtained by the mean of DFT calculations (in the gas phase), for **16a** of $\Delta G_{theo}^{298} = 13.0\ kcal/mol$ (other theoretical investigations are still on-going at the moment).

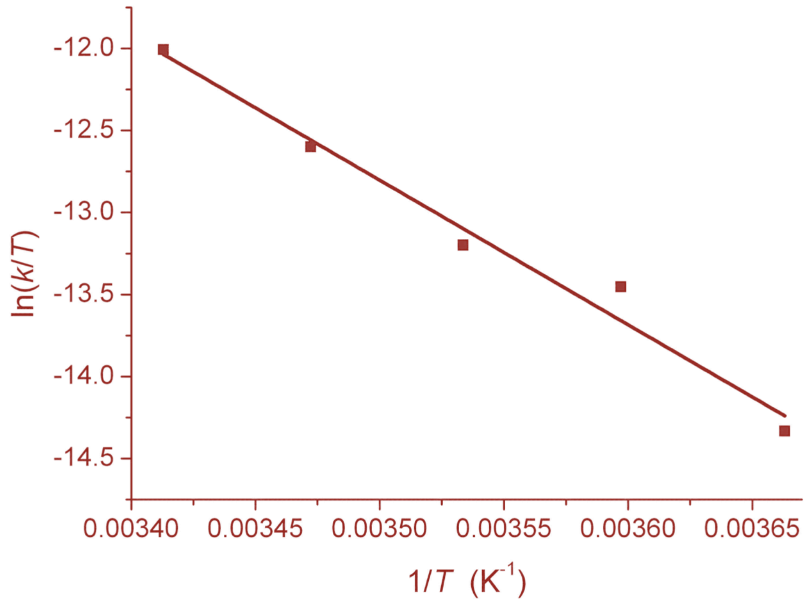

Figure 172: Eyring plot of ln(*k/T*) vs T^{-1} (K^{-1}) for the isomerization of **16a** into **17a** - ^{1}H NMR (600 MHz) line-shape between 273(1) and 293(1) K in toluene.

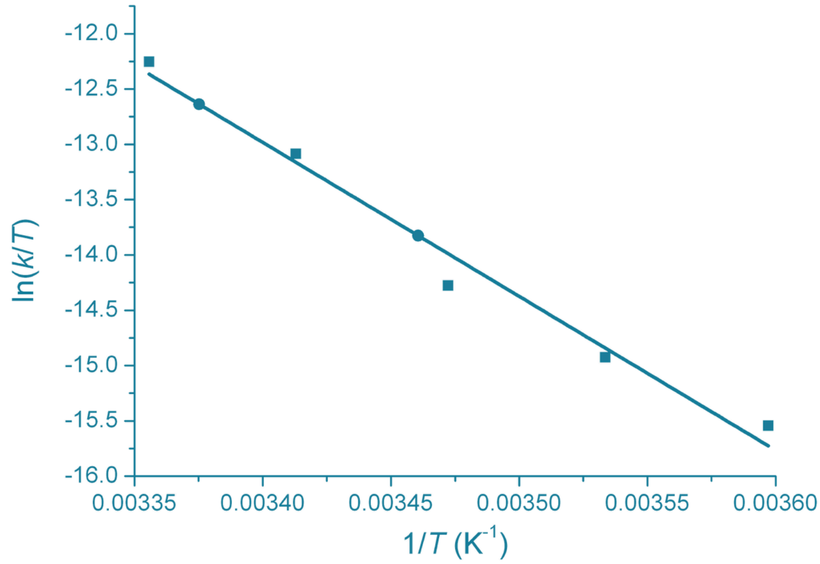

Figure 173: Eyring plot of ln(*k/T*) vs T^{-1} (K^{-1}) for the isomerization of **16b** into **17b** - ^{1}H NMR (600 MHz) line-shape between 278(1) and 298(1) K in toluene.

Due to the problems in the synthesis of **16c** and **16j** in ether, changes in the reaction had to be made, namely, changing the solvent (by THF, Figure 174), a prolonged reaction time and heating at 50°C for 1h. These conditions permitted to successfully produce **17c** and **17j** in the same range of yields as previous **16** compounds (40-50 %). Unfortunately, compounds **16c** and **16j** were not observed under these thermodynamically driven conditions.

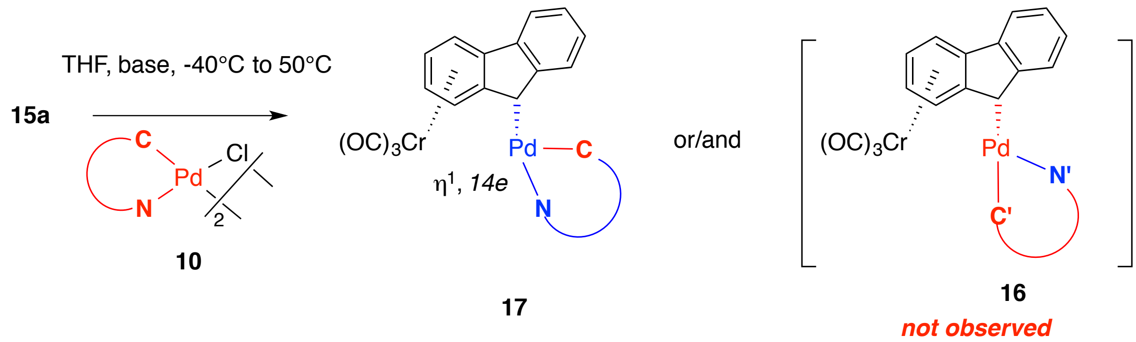

Figure 174: New experimental conditions used for the synthesis of compounds **17c**, **17j**.

Structural characterization by means of X-ray diffraction analysis was also successful with palladium complexes **17c**, **17j,** as well as for compounds **17a, 17b, 17f, 17i** (Figure 175-Figure 180):

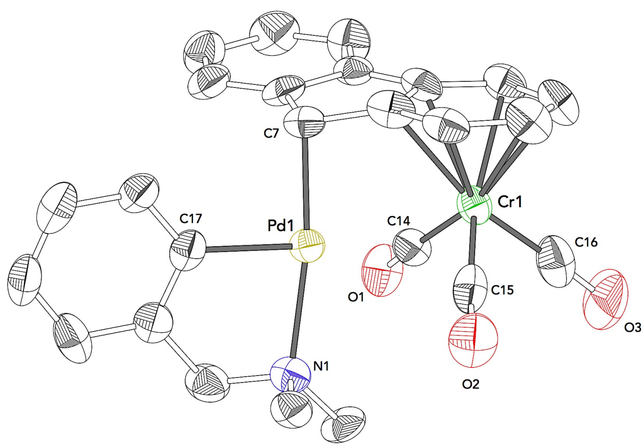

Compound **17a**
Space Group: **P -1**
R-Factor (%): **8.38**

N°	A	B	C	Lengths (Å)	Angles (°)
1	Cr_1	Pd_1	-	2.915(1)	-
2	Cr_1	C_{14}	-	1.85(1)	-
3	Cr_1	C_{15}	-	1.85(1)	-
4	Cr_1	C_{16}	-	1.84(1)	-
5	C_{14}	O_1	-	1.14(1)	-
6	C_{15}	O_2	-	1.17(1)	-
7	C_{16}	O_3	-	1.16(1)	-
8	Pd_1	C_7	-	2.068(8)	-
9	Pd_1	C_{17}	-	2.034(8)	-
10	Pd_1	N_1	-	2.181(6)	-
11	Pd_1	C_{14}	-	2.525(8)	-
12	Pd_1	C_{15}	-	2.92(1)	-
13	Cr_1	C_{14}	O_1	-	170.2(8)
14	Cr_1	C_{15}	O_2	-	175.0(8)
15	Cr_1	C_{16}	O_3	-	177.5(9)
16	C_{14}	Cr_1	C_{15}	-	99.7(4)

Figure 175: X-ray structure and selected interatomic distances of compound **17a**.

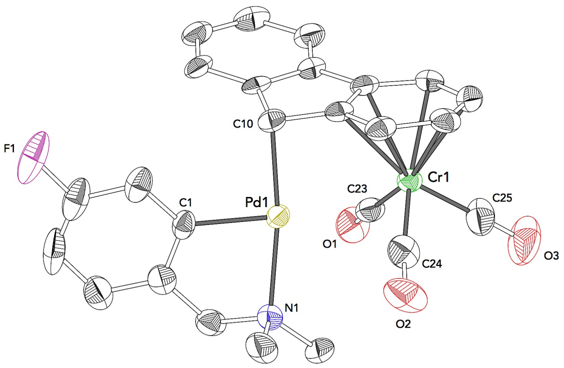

Compound **17b**
Space Group: **P 2_1/c**
R-Factor (%): **3.91**

N°	*A*	*B*	*C*	*Lengths (Å)*	*Angles (°)*
1	Cr_1	Pd_1	-	2.9179(6)	-
2	Cr_1	C_{23}	-	1.862(4)	-
3	Cr_1	C_{24}	-	1.841(5)	-
4	Cr_1	C_{25}	-	1.838(4)	-
5	C_{23}	O_1	-	1.148(5)	-
6	C_{24}	O_2	-	1.154(6)	-
7	C_{25}	O_3	-	1.150(5)	-
8	Pd_1	C_{10}	-	2.095(3)	-
9	Pd_1	C_1	-	2.018(3)	-
10	Pd_1	N_1	-	2.188(3)	-
11	Pd_1	C_{23}	-	2.627(4)	-
12	Pd_1	C_{24}	-	2.911(5)	-
13	Cr_1	C_{23}	O_1	-	170.8(3)
14	Cr_1	C_{24}	O_2	-	173.9(4)
15	Cr_1	C_{25}	O_3	-	178.8(4)
16	C_{23}	Cr_1	C_{24}	-	98.9(2)

Figure 176: X-ray structure and selected interatomic distances of compound **17b**.

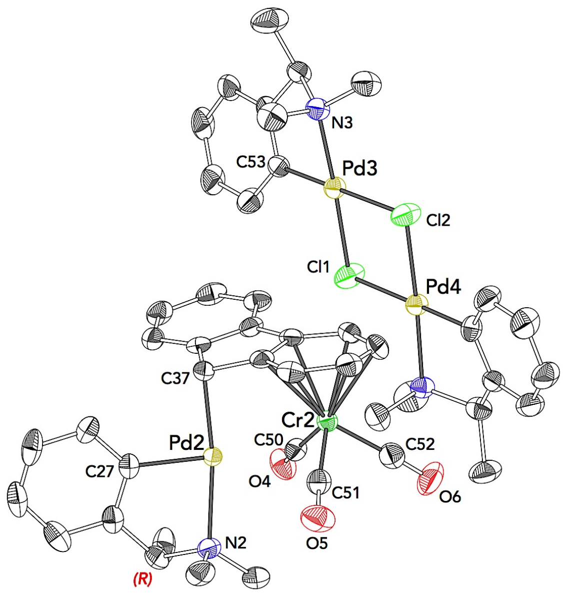

Compound (1*R*)-**17c**
Space Group: **P 1**
R-Factor (%): **3.07**

N°	*A*	*B*	*C*	*Lengths (Å)*	*Angles (°)*
1	Cr_2	Pd_2	-	2.894(1)	-
2	Cr_2	C_{50}	-	1.863(7)	-
3	Cr_2	C_{51}	-	1.835(6)	-
4	Cr_2	C_{52}	-	1.864(6)	-
5	C_{50}	O_4	-	1.153(9)	-
6	C_{51}	O_5	-	1.146(7)	-
7	C_{52}	O_6	-	1.136(8)	-
8	Pd_2	C_{37}	-	2.082(6)	-
9	Pd_2	N_2	-	2.216(5)	-
10	Pd_2	C_{27}	-	2.027(5)	-
11	Pd_2	C_{50}	-	2.479(6)	-
12	Pd_2	C_{51}	-	2.895(6)	-
13	Pd_3	Cl_1	-	2.327(2)	-
14	Pd_3	Cl_2	-	2.483(2)	-
15	Pd_3	N_3	-	2.075(7)	-
16	Pd_3	C_{53}	-	1.970(6)	-
17	Pd_4	Cl_1	-	2.476(2)	-
18	Pd_4	Cl_2	-	2.331(2)	-
19	Pd_4	N_4	-	2.076(7)	-
20	Pd_4	C_{63}	-	1.979(6)	-
21	Cr_2	C_{50}	O_4	-	170.0(5)
22	Cr_2	C_{51}	O_5	-	174.4(6)
23	Cr_2	C_{52}	O_6	-	177.6(6)
24	C_{50}	Cr_2	C_{51}	-	99.1(3)
25	Pd_3	Cl_1	Pd_4	-	94.68(6)
26	Pd_3	Cl_2	Pd_4	-	94.97(6)

Figure 177: X-ray structure and selected interatomic distances of compound (1R)-**17c**.

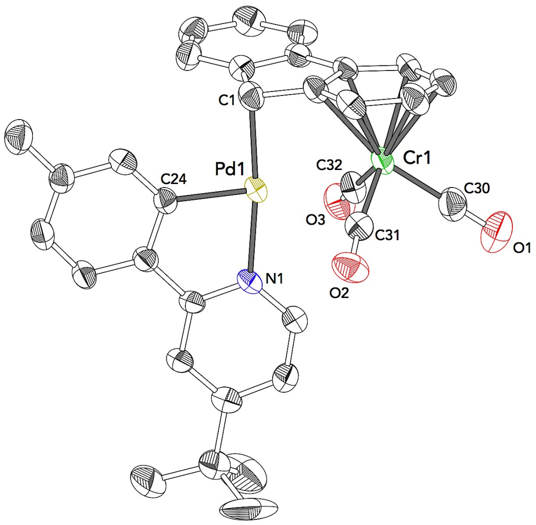

Compound **17f**
Space Group: **P 2_1/c**
R-Factor (%): **6.55**

N°	A	B	C	Lengths (Å)	Angles (°)
1	Cr_1	Pd_1	-	2.8625(7)	-
2	Cr_1	C_{30}	-	1.844(5)	-
3	Cr_1	C_{31}	-	1.847(4)	-
4	Cr_1	C_{32}	-	1.851(4)	-
5	C_{30}	O_1	-	1.152(6)	-
6	C_{31}	O_2	-	1.158(6)	-
7	C_{32}	O_3	-	1.162(5)	-
8	Pd_1	C_1	-	2.097(5)	-
9	Pd_1	N_1	-	2.112(4)	-
10	Pd_1	C_{24}	-	2.018(4)	-
11	Pd_1	C_{31}	-	2.660(4)	-
12	Pd_1	C_{32}	-	2.647(4)	-
13	Cr_1	C_{30}	O_1	-	177.6(4)
14	Cr_1	C_{31}	O_2	-	173.2(2)
15	Cr_1	C_{32}	O_3	-	173.7(4)
16	C_{31}	Cr_1	C_{32}	-	98.4(2)

Figure 178: X-ray structure and selected interatomic distances of compound **17f**.

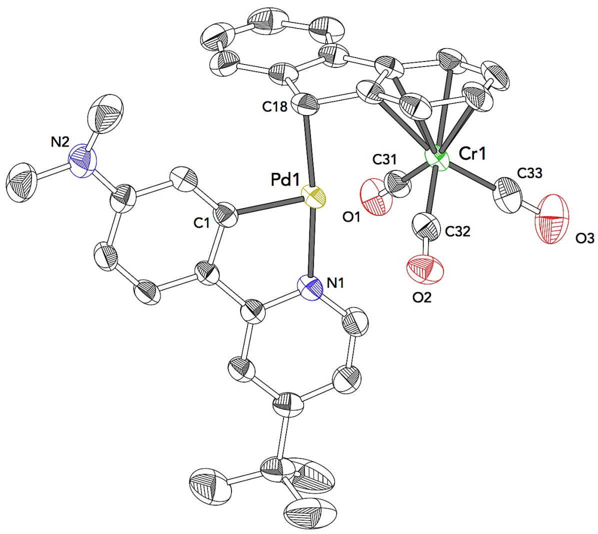

Compound **17i**
Space Group: **P 2_1/c**
R-Factor (%): **3.04**

N°	A	B	C	Lengths (Å)	Angles (°)
1	Cr_1	Pd_1	-	2.8577(4)	-
2	Cr_1	C_{31}	-	1.862(2)	-
3	Cr_1	C_{32}	-	1.849(2)	-
4	Cr_1	C_{33}	-	1.848(2)	-
5	C_{31}	O_1	-	1.153(3)	-
6	C_{32}	O_2	-	1.153(3)	-
7	C_{33}	O_3	-	1.150(3)	-
8	Pd_1	C_{18}	-	2.098(2)	-
9	Pd_1	C_1	-	2.012(2)	-
10	Pd_1	N_1	-	2.111(2)	-
11	Pd_1	C_{31}	-	2.648(2)	-
12	Pd_1	C_{32}	-	2.649(2)	-
13	Cr_1	C_{31}	O_1	-	174.5(2)
14	Cr_1	C_{32}	O_2	-	173.6(2)
15	Cr_1	C_{33}	O_3	-	177.2(2)
16	C_{31}	Cr_1	C_{32}	-	98.66(9)

Figure 179: X-ray structure and selected interatomic distances of compound **17i**.

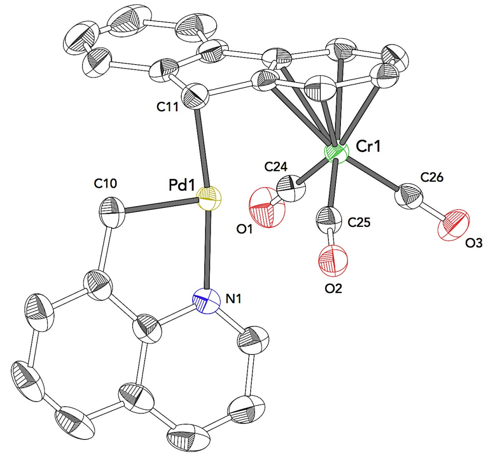

Compound **17j**
Space Group: **P b c a**
R-Factor (%): **2.47**

N°	A	B	C	Lengths (Å)	Angles (°)
1	Cr_1	Pd_1	-	2.8368(4)	-
2	Cr_1	C_{24}	-	1.861(2)	-
3	Cr_1	C_{25}	-	1.859(2)	-
4	Cr_1	C_{26}	-	1.833(2)	-
5	C_{24}	O_1	-	1.152(3)	-
6	C_{25}	O_2	-	1.158(3)	-
7	C_{26}	O_3	-	1.155(3)	-
8	Pd_1	C_{11}	-	2.116(2)	-
9	Pd_1	C_{10}	-	2.044(2)	-
10	Pd_1	N_1	-	2.106(2)	-
11	Pd_1	C_{24}	-	2.700(2)	-
12	Pd_1	C_{25}	-	2.532(2)	-
13	Cr_1	C_{24}	O_1	-	173.0(2)
14	Cr_1	C_{25}	O_2	-	170.4(2)
15	Cr_1	C_{26}	O_3	-	179.0(2)
16	C_{24}	Cr_1	C_{25}	-	99.7(1)

Figure 180: X-ray structure and selected interatomic distances of compound **17j**.

The X-ray structures of bimetallics **17** argue in favour of a η^1-*syn*-facial coordination mode of the metal centre to the fluorene ligand (hemichelation). The Cr−Pd distances of bimetallics **17** are all in the range of 2.837−2.918 Å (similar to the distance observed for bimetallics **12**). In all cases these distances are longer than the associated ones in compound **16**.

Bis-chromium fluorenyl anion **18b** (hemichelating ligand, Figure 181) was used in an attempt to improve the stability of **16** derivatives, by avoiding the isomerization process. The presence of a second chromium unit could reasonably stabilize, thanks to an improved charge depletion on the benzylic position, the species where the two δ^- charged carbons (benzylic and [NC]chelate) are in a *trans* position.

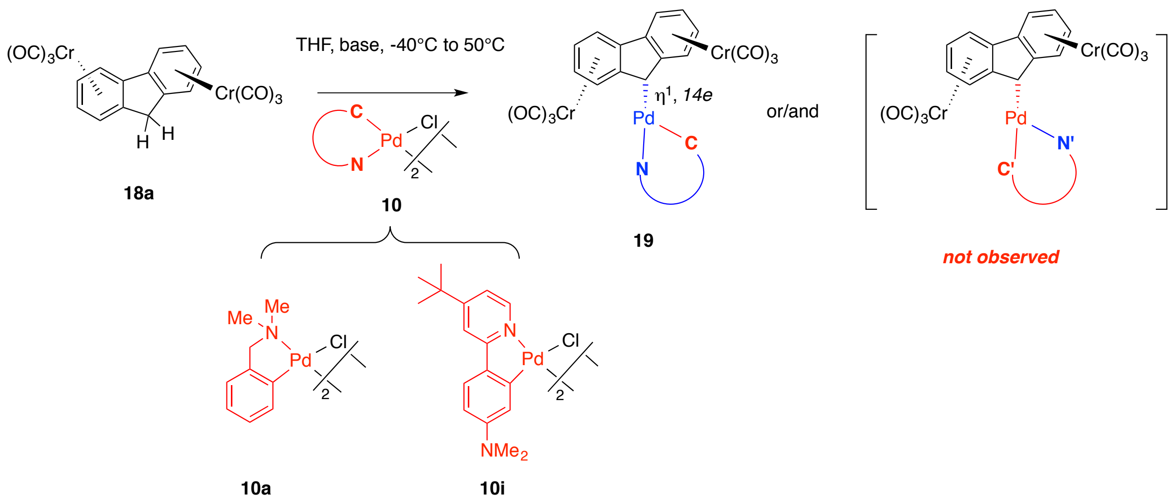

Figure 181: The ambiphilic character of anion **18b** allows only one orientation for the metallacycle (**N**-**Pd**-**C**).

Unfortunately, due to the very low solubility of compound **15a** in ether (anion **15b** could not be formed), the conditions had to be changed and THF was used. Even in these conditions, it was necessary to heat the reaction mixture before treatment to displace the equilibrium toward the formation of **19**, otherwise a huge amount (*i.e.* ~60 %) of **18a** would remain at the end of the reaction. Thus, the constraints of such thermodynamic conditions represent a serious obstacle for the formation of the expected **17** analogues with a bis-chromium unit.

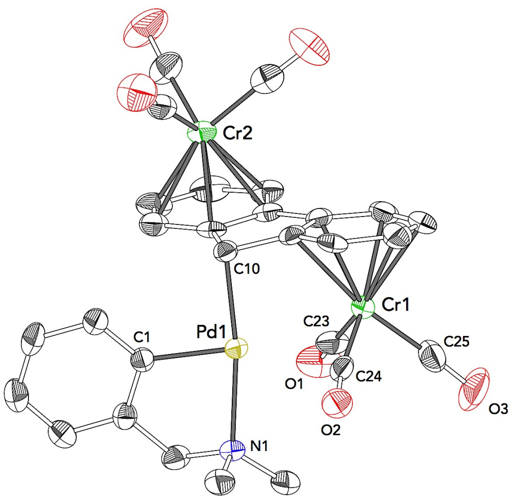

Compound **19a**
Space Group: **P -1**
R-Factor (%): **3.81**

N°	*A*	*B*	*C*	*Lengths (Å)*	*Angles (°)*
1	Cr_1	Pd_1	-	2.8558(7)	-
2	Cr_1	C_{23}	-	1.845(4)	-
3	Cr_1	C_{24}	-	1.858(4)	-
4	Cr_1	C_{25}	-	1.834(4)	-
5	C_{23}	O_1	-	1.158(5)	-
6	C_{24}	O_2	-	1.153(4)	-
7	C_{25}	O_3	-	1.155(5)	-
8	Pd_1	C_{10}	-	2.095(3)	-
9	Pd_1	C_1	-	2.025(4)	-
10	Pd_1	N_1	-	2.204(3)	-
11	Pd_1	C_{23}	-	2.677(5)	-
12	Pd_1	C_{24}	-	2.542(4)	-
13	Cr_1	C_{23}	O_1	-	172.1(4)
14	Cr_1	C_{24}	O_2	-	168.9(4)
15	Cr_1	C_{25}	O_3	-	176.9(4)
16	C_{23}	Cr_1	C_{24}	-	100.5(2)

Figure 182: X-ray structure and selected interatomic distances of compound **19a**.

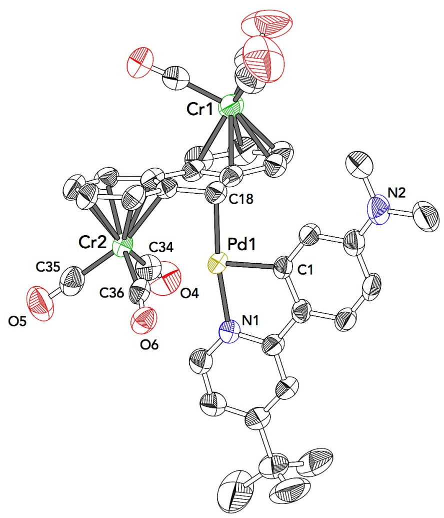

Compound **19i**
Space Group: **P 2_1/c**
R-Factor (%): **5.82**

N°	A	B	C	Lengths (Å)	Angles (°)
1	Cr_2	Pd_1	-	2.9021(7)	-
2	Cr_1	C_{34}	-	1.846(5)	-
3	Cr_1	C_{35}	-	1.848(5)	-
4	Cr_1	C_{36}	-	1.861(5)	-
5	C_{34}	O_4	-	1.163(6)	-
6	C_{35}	O_5	-	1.152(7)	-
7	C_{36}	O_6	-	1.158(6)	-
8	Pd_1	C_{18}	-	2.095(4)	-
9	Pd_1	C_1	-	2.018(4)	-
10	Pd_1	N_1	-	2.109(4)	-
11	Pd_1	C_{34}	-	2.880(5)	-
12	Pd_1	C_{36}	-	2.557(4)	-
13	Cr_2	C_{34}	O_4	-	174.7(5)
14	Cr_2	C_{35}	O_5	-	174.9(5)
15	Cr_2	C_{36}	O_6	-	170.5(4)
16	C_{34}	Cr_2	C_{36}	-	98.5(2)

Figure 183: X-ray structure and selected interatomic distances of compound **19i**.

(ATR)-FT-IR spectra of the *syn*-facial complexes are characterized by the lifted degeneracy of the carbonyl C−O stretching E band (the A band appears at *ca.* 1956−1931 cm^{-1}) that gives rise to two distinct bands at *ca.* 1880 (s) and 1850 (vs) cm^{-1} (Figure 184). This spectroscopic peculiarity is typical of the lack of local C_{3v} symmetry[987-990] at the $Cr(CO)_3$ moiety in the solid state. The ^{13}C NMR spectra of **16**, **17** and **19** present the typical signature of a rotation-hindered $Cr(CO)_3$ moiety in an asymmetric local environment[991 - 993] that is materialized by three broad signals at around δ 240, 238, and 234 ppm.

[987] [N°736] van Meurs, F.; Baas, J. M. A.; van Bekkum, H. *J. Organomet. Chem.* **1977**, *129*, 347.

[988] [N°828] Lokshin, B. V.; Rusach, E. B.; Kolobova, N. E.; Makarov, Y. V.; Ustynyuk, N. A.; Zdanovich, V. I., . . . Setkina, V. N. *J. Organomet. Chem.* **1976**, *108*, 353.

[989] [N°807] W. Neuse, E. *J. Organomet. Chem.* **1975**, *99*, 287.

[990] [N°808] Adams, D. M.; Squire, A. *J. Chem. Soc., Dalton Trans.* **1974**, 558.

[991] [N°609] Djukic, J. P.; Michon, C.; Maisse-Francois, A.; Allagapen, R.; Pfeffer, M.; Dotz, K. H., . . . Fischer, J. *Chem. Eur. J.* **2000**, *6*, 1064.

[992] [N°608] Djukic, J. P.; Maisse-Francois, A.; Pfeffer, M.; Dotz, K. H.; De Cian, A.; Fischer, J. *Organometallics* **2000**, *19*, 5484.

[993] [N°604] Djukic, J. P.; Pfeffer, M.; Dotz, K. H. *C.R. Acad. Sci. Paris, Ser. IIc* **1999**, *2*, 403.

Cmpds	***Reciprocal wavelengths (cm^{-1})***		
15a	1942	1885	1850
18a	1932		1850
16a	1944	1876	1839
17a	1940	1886	1843
16b	1956	1922	1829
17b	1945	1883	1843
16f	1945	1875	1858
17f	1952	1880	1857
16i	1948	1885	1860
17i	1937	1886	1849
17j	1931	1873	1849
17c	1943	1886	1848
19a	1942	1892	1855
19i	1946	1887	1866

Figure 184: IR vibrations of carbonyl groups.

5.2 - Conclusion.

The new hemichelates **16, 17** and **19**, constitute the first arguments in favour of the extensibility of the concept of hemichelation, which is now not only limited to the tricarbonyl(η^6-indenyl)chromium anion, a conventional heteroditopic ligand capable of chelating a metal centre through covalent and noncovalent bonding, but also to other analogues (*e.g.* fluorene). At the moment of the writing of the thesis, the structural cohesion of these species was not yet thoroughly addressed by DFT methods. However, a reasonable assumption is that the stabilization stems from a compensation of insufficient donor/acceptor Cr-Pd bonding by non-covalent interactions of preponderant attractive Coulombic nature, as it was the case for compounds **7**, **12** and **13**. The *syn*-facial η^1 coordination of the fluorenyl ligand to Pd is thermodynamically preferred over the *syn*-facial and *antara*-facial η^3 modes as a consequence of the charge depletion induced by the aromaticity of the phenyl ring (**15a**) or due to an incorporation of a second chromium unit (**18a**). An eventual fluxional character is thus prevented and hemichelation remains the preferred coordination mode. These results lay the ground for further possible extensions of the concept of hemichelation toward other ligands as well as other metal centres.

6 - Extension of the concept of hemichelation to the allylbenzene unit.

6.1 - Purpose.

In our continued effort to analyse the modes of stabilization of electron-deficient centres by noncovalent interactions, the present section will disclose an asset of the hemichelation concept by a very specific arene unit, namely: the allylbenzene. In this case the metal centre has two possibilities (Figure 185):

- To establish a classical η^3 coordination mode, thus, forming a saturated 16-electron Pd centre (red).
- To establish a hemichelation with the $Cr(CO)_3$ unit, leading to an unsaturated 14 electron Pd centre (blue).

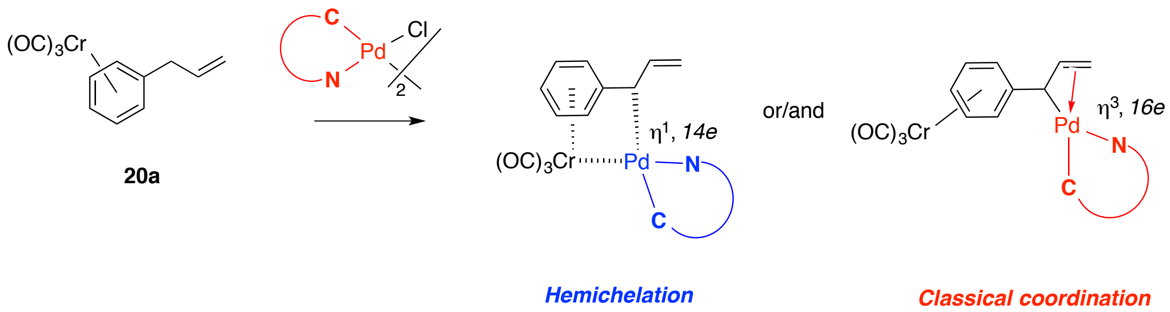

Figure 185: The anion **20b** can hypothetically bind the palladium centre by two different kind of coordination modes (classical η^3) or hemichelation.

6.2 - Experimental aspects.

For the three studied cases (Figure 186) it was found that only saturated 16 electron Pd(II) complexes are formed where the metal centre is coordinated at the allylbenzene benzylic position in a η^3 manner involving the allylic double bond of the arene unit. Optimal conversions were achieved when palladacycles **10a**, **10b** or **10i** reacted with anion **20b** in a dry mixture of THF (preferred to ether where compound **20a** is rather insoluble) at −40 °C. The corresponding *antara*-facial complexes **21a, 21b** and **21i** were isolated mostly by recrystallization below 0°C to prevent decomposition (yields spanning 40–57 %).

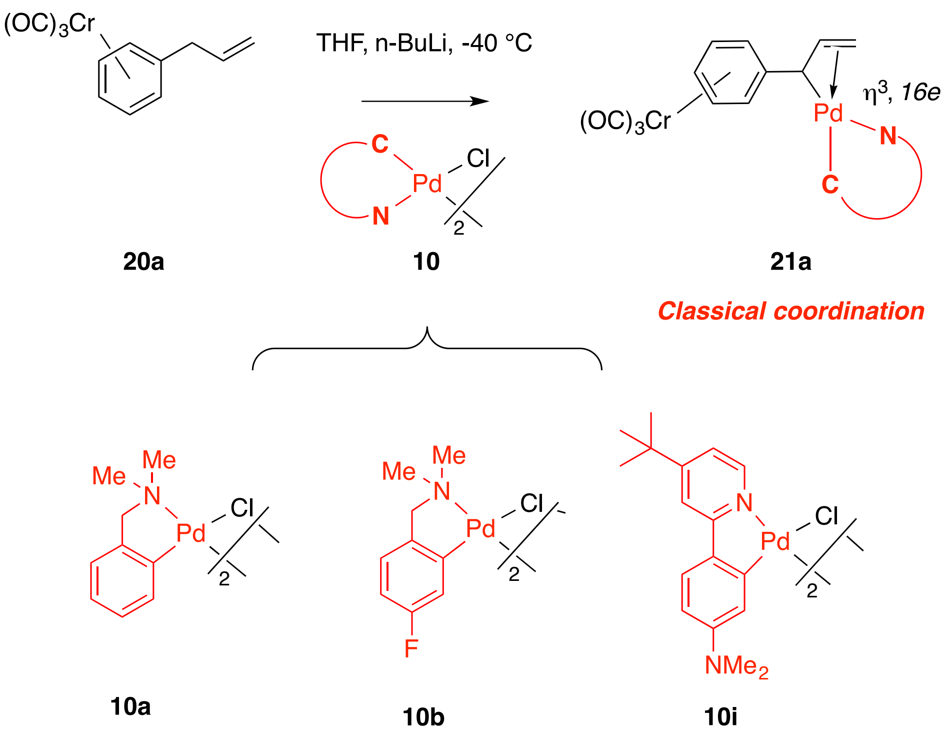

Figure 186: The ambiphilic character of anion **20b** leads upon reaction to the formation of a saturated Pd metal centre coordinated fashion η^3 at the benzylic position.

Compounds **21** have been characterized by the mean of X-ray diffraction analysis (Figure 187 to Figure 189). They display, at the solid state a classical allylic coordination type of the Pd centre to the allylbenzene unit but quite not in the expected hemichelation mode:

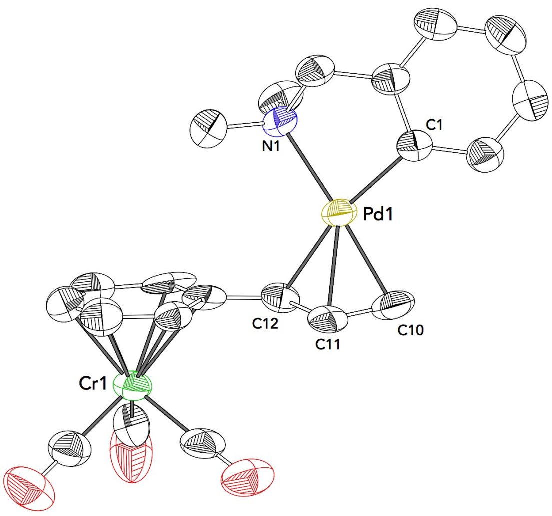

N°	A	B	C	Lengths (Å)	Angles (°)
1	Pd_1	C_{10}	-	2.101(5)	-
2	Pd_1	C_{11}	-	2.11(1)	-
3	Pd_1	C_{12}	-	2.247(9)	-
4	Pd_1	N_1	-	2.144(3)	-
5	Pd_1	C_1	-	2.022(4)	-
6	C_{10}	C_{11}	-	1.31(1)	-
7	C_{11}	C_{12}	-	1.44(1)	-

Compound **21a**
Space Group: **P -1**
R-Factor (%): **5.33**

Figure 187: X-ray structure and selected interatomic distances of compound **21a**.

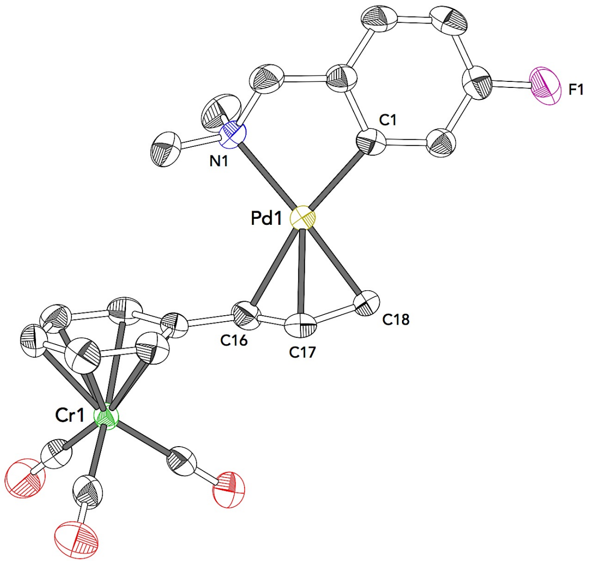

N°	A	B	C	Lengths (Å)	Angles (°)
1	Pd_1	C_{18}	-	2.096(3)	-
2	Pd_1	C_{17}	-	2.146(3)	-
3	Pd_1	C_{16}	-	2.276(3)	-
4	Pd_1	N_1	-	2.149(3)	-
5	Pd_1	C_1	-	2.021(2)	-
6	C_{18}	C_{17}	-	1.420(4)	-
7	C_{17}	C_{16}	-	1.373(4)	-

Compound **21b**
Space Group: **P 2_1/c**
R-Factor (%): **2.75**

Figure 188: X-ray structure and selected interatomic distances of compound **21b**.

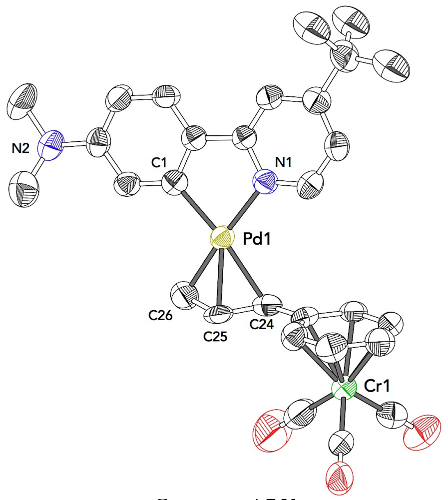

Compound **21i**
Space Group: **C 2/c**
R-Factor (%): **7.08**

N°	*A*	*B*	*C*	*Lengths (Å)*	*Angles (°)*
1	Pd_1	C_{26}	-	2.105(6)	-
2	Pd_1	C_{25}	-	2.135(6)	-
3	Pd_1	C_{24}	-	2.256(5)	-
4	Pd_1	N_1	-	2.082(4)	-
5	Pd_1	C_1	-	2.025(5)	-
6	C_{26}	C_{25}	-	1.393(8)	-
7	C_{25}	C_{24}	-	1.379(7)	-

Figure 189: X-ray structure and selected interatomic distances of compound **21i**.

Worthy to note are the multiple signals associated with compounds **21** in ^{1}H NMR spectroscopy at room temperature, which progressively disappear upon decreasing the temperature. This phenomenon might be associated to conformational exchanges taking place within **21** (*i.e.*: Free rotation around C_{24}) occurring at room temperature and limited at low temperature.

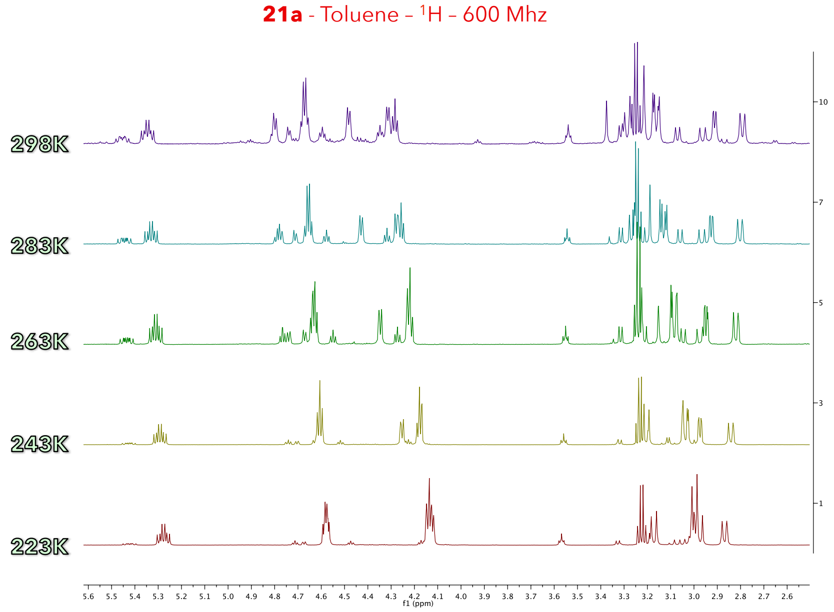

Figure 190: ^{1}H NMR variable temperature investigations at subambiant temperatures revealing the simplification of the ^{1}H signals leading to the expected spectrum of **21a**.

It is important to mention that compounds **21a**, **21b** and **21i** have the disadvantage of being air sensitive and kinetically unstable at room temperature generally decomposing within a few hours in two subproducts namely, **22** and **23** (Figure 191).

21

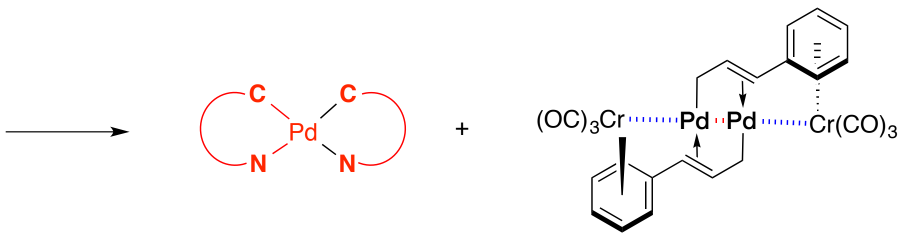

22 **23**

Figure 191: Compound **21** decomposes at room temperature into homoleptic compound **22** and a rare example of bis-Pd(I) bridged tetrametallic compound **23**.

The subproducts **22** and **23** are respectively the classical homoleptic complexes as well as a rare example of tetrametallic Cr(0)-Pd(I)-Pd(I)-Cr(0) species (yields for **23** spanning 20-30 %). Worthy to note, the proportion of **23** formed in the decomposition process is higher for **21a** and **21b** than for **21i,** where the formation of the homoleptic compound is favoured. A reasonable rationale could be that the phenylpyridine is a more robust and rigid chelate than the N-N-dimethylbenzylamine, in other words it is more solidly anchored to the Pd centre and thus, harder to remove, a necessary condition for the formation of **23**. Another necessary condition is the reduction of the palladium centre (from oxidation state II to putative I), which could be accounted for the oxidation of the chromium centre. It would explain the presence of unmetallated allylbenzene organic ligand in the reaction mixture. X-ray diffraction structures have been obtained for compounds **22a**, **22b**, as well as for compound **23**.

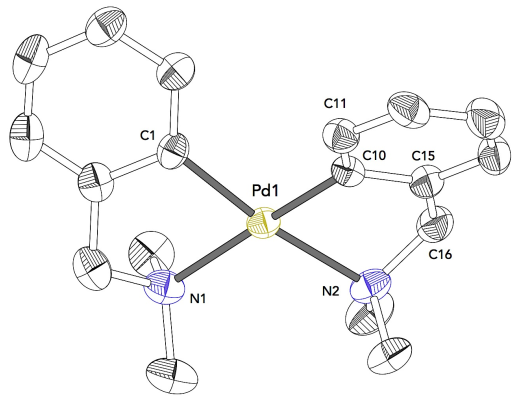

N°	A	B	C	D	Lengths (Å)	Angles (°)
1	Pd_1	C_1	-	-	2.001(3)	-
2	Pd_1	C_{10}	-	-	1.998(3)	-
3	Pd_1	N_1	-	-	2.210(3)	-
4	Pd_1	N_2	-	-	2.217(3)	-
5	C_{11}	C_{10}	Pd_1	C_1	-	33.6(3)
6	C_{10}	C_{15}	C_{16}	N_2	-	-33.5(4)

Compound **22a**
Space Group: **P b c a**
R-Factor (%): **4.27**

Figure 192: X-ray structure and selected interatomic distances of compound **22a**.

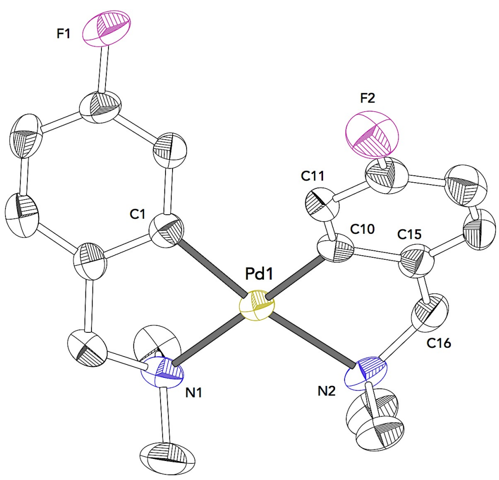

N°	A	B	C	D	Lengths (Å)	Angles (°)
1	Pd_1	C_1	-	-	1.199(4)	-
2	Pd_1	C_{10}	-	-	1.991(3)	-
3	Pd_1	N_1	-	-	2.203(3)	-
4	Pd_1	N_2	-	-	2.210(3)	-
5	C_{11}	C_{10}	Pd_1	C_1	-	34.4(3)
6	C_{10}	C_{15}	C_{16}	N_2	-	-32.9(4)

Compound **22b**
Space Group: **P b c a**
R-Factor (%): **4.65**

Figure 193: X-ray structure and selected interatomic distances of compound **22b**.

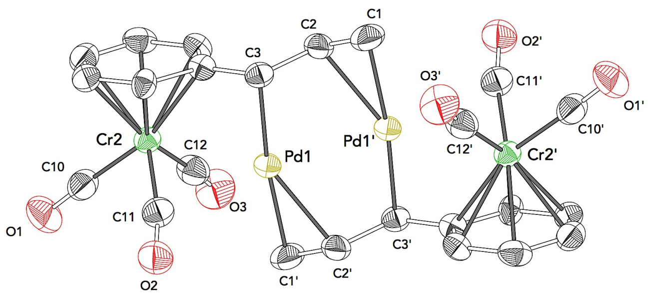

Compound **23**
Space Group: **P 2_1/c**
R-Factor (%): **3.89**

N°	A	B	C	D	Lengths (Å)	Angles (°)
1	Cr_2	Pd_1	-	-	2.786(1)	-
2	Pd_1	$Pd_{1'}$	-	-	2.749(1)	
3	Cr_2	C_{10}	-	-	1.837(3)	-
4	Cr_2	C_{11}	-	-	1.872(2)	-
5	Cr_2	C_{12}	-	-	1.851(3)	-
6	C_{10}	O_1	-	-	1.152(4)	-
7	C_{11}	O_2	-	-	1.149(3)	-
8	C_{12}	O_3	-	-	1.151(4)	-
9	C_1	C_2	-	-	1.379(6)	-
10	C_2	C_3	-	-	1.441(6)	-
11	Pd_1	$C_{1'}$	-	-	2.174(4)	-
12	Pd_1	$C_{2'}$	-	-	2.271(5)	-
13	Pd_1	C_3	-	-	2.164(4)	-
14	Pd_1	C_{11}	-	-	2.526(3)	-
15	Pd_1	C_{12}	-	-	2.895(3)	-
16	Cr_2	Pd_1	$Pd_{1'}$	-	-	151.38(6)
17	Cr_2	C_{10}	O_1	-	-	177.3(2)
18	Cr_2	C_{11}	O_2	-	-	170.3(2)
19	Cr_2	C_{12}	O_3	-	-	172.3(3)
20	C_{11}	Cr_2	C_{12}	-	-	95.2(1)
21	Cr_2	Pd_1	$Pd_{1'}$	$Cr_{2'}$	-	180.0(8)

Figure 194: X-ray structure and selected interatomic distances of compound **23**.

Figure 194 displays an apparently new case of *syn*-facial hemichelates of palladium. The metal distances Cr–Pd and Pd-Pd are respectively 2.79 and 2.75 Å, which is in the approximate range of the sum of empirical van der Waals radii[994] for Cr (1.4 Å)/Pd (1.4 Å), as well as for Pd (1.4 Å)/ Pd (1.4 Å). Compound **23** was found to be stable for days at room temperature in the solid state but much more reactive once in solution, where the formation of small amounts of **24** could be observed as well as other untraceable products. Moreover it was found that small yellow crystals, corresponding to **24**, started to grow, after a few days, over the red crystals of **23** that were kept in the mother solution of the diffusion tubes.

[994] [N°806] Slater, J. C. *J. Chem. Phys.* **1964**, *41*, 3199.

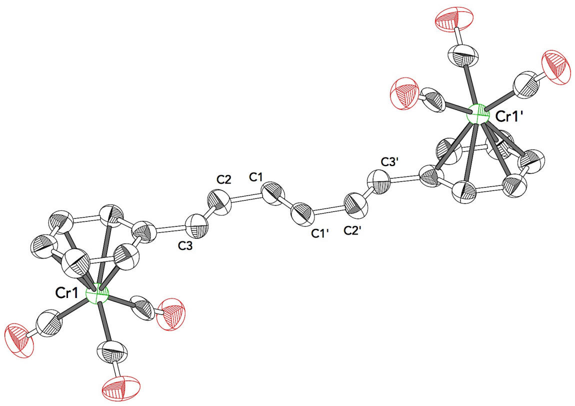

N°	A	B	C	D	Lengths (Å)	Angles (°)
1	C_1	C_2	-	-	1.510(9)	-
2	C_2	C_3	-	-	1.309(8)	-
3	C_1	$C_{1'}$	-	-	1.509(9)	-

Compound **24**
Space Group: **P 2_1/c**
R-Factor (%): **8.81**

Figure 195: X-ray structure and selected interatomic distances of compound **24**.

6.3 - Conclusion.

At the moment of the writing of the thesis, the theoretical calculations associated to these compounds, especially for **23**, have not yet been finished and are still in progress. A thoughtful analysis on the apparent specific relationship between the Pd(I) centres as-well as the hypothetic communication between the two Cr(0) centres toward the two bridging palladiums is on its way. For sure, NCIs have a role to play in this new heterodox hemichelation.

7 - Extension of the concept of hemichelation to bridged indenyls.

7.1 - Purpose and experimental aspects.

The present section will argue for the possibility of hemichelation to simultaneously stabilize on a single molecule two electron-deficient centres. Thus, a very specific arene unit has been chosen, namely the 1,2-bis(3-indenyl)ethane. The procedure used for the synthesis of the tetrametallic complex bearing two potentially electron deficient palladium centres followed our standard procedures (Figure 196), the only major difference residing in the stoichiometric amounts used, as-well as the "tolerance" of the substrate toward a double deprotonation, which is possible in the present case because of the stabilization of the negative charges by the two chromium units.

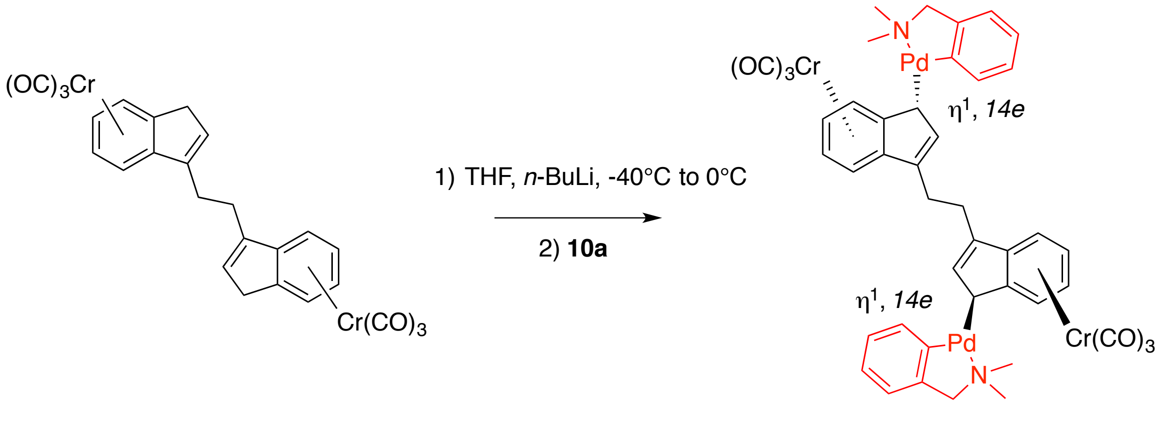

25a **26a**

Figure 196: The ambiphilic character of the anion associated to **25a** leads, upon reaction, to the formation of a new palladium hemichelate.

The yield of the reaction was found to be slightly lower than for previous studied cases (17 %). This is due to the difficulty inherent to the double deprotonation of **25a**, which generated some untraceable side products. The best conditions were achieved when palladacycle **10a** was reacted with anion **25b** in a dry mixture of THF at −40 °C (**25a** being rather insoluble in ether). The corresponding bis-*syn*-facial complex **26a** was isolated after evaporation of the solvent at 0°C and by recrystallization. Structural characterization by means of X-ray diffraction analysis was successful (Figure 197).

[995] [N°801] Ryabov, A. D.; Van Eldik, R.; Le Borgne, G.; Pfeffer, M. *Organometallics* **1993**, *12*, 1386.

[996] [N°802] Gaunt, J. C.; Shaw, B. L. *J. Organomet. Chem.* **1975**, *102*, 511.

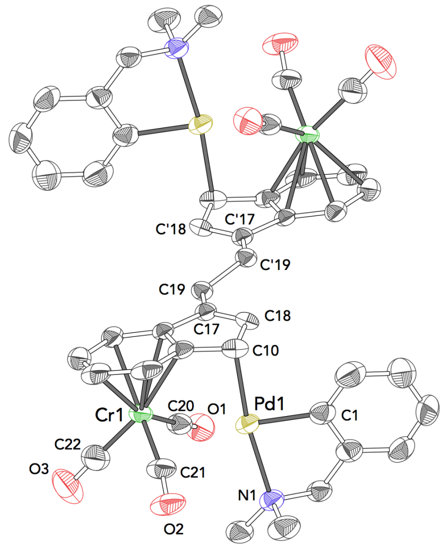

Compound **26a**
Space Group: **P -1**
R-Factor (%): **3.25**

N°	A	B	C	D	Lengths (Å)	Angles (°)
1	Cr_1	Pd_1	-	-	2.8929(4)	-
	Cr_1	C_{20}	-	-	1.853(2)	
2	Cr_1	C_{21}	-	-	1.837(3)	-
3	Cr_1	C_{22}	-	-	1.832(3)	-
4	C_{20}	O_1	-	-	1.151(3)	-
5	C_{21}	O_2	-	-	1.156(3)	-
6	C_{22}	O_3	-	-	1.155(4)	-
7	Pd_1	C_{10}	-	-	2.110(2)	-
8	Pd_1	C_1	-	-	2.020(3)	-
9	Pd_1	N_1	-	-	2.192(1)	-
10	Pd_1	C_{20}	-	-	2.647(3)	-
11	Pd_1	C_{21}	-	-	2.649(3)	-
12	C_{10}	C_{18}	-	-	1.471(3)	-
13	C_{18}	C_{17}	-	-	1.358(3)	-
14	C_{17}	C_{19}	-	-	1.493(3)	-
15	C_{19}	$C_{19'}$	-	-	1.521(3)	-
16	Cr_1	C_{20}	O_1	-	-	173.1(2)
17	Cr_1	C_{21}	O_2	-	-	171.2(2)
18	Cr_1	C_{22}	O_3	-	-	178.4(3)
19	C_{20}	Cr_1	C_{21}	-	-	98.1(1)

Figure 197: X-ray structure and selected interatomic distances of compound **26a**.

Compound **26a** constitutes a new case of *syn*-facial hemichelate of palladium, with the high specificity of bearing two unsaturated metal centres stabilized by hemichelation. The Pd metal centres, as usual, are found to be in short contact with one of the vicinal Cr-bound CO ligands and prefer an η^1 coordination mode to a η^3 one at the benzylic indenyl. The Cr–Pd distance lies in the range of 2.89 Å, which is in the approximate range of the sum of empirical van der Waals radii[997] for Cr (1.4 Å)/Pd (1.4 Å). The (ATR)-FT-IR spectrum is characterized by the lifted degeneracy of the carbonyl C–O stretching E band (the A band appears at *ca.* 1936 cm^{-1}) that gives rise to two distinct bands at *ca.* 1875 (s) and 1842 (vs) cm^{-1}. The ^{13}C NMR spectra of **26a** presents the typical signature of a rotation-hindered $Cr(CO)_3$ moiety in an asymmetric local environment[998-1000] that is materialized by three broad signals at around δ 239, 236, and 233 ppm.

[997] [N°806] Slater, J. C. *J. Chem. Phys.* **1964**, *41*, 3199.

[998] [N°609] Djukic, J. P.; Michon, C.; Maisse-Francois, A.; Allagapen, R.; Pfeffer, M.; Dotz, K. H., . . . Fischer, J. *Chem. Eur. J.* **2000**, *6*, 1064.

[999] [N°608] Djukic, J. P.; Maisse-Francois, A.; Pfeffer, M.; Dotz, K. H.; De Cian, A.; Fischer, J. *Organometallics* **2000**, *19*, 5484.

[1000] [N°604] Djukic, J. P.; Pfeffer, M.; Dotz, K. H. *C.R. Acad. Sci. Paris, Ser. IIc* **1999**, *2*, 403.

7.2 - Conclusion.

To conclude, **26a** constitutes the first case of a molecule bearing two electron-deficient Pd (14 electron) centre which are stabilized by the mean of hemichelation, thus, forming an unprecedented air-stable and solution-persistent neutral T-shaped tetrametallic complex. More heteroditopic ligands (**27a** and **28a**) were tried in order to form other tetrametallic species (Figure 198):

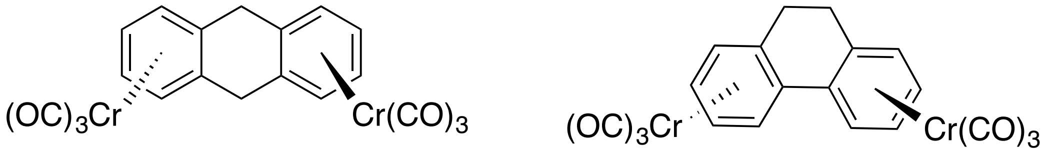

27a **28a**

Figure 198: Other heteroditopic ligands tested in order to synthesize another tetrametallic complex.

Nevertheless no stable four-metal-species could be isolated. The generation of a double negative charge on these ligands could not easily be accessed even at -80 °C. The only highly reactive species, which could be observed, was that shown in Figure 199. This is not the expected tetrametallic complex, but rather a trimetallic one.

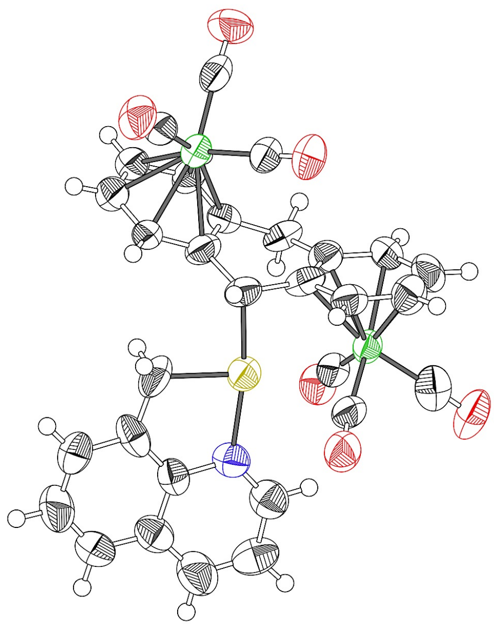

Figure 199: X-ray structure of the bimetallic obtained while trying to synthesis another tetrametallic complex **29j**.

8 - Chapter Conclusion.

Rare examples of persistent coordinatively unsaturated Pd(II)/Pt(II) complexes where reported. The *syn*-facial η^1 coordination preference of the metal centre at the benzylic position of several heteroditopic ligands (Figure 200) is thermodynamically preferred over *syn*-facial or *antara*-facial η^3 modes.

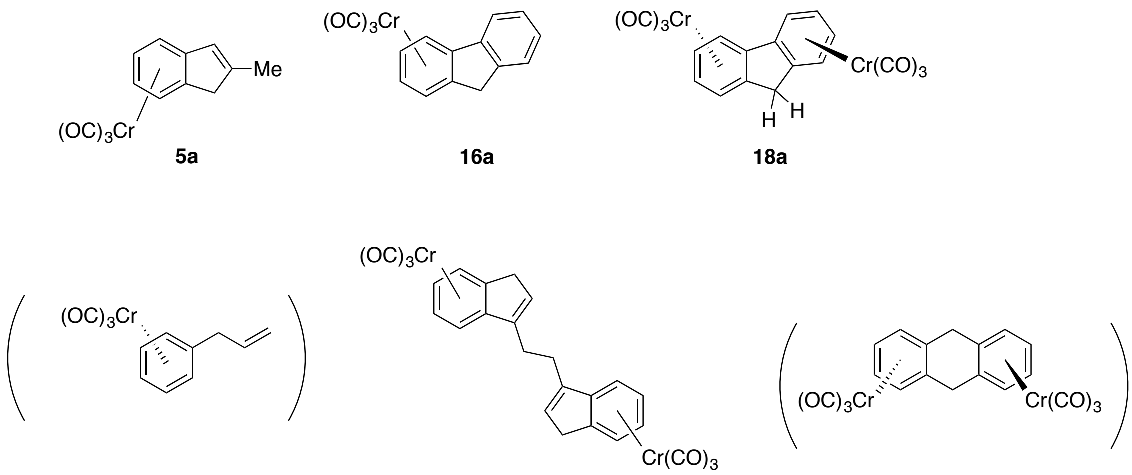

5a **16a** **18a**

20a **25a** **27a**

Figure 200: Heteroditopic ligand used to form Pd/Pt hemichelates.

In several cases fluxionality was observed (*i.e.* a rapid haptotropy of the metal centre between two limiting benzylic positions) as a direct consequence of the evanescence of the polar intermetallic interaction.[1001,1002] Nevertheless, fluxionality is only a side feature of such hemichelates (*e.g.* fluorene hemichelates). These results highlight the cohesive role of non-covalent interactions (electron correlation, London force, and Coulombic attraction) in loose but manageable donor/acceptor metal-based Lewis pairs.

1001 [N°559] Hyla-Kryspin, I.; Grimme, S.; Djukic, J. P. *Organometallics* **2009**, *28*, 1001.

1002 [N°562] Schwabe, T.; Grimme, S.; Djukic, J.-P. *J. Am. Chem. Soc.* **2009**, *131*, 14156.

IV

An excursion into non-covalence

Group 9 Transition Metals

This chapter describes an extension of the concept of HEMICHELATION to other transition-metals, namely Rh(I).

Chapter IV - Extension of Hemichelation to other transition metals: The case of Rh(I).

1 - Introduction.

Hemichelation is emerging as a new mode of coordination where non-covalent interactions crucially contribute to the cohesion of electron-unsaturated organometallic complexes. This chapter discloses a new unprecedented demonstration of this novel concept of coordination chemistry to a Group 9 transition metal, *i.e.* Rh(I). *Hemichelation* can be achieved, as largely shown in chapter III, with ambiphilic anionic ligands such as the (η^6-indenyl)tricarbonylchromium anion **5b** prepared from **5a** by benzylic deprotonation, which can bind Pd(II) and Pt(II) centres (Figure 79, Figure 117) by means of 1) a covalent bond to the benzylic position and 2) non-covalent interactions of dominating Coulombic character with the proximal $Cr(CO)_3$ moiety (Figure 161), leading to persistent and manageable 14 valence electron complexes of group 10 metals (Figure 201).

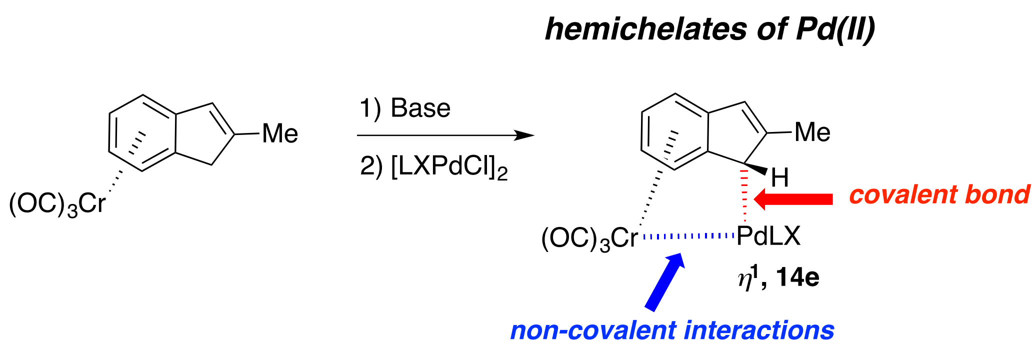

5a **7, 12**

Figure 201: Formation of *hemichelates* of group 10 transition metals.

2 - Purpose.

The present chapter discloses the first extension of the concept of *hemichelation* to Rh(I) centres with a hemichelating ambiphilic anionic ligand of electronic properties chosen so as to promote structural cohesion by non-covalent inter-metallic interactions. Indeed, by appropriate tuning of the electronic properties of the ambiphilic ligand, new truly coordination-unsaturated Rh(I) complexes can be synthesized in a manageable form.

3 - First approach.

From the experience acquired with the stabilization of Pd(II) and Pt(II) hemichelates, the anion derived from **5a** looked promising because of the slight steric hindrance of the methyl group at the 2 position which could purportedly orient the coordination of the Rh(I) centre in a *syn*-facial manner so as to give exclusively the formation of a η^1-bonded Rh hemichelate (Figure 202).

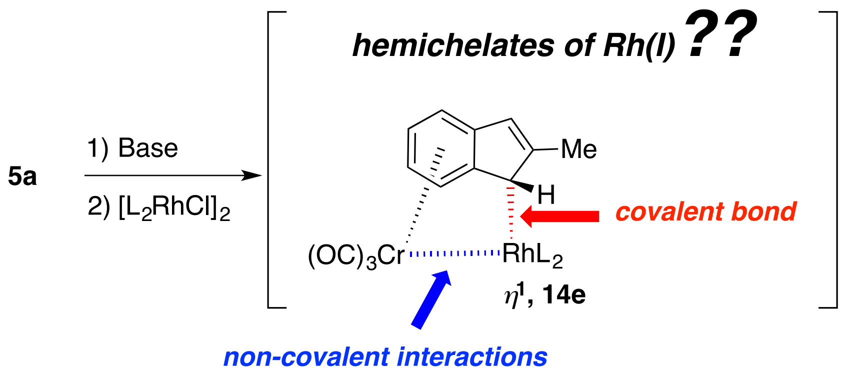

Figure 202: Expected formation of Rh(I) hemichelation by using **5a** as an heteroditopic ligand.

In fact the reaction of the anion of **5a** with $[Rh(cod)Cl]_2$,[1003] $[Rh(nbd)Cl]_2$[1004] and $[Rh(CO)_2Cl]_2$[1005] (Figure 203) produced compounds akin to those already reported by Ceccon et *al.* in several reports.[1006-1011]

[1003] [N°842] Giordano, G.; Crabtree, R. H. *Inorg. Synth.* **1990**, *28*, 88.

[1004] [N°843] Abel, E. W.; Bennett, M. A.; Wilkinson, G. *J. Chem. Soc. A* **1959**, 3178.

[1005] [N°844] Hanh Nguyen, D.; Lassauque, N.; Vendier, L.; Mallet-Ladeira, S.; Le Berre, C.; Serp, P.; Kalck, P. *Eur. J. Inorg. Chem.* **2014**, *2014*, 326.

[1006] [N°845] Bonifaci, C.; Ceccon, A.; Gambaro, A.; Ganis, P.; Santi, S.; Valle, G.; Venzo, A. *J. Organomet. Chem.* **1995**, *492*, 35.

[1007] [N°560] Bonifaci, C.; Ceccon, A.; Santi, S.; Mealli, C.; Zoellner, R. W. *Inorg Chim Acta* **1995**, *240*, 541.

[1008] [N°573] Bonifaci, C.; Ceccon, A.; Gambaro, A.; Ganis, P.; Santi, S.; Venzo, A. *Organometallics* **1995**, *14*, 2430.

[1009] [N°846] Ceccon, A.; Elsevier, C. J.; Ernsting, J. M.; Gambaro, A.; Santi, S.; Venzo, A. *Inorg. Chim. Acta* **1993**, *204*, 15.

[1010] [N°574] Bonifaci, C.; Ceccon, A.; Gambaro, A.; Ganis, P.; Santi, S.; Valle, G.; Venzo, A. *Organometallics* **1993**, *12*, 4211.

[1011] [N°575] Ceccon, A.; Gambaro, A.; Santi, S.; Valle, G.; Venzo, A. *J. Chem. Soc., Chem. Commun.* **1989**, 51.

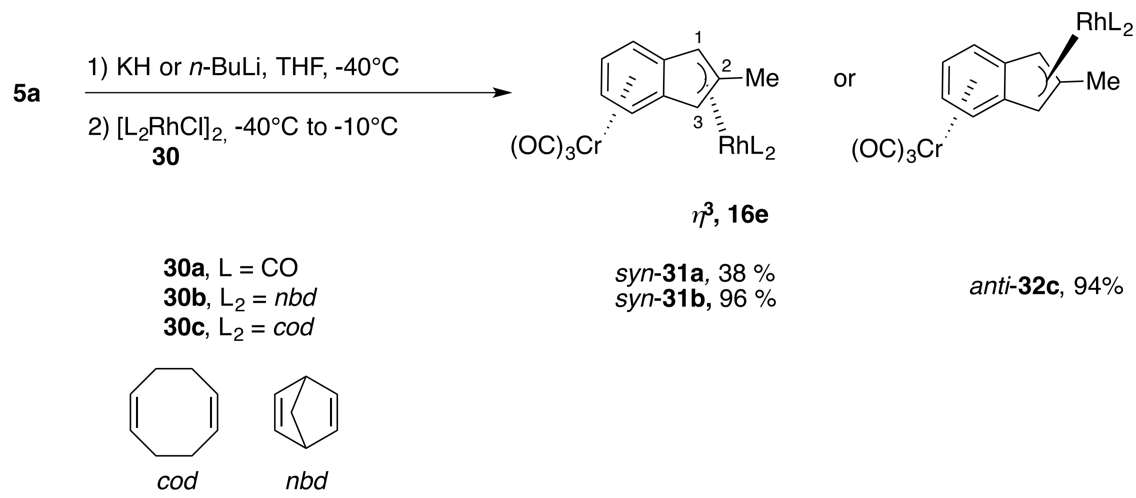

Figure 203: First approach for the synthesis of Rh(I) hemichelates.

These compounds, namely *syn*-**31a**, *syn*-**31b** and *anti*-**32c** (Figure 203) were isolated pure and structurally characterized by X-ray diffraction analysis.

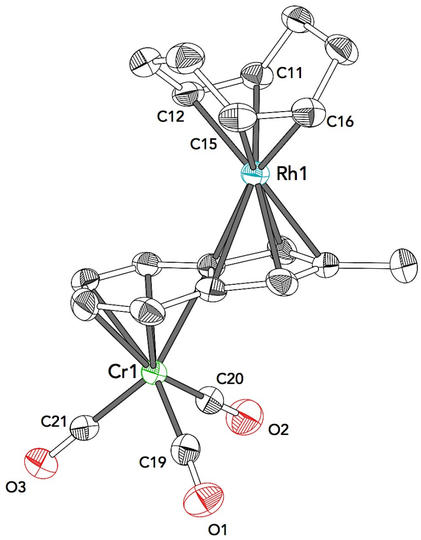

Compound *anti*-**32c**
Space Group: **P -1**
R-Factor (%): **3.99**

N°	A	B	C	Lengths (Å)	Angles (°)
1	Rh_1	C_{11}	-	2.170(3)	-
2	Rh_1	C_{12}	-	2.137(4)	-
3	Rh_1	C_{15}	-	2.140(3)	-
4	Rh_1	C_{16}	-	2.106(3)	-
5	Rh_1	C_1	-	2.377(4)	-
6	Rh_1	C_6	-	2.334(3)	-
7	Rh_1	C_7	-	2.248(3)	-
8	Rh_1	C_8	-	2.276(3)	-
9	Rh_1	C_9	-	2.223(4)	-
10	Cr_1	C_{19}	-	1.838(4)	-
11	Cr_1	C_{20}	-	1.841(3)	-
12	Cr_1	C_{21}	-	1.827(3)	-
13	C_{19}	O_1	-	1.152(5)	-
14	C_{20}	O_2	-	1.155(3)	-
15	C_{21}	O_3	-	1.159(4)	-
16	Cr_1	C_{19}	O_1	-	176.8(3)
17	Cr_1	C_{20}	O_2	-	179.6(3)
18	Cr_1	C_{21}	O_3	-	178.8(3)
19	C_{19}	Cr_1	C_{20}	-	87.3(1)

Figure 204: X-ray structure and selected interatomic distances of compound *anti*-**32c**.

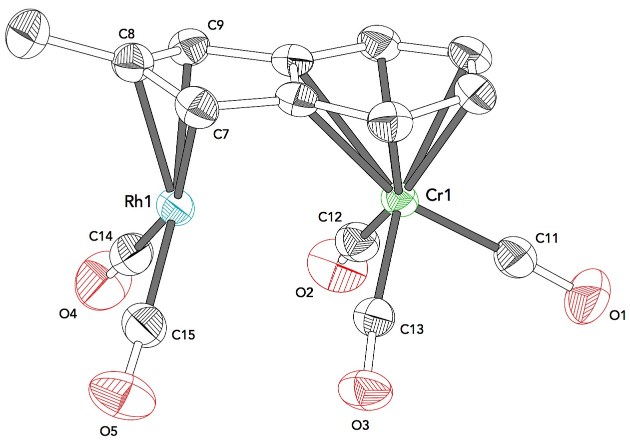

Compound *syn*-**31a**
Space Group: **P 2_1/c**
R-Factor (%): **1.89**

N°	*A*	*B*	*C*	*Lengths (Å)*	*Angles (°)*
1	Rh_1	Cr_1	-	3.0641(5)	
2	Rh_1	C_7	-	2.210(2)	-
3	Rh_1	C_8	-	2.191(2)	-
4	Rh_1	C_9	-	2.221(1)	-
5	Rh_1	C_{14}	-	1.882(2)	-
6	Rh_1	C_{15}	-	1.879(2)	-
7	Rh_1	C_{12}	-	3.130(2)	-
8	Rh_1	C_{13}	-	3.171(2)	-
9	C_{14}	O_4	-	1.132(3)	-
10	C_{15}	O_5	-	1.135(2)	-
11	Cr_1	C_{11}	-	1.821(2)	-
12	Cr_1	C_{12}	-	1.854(2)	-
13	Cr_1	C_{13}	-	1.853(1)	-
14	C_{11}	O_1	-	1.155(2)	-
15	C_{12}	O_2	-	1.156(2)	-
16	C_{13}	O_3	-	1.152(2)	-
17	Rh_1	C_{14}	O_4	-	178.2(2)
18	Rh_1	C_{15}	O_5	-	177.8(2)
19	Cr_1	C_{11}	O_1	-	178.0(1)
20	Cr_1	C_{12}	O_2	-	174.8(1)
21	Cr_1	C_{13}	O_3	-	175.0(1)
22	C_{12}	Cr_1	C_{13}	-	95.16(7)
23	C_{14}	Rh_1	C_{15}	-	92.42(8)

Figure 205: X-ray structure and selected interatomic distances of compound *syn*-**31a**.

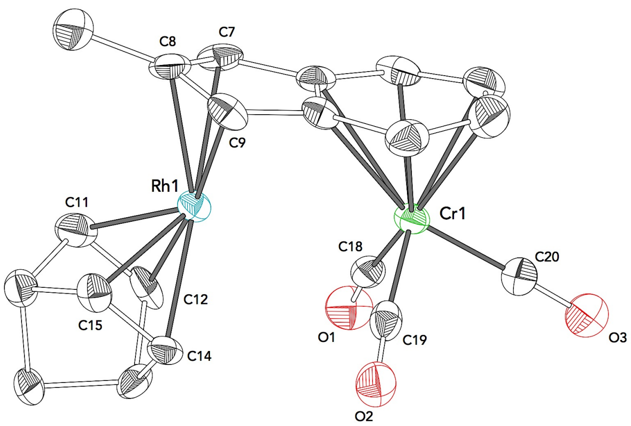

Compound *syn*-**31b**
Space Group: **C 2/c**
R-Factor (%): **4.82**

N°	*A*	*B*	*C*	*Lengths (Å)*	*Angles (°)*
1	Rh_1	Cr_1	-	3.156(1)	-
2	Rh_1	C_7	-	2.223(8)	-
3	Rh_1	C_8	-	2.190(8)	-
4	Rh_1	C_9	-	2.248(9)	-
5	Rh_1	C_{11}	-	2.104(7)	-
6	Rh_1	C_{12}	-	2.155(8)	-
7	Rh_1	C_{14}	-	2.173(7)	-
8	Rh_1	C_{15}	-	2.126(6)	-
9	Rh_1	C_{18}	-	3.196(7)	-
10	Rh_1	C_{19}	-	3.341(5)	-
11	Cr_1	C_{18}	-	1.855(7)	-
12	Cr_1	C_{19}	-	1.840(7)	-
13	Cr_1	C_{20}	-	1.820(6)	-
14	C_{18}	O_1	-	1.160(9)	-
17	C_{19}	O_2	-	1.158(8)	-
18	C_{20}	O_3	-	1.160(8)	-
19	Cr_1	C_{18}	O_1	-	173.5(6)
20	Cr_1	C_{19}	O_2	-	175.0(6)
21	Cr_1	C_{20}	O_3	-	178.5(6)
22	C_{18}	Cr_1	C_{19}	-	94.0(3)

Figure 206: X-ray structure and selected interatomic distances of compound *syn*-**31b**.

In *anti*-**32c** (Figure 204), the bulky [Rh(cod)] fragment was found to bind in an *anti*-facial manner, whereas in *syn*-**31a** (Figure 205) and *syn*-**31b** (Figure 206) the respective [Rh(CO)$_2$] and [Rh(nbd)] fragments where found to bind in a *syn*-facial manner (Figure 203). In the latter two cases, the Rh(I) centre (16 electrons) was found to bind in a η^3 mode to the 1,2,3 positions of the indenyl, quite not in the expected hemichelation η^1 bonding mode. In *anti*-**32c** the Rh(I) centre (formally 18 electrons) was clearly engaged in a dissymmetric η^2: η^3 coordination mode with the 5-membered ring (Figure 203). Ceccon and coworkers[1012-1016] demonstrated indeed that, with a similar anion prepared from tricarbonyl(η^6-indene)chromium, reactions of [RhL$_2$Cl]$_2$ complexes would lead under thermodynamic control to the *syn*-facial η^3 coordination of the Rh centre to the 5-membered ring when the L$_2$ moiety operates limited steric hindrance (Figure 207).

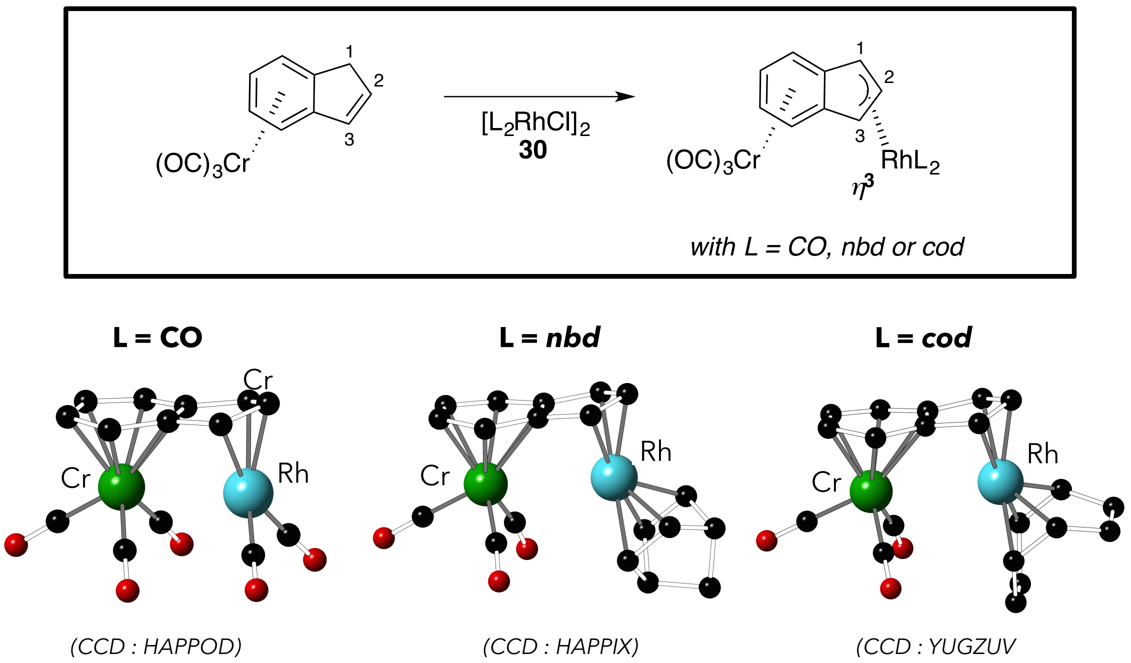

Figure 207: Ceccon and coworkers demonstrated the *syn*-facial selectivity and η^3 coordination mode of the metal centre for some analogues.

[1012] [N°845] Bonifaci, C.; Ceccon, A.; Gambaro, A.; Ganis, P.; Santi, S.; Valle, G.; Venzo, A. *J. Organomet. Chem.* **1995**, *492*, 35.

[1013] [N°560] Bonifaci, C.; Ceccon, A.; Santi, S.; Mealli, C.; Zoellner, R. W. *Inorg Chim Acta* **1995**, *240*, 541.

[1014] [N°573] Bonifaci, C.; Ceccon, A.; Gambaro, A.; Ganis, P.; Santi, S.; Venzo, A. *Organometallics* **1995**, *14*, 2430.

[1015] [N°846] Ceccon, A.; Elsevier, C. J.; Ernsting, J. M.; Gambaro, A.; Santi, S.; Venzo, A. *Inorg. Chim. Acta* **1993**, *204*, 15.

[1016] [N°574] Bonifaci, C.; Ceccon, A.; Gambaro, A.; Ganis, P.; Santi, S.; Valle, G.; Venzo, A. *Organometallics* **1993**, *12*, 4211.

Worthy to note that a slight modification of the experimental conditions (replacement of the THF with diethyl ether as solvent, Figure 208) led to the formation of a Rh (III) dimer where the $RhCO_2$ fragment was found to be bound at the indenyl benzylic position in an *anti*-facial manner (namely *anti*-**32b**), with a bridging carbonyl group (IR typical band located at 1712 cm^{-1}) between the two metal centres. This compound, resulting from an oxidation of the rhodium (Rh(I) to Rh(III)) under these conditions, was found to be highly reactive, generally decomposing within an hour in solution at room temperature into **5a** and other untraceable subspecies.

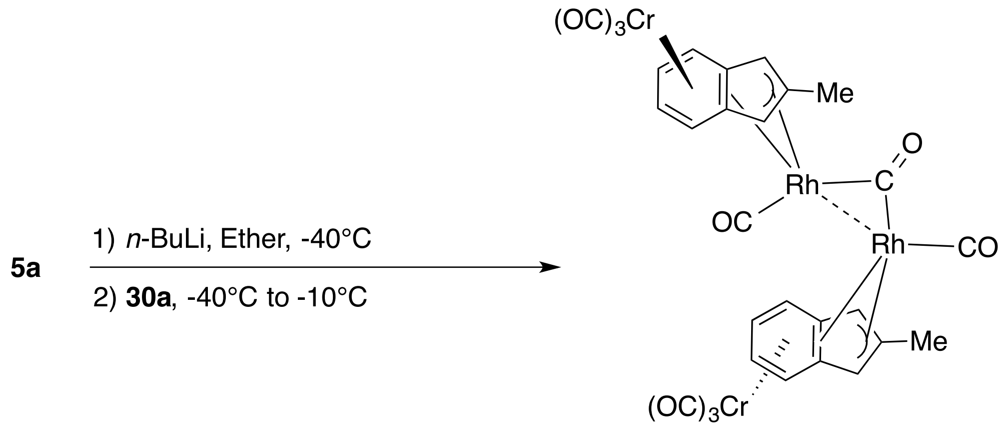

anti-**32a**, 27%

Figure 208: Formation of *anti*-**32a** after a slight modification of the experimental conditions.

Nevertheless, this compound was fully characterized, especially by means of X-ray diffraction analysis (Figure 209). The Rh(III) centre (formally 18 electrons) was found, very similarly to *anti*-**32c,** engaged in a dissymmetric η^2: η^3 coordination mode with the 5-membered ring.

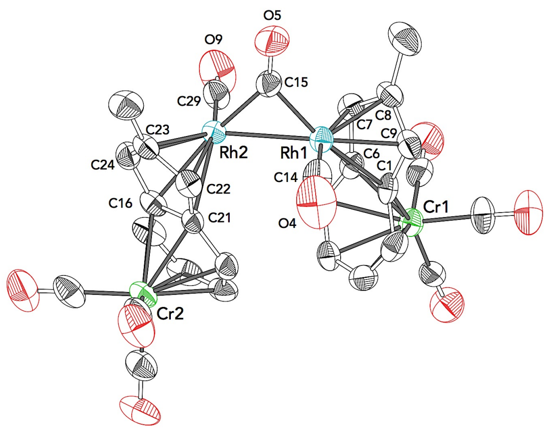

Compound *anti*-**32a**
Space Group: **P 2$_1$/c**
R-Factor (%): **5.73**

N°	*A*	*B*	*C*	*Lengths (Å)*	*Angles (°)*
1	Rh$_1$	Rh$_2$	-	2.6756(7)	-
2	Rh$_1$	C$_1$	-	2.372(6)	-
3	Rh$_1$	C$_6$	-	2.406(6)	-
4	Rh$_1$	C$_7$	-	2.243(6)	-
5	Rh$_1$	C$_8$	-	2.245(6)	-
6	Rh$_1$	C$_9$	-	2.219(6)	-
7	Rh$_1$	C$_{14}$	-	1.866(8)	-
8	Rh$_1$	C$_{15}$	-	1.991(7)	-
9	Rh$_2$	C$_{16}$	-	2.344(6)	-
10	Rh$_2$	C$_{21}$	-	2.356(6)	-
11	Rh$_2$	C$_{22}$	-	2.257(6)	-
12	Rh$_2$	C$_{23}$	-	2.288(5)	-
13	Rh$_2$	C$_{24}$	-	2.220(6)	-
14	Rh$_2$	C$_{15}$	-	1.971(7)	-
15	Rh$_2$	C$_{29}$	-	1.855(6)	-
16	C$_{14}$	O$_4$	-	1.133(9)	-
17	C$_{15}$	O$_5$	-	1.177(9)	-
18	C$_{29}$	O$_9$	-	1.140(8)	-
19	Rh$_1$	C$_{15}$	Rh$_2$	-	85.0(3)
20	Rh$_1$	C$_{14}$	O$_4$	-	176.8(7)
21	Rh$_1$	C$_{15}$	O$_5$	-	135.3(6)
22	Rh$_2$	C$_{29}$	O$_9$	-	178.2(6)
23	Rh$_2$	C$_{15}$	O$_5$	-	139.8(6)

Figure 209: X-ray structure and selected interatomic distances of compound *anti*-**32a**.

As has already been pointed out, the thermodynamic preference for the *syn*-facial products over the *anti*-facial ones was recently rationalized by Grimme *et al.*[1017] as a direct consequence of the attractive stabilizing and driving effects of electron correlation and dispersion force acting between the $Cr(CO)_3$ moiety and the η^3-bonded RhL_2 fragment (Figure 210).

Figure 210: Investigation by Grimme *et al.*[137] of the differences in intrafragment (diagonalentries) and interfragment (off-diagonal entries) correlation energies (kcal.mol^{-1}) between *syn*-bimetallic and *anti*-bimetallic at the SCS-MP2 level © American Chemical Society. *(Figure removed because subjected to copyright).*

[1017] [N°562] Schwabe, T.; Grimme, S.; Djukic, J.-P. *J. Am. Chem. Soc.* **2009**, *131*, 14156.

Keeping in perspective the synthesis of Rh(I) 14 electron hemichelates, it became clear that the electronic properties of the ambiphilic ligand had to be tuned in order to preclude completely the possibility of a η^3 coordination of the Rh centre, this without compromising the *syn*-facial selectivity of the binding of the [RhL_2] fragment. In other words, the structure of the ambiphilic ligand had to be changed so as to leave no other choice to the Rh(I) but to form a *hemichelate*.

4 - New approach.

It was found that the most promising way to achieve this goal was by using a parent of **5a** containing a fluorenyl motive instead of the indenyl.[1018] Like shown in (Figure 163), analysis of the partial natural charges (Natural Population Analysis)[1019] of singlet ground state geometries of **5a**, **15a** and **18a** (throughout this computed models were optimized at the ZORA-TPSS[1020]-D3(BJ)[1021] / all electron TZP level) indicates that the strongest depletion of charge density at the aromatic carbons at the 2,3 positions occurs with **18a**. This depletion is a necessary condition to prevent a η^3 bonding mode to the Rh(I) centre, which therefore made **18a** a reasonable candidate for attempting the synthesis of Rh(I) hemichelates.

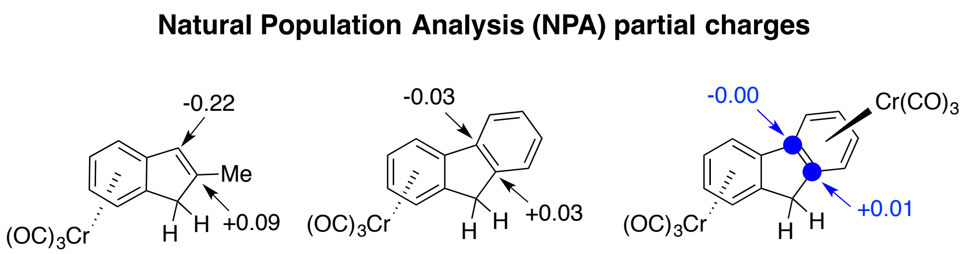

5a **15a** **18a**

Figure 211: Natural partial charges (NPA) at C_2 and C_3 positions in **5a**, **15a** and **18a** computed from gas phase singlet ground state geometries optimized at the ZORA-TPSS-D3(BJ)/all electron TZP level.

[1018] [N°847] Werlé, C.; Bailly, C.; Karmazin-Brelot, L.; Le Goff, X.-F.; Pfeffer, M.; Djukic, J.-P. *Angew. Chem. Int. Ed. Engl.* **2014**, *53*, 9827.

[1019] [N°813] Weinhold, F.; Landis, C. R. *Valency and Bonding, a Natural Bond Orbital Donor-Acceptor Perspective*; University Press: Cambridge, UK, **2005**.

[1020] [N°743] Tao, J.; Perdew, J. P.; Staroverov, V. N.; Scuseria, G. E. *Phys. Rev. Lett.* **2003**, *91*, 146401.

[1021] [N°187] Grimme, S.; Ehrlich, S.; Goerigk, L. *J. Comput. Chem.* **2011**, *32*, 1456.

Complex **18a**[1022] was readily synthesized and isolated in 50 % yield as the major product of the thermolysis of excess $Cr(CO)_6$ in the presence of fluorene and catalytic amounts of naphthalene in a refluxing 1:10 mixture of THF and di-*n*-butylether for *ca.* 6 days. Complex **18a** was subsequently deprotonated by reaction with *n*-BuLi at a subambient temperature and reacted in two separate experiments with $[Rh(CO)_2Cl]_2$ and $[Rh(nbd)Cl]_2$ yielding single products, respectively *syn*-**33a** and *syn*-**33b** (Figure 212).

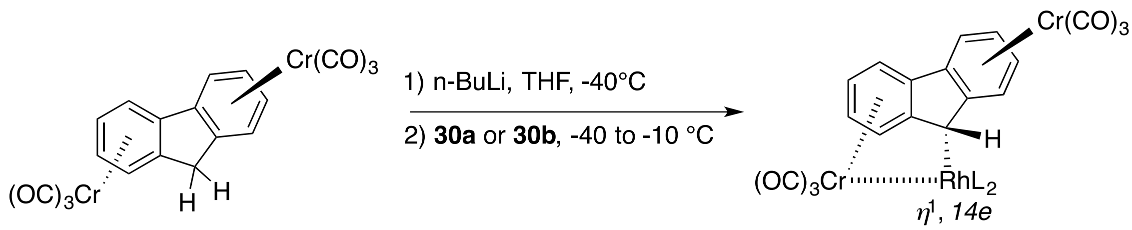

18a

syn-**33a**, 30%, L= *CO*
syn-**33b**, 70%, L_2= *nbd*

Figure 212: Formation of hemichelates *syn*-**33a** and *syn*-**33b** by sequential deprotonation and metalation of the benzylic position of **18a**.

Those two complexes proved to be unstable in solution at room temperature and to generally decompose into **18a** and untraceable material. Isolation of the products was however possible by repeated recrystallizations at temperatures around -20 °C. Analyses by ^{13}C and ^{1}H NMR spectroscopy were therefore carried out below -20 °C in dry [D_8]toluene or [D]chloroform. The most notable ^{13}C NMR spectral feature common to *syn*-**33a** and *syn*-**33b** is the signature of the $Cr(CO)_3$ moiety proximal to Rh, which appears as three broad signals of low intensity at *ca.* 234.4, 233.7 and 227.1 ppm (Figure 213). In the case of *syn*-**33a**, the $Rh(CO)_2$ moiety resonates as two distinct signals in the ^{13}C NMR spectrum, *i.e.* a broad signal at 182.6 ppm and a well resolved doublet at 191.6 ppm displaying a Rh-C_{CO} coupling constant of 69 Hz, which suggests that the $Rh(CO)_2$ moiety undergoes a fast rotational exchange around the Rh-$C_{benzylic}$ axis producing a time-averaged signal for the equatorial Rh-bound carbonyl ligand and a fine doublet for the axial Rh-bound CO ligand (Figure 213). Quite notable is also the

[1022] [N°848] Ceccon, A.; Gambaro, A.; Venzo, A.; Lucchini, V.; Bitterwolf, T. E.; Shade, J. *J. Organomet. Chem.* **1988**, *349*, 315.

^{13}C NMR response of the benzylic CH fragment at 37.3 and 26.3 ppm for *syn*-**33a** and *syn*-**33b** respectively (Figure 213): with both complexes, this signal is a doublet of scalar ^{1}H-^{103}Rh coupling constant amounting to *ca.* 1.5 Hz. The ^{13}C signal arising from this fragment with *syn*-**33b** is a resolved doublet ($J_{H\text{-}Rh}$= 15 Hz) whereas with *syn*-**33a** it is a broad and barely resolved doublet ($J_{H\text{-}Rh}$= 6.9 Hz), which supports the assumption of a conformational exchange of the $Rh(CO)_2$ moiety.

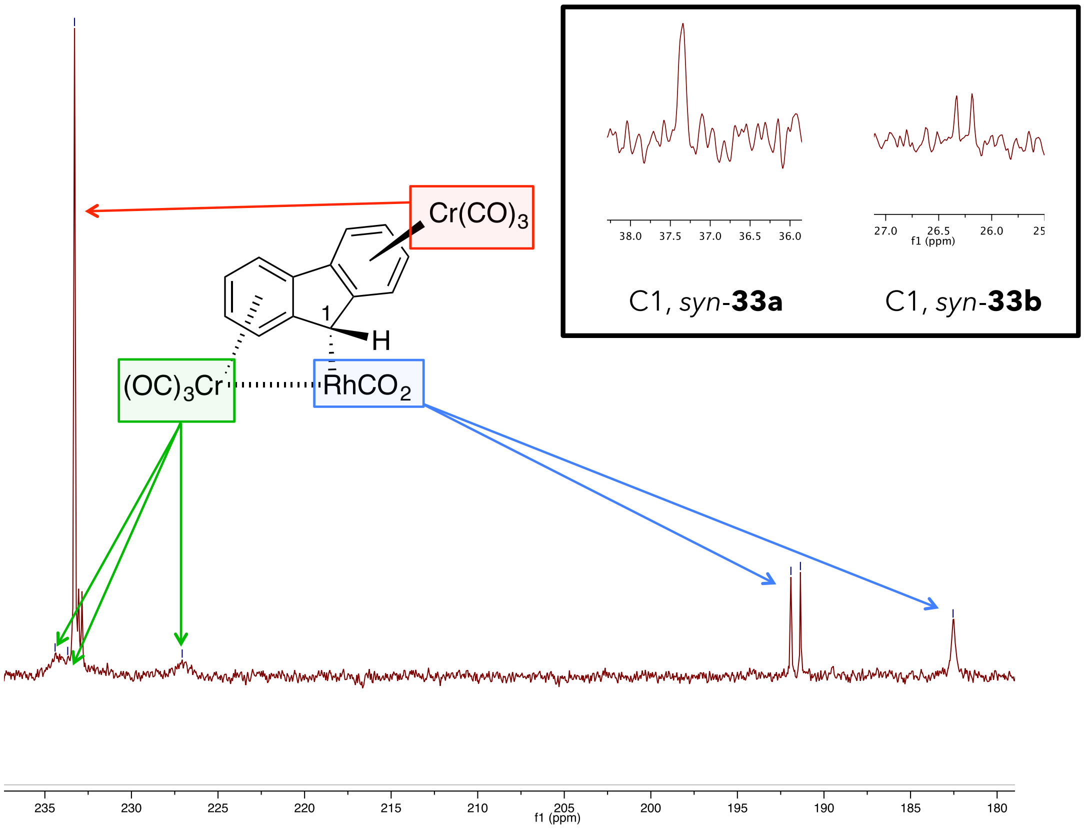

Figure 213: Most notable ^{13}C NMR spectral features for the Rh(I) hemichelates.

The structures of *syn*-**33a** and *syn*-**33b** (Figure 214, Figure 215) were resolved by X-ray diffraction analyses of crystals grown at -20°C.

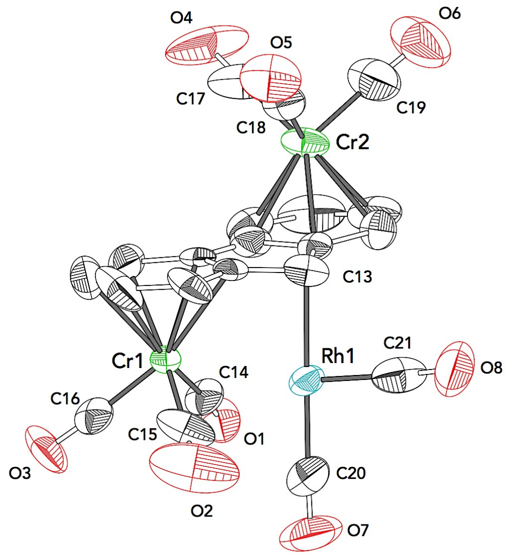

Compound *syn*-**33a**
Space Group: **P 2_1**
R-Factor (%): **9.97**

N°	A	B	C	Lengths (Å)	Angles (°)
1	Rh_1	Cr_1	-	2.802(3)	-
2	Rh_1	C_{13}	-	2.16(2)	-
3	Rh_1	C_{20}	-	1.88(3)	-
4	Rh_1	C_{21}	-	1.86(3)	-
5	Rh_1	C_{14}	-	2.64(2)	-
6	Rh_1	C_{15}	-	2.76(3)	-
7	C_{20}	O_7	-	1.13(5)	-
8	C_{21}	O_8	-	1.13(4)	-
9	Cr_1	C_{14}	-	1.82(2)	-
10	Cr_1	C_{15}	-	1.88(4)	-
11	Cr_1	C_{16}	-	1.83(2)	-
12	C_{14}	O_1	-	1.21(3)	-
13	C_{15}	O_2	-	1.15(5)	-
14	C_{16}	O_3	-	1.16(3)	-
15	Rh_1	C_{20}	O_7	-	177(3)
16	Rh_1	C_{21}	O_8	-	176(3)
17	Cr_1	C_{14}	O_1	-	170(2)
18	Cr_1	C_{15}	O_2	-	175(3)
19	Cr_1	C_{16}	O_3	-	177(2)
20	C_{14}	Cr_1	C_{15}	-	100(1)

Figure 214: X-ray structure and selected interatomic distances of compound *syn*-**33a**.

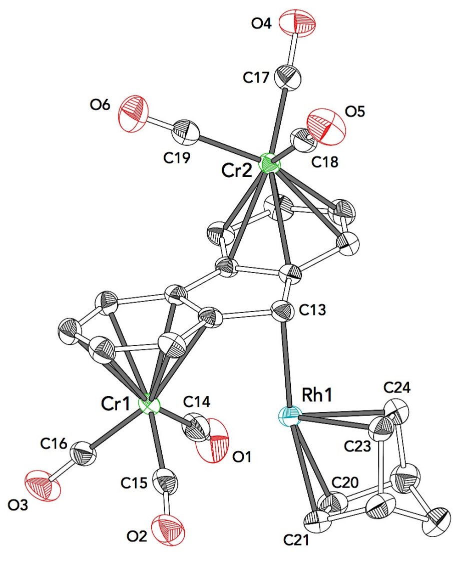

Compound *syn*-**33b**
Space Group: **P -1**
R-Factor (%): **2.06**

N°	A	B	C	Lengths (Å)	Angles (°)
1	Rh_1	Cr_1	-	2.8238(3)	-
2	Rh_1	C_{13}	-	2.172(1)	-
3	Rh_1	C_{14}	-	2.506(2)	
4	Rh_1	C_{15}	-	2.954(2)	
5	Rh_1	C_{20}	-	2.198(1)	-
6	Rh_1	C_{21}	-	2.195(2)	-
7	Rh_1	C_{23}	-	2.113(2)	-
8	Rh_1	C_{24}	-	2.126(2)	-
9	Cr_1	C_{14}	-	1.871(1)	-
10	Cr_1	C_{15}	-	1.849(2)	-
11	Cr_1	C_{16}	-	1.838(2)	-
12	C_{14}	O_1	-	1.158(2)	-
16	C_{15}	O_2	-	1.155(2)	-
17	C_{16}	O_3	-	1.149(2)	-
21	Cr_1	C_{14}	O_1	-	166.1(1)
22	Cr_1	C_{15}	O_2	-	173.0(1)
23	Cr_1	C_{16}	O_3	-	178.3(1)
24	C_{14}	Cr_1	C_{15}	-	98.24(7)

Figure 215: X-ray structure and selected interatomic distances of compound *syn*-**33b**.

In both cases, the [RhL_2] fragment is η^1-bonded to the fluorenyl ligand at the benzylic carbon and the Rh atom is distant by *ca.* 2.81 Å from the Cr centre, *i.e.* about the sum of van der Waals radii for the two metals.[1023] In both cases, the $Cr(CO)_3$ group proximal to the RhL_2 moiety is only slightly distorted and adopts an anti-eclipsed conformation with respect to the benzylic position materialized by atom C_{13} (Figure 214).

5 - Theoretical aspects.

Theoretical analysis of the Rh-$C_{benzylic}$ bond in models *syn*-**33a** (*wbi*= 0.31) and *syn*-**33b** (*wbi*= 0.37) by the Natural Bond Orbital method[1024] points to a coordinative *s* bond wherein the partially negatively charged carbon atom (NPA $qC_{benzylic}$~ -0.42) contributes by an orbital hybridization of marked *p* character (sp^8 in *syn*-**33a** and *syn*-**33b,** bonding orbital population ~1.7 electron) to the bond with Rh.

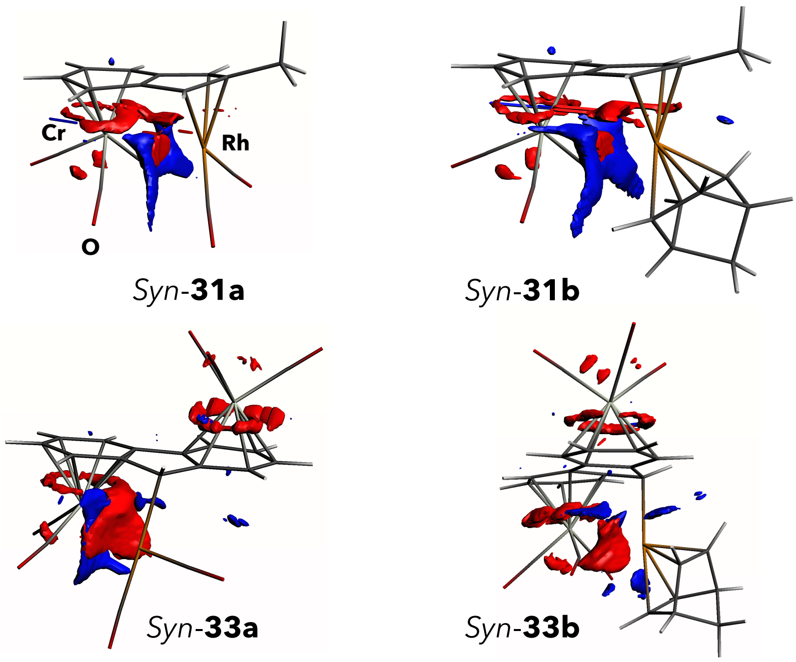

Figure 216: Plots of non-covalent interaction (NCI) regions materialized by *reduced density gradient* isosurfaces (cut-off value *s*= 0.02 a.u., ρ=0.05 a.u.) coloured according to the sign of the signed density $\lambda_2\rho$ for gas-phase relaxed singlet ground state models of Rh-containing complexes *syn*-**31a**, *syn*-**31b**, *syn*-**33a** and *syn*-**33b**; red and blue colours are associated to negatively (attractive) and positively (repulsive) signed terms respectively.

[1023] [N°849] Bondi, A. *J. Phys. Chem.* **1964**, *68*, 441.

[1024] [N°813] Weinhold, F.; Landis, C. R. *Valency and Bonding, a Natural Bond Orbital Donor-Acceptor Perspective*; University Press: Cambridge, UK, **2005**.

Further analysis of *syn*-**33a** and *syn*-**33b** by Yang's treatment of the reduced density gradient, which reveals the spatial distribution of intimate non-covalent interactions (NCI),[1025, 1026] indicates that the [RhL_2] fragments interact with the neighbouring $Cr(CO)_3$ moiety through attractive non-covalent interactions (red-coloured isosurfaces, Figure 216).

Analysis of the topology of the electron density by the theory of Atoms In Molecule (AIM)[1027] reveals a *bond critical point* (3, -1) (BCP) for the Cr-Rh segment in *syn*-**33a** of low electron density *r* amounting to 0.04 a.u. (Figure 217 and Figure 218). In the case of *syn*-**33b,** no BCP is found in the Cr-Rh segment (Figure 217 and Figure 218).

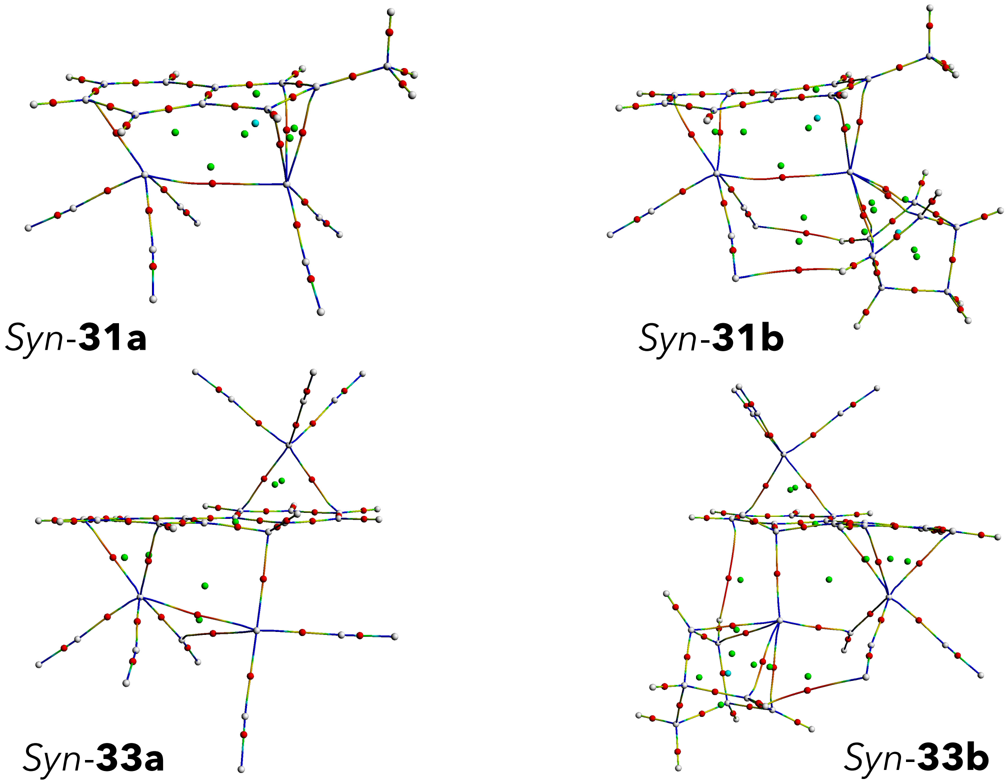

Figure 217: Atom-in-molecules analysis of the electron density topology for *syn*-**31a**, *syn*-**31b**, *syn*-**33a** and *syn*-**33b**. Red and green dots are associated to Bond (BCP) and Ring (RCP) Critical Points respectively. Grey spheres materialize the atomic critical points scaled by the associated density.

[1025] [N°629] Contreras-García, J.; Johnson, E. R.; Keinan, S.; Chaudret, R.; Piquemal, J.-P.; Beratan, D. N.; Yang, W. *J. Chem. Theory Comput.* **2011**, *7*, 625.

[1026] [N°630] Johnson, E. R.; Keinan, S.; Mori-Sánchez, P.; Contreras-García, J.; Cohen, A. J.; Yang, W. *J. Am. Chem. Soc.* **2010**, *132*, 6498.

[1027] [N°755] Bader, R. F. W. In *Atoms in Molecules: A Quantum Theory*; Clarendon: Oxford, **1990**.

It is generally considered that *r* values of a magnitude of 10^{-2} au and negative values of the laplacian $-¼\nabla^2\rho$ at a BCP are associated with closed-shell interactions, *i.e.* van der Waals type of non-covalent interactions.[1028] This is well exemplified by the *r* values at BCP for models *syn*-**31a** and *syn*-**31b** (Figure 218) for which it is evident, from NCI plots (Figure 216), that the metal-metal interaction is non-covalently attractive.[1029]

parameters	*syn*-***31a***	*syn*-***31b***	*syn*-***33a***	*syn*-***33b***
d(Cr-Rh) (Å)	3.062	3.135	2.776	2.679
d(Rh-$C_{benzylic}$) (Å)	2.231[a]	2.254[a]	2.213	2.203
q(Cr)[b]	-0.82	-0.80	-0.81	-0.80
q(Rh)[b]	+0.22	+0.53	+0.10	+0.44
$\Delta\Delta E_{int}$($Cr(CO)_3$…fragmt)[c] (kcal/mol)	-6.0	-12.5	-37.9	-40.0
ρ (3,-1; Cr-Rh) (au)[d]	0.0245	0.0214	0.0403	no BCP
$-¼\nabla^2\rho$ (3,-1; Cr-Rh) (au)[d]	-0.0080	-0.0083	-0.0113	-
wbi(Cr-Rh)[e]	0.05	0.06	0.14	0.18

[a] averaged value. [b] from Natural Population Analysis. [c] ΔE_{int}($Cr(CO)_3$…fragment) for **5a**= -73.9 kcal/mol, ΔE_{int}($Cr(CO)_3$…fragment) for **18a**= -72.1 kcal/mol; $\Delta\Delta E_{int}(Cr(CO)_3…fragment)_i = \Delta E_{int}(Cr(CO)_3…fragment)_i - \Delta E_{int}(Cr(CO)_3…fragment)_{ref}$. [d] the density ρ and the Laplacian of the density $\nabla^2\rho$ at BCP (3,-1) were computed with Bader's AIM method. [e] Wiberg's bond indice.[1030]

Figure 218: Selected structural and electronic information on gas phase singlet ground state model structures of *syn*-**31a**, *syn*-**31b**, *syn*-**33a** and *syn*-**33b**.

ETS-NOCV analyses of the interaction of the prepared $Cr(CO)_3$ moiety with the remaining organo-rhodium entity in *syn*-**33a** and *syn*-**33b** rationalize the slight shift of *ca.* 9 cm^{-1} to higher frequencies of the vibrational IR C-O stretching bands of the $Cr(CO)_3$ moiety in *syn*-**33a** and *syn*-**33b** as compared to reference compound **18a**.

[1028] [N°754] Popelier, P. *Atoms in Molecules, An Introduction*; Prentice Hall, Harlow, England, **2000**.

[1029] [N°630] Johnson, E. R.; Keinan, S.; Mori-Sánchez, P.; Contreras-García, J.; Cohen, A. J.; Yang, W. *J. Am. Chem. Soc.* **2010**, *132*, 6498.

[1030] [N°850] Wiberg, K. B. *Tetrahedron Lett.* **1968**, *24*, 1083.

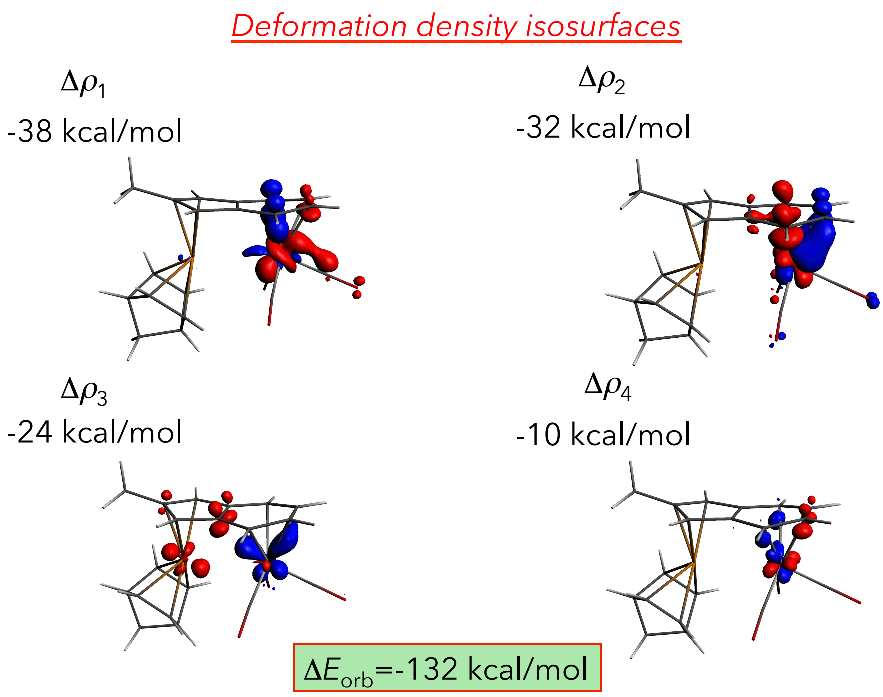

Figure 219: ETS-NOCV deformation densities $\Delta\rho$ and the associated orbital interaction energies for the interaction of prepared $Cr(CO)_3$ with the Rh-fluorenyl fragment of *syn*-**31a** and *syn*-**31b**. Red and blue-colored isosurfaces materialize regions where charge density depletion and build up occur respectively upon interaction of the two considered prepared fragments: electron density transfer operates from red-coloured areas to blue ones upon bonding. Density isosurface contour = 0.005 e/bohr^3.

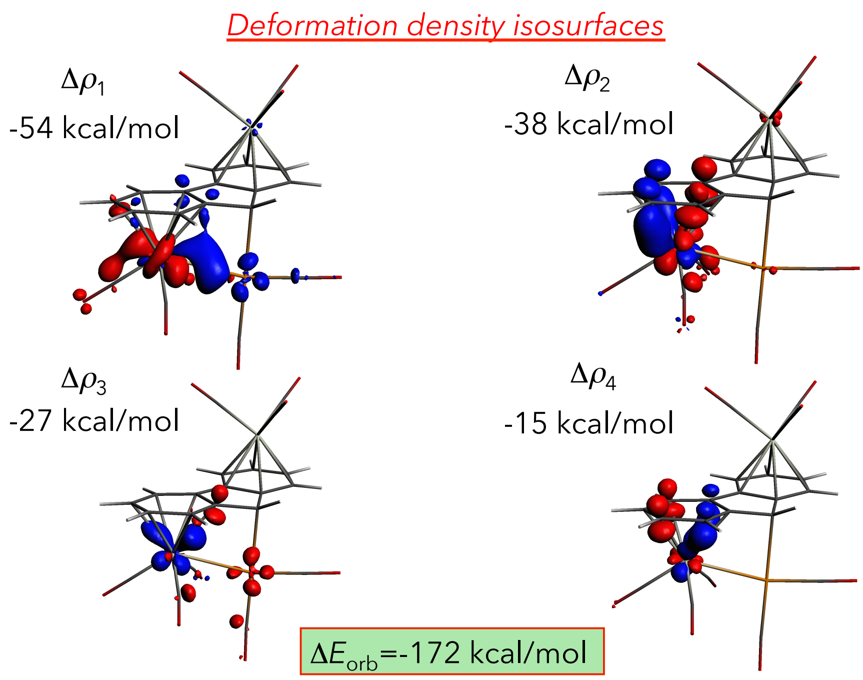

Figure 220: ETS-NOCV deformation densities $\Delta\rho$ and the associated orbital interaction energies for the interaction of prepared $Cr(CO)_3$ with the Rh-fluorenyl fragment of *syn*-**33a** and *syn*-**33b**. Red and blue-colored isosurfaces materialize regions where charge density depletion and build up occur respectively upon interaction of the two considered prepared fragments: electron density transfer operates from red-coloured areas to blue ones upon bonding. Density isosurface contour = 0.005 e/bohr^3.

Deformation density plot $\Delta\rho_1$ (Figure 220) indicates that in *syn*-**33a** a portion of electron density is transferred from the Cr(CO)$_3$ fragment towards the intermetallic space and the Rh centre with minor backdonation contribution from the Rh to the Cr center ($\Delta\rho_3$, Figure 220). This suggests that in the Rh-hemichelates reported herewith some Cr→Rh donor-acceptor character residually exists, which slighly dominates the Rh→Cr backdonation. Natural partial charges[1031] (NPA) at Rh and Cr outline the key role of the attractive coulombic contribution to the stabilization of *syn*-**33a** and *syn*-**33b**, which receives also the support of favorable dispersion and orbital interaction energy terms in the compensation of Pauli repulsion. This is illustrated by a larger difference in inter-fragment interaction energy $\Delta\Delta E_{int}$ for *syn*-**33a** and *syn*-**33b** (**18a** is the reference) than for *syn*-**31a** and *syn*-**31b** (**5a** is the reference); $\Delta\Delta E_{int}$ is used here as a measure of the energetic structural cohesion of a given complex with respect to a structure-related reference for a pertinent fragment interaction scheme (here the (CO)$_3$Cr-to-arene bonding, see Figure 221).

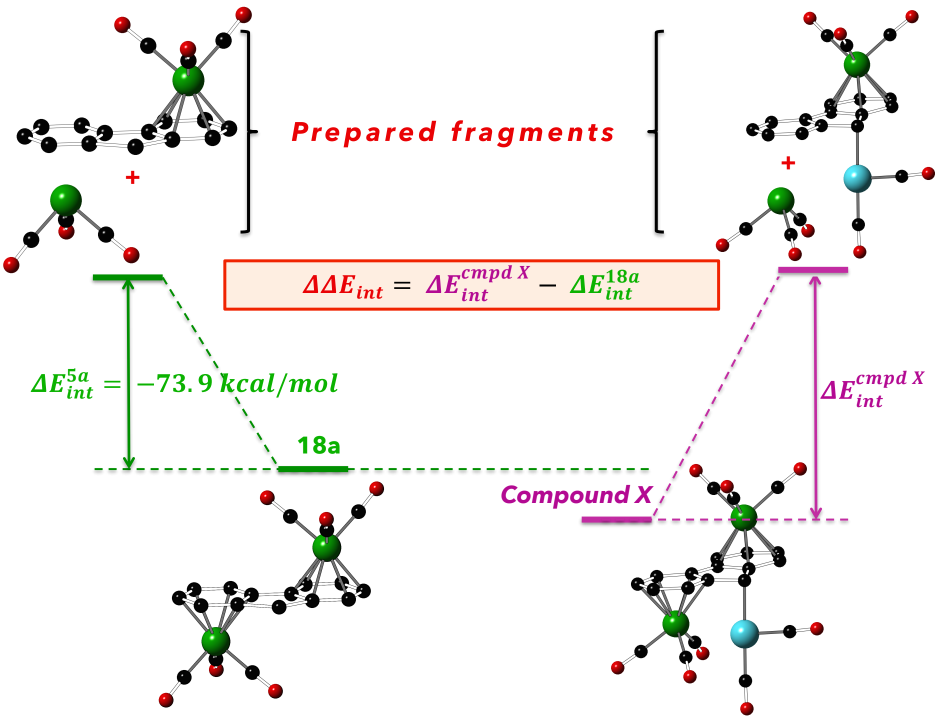

Figure 221: Considered fragments for the energy decomposition analysis.

1031 [N°813] Weinhold, F.; Landis, C. R. *Valency and Bonding, a Natural Bond Orbital Donor-Acceptor Perspective*; University Press: Cambridge, UK, **2005**.

The attractive coulombic contribution to the $(CO)_3$Cr-to-arene bonding is evaluated to be by one order of magnitude stronger in the Rh hemichelates disclosed here than in Ceccon's type of *syn*-facial bimetallic compounds *syn*-**31a** and *syn*-**31b**.

6 - Conclusion.

In summary, this study demonstrates that the concept of *hemichelation* applies to Rh^{I} complexes.

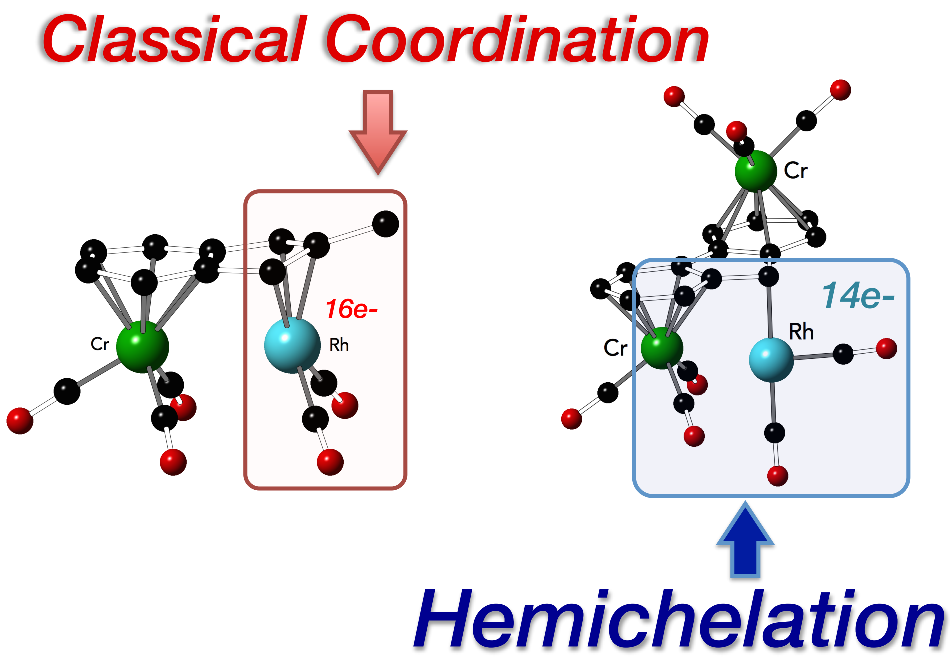

Figure 222: Illustration of the difference between the classical coordination and the hemichelation for Rh(I) derivatives.

The use of the ambiphilic fluorenyl anion enables the formation of relatively persistent hemichelates (Figure 222) wherein the Rh atom holds formally an unsaturated 14 valence electron shell with a loose but stabilizing non-covalent interaction at its fourth coordination site. Apart from validating the whole concept of *hemichelation*, this study points out the multifaceted role played by the arene-bound $Cr(CO)_3$ moiety in the cohesion of unusual organometallic architectures. These results also broaden the potential lying behind *hemichelation*, which offers a new alternative for the production of coordinatively unsaturated and potentially reactive metal centres.

V

An excursion into non-covalence

Conclusions and Perspectives

This chapter will present the conclusions and perspectives of this work.

Chapter V - Conclusions and perspectives.

The core focus of this PhD thesis was to highlight, understand and describe specific "anomalies" that organometallic chemistry carries and which could not be reasonably explained by the "universally accepted paradigm" without the consideration of one key parameter, namely: *noncocalent interactions (NCIs)*. We saw in the introduction that they are very important macroscopic phenomenons, which could not be completely understood without taking into account the NCIs (*e.g.* properties of the water molecule, protein folding process, the gecko climbing skills…). We also saw that the transition metal chemistry conceals number of "heterodox"[1032] cases, which deserve some specific attention in order to find the right reasons for their behaviour, and the right answers to their atypical features. Certainly, NCIs is one of these answers. One major drawback related to non-covalence in general is that this type of subtle interaction is difficult to observe and their effect cannot be easily quantified. Indeed, NCIs cannot be easily visualized or measured, as other physical parameters can be. Some specific tools are needed, *i.e*. experiments and theory. The huge amount of improvements in terms of computer technology (always faster and more efficient), software's development, Quantum theoretical methods (especially in the field of DFT), as well as experimental characterization methods (vibration rotation spectroscopy, UV and IR hole burning, REMPI, ZEKE spectroscopy…) constitute much accurate data to properly look at the non-covalent scale.

Figure 223: The methodology we applied for the investigation of NCIs during this PhD thesis. *(Figure removed because subjected to copyright).*

[1032] [N°560] Bonifaci, C.; Ceccon, A.; Santi, S.; Mealli, C.; Zoellner, R. W. *Inorg Chim Acta* **1995**, *240*, 541.

It is part of this PhD thesis to provide the methodology that we have elaborated for the study of NCIs especially in the organometallic chemistry field. Our approach consists in a subtle association of chemical synthesis, physical chemistry and Quantum mechanics, which are all three inseparable facets of a prism surrounding the NCIs and, like for the Newton prism, put the light on them (Figure 223).

We aimed first to synthesize Re analogues[1033] of the formally electron-unsaturated 6-membered cyclomanganated 2-oxazoline derivatives (Figure 224) studied by Djukic *et al*,[1034] as we estimated that two crucial issues needed to be further addressed in order to achieve a comprehensive understanding of this specific molecular system. The first aspect was to properly evaluate the interconversion in solution of the heterobimetallic isomers by the use of ^{1}H NMR spectroscopy, which remained impossible in the case of the cyclomanganated derivatives due to the recurrence of radical species. The Second one was, by the means of DFT, to evaluate the contribution of NCIs in the molecular cohesion of the electron-unsaturated system.

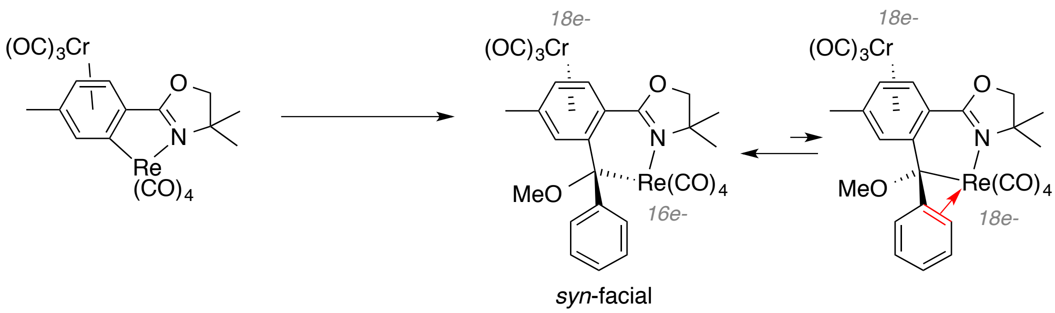

Figure 224: Expected formation of two "pseudoconformers". A *syn*-facial electron-unsaturated 18-16 electrons isomer and an electron-saturated 18-18 electrons isomer.

Unfortunately, the reactivity of complex **2** towards diazomethanes was found to be in no way straightforward. The planned carbene mono-insertion products **3a** and **4a** were not isolated (Figure 225), but rather electron-saturated 18-18 electrons complexes were obtained (Figure 226).

[1033] [N°612] Werlé, C.; Le Goff, X. F.; Djukic, J. P. *J. Organomet. Chem.* **2014**, *751*, 754.

[1034] [N°608] Djukic, J. P.; Maisse-Francois, A.; Pfeffer, M.; Dotz, K. H.; De Cian, A.; Fischer, J. *Organometallics* **2000**, *19*, 5484.

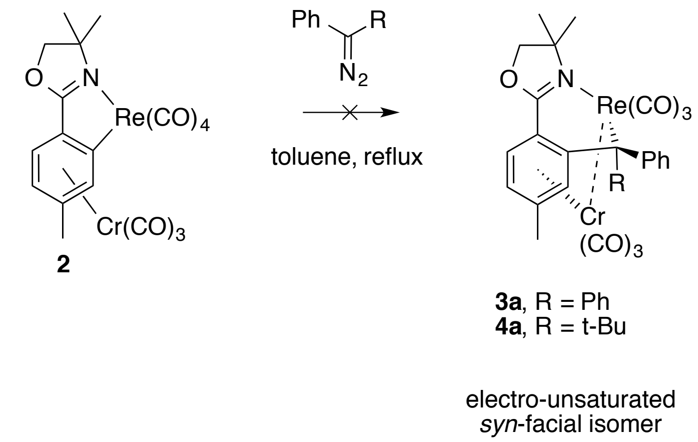

Figure 225: Expected formation of electron unsaturated heterobimetallic species.

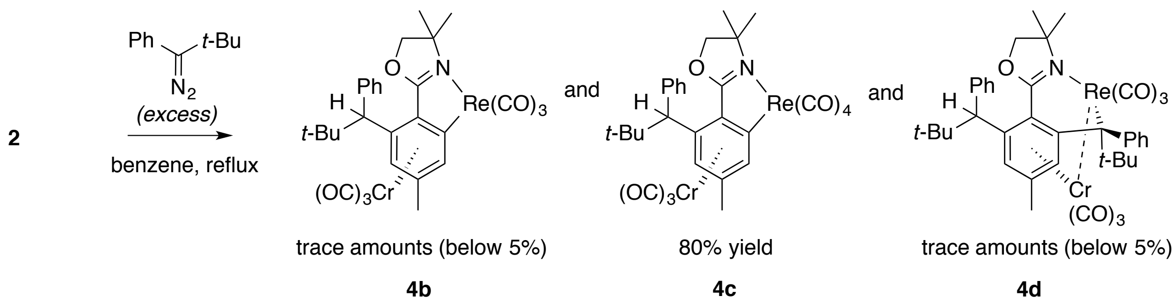

Figure 226: Reaction of **2** with (t-Bu)(Ph)CN_2.

Only compound **4d** (isolated on a trace amount), which stems from a reaction of **4c** or **4b** with a second equivalent of (t-Bu)(Ph)CN_2, displayed the typical structure of 18-16 electron *syn*-facial Cr-Re complexes. Preliminary theoretical analyses of the intermetallic interaction using Yang's[1035, 1036] electron density topology-based analysis of non-covalent interactions regions, established a typical bonded non-covalent interaction (red-coloured isosurfaces) between the Re and the Cr centres (Figure 227). Bader's AIM analysis stressed the absence of any bond critical point in the Cr-Re segment.

[1035] [N°629] Contreras-García, J.; Johnson, E. R.; Keinan, S.; Chaudret, R.; Piquemal, J.-P.; Beratan, D. N.; Yang, W. *J. Chem. Theory Comput.* **2011**, *7*, 625.
[1036] [N°630] Johnson, E. R.; Keinan, S.; Mori-Sánchez, P.; Contreras-García, J.; Cohen, A. J.; Yang, W. *J. Am. Chem. Soc.* **2010**, *132*, 6498.

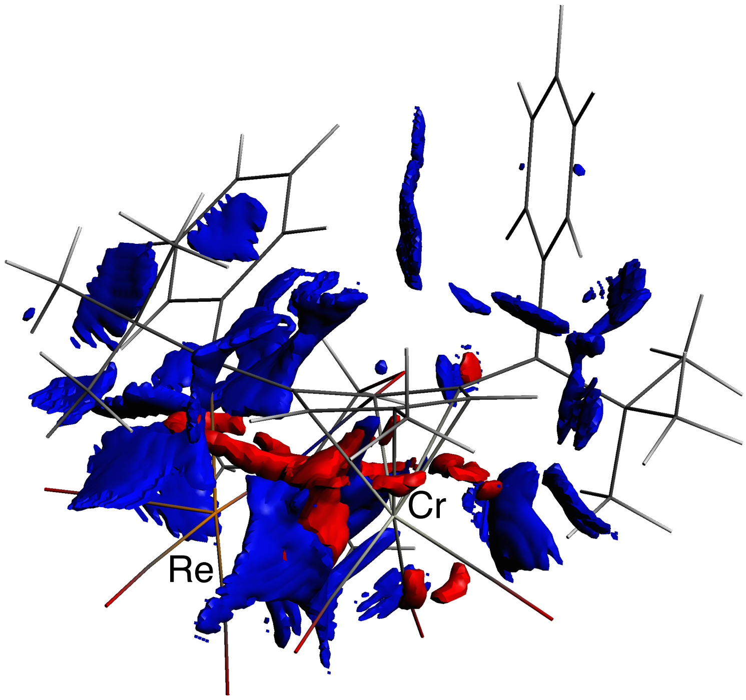

Figure 227: ADFview 2013 plot of NCI regions materialized by reduced density gradient sisosurfaces (cutoff value s= 0.02 au, ρ= 0.05) coloured according to the signed density $\lambda_2\rho$ (red and blue colours are assigned to negative and positive signs respectively) for the gas-phase singlet ground state geometry of **4d** computed at the ZORA-PBE-D3(BJ)/all electron TZP level).

After these difficulties, we decided to quickly change our approach in the investigation of non-covalent interactions. A new class of metals, as well as another kind of bridging ligands were chosen. The indenyl derivatives as ligand and the palladium as a metal centre looked promising to us. The reason for this choice was quite simple: the indenyl effect, which can be considered as a form of intrinsic hemilability (see chapter III), correlated with the unique properties induced by the presence of the $Cr(CO)_3$ moiety, appeared as new promising characteristics in the stabilisation of coordinative unsaturated transition metal complexes. A rational method of synthesis and characterization, determination of the electronic structure, and dynamic behaviour of electron deficient species have thus been developed. This method takes advantage of the ambiphilic character of the tricarbonyl(η^6-arene)chromium anion (Figure 228), whose main property is to behave as a conventional heteroditopic ligand, capable of chelating a metal centre through covalent and noncovalent bonding, preserving its unsaturated valence shell.

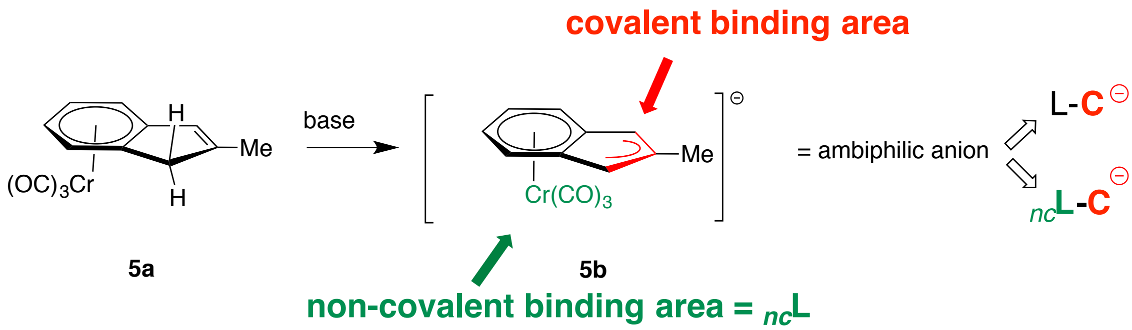

Figure 228: Ambiphilic character of anion **5b**.

Rare examples of persistent coordinatively unsaturated Pd(II)/Pt(II) complexes have been reported (Figure 229).[1037,1038] The *syn*-facial η^1 coordination preference of the metal centre at the benzylic position of several heteroditopic ligands stems from a thermodynamically preference over *syn*-facial or *antara*-facial η^3 modes.

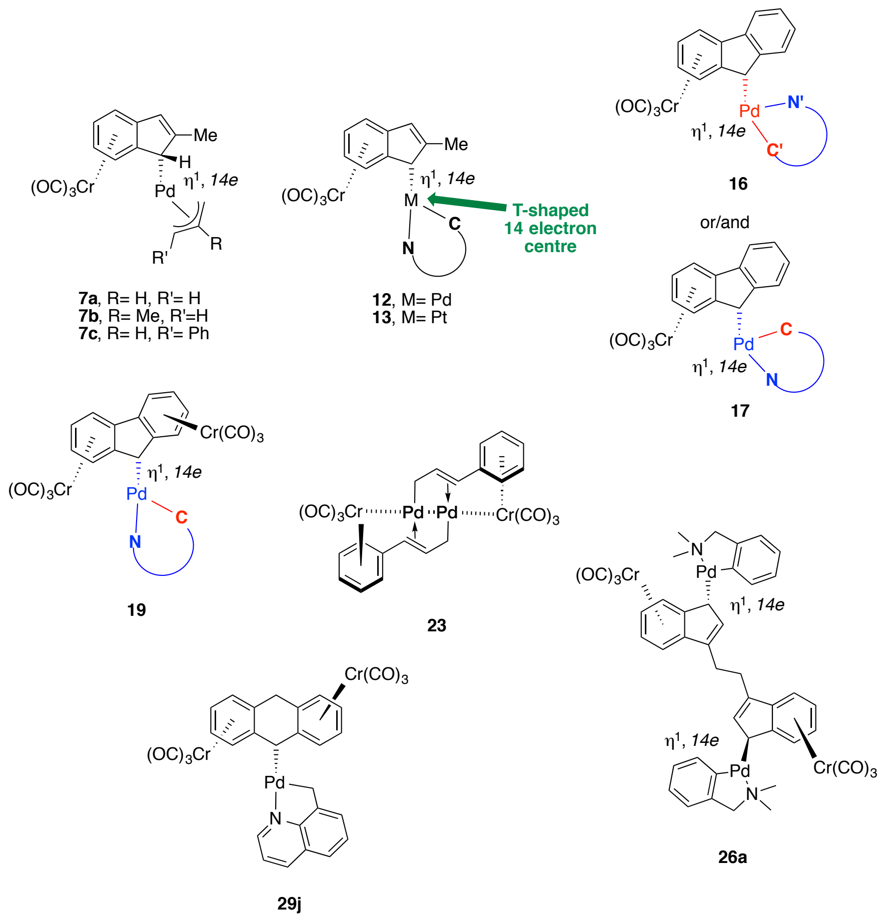

Figure 229: List of the coordinatively unsaturated Pd(II)/Pt(II) complexes synthesized.

[1037] [N°733] Werlé, C.; Hamdaoui, M.; Bailly, C.; Le Goff, X. F.; Brelot, L.; Djukic, J. P. *J. Am. Chem. Soc.* **2013**, *135*, 1715.

[1038] [N°732] Werlé, C.; Bailly, C.; Karmazin-Brelot, L.; Le Goff, X. F.; Ricard, L.; Djukic, J. P. *J. Am. Chem. Soc.* **2013**, *135*, 17839.

In several cases fluxionality was observed (*i.e.* a rapid haptotropy of the metal centre between two limiting benzylic positions) as a direct consequence of the evanescence of the polar intermetallic interaction.[1039,1040]

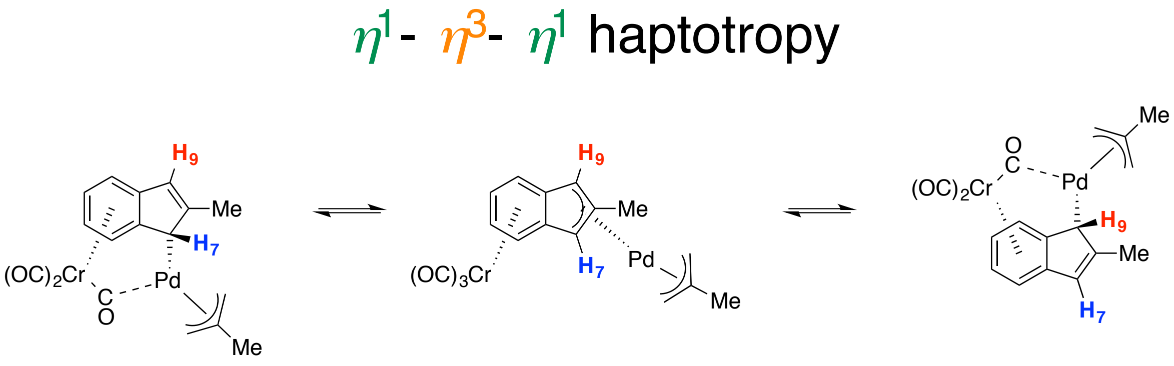

η^1-**7b** η^3-**7b** η^1-**7b**

Figure 230: Supposed fluxional behavior of the Pd centre.

Nevertheless, fluxionality does not constitute essential criteria in the formation of hemichelates (*e.g.* fluorene hemichelates). All of these results highlight the cohesive role of non-covalent interactions (electron correlation, London force, and Coulombic attraction) in loose but manageable donor/acceptor metal-based Lewis pairs. We proposed to name "*hemi*chelation" (Figure 231) any half-covalent/half noncovalent bonding-relationship similar to that existing between the ambiphilic heteroditopic tricarbonyl(η^6-indenyl) chromium ligand and the electron-unsaturated Pd(II) or Pt(II) centres.

[1039] [N°559] Hyla-Kryspin, I.; Grimme, S.; Djukic, J. P. *Organometallics* **2009**, *28*, 1001.

[1040] [N°562] Schwabe, T.; Grimme, S.; Djukic, J.-P. *J. Am. Chem. Soc.* **2009**, *131*, 14156.

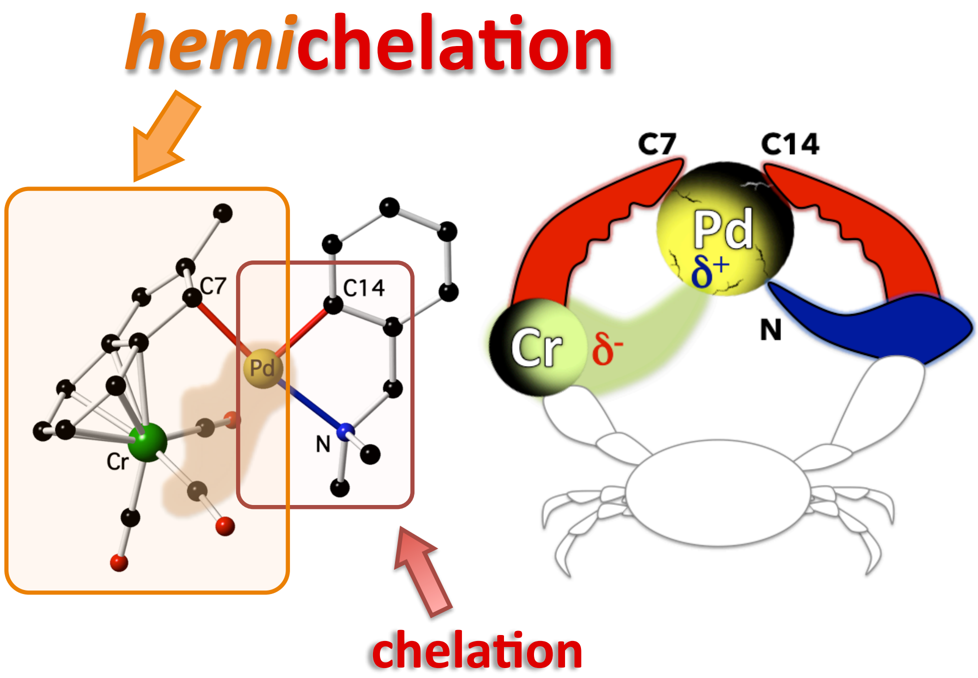

Figure 231: Illustration of the concept of *hemichelation*.

Worthy to note is that the concept of *hemichelation* could readily be extended to Rh(I) centres[1041] with a hemichelating ambiphilic anionic ligand with the adequate electronic properties in order to promote structural cohesion by non-covalent inter-metallic interactions. It was found that the most promising way to achieve this goal was by using a parent of **5a** containing a fluorenyl motive instead of the indenyl. Like shown in (Figure 163), analysis of the partial natural charges indicates that the strongest depletion of charge density at the aromatic carbons at the 2,3 positions occurs with **18a**.

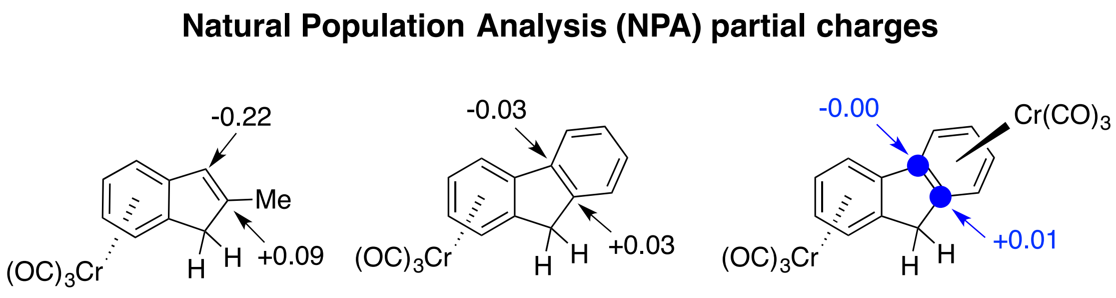

5a **15a** **18a**

Figure 232: Natural partial charges (NPA) at C_2 and C_3 positions in **5a**, **15a** and **18a** computed from gas phase singlet ground state geometries optimized at the ZORA-TPSS-D3(BJ)/all electron TZP level.

[1041] [N°847] Werlé, C.; Bailly, C.; Karmazin-Brelot, L.; Le Goff, X.-F.; Pfeffer, M.; Djukic, J.-P. *Angew. Chem. Int. Ed. Engl.* **2014**, *53*, 9827.

This depletion is a necessary condition to prevent a η^3 bonding mode to the Rh(I) centre, which therefore made **18a** a reasonable candidate for attempting the synthesis of Rh(I) hemichelates. This provides a new step forward in the rational method we developed: by appropriately tuning the electronic properties of the ambiphilic ligand, new truly coordination-unsaturated Rh(I) (14 valence electron shell) complexes with a loose but stabilizing non-covalent interaction at its fourth coordination site can be synthesized in a manageable form (Figure 233).

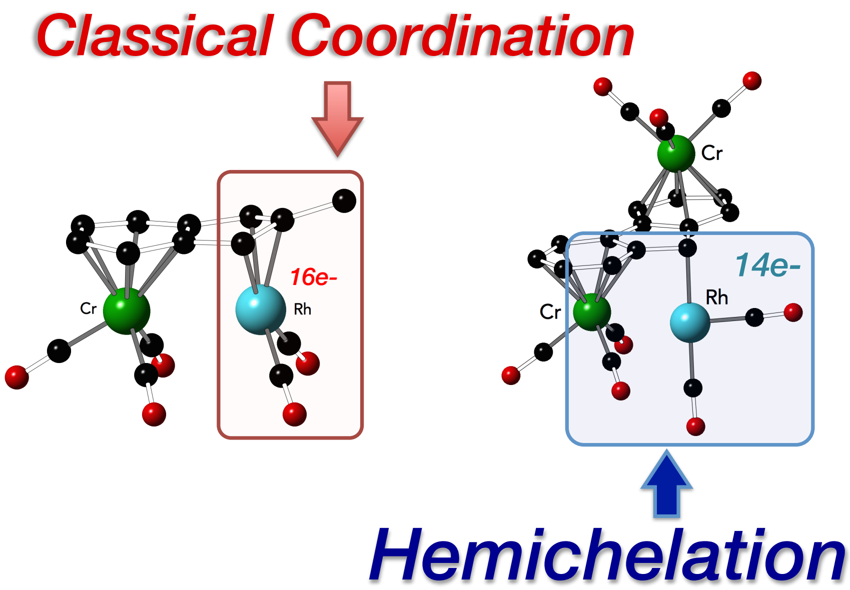

Figure 233: Illustration of the difference between the classical coordination and the hemichelation for Rh(I) derivatives.

This approach significantly broadens the potential lying behind *hemichelation*, offering a new alternative for the production of coordinatively unsaturated metal centres.

The synthesis of new hemichelates that will argue in favour of the solidity of this concept brings us to contemplate some perspectives to this work. Therefore, modulations that can preponderantly lead to new hemichelates are:

- The modification of the hemichelating ligand,
- The variation of the arene metal (*e.g.* replacement of Cr by Mo, W,…),
- The consideration of new potential electron-unsaturated metals (*e.g.* Ir, Ru, Os,…)

Another important perspective lies in the determination of possible applications of these coordinatively unsaturated complexes, and so, of potentially reactive metal centres which are thought to take part in a number of catalytic processes as pivotal intermediates[1042-1044].

Finally, the stabilization of such kinetically unstable species that are electron-unsaturated from the standpoint of the so-called Sidwick-Langmuir 18 valence electrons rule,[1045-1047] represents a great challenge which still has to be explored. Moreover, in view of the number of such heterodox cases, which are becoming more and more prevalent, it might indeed be that the field of organometallic chemistry starts to move toward a ***new paradigm where NCIs are preponderant and the 18-electron rule is ruled out.***

[1042] [N°705] Faza, R. Á. O. N.; de Lera, A. R.; Cárdenas, D. J. *Adv. Synth. Catal.* **2007**, *349*, 887.

[1043] [N°706] Sergeev, A. G.; Spannenberg, A.; Beller, M. *J. Am. Chem. Soc.* **2008**, *130*, 15549.

[1044] [N°707] Marrone, A.; Re, N.; Romeo, R. *Organometallics* **2008**, *27*, 2215.

[1045] [N°708] Jensen, W. B. *J. Chem. Educ.* **2005**, *82*, 28.

[1046] [N°709] Langmuir, I. *Science* **1921**, *54*, 59.

[1047] [N°710] Pyykkö, P. *J. Organomet. Chem.* **2006**, *691*, 4336.

VI

An excursion into non-covalence

Experimental Section

Chapter VI - Experimental section.

1 - Experimental methods of chapter II compounds.

1.1 - Generalities.

All experiments were carried out under a dry argon atmosphere using the standard Schlenk technique. Hexacarbonylchromium was purchased from ABCR. Chem. Co. Celite 545 was purchased from VWR Prolabo. All solvents were distilled over sodium or CaH_2 under argon. Deuterated solvents were dried over sodium or CaH_2 and purified by trap-to-trap techniques, degassed by freeze-pump-thaw cycles and stored under argon. ^{1}H, ^{13}C NMR spectra were measured on Bruker DPX 300, 400, Avance I 500 and Avance III 600 spectrometers. Chemical shifts (expressed in parts per million) were referenced against solvent peaks or external references (assignments are related to the atom numbering scheme given in the experimental part). IR spectra were acquired with a FT-IR Bruker alpha spectrometer using an ATR solid-state sample cell. Diazoalkanes were produced by the yellow HgO oxidation of hydrazones following literature procedures[1048,1049] and were used without further purification: this method generally ensures a high purity in diazoalkane even though unavoidable contamination by the ketone serving as substrate to make the hydrazone may exist.

[1048] [N°851] Javed, M. I.; Brewer, M. *Org. Lett. 9* **2007**, *9*, 1789.

[1049] [N°852] Ishiguro, K.; Ikeda, M.; Sawaki, Y. *J. Org. Chem.* **1992**, *57*, 3057.

1.2 - Synthesis and characterizations.

1.2.1 - Compound 2.

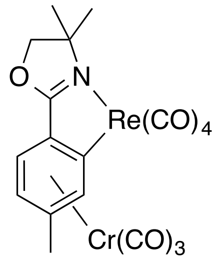

2

Synthesis:

A mixture of **1**, (1.8 g, 5.53 mmol), $PhCH_2Re(CO)_5$ (3.003 g, 7.19 mmol) dissolved in heptane (20 mL) was refluxed under argon for 7 h. The solvent was then removed under reduced pressure, the residue redissolved in a small volume of CH_2Cl_2 and silica gel added. The resulting suspension was stripped of solvent under reduced pressure and the coated silica gel loaded on the top of silica gel column packed in dry *n*-hexane. The orange band containing **2** was eluted with a mixture of hexane and CH_2Cl_2 (6:4) and the fraction stripped of solvents under reduced pressure to afford an intense-orange crystalline solid (1.510 g, 44 % yield).

Characterizations:

Calcd for $C_{19}H_{14}CrNO_8Re$: C, 36.66; H, 2.27; N, 2.25. Found: C, 36.68; H, 2.37; N, 2.18. HRMS-ESI (m/z): $[M]^+$ calcd for $C_{19}H_{14}CrNO_8Re$, 622.9682; found, 622.9659. IR (cm^{-1}) ν(CO): 2095 (s), 1971 (vs), 1927 (vs), 1881 (vs), 1860 (vs).

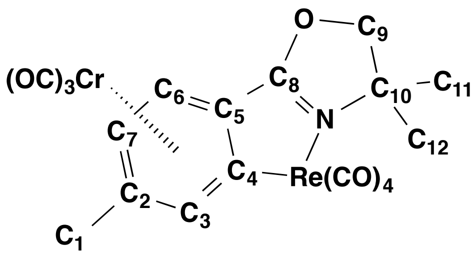

^{1}H NMR (400 MHz, $CDCl_3$, 298 K) δ 5.91 (d, J = 1.5 Hz, 1H, H_3), 5.59 (d, J = 6.5 Hz, 1H, H_6), 5.28 (dd, J = 6.5, 1.5 Hz, 1H, H_7), 4.62–4.42 (m, 2H, H_9), 2.21 (s, 3H, H_1), 1.46 (s, 3H, H_{11}), 1.42 (s, 3H, H_{12}). ^{13}C NMR (151 MHz, $CDCl_3$, 298 K) δ 234.48, 190.74, 188.67, 185.19, 184.40, 178.70, 122.53, 110.05, 108.51, 97.90, 93.11, 93.11, 91.35, 81.74, 67.48, 28.16, 27.76, 21.18, 21.17.

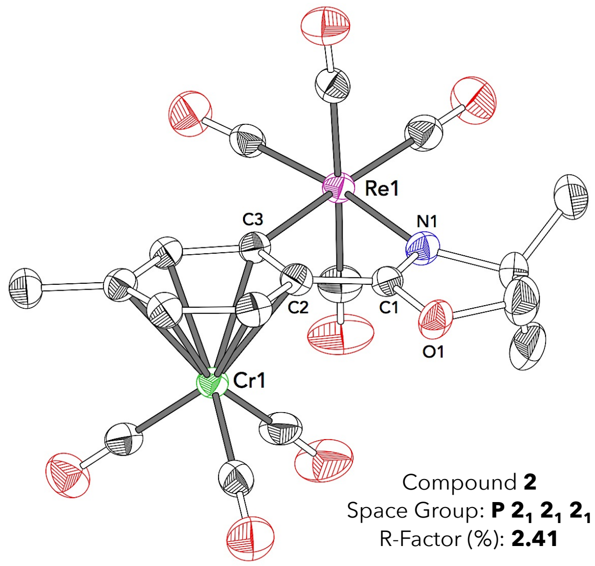

Compound **2**
Space Group: **P 2_1 2_1 2_1**
R-Factor (%): **2.41**

N°	*A*	*B*	*C*	*D*	*Lengths (Å)*	*Torsion Angles (°)*
1	Re_1	N_1	-	-	2.187(3)	-
2	Re_1	C_3	-	-	2.190(3)	-
3	Re_1	C_3	C_2	C_1	-	-12.1(4)
4	Re_1	N_1	C_1	C_2	-	1.8(4)

1.2.2 - Compound 3b.

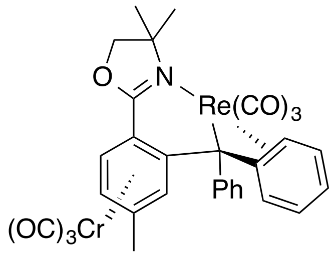

3b

Synthesis:

Compound **2** (0.500 g, 0.80 mmol) and Ph_2CN_2 (0.468 g, 2.41 mmol) were dissolved in dry and degassed heptane. The mixture was then brought to reflux for 4 h until a reddish precipitate appeared. An additional amount of Ph_2CN_2 (0.468 g, 2.41 mmol) was added to the medium, and the suspension was refluxed for additional 30 min. The reaction mixture was then cooled to room temperature and the solvent evaporated under reduced pressure to afford a solid. The latter was dissolved in CH_2Cl_2, and SiO_2 was added. The solvent was evaporated in vacuo and the coated silica gel loaded on the top of a SiO_2 column packed in hexane. Chromatography on SiO_2 and elution with a hexane/CH_2Cl_2 mixture (5:5) yielded a red-coloured complex (0.49 g, 80% yield).

Characterizations:

Calcd for $C_{31}H_{24}CrNO_7Re$: C, 48.94; H, 3.18; N, 1.84. Found: C, 48.86; H, 3.41; N, 1.74. HRMS-ESI (m/z): $[M]^+$ calcd for $C_{31}H_{24}CrNO_7Re$, 761.0515; found, 761.0520. IR (cm^{-1}) ν(CO): 2004 (s), 1963 (s), 1919 (s) 1886 (s), 1866 (vs).

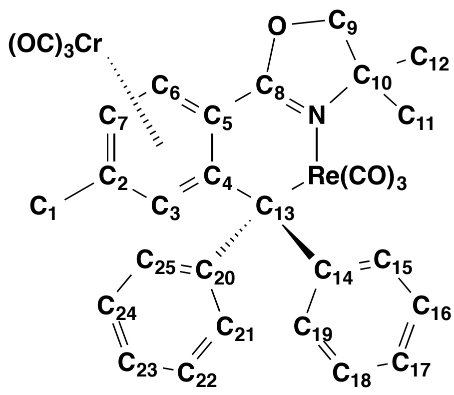

^{1}H NMR (500 MHz, Tol, 227 K) δ 8.30 (d, J = 8.7 Hz, 1H, H_{19}), 7.91 (d, J = 7.9 Hz, 1H, H_{21}), 7.32 (t, J = 7.6 Hz, 1H, H_{22}), 7.04 (d, J = 7.5 Hz, 1H, H_{25}), 6.92 (tt, J = 16.2, 7.5 Hz, 4H, H_{18}, H_{16}, H_{24}, H_{23}), 6.58 (t, J = 7.5 Hz, 1H, H_{17}), 6.33 (d, J = 7.2 Hz, 1H, H_{15}), 5.59 (d, J = 6.8 Hz, 1H, H_6), 4.96 (s, 1H, H_3), 3.80 (d, J = 6.9 Hz, 1H, H_7), 3.37 (d, J = 8.6 Hz, 1H, H_{9a}), 3.03 (d, J = 8.6 Hz, 1H, H_{9b}), 1.15 (s, 3H, H_1), 0.71 (s, 3H, H_{11}), 0.12 (s, 3H, H_{12}).^{13}C NMR (151 MHz, $CDCl_3$, 299 K) δ 232.66, 195.66, 195.05, 194.40, 166.28, 147.85, 138.53, 131.41, 128.87, 128.72, 126.39, 126.25, 126.08, 125.80, 124.98, 121.50, 109.50, 107.47, 95.60, 94.11, 92.13, 89.52, 79.77, 72.92, 27.78, 27.25, 26.73, 25.91, 21.23, 20.94.

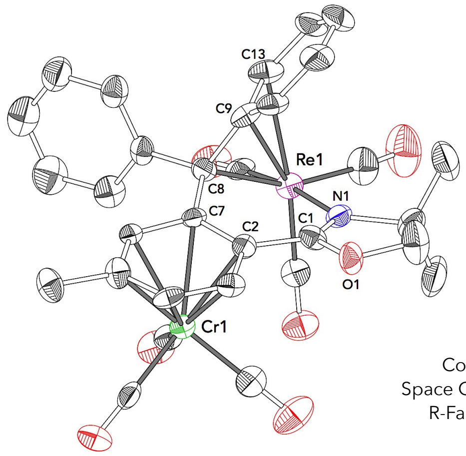

Compound **3b**
Space Group: **P 2_1 2_1 2_1**
R-Factor (%): **4.13**

N°	*A*	*B*	*C*	*D*	*Lengths (Å)*	*Angles (°)*	*Torsion Angles (°)*
1	Re_1	C_8	-	-	2.290(8)	-	-
2	Re_1	C_9	-	-	2.445(7)	-	-
3	Re_1	N_1	-	-	2.180(6)	-	-
4	Re_1	C_8	C_7	-	-	116.4(5)	-
5	C_9	C_8	C_7	-	-	116.0(6)	-
6	Re_1	C_8	C_7	C_2	-	-	38.1(8)
7	Re_1	N_1	C_1	C_2	-	-	-2(1)

1.2.3 - Compound 4c.

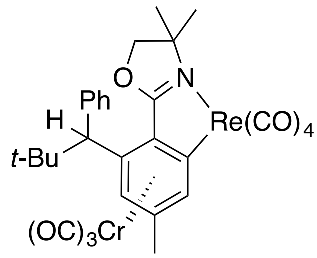

4c

Synthesis:

Compound **2** (0.200 g, 0.32 mmol) and (*t*-Bu)(Ph)CN_2 (0.168 g, 0.96 mmol) were dissolved in dry and degassed benzene. The mixture was then brought to reflux for 43 h until a reddish precipitate appeared. The reaction mixture was then cooled to room temperature and the solvent evaporated under reduced pressure. The resulting residue was dissolved in CH_2Cl_2, and SiO_2 was added. The solvent was stripped under reduced pressure and the coated silica gel loaded on the top of a SiO_2 column packed in *n*-hexane. Chromatography through SiO_2 and elution with a hexane/CH_2Cl_2 mixture (5:5) yielded an orange complex that was recovered neat after recrystallization from a CH_2Cl_2/pentane mixture (0.170 g, 71 % yield).

Characterizations:

Calcd for $C_{30}H_{28}CrNO_8ReCr{\bullet}0.25CH_2Cl_2$: C, 45.99; H, 3.64; N, 1.77. Found: C, 45.77; H, 3.92; N, 1.69. HRMS-ESI (m/z): $[M]^+$ calcd for $C_{30}H_{28}CrNO_8Re$, 769.0778; found, 769.0772. IR (cm^{-1}) ν(CO): 2093 (s), 2004 (s), 1980 (vs), 1945 (vs), 1924 (vs), 1878 (vs), 1849 (vs).

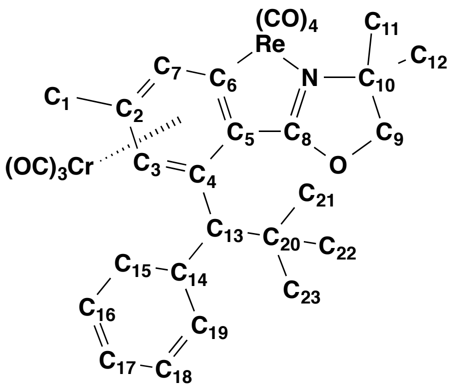

[1]H NMR (500 MHz, $CDCl_3$, 300 K) δ 7.08–6.93 (m, 3H, H_{18}, H_{17}, H_{16}), 6.80 (d, J = 7.2 Hz, 2H, H_{19}, H_{15}), 5.66 (s, 1H, H_3), 5.58 (s, 1H, H_7), 4.39 (s, 1H, H_{13}), 4.33 (d, J = 8.5 Hz, 1H, H_{9b}), 4.05 (d, J = 8.6 Hz, 1H, H_{9a}), 2.29 (s, 3H, H_1), 1.22 (s, 3H, H_{12}), 1.06 (s, 9H, H_{23}, H_{21}, H_{22}), 0.82 (s, 3H, H_{11}). [13]C NMR (126 MHz, $CDCl_3$, 300 K) δ 234.51, 191.15, 188.70, 184.97, 183.99, 178.73, 143.86, 131.49, 126.91, 126.49, 126.09, 118.55, 108.56, 105.74, 94.75, 94.70, 80.58, 66.15, 54.23, 34.20, 29.86, 27.53, 27.21, 21.46.

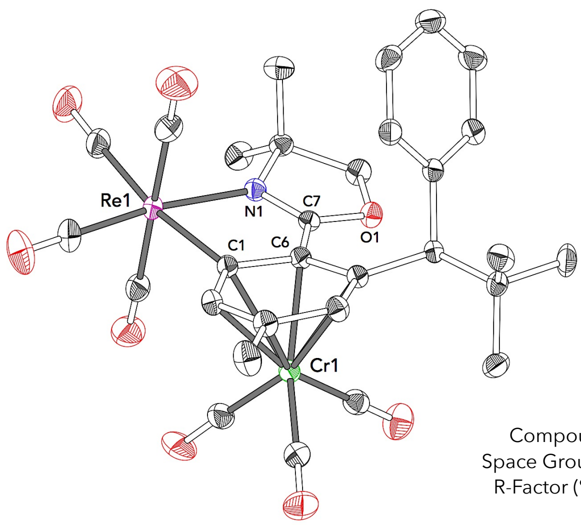

Compound **4c**
Space Group: **P 2_1/c**
R-Factor (%): **2.43**

N°	*A*	*B*	*C*	*D*	*Lengths (Å)*	*Angles (°)*	*Torsion Angles (°)*
1	Re_1	C_1	-	-	2.190(2)	-	-
2	Re_1	N_1	-	-	2.157(2)	-	-
4	N_1	Re_1	C_1	-	-	75.08(8)	-
7	Re_1	C_1	C_6	C_7	-	-	-10.1(2)
8	Re_1	N_1	C_7	C_6	-	-	-8.4(3)

2 - Experimental methods of chapter III compounds.

2.1 - Generalities.

All experiments were carried out under a dry argon atmosphere using the standard Schlenk technique or in an argon-filled glove box when necessary. *n*-Butyllithium was purchased from Aldrich Chem. Co as a 1.6 M solution in hexanes, hexacarbonylchromium was purchased from ABCR and 2-methyl-1*H*-indene (98 %) was purchased from Aldrich Chem. Co. Celite 545 was purchased from VWR Prolabo. 4-(*t*-Butyl)-2-(*p*-tolyl)pyridine was prepared according to a literature procedure.[1050] The palladacycles used in this study **10**[1051 - 1055] and platinacycle **11a**[1056] were prepared according to literature procedures. Anhydrous tetrahydrofurane (abbr. THF) and diethylether (ether) were distilled from purple solutions of Na/benzophenone under argon. All other solvents were distilled over sodium or CaH_2 under argon. Deuterated solvents were dried over sodium or CaH_2 and purified by trap-to-trap techniques, degassed by freeze-pump-thaw cycles and stored under argon. ^{1}H, ^{13}C NMR spectra were obtained on Bruker DPX 300, 400, Avance I 500 and Avance III 600 spectrometers. Chemical shifts (expressed in parts per million) were referenced against solvent peaks or external references. ^{195}Pt NMR spectra were referenced against Na_2PtCl_4 in D_2O. Infrared spectra of powdered amorphous samples were acquired with a Fourier transform−IR Bruker alpha spectrometer using an ATR solid-state sample cell. Circular dichroism absorption spectropolarimetry was carried out with a UV−visible Jasco J-810 CD spectrometer using a 0.1 mm optical path quartz cell at 20.0 ± 0.1 °C. The determination of specific rotations $[\alpha]$ was performed with a Perkin-Elmer 341 polarimeter at 589 nm (Na) using a thermostatted (20.0 ± 0.1 °C) 10 cm optical path quartz cell.

[1050] [N°853] Djukic, J.-P.; Parkhomenko, K.; Hijazi, A.; Chemmi, A.; Allouche, L.; Brelot, L., . . . Le Goff, X.-F. *Dalton Trans.* **2009**, 2695.

[1051] [N°800] Berger, A.; de Cian, A.; Djukic, J.-P.; Fischer, J.; Pfeffer, M. *Organometallics* **2001**, *20*, 3230.

[1052] [N°801] Ryabov, A. D.; Van Eldik, R.; Le Borgne, G.; Pfeffer, M. *Organometallics* **1993**, *12*, 1386.

[1053] [N°802] Gaunt, J. C.; Shaw, B. L. *J. Organomet. Chem.* **1975**, *102*, 511.

[1054] [N°803] Otsuka, S.; Nakamura, A.; Kano, T.; Tani, K. *J. Am. Chem. Soc.* **1971**, *93*, 4301.

[1055] [N°769] Cope, A. C.; Friedrich, E. C. *J. Am. Chem. Soc.* **1968**, *90*, 909.

[1056] [N°804] Schmulling, M.; Ryabov, A. D.; van Eldik, R. *J. Chem. Soc., Chem. Commun.* **1992**, 1609.

2.2 - Computational Details.

Computations were performed with methods of the Density Functional Theory, that is, the Perdew−Burke−Ernzerhof (PBE) GGA functional,[1057] as well as the Tao-Perdew-Staroverov-Scuseria *(TPSS)* meta-GGA functional[1058] implemented in the Amsterdam Density Functional package[1059-1061] (ADF2012 or ADF2013 versions) and augmented with Grimme's DFT-D3(BJ) implementation of Dispersion with a Becke-Johnson (BJ) damping function.[1062,1063] The PBE0[1064, 1065]-dDsC29[1066] hybrid functional was also used particularly in the perspective of QTAIM and NCI region analyses. Within the *PBE* scheme electron correlation was treated within the local density approximation *(LDA)* in the PW92[1067] parametrization. Unless otherwise stated, all computations were carried out using scalar relativistic corrections within the *Zeroth Order Regular Approximation* using *ad hoc* all-electron (AE) basis sets: polarized triple-ζ (TZP) Slater type orbitals were used in this study. Natural Population analyses (NPA) were carried out on geometries of models relaxed at the (ZORA) *PBE*-D3(BJ) level using AE-TZP basis sets. Geometry optimizations by energy gradient minimization were carried out in all cases with an integration grid comprised between 4.5 and 7.5, an energy gradient convergence criterion of 10^{-3} au and tight to very tight SCF convergence criteria. All ground state were computed using the (ZORA) *PBE*-D3(BJ) and the TPSS-D3(BJ) functionals associated with all electron TZP basis sets for all elements. The COSMO treatment of solvation (with toluene) was applied using the procedure implemented within the ADF package with Klaamt's adjustment of the van der Waals radii of

---

1057 [N°170] Perdew, J. P.; Burke, K.; Ernzerhof, M. *Phys. Rev. Lett.* **1996**, *77*, 3865.

1058 [N°743] Tao, J.; Perdew, J. P.; Staroverov, V. N.; Scuseria, G. E. *Phys. Rev. Lett.* **2003**, *91*, 146401.

1059 [N°821] te Velde, G.; Bickelhaupt, F. M.; Baerends, E. J.; Fonseca Guerra, C.; van Gisbergen, S. J. A.; Snijders, J. G.; Ziegler, T. *J. Comp. Chem.* **2001**, *22*, 931.

1060 [N°854] In *Amsterdam Density Functional ADF2012*; SCM: Theoretical Chemistry, Vrije Universiteit, Amsterdam, The Netherlands.

1061 [N°855] Brown, D. A.; Fitzpatrick, N. J.; Glass, W. K.; Ahmed, H. A.; Cunningham, D.; McArdle, P. *J. Organomet. Chem.* **1993**, *455*, 157.

1062 [N°738] Grimme, S.; Antony, J.; Ehrlich, S.; Krieg, H. *J. Chem. Phys.* **2010**, *132*, 154104.

1063 [N°187] Grimme, S.; Ehrlich, S.; Goerigk, L. *J. Comput. Chem.* **2011**, *32*, 1456.

1064 [N°744] Ernzerhof, M.; Scuseria, G. E. *J. Chem. Phys.* **1999**, *110*, 5029.

1065 [N°745] Adamo, C.; Barone, V. *J. Chem. Phys.* **1999**, *110*, 6158.

1066 [N°740] Steinmann, S. N.; Corminboeuf, C. *J. Chem. Theory Comput.* **2011**, *7*, 3567.

1067 [N°856] Perdew, J. P.; Wang, Y. *Phys. Rev. B* **1992**, *45*, 13244.

atoms.[1068] Counterpoise correction for basis set superposition error (BSSE) was neglected throughout this study. ETS-NOCV analyses, simulations of NMR spectra, and TDDFT computations of CD spectra as well as calculations of vibrational modes (analytical second derivative frequencies and two point numerical integration for COSMO geometries) were performed with optimized geometries using ADF2012 or ADF2013 versions subroutines. TDDFT calculation were performed from geometries relaxed at the PBE-D3(BJ) level with the model potential SAOP[1069] or with the hybrid functional PBE0 using ad hoc all electron ZORA QZ4P basis sets. Vibrational modes were computed in all cases to verify that the optimized geometries were either related to energy minima: statistical thermodynamic data at 298.15 K were extracted for further determination of enthalpies and variations of Gibbs free energies by conventional methods. For the allyl-Pd cases, Natural atomic orbital (NAO) and natural bond orbital (NBO) analyses as well as Wiberg indice determinations were performed with the GENNBO[1070] 5.0 module of ADF. AIM and ELF analyses were carried out using the modules embedded within ADF2012. Representations of molecular structures and orbitals were drawn using *ADFview* v12. For the cyclometallated cases, Natural population analyses (NPA) as well as Wiberg indice determination were performed with geometries of models relaxed at the (ZORA) PBE-D3(BJ) level using all electron TZP basis sets with the GENNBO 5.0 module of ADF. QTAIM and NCI region analyses were carried out using the modules embedded within ADF2013.01. Representations of molecular structures and isosurfaces were produced with ADFview 2013.

2.3 - X-ray diffraction analyses.

Reflections were collected with a Nonius KappaCCD and with an APEX diffractometer equipped with an Oxford Cryosystem liquid N_2 device, using Mo Kα radiation (λ = 0.71073 Å). The crystal detector distance was 38 mm. The cell parameters were determined (APEX2 software[1071]) from reflections taken from three sets of 12 frames,

[1068] [N°758] Klamt, A.; Schuurmann, G. *J. Chem. Soc., Perkin Trans. 2* **1993**, 799.

[1069] [N°759] Gritsenko, O. V.; Schipper, P. R. T.; Baerends, E. J. *Chem. Phys. Lett.* **1999**, *302*, 199.

[1070] [N°813] Weinhold, F.; Landis, C. R. *Valency and Bonding, a Natural Bond Orbital Donor-Acceptor Perspective*; University Press: Cambridge, UK, **2005**.

[1071] [N°857] In *M86-E01078 APEX2 User Manual*: Bruker AXS Inc.: Madison, USA, **2006**.

each at 10 s exposures. The structures were solved by direct methods using the program SHELXS-97.[1072] The refinement and all further calculations were carried out using SHELXL-97.[1073] The crystal structures acquired with the Nonius Kappa CCD were solved using SIR-97[1074] and refined with SHELXL-97. The refinement and all further calculations were carried out using SHELXL-97. The H-atoms were included in calculated positions and treated as riding atoms using SHELXL default parameters. The non-H atoms were refined anisotropically, using weighted full-matrix least-squares on F^2. A semiempirical absorption correction was applied using SADABS in APEX2.

2.4 - Dynamic NMR line shape analysis of 7b in toluene.

The investigation was carried out with a solution of complex **7b** in d_8-toluene that was obtained by the gradual enrichment in deuterated solvent of an original benzene mother solution of the complex. This enrichment was achieved by repeating several times a dilution-concentration cycle with addition of deuterated solvent. The solution was then filtered through a pad of celite and introduced into a 5 mm outer diameter NMR sample tube, which was sealed under argon. All experiments were carried out with a Bruker Avance III spectrometer (^{1}H at 600 MHz) between -60°C and + 25°C. Spectra were analysed with the Spinwork3 software, in which an embedded version of the DNMR3 algorithm[1075] is implemented. The latter enables a full non-recurrent line shape analysis.[1076] In our investigation, the T_2 of the considered protons were assumed to be *ca.* 0.5 s. The chemical shifts of the relevant protons at the low exchange rate limit were approximated by computing the theoretical ^{1}H NMR spectrum of **7b** in toluene (COSMO) at two different levels of theory ((ZORA)-PBE-D3(BJ)/AE-TZP and (ZORA)-SAOP/AE-TZP from a minimum optimized in the ground state at the PBE-D3(BJ) level). The corresponding calculated spectra provided identical peak separation $\Delta\delta$ of 0.27 ppm for the protons submitted to the effects of chemical exchange, *i.e.* H_7 and H_9. This

[1072][N°858] Sheldrick, G. *Acta Cryst. Sect. A* **1990**, *46*, 467.
[1073][N°859] Sheldrick, G. M.; Universität Göttingen: Göttingen, Germany, **1998**.
[1074][N°860] Altomare, A.; Burla, M. C.; Camalli, M.; Cascarano, G. L.; Giacovazzo, C.; Guagliardi, A., . . . Spagna, R. *J. Appl. Cryst.* **1999**, *32*, 115.
[1075] [N°760] Binsch, G.; Kleier, D. A. *QCPE No. 165*; Indiana University, **1970**.
[1076] [N°756] Sandstrom, J. *Dynamic NMR Spectroscopy*; Academic Press: New York, **1982**.

value was subsequently used as the peak separation at the slow exchange limit in the simulation procedure to fit the simulated lorentzian to the experimental signal, taking also into account the frequency drift induced by temperature. The portion of the Eyring plot that was fit by the root mean-square method comprised values measured in the -60(1)°C to -10(1) °C interval. Other points of the curve that diverged significantly were related to exchange rates at 0, 10 and 25 °C, the accuracy of which was found difficult to improve.

2.5 - Synthesis and characterizations.

2.5.1 - Compound 5a.

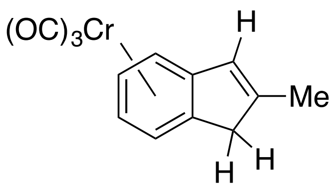

5a

Synthesis:

$Cr(CO)_6$ (5.0 g, 22.7 mmol), 2-methyl-1*H*-indene (3.3 mL, 25 mmol), THF (15 mL), and di-nbutylether (150 mL) were gently refluxed for 95 h under a permanent flow of argon. The resulting yellow solution was evaporated to dryness and the resulting residue was adsorbed on silica gel. Chromatographic separation was performed on silica gel using a mixture of CH_2Cl_2 and pentane (5:5) as eluent. The product was eluted as a yellow solution, which afforded a canary yellow solid upon removal of the solvents under reduced pressure (5.49 g, 20.6 mmol, 91 %).

Characterizations:

Calcd for $C_{13}H_{10}CrO_3$•$0.1CH_2Cl_2$: C, 57.28; H, 3.74. Found: C, 57.09; H, 3.85. HRMS-ESI (m/z): $[M+Na]^+$ calcd for $C_{13}H_{10}CrO_3$, 288,9927; found, 288.9934. IR (cm^{-1}) ν(CO): 1935 (s), 1839 (vs).

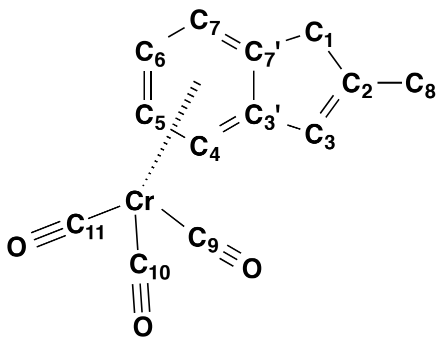

^{1}H NMR (500 MHz, C_6D_6, 300 K) δ 5.52 (s, 1H, H3), 4.98 (d, J = 5.9 Hz, 1H, H_4), 4.90 (d, J = 6.0 Hz, 1H, H_7), 4.55 – 4.40 (m, 2H, H_5, H_6), 2.79 (d, J = 22.5 Hz, 1H, H_{1a}), 2.53 (d, J = 22.4 Hz, 1H, H_{1b}), 1.57 (s, 3H, H_8). ^{13}C NMR (126 MHz, C_6D_6, 230 K) δ 234.68 (C_{10}, C_{11}, C_9), 149.99 (C_2), 124.31 (C_3), 117.77 ($C_{3'}$), 112.60 ($C_{7'}$), 90.85 (C_6), 90.21 (C_4), 89.71 (C_5), 87.21 (C_7), 42.36 (C_1), 16.30 (C_8).

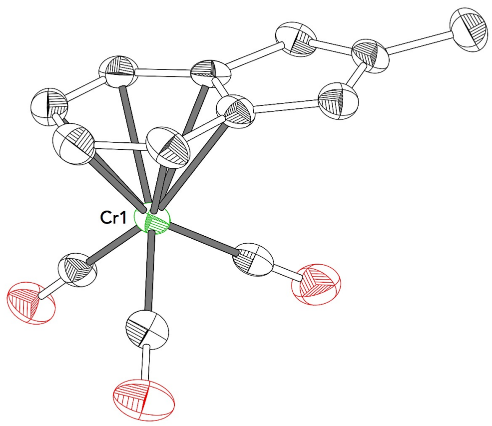

Compound **5a**
Space Group: **P 2_1 2_1 2_1**
R-Factor (%): **4.25**

N°	A	B	Lengths (Å)
1	C_9	C_8	1.428(5)
2	C_8	C_7	1.417(4)

2.5.2 - Compound 7a.

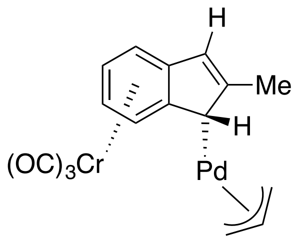

7a

Synthesis:

Compound **5a** (0.200 g, 0.75 mmol) was dissolved in THF (5 mL) and treated with 1.1 equivalent of *n*-BuLi (0.52 mL, 0.83 mmol) at -40°C under argon. The resulting solution was transferred via cannula after 10 min to another schlenk containing bis[(η^3-allyl)chloridopalladium] (137 mg, 0.5 eq., 0.38 mmol). The resulting solution was stirred for 1h15 whilst slowly warmed to -25°C and chilled toluene (5 mL) was added. The resulting mixture was then concentrated to *ca.* 3 mL, cold cyclohexane was added and the resulting mixture filtered through celite. The red-colored eluate was again concentrated under reduced pressure; chilled toluene (3 mL) and CH_2Cl_2 (3 mL) were added to favour the displacement of THF as the latter proved to be detrimental to the stability of the complex. The resulting solution was further concentrated to *ca.* 2 mL. For evaporation of the solvent would lead to irremediable decomposition of the new product, further characterizations were carried out either with wet crystals or with the mother solution. NMR analysis indicated quantitative conversion of **5a** into **7a**. Crystals were grown by diffusion of the mother solution in dry *n*-heptane.

Characterizations:

Calcd for $C_{16}H_{14}CrO_3Pd{\bullet}1/3CH_2Cl_2$: C, 44.48; H, 3.35. Found: C, 44.24; H, 3.54. HRMS-ESI (m/z): $[M + H]^+$ calcd for $C_{16}H_{14}CrO_3Pd$, 412.9456; found, 412.9512. IR (cm^{-1}) ν(CO): 1928 (s), 1843 (vs).

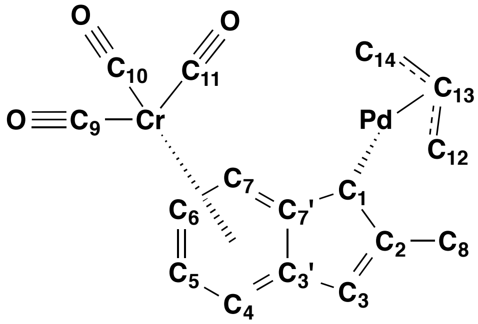

^{1}H NMR (500 MHz, C_6D_6, 300 K) δ 5.38 (s, 2H, H_1, H_3), 5.21 (dd, J = 4.8, 2.8 Hz, 2H, H_4, H_7), 4.85 – 4.71 (m, 1H, H_{13}), 4.59 (dd, J = 5.0, 2.8 Hz, 2H, H_5, H_6), 4.12 (d, J = 7.0 Hz, 2H, H_{12a}, H_{14a}), 2.66 (d, J = 12.6 Hz, 2H, H_{12b}, H_{14b}), 2.12 (s, 3H, H_8). ^{13}C NMR (126 MHz, C_6D_6, 300 K) δ 239.08 (bs, C_{11}), 235.36 (bs, C_{10}, C_9), 155.25 (C_2), 111.56 (C_{13}), 109.25 ($C_{3'}$, $C_{7'}$), 91.77 (C_4, C_7), 88.94 (C_5, C_6), 80.17 (bs, C_1, C_3), 70.06 (C_{12}, C_{14}), 17.02 (C_8).

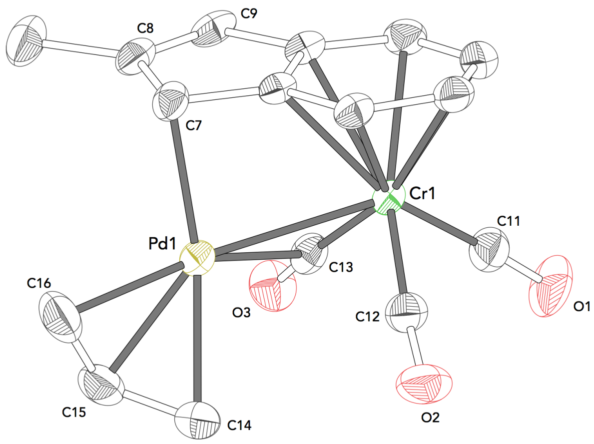

Compound **7a**
Space Group: **P 2_1/c**
R-Factor (%): **4.07**

N°	*A*	*B*	*C*	*Lengths (Å)*	*Angles (°)*
1	Pd_1	Cr_1	-	2.7542(5)	-
2	Pd_1	C_{13}	-	2.428(4)	-
3	Cr_1	C_{13}	-	1.873(4)	-
4	Cr_1	C_{12}	-	1.840(5)	-
5	Cr_1	C_{11}	-	1.832(4)	-
6	Pd_1	C_7	-	2.175(5)	-
7	Pd_1	C_8	-	2.950(5)	-
8	Pd_1	C_{16}	-	2.147(4)	-
9	Pd_1	C_{15}	-	2.133(3)	-
10	Pd_1	C_{14}	-	2.174(5)	-
11	Cr_1	C_{13}	O_3	-	169.2(4)
12	Cr_1	C_{12}	O_2	-	175.7(4)
13	Cr_1	C_{11}	O_1	-	177.2(4)

2.5.3 - Compound 7b.

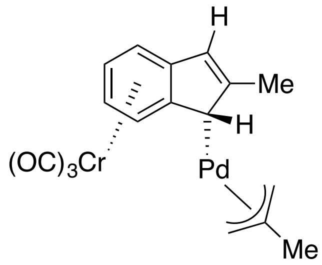

7b

Synthesis:

Compound **5a** (0.200 g, 0.75 mmol) was dissolved in THF (5 mL) and the resulting solution treated with *n*-BuLi (0.52 mL, 1.1 eq, 0.83 mmol) at -40 °C under argon. The resulting solution was transferred after 10 min via cannula to another schlenk containing bis[(η^3-2-methylallyl)chloridopalladium] (148 mg, 0.5 eq, 0.38 mmol). The mixture was stirred for 1h15, whilst slowly warmed from -40 °C to -25 °C. Chilled toluene (5 mL) was added to quench the reaction and the reaction mixture was concentrated to ca. 3-4 mL under reduced pressure. Chilled cyclohexane was added and the resulting mixture was filtered through celite. The resulting red-colored eluate was once more concentrated under reduced pressure, chilled toluene and CH_2Cl_2 (both 3 mL) and the resulting solution concentrated to a final volume of *ca.* 3 mL. Further analyses were performed as described previously for **7a**.

Characterizations:

Calcd for $C_{17}H_{16}CrO_3Pd{\bullet}1CH_2Cl_2$: C, 42.25; H, 3.55. Found: C, 42.08; H, 3.68. HRMS-ESI (m/z): $[M + H]^+$ calcd for $C_{17}H_{16}CrO_3Pd$, 426.9612; found, 426.9655. IR (cm^{-1}) ν(CO): 1932 (s), 1865 (s), 1836 (vs).

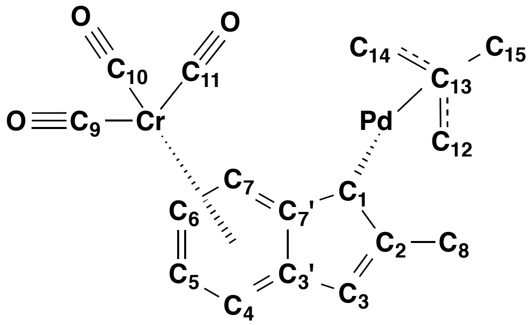

^{1}H NMR (300 MHz, C_6D_6, 298 K) δ 5.42 (s, 2H, H_1, H_3), 5.23 (dd, J = 4.9, 2.8 Hz, 2H, H_4, H_7), 4.58 (dd, J = 5.0, 2.8 Hz, 2H, H_5, H_6), 4.03 (s, 2H, H_{12a}, H_{14a}), 2.62 (s, 2H, H_{12b}, H_{14b}), 2.18 (s, 3H, H_8), 1.52 (s, 3H, H_{15}). ^{13}C NMR (126 MHz, C_6D_6, 300 K) δ 239.29 (bs, C_{11}), 235.66 (bs, C_{10}, C_9), 155.22 (C_2), 126.99 (C_{13}), 109.23 ($C_{3'}$, $C_{7'}$), 91.79 (C_4, C_7), 88.89 (C_5, C_6), 79.96 (bs, C_1, C_3), 69.16 (C_{12}, C_{14}), 22.86 (C_{15}), 16.97 (C_8).

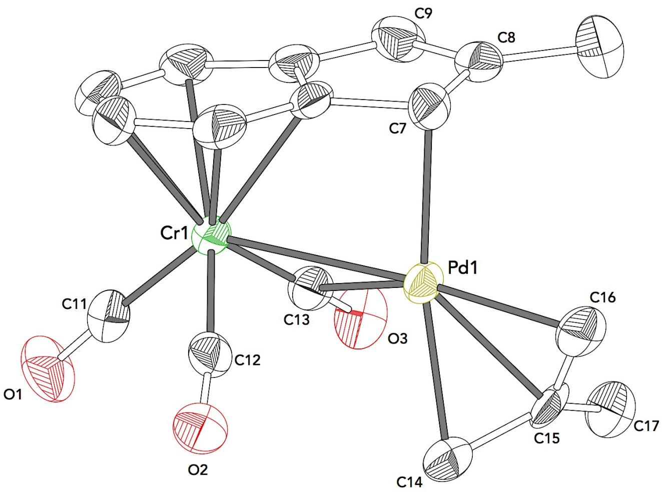

Compound **7b**
Space Group: **P -1**
R-Factor (%): **3.87**

N°	*A*	*B*	*C*	*Lengths (Å)*	*Angles (°)*
1	Pd_1	Cr_1	-	2.7465(6)	-
2	Pd_1	C_{13}	-	2.443(4)	-
3	Cr_1	C_{13}	-	1.862(4)	-
4	Cr_1	C_{12}	-	1.846(3)	-
5	Cr_1	C_{11}	-	1.853(4)	-
6	Pd_1	C_7	-	2.184(4)	-
7	Pd_1	C_8	-	2.868(5)	-
8	Pd_1	C_{16}	-	2.152(3)	-
9	Pd_1	C_{15}	-	2.146(3)	-
10	Pd_1	C_{14}	-	2.168(4)	-
11	Cr_1	C_{13}	O_3	-	169.5(3)
12	Cr_1	C_{12}	O_2	-	174.4(3)
13	Cr_1	C_{11}	O_1	-	177.5(3)

2.5.4 - Compound 7c.

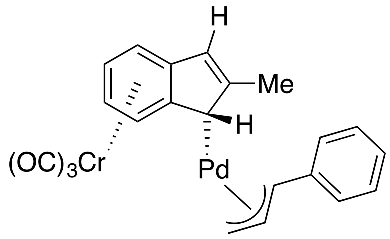

7c

Synthesis:

A solution of compound **5a** (0.200 g, 0.75 mmol) in THF (5 mL) was treated with *n*-BuLi (0.52 mL, 1.1 eq, 0.83 mmol) at -40°C under argon. After 10 min, the resulting solution was transferred via cannula to another schlenk tube containing neat bis[(η^3-1-phenylallyl)chloridopalladium] (195 mg, 0.5 eq 0.38 mmol). The resulting solution was slowly warmed for 1h15 up to -25°C and chilled toluene (5 mL) was added. The resulting mixture was concentrated to *ca.* 3-4 mL, chilled cyclohexane was added and the resulting solution was filtered through celite. The red-colored eluate was concentrated under reduced pressure, chilled toluene (3 mL) and CH_2Cl_2 (3 mL) were added and the resulting solution once more concentrated to *ca.* 3 mL. ^{1}H NMR analysis of this solution indicated the quantitative conversion of **5a** into **7c**. At this stage it was noticed that the new product, *i.e.* **7c**, had a longer life-time (a few minutes) in the solid state than **7a-b**. Crystals suitable for structural X-ray diffraction analysis were grown as previously described for **7a-b**.

Characterizations:

Calcd for $C_{22}H_{18}CrO_3Pd{\bullet}0.1CH_2Cl_2$: C, 53.38; H, 3.69. Found: C, 53.22; H, 3.99. HRMS-ESI (m/z): $[M + H]^+$ calcd for $C_{22}H_{18}CrO_3Pd$, 488,9769; found, 488.9707. IR (cm^{-1}) ν(CO): 1941 (s), 1864 (s) 1821 (vs).

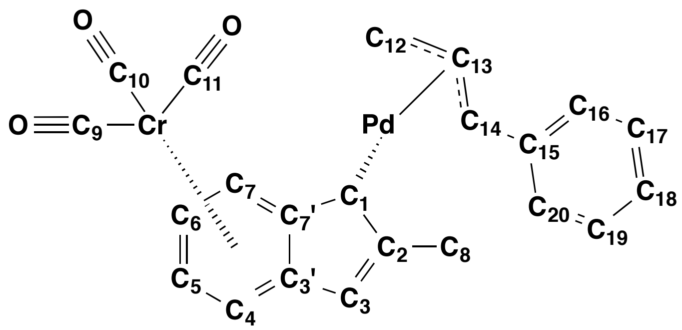

[1]H NMR (500 MHz, $CDCl_3$, 300 K) δ 7.45 (d, J = 7.6 Hz, 2H, H_{16}, H_{20}), 7.34 (dd, J = 13.7, 6.1 Hz, 2H, H_{17}, H_{19}), 7.22 (t, J = 7.3 Hz, 1H, H_{18}), 5.94 (d, J = 6.5 Hz, 1H, H_4), 5.84 (d, J = 6.5 Hz, 1H, H_7), 5.79 – 5.70 (m, 1H, H_{13}), 5.38 (t, J = 6.4 Hz, 1H, H_5), 5.35 (s, 1H, H_3), 5.31 (t, J = 6.2 Hz, 1H, H_6), 5.03 (bs, 1H, H_1), 4.64 (d, J = 12.0 Hz, 1H, H_{14}), 4.17 (d, J = 7.0 Hz, 1H, H_{12a}), 2.85 (d, J = 12.4 Hz, 1H, H_{12b}), 1.92 (s, 3H, H_8). [13]C NMR (126 MHz, $CDCl_3$, 300 K) δ 238.40 (bs, C_{11}), 235.77 (bs, C_{10}), 235.10 (bs, C_9), 155.64 (C_2), 138.61 (C_{15}), 128.87 (C_{17}, C_{19}), 127.07 (C_{18}), 126.94 (C_{16}, C_{20}), 109.61 ($C_{7'}$), 109.15 ($C_{3'}$), 106.61 (C_{13}), 91.77 (C_7), 91.75 (C_4), 90.23 (C_{14}), 89.34 (bs, C_1, C_3), 88.63 (bs, C_5, C_6), 67.39 (bs, C_{12}), 16.39 (C_8).

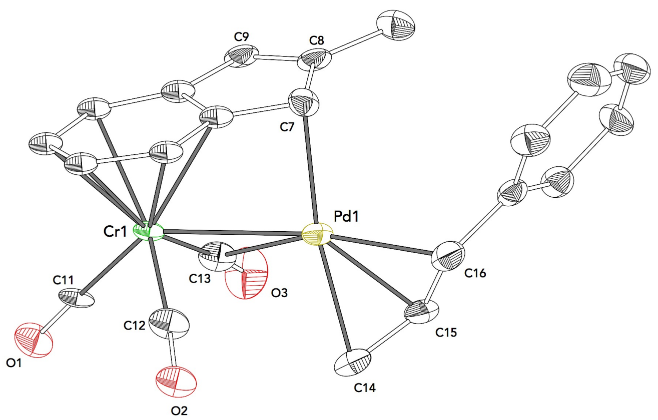

Compound **7c**
Space Group: **P 2_1/c**
R-Factor (%): **8.2**

N°	A	B	C	Lengths (Å)	Angles (°)
1	Pd_1	Cr_1	-	2.737(2)	-
2	Pd_1	C_{13}	-	2.340(1)	-
3	Cr_1	C_{13}	-	1.860(1)	-
4	Cr_1	C_{12}	-	1.850(1)	-
5	Cr_1	C_{11}	-	1.845(9)	-
6	Pd_1	C_7	-	2.193(9)	-
7	Pd_1	C_8	-	2.932(9)	-
8	Pd_1	C_{16}	-	2.218(9)	-
9	Pd_1	C_{15}	-	2.139(9)	-
10	Pd_1	C_{14}	-	2.160(1)	-
11	Cr_1	C_{13}	O_3	-	167.2(9)
12	Cr_1	C_{12}	O_2	-	175.5(9)
13	Cr_1	C_{11}	O_1	-	178.1(8)

2.5.5 - Compound 8a.

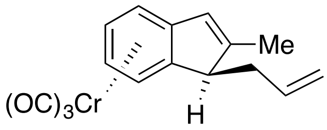

8a

Synthesis:

A mother solution of **7a** made from **5a** (200 mg, 0.75 mmol) was allowed to stir at room temperature for 30 min, leading to the precipitation of «palladium black» into the blackbrownish solution. After removal of the solvents, separation of the main product of decomposition was performed by flash chromatography over silica by a 7:3 Pentane/CH_2Cl_2 mixture. Evaporation of the solvent from the main eluate afforded a yellow solid (156 mg, 0.51 mmol, 68 % yield).

Characterizations:

Calcd for $C_{16}H_{14}CrO_3$•0.1CH_2Cl_2: C, 61.43; H, 4.55. Found: C, 61.36; H, 4.86. HRMS-ESI (m/z): $[M+Na]^+$ calcd for $C_{16}H_{14}CrO_3$, 329,0240; found, 329.0238. IR (cm^{-1}) ν(CO): 1951 (s), 1829 (vs).

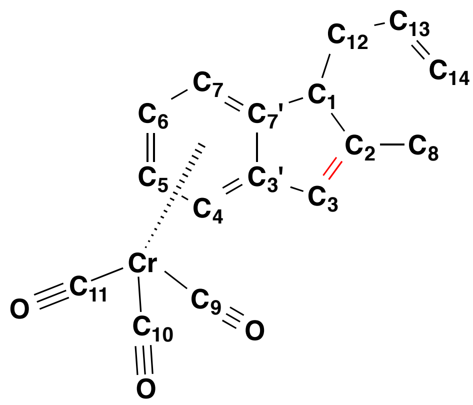

^{1}H NMR (500 MHz, C_6D_6, 300 K) δ 5.49 (s, 1H, H_3), 5.18 – 5.07 (m, 2H, H_4, H_{13}), 4.82 – 4.71 (m, 3H, H_7, H_{14}), 4.41 (dd, J = 4.2, 3.0 Hz, 2H, H_5, H_6), 3.03 (t, J = 5.7 Hz, 1H, H_1), 2.15 – 2.05 (m, 1H, H_{12a}), 1.95 – 1.84 (m, 1H, H_{12b}), 1.53 (s, 3H, H_8). ^{13}C NMR (126 MHz, C_6D_6, 300 K) δ 234.51 (C_{10}, C_{11}, C_9), 151.95 (C_2), 133.64 (C_{14}), 124.23 (C_3), 117.64 (C_{13}), 116.61 ($C_{7'}$), 115.97 ($C_{3'}$), 90.84 (C_6), 89.82 (C_4), 89.41 (C_5), 86.84 (C_7), 51.99 (C_1), 35.25 (C_{12}), 14.93 (C_8).

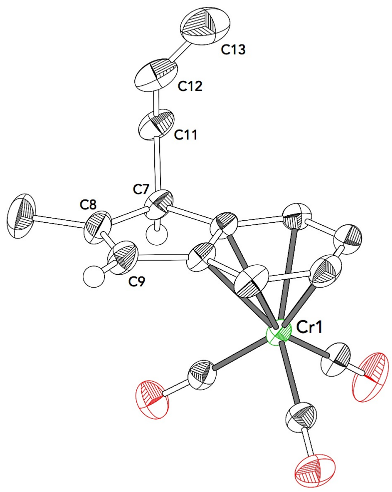

Compound **8a**
Space Group: **P 2_1/c**
R-Factor (%): **2.83**

N°	A	B	Lengths (Å)
1	C_7	C_{11}	1.542(2)
2	C_{11}	C_{12}	1.497(2)
3	C_{12}	C_{13}	1.316(3)
4	C_7	C_8	1.517(2)
5	C_8	C_9	1.344(1)

2.5.6 - Compounds 8b and 8d.

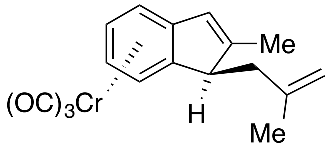

and

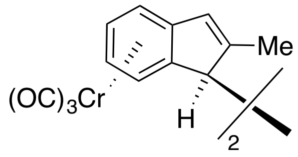

8b **8d**

Synthesis:

A mother solution of **7b** made from **5a** (200 mg, 0.75 mmol) was allowed to stirr at room temperature for 2 hours at room temperature exposed to air, which induced the precipitation of «palladium black». After removal of the solvents, column chromatography was performed over silica by eluting with a dry Pentane/CH_2Cl_2 mixture (7:3 and 5:5) leading to two different products, *i.e.* **8b** (105 mg, 0.33 mmol, 44 % yield) and **8d** (18 mg, 0.03 mmol, 5 % yield), as yellow solids.

Characterizations:

Compound 8b:

Calcd for $C_{17}H_{16}CrO_3$•$0.1CH_2Cl_2$: C, 62.47; H, 4.97. Found: C, 62.27; H, 5.13. HRMS-ESI (m/z): $[M+Na]^+$ calcd for $C_{17}H_{16}CrO_3$, 343,0397; found, 343.0380. IR (cm^{-1}) ν(CO): 1949(s), 1867(s), 1834(vs).

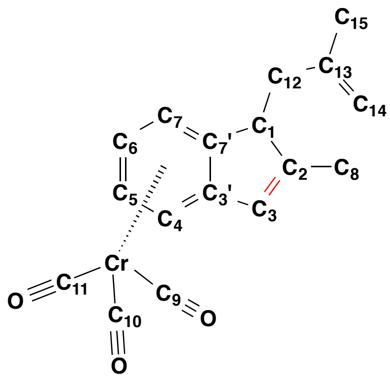

[1]H NMR (500 MHz, C_6D_6, 300 K) δ 5.53 (s, 1H, H_3), 5.30 (d, J = 6.0 Hz, 1H, H_4), 4.83 (d, J = 6.0 Hz, 1H, H_7), 4.68 (s, 1H, H_{14b}), 4.53 (s, 1H, H_{14a}), 4.48 – 4.37 (m, 2H, H_5, H_6), 3.28 (dd, J = 8.8, 4.8 Hz, 1H, H_1), 2.13 (dd, J = 14.2, 4.5 Hz, 1H, H_{12a}), 1.68 (dd, J = 14.3, 9.2 Hz, 1H, H_{12b}), 1.57 (s, 3H, H_8), 1.42 (s, 3H, H_{15}). [13]C NMR (126 MHz, C_6D_6, 300 K) δ 234.56 (C_{10}, C_{11}, C_9), 152.82 (C_2), 142.37 (C_{13}), 123.92 (C_3), 116.53 ($C_{3'}$), 116.24 ($C_{7'}$), 113.91 (C_{14}), 91.17 (C_6), 90.36 (C_4), 89.26 (C_5), 86.86 (C_7), 50.79 (C_1), 39.92 (C_{12}), 22.37 (C_{15}), 15.05 (C_8).

Compound 8d:

Calcd for $C_{26}H_{18}Cr_2O_6$•1.25CH_2Cl_2: C, 51.41; H, 3.25. Found: C, 51.39; H, 3.55. HRMS-ESI (m/z): $[M+Na]^+$ calcd for $C_{26}H_{18}Cr_2O_6$, 552,9806; found, 552.9807. IR (cm^{-1}) ν(CO): 1946 (s), 1862 (s) 1851 (vs).

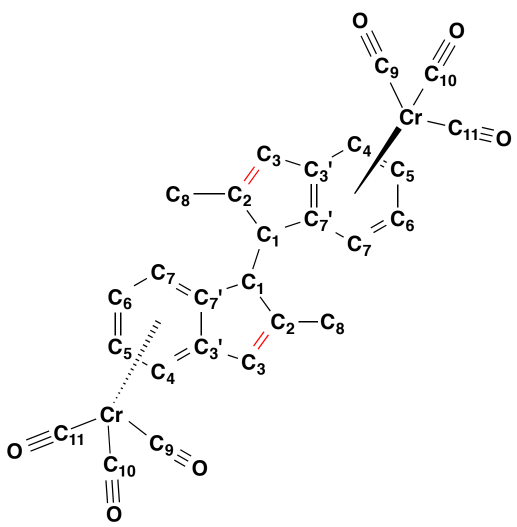

Mixture of two diastereomers in 1:1 ratio:

^{1}H NMR (600 MHz, C_6D_6, 338 K) δ 5.64 (s, 2H, H_{3a}), 4.92 (d, J = 6.3 Hz, 2H, H_{4a}), 4.69 (d, J = 6.3 Hz, 2H, H_{7a}), 4.30 (t, J = 6.6 Hz, 2H, H_{6a}), 4.17 (d, J = 8.4 Hz, 2H, H_{5a}), 3.63 (s, 2H, H_{1a}), 1.59 (br s, 6H, H_{8a}). ^{13}C NMR (151 MHz, C_6D_6, 338 K) δ 233.94 (C_{10a}, C_{11a}, C_{9a}), 148.55 (C_{2a}), 126.07 (C_{3a}), 115.24 ($C_{3'a}$), 110.45 ($C_{7'a}$), 91.74 (C_{6a}), 88.86 (C_{4a}), 88.80 (C_{5a}), 86.08 (C_{7a}), 54.20 (C_{1a}), 16.94 (C_{8a}).

Second set:

^{1}H NMR (600 MHz, C_6D_6, 338 K) δ 5.48 (s, 2H, H_{3b}), 4.79 (d, J = 6.2 Hz, 2H, H_{4b}), 4.74 (br, 2H, H_{7b}), 4.43 (s, 2H, H_{5b}), 4.29 (t, J = 6.5 Hz, 2H, H_{6b}), 3.73 (s, 2H, H_{1b}), 1.43 (br s, 6H, H_{8b}). ^{13}C NMR (151 MHz, C_6D_6, 338 K) δ 233.69 (C_{10b}, C_{11b}, C_{9b}), 149.05 (C_{2b}), 126.04 (C_{3b}), 116.09 ($C_{3'b}$), 112.22 ($C_{7'b}$), 90.64 (C_{5b}), 90.49 (C_{6b}), 90.08 (C_{7b}), 86.10 (C_{4b}), 54.39 (C_{1b}), 16.09 (C_{8b}).

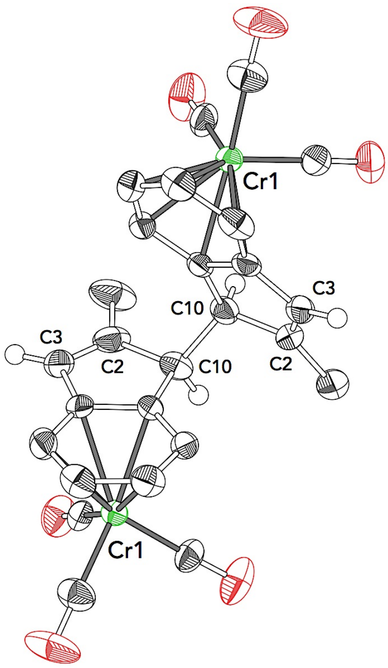

Compound **8d**
Space Group: **C 2/c**
R-Factor (%): **4.62**

N°	*A*	*B*	*Lengths (Å)*
1	C_{10}	C_{10}	1.534(5)
2	C_{10}	C_2	1.534(5)
3	C_2	C_3	1.336(6)

2.5.7 - Compound 8c.

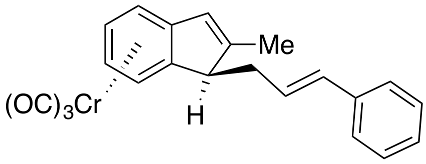

8c

Synthesis:

Compound **7c** (100 mg, 0.20 mmol) and triphenylphosphine (80 mg, 0.31 mmol) were dissolved in 5 mL of benzene under argon. The resulting solution was stirred at room temperature for 15 min, during which period a significant precipitate of «palladium black» was formed. The resulting mixture was stripped of solvents and the residue adsorbed on silica gel. The coated silica gel was loaded on the top of a silica gel column packed in pentane. A band containing compound **8c** was eluted with a 7:3 mixture of pentane and dichloromethane. A subsequent band containing **8d** was eluted with a 5:5 mixture of pentane and dichloromethane. The two complexes, *i.e.* **8c** (31 mg, 0.08 mmol, 20 % yield) and **8d** (56 mg, 0.11 mmol, 26 % yield) were recovered as yellow powders upon removal of the solvents and subsequent recrystallization from dry pentane.

Characterizations:

Calcd for $C_{22}H_{18}CrO_3$•$0.25CH_2Cl_2$: C, 66.21; H, 4.62. Found: C, 66.00; H, 4.82. HRMS-ESI (m/z): $[M]^+$ calcd for $C_{22}H_{18}CrO_3$, 382,0661; found, 382.0622. IR (cm^{-1}) ν(CO): 1949(s), 1856(vs).

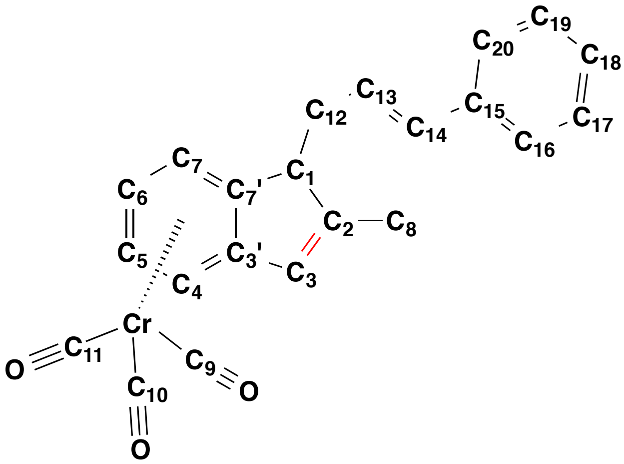

^{1}H NMR (400 MHz, $CDCl_3$, 298 K) δ 7.21 – 7.09 (m, 5H, H_{16}, H_{17}, H_{18}, H_{19}, H_{20}), 6.31 (d, J = 15.7 Hz, 1H, H_{14}), 6.02 (s, 1H, H_3), 5.83 (dt, J = 15.1, 7.1 Hz, 1H, H_{13}), 5.69 (d, J = 5.9 Hz, 1H, H_4), 5.46 (d, J = 5.9 Hz, 1H, H_7), 5.18 – 4.99 (m, 2H, H_5, H_6), 3.45 (t, J = 6.0 Hz, 1H, H_1), 2.83 – 2.69 (m, 1H, H_{12a}), 2.51 – 2.37 (m, 1H, H_{12b}), 1.97 (s, 3H, H_8). ^{13}C NMR (126 MHz, $CDCl_3$, 300 K) δ 234.15 (C_{10}, C_{11}, C_9), 152.52 (C_2), 137.05 (C_{15}), 133.31 (C_{14}), 128.74 (C_{17}, C_{19}), 127.63 (C_{18}), 126.26 (C_{16}, C_{20}), 125.22 (C_{13}), 124.19 (C_3), 116.80 ($C_{3'}$), 116.32 ($C_{7'}$), 91.18 (C_6), 90.14 (C_4), 89.94 (C_5), 87.35 (C_7), 52.58 (C_1), 34.91 (C_{12}), 15.61 (C_8).

2.5.8 - Compound 9a.

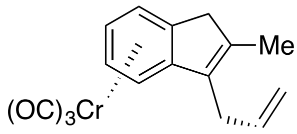

9a

Synthesis:

Slow filtration of a benzene or toluene solution of **8a** through basic activated alumina led to the quantitative formation of compound **9a**, which was isolated pure as an orange solid.

Characterizations:

Calcd for $C_{16}H_{14}CrO_3 \cdot 0.1CH_2Cl_2$: C, 61.43; H, 4.55. Found: C, 61.62; H, 4.76. HRMS-ESI (m/z): $[M]^+$ calcd for $C_{16}H_{14}CrO_3$, 306,0348; found, 306.0336. IR (cm^{-1}) ν(CO): 1938 (s), 1843 (vs).

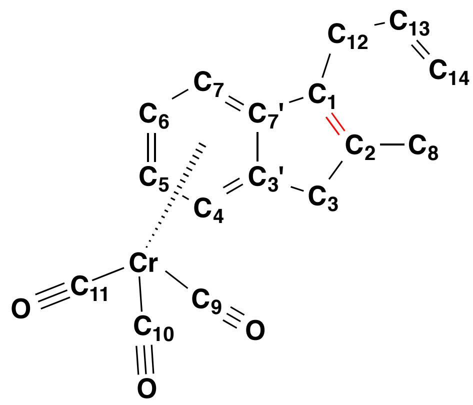

[1]H NMR (500 MHz, C_6D_6, 300 K) δ 5.67 (ddt, J = 16.4, 10.1, 6.2 Hz, 1H, H_{13}), 5.09 – 4.89 (m, 4H, H_4, H_7, H_{14}), 4.52 – 4.40 (m, 2H, H_5, H_6), 2.82 (d, J = 22.4 Hz, 1H, H_{3a}), 2.77 (d, J = 5.9 Hz, 2H, H_{12}), 2.56 (d, J = 22.4 Hz, 1H, H_{3b}), 1.50 (s, 3H, H_8). [13]C NMR (126 MHz, C_6D_6, 300 K) δ 234.57 (C_{10}, C_{11}, C_9), 142.88 (C_2), 134.56 (C_{13}), 131.94 (C_1), 117.95 ($C_{7'}$), 116.27 (C_{14}), 112.02 ($C_{3'}$), 90.33 (C_6), 90.03 (C_5), 89.72 (C_4), 86.73 (C_7), 42.31 (C_3), 29.36 (C_{12}), 13.58 (C_8).

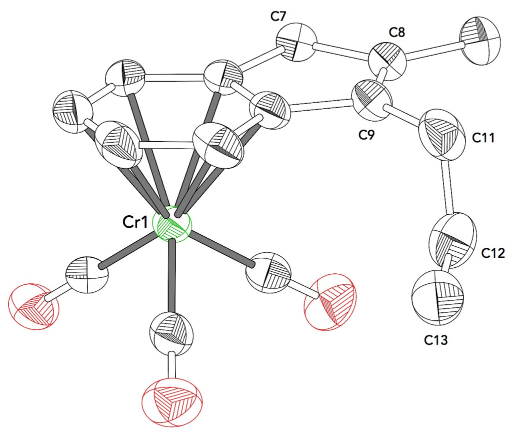

Compound **9a**
Space Group: **P 2_1/c**
R-Factor (%): **4.04**

N°	*A*	*B*	*Lengths (Å)*
1	C_7	C_8	1.508(2)
2	C_8	C_9	1.344(3)
3	C_{11}	C_{12}	1.508(4)
4	C_{12}	C_{13}	1.308(4)

2.5.9 - Compound 9b.

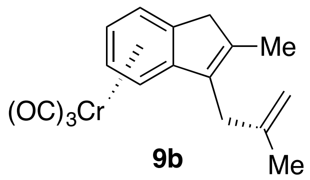

9b

Synthesis:

Slow filtration of a benzene or toluene solution of **8b** through basic activated alumina led to the quantitative formation of compound **9b**, which was isolated pure as an orange solid.

Characterizations:

Calcd for $C_{17}H_{16}CrO_3$•1/4CH_2Cl_2: C, 60.66; H, 4.87. Found: C, 60.96; H, 5.01. HRMS-ESI (m/z): $[M+Na]^+$ calcd for $C_{17}H_{16}CrO_3$, 343,0397; found, 343.0396. IR (cm^{-1}) ν(CO): 1939(s), 1843(vs).

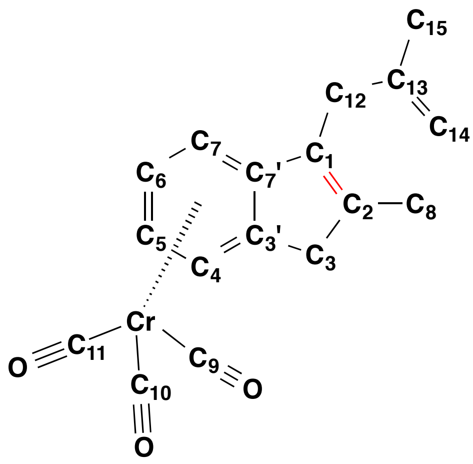

^{1}H NMR (500 MHz, C_6D_6, 300 K) δ 5.20 (d, J = 5.7 Hz, 1H, H_7), 4.92 (d, J = 5.4 Hz, 1H, H_4), 4.81 (s, 1H, H_{14b}), 4.69 (s, 1H, H_{14a}), 4.53 – 4.46 (m, 1H, H_5), 4.46 – 4.40 (m, 1H, H_6), 2.87 (d, J = 22.6 Hz, 1H, H_{3b}), 2.77 (br s, 2H, H_{12}), 2.60 (d, J = 22.2 Hz, 1H, H_{3a}), 1.58 (s, 3H, H_{15}), 1.52 (s, 3H, H_8). ^{13}C NMR (126 MHz, C_6D_6, 300 K) δ 234.56 (C_{10}, C_{11}, C_9), 143.30 (C_2), 142.29 (C_{13}), 131.91 ($C_{7'}$), 118.01 ($C_{3'}$), 112.34 (C_{14}), 112.30 (C_1), 90.52 (C_5), 89.87 (C_6), 89.26 (C_4), 87.37 (C_7), 42.32 (C_3), 33.65 (C_{12}), 22.23 (C_{15}), 13.72 (C_8).

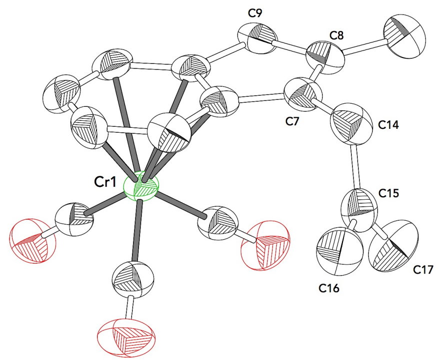

Compound **9b**
Space Group: **P 2_1/c**
R-Factor (%): **3.65**

N°	*A*	*B*	*Lengths (Å)*
1	C_9	C_8	1.507(3)
2	C_8	C_7	1.346(3)
3	C_{14}	C_{15}	1.514(4)
4	C_{15}	C_{16}	1.317(4)
5	C_{15}	C_{17}	1.495(4)

2.5.10 - Compound 9c.

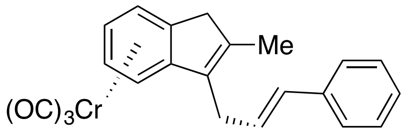

9c

Synthesis:

Slow filtration of a benzene or toluene solution of **8c** through basic activated alumina led to the quantitative formation of compound **9c**, which was isolated pure as an orange solid.

Characterizations:

Calcd for $C_{22}H_{18}CrO_3$•$0.1C_5H_{12}$: C, 69.37; H, 4.97. Found: C, 69.07; H, 5.23. HRMS-ESI (m/z): $[M]^+$ calcd for $C_{22}H_{18}CrO_3$, 382,0661; found, 382.0651. IR (cm^{-1}) ν(CO): 1944(s), 1848(vs).

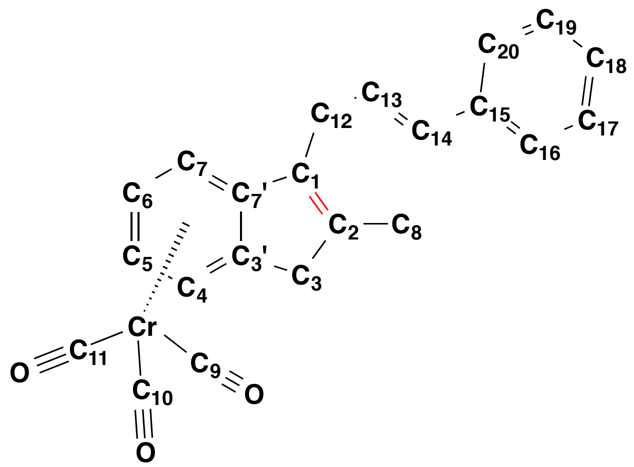

[1]H NMR (600 MHz, $CDCl_3$, 298 K) δ 7.26 – 7.07 (m, 5H, H_{16}, H_{17}, H_{18}, H_{19}, H_{20}), 6.40 (d, J = 16.1 Hz, 1H, H_{14}), 6.14 (dt, J = 15.8, 6.5 Hz, 1H, H_{13}), 5.66 (d, J = 5.9 Hz, 1H, H_7), 5.54 (d, J = 5.9 Hz, 1H, H_4), 5.14 – 5.04 (m, 2H, H_5, H_6), 3.40 – 3.14 (m, 4H, H_3, H_{12}), 1.96 (s, 3H, H_8). [13]C NMR (126 MHz, $CDCl_3$, 300 K) δ 234.24 (C_{10}, C_{11}, C_9), 143.45 (C_2), 137.24 (C_{15}), 132.11 (C_1), 131.70 (C_{14}), 128.66 (C_{16}, C_{20}), 127.43 (C_{18}), 126.31 (C_{17}, C_{19}), 126.16 (C_{13}), 118.36 ($C_{7'}$), 112.37 ($C_{3'}$), 90.78 (C_5), 90.42 (C_6), 90.16 (C_7), 87.03 (C_4), 42.80 (C_3), 28.68 (C_{12}), 14.33 (C_8).

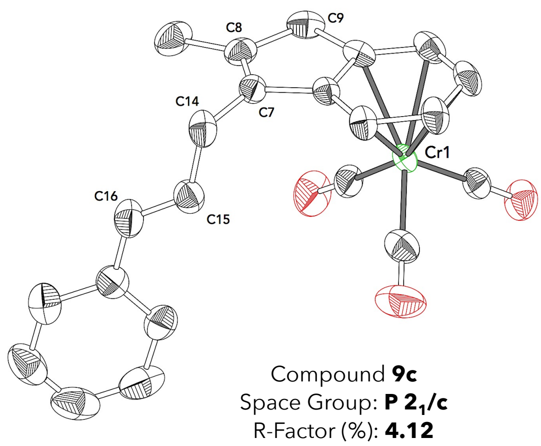

Compound **9c**
Space Group: **P 2_1/c**
R-Factor (%): **4.12**

N°	*A*	*B*	*Lengths (Å)*
1	C_9	C_8	1.511(2)
2	C_8	C_7	1.341(3)
3	C_{14}	C_{15}	1.513(3)
4	C_{15}	C_{16}	1.318(2)

2.5.11 - Compound 9d.

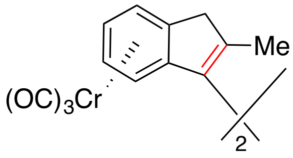

9d

Synthesis:

9d was obtained as an orange solid in quantitative yield by slow filtration of a benzene solution of **8d** through basic activated alumina.

Characterizations:

Calcd for $C_{26}H_{18}Cr_2O_6$•$2CH_2Cl_2$: C, 48.02; H, 3.17. Found: C, 48.30; H, 3.53. HRMS-ESI (m/z): $[M+Na]^+$ calcd for $C_{26}H_{18}Cr_2O_6$, 552,9806; found, 552.9784. IR (cm^{-1}) ν(CO): 1936 (s), 1855 (s) 1843 (vs).

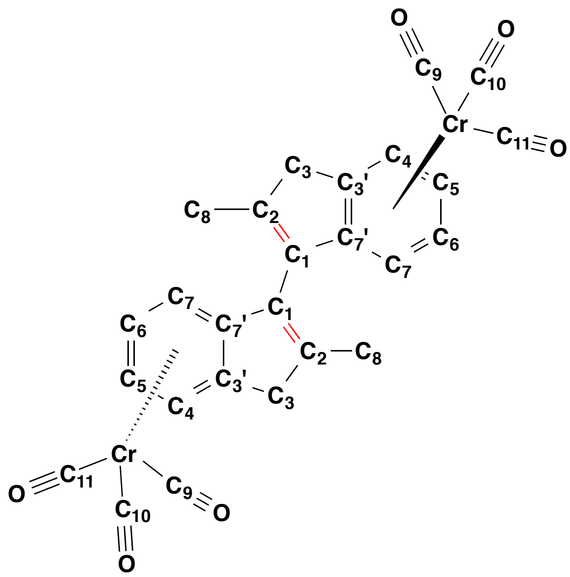

[1]H NMR (500 MHz, C_6D_6, 300 K) δ 4.95 (d, J = 6.2 Hz, 2H, H_7), 4.74 (d, J = 6.2 Hz, 2H, H_4), 4.48 (t, J = 6.3 Hz, 2H, H_6), 4.31 (t, J = 6.2 Hz, 2H, H_5), 2.96 (d, J = 22.8 Hz, 2H, H_{3a}), 2.71 (d, J = 22.9 Hz, 2H, H_{3b}), 1.75 (s, 6H, H_8). [13]C NMR (126 MHz, C_6D_6, 300 K) δ 234.14 (C_{10}, C_9, C_{11}), 149.06 (C_2), 127.68 (C_1), 117.15 ($C_{7'}$), 112.28 ($C_{3'}$), 90.81 (C_6), 89.71 (C_5), 89.47 (C_7), 87.13 (C_4), 42.69 (C_3), 15.33 (C_8).

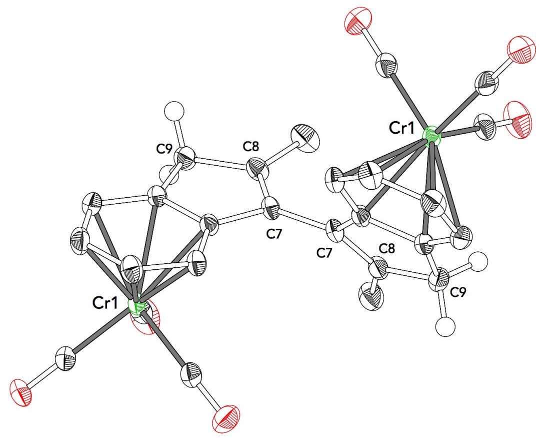

Compound **9d**
Space Group: **C 2/c**
R-Factor (%): **3.67**

N°	*A*	*B*	*Lengths (Å)*
1	C_9	C_8	1.510(2)
2	C_8	C_7	1.347(2)

2.5.12 - Compound 10f.

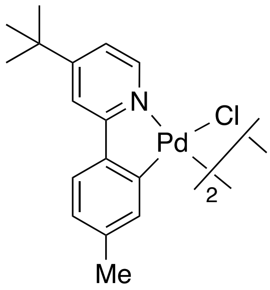

10f

Synthesis:

A mixture containing palladium(II) chloride (1.0 g, 5.64 mmol), potassium chloride (0.841 g, 11.28 mmol), and 4-(*t*-butyl)-2-(*p*-tolyl)pyridine (3.81 g, 16.92 mmol) in 50 mL of degassed methanol was refluxed under argon for 36 h. After the solution was cooled to room temperature, the resulting white suspension was filtered and washed with cold methanol and pentane, and eventually dried under reduced pressure to afford off white colored compound **10f** (1.875 g, 91 % yield).

Characterizations:

Calcd for $C_{32}H_{36}Cl_2N_2Pd_2$: C, 52.48; H, 4.95; N, 3.82. Found: C, 52.31; H, 5.10; N, 3.80. HRMS-ESI (*m/z*): $[M+H]^+$ calcd for $C_{32}H_{36}Cl_2N_2Pd_2$, 731.0398; found, 731.0451.

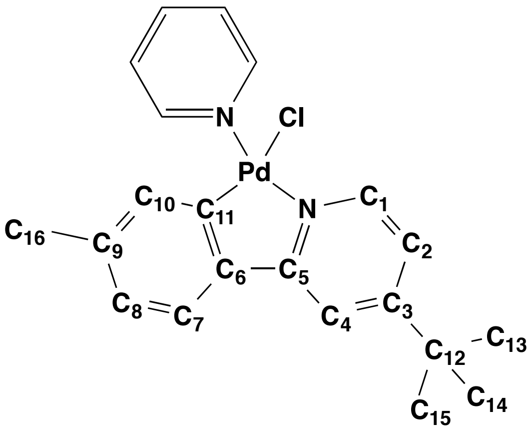

^{1}H NMR (500 MHz, C_6D_6, + Pyr-d_5, 293 K) δ 9.93 (d, J = 6.1 Hz, 1H, H_1), 7.38 (s, 1H, H_4), 7.37 (d, J = 6.4 Hz, 1H, H_7), 6.94 – 6.87 (m, 1H, H_8), 6.44 (dd, J = 6.2, 2.1 Hz, 1H, H_2), 6.31 (s, 1H, H_{10}), 2.05 (s, 3H, H_{16}), 0.93 (s, 9H, H_{14}, H_{15}, H_{13}).

^{13}C NMR (126 MHz, C_6D_6, + Pyr-d_5, 293 K) δ 165.91 (C_5), 162.69 (C_3), 156.87 (C_{11}), 152.62 (C_1), 144.23 (C_6), 139.28 (C_9), 134.08 (C_{10}), 125.47 (C_8), 123.36 (C_7), 119.24 (C_2), 114.67 (C_4), 34.86 (C_{12}), 30.03 (C_{14}, C_{15}, C_{13}), 21.93 (C_{16}).

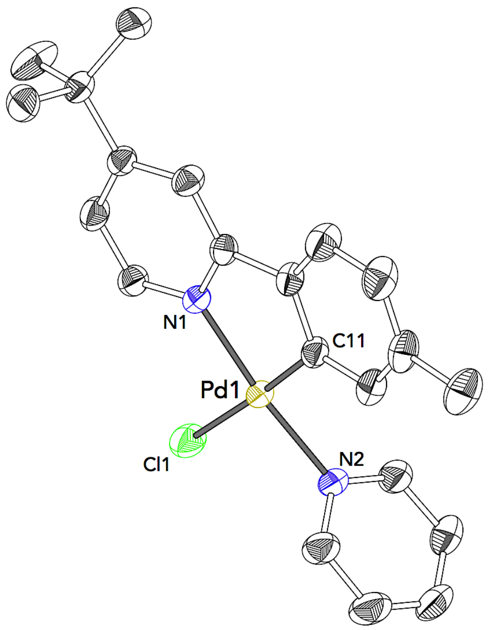

Compound **10f**
Space Group: **P -1**
R-Factor (%): **2.88**

N°	*A*	*B*	*C*	*Lengths (Å)*	*Angles (°)*
1	Pd_1	Cl_1	-	2.4099(5)	-
2	Pd_1	N1	-	2.028(1)	-
3	Pd_1	N_2	-	2.030(2)	-
4	Pd_1	C_{11}	-	1.986(2)	-

2.5.13 - Compound 10i.

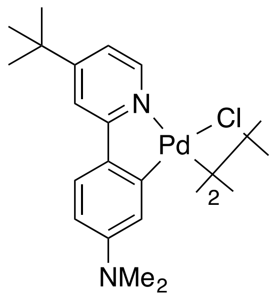

10i

Synthesis:

A mixture containing palladium (II) acetate (1.5 g, 6.68 mmol), and 4-(4-(*tert*-butyl)pyridin-2-yl)-*N*,*N*-dimethylaniline (1.7 g, 6.68 mmol) in 10 mL of dry degassed 1,2-dichloroéthane (DCE) was stirred for 18 h at room temperature. The resulting mixture was filtrated over celite and solvents removed under vacuo. The crude solid was, without further purifications dissolved in a acetone:H_2O (3:1, 20 mL) mixture of solvent and an excess of LiCl was added. After stirring at room temperature for 1 h an extraction with dichloromethane (3 times 15 mL) was performed. The combined organic layers were dried over $MgSO_4$ and the solvent was removed under reduced pressure. Finally recristallisation in a dichloromethane/pentane mixture of solvents led to the expected yellowish compound (2.419 g, 3.06 mmol, 92 % yield).

Characterizations:

Calcd for $C_{34}H_{42}Cl_2N_4Pd_2$•$0.1CH_2Cl_2$: C, 51.26; H, 5.32; N, 7.01. Found: C, 51.13; H, 5.37; N, 6.97. HRMS-ESI (*m/z*): $[M+1Na]^+$ calcd for $C_{34}H_{42}Cl_2N_4Pd_2$, 789.0929; found, 789.0872.

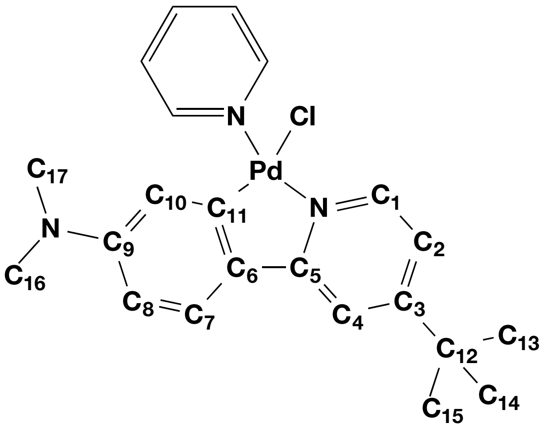

[1]H NMR (400 MHz, C_6D_6 + Pyr-d_5, 298 K) δ 9.90 (d, J = 6.2 Hz, 1H, H_1), 7.43 (d, J = 8.6 Hz, 1H, H_7), 7.33 (d, J = 2.1 Hz, 1H, H_4), 6.44 (dd, J = 8.6, 2.5 Hz, 1H, H_8), 6.40 (dd, J = 6.3, 2.1 Hz, 1H, H_2), 5.66 (d, J = 2.5 Hz, 1H, H_{10}), 2.41 (s, 6H, H_{17}, H_{16}), 0.96 (s, 9H, H_{14}, H_{15}, H_{13}). [13]C NMR (101 MHz, C_6D_6 + Pyr-d_5, 298 K) δ 166.55 (C_5), 162.19 (C_3), 158.24 (C_{11}), 152.30 (C_1), 150.75 (C_9), 134.79 (C_6), 124.42 (C_7), 117.49 (C_2), 116.49 (C_{10}), 113.46 (C_4), 108.49 (C_8), 39.71 (C_{17}, C_{16}), 34.81 (C_{12}), 30.09 (C_{14}, C_{15}, C_{13}).

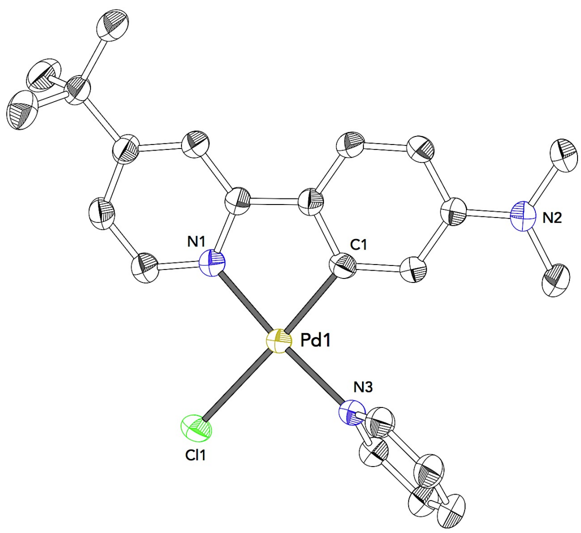

Compound **10i**
Space Group: **P -1**
R-Factor (%): **4.35**

N°	A	B	C	Lengths (Å)	Angles (°)
1	Pd_1	Cl_1	-	2.4116(6)	-
2	Pd_1	N_1	-	2.032(2)	-
3	Pd_1	C_1	-	1.972(2)	-
4	Pd_1	N_3	-	2.040(2)	-

2.5.14 - Standard procedure for the synthesis of 12a, 12c, 12d, 12e, 12g, 14h.

Compound **5a** was dissolved in diethyl ether (2 mL) and treated with *n*-BuLi at −40 °C under argon. The resulting solution was transferred after 10 min via canula to another Schlenk vessel containing a toluene (3 mL) solution of **10**. The resulting solution was stirred for 2 h while the temperature was slowly raised to −10 °C and filtered thrice through Celite to remove palladium black residues. The resulting filtrate was further concentrated to *ca.* 2 mL, and recrystallizations from a dichloromethane/benzene/ pentane mixture of solvents yielded the expected orange solid.

2.5.14.1 - Compound 12a.

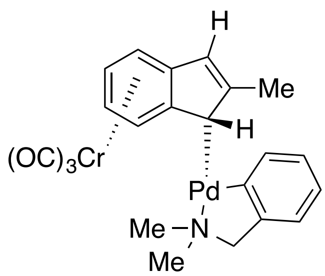

12a

Synthesis:

5a (0.250 g, 0.94 mmol), *n*-BuLi (0.59 mL, 0.94 mmol), **10a** (0.259 g, 0.47 mmol): **12a** (0.233 g, 49 % yield).

Characterizations:

Calcd for $C_{22}H_{21}CrNO_3Pd{\bullet}0.1CH_2Cl_2$: C, 51.61; H, 4.15; N, 2.72. Found: C, 51.67; H, 4.29; N, 2.74. HRMS-ESI (*m/z*): $[M]^+$ calcd for $C_{22}H_{21}CrNO_3Pd$, 504.9961; found, 504.9956. IR (cm^{-1}) ν(CO): 1954 (s), 1877 (s), 1841 (vs).

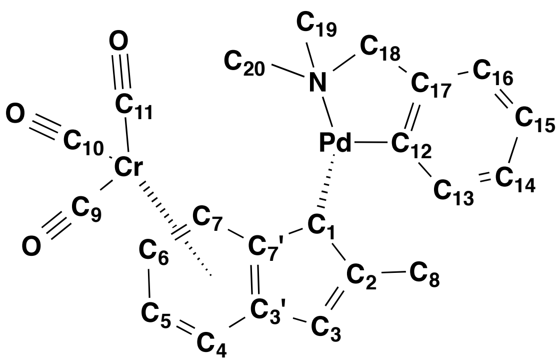

[1]H NMR (500 MHz, C_6D_6, 293 K) δ 7.87 (d, J = 7.3 Hz, 1H, H_{13}), 7.28 (t, J = 7.4 Hz, 1H, H_{14}), 7.19 – 7.17 (m, 1H, H_{15}), 7.03 (d, J = 7.3 Hz, 1H, H_{16}), 5.55 (s, 1H, H_3), 5.23 (d, J = 6.3 Hz, 1H, H_4), 5.17 (d, J = 6.6 Hz, 1H, H_7), 4.94 (t, J = 6.9 Hz, 1H, H_6), 4.45 (s, 1H, H_1), 4.10 (t, J = 6.4 Hz, 1H, H_5), 3.90 (d, J = 12.9 Hz, 1H, H_{18a}), 2.93 (d, J = 12.9 Hz, 1H, H_{18b}), 2.41 (s, 3H, H_{19}), 2.34 (s, 3H, H_{20}), 2.15 (d, J = 1.0 Hz, 3H, H_8). [13]C NMR (126 MHz, C_6D_6, 293 K) δ 239.39 (bs, C_{11}), 237.17 (bs, C_{10}), 234.09 (bs, C_9), 162.11 (C_2), 160.16 (C_{12}), 147.86 (C_{17}), 133.89 (C_{13}), 126.13 (C_{14}), 124.45 (C_{15}), 123.70 (C_{16}), 115.44 ($C_{3'}$), 112.11 (C_3), 107.93 ($C_{7'}$), 94.70 (C_4), 93.39 (C_6), 90.11 (C_7), 87.97 (C_5), 73.86 (C_{18}), 51.14 (C_{19}), 49.70 (C_1), 49.46 (C_{20}), 17.99 (C_8).

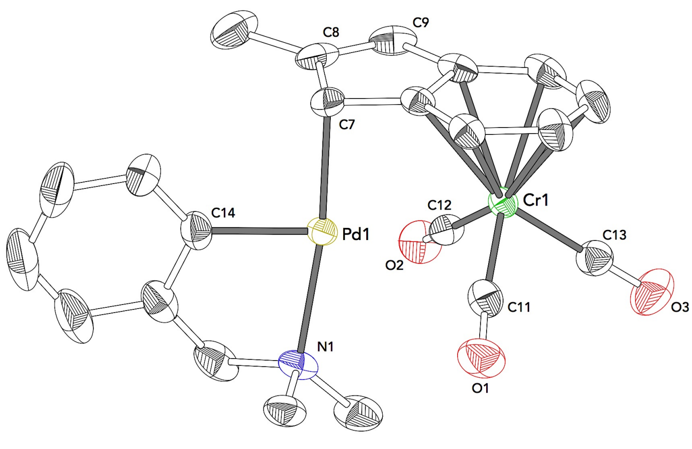

Compound **12a**
Space Group: **P 2_1/c**
R-Factor (%): **2.28**

N°	*A*	*B*	*C*	*Lengths (Å)*	*Angles (°)*
1	Pd_1	Cr_1	-	2.9290(3)	-
2	Pd_1	C_7	-	2.108(2)	-
3	Pd_1	C_8	-	2.913(2)	-
4	Pd_1	C_{14}	-	2.016(2)	-
5	Pd_1	N_1	-	2.206(2)	-
6	Pd_1	C_{11}	-	2.962(2)	-
7	Pd_1	C_{12}	-	2.572(2)	-
8	Cr_1	C_{11}	-	1.835(2)	-
9	Cr_1	C_{12}	-	1.856(2)	-
10	Cr_1	C_{13}	-	1.850(1)	-
11	C_{11}	O_1	-	1.158(2)	-
12	C_{12}	O_2	-	1.157(2)	-
13	C_{13}	O_3	-	1.143(2)	-
14	Cr_1	C_{11}	O_1	-	174.0(2)
15	Cr_1	C_{12}	O_2	-	170.8(2)
16	Cr_1	C_{13}	O_3	-	178.7(2)

2.5.14.2 - Compound 12c.

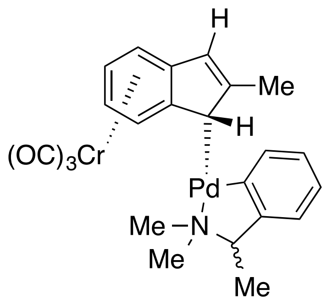

(1*R*)-**12c**
(1*S*)-**12c**

Synthesis:

5a (0.200 g, 0.75 mmol), *n*-BuLi (0.52 mL, 0.83 mmol), **10c** (0.262 g, 0.45 mmol): **12c** (0.233 g, 60 %).

Characterizations:

Calcd for $C_{23}H_{23}CrNO_3Pd$: C, 53.14; H, 4.46; N, 2.69. Found: C, 53.18; H, 4.65; N, 2.69. HRMS-ESI (*m/z*): $[M]^+$ calcd for $C_{23}H_{23}CrNO_3Pd$, 519.0118; found, 519.0169. IR (cm^{-1}) ν(CO): 1941 (s), 1891 (s), 1832 (vs).

(1*S*)-**12c** (mixture of diastereomers): $[\alpha]_D^{20}$ +132.7° (*c* 0.052, CH_2Cl_2); $[\alpha]_D^{20}$ +188.5° (*c* 0.052, benzene). CD (CH_2Cl_2) λ_{max} (Mol. Ellip.) 300 (9012), 330 (-4506), 410 (8405), 470 (-3874); CD (benzene) λ_{max} (Mol. Ellip.) 300 (13750), 330 (-2766), 410 (11009), 470 (-4573).

(1*R*)-**12c** (mixture of diastereomers): $[\alpha]_D^{20}$ -167.3° (*c* 0.052, CH_2Cl_2); $[\alpha]_D^{20}$ -244.2° (*c* 0.052, benzene). CD (CH_2Cl_2) λ_{max} (Mol. Ellip.) 300 (-12811), 330 (3510), 410 (-11483), 470 (4078); CD (benzene) λ_{max} (Mol. Ellip.) 300 (-17554), 330 (2527), 410 (-13498), 470 (4113).

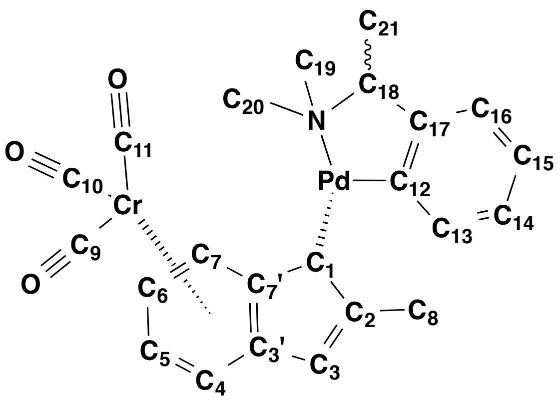

^{1}H NMR (500 MHz, C_6D_6, 300 K) δ 7.79 (d, J = 7.6 Hz, 1H, H_{13}), 7.23 (td, J = 7.4, 1.6 Hz, 1H, H_{14}), 7.13 (td, J = 7.4, 1.2 Hz, 1H, H_{15}), 6.99 (dd, J = 7.3, 1.5 Hz, 1H, H_{16}), 5.61 (s, 1H, H_3), 5.26 (d, J = 6.8 Hz, 1H, H_4), 5.18 (d, J = 6.6 Hz, 1H, H_7), 4.98 (td, J = 6.5, 0.9 Hz, 1H, H_6), 4.39 (s, 1H, H_1), 4.09 (td, J = 6.4, 1.0 Hz, 1H, H_5), 2.90 (q, J = 6.4 Hz, 1H, H_{18}), 2.56 (s, 3H, H_{20}), 2.35 (s, 3H, H_{19}), 2.11 (s, 3H, H_8), 1.57 (d, J = 6.4 Hz, 3H, H_{21}). ^{13}C NMR (126 MHz, C_6D_6, 300 K) δ 239.46 (bs, C_{11}), 237.31 (bs, C_{10}), 235.11 (bs, C_9), 161.83 (C_2), 156.96 (C_{17}), 155.03 (C_{12}), 133.90 (C_{16}), 125.92 (C_{15}), 124.58 (C_{14}), 122.96 (C_{13}), 115.74 ($C_{3'}$), 111.70 (C_3), 108.10 ($C_{7'}$), 94.99 (C_4), 93.65 (C_6), 90.10 (C_7), 87.72 (C_5), 77.88 (C_{18}), 51.36 (C_{19}), 50.76 (C_1), 47.70 (C_{20}), 23.88 (bs, C_{21}), 17.79 (C_8).

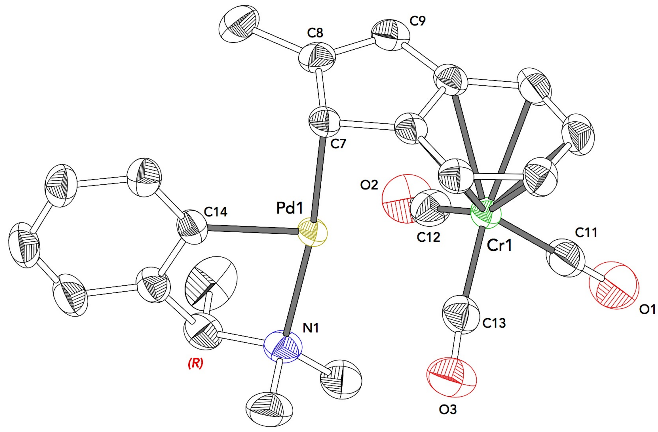

Compound (1*R*)-**12c**
Space Group: **P 2_1**
R-Factor (%): **1.41**
Flack' s parameter x = **0.018(10)**

N°	*A*	*B*	*C*	*Lengths (Å)*	*Angles (°)*
1	Pd_1	Cr_1	-	2.921(2)	-
2	Pd_1	C_7	-	2.113(2)	-
3	Pd_1	C_8	-	2.919(2)	-
4	Pd_1	C_{14}	-	2.018(1)	-
5	Pd_1	N_1	-	2.198(2)	-
6	Pd_1	C_{12}	-	2.548(1)	-
7	Pd_1	C_{13}	-	2.917(1)	-
8	Cr_1	C_{11}	-	1.847(2)	-
9	Cr_1	C_{12}	-	2.857(1)	-
10	Cr_1	C_{13}	-	2.847(2)	-
11	C_{11}	O_1	-	1.148(3)	-
12	C_{12}	O_2	-	1.161(2)	-
13	C_{13}	O_3	-	1.151(2)	-
14	Cr_1	C_{11}	O_1	-	178.2(2)
15	Cr_1	C_{12}	O_2	-	168.8(1)
16	Cr_1	C_{13}	O_3	-	173.4(1)

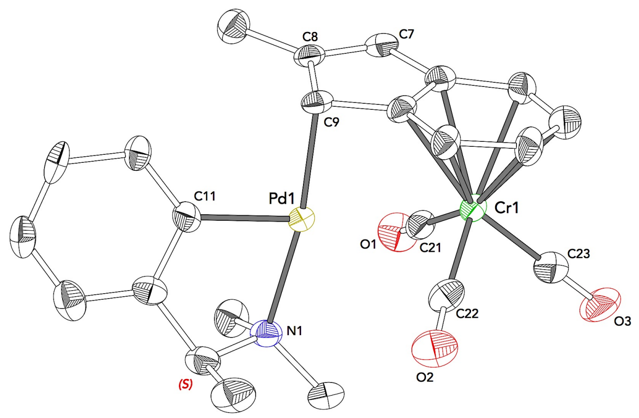

Compound (1*S*)-**12c**
Space Group: **P 2$_1$**
R-Factor (%): **4.04**
Flack' s parameter x = **0.02(3)**

N°	*A*	*B*	*C*	*Lengths (Å)*	*Angles (°)*
1	Pd$_1$	Cr$_1$	-	2.932(1)	-
2	Pd$_1$	C$_9$	-	2.107(5)	-
3	Pd$_1$	C$_8$	-	2.859(5)	-
4	Pd$_1$	C$_{11}$	-	2.001(6)	-
5	Pd$_1$	N$_1$	-	2.185(5)	-
6	Pd$_1$	C$_{21}$	-	2.572(7)	-
7	Pd$_1$	C$_{22}$	-	2.971(6)	-
8	Cr$_1$	C$_{21}$	-	1.844(6)	-
9	Cr$_1$	C$_{22}$	-	1.858(7)	-
10	Cr$_1$	C$_{23}$	-	1.834(7)	-
11	C$_{21}$	O$_1$	-	1.175(8)	-
12	C$_{22}$	O$_2$	-	1.147(8)	-
13	C$_{23}$	O$_3$	-	1.161(8)	-
14	Cr$_1$	C$_{21}$	O$_1$	-	169.4(6)
15	Cr$_1$	C$_{22}$	O$_2$	-	174.8(6)
16	Cr$_1$	C$_{23}$	O$_3$	-	179.4(6)

2.5.14.3 - Compound (1*R*)-12d.

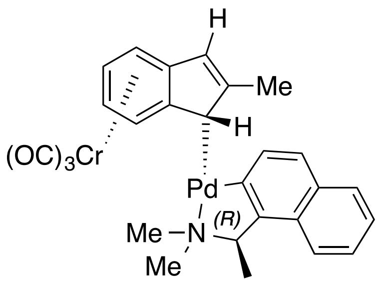

(1*R*)-**12d**

Synthesis:

5a (0.200 g, 0.75 mmol), *n*-BuLi (0.52 mL, 0.83 mmol), **10d** (0.261 g, 0.38 mmol): **12d** (0.313 g, 73 %).

Characterizations:

Calcd for $C_{27}H_{25}CrNO_3Pd$: C, 56.90; H, 4.42; N, 2.46. Found: C, 56.77; H, 4.41; N, 2.29.
HRMS-ESI (*m/z*): $[M+Na]^+$ calcd for $C_{27}H_{25}CrNO_3Pd$, 592.0167; found, 592.0236.
IR (cm^{-1}) ν(CO): 1935 (s), 1865 (s), 1843 (vs).

$[\alpha]_D^{20}$ -267.3° (*c* 0.052, benzene). CD (benzene, 293 K) λ_{max}(Mol. Ellip.) 305 (-5494), 312 (-10368), 322 (-3091), 338 (-11253), 366 (-7094), 413 (-17765), 470 (3442), 530 (-384).

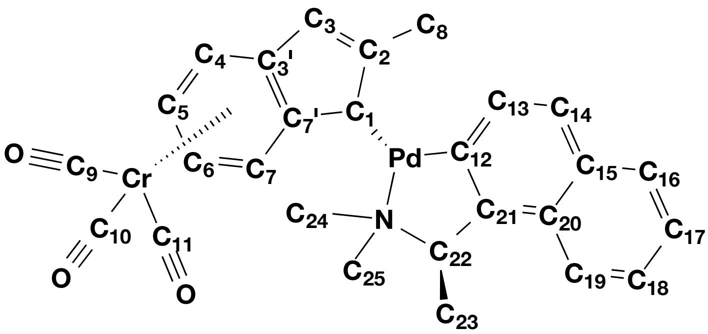

^{1}H NMR (500 MHz, C_6D_6, 293 K) δ 8.06 (d, J = 8.3 Hz, 1H, H_{13}), 7.82 (d, J = 7.6 Hz, 1H, H_{16}), 7.70 (d, J = 8.5 Hz, 1H, H_{14}), 7.58 (d, J = 7.6 Hz, 1H, H_{19}), 7.37 – 7.30 (m, 2H, H_{17}, H_{18}), 5.62 (s, 1H, H_3), 5.27 (d, J = 6.4 Hz, 1H, H_4), 5.17 (d, J = 6.7 Hz, 1H, H_7), 4.98 (td, J = 6.5, 0.9 Hz, 1H, H_6), 4.44 (s, 1H, H_1), 4.08 (td, J = 6.4, 1.1 Hz, 1H, H_5), 3.80 (q, J = 6.4 Hz, 1H, H_{22}), 2.54 (s, 3H, H_{24}), 2.45 (s, 3H, H_{25}), 2.03 (s, 3H, H_8), 1.72 (d, J = 6.4 Hz, 3H, H_{23}). ^{13}C NMR (126 MHz, C_6D_6, 293 K) δ 239.53 (bs, C_{11}), 237.31 (bs, C_{10}), 235.24 (bs, C_9), 161.78 (C_2), 156.99 (C_{12}), 148.46 (C_{21}), 132.74 (C_{13}), 132.39 (C_{15}), 130.09 (C_{20}), 129.40 (C_{16}), 125.88 (C_{17}), 125.55 (C_{14}), 124.13 (C_{18}), 124.10 (C_{19}), 115.90 ($C_{7'}$), 111.54 (C_3), 108.03 ($C_{3'}$), 95.03 (C_4), 93.81 (C_6), 90.17 (C_7), 87.72 (C_5), 74.44 (C_{22}), 51.47 (C_{24}), 51.23 (C_1), 48.16 (C_{25}), 22.30 (C_{23}), 17.73 (C_8).

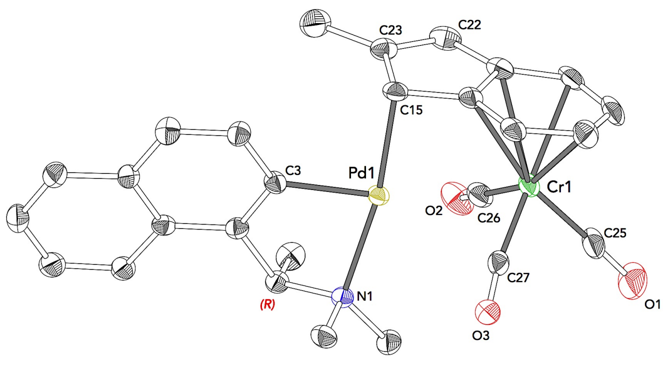

Compound (1*R*)-**12d**
Space Group: **P 2_1**
R-Factor (%): **2.92**
Flack' s parameter x = **0.02(3)**

N°	*A*	*B*	*C*	*Lengths (Å)*	*Angles (°)*
1	Pd_1	Cr_1	-	2.9294(5)	-
2	Pd_1	C_{15}	-	2.117(3)	-
3	Pd_1	C_{23}	-	2.886(3)	-
4	Pd_1	C_3	-	2.017(2)	-
5	Pd_1	N_1	-	2.170(2)	-
6	Pd_1	C_{26}	-	2.700(5)	-
7	Pd_1	C_{27}	-	2.737(5)	-
8	Cr_1	C_{25}	-	1.838(3)	-
9	Cr_1	C_{26}	-	1.861(5)	-
10	Cr_1	C_{27}	-	1.849(5)	-
11	C_{25}	O_1	-	1.148(4)	-
12	C_{26}	O_2	-	1.149(6)	-
13	C_{27}	O_3	-	1.156(6)	-
14	Cr_1	C_{25}	O_1	-	178.4(4)
15	Cr_1	C_{26}	O_2	-	171.3(4)
16	Cr_1	C_{27}	O_3	-	171.3(4)

2.5.14.4 - Compound 12e.

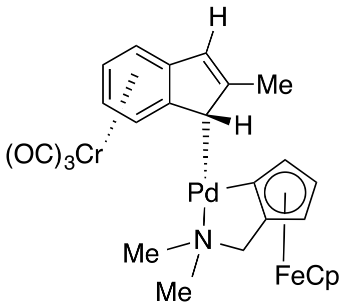

12e

Synthesis:

5a (0.200 g, 0.75 mmol), *n*-BuLi (0.52 mL, 0.83 mmol, **10e** (0.346 g, 0.45 mmol): **12e** (0.397 g, 86 % yield).

Characterizations:

Calcd for $C_{26}H_{25}CrFeNO_3Pd$: C, 50.88; H, 4.11; N, 2.28. Found: C, 50.97; H, 4.37; N, 2.26. HRMS-ESI (*m/z*): $[M]^+$ calcd for $C_{26}H_{25}CrFeNO_3Pd$, 612.9624; found, 612.9593. IR (cm^{-1}) ν(CO): 1941 (s), 1872 (s), 1843 (vs).

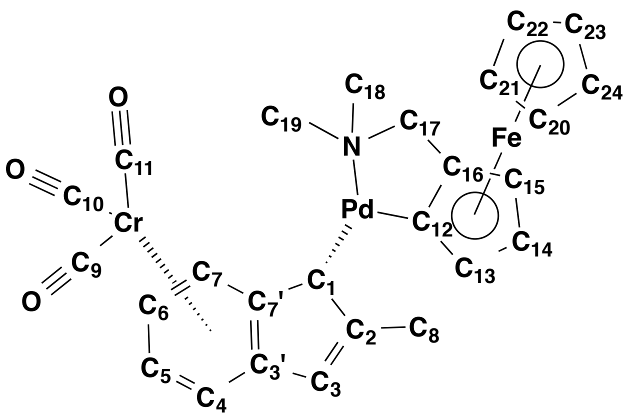

^1H NMR (500 MHz, C_6D_6, 300 K) δ 5.80 – 5.71 (m, 1H, H_4), 5.60 (s, 1H, H_3), 5.22 (d, J = 6.7 Hz, 1H, H_7), 5.00 (td, J = 6.6, 0.9 Hz, 1H, H_6), 4.86 (s, 1H, H_1), 4.39 (dd, J = 2.1, 0.8 Hz, 1H, H_{15}), 4.35 (td, J = 6.4, 1.0 Hz, 1H, H_5), 4.27 (s, 5H, H_{21}, H_{20}, H_{24}, H_{23}, H_{22}), 4.21 – 4.17 (m, 1H, H_{13}), 4.16 (t, J = 2.2 Hz, 1H, H_{14}), 4.03 (d, J = 13.0 Hz, 1H, H_{17a}), 2.51 (d, J = 13.0 Hz, 1H, H_{17b}), 2.40 (d, J = 1.1 Hz, 3H, H_8), 2.37 (s, 3H, H_{19}), 2.24 (s, 3H, H_{18}). ^{13}C NMR (126 MHz, C_6D_6, 300 K) δ 238.88 (bs, C_{11}), 238.12 (bs, C_{10}), 234.84 (bs, C_9), 160.26 (C_2), 116.74 ($C_{3'}$), 112.01 (C_3), 107.46 (C_{16}), 106.73 ($C_{7'}$), 94.82 (C_4), 94.25 (C_{12}), 93.25 (C_6), 91.76 (C_7), 88.47 (C_5), 70.15 (C_{21}, C_{20}, C_{24}, C_{23}, C_{22}), 70.04 (C_{15}), 67.46 (C_{17}), 66.79 (C_{14}), 64.11 (C_{13}), 50.98 (C_{19}), 50.48 (C_{18}), 45.47 (C_1), 17.94 (C_8).

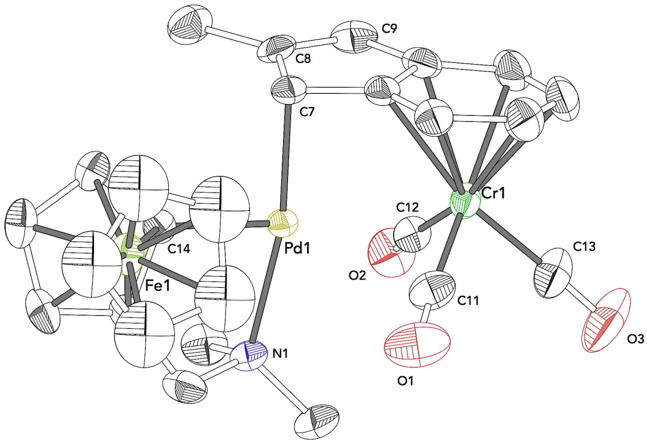

Compound **12e**
Space Group: **P 2_1/c**
R-Factor (%): **4.12**

N°	*A*	*B*	*C*	*Lengths (Å)*	*Angles (°)*
1	Pd_1	Cr_1	-	2.8505(7)	-
2	Pd_1	C_7	-	2.111(3)	-
3	Pd_1	C_8	-	2.835(3)	-
4	Pd_1	C_{14}	-	2.004(3)	-
5	Pd_1	N_1	-	2.212(3)	-
6	Pd_1	C_{11}	-	2.763(4)	-
7	Pd_1	C_{12}	-	2.567(3)	-
8	Cr_1	C_{11}	-	1.839(3)	-
9	Cr_1	C_{12}	-	1.857(4)	-
10	Cr_1	C_{13}	-	1.841(3)	-
11	C_{11}	O_1	-	1.152(4)	-
12	C_{12}	O_2	-	1.157(5)	-
13	C_{13}	O_3	-	1.146(4)	-
14	Cr_1	C_{11}	O_1	-	174.3(3)
15	Cr_1	C_{12}	O_2	-	169.3(3)
16	Cr_1	C_{13}	O_3	-	177.8(4)

2.5.14.5 - Compound 12g.

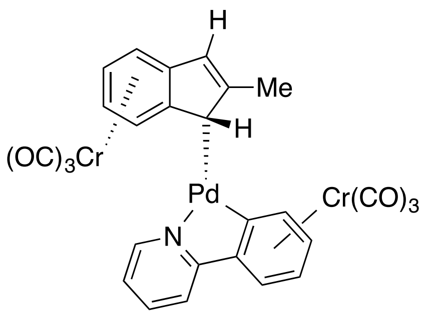

12g

Synthesis:

5a (0.150 g, 0.56 mmol), *n*-BuLi (0.35 mL, 0.56 mmol), **10g** (0.248 g, 0.29 mmol): **12g** (0.203 g, 54 % yield).

Characterizations:

Elem. Anal. Calcd for $C_{27}H_{17}Cr_2NO_6Pd{\bullet}1.25CH_2Cl_2$: C, 44.18; H, 2.56; N, 1.82. Found: C, 44.03; H, 2.92; N, 1.72. HRMS-ESI (*m/z*): $[M+H]^+$ calcd for $C_{27}H_{17}Cr_2NO_6Pd$, 661.8974; found, 661.9021. IR (cm^{-1}) ν(CO): 1874 (s), 1940 (s), 1911 (s), 1876 (vs), 1851 (vs).

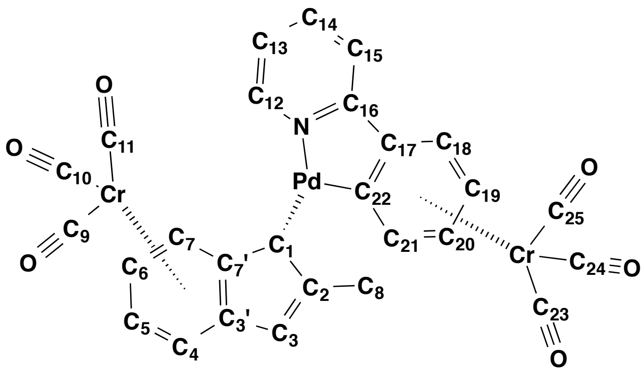

^{1}H NMR (500 MHz, C_6D_6, 293 K) δ 8.47 (d, J = 4.9 Hz, 1H, H_{12}), 6.64 (t, J = 7.7 Hz, 1H, H_{14}), 6.55 (d, J = 7.8 Hz, 1H, H_{15}), 6.13 (t, J = 6.4 Hz, 1H, H_{13}), 5.95 (d, J = 6.5 Hz, 1H, H_4), 5.63 (d, J = 6.2 Hz, 1H, H_{18}), 5.54 (s, 1H, H_3), 5.24 (d, J = 6.7 Hz, 1H, H_{21}), 5.14 - 5.06 (m, 2H, H_7, H_{19}), 4.93 (t, J = 6.4 Hz, 1H, H_6), 4.68 - 4.58 (m, 1H, H_{20}), 4.28 (s, 1H, H_1), 4.18 (t, J = 6.1 Hz, 1H, H_5), 2.23 (d, J = 1.9 Hz, 3H, H_8). ^{13}C NMR (126 MHz, C_6D_6, 293 K) δ 238.30 (bs, C_{11}), 236.69 (bs, C_{10}), 234.83 (C_{23}, C_{25}, C_{24}), 233.61 (bs, C_9), 163.08 (C_{16}), 159.85 (C_2), 153.17 (C_{12}), 137.68 (C_{14}), 127.53 (C_{17}), 123.04 (C_{13}), 118.13 (C_{15}), 114.32 ($C_{3'}$), 114.21 (C_3), 111.09 (C_{22}), 107.99 ($C_{7'}$), 96.38 (C_{19}), 96.28 (C_{18}), 95.12 (C_4), 93.46 (C_6), 92.69 (C_{21}), 90.86 (C_7), 89.20 (C_5), 88.94 (C_{20}), 49.59 (C_1), 17.31 (C_8).

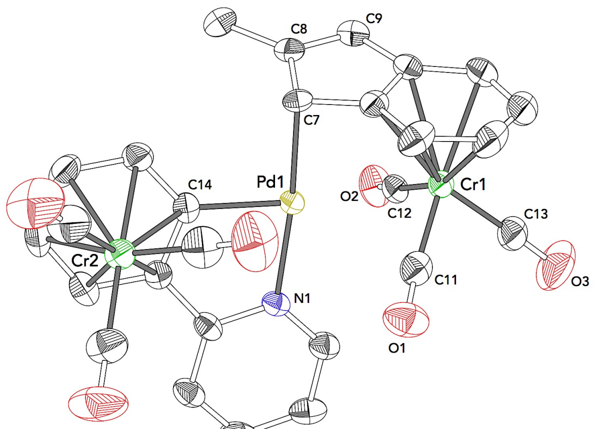

Compound **12g**
Space Group: **P b c a**
R-Factor (%): **4.71**

N°	A	B	C	Lengths (Å)	Angles (°)
1	Pd_1	Cr_1	-	2.8392(5)	-
2	Pd_1	C_7	-	2.112(3)	-
3	Pd_1	C_8	-	2.888(3)	-
4	Pd_1	C_{14}	-	2.013(3)	-
5	Pd_1	N_1	-	2.111(3)	-
6	Pd_1	C_{11}	-	2.806(3)	-
7	Pd_1	C_{12}	-	2.515(3)	-
8	Cr_1	C_{11}	-	1.850(3)	-
9	Cr_1	C_{12}	-	1.849(3)	-
10	Cr_1	C_{13}	-	1.843(4)	-
11	C_{11}	O_1	-	1.153(5)	-
12	C_{12}	O_2	-	1.159(4)	-
13	C_{13}	O_3	-	1.148(5)	-
14	Cr_1	C_{11}	O_1	-	173.3(3)
15	Cr_1	C_{12}	O_2	-	169.4(3)
16	Cr_1	C_{13}	O_3	-	178.1(3)

2.5.14.6 - Compound 14h.

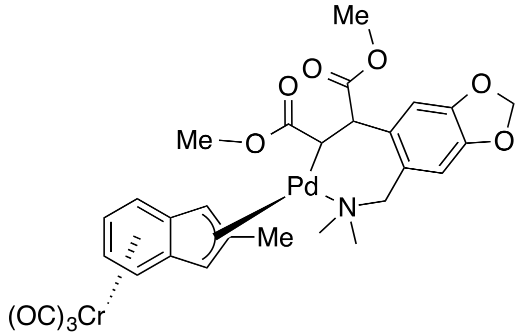

14h

Synthesis:

5a (0.150 g, 0.56 mmol), *n*-BuLi (0.35 mL, 0.56 mmol), **10h** (0.313 g, 0.29 mmol): **14h** (0.160 g, 41 % yield).

Characterizations:

Calcd for $C_{29}H_{27}CrNO_9Pd{\bullet}0.1CH_2Cl_2$: C, 49.90; H, 3.91; N, 2.00. Found: C, 49.90; H, 4.23; N, 1.85. HRMS-ESI (*m/z*): $[M]^+$ calcd for $C_{29}H_{27}CrNO_9Pd$, 691.0126; found, 691.0139. IR (cm^{-1}) ν(CO): 1942 (s), 1851 (vs), 1695 (vs).

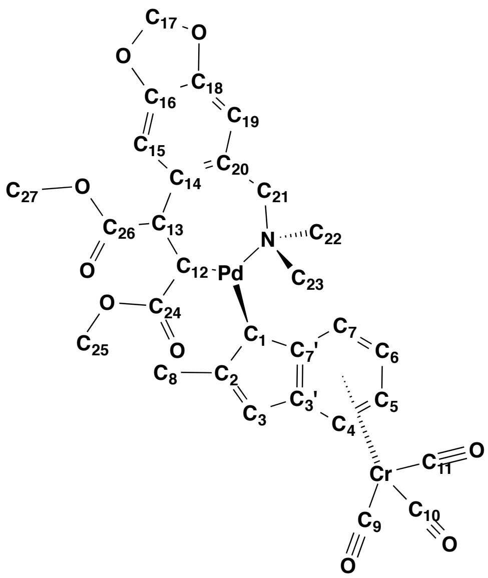

^{1}H NMR (600 MHz, C_6D_6, 298 K) δ 6.91 (s, 1H, H_{15}), 6.07 (s, 1H, H_{19}), 5.32 (dd, J = 9.8, 1.2 Hz, 2H, H_{17}), 4.76 (d, J = 2.0 Hz, 1H, H_3), 4.50 (d, J = 6.1 Hz, 1H, H_4), 4.30 (t, J = 5.6 Hz, 2H, H_5, H_6), 4.27 (d, J = 5.9 Hz, 1H, H_7), 4.11 (d, J = 1.5 Hz, 1H, H_1), 3.69 (s, 3H, H_{25}), 3.43 (s, 3H, H_{27}), 3.40 (d, J = 11.8 Hz, 1H, H_{21a}), 2.10 (s, 3H, H_8), 2.07 (s, 3H, H_{22}), 1.86 (s, 3H, H_{23}), 1.82 (d, J = 11.9 Hz, 1H, H_{21b}). ^{13}C NMR (151 MHz, C_6D_6, 298 K) δ 236.51 (C_{10}, C_{11}, C_9), 176.90 (C_{12}), 173.82 (C_{24}), 162.63 (C_{26}), 147.41 (C_{16}), 145.93 (C_{18}), 137.38 (C_2), 135.83 (C_{20}), 129.22 (C_{13}), 127.41 (C_{14}), 112.61 (C_{15}), 110.38 (C_{19}), 108.45 ($C_{3'}$), 104.74 ($C_{7'}$), 101.20 (C_{17}), 88.97 (C_7), 87.73 (C_5), 85.67 (C_4), 83.20 (C_1), 81.68 (C_6), 66.50 (C_3), 64.68 (C_{21}), 53.53 (C_{22}), 52.30 (C_{23}), 51.40 (C_{27}), 51.02 (C_{25}), 16.88 (C_8).

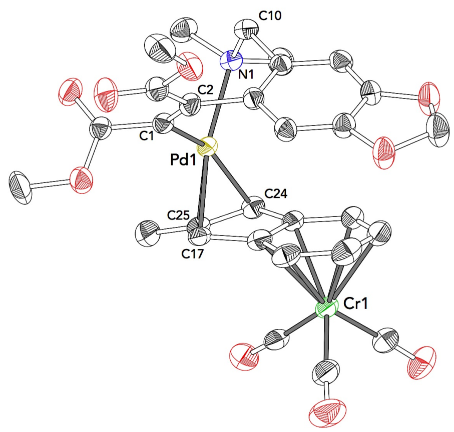

Compound **14h**
Space Group: **P -1**
R-Factor (%): **3.62**

N°	*A*	*B*	*C*	*Lengths (Å)*	*Angles (°)*
1	Pd_1	C_{17}	-	2.132(2)	-
2	Pd_1	C_{24}	-	2.319(2)	-
3	Pd_1	C_{25}	-	2.177(2)	-
4	Pd_1	C_1	-	2.011(2)	-
5	Pd_1	N_1	-	2.142(2)	-

2.5.15 - Compounds 12b and 14b.

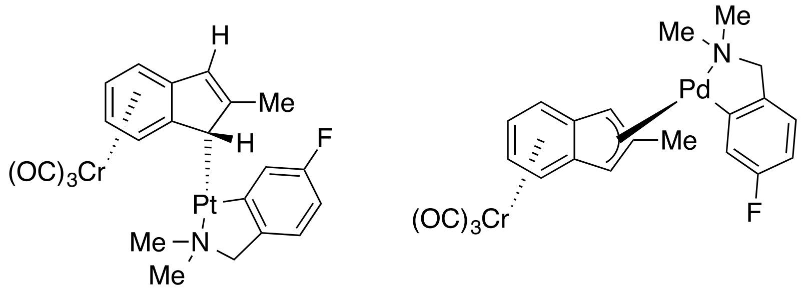

12b **14b**

Synthesis:

5a (0.200 g, 0.75 mmol) was dissolved in an ether/toluene mixture (2:1, 3 mL) and treated with 1.1 equiv of *n*-BuLi (0.52 mL, 0.83 mmol) at −40 °C under argon. The resulting anion solution was transferred after 10 min via canula to another Schlenk vessel containing a toluene (3 mL) solution of **10b** (0.221 g, 0.38 mmol). The resulting solution was stirred 1 h while temperature was slowly raised up to −5 °C and filtered through Celite. The dark red filtrate was concentrated to *ca.* 2 mL and recrystallization from a CH_2Cl_2/*n*-pentane mixture of solvents gave a pure orange solid (**12b**, 0.089 g, 23 %). The reddish solid retained on the top of the Celite pad was recovered with dichloromethane and recrystallized from *n*-pentane to afford **14b** as an orange solid (0.085 g, 22 %).

Characterizations:

Compound 12b:

Calcd for $C_{22}H_{20}CrFNO_3Pd{\bullet}0.1CH_2Cl_2$: C, 49.87; H, 3.82; N, 2.63. Found: C, 49.89; H, 4.01; N, 2.83. HRMS-ESI (*m/z*): $[M]^+$ calcd for $C_{22}H_{20}CrFNO_3Pd$, 522.9867; found, 522.9889. IR (cm^{-1}) ν(CO): 1956(s), 1886(s), 1847(vs).

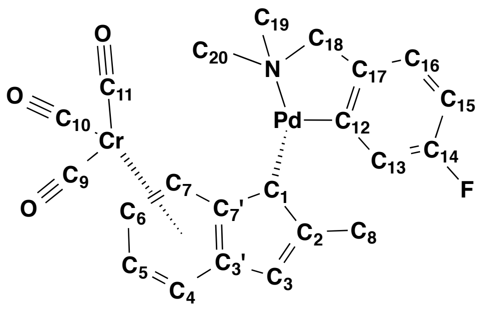

^{1}H NMR (500 MHz, C_6D_6, 293 K) δ 7.70 (dd, J = 9.2, 2.4 Hz, 1H, H_{13}), 6.94 – 6.76 (m, 2H, H_{15}, H_{16}), 5.48 (s, 1H, H_3), 5.14 (d, J = 6.4 Hz, 1H, H_4), 5.11 (d, J = 6.6 Hz, 1H, H_7), 4.91 (td, J = 6.5, 0.9 Hz, 1H, H_6), 4.21 (s, 1H, H_1), 4.08 (td, J = 6.4, 1.0 Hz, 1H, H_5), 3.77 (d, J = 12.8 Hz, 1H, H_{18a}), 2.86 (d, J = 12.8 Hz, 1H, H_{18b}), 2.35 (s, 3H, H_{19}), 2.29 (s, 3H, H_{20}), 2.07 (d, J = 1.1 Hz, 3H, H_8). ^{13}C NMR (126 MHz, C_6D_6, 293 K) δ 239.20 (bs, C_9), 237.01 (bs, C_{10}), 233.85 (bs, C_{11}), 163.02 (d, J = 1.9 Hz, C_{12}), 161.86 (C_2), 161.55 (d, J = 247.6 Hz, C_{14}), 143.38 (d, J = 2.6 Hz, C_{17}), 124.41 (d, J = 7.1 Hz, C_{16}), 120.37 (d, J = 17.7 Hz, C_{13}), 115.21 ($C_{3'}$), 112.65 (C_3), 110.70 (d, J = 22.0 Hz, C_{15}), 107.74 ($C_{7'}$), 94.65 (C_4), 93.43 (C_6), 90.32 (C_7), 88.22 (C_5), 73.17 (d, J = 0.8 Hz, C_{18}), 50.96 (C_{20}), 49.49 (C_1), 49.25 (C_{19}), 17.80 (C_8). ^{19}F NMR (282 MHz, C_6D_6, 298 K) δ -116.7.

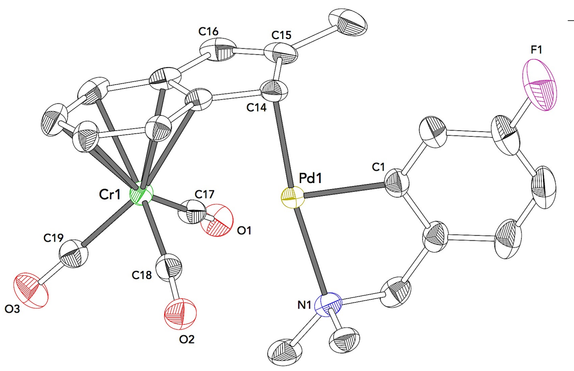

Compound **12b**
Space Group: **P 2_1/c**
R-Factor (%): **2.75**

N°	A	B	C	Lengths (Å)	Angles (°)
1	Pd_1	Cr_1	-	2.9125(5)	-
2	Pd_1	C_{14}	-	2.111(3)	-
3	Pd_1	C_{15}	-	2.908(3)	-
4	Pd_1	C_1	-	2.017(2)	-
5	Pd_1	N_1	-	2.203(2)	-
6	Pd_1	C_{17}	-	2.604(2)	-
7	Pd_1	C_{18}	-	2.867(2)	-
8	Cr_1	C_{17}	-	1.854(3)	-
9	Cr_1	C_{18}	-	1.840(3)	-
10	Cr_1	C_{19}	-	1.855(2)	-
11	C_{17}	O_1	-	1.160(3)	-
12	C_{18}	O_2	-	1.153(3)	-
13	C_{19}	O_3	-	1.142(3)	-
14	Cr_1	C_{17}	O_1	-	171.7(2)
15	Cr_1	C_{18}	O_2	-	174.1(2)
16	Cr_1	C_{19}	O_3	-	178.6(2)

Compound 14b:

Calcd for $C_{22}H_{20}CrFNO_3Pd{\bullet}0.25CH_2Cl_2$: C, 49.03; H, 3.79; N, 2.57. Found: C, 48.70; H, 3.95; N, 2.76. HRMS-ESI (*m/z*): $[M]^+$ calcd for $C_{22}H_{20}CrFNO_3Pd$, 522.9867; found, 522.9924. IR (cm^{-1}) ν(CO): 1933(s), 1843(vs).

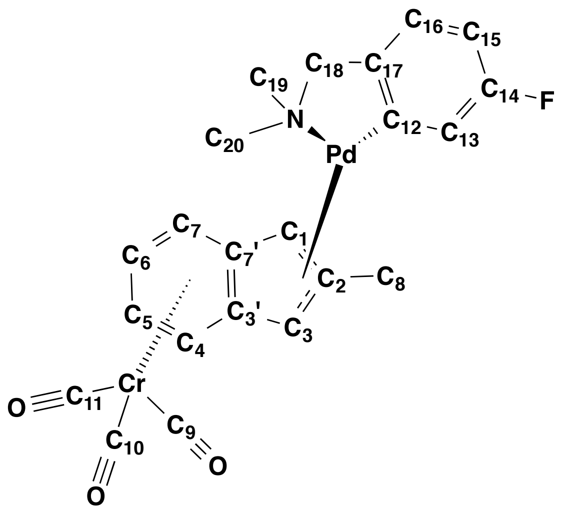

^{1}H NMR (500 MHz, C_6D_6, 293 K) δ 7.33 (dd, J = 11.1, 2.7 Hz, 1H, H_{13}), 6.77 – 6.65 (m, 1H, H_{15}), 6.46 (dd, J = 7.8, 5.2 Hz, 1H, H_{16}), 5.00 – 4.87 (m, 2H, H_4, H_7), 4.47 (t, J = 6.1 Hz, 1H, H_6), 4.41 (s, 1H, H_3), 4.38 (t, J = 6.2 Hz, 1H, H_5), 4.02 (s, 1H, H_1), 2.82 (d, J = 13.8 Hz, 1H, H_{18a}), 2.58 (d, J = 13.4 Hz, 1H, H_{18b}), 2.14 (s, 3H, H_8), 1.89 (s, 3H, H_{19}), 1.77 (s, 3H, H_{20}). ^{13}C NMR (126 MHz, C_6D_6, 293 K) δ 236.83 (C_{10}, C_{11}, C_9), 160.66 (d, J = 249.3 Hz, C_{14}), 156.31 (d, J = 2.9 Hz, C_{12}), 143.80 (d, J = 2.5 Hz, C_{17}), 139.10 (C_2), 127.04 (d, J = 17.0 Hz, C_{13}), 122.72 (d, J = 7.1 Hz, C_{16}), 111.50 (d, J = 22.1 Hz, C_{15}), 108.25 ($C_{3'}$), 107.80 ($C_{7'}$), 89.23 (C_5), 88.71 (C_6), 83.84 (C_4), 83.30 (C_7), 83.23 (C_3), 71.13 (C_{18}), 65.74 (C_1), 54.15 (C_{20}), 52.23 (C_{19}), 17.43 (C_8). ^{19}F NMR (282 MHz, C_6D_6, 298 K) δ -116.6.

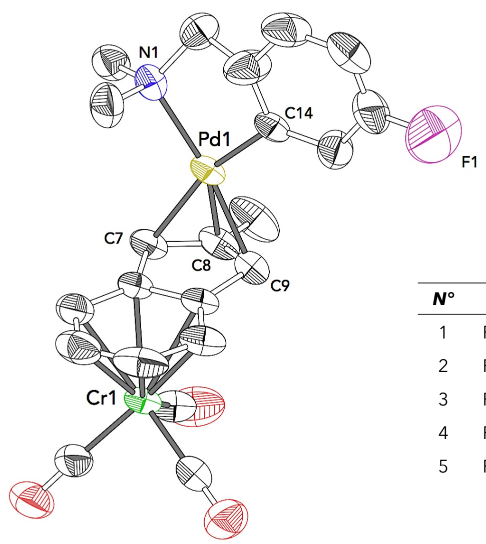

Compound **14b**
Space Group: **P 2_1/c**
R-Factor (%): **3.61**

N°	*A*	*B*	*C*	*Lengths (Å)*	*Angles (°)*
1	Pd_1	C_7	-	2.351(3)	-
2	Pd_1	C_8	-	2.189(3)	-
3	Pd_1	C_9	-	2.161(2)	-
4	Pd_1	C_{14}	-	2.010(4)	-
5	Pd_1	N_1	-	2.109(2)	-

2.5.16 - Compound 12f.

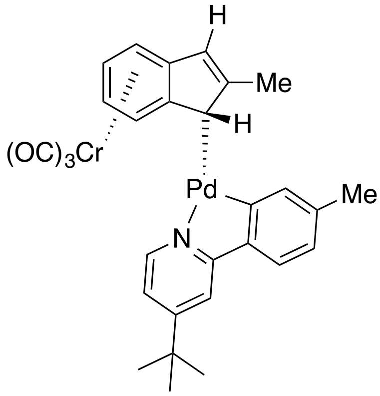

12f

Synthesis:

Compound **5a** (0.200 g, 0.75 mmol) was dissolved in tetrahydrofurane (THF) (5 mL) and treated with *n*-BuLi (0.52 mL, 0.83 mmol) at −40 °C under argon. The resulting solution was transferred after 10 min via canula to another Schlenk vessel containing 0.7 equiv. of **10f** (0.385 g, 0.53 mmol). The solution was stirred for 3 h while temperature was slowly raised to room temperature. Chilled toluene (5 mL) was added to the solution and the resulting suspension was filtered through Celite to remove residues of palladium black. The filtrate was further concentrated to *ca.* 2 mL and *n*-pentane was added to induce precipitation. The supernatant was removed and evaporation of the solvents under reduced pressure afforded **12f** as an orange solid (0.280 g, 63 % yield), which displayed low solubility in almost all common solvents.

Characterizations:

Elem. Anal. Calcd for $C_{29}H_{27}CrNO_3Pd{\bullet}0.6CH_2Cl_2$: C, 54.96; H, 4.39; N, 2.17. Found: C, 54.98; H, 4.60; N, 2.19. HRMS-ESI (*m/z*): $[M+H]^+$ calcd for $C_{29}H_{27}CrNO_3Pd$, 596.0504; found, 596.0506. IR (cm^{-1}) ν(CO): 1948 (s), 1887 (s), 1843 (vs).

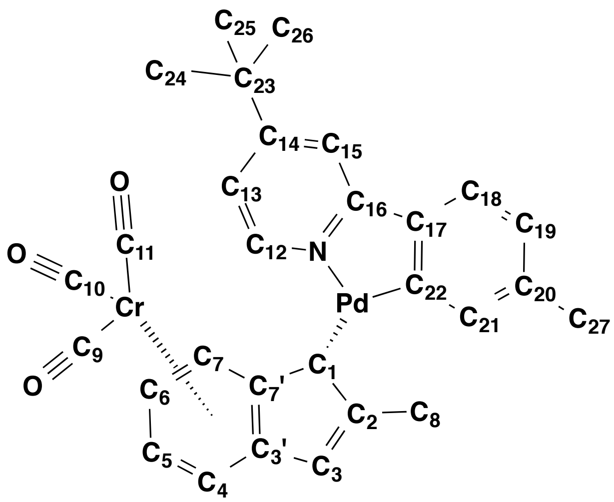

^{1}H NMR (500 MHz, $CDCl_3$, 300 K) δ 8.25 (d, J = 6.0 Hz, 1H, H_{12}), 7.79 (s, 1H, H_{21}), 7.72 (d, J = 1.8 Hz, 1H, H_{15}), 7.62 (d, J = 7.9 Hz, 1H, H_{18}), 7.06 (dd, J = 6.1, 2.1 Hz, 1H, H_{13}), 7.02 (d, J = 7.9 Hz, 1H, H_{19}), 6.04 (d, J = 6.4 Hz, 1H, H_4), 5.96 (d, J = 6.5 Hz, 1H, H_7), 5.88 (t, J = 6.5 Hz, 1H, H_6), 5.79 (s, 1H, H_3), 5.14 – 5.06 (m, 1H, H_5), 4.71 (s, 1H, H_1), 2.47 (s, 3H, H_{27}), 2.40 – 2.37 (m, 3H, H_8), 1.33 (s, 9H, H_{25}, H_{26}, H_{24}). ^{13}C NMR (126 MHz, $CDCl_3$, 300 K) δ 241.37 (bs, C_{11}), 237.59 (bs, C_{10}), 233.45 (bs, C_9), 165.07 (C_{16}), 162.90 (C_{20}), 162.01 (C_{14}), 161.74 (C_2), 152.69 (C_{12}), 144.67 (C_{17}), 139.57 (C_{22}), 135.67 (C_{21}), 125.27 (C_{19}), 124.17 (C_{18}), 119.62 (C_{13}), 115.45 (C_{15}), 115.42 ($C_{7'}$), 112.65 (C_3), 108.36 ($C_{3'}$), 95.16 (C_4), 93.46 (C_6), 90.13 (C_7), 88.10 (C_5), 50.48 (C_1), 35.27 (C_{23}), 30.50 (C_{25}, C_{26}, C_{24}), 22.49 (C_{27}), 17.69 (C_8).

2.5.17 - Compound 13a.

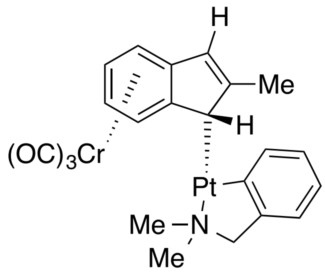

Synthesis:

Compounds **13a** (0.282 g, 0.66 mmol) was stirred in chloroform for 13 h in the presence of excess amounts of Me_2S. The reaction mixture was subsequently filtered through Celite, and the filtrate was stripped of solvent under reduced pressure. The resulting light yellow residue was thoroughly dried under reduced pressure and subsequently dissolved in dry toluene (2 mL). The resulting solution was hence treated with a fresh solution of complex **5b** prepared from **5a** (0.160 g, 0.60 mmol) by treatment with *n*-BuLi (0.41 mL, 0.66 mmol), and the resulting mixture was slowly stirred and warmed from −40 °C to room temperature in 4 h. The resulting reaction medium was filtered through Celite to remove insoluble materials and strip the solvent. The solid residue was recrystallized from a benzene/pentane mixture to afford orange crystals of compound **13a** (0.043 g, 12 % yield).

Characterizations:

Calcd for $C_{22}H_{21}CrNO_3Pt$•0.3 CH_2Cl_2: C, 43.20; H, 3.51; N, 2.26. Found: C, 43.02; H, 3.80; N, 2.23. HRMS-ESI (*m/z*): $[M+H]^+$ calcd for $C_{22}H_{21}CrNO_3Pt$, 595.0647; found, 595.0671. IR (cm^{-1}) ν(CO): 1953(s), 1872(s), 1818(s).

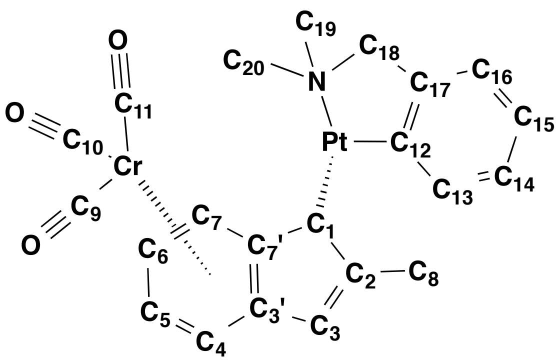

^{1}H NMR (600 MHz, C_6D_6, 298 K) δ 7.95 (dd, J = 75.2, 7.5 Hz, 1H, H_{13}), 7.34 – 7.27 (m, 1H, H_{14}), 7.24 (t, J = 7.1 Hz, 1H, H_{15}), 7.11 (d, J = 7.2 Hz, 1H, H_{16}), 5.57 – 5.47 (m, 2H, H_3, H_7), 5.36 (d, J = 6.5 Hz, 1H, H_4), 4.96 (d, J = 134.7 Hz, 1H, H_1), 4.70 (t, J = 6.5 Hz, 1H, H_5), 4.30 (t, J = 6.3 Hz, 1H, H_6), 3.78 (d, J = 12.7 Hz, 1H, H_{18a}), 3.00 (dd, J = 62.0, 12.7 Hz, 1H, H_{18b}), 2.49 (s, 3H, H_{19}), 2.46 (s, 3H, H_{20}), 2.16 (s, 3H, H_8). ^{13}C NMR (126 MHz, C_6D_6, 293 K) δ 240.87 (bs, C_{11}), 238.57 (bs, C_{10}), 236.87 (bs, C_9), 165.84 (C_2), 155.31 (C_{12}), 148.10 ($C_{3'}$), 131.33 (C_{13}), 126.50 (C_{14}), 124.25 (C_{15}), 123.47 (C_{16}), 116.96 ($C_{7'}$), 111.79 (C_{17}), 111.49 (C_3), 94.48 (C_7), 93.81 (C_5), 91.77 (C_4), 91.14 (C_6), 75.68 (C_{18}), 51.90 (C_{19}), 50.46 (C_{20}), 36.16 (C_1), 17.57 (C_8). ^{195}Pt NMR (86 MHz, Tol, 298 K) δ -2524.5.

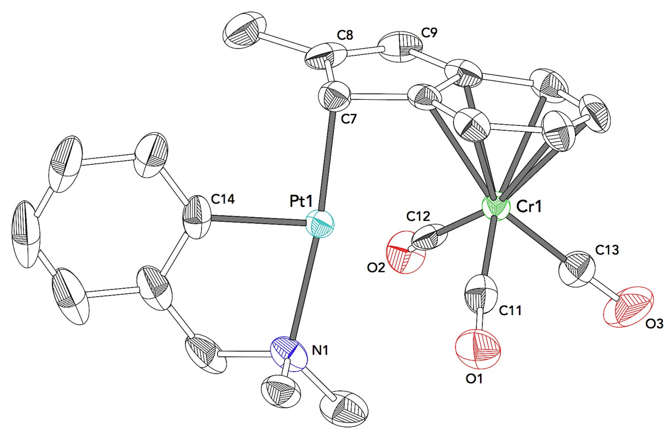

Compound **13a**
Space Group: **P 2_1/c**
R-Factor (%): **4.01**

N°	*A*	*B*	*C*	*Lengths (Å)*	*Angles (°)*
1	Pd_1	Cr_1	-	2.8834(6)	-
2	Pd_1	C_7	-	2.099(5)	-
3	Pd_1	C_8	-	2.929(5)	-
4	Pd_1	C_{14}	-	2.017(3)	-
5	Pd_1	N_1	-	2.183(4)	-
6	Pd_1	C_{11}	-	3.024(4)	-
7	Pd_1	C_{12}	-	2.408(4)	-
8	Cr_1	C_{11}	-	1.841(5)	-
9	Cr_1	C_{12}	-	1.876(5)	-
10	Cr_1	C_{13}	-	1.844(3)	-
11	C_{11}	O_1	-	1.155(6)	-
12	C_{12}	O_2	-	1.161(6)	-
13	C_{13}	O_3	-	1.144(4)	-
14	Cr_1	C_{11}	O_1	-	174.8(4)
15	Cr_1	C_{12}	O_2	-	163.2(4)
16	Cr_1	C_{13}	O_3	-	178.4(4)

2.5.18 - Compounds (p*R*)-5a and (p*S*-5a).

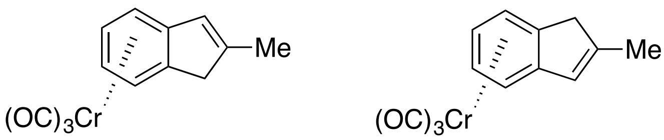

(p*R*)-**5a** (p*S*)-**5a**

Synthesis:

A solution of (1*R*)-**12c** or (1*S*)-**12c** (0.100 g, 0.09 mmol) and acetic acid (0.1 mL, 1.73 mmol) in dry dichloromethane (2 mL) was stirred under argon at room temperature during 15 min. The solvent was then removed under vacuo, and the residue was treated by flash chromatography on silica gel using a mixture of CH_2Cl_2 and pentane (5:5) as eluent. The product was recovered as a yellow-colored powder upon removal of the solvents under reduced pressure.

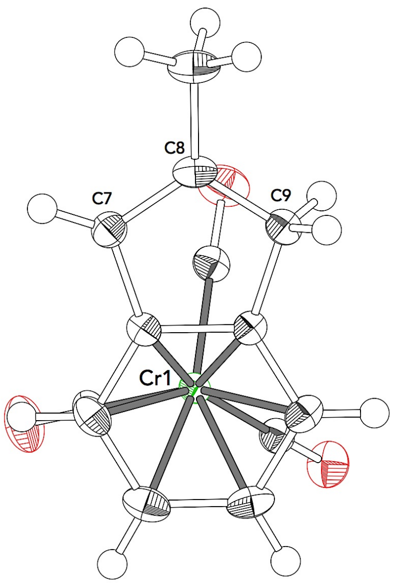

Compound (p*R*)-**5a**
Space Group: **P 2_1 2_1 2_1**
R-Factor (%): **2.47**
Flack' s parameter x = **0.001(16)**

N°	*A*	*B*	*Lengths (Å)*
1	C_7	C_8	1.415(2)
2	C_8	C_9	1.436(2)

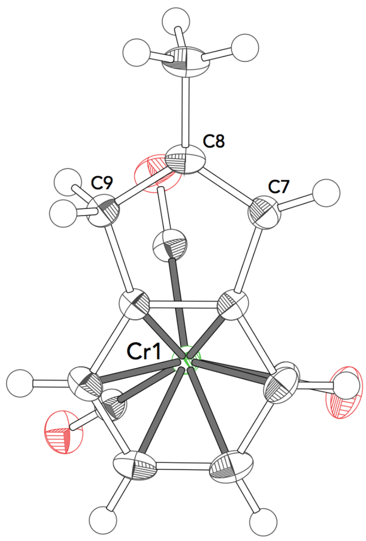

Compound (p*S*)-**5a**
Space Group: **P 2_1 2_1 2_1**
R-Factor (%): **2.29**
Flack' s parameter x = -**0.005(14)**

N°	*A*	*B*	*Lengths (Å)*
1	C_7	C_8	1.408(2)
2	C_8	C_9	1.444(2)

2.5.19 - Benzylic deuteration of 5a.

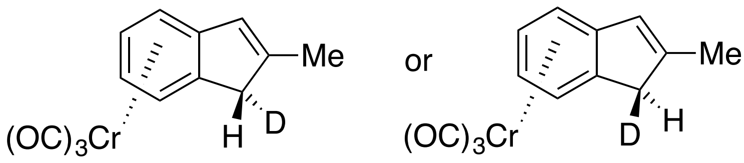

Compound **5a** (0.200 g, 0.75 mmol) was dissolved in diethyl ether (2 mL) and treated with 1.1 equiv of *n*-BuLi (0.52 mL, 0.83 mmol) at −40 °C under argon. Deuterium oxide (0.30 mL, 15 mmol) was added after 10 min to the resulting anion solution, and the reaction mixture was stirred during 3 h while temperature was warmed to 0 °C. Solvent was then removed under vacuum and the resulting residue was purified by silica gel column chromatography using a mixture of CH_2Cl_2 and pentane (1:1) as eluent. Evaporation of the yellow band led to the pure solid-state compound d_1-**5a** (107 mg, 54 % yield), which was analyzed by ^{1}H NMR spectroscopy.

2.5.20 - Deutero-depalladation of (1*R*)-12c.

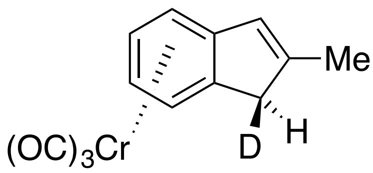

Compound (1*R*)-**12c** (10 mg, 0.02 mmol), CD_3CO_2D (0.01 mL, 0.15 mmol) in dry dichloromethane (2 mL) was stirred under argon at room temperature during 30 min. The solvent was then removed under reduced pressure. The residue was dissolved in a minimum amount of CH_2Cl_2 and eluted through a short column of silica gel with a mixture of CH_2Cl_2 and pentane (1:1). The yellow band containing d_1-**5a** was recovered, evaporated to dryness (2 mg, 39 % yield), and further analyzed by ^{1}H NMR.

2.5.21 - Compound 15a.

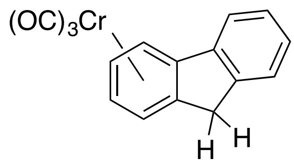

15a

Synthesis:

$Cr(CO)_6$ (5.0 g, 22.72 mmol), fluorene (11.330 g, 68.16 mmol), THF (15 mL), and *n*-dibutylether (150 mL) were gently refluxed for 116 h under a permanent flow of argon. The resulting orange/red solution was evaporated to dryness and the resulting residue was adsorbed on silica gel. Chromatographic separation was performed on silica gel using a mixture of CH_2Cl_2 and pentane (1:1 to 1:0) as eluent. The product was eluted as a yellow solution, which afforded a yellow solid upon removal of the solvents under reduced pressure (4.624 g, 15.30 mmol, 67 %).

Characterizations:

Calcd for $C_{16}H_{10}CrO_3{\bullet}CH_2Cl_2$: C, 62.23; H, 3.31. Found: C, 62.61; H, 3.36. HRMS-ESI (*m/z*): $[M+1Na]^+$ calcd for $C_{16}H_{10}CrO_3$, 324.9927; found, 324.9886. IR (cm^{-1}) ν(CO): 1942 (s), 1885 (s) 1850 (vs).

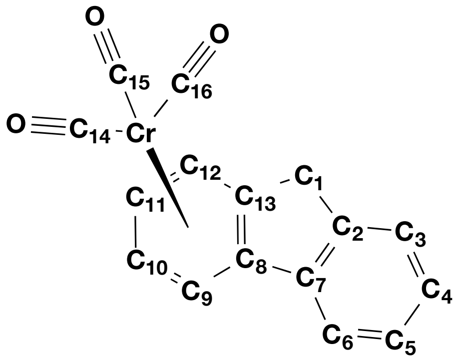

^{1}H NMR (300 MHz, C_6D_6, 298 K) δ 7.10 – 6.94 (m, 4H, H_3, H_6, H_5, H_4), 5.23 (dd, J = 4.7, 2.7 Hz, 1H, H_9), 4.90 (dd, J = 4.4, 2.8 Hz, 1H, H_{12}), 4.49 (dd, J = 4.7, 2.7 Hz, 2H, H_{10}, H_{11}), 3.39 (d, J = 21.4 Hz, 1H, H_{1a}), 3.08 (d, J = 21.5 Hz, 1H, H_{1b}). ^{13}C NMR (126 MHz, C_6D_6, 293 K) δ 233.67 (C_{15}, C_{16}, C_{14}), 142.16 (C_7), 138.84 (C_2), 128.57 (C_4), 127.46 (C_6), 125.11 (C_5), 120.20 (C_3), 112.50 (C_{13}), 110.74 (C_8), 91.12 (C_{10}), 90.59 (C_{11}), 90.13 (C_9), 86.11 (C_{12}), 36.59 (C_1).

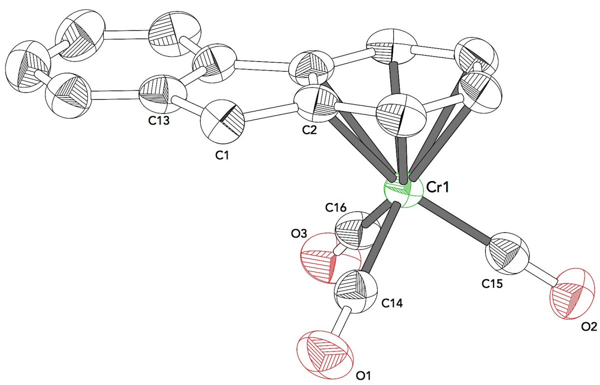

Compound **15a**
Space Group: **P 2_1 2_1 2_1**
R-Factor (%): **3.87**

N°	*A*	*B*	*C*	*Lengths (Å)*	*Angles (°)*
1	Cr_1	C_{14}	-	1.840(3)	-
2	Cr_1	C_{15}	-	1.833(3)	-
3	Cr_1	C_{16}	-	1.839(3)	-
4	C_1	C_2	-	1.513(4)	-
5	C_1	C_{13}	-	1.504(4)	-
6	C_{14}	O_1	-	1.156(4)	-
7	C_{15}	O_2	-	1.155(4)	-
8	C_{16}	O_3	-	1.153(4)	-
9	Cr_1	C_{14}	O_1	-	179.2(3)
10	Cr_1	C_{15}	O_2	-	178.7(3)
11	Cr_1	C_{16}	O_3	-	178.2(3)
12	C_{14}	Cr_1	C_{16}	-	88.4(1)

2.5.22 - Standard procedure for the synthesis of 16 and for the isomerization process of 16 into 17.

Standard procedure for the synthesis of bimetallic compounds 16.

Tricarbonyl(η^6-fluorene)chromium(0) was dissolved in diethyl ether (5 mL) and treated with *n*-BuLi at -40°C under argon. The resulting solution was transferred after 30 min *via* canula to another Schlenk vessel containing a diethyl ether (3 mL) solution of the corresponding [Pd(μ-Cl)(Metalacycle)]$_2$. The resulting solution was stirred for 2 h whilst temperature was slowly raised to -10 °C and a reddish solid precipitates. Solvent was then removed and the residue washed with cold diethyl ether (15 mL). Finally, filtration over celite and recrystallization from a dichloromethane/pentane mixture of solvents led to the expected red solid **16**.

Standard procedure for the isomerization of 16 into 17.

The bimetallic complex **16** was dissolved under argon in dry benzene (5 mL) and stirred at 40°C during 2 hours leading quantitatively to the expected bimetallic compound **17**.

2.5.22.1 - Compounds 16a and 17a.

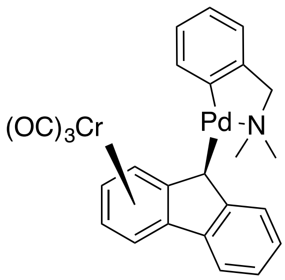

16a

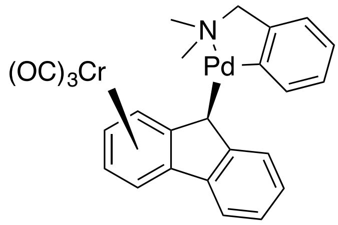

17a

Synthesis:

15a (0.200 g, 0.66 mmol), *n*-BuLi (0.45 mL, 0.73 mmol), **10a** (0.186 g, 0.34 mmol): bimetallic compound **16a** (0.160 g, 0.30 mmol, 45 % yield).

Characterizations:

Calcd for $C_{25}H_{21}CrNO_3Pd$: C, 55.42; H, 3.91; N, 2.58. Found: C, 55.39; H, 4.22; N, 2.79. HRMS-ESI (*m/z*): $[M+1H]^+$ calcd for $C_{25}H_{21}CrNO_3Pd$, 542.0034; found, 541.9968.

Compound 16a:

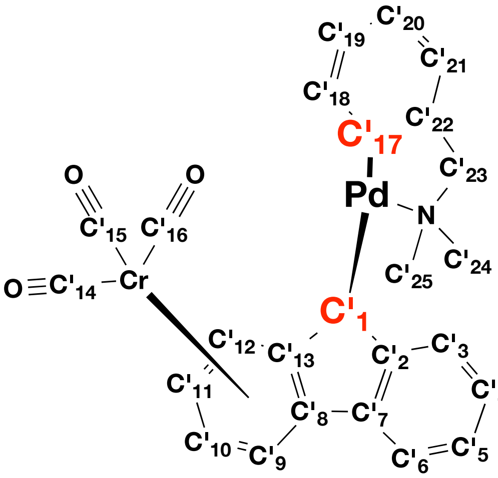

IR (cm^{-1}) ν(CO): 1944 (s), 1876 (s), 1839 (vs).

^{1}H NMR (600 MHz, Tol, 223K) δ 7.52 (d, J = 7.7 Hz, 1H, H'$_6$), 7.43 (d, J = 6.8 Hz, 1H, H'$_{18}$), 7.36 – 7.32 (m, 2H, H'$_4$, H'$_3$), 7.24 – 7.19 (m, 1H, H'$_5$), 7.03 – 6.97 (m, 2H, H'$_{19}$, H'$_{20}$), 6.92 (d, J = 7.2 Hz, 1H, H'$_{21}$), 5.64 (d, J = 6.5 Hz, 1H, H'$_9$), 5.53 (d, J = 6.5 Hz, 1H, H'$_{12}$), 4.77 (t, J = 6.6 Hz, 1H, H'$_{11}$), 4.32 (t, J = 6.4 Hz, 1H, H'$_{10}$), 4.15 (s, 1H, H'$_1$), 3.93 (d, J = 13.4 Hz, 1H, H'$_{23a}$), 2.81 (d, J = 11.0 Hz, 1H, H'$_{23b}$), 2.42 (s, 3H, H'$_{24}$), 2.08 (s, 3H, H'$_{25}$). ^{13}C NMR (151 MHz, Tol, 223K) δ 241.33 (C'$_{16}$), 238.35 (C'$_{15}$), 234.09 (C'$_{14}$), 163.03 (C'17), 147.80 (C'$_{22}$), 146.58 (C'$_2$), 139.00 (C'$_{18}$), 129.01 (C'$_7$), 128.45 (C'$_3$), 124.80 (C'$_{19}$), 124.25 (C'$_{20}$), 122.27 (C'$_6$), 121.90 (C'$_{21}$), 121.00 (C'$_5$), 118.05 (C'$_4$), 114.19 (C'$_8$), 102.39 (C'$_{13}$), 91.39 (C'$_{10}$), 90.70 (C'$_{12}$), 90.32 (C'$_9$), 89.82 (C'$_{11}$), 74.46 (C'$_{23}$), 54.20 (C'$_1$), 51.97 (C'$_{25}$), 51.56 (C'$_{24}$).

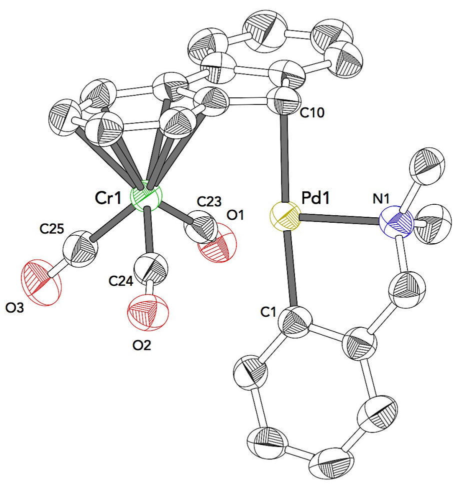

Compound **16a**
Space Group: **C 2/c**
R-Factor (%): **4.66**

N°	A	B	C	Lengths (Å)	Angles (°)
1	Cr_1	Pd_1	-	2.7123(9)	-
2	Cr_1	C_{23}	-	1.898(6)	-
3	Cr_1	C_{24}	-	1.851(4)	-
4	Cr_1	C_{25}	-	1.843(4)	-
5	C_{23}	O_1	-	1.163(7)	-
6	C_{24}	O_2	-	1.151(5)	-
7	C_{25}	O_3	-	1.145(5)	-
8	Pd_1	C_{10}	-	2.230(4)	-
9	Pd_1	N_1	-	2.169(4)	-
10	Pd_1	C_1	-	2.045(4)	-
11	Pd_1	C_{23}	-	2.204(4)	-
12	Pd_1	C_{24}	-	3.033(6)	-
13	Cr_1	C_{23}	O_1	-	160.8(4)
14	Cr_1	C_{24}	O_2	-	173.8(4)
15	Cr_1	C_{25}	O_3	-	177.4(4)
16	C_{23}	Cr_1	C_{24}	-	103.4(2)

Compound 17a:

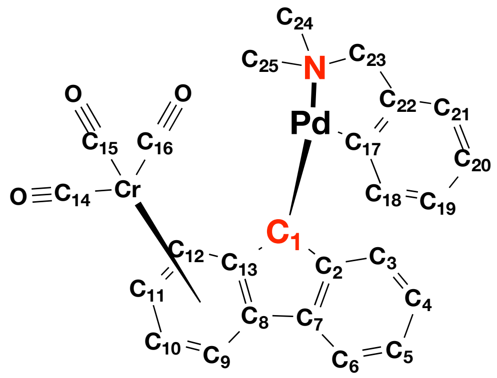

IR (cm^{-1}) ν(CO): 1940 (s), 1886 (s), 1843 (vs).

^{1}H NMR (600 MHz, C_6D_6, 298 K) δ 8.23 (d, J = 7.4 Hz, 1H, H_{18}), 7.71 – 7.67 (m, 1H, H_6), 7.42 (td, J = 7.4, 1.5 Hz, 1H, H_{19}), 7.26 – 7.24 (m, 1H, H_3), 7.22 (td, J = 7.4, 1.1 Hz, 1H, H_{20}), 7.00 (d, J = 7.2 Hz, 1H, H_{21}), 6.97 – 6.90 (m, 2H, H_5, H_4), 5.42 (d, J = 6.5 Hz, 1H, H_9), 5.20 (d, J = 6.4 Hz, 1H, H_{12}), 4.99 (t, J = 6.4 Hz, 1H, H_{10}), 4.85 (s, 1H, H_1), 4.23 – 4.14 (m, 1H, H_{11}), 3.58 (d, J = 12.9 Hz, 1H, H_{23a}), 2.82 (d, J = 12.9 Hz, 1H, H_{23b}), 2.33 (s, 3H, H_{24}), 2.17 (s, 3H, H_{25}). ^{13}C NMR (151 MHz, C_6D_6, 301 K) δ 237.28 (bs, C_{16}), 236.16 (bs, C_{15}), 232.68 (bs, C_{14}), 160.86 (C_{17}), 151.01 (C_7), 147.40 (C_{22}), 133.23 (C_{18}), 130.05 (C_2), 129.40 (C_5), 125.92 (C_{19}), 124.01 (C_{20}), 123.50 (C_{21}), 122.91 (C_6), 122.50 (C_4), 121.11 (C_3), 108.78 (C_8), 108.51 (C_{13}), 94.88 (C_{12}), 92.85 (C_{10}), 90.22 (C_{11}), 88.44 (C_9), 73.04 (C_{23}), 50.12 (C_{25}), 48.81 (C_{24}), 41.46 (C_1).

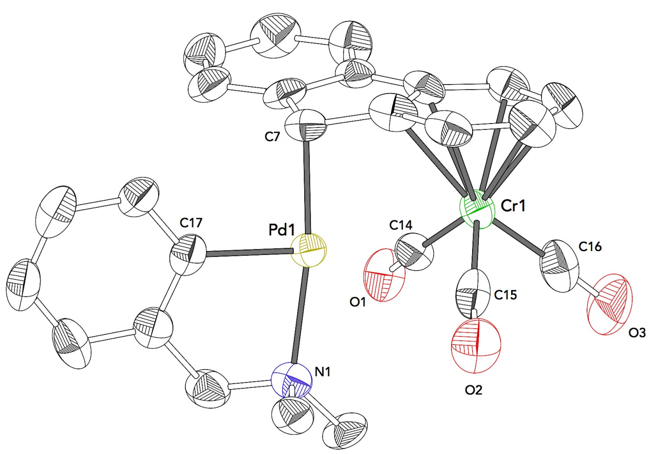

Compound **17a**
Space Group: **P -1**
R-Factor (%): **8.38**

N°	A	B	C	Lengths (Å)	Angles (°)
1	Cr_1	Pd_1	-	2.915(1)	-
2	Cr_1	C_{14}	-	1.85(1)	-
3	Cr_1	C_{15}	-	1.85(1)	-
4	Cr_1	C_{16}	-	1.84(1)	-
5	C_{14}	O_1	-	1.14(1)	-
6	C_{15}	O_2	-	1.17(1)	-
7	C_{16}	O_3	-	1.16(1)	-
8	Pd_1	C_7	-	2.068(8)	-
9	Pd_1	C_{17}	-	2.034(8)	-
10	Pd_1	N_1	-	2.181(6)	-
11	Pd_1	C_{14}	-	2.525(8)	-
12	Pd_1	C_{15}	-	2.92(1)	-
13	Cr_1	C_{14}	O_1	-	170.2(8)
14	Cr_1	C_{15}	O_2	-	175.0(8)
15	Cr_1	C_{16}	O_3	-	177.5(9)
16	C_{14}	Cr_1	C_{15}	-	99.7(4)

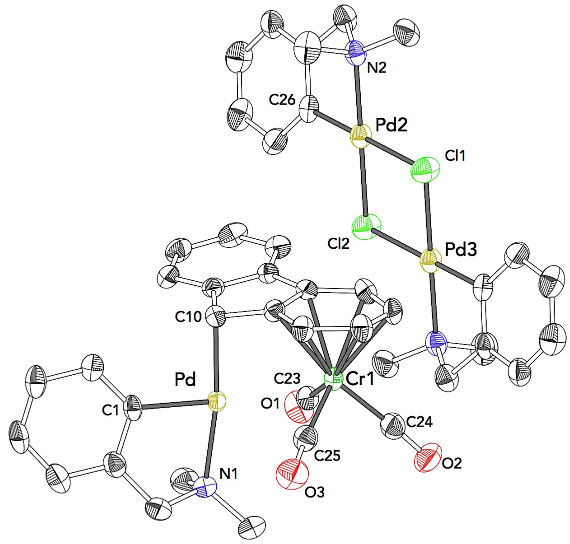

Compound **17a**
Space Group: **P -1**
R-Factor (%): **4.31**

N°	*A*	*B*	*C*	*Lengths (Å)*	*Angles (°)*
1	Cr_1	Pd_1	-	2.8615(7)	-
2	Cr_1	C_{23}	-	1.856(3)	-
3	Cr_1	C_{24}	-	1.842(4)	-
4	Cr_1	C_{25}	-	1.843(3)	-
5	C_{23}	O_1	-	1.161(4)	-
6	C_{24}	O_2	-	1.151(5)	-
7	C_{25}	O_3	-	1.162(4)	-
8	Pd_1	C_{10}	-	2.079(3)	-
9	Pd_1	N_1	-	2.211(3)	-
10	Pd_1	C_1	-	2.031(3)	-
11	Pd_1	C_{23}	-	2.531(4)	-
12	Pd_1	C_{25}	-	2.675(4)	-
13	Pd_2	Cl_1	-	2.4710(9)	-
14	Pd_2	Cl_2	-	2.3376(9)	-
15	Pd_2	N_2	-	2.083(3)	-
16	Pd_2	C_{26}	-	1.972(4)	-
17	Pd_3	Cl_1	-	2.3376(9)	-
18	Pd_3	Cl_2	-	2.4710(9)	-
19	Cr_1	C_{23}	O_1	-	169.4(3)
20	Cr_1	C_{24}	O_2	-	176.5(3)
21	Cr_1	C_{25}	O_3	-	173.2(3)
22	C_{23}	Cr_1	C_{24}	-	100.3(2)
23	Pd_2	Cl_1	Pd_3	-	94.07(3)
24	Pd_2	Cl_2	Pd_3	-	94.07(3)

2.5.22.2 - Compounds 16b and 17b.

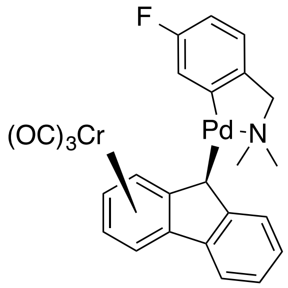

16b

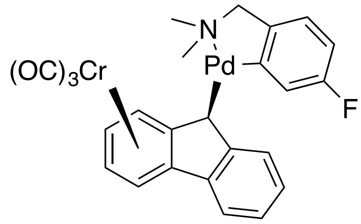

17b

Synthesis:

15a (0.200 g, 0.66 mmol), *n*-BuLi (0.45 mL, 0.73 mmol), **10b** (0.198 g, 0.34 mmol): bimetallic compound **16b** (0.109 g, 0.22 mmol, 33 % yield).

Characterizations:

Calcd for $C_{25}H_{20}CrFNO_3Pd{\bullet}0.1CH_2Cl_2$: C, 53.04; H, 3.58; N, 2.46. Found: C, 53.07; H, 3.76; N, 2.18. HRMS-ESI (*m/z*): $[M+1H]^+$ calcd for $C_{25}H_{20}CrFNO_3Pd$, 559.9940; found, 559.9936.

Compound 16b:

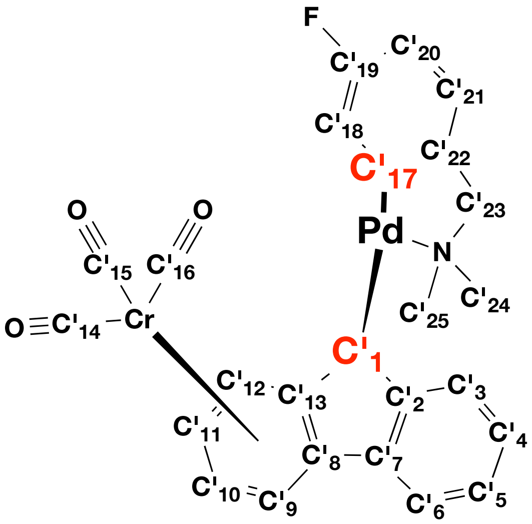

IR (cm^{-1}) ν(CO): 1956 (s), 1922 (vs), 1829 (s).

^{1}H NMR (600 MHz, Tol, 223 K) δ 7.44 (d, J = 7.8 Hz, 1H, H'$_6$), 7.34 – 7.28 (m, 3H, H'$_{18}$, H'$_4$, H'$_3$), 7.22 – 7.16 (m, 1H, H'$_5$), 6.75 – 6.68 (m, 2H, H'$_{20}$, H'$_{21}$), 5.53 (d, J = 6.5 Hz, 1H, H'$_9$), 5.39 (d, J = 6.5 Hz, 1H, H'$_{12}$), 4.71 (t, J = 6.3 Hz, 1H, H'$_{11}$), 4.24 (t, J = 6.6 Hz, 1H, H'$_{10}$), 4.07 (s, 1H, H'$_1$), 3.83 (d, J = 13.3 Hz, 1H, H'$_{23a}$), 2.73 (d, J = 13.4 Hz, 1H, H'$_{23b}$), 2.39 (s, 3H, H'$_{24}$), 2.04 (s, 3H, H'$_{25}$). ^{13}C NMR (151 MHz, Tol, 223 K) δ 240.37 (C'$_{16}$), 238.15 (C'$_{15}$), 233.68 (C'$_{14}$), 166.75 (d, J = 1.5 Hz, C'$_{22}$), 161.23 (d, J = 238.3 Hz, C'$_{19}$), 147.05 (C'$_7$), 142.91 (d, J = 2.1 Hz, C'$_{17}$), 129.46 (C'$_2$), 128.61 (C'$_4$), 124.50 (d, J = 18.7 Hz, C'$_{18}$), 122.67 (d, J = 6.2 Hz, C'$_{21}$), 122.43 (C'$_6$), 121.29 (C'$_5$), 118.21 (C'$_3$), 113.85 (C'$_8$), 110.33 (d, J = 23.4 Hz, C'$_{20}$), 102.49 (C'$_{13}$), 91.55 (C'$_{10}$), 90.91 (C'$_{12}$), 90.55 (C'$_9$), 90.24 (C'$_{11}$), 73.79 (C'$_{23}$), 53.38 (C'$_1$), 51.82 (C'$_{24}$), 49.70 (C'$_{25}$). ^{19}F NMR (282 MHz, Tol, 296 K) δ -115.84.

Compound 17b:

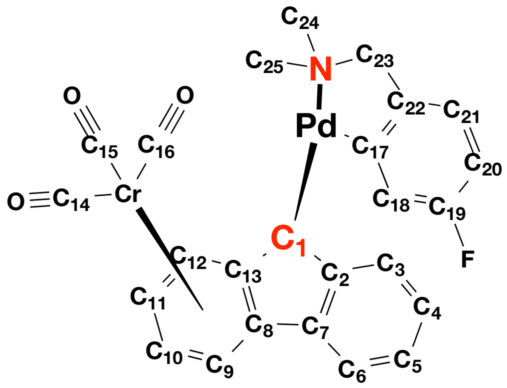

IR (cm^{-1}) ν(CO): 1945 (vs), 1883 (s) 1843 (vs).

^{1}H NMR (500 MHz, 293 K, C_6D_6) δ 8.09 (dd, J = 9.0, 2.2 Hz, 1H, H_{18}), 7.66 (d, J = 7.3 Hz, 1H, H_6), 7.19 (d, J = 7.2 Hz, 1H, H_3), 6.96 – 6.88 (m, 3H, H_{20}, H_5, H_4), 6.79 (dd, J = 7.9, 5.6 Hz, 1H, H_{21}), 5.38 – 5.33 (m, 1H, H_9), 5.10 (d, J = 6.4 Hz, 1H, H_{12}), 4.96 (t, J = 6.4 Hz, 1H, H_{10}), 4.62 (s, 1H, H_1), 4.16 (t, J = 6.4 Hz, 1H, H_{11}), 3.49 – 3.43 (m, 1H, H_{23a}), 2.72 (d, J = 12.8 Hz, 1H, H_{23b}), 2.26 (s, 3H, H_{24}), 2.11 (s, 3H, H_{25}). ^{13}C NMR (126 MHz, C_6D_6, 293 K) δ 237.80 (bs, C_{16}), 236.15 (bs, C_{15}), 232.34 (bs, C_{14}), 164.21 (d, J = 1.4 Hz, C_{17}), 161.82 (d, J = 247.5 Hz, C_{19}), 150.96 (C_7), 143.34 (d, J = 2.5 Hz, C_{22}), 130.51 (C_2), 130.01 (C_4), 124.61 (d, J = 7.0 Hz, C_{21}), 123.21 (C_6), 123.14 (C_5), 121.53 (C_3), 120.02 (d, J = 17.4 Hz, C_{18}), 110.62 (d, J = 21.9 Hz, C_{20}), 109.06 (C_8), 108.48 (C_{13}), 95.22 (C_{12}), 93.35 (C_{10}), 90.78 (C_{11}), 88.98 (C_9), 72.72 (C_{23}), 50.33 (C_{25}), 48.95 (C_{24}), 41.86 (C_1). ^{19}F NMR (282 MHz, Tol, 296 K) δ -116.42.

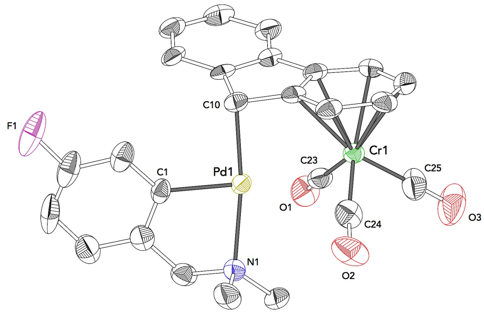

Compound **17b**
Space Group: **P 2_1/c**
R-Factor (%): **3.91**

N°	A	B	C	Lengths (Å)	Angles (°)
1	Cr_1	Pd_1	-	2.9179(6)	-
2	Cr_1	C_{23}	-	1.862(4)	-
3	Cr_1	C_{24}	-	1.841(5)	-
4	Cr_1	C_{25}	-	1.838(4)	-
5	C_{23}	O_1	-	1.148(5)	-
6	C_{24}	O_2	-	1.154(6)	-
7	C_{25}	O_3	-	1.150(5)	-
8	Pd_1	C_{10}	-	2.095(3)	-
9	Pd_1	C_1	-	2.018(3)	-
10	Pd_1	N_1	-	2.188(3)	-
11	Pd_1	C_{23}	-	2.627(4)	-
12	Pd_1	C_{24}	-	2.911(5)	-
13	Cr_1	C_{23}	O_1	-	170.8(3)
14	Cr_1	C_{24}	O_2	-	173.9(4)
15	Cr_1	C_{25}	O_3	-	178.8(4)
16	C_{23}	Cr_1	C_{24}	-	98.9(2)

2.5.22.3 - Compounds 16f and 17f.

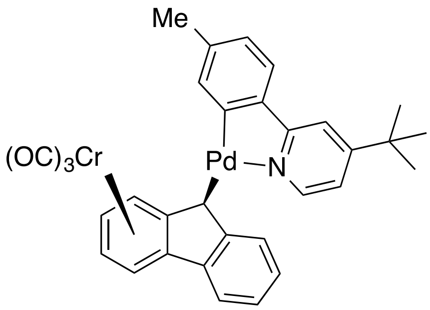

16f

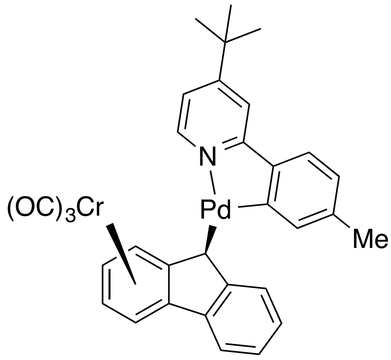

17f

Synthesis:

15a (0.200 g, 0.66 mmol), *n*-BuLi (0.45 mL, 0.73 mmol), **10f** (0.247 g, 0.34 mmol): bimetallic compound **16f** (0.231 g, 0.39 mmol, 59 % yield).

Characterizations:

Calcd for $C_{32}H_{27}CrNO_3Pd{\bullet}0.4CH_2Cl_2$: C, 58.44; H, 4.21; N, 2.10. Found: C, 58.37; H, 4.29; N, 2.06. HRMS-ESI (*m/z*): $[M+1H]^+$ calcd for $C_{32}H_{27}CrNO_3Pd$, 632.0504; found, 632.0572.

Compound 16f:

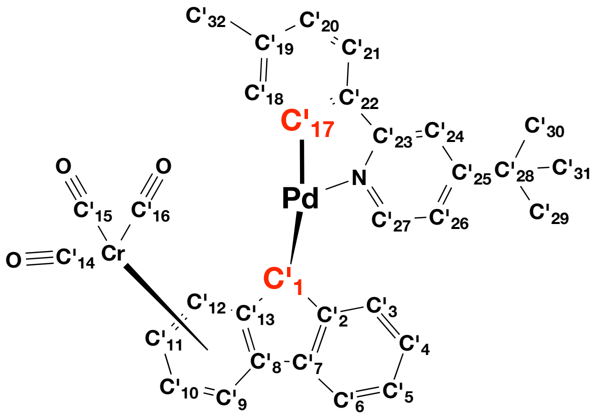

IR (cm^{-1}) ν(CO): 1945 (s), 1875 (s), 1858 (vs).

^{1}H NMR (600 MHz, Tol, 223 K) δ 8.84 (d, J = 6.1 Hz, 1H, H'_{27}), 7.68 (d, J = 8.0 Hz, 1H, H'_{6}), 7.53 (d, J = 7.7 Hz, 1H, H'_{3}), 7.44 (d, J = 1.3 Hz, 1H, H'_{18}), 7.39 (d, J = 1.9 Hz, 1H, H'_{24}), 7.31 (d, J = 8.1 Hz, 1H, H'_{21}), 7.20 (t, J = 7.5 Hz, 1H, H'_{5}), 7.16 – 7.10 (m, 1H, H'_{4}), 6.80 (d, J = 7.4 Hz, 1H, H'_{20}), 6.55 (dd, J = 6.0, 2.1 Hz, 1H, H'_{26}), 5.55 (d, J = 6.4 Hz, 1H, H'_{9}), 5.50 (d, J = 6.6 Hz, 1H, H'_{12}), 4.93 (t, J = 6.4 Hz, 1H, H'_{11}), 4.63 (s, 1H, H'_{1}), 4.43 (td, J = 6.4, 1.1 Hz, 1H, H'_{10}), 2.22 (s, 3H, H'_{32}), 1.05 (s, 9H, H'30, H'31, H'29). ^{13}C NMR (151 MHz, Tol, 213 K) δ 241.56 (C'_{16}), 238.33 (C'_{15}), 233.21 (C'_{14}), 170.26 (C'_{17}), 167.52 (C'_{23}), 161.32 (C'_{25}), 147.78 (C'_{27}), 146.89 (C'_{7}), 143.69 (C'_{22}), 140.48 (C'_{18}), 139.39 (C'_{19}), 129.58 (C'_{2}), 129.07 (C'_{5}), 124.65 (C'_{20}), 123.82 (C'_{21}), 122.21 (C'_{3}), 121.17 (C'_{4}), 119.05 (C'_{6}), 119.02 (C'_{26}), 115.72 (C'_{24}), 114.62 (C'_{8}), 103.69 (C'_{13}), 91.92 (C'_{9}), 91.59 (C'_{12}), 91.37 (C'_{11}), 91.08 (C'_{10}), 54.83 (C'_{1}), 34.70 (C'_{28}), 29.75 (C'_{30}, C'_{31}, C'_{29}), 22.22 (C'_{32}).

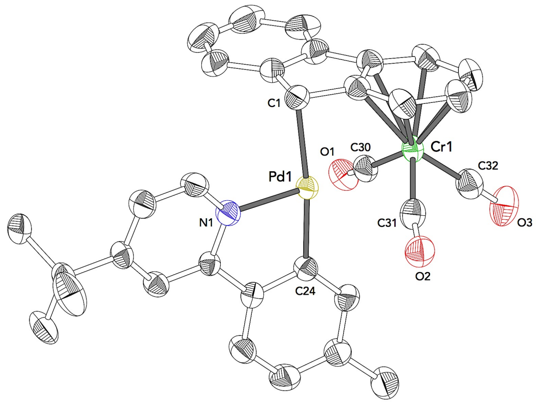

Compound **16f**
Space Group: **P c a 2$_1$**
R-Factor (%): **3.95**

N°	*A*	*B*	*C*	*Lengths (Å)*	*Angles (°)*
1	Cr_1	Pd_1	-	2.698(1)	-
2	Cr_1	C_{30}	-	1.880(4)	-
3	Cr_1	C_{31}	-	1.866(6)	-
4	Cr_1	C_{32}	-	1.846(6)	-
5	C_{30}	O_1	-	1.153(6)	-
6	C_{31}	O_2	-	1.151(7)	-
7	C_{32}	O_3	-	1.148(8)	-
8	Pd_1	C_1	-	2.254(5)	-
9	Pd_1	N_1	-	2.079(5)	-
10	Pd_1	C_{24}	-	2.040(5)	-
11	Pd_1	C_{30}	-	2.425(6)	-
12	Pd_1	C_{31}	-	2.626(5)	-
13	Cr_1	C_{30}	O_1	-	167.0(5)
14	Cr_1	C_{31}	O_2	-	170.8(5)
15	Cr_1	C_{32}	O_3	-	178.9(6)
16	C_{30}	Cr_1	C_{31}	-	103.6(2)

Compound 17f:

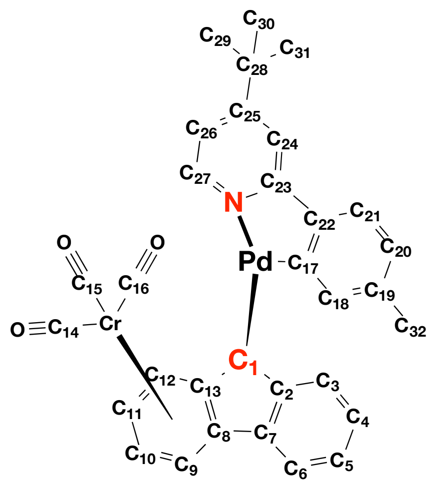

IR (cm^{-1}) ν(CO): 1952 (s), 1880 (s), 1857 (vs).

^{1}H NMR (500 MHz, C_6D_6, 293 K) δ 8.46 (s, 1H, H_{18}), 8.44 (dd, J = 6.1, 0.6 Hz, 1H, H_{27}), 8.07 (d, J = 7.9 Hz, 1H, H_6), 7.55 (d, J = 7.9 Hz, 1H, H_{21}), 7.35 (d, J = 2.1 Hz, 1H, H_{24}), 7.34 – 7.29 (m, 1H, H_3), 7.11 – 7.06 (m, 2H, H_5, H_{20}), 7.03 – 6.96 (m, 1H, H_4), 6.26 (dd, J = 6.1, 2.1 Hz, 1H, H_{26}), 5.42 (d, J = 6.5 Hz, 1H, H_9), 5.34 (d, J = 6.5 Hz, 1H, H_{12}), 5.10 (s, 1H, H_1), 5.08 (t, J = 6.4 Hz, 1H, H_{10}), 4.27 (td, J = 6.4, 1.0 Hz, 1H, H_{11}), 2.55 (s, 3H, H_{32}), 0.83 (s, 9H, H_{30}, H_{31}, H_{29}). ^{13}C NMR (126 MHz, C_6D_6, 293 K) δ 237.62 (bs, C_{16}), 236.89 (bs, C_{15}), 232.04 (bs, C_{14}), 165.52 (C_{17}), 165.39 (C_{23}), 161.38 (C_{25}), 151.91 (C_{27}), 150.86 (C_7), 145.19 (C_{22}), 139.53 (C_{19}), 135.54 (C_{18}), 130.95 (C_2), 129.90 (C_5), 125.29 (C_{20}), 124.54 (C_{21}), 122.94 (C_4), 122.70 (C_6), 121.74 (C_3), 119.47 (C_{26}), 115.28 (C_{24}), 109.37 (C_{13}), 109.17 (C_8), 95.66 (C_{12}), 93.17 (C_{10}), 90.53 (C_{11}), 88.88 (C_9), 43.49 (C_1), 34.65 (C_{28}), 29.48 (C_{30}, C_{31}, C_{29}), 22.39 (C_{32}).

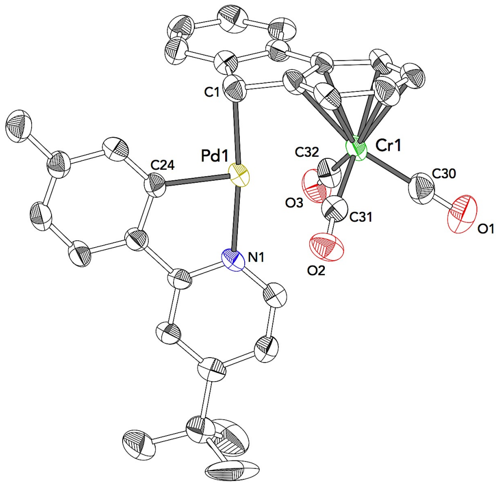

Compound **17f**
Space Group: **P 2_1/c**
R-Factor (%): **6.55**

N°	***A***	***B***	***C***	***Lengths (Å)***	***Angles (°)***
1	Cr_1	Pd_1	-	2.8625(7)	-
2	Cr_1	C_{30}	-	1.844(5)	-
3	Cr_1	C_{31}	-	1.847(4)	-
4	Cr_1	C_{32}	-	1.851(4)	-
5	C_{30}	O_1	-	1.152(6)	-
6	C_{31}	O_2	-	1.158(6)	-
7	C_{32}	O_3	-	1.162(5)	-
8	Pd_1	C_1	-	2.097(5)	-
9	Pd_1	N_1	-	2.112(4)	-
10	Pd_1	C_{24}	-	2.018(4)	-
11	Pd_1	C_{31}	-	2.660(4)	-
12	Pd_1	C_{32}	-	2.647(4)	-
13	Cr_1	C_{30}	O_1	-	177.6(4)
14	Cr_1	C_{31}	O_2	-	173.2(2)
15	Cr_1	C_{32}	O_3	-	173.7(4)
16	C_{31}	Cr_1	C_{32}	-	98.4(2)

2.5.22.4 - Compounds 16i and 17i.

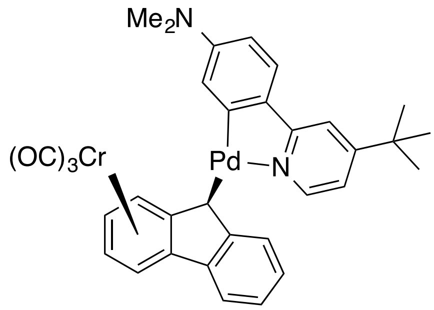

16i

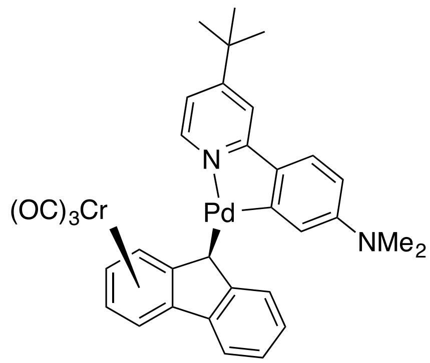

17i

Synthesis:

15a (0.200 g, 0.66 mmol), *n*-BuLi (0.45 mL, 0.73 mmol), **10i** (0.267 g, 0.34 mmol): bimetallic compound **16i** (0.184 g, 0.28 mmol, 42 % yield).

Characterizations:

Calcd for $C_{33}H_{30}CrN_2O_3Pd{\bullet}1.1CH_2Cl_2$: C, 54.29; H, 4.30; N, 3.71. Found: C, 53.95; H, 4.69; N, 3.62. HRMS-ESI (*m/z*): $[M+1H]^+$ calcd for $C_{33}H_{30}CrN_2O_3Pd$, 661.0769; found, 661.0734.

Compound **16i**:

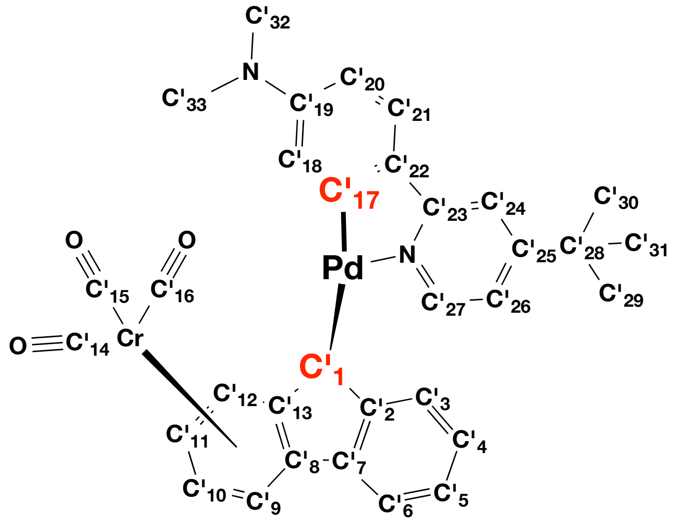

IR (cm^{-1}) ν(CO): 1948 (s), 1885 (s), 1860 (vs).

^{1}H NMR (600 MHz, Tol, 223 K) δ 8.82 (d, J = 6.0 Hz, 1H, H'_{27}), 7.71 (d, J = 8.1 Hz, 1H, H'_{6}), 7.56 (d, J = 8.1 Hz, 1H, H'_{3}), 7.42 (d, J = 9.0 Hz, 1H, H'_{21}), 7.38 (d, J = 2.0 Hz, 1H, H'_{24}), 7.22 – 7.16 (m, 1H, H'_{5}), 7.16 – 7.10 (m, 1H, H'_{4}), 6.78 (d, J = 2.5 Hz, 1H, H'_{18}), 6.49 (dd, J = 6.0, 2.0 Hz, 1H, H'_{26}), 6.27 (dd, J = 8.6, 2.6 Hz, 1H, H'_{20}), 5.57 (d, J = 6.9 Hz, 2H, H'_{12}, H'_{9}), 4.93 (t, J = 6.7 Hz, 1H, H'_{10}), 4.66 (s, 1H, H'_{1}), 4.47 (t, J = 6.3 Hz, 1H, H'_{11}), 2.63 (s, 6H, H'_{32}, H'_{33}), 1.10 (s, 9H, H'_{30}, H'_{31}, H'_{29}).

Fast acquisition at room temperature in order to get the carbonyl signals which couldn't be obtained due to the low solubility of the trans species at low temperature in toluene:

^{13}C NMR (126 MHz, C_6D_6, 293 K) δ 242.08 (C'_{16}), 238.85 (C'_{15}), 233.86 (C'_{14}).

^{13}C NMR (151 MHz, Tol, 223 K) δ 170.95 (C'_{17}), 168.15 (C'_{23}), 160.49 (C'_{25}), 149.84 (C'_{19}), 147.48 (C'_{27}), 147.19 (C'_{7}), 133.80 (C'_{22}), 129.28 (C'_{2}), 128.19 (C'_{5}), 125.02 (C'_{21}), 122.37 (C'_{18}), 121.91 (C'_{3}), 120.87 (C'_{4}), 118.99 (C'_{6}), 116.76 (C'_{26}), 114.71 (C'_{13}) 114.42 (C'_{24}), 107.36 (C'_{20}), 103.63 (C'_{8}), 91.41 (C'_{12}, C'_{9}), 90.98 (C'_{11}), 90.35 (C'_{10}), 54.83 (C'_{1}), 39.55 (C'_{32}, C'_{33}), 34.86 (C'_{28}), 29.79 (C'_{30}, C'_{31}, C'_{29}).

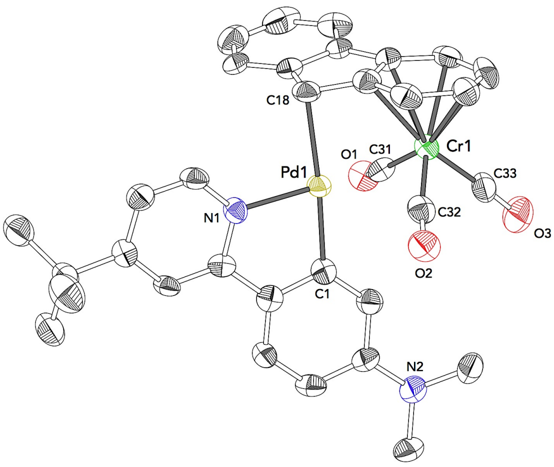

Compound **16i**
Space Group: **P -1**
R-Factor (%): **4.6**

N°	*A*	*B*	*C*	*Lengths (Å)*	*Angles (°)*
1	Cr_1	Pd_1	-	2.6776(9)	-
2	Cr_1	C_{31}	-	1.896(7)	-
3	Cr_1	C_{32}	-	1.856(7)	-
4	Cr_1	C_{33}	-	1.843(5)	-
5	C_{31}	O_1	-	1.153(8)	-
6	C_{32}	O_2	-	1.154(8)	-
7	C_{33}	O_3	-	1.152(6)	-
8	Pd_1	C_{18}	-	2.269(5)	-
9	Pd_1	N_1	-	2.092(4)	-
10	Pd_1	C_1	-	2.057(5)	-
11	Pd_1	C_{31}	-	2.289(5)	-
12	Pd_1	C_{32}	-	2.610(7)	-
13	Cr_1	C_{31}	O_1	-	163.8(5)
14	Cr_1	C_{32}	O_2	-	171.6(5)
15	Cr_1	C_{33}	O_3	-	177.0(5)
16	C_{31}	Cr_1	C_{32}	-	103.1(3)

Compound 17i:

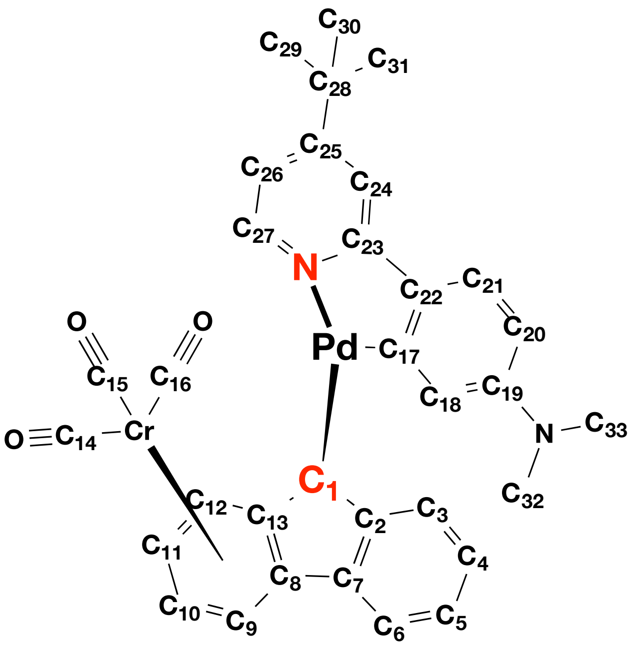

IR (cm^{-1}) ν(CO): 1937 (s), 1886 (s), 1849 (vs).

^{1}H NMR (500 MHz, C_6D_6, 293 K) δ 8.51 (d, J = 6.1 Hz, 1H, H_{27}), 8.25 (d, J = 7.9 Hz, 1H, H_6), 8.11 (d, J = 2.6 Hz, 1H, H_{18}), 7.74 (d, J = 8.6 Hz, 1H, H_{21}), 7.36 – 7.29 (m, 2H, H_3, H_{24}), 7.12 – 7.06 (m, 1H, H_5), 7.05 – 6.98 (m, 1H, H_4), 6.73 (dd, J = 8.6, 2.5 Hz, 1H, H_{20}), 6.32 (dd, J = 6.1, 2.1 Hz, 1H, H_{26}), 5.63 (d, J = 6.4 Hz, 1H, H_9), 5.57 (d, J = 6.5 Hz, 1H, H_{12}), 5.12 – 5.04 (m, 2H, H1, H_{10}), 4.37 (td, J = 6.5, 1.1 Hz, 1H, H_{11}), 3.10 (s, 6H, H_{32}, H_{33}), 1.08 (s, 9H, H_{30}, H_{31}, H_{29}).

^{13}C NMR (126 MHz, C_6D_6, 293 K) δ 237.86 (bs, C_{16}), 237.07 (bs, C_{15}), 232.32 (bs, C_{14}), 166.55 (C_{19}), 166.07 (C_{25}), 160.86 (C_{23}), 151.71 (C_{27}), 151.41 (C_{17}), 150.99 (C_7), 136.41 (C_{22}), 130.98 (C_2), 129.80 (C_5), 125.66 (C_{21}), 122.99 (C_6), 122.75 (C_4), 121.75 (C_3), 118.15 (C_{18}), 117.88 (C_{26}), 114.22 (C_{24}), 109.73 (C_{13}), 109.01 (C_8), 108.65 (C_{20}), 95.60 (C_{12}), 93.08 (C_{10}), 90.45 (C_{11}), 88.72 (C_9), 44.17 (C_1), 40.39 (C_{32}, C_{33}), 34.61 (C_{28}), 30.02 (C_{30}, C_{31}, C_{29}).

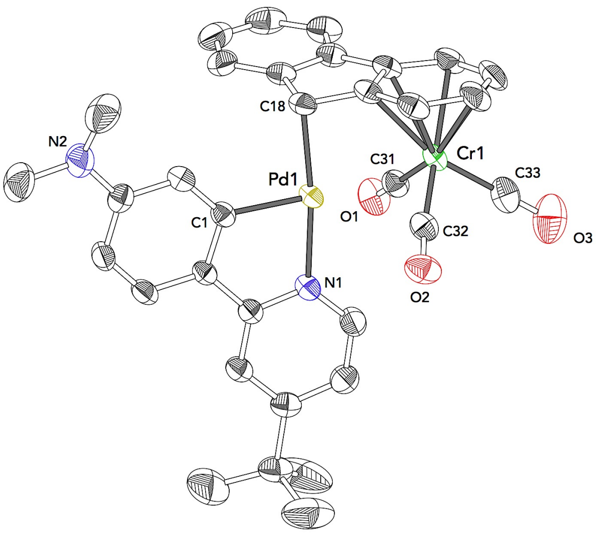

Compound **17i**
Space Group: **P 2_1/c**
R-Factor (%): **3.04**

N°	A	B	C	Lengths (Å)	Angles (°)
1	Cr_1	Pd_1	-	2.8577(4)	-
2	Cr_1	C_{31}	-	1.862(2)	-
3	Cr_1	C_{32}	-	1.849(2)	-
4	Cr_1	C_{33}	-	1.848(2)	-
5	C_{31}	O_1	-	1.153(3)	-
6	C_{32}	O_2	-	1.153(3)	-
7	C_{33}	O_3	-	1.150(3)	-
8	Pd_1	C_{18}	-	2.098(2)	-
9	Pd_1	C_1	-	2.012(2)	-
10	Pd_1	N_1	-	2.111(2)	-
11	Pd_1	C_{31}	-	2.648(2)	-
12	Pd_1	C_{32}	-	2.649(2)	-
13	Cr_1	C_{31}	O_1	-	174.5(2)
14	Cr_1	C_{32}	O_2	-	173.6(2)
15	Cr_1	C_{33}	O_3	-	177.2(2)
16	C_{31}	Cr_1	C_{32}	-	98.66(9)

2.5.23 - Compound 18a.

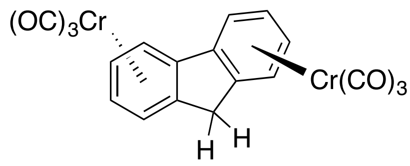

18a

Synthesis:

$Cr(CO)_6$ (9.929 g, 45.12 mmol), fluorene (3.0 g, 18.05 mmol), naphtalene (0.289 g, 2.26 mmol), THF (15 mL), and di-*n*butylether (150 mL) were gently refluxed for 140 h under a permanent flow of argon. The resulting orange/red solution was evaporated to dryness and the resulting residue was adsorbed on silica gel. Chromatographic separation was performed on silica gel using a mixture of CH_2Cl_2 and acetone (95:5) as eluent. The product was eluted as an orange solution, which afforded an orange solid upon removal of the solvents under reduced pressure (3.93 g, 8.97 mmol, 50 %).

Characterizations:

Calcd for $C_{19}H_{10}Cr_2O_6$: C, 52.07; H, 2.30. Found: C, 51.73; H, 2.40. HRMS-ESI (*m/z*): $[M+1Na]^+$ calcd for $C_{19}H_{10}Cr_2O_6$, 460.9180; found, 460.9238. IR (cm^{-1}) ν(CO): 1932 (s), 1850 (vs).

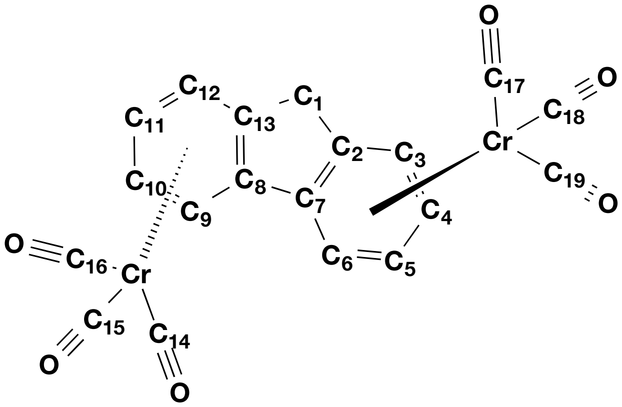

^{1}H NMR (600 MHz, 298 K, C_6D_6) δ 4.80 (d, J = 3.6 Hz, 2H, H_9, H_6), 4.60 (d, J = 5.9 Hz, 2H, H_{12}, H_3), 4.39 – 4.32 (m, 2H, H_{11}, H_4), 4.33 – 4.26 (m, 2H, H_{10}, H_5), 3.10 (s, 2H, H_1). ^{13}C NMR (151 MHz, C_6D_6, 298 K) δ 232.84 (C_{15}, C_{16}, C_{14}, C_{18}, C_{19}, C_{17}), 110.49 (C_2, C_{13}), 106.81 (C_7, C_8), 91.86 (C_{11}, C_4), 90.12 (C_{10}, C_5), 89.35 (C_{12}, C_3), 85.47 (C_9, C_6), 36.04 (C_1).

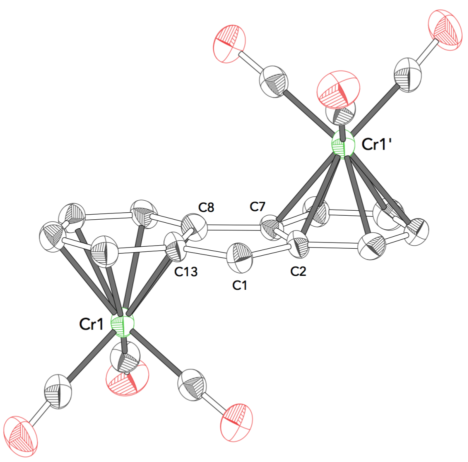

Compound **18a**
Space Group: **P -1**
R-Factor (%): **3.26**

N°	*A*	*B*	*C*	*D*	*Lengths (Å)*	*Angles (°)*
1	C_1	C_2	-	-	1.517(7)	-
2	C_{13}	C_1	-	-	1.514(7)	-
3	C_{13}	C_8	-	-	1.43(1)	-
4	C_2	C_7	-	-	1.387(9)	-

2.5.24 - Standard procedure for the synthesis of (1*R*)-17c, 17j and 19.

15a or **18a** was dissolved in THF (5 mL) and treated with *n*-BuLi at -40°C under argon. The resulting solution was transferred after 1 h *via* canula to another Schlenk vessel containing a THF (3 mL) solution of the corresponding [Pd(μ-Cl)(Metalacycle)]$_2$. The resulting solution was stirred for 1 h whilst temperature was slowly raised to -10 °C, then 1 h at room temperature and finally heated during one more hour at 50 °C. After cooling down to room temperature, filtration over celite was performed. Solvents were removed under reduced pressure. The brownish solid was recristallized in a dichloromethane/benzene/pentane mixture of solvents leading to the expected orange solid.

2.5.24.1 - Compound (1*R*)-17c.

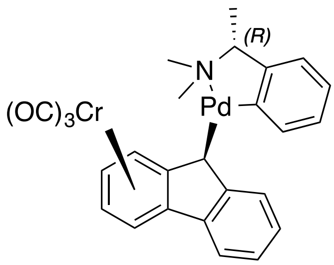

(1R)-17c

Synthesis:

15a (0.200 g, 0.66 mmol), *n*-BuLi (0.45 mL, 0.73 mmol), (1*R*)-**10c** (0.191 g, 0.34 mmol): bimetallic compound (1*R*)-**17c** (0.148 g, 0.27 mmol, 40 % yield).

Characterizations:

Calcd for $C_{26}H_{23}CrNO_3Pd$: C, 56.18; H, 4.17; N, 2.52. Found: C, 56.57; H, 4.41; N, 2.45. HRMS-ESI (*m/z*): $[M+1Na]^+$ calcd for $C_{26}H_{23}CrNO_3Pd$, 578.0010; found, 577.9961. IR (cm^{-1}) ν(CO): 1943 (s), 1886 (s), 1848 (vs). $[\alpha]_D^{20}$ -290.4° (*c* 0.052, benzene).

CD (benzene, 293 K) λ_{max} (Mol. Ellip.) 315 (5711), 350 (-2429), 390 (1476), 440 (-1823), 480 (-3920), 600 (-269).

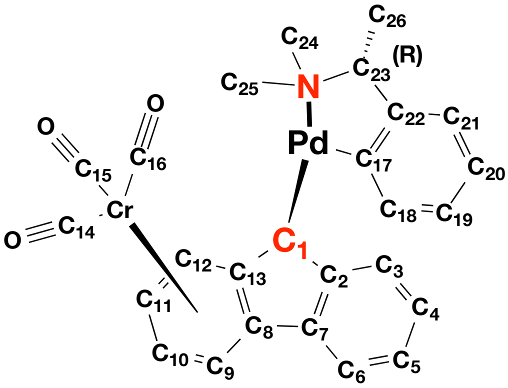

^{1}H NMR (600 MHz, Tol, 223 K) δ 8.17 (d, J = 7.5 Hz, 1H, H_{18}), 7.55 (d, J = 7.9 Hz, 1H, H_6), 7.43 (td, J = 7.4, 1.5 Hz, 1H, H_{19}), 7.29 – 7.23 (m, 2H, H_3, H_{20}), 7.00 (s, 2H, H_4, H_{21}), 6.92 (t, J = 7.4 Hz, 1H, H_5), 5.08 (d, J = 6.6 Hz, 1H, H_9), 5.03 (d, J = 6.5 Hz, 1H, H_{12}), 4.88 (t, J = 6.5 Hz, 1H, H_{10}), 4.71 (s, 1H, H_1), 3.98 (t, J = 6.4 Hz, 1H, H_{11}), 2.54 (q, J = 6.4 Hz, 1H, H_{23}), 2.47 (s, 3H, H_{24}), 2.15 (s, 3H, H_{25}), 1.23 (d, J = 6.3 Hz, 3H, H_{26}). ^{13}C NMR (151 MHz, Tol, 223 K) δ 238.10 (C_{16}), 236.58 (C_{15}), 233.29 (C_{14}), 158.15 (C_{17}), 154.77 (C_{22}), 151.20 (C_7), 133.24 (C_{18}), 129.71 (C_2), 129.07 (C_5), 125.86 (C_{19}), 124.25 (C_{20}), 123.39 (C_6), 122.83 (C_{21}), 122.39 (C_4), 121.20 (C_3), 108.95 (C_8), 108.46 (C_{13}), 95.16 (C_{12}), 93.29 (C_{10}), 90.02 (C_{11}), 88.76 (C_9), 76.74 (C_{23}), 50.52 (C_{24}), 46.46 (C_{25}), 42.21 (C_1), 24.03 (C_{26}).

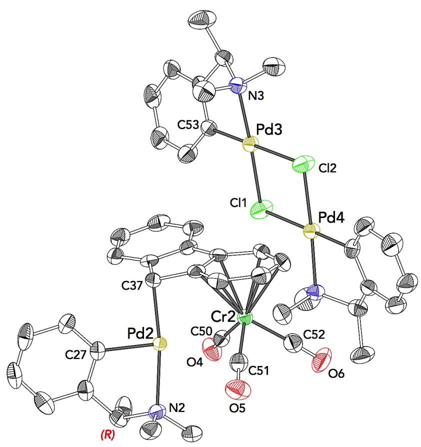

Compound (1*R*)-**17c**
Space Group: **P 1**
R-Factor (%): **3.07**

N°	A	B	C	Lengths (Å)	Angles (°)
1	Cr_2	Pd_2	-	2.894(1)	-
2	Cr_2	C_{50}	-	1.863(7)	-
3	Cr_2	C_{51}	-	1.835(6)	-
4	Cr_2	C_{52}	-	1.864(6)	-
5	C_{50}	O_4	-	1.153(9)	-
6	C_{51}	O_5	-	1.146(7)	-
7	C_{52}	O_6	-	1.136(8)	-
8	Pd_2	C_{37}	-	2.082(6)	-
9	Pd_2	N_2	-	2.216(5)	-
10	Pd_2	C_{27}	-	2.027(5)	-
11	Pd_2	C_{50}	-	2.479(6)	-
12	Pd_2	C_{51}	-	2.895(6)	-
13	Pd_3	Cl_1	-	2.327(2)	-
14	Pd_3	Cl_2	-	2.483(2)	-
15	Pd_3	N_3	-	2.075(7)	-
16	Pd_3	C_{53}	-	1.970(6)	-
17	Pd_4	Cl_1	-	2.476(2)	-
18	Pd_4	Cl_2	-	2.331(2)	-
19	Pd_4	N_4	-	2.076(7)	-
20	Pd_4	C_{63}	-	1.979(6)	-
21	Cr_2	C_{50}	O_4	-	170.0(5)
22	Cr_2	C_{51}	O_5	-	174.4(6)
23	Cr_2	C_{52}	O_6	-	177.6(6)
24	C_{50}	Cr_2	C_{51}	-	99.1(3)
25	Pd_3	Cl_1	Pd_4	-	94.68(6)
26	Pd_3	Cl_2	Pd_4	-	94.97(6)

2.5.24.2 - Compound 17j.

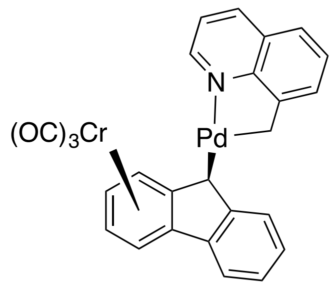

17j

Synthesis:

15a (0.200 g, 0.66 mmol), *n*-BuLi (0.45 mL, 0.73 mmol), **10j** (0.199 g, 0.35 mmol): bimetallic compound **17j** (0.175 g, 0.32 mmol, 48 % yield).

Characterizations:

Calcd for $C_{26}H_{17}CrNO_3Pd{\bullet}0.1CH_2Cl_2$: C, 56.15; H, 3.11; N, 2.51. Found: C, 56.28; H, 3.29; N, 2.75. HRMS-ESI (*m/z*): $[M+1Na]^+$ calcd for $C_{26}H_{17}CrNO_3Pd$, 571.4541; found, 571.9518. IR (cm^{-1}) ν(CO): 1931 (s), 1873 (s), 1849 (vs).

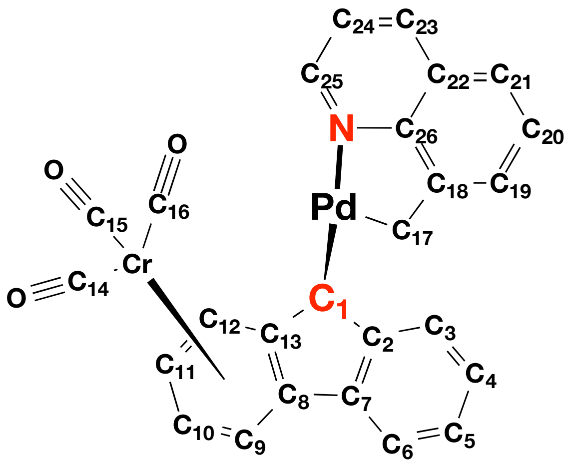

^{1}H NMR (600 MHz, C_6D_6, 298 K) δ 8.72 (dd, J = 4.9, 1.6 Hz, 1H, H_{25}), 7.69 (d, J = 7.9 Hz, 1H, H_6), 7.52 (d, J = 7.1 Hz, 1H, H_{21}), 7.40 (d, J = 7.5 Hz, 1H, H_3), 7.26 – 7.19 (m, 2H, H_5, H_{23}), 7.11 – 7.05 (m, 2H, H_4, H_{20}), 6.95 (d, J = 8.0 Hz, 1H, H_{19}), 6.35 (dd, J = 8.2, 4.9 Hz, 1H, H_{24}), 5.56 (d, J = 6.6 Hz, 1H, H_9), 5.33 (d, J = 6.5 Hz, 1H, H_{12}), 5.08 (t, J = 6.4 Hz, 1H, H_{10}), 4.74 (s, 1H, H_1), 4.30 (t, J = 6.4 Hz, 1H, H_{11}), 4.25 (d, J = 13.9 Hz, 1H, H_{17a}), 3.69 (d, J = 13.9 Hz, 1H, H_{17b}). ^{13}C NMR (126 MHz, C_6D_6, 293 K) δ 238.14 (bs, C_{16}), 237.97 (bs, C_{15}), 232.94 (bs, C_{14}), 153.41 (C_{26}), 152.28 (C_{25}), 151.26 (C_7), 151.19 (C_{18}), 136.90 (C_{23}), 130.31 (C_2), 129.64 (C_{21}), 129.59 (C_5), 129.46 (C_{22}), 127.53 (C_{20}), 123.58 (C_{19}), 122.20 (C_4), 121.86 (C_3), 121.70 (C_{24}), 121.26 (C_6), 109.17 (C_8), 107.95 (C_{13}), 94.32 (C_{12}), 92.28 (C_{10}), 90.15 (C_{11}), 89.44 (C_9), 38.95 (C_{17}), 34.60 (C_1).

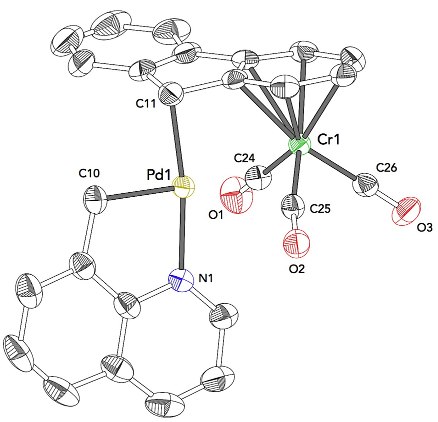

Compound **17j**
Space Group: **P b c a**
R-Factor (%): **2.47**

N°	A	B	C	Lengths (Å)	Angles (°)
1	Cr_1	Pd_1	-	2.8368(4)	-
2	Cr_1	C_{24}	-	1.861(2)	-
3	Cr_1	C_{25}	-	1.859(2)	-
4	Cr_1	C_{26}	-	1.833(2)	-
5	C_{24}	O_1	-	1.152(3)	-
6	C_{25}	O_2	-	1.158(3)	-
7	C_{26}	O_3	-	1.155(3)	-
8	Pd_1	C_{11}	-	2.116(2)	-
9	Pd_1	C_{10}	-	2.044(2)	-
10	Pd_1	N_1	-	2.106(2)	-
11	Pd_1	C_{24}	-	2.700(2)	-
12	Pd_1	C_{25}	-	2.532(2)	-
13	Cr_1	C_{24}	O_1	-	173.0(2)
14	Cr_1	C_{25}	O_2	-	170.4(2)
15	Cr_1	C_{26}	O_3	-	179.0(2)
16	C_{24}	Cr_1	C_{25}	-	99.7(1)

2.5.24.3 - Compound 19a.

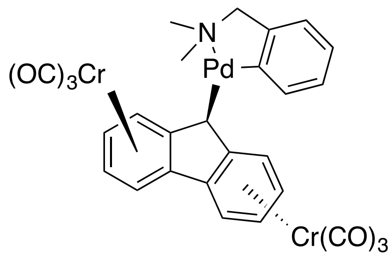

19a

Synthesis:

18a (0.200 g, 0.46 mmol), *n*-BuLi (0.31 mL, 0.50 mmol), **10a** (0.128 g, 0.23 mmol): bimetallic compound **19a** (0.170 g, 0.25 mmol, 55 % yield).

Characterizations:

Calcd for $C_{28}H_{21}Cr_2NO_6Pd$: C, 49.61; H, 3.12; N, 2.07. Found: C, 49.58; H, 3.25; N, 1.96.

HRMS-ESI (*m/z*): $[M+1H]^+$ calcd for $C_{28}H_{21}Cr_2NO_6Pd$, 677.9287; found, 677.9283.

IR (cm^{-1}) ν(CO): 1942 (s), 1892 (s), 1855 (vs).

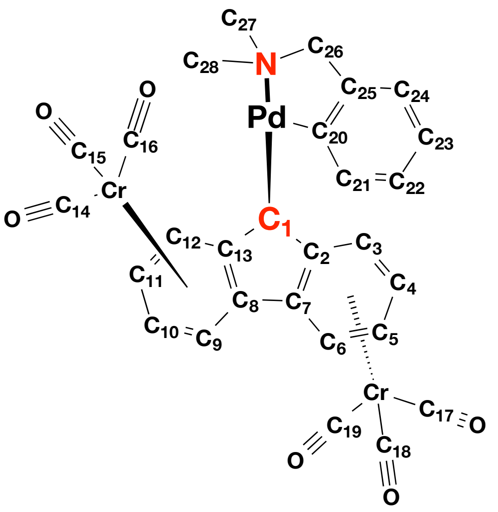

^{1}H NMR (600 MHz, C_6D_6, 298 K) δ 7.96 (d, J = 7.5 Hz, 1H, H_{21}), 7.31 (t, J = 7.7 Hz, 1H, H_{22}), 7.19 – 7.13 (m, 1H, H_{23}), 6.94 (d, J = 7.5 Hz, 1H, H_{24}), 5.50 (d, J = 6.7 Hz, 1H, H_9), 5.22 (d, J = 6.4 Hz, 1H, H_{12}), 4.98 (d, J = 6.5 Hz, 1H, H_6), 4.87 – 4.77 (m, 2H, H_5, H_3), 4.48 (s, 1H, H_1), 4.40 (t, J = 6.4 Hz, 1H, H_{10}), 4.23 (t, J = 6.2 Hz, 1H, H_{11}), 3.97 (t, J = 6.4 Hz, 1H, H_4), 3.69 (d, J = 13.0 Hz, 1H, H_{26a}), 2.68 (d, J = 13.0 Hz, 1H, H_{26b}), 2.24 (s, 3H, H_{27}), 2.15 (s, 3H, H_{28}). ^{13}C NMR (151 MHz, C_6D_6, 298 K) δ 236.77 (bs, C_{16}), 235.14 (bs, C_{15}), 234.01 (C_{18}, C_{17}, C_{19}), 232.88 (bs, C_{14}), 160.24 (C_{20}), 147.47 (C_{25}), 132.86 (C_{21}), 126.88 (C_{22}), 124.87 (C_{23}), 124.07 (C_{24}), 123.57 (C_8), 109.18 (C_2), 108.35 (C_7), 96.69 (C_{13}), 94.94 (C_{10}), 94.70 (C_3), 94.07 (C_5), 91.59 (C_4), 88.94 (C_{12}), 87.46 (C_6), 87.09 (C_{11}), 85.49 (C_9), 73.41 (C_{26}), 50.59 (C_{28}), 49.11 (C_{27}), 41.12 (C_1).

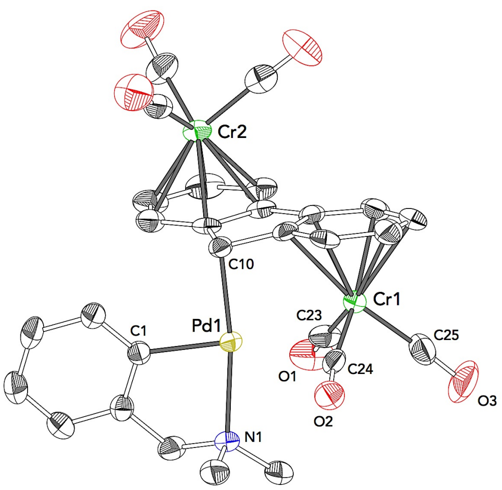

Compound **19a**
Space Group: **P -1**
R-Factor (%): **3.81**

N°	A	B	C	Lengths (Å)	Angles (°)
1	Cr_1	Pd_1	-	2.8558(7)	-
2	Cr_1	C_{23}	-	1.845(4)	-
3	Cr_1	C_{24}	-	1.858(4)	-
4	Cr_1	C_{25}	-	1.834(4)	-
5	C_{23}	O_1	-	1.158(5)	-
6	C_{24}	O_2	-	1.153(4)	-
7	C_{25}	O_3	-	1.155(5)	-
8	Pd_1	C_{10}	-	2.095(3)	-
9	Pd_1	C_1	-	2.025(4)	-
10	Pd_1	N_1	-	2.204(3)	-
11	Pd_1	C_{23}	-	2.677(5)	-
12	Pd_1	C_{24}	-	2.542(4)	-
13	Cr_1	C_{23}	O_1	-	172.1(4)
14	Cr_1	C_{24}	O_2	-	168.9(4)
15	Cr_1	C_{25}	O_3	-	176.9(4)
16	C_{23}	Cr_1	C_{24}	-	100.5(2)

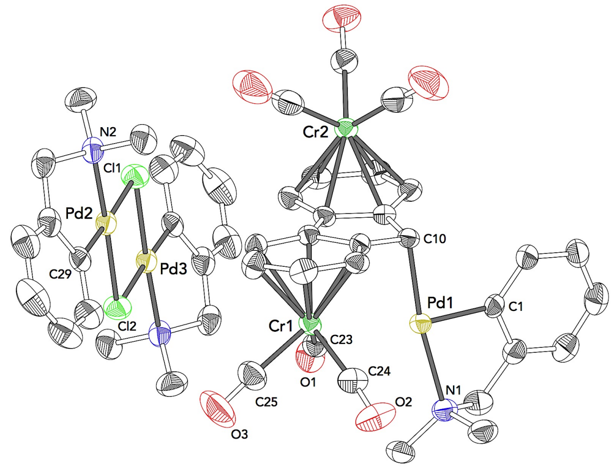

Compound **19a**
Space Group: **P -1**
R-Factor (%): **3.3**

N°	A	B	C	Lengths (Å)	Angles (°)
1	Cr_1	Pd_1	-	2.9608(4)	-
2	Cr_1	C_{23}	-	1.850(4)	-
3	Cr_1	C_{24}	-	1.843(3)	-
4	Cr_1	C_{25}	-	1.851(3)	-
5	C_{23}	O_1	-	1.158(5)	-
6	C_{24}	O_2	-	1.155(4)	-
7	C_{25}	O_3	-	1.146(4)	-
8	Pd_1	C_{10}	-	2.080(2)	-
9	Pd_1	C_1	-	2.021(3)	-
10	Pd_1	N_1	-	2.196(2)	-
11	Pd_1	C_{23}	-	2.593(3)	-
12	Pd_1	C_{24}	-	2.981(4)	-
13	Pd_2	Cl_1	-	2.4725(9)	-
14	Pd_2	Cl_2	-	2.3308(5)	-
15	Pd_2	N_2	-	2.078(2)	-
16	Pd_2	C_{29}	-	1.987(4)	-
17	Pd_3	Cl_1	-	2.3308(5)	-
18	Pd_3	Cl_2	-	2.4725(9)	-
19	Cr_1	C_{23}	O_1	-	169.9(3)
20	Cr_1	C_{24}	O_2	-	174.1(3)
21	Cr_1	C_{25}	O_3	-	177.6(3)
22	C_{23}	Cr_1	C_{24}	-	98.7(1)
23	Pd_2	Cl_1	Pd_3	-	93.76(3)
24	Pd_2	Cl_2	Pd_3	-	93.76(3)

2.5.24.4 - Compound 19i.

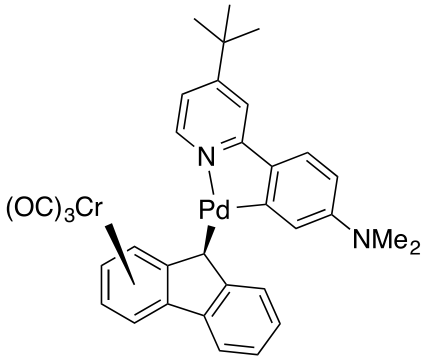

19i

Synthesis:

18a (0.200 g, 0.46 mmol), *n*-BuLi (0.31 mL, 0.50 mmol), **10i** (0.184 g, 0.23 mmol): bimetallic compound **19i** (0.182 g, 0.23 mmol, 50 % yield).

Characterizations:

Calcd for $C_{36}H_{30}Cr_2N_2O_6Pd$: C, 54.25; H, 3.79; N, 3.51. Found: C, 53.86; H, 4.10; N, 3.90. HRMS-ESI (*m/z*): $[M+1H]^+$ calcd for $C_{36}H_{30}Cr_2N_2O_6Pd$, 797.0022; found, 797.0077. IR (cm^{-1}) ν(CO): 1946 (s), 1887 (s), 1866 (vs).

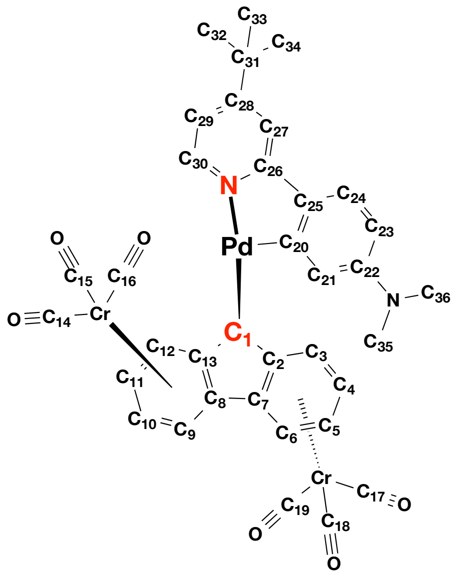

^{1}H NMR (500 MHz, C_6D_6, 293 K) δ 8.33 (d, J = 6.1 Hz, 1H, H_{30}), 7.76 (d, J = 2.5 Hz, 1H, H_{21}), 7.59 (d, J = 8.7 Hz, 1H, H_{24}), 7.31 (d, J = 2.2 Hz, 1H, H_{27}), 6.59 (dd, J = 8.7, 2.5 Hz, 1H, H_{23}), 6.23 (dd, J = 6.1, 2.0 Hz, 1H, H_{29}), 6.03 (d, J = 6.8 Hz, 1H, H_9), 5.27 (d, J = 6.5 Hz, 1H, H_{12}), 5.03 (d, J = 6.6 Hz, 1H, H_6), 5.01 (d, J = 6.5 Hz, 1H, H_3), 4.90 (t, J = 6.5 Hz, 1H, H_5), 4.76 (s, 1H, H_1), 4.52 (t, J = 6.3 Hz, 1H, H_{10}), 4.40 (t, J = 6.3 Hz, 1H, H_{11}), 4.05 (td, J = 6.5, 1.1 Hz, 1H, H_4), 2.90 (s, 6H, H_{35}, H_{36}), 0.86 (s, 9H, H_{33}, H_{34}, H_{32}). ^{13}C NMR (126 MHz, C_6D_6, 293 K) δ 236.16 (bs, C_{16}), 235.73 (bs, C_{15}), 234.54 (C_{17}, C_{18}, C_{19}), 232.16 (bs, C_{14}), 166.02 (C_{28}), 165.21 (C_{20}), 161.51 (C_{26}), 151.49 (C_{30}, C_{22}), 135.76 (C_{25}), 126.02 (C_{24}), 121.80 (C_8), 118.08 (C_{29}), 117.03 (C_{21}), 114.33 (C_{27}), 110.53 (C_2), 108.75 (C_{23}), 108.31 (C_7), 98.41 (C_{13}), 95.43 (C_3), 94.30 (C_{10}), 94.09 (C_5), 91.57 (C_4), 88.76 (C_{12}), 87.94 (C_{11}), 87.86 (C_6), 85.94 (C_9), 43.55 (C_1), 40.15 (C_{35}, C_{36}), 34.68 (C_{31}), 29.97 (C_{33}, C_{34}, C_{32}).

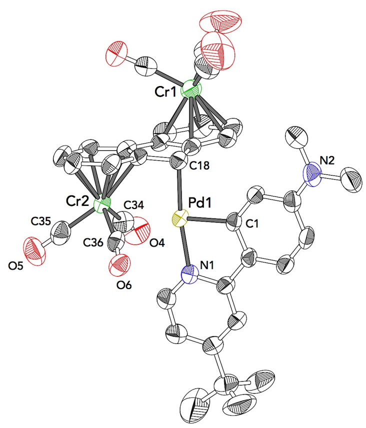

Compound **19i**
Space Group: **P 2_1/c**
R-Factor (%): **5.82**

N°	A	B	C	Lengths (Å)	Angles (°)
1	Cr_2	Pd_1	-	2.9021(7)	-
2	Cr_1	C_{34}	-	1.846(5)	-
3	Cr_1	C_{35}	-	1.848(5)	-
4	Cr_1	C_{36}	-	1.861(5)	-
5	C_{34}	O_4	-	1.163(6)	-
6	C_{35}	O_5	-	1.152(7)	-
7	C_{36}	O_6	-	1.158(6)	-
8	Pd_1	C_{18}	-	2.095(4)	-
9	Pd_1	C_1	-	2.018(4)	-
10	Pd_1	N_1	-	2.109(4)	-
11	Pd_1	C_{34}	-	2.880(5)	-
12	Pd_1	C_{36}	-	2.557(4)	-
13	Cr_2	C_{34}	O_4	-	174.7(5)
14	Cr_2	C_{35}	O_5	-	174.9(5)
15	Cr_2	C_{36}	O_6	-	170.5(4)
16	C_{34}	Cr_2	C_{36}	-	98.5(2)

2.5.25 - Compound 20a.

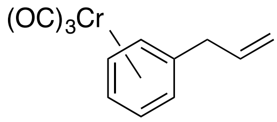

20a

Synthesis:

$Cr(CO)_6$ (7.0 g, 31.81 mmol), allylbenzene (7.59 mL, 57.26 mmol), THF (15 mL), and di-*n*-butylether (150 mL) were gently refluxed for 144 h under a permanent flow of argon. The resulting orange/red solution was evaporated to dryness and the resulting residue was adsorbed on silica gel. Chromatographic separation was performed on silica gel using a mixture of CH_2Cl_2 and pentane (1:1 to 1:0) as eluent. The product was eluted as a yellow solution, which afforded yellow oil upon removal of the solvents under reduced pressure (5.500 g, 21.64 mmol, 68 %).

Characterizations:

Calcd for $C_{12}H_{10}CrO_3$: C, 56.70; H, 3.97. Found: C, 56.78; H, 3.95. HRMS-ESI (*m/z*): $[M]^+$ calcd for $C_{12}H_{10}CrO_3$, 254.0035; found, 254.0039. IR (cm^{-1}) ν(CO): 1951 (s), 1851 (vs).

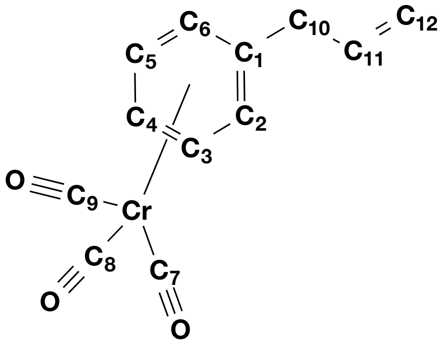

^{1}H NMR (300 MHz, C_6D_6, 298 K) δ 5.54 (ddt, J = 16.8, 10.0, 6.7 Hz, 1H, H_{11}), 4.87 (dq, J = 10.1, 1.3 Hz, 1H, H_{12a}), 4.78 (dd, J = 17.0, 1.6 Hz, 1H, H_{12b}), 4.44 (t, J = 6.4 Hz, 2H, H_3, H_5), 4.36 – 4.31 (m, 2H, H_2, H_6), 4.29 – 4.21 (m, 1H, H_4), 2.58 (dt, J = 6.8, 1.4 Hz, 2H, H_{10}). ^{13}C NMR (101 MHz, C_6D_6, 298 K) δ 233.54 (C_8, C_9, C_7), 135.08 (C_{11}), 117.86 (C_{12}), 111.01 (C_1), 93.43 (C_3, C_5), 92.47 (C_2, C_6), 90.33 (C_4), 38.67 (C_{10}).

2.5.26 - Standard procedure for the synthesis of 21.

20a was dissolved in THF (5 mL) and treated with *n*-BuLi at -40°C under argon. The resulting solution was transferred after 30 min *via* canula to another Schlenk vessel containing a THF (3 mL) solution of corresponding [Pd(μ-Cl)(Metalacycle)]$_2$. The resulting solution was stirred for 30 min whilst temperature was slowly raised to -20 °C. At this temperature the solvent was removed and the residue extracted with cold diethyl ether. Finally filtration over celite and recrystallization from a dichloromethane/pentane mixture of solvents led to the expected yellowish solid.

2.5.26.1 - Compound 21a.

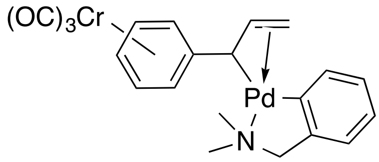

21a

Synthesis:

20a (0.200 g, 0.79 mmol), *n*-BuLi (0.54 mL, 0.87 mmol), **10a** (0.226 g, 0.41 mmol): bimetallic compound **21a** (0.220 g, 0.22 mmol, 57 % yield).

Characterizations:

Calcd for $C_{21}H_{21}CrNO_3Pd{\bullet}0.4CH_2Cl_2$: C, 48.70; H, 4.16; N, 2.65. Found: C, 48.63; H, 4.15; N, 2.29. HRMS-ESI (*m/z*): $[M+1H]^+$ calcd for $C_{21}H_{21}CrNO_3Pd$, 494.0034; found, 494.0035. IR (cm^{-1}) ν(CO): 1950 (s), 1896 (s) 1860 (vs).

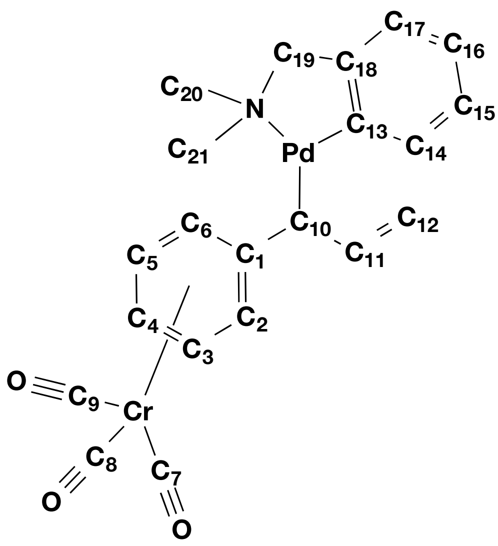

^{1}H NMR (600 MHz, Tol, 223 K) δ 7.82 (dd, J = 5.7, 2.9 Hz, 1H, H_{14}), 7.22 – 7.17 (m, 2H, H_{15}, H_{16}), 7.05 (d, J = 5.7 Hz, 1H, H_{17}), 5.30 (td, J = 12.2, 7.1 Hz, 1H, H_{11}), 4.60 (q, J = 5.6 Hz, 2H, H_{3}, H_{5}), 4.18 – 4.13 (m, 3H, H_{2}, H_{4}, H_{6}), 3.19 (d, J = 10.3 Hz, 1H, H_{19a}), 3.04 – 2.97 (m, 3H, H_{10}, H_{12a}, H_{19b}), 2.88 (d, J = 11.9 Hz, 1H, H_{12b}), 1.89 (s, 3H, H_{21}), 1.68 (s, 3H, H_{20}). ^{13}C NMR (151 MHz, Tol, 223 K) δ 234.17 (C_{9}, C_{8}, C_{7}), 161.50 (C_{13}), 148.47 (C_{18}), 140.30 (C_{14}), 126.04 (C_{15}), 124.65 (C_{16}), 122.42 (C_{17}), 113.42 (C_{11}), 112.99 (C_{1}), 94.43 (C_{3}, C_{5}), 90.12 (C_{6}), 87.56 (C_{4}), 85.14 (C_{2}), 75.03 (C_{10}), 72.37 (C_{19}), 50.42 (C_{20}), 49.96 (C_{21}), 45.94 (C_{12}).

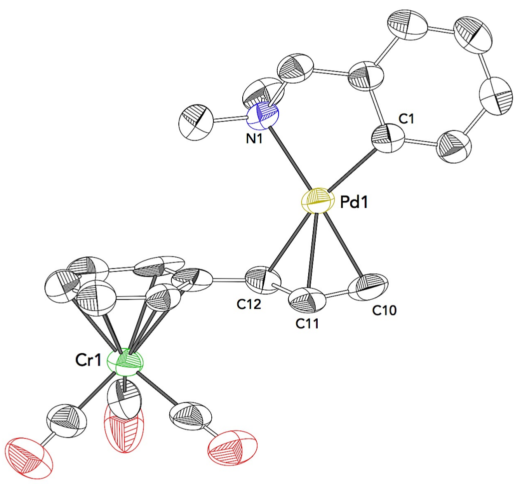

Compound **21a**
Space Group: **P -1**
R-Factor (%): **5.33**

N°	*A*	*B*	*C*	*Lengths (Å)*	*Angles (°)*
1	Pd_1	C_{10}	-	2.101(5)	-
2	Pd_1	C_{11}	-	2.11(1)	-
3	Pd_1	C_{12}	-	2.247(9)	-
4	Pd_1	N_1	-	2.144(3)	-
5	Pd_1	C_1	-	2.022(4)	-
6	C_{10}	C_{11}	-	1.31(1)	-
7	C_{11}	C_{12}	-	1.44(1)	-

2.5.26.2 - Compound 21b.

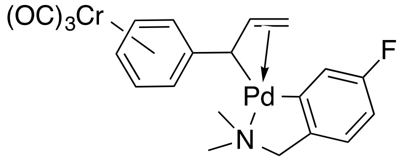

21b

Synthesis:

20a (0.200 g, 0.79 mmol), *n*-BuLi (0.54 mL, 0.87 mmol), **10b** (0.241 g, 0.41 mmol): bimetallic compound **21b** (0.171 g, 0.33 mmol, 42 % yield).

Characterizations:

Calcd for $C_{21}H_{20}CrFNO_3Pd$: C, 49.28; H, 3.94; N, 2.74. Found: C, 49.18; H, 4.08; N, 2.70.
HRMS-ESI (*m/z*): $[M+1H]^+$ calcd for $C_{21}H_{20}CrFNO_3Pd$, 511.9940; found, 511.9963.
IR (cm^{-1}) ν(CO): 1959 (s), 1940 (s) 1858 (vs).

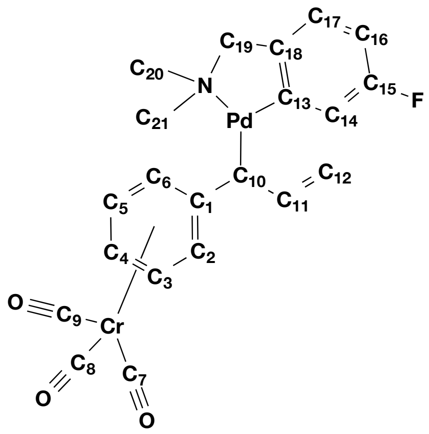

^{1}H NMR (600 MHz, Tol, 233 K) δ 7.66 (dd, J = 7.9, 2.6 Hz, 1H, H_{14}), 6.89 – 6.84 (m, 1H, H_{16}), 6.82 (d, J = 5.1 Hz, 1H, H_{17}), 5.17 (td, J = 12.3, 7.1 Hz, 1H, H_{11}), 4.59 – 4.55 (m, 2H, H_3, H_5), 4.16 (t, J = 6.2 Hz, 1H, H_4), 4.14 (d, J = 6.8 Hz, 2H, H_2, H_6), 3.06 (d, J = 13.4 Hz, 1H, H_{19a}), 2.97 – 2.85 (m, 3H, H_{10}, H_{12a}, H_{19b}), 2.72 (dt, J = 11.8, 1.4 Hz, 1H, H_{12b}), 1.84 (s, 3H, H_{20}), 1.62 (s, 3H, H_{21}). ^{13}C NMR (151 MHz, Tol, 233 K) δ 233.92 (C_9, C_8, C_7), 164.54 (d, J = 1.6 Hz, C_{13}), 160.87 (d, J = 248.2 Hz, C_{15}), 143.80 (d, J = 2.2 Hz, C_{18}), 125.91 (d, J = 15.3 Hz, C_{14}), 123.06 (d, J = 7.1 Hz, C_{17}), 113.20 (C_{11}), 112.53 (C_1), 110.74 (d, J = 22.2 Hz, C_{16}), 94.11 (C_3), 94.09 (C_5), 90.22 (C_6), 87.75 (C_4), 85.25 (C_2), 75.47 (C_{10}), 71.75 (C_{19}), 50.25 (C_{20}), 49.80 (C_{21}), 46.26 (C_{12}). ^{19}F NMR (282 MHz, C_6D_6) δ -118.53.

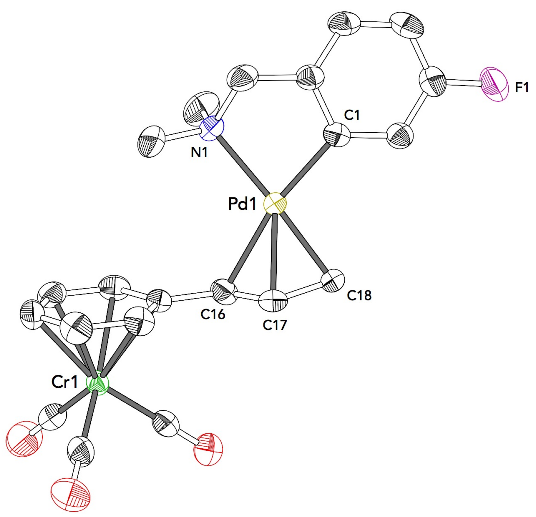

N°	A	B	C	Lengths (Å)	Angles (°)
1	Pd_1	C_{18}	-	2.096(3)	-
2	Pd_1	C_{17}	-	2.146(3)	-
3	Pd_1	C_{16}	-	2.276(3)	-
4	Pd_1	N_1	-	2.149(3)	-
5	Pd_1	C_1	-	2.021(2)	-
6	C_{18}	C_{17}	-	1.420(4)	-
7	C_{17}	C_{16}	-	1.373(4)	-

Compound **21b**
Space Group: **P 2_1/c**
R-Factor (%): **2.75**

2.5.26.3 - Compound 21i.

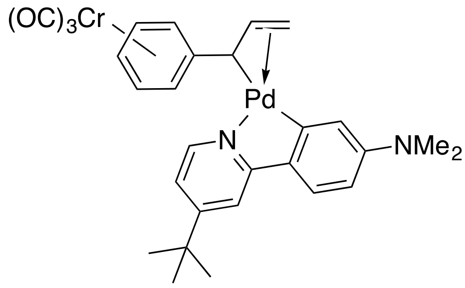

21i

Synthesis:

20a (0.200 g, 0.79 mmol), *n*-BuLi (0.54 mL, 0.87 mmol), **10i** (0.317 g, 0.40 mmol): bimetallic compound **21i** (0.247 g, 0.40 mmol, 51 % yield).

Characterizations:

Calcd for $C_{29}H_{30}CrN_2O_3Pd$: C, 56.82; H, 4.93; N, 4.54. Found: C, 56.66; H, 5.03; N, 4.77.

HRMS-ESI (*m/z*): $[M+1Na]^+$ calcd for $C_{29}H_{30}CrN_2O_3Pd$, 635.0589; found, 635.0573.

IR (cm^{-1}) ν(CO): 1951 (s), 1866 (vs).

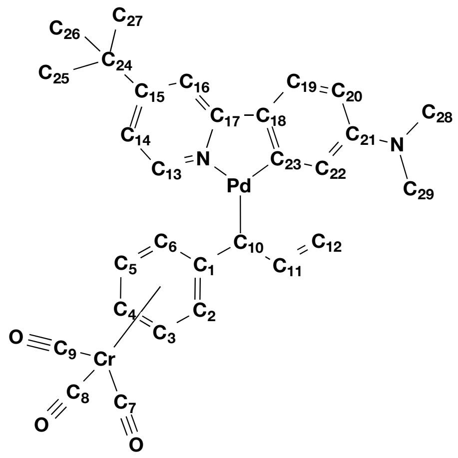

^{1}H NMR (600 MHz, Tol, 233 K) δ 8.26 (d, J = 5.9 Hz, 1H, H_{13}), 7.78 (d, J = 8.7 Hz, 1H, H_{19}), 7.68 (d, J = 2.0 Hz, 1H, H_{16}), 6.48 (dd, J = 8.6, 2.6 Hz, 1H, H_{20}), 6.44 (dd, J = 5.9, 2.1 Hz, 1H, H_{14}), 6.15 (d, J = 2.5 Hz, 1H, H_{22}), 5.94 (q, J = 11.3, 10.8 Hz, 1H, H_{11}), 5.08 (d, J = 6.9 Hz, 1H, H_2), 4.55 (q, J = 6.3 Hz, 1H, H_5), 4.45 (d, J = 6.3 Hz, 1H, H_6), 4.35 (t, J = 6.6 Hz, 1H, H_3), 4.18 (t, J = 6.3 Hz, 1H, H_4), 3.72 (d, J = 8.2 Hz, 1H, H_{12a}), 3.43 (d, J = 14.0 Hz, 1H, H_{12b}), 3.15 (d, J = 10.9 Hz, 1H, H_{10}), 2.51 (s, 6H, H_{29}, H_{28}), 1.13 (s, 9H, H_{25}, H_{26}, H_{27}). ^{13}C NMR (151 MHz, Tol, 233 K) δ 234.45 (C_8, C_9, C_7), 166.77 (C_{23}), 166.00 (C_{17}), 161.69 (C_{15}), 154.12 (C_{13}), 150.27 (C_{21}), 135.84 (C_{18}), 124.65 (C_{19}), 119.42 (C_{22}), 118.07 (C_{14}), 116.83 (C_1), 116.38 (C_{11}), 114.67 (C_{16}), 107.99 (C_{20}), 95.52 (C_3), 94.81 (C_5), 92.11 (C_6), 88.85 (C_2), 87.30 (C_4), 69.05 (C_{12}), 55.09 (C_{10}), 40.50 (C_{29}, C_{28}), 34.87 (C_{24}), 29.90 (C_{25}, C_{26}, C_{27}).

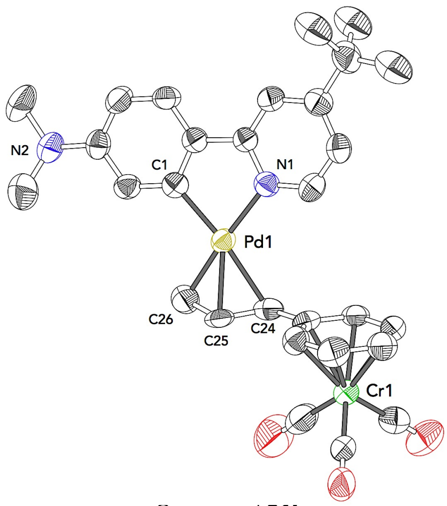

Compound **21i**
Space Group: **C 2/c**
R-Factor (%): **7.08**

N°	*A*	*B*	*C*	*Lengths (Å)*	*Angles (°)*
1	Pd_1	C_{26}	-	2.105(6)	-
2	Pd_1	C_{25}	-	2.135(6)	-
3	Pd_1	C_{24}	-	2.256(5)	-
4	Pd_1	N_1	-	2.082(4)	-
5	Pd_1	C_1	-	2.025(5)	-
6	C_{26}	C_{25}	-	1.393(8)	-
7	C_{25}	C_{24}	-	1.379(7)	-

2.5.27 - Standard procedure for the synthesis of 23.

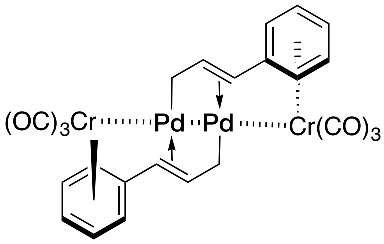

23

Synthesis:

Bimetallic **21a**, **21b**, or **21c** was dissolved under argon in dry benzene and left in solution for 12 hours, leading to the formation of red crystals associated to the Pd(I)-Pd(I) species. The solution was then removed, and crystals carefully recovered under argon and dried under vacuum.

Best yields by using bimetallic **21a** (0.200 g, 0.41 mmol), benzene (5 mL): Pd(I)-Pd(I) compound (0.032 g, 0.04 mmol, 22 % yield).

Characterizations:

Analysis performed on crystals of **23**: Calcd for $C_{24}H_{18}Cr_2O_6Pd_2{\bullet}0.5C_6H_6$: C, 42.60; H, 3.18. Found: C, 42.79; H, 2.99. IR (cm^{-1}) ν(CO): 1928 (s), 1874 (s), 1835 (vs).

In this case it was not possible to get the molecular mass of the Pd(I)-Pd(I) complex by ESI-TOF-MS, but we were able to obtain the mass associated to the related oxidized Pd(II) species:

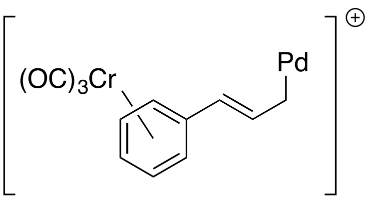

HRMS-ESI (*m/z*): $[M]^+$ calcd for $C_{12}H_9CrO_3Pd$, 358.8992; found, 358.8990.

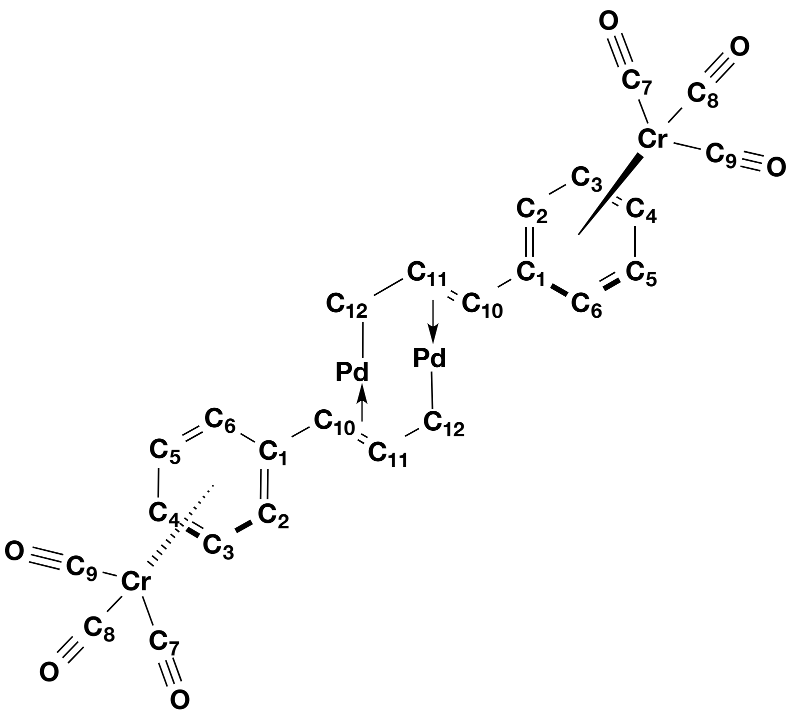

[1]H NMR (600 MHz, C_6D_6, 298 K) δ 5.81 – 5.72 (m, 2H, H_{11}), 5.56 (d, J = 15.8 Hz, 2H, H_{10}), 4.76 – 4.70 (m, 4H, H_2, H_6), 4.54 (t, J = 6.5 Hz, 4H, H_3, H_5), 4.32 (tt, J = 6.2, 1.0 Hz, 2H, H_4), 1.99 – 1.94 (m, 4H, H_{12}). [13]C NMR (151 MHz, C_6D_6, 298 K) δ 233.65 (C_8, C_9, C_7), 132.17 (C_{11}), 127.62 (C_{10}), 106.34 (C_1), 93.07 (C_3, C_5), 90.78 (C_4), 90.31 (C_2, C_6), 32.33 (C_{12}).

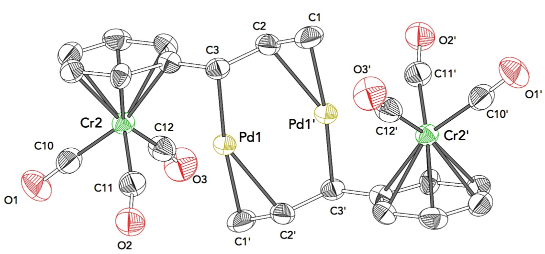

Compound **23**
Space Group: **P 2_1/c**
R-Factor (%): **3.89**

N°	A	B	C	D	Lengths (Å)	Angles (°)
1	Cr_2	Pd_1	-	-	2.786(1)	-
2	Pd_1	$Pd_{1'}$	-	-	2.749(1)	
3	Cr_2	C_{10}	-	-	1.837(3)	-
4	Cr_2	C_{11}	-	-	1.872(2)	-
5	Cr_2	C_{12}	-	-	1.851(3)	-
6	C_{10}	O_1	-	-	1.152(4)	-
7	C_{11}	O_2	-	-	1.149(3)	-
8	C_{12}	O_3	-	-	1.151(4)	-
9	C_1	C_2	-	-	1.379(6)	-
10	C_2	C_3	-	-	1.441(6)	-
11	Pd_1	$C_{1'}$	-	-	2.174(4)	-
12	Pd_1	$C_{2'}$	-	-	2.271(5)	-
13	Pd_1	C_3	-	-	2.164(4)	-
14	Pd_1	C_{11}	-	-	2.526(3)	-
15	Pd_1	C_{12}	-	-	2.895(3)	-
16	Cr_2	Pd_1	$Pd_{1'}$	-	-	151.38(6)
17	Cr_2	C_{10}	O_1	-	-	177.3(2)
18	Cr_2	C_{11}	O_2	-	-	170.3(2)
19	Cr_2	C_{12}	O_3	-	-	172.3(3)
20	C_{11}	Cr_2	C_{12}	-	-	95.2(1)
21	Cr_2	Pd_1	$Pd_{1'}$	$Cr_{2'}$	-	180.0(8)

2.5.28 - Compound 24.

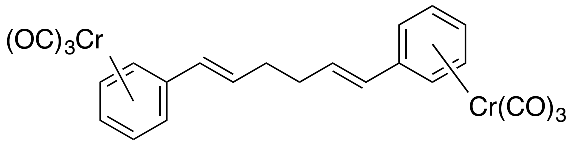

24

HRMS-ESI (*m/z*): [M+1Na]$^+$ calcd for $C_{24}H_{18}Cr_2O_6$, 528.9806; found, 528.9808.

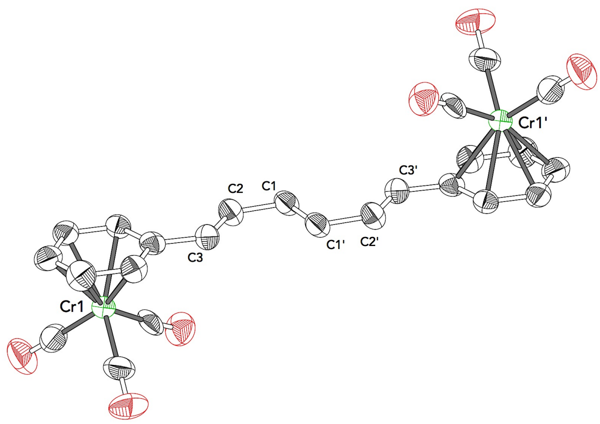

N°	A	B	C	D	Lengths (Å)	Angles (°)
1	C_1	C_2	-	-	1.510(9)	-
2	C_2	C_3	-	-	1.309(8)	-
3	C_1	$C_{1'}$	-	-	1.509(9)	-

Compound **24**
Space Group: **P 2_1/c**
R-Factor (%): **8.81**

2.5.29 - Compound 25a.

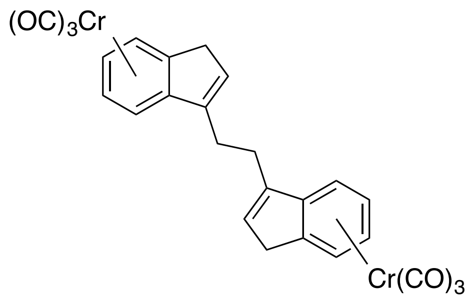

25a

Synthesis:

$Cr(CO)_6$ (11.499 g, 52.25 mmol), 1,2-Bis(3-indenyl)ethane (5.0 g, 19.35 mmol), naphtalen (0.335 g, 2.61 mmol), THF (15 mL), and di-*n*butylether (150 mL) were gently refluxed for 135 h under a permanent flow of argon. The resulting orange/red solution was evaporated to dryness and the resulting residue was adsorbed on silica gel. Chromatographic separation was performed on silica gel using a mixture of CH_2Cl_2 and pentane (1:1 to 1:0) as eluent. The product was eluted as a orange solution, which afforded a orange solid upon removal of the solvents under reduced pressure (1.57 g, 19.35 mmol, 15 %).

Characterizations:

Calcd for $C_{26}H_{18}Cr_2O_6$: C, 58.88; H, 3.42. Found: C, 59.10; H, 3.75. HRMS-ESI (*m/z*): $[M+1Na]^+$ calcd for $C_{26}H_{18}Cr_2O_6$, 552.9806; found, 552.9810. IR (cm^{-1}) ν(CO): 1940 (s), 1840 (vs).

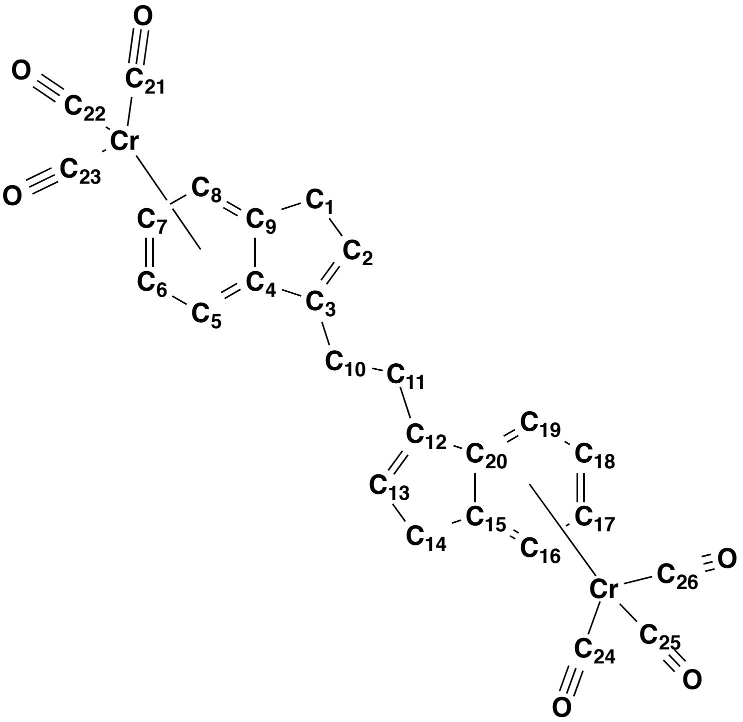

Isomer A:

^{1}H NMR (500 MHz, C_6D_6, 293 K) δ 5.69 (bd, J = 26.2 Hz, 4H, H_2, H_{13}), 5.24 (d, J = 6.2 Hz, 2H, H_5), 4.91 (d, J = 6.2 Hz, 2H, H_8), 4.53 – 4.45 (m, 2H, H_7, H_{17}), 4.45 – 4.36 (m, 2H, H_6, H_{18}), 2.90 (dd, J = 23.0, 7.3 Hz, 1H, H_{1a}, H_{14a}), 2.68 (d, J = 23.0 Hz, 1H, H_{1b}, H_{14b}), 2.52 – 2.38 (m, 2H, H_{10}), 2.37 – 2.27 (m, 2H, H_{11}). ^{13}C NMR (126 MHz, C_6D_6, 293 K) δ 234.32 (C_{22}, C_{21}, C_{23}, C_{25}, C_{24}, C_{26}), 141.21 (C_3, C_{12}), 130.79 (C_2, C_{13}), 114.87 (C_4, C_{20}), 114.53 (C_9, C_{15}), 91.37 (C_7, C_{17}), 90.05 (C_6, C_{18}), 89.80 (C_8, C_{16}), 87.30 (C_5, C_{19}), 37.88 (C_1, C_{14}), 25.15 (C_{10}, C_{11}).

Isomer B:

^{1}H NMR (500 MHz, C_6D_6, 293 K) δ 5.69 (bd, J = 26.2 Hz, 2H, H_2, H_{13}), 5.01 (d, J = 6.2 Hz, 2H, H_5, H_{19}), 4.95 (d, J = 6.2 Hz, 2H, H_8, H_{16}), 4.53 – 4.45 (m, 2H, H_7, H_{17}), 4.45 – 4.36 (m, 2H, H_6, H_{18}), 2.90 (dd, J = 23.0, 7.3 Hz, 2H, H_{1a}, H_{14a}), 2.68 (d, J = 23.0 Hz, 2H, H_{1b}, H_{14b}), 2.52 – 2.38 (m, 2H, H_{10}), 2.37 – 2.27 (m, 2H, H_{11}). ^{13}C NMR (126 MHz, C_6D_6, 293 K) δ 234.24 (C_{22}, C_{21}, C_{23}, C_{25}, C_{24}, C_{26}), 141.53 (C_3, C_{12}), 130.37 (C_2, C_{13}), 115.18 (C_4, C_{20}), 114.00 (C_9, C_{15}), 90.87 (C_7, C_{17}), 90.28 (C_6, C_{18}), 90.09 (C_8, C_{16}), 86.70 (C_5, C_{19}), 37.89 (C_1, C_{14}), 24.95 (C_{10}, C_{11}).

2.5.30 - Compound 26a.

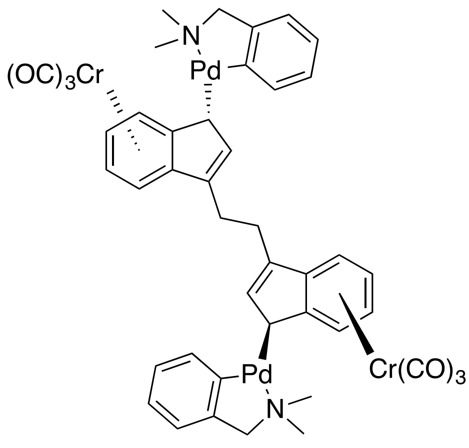

26a

Synthesis:

25a (0.100 g, 0.19 mmol) was dissolved in THF (5 mL) and treated with *n*-BuLi (0.26 mL, 0.41 mmol) at -40 °C under argon. The resulting solution was transferred after 30 min *via* canula to another Schlenk vessel containing a THF (3 mL) solution of **10a** (0.115 g, 0.21 mmol). The resulting solution was stirred for 1 hour whilst temperature was slowly raised to -5 °C. At this temperature, the solvent was removed under reduced pressure. The residue was then washed with cold diethyl ether to remove soluble impurities. Finally extraction with dichloromethane was performed, followed by a filtration over celite and recrystallization from a dichloromethane/pentane mixture of solvents, which led to the expected orange solid (0.033 g, 0.03 mmol, 17 % yield).

Characterizations:

Calcd for $C_{44}H_{40}Cr_2N_2O_6Pd_2{\bullet}0.2CH_2Cl_2$: C, 51.71; H, 3.97; N, 2.73. Found: C, 51.73; H, 4.10; N, 2.66. HRMS-ESI (*m/z*): $[M]^+$ calcd for $C_{44}H_{40}Cr_2N_2O_6Pd_2$, 1007.9766; found, 1007.9869. IR (cm^{-1}) ν(CO): 1936 (s), 1875 (s), 1842 (vs).

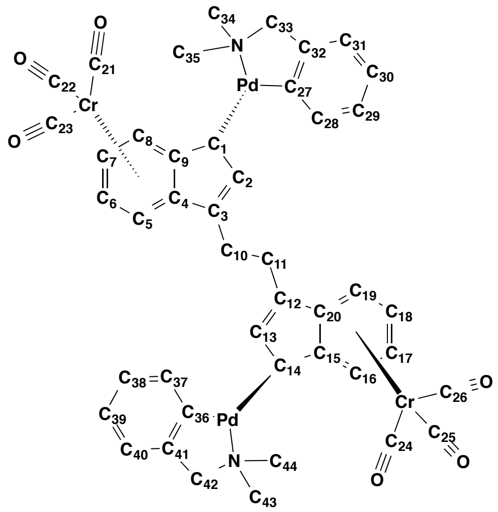

^{1}H NMR (500 MHz, $CDCl_3$, 293 K) δ 7.63 (d, J = 7.4 Hz, 2H, H_{28}, H_{37}), 7.19 (t, J = 7.3 Hz, 2H, H_{29}, H_{38}), 7.16 (d, J = 6.1 Hz, 2H, H_{31}, H_{40}), 7.11 (t, J = 7.3 Hz, 2H, H_{30}, H_{39}), 6.77 (d, J = 2.1 Hz, 2H, H_2, H_{13}), 6.02 (d, J = 6.7 Hz, 2H, H_5, H_{19}), 5.97 (d, J = 6.4 Hz, 2H, H_8, H_{16}), 5.93 (t, J = 6.2 Hz, 2H, H_6, H_{18}), 5.09 (t, J = 6.4 Hz, 2H, H_7, H_{17}), 4.47 (d, J = 2.1 Hz, 2H, H_1, H_{14}), 3.92 (d, J = 13.1 Hz, 2H, H_{33a}, H_{42a}), 3.64 (d, J = 13.1 Hz, 2H, H_{33b}, H_{42b}), 2.65 (s, 6H, H_{34}, H_{43}), 2.51 (s, 6H, H_{35}, H_{44}), 2.48 (s, 4H, H_{10}, H_{11}). ^{13}C NMR (126 MHz, $CDCl_3$, 293 K) δ 238.70 (bs, C_{23}, C_{26}), 236.44 (bs, C_{22}, C_{25}), 232.75 (bs, C_{21}, C_{24}), 156.50 (C_{27}, C_{36}), 148.03 (C_{32}, C_{41}), 141.28 (C_2, C_{13}), 132.18 (C_{28}, C_{37}), 126.19 (C_{29}, C_{38}), 124.39 (C_{30}, C_{39}), 124.30 (C_3, C_{12}), 123.66 (C_{31}, C_{40}), 116.17 (C_4, C_{20}), 106.45 (C_9, C_{15}), 95.89 (C_8, C_{16}), 94.16 (C_6, C_{18}), 90.35 (C_5, C_{19}), 88.44 (C_7, C_{17}), 73.49 (C_{33}, C_{42}), 51.01 (C_{35}, C_{44}), 50.35 (C_{34}, C_{43}), 46.29 (C_1, C_{14}), 25.95 (C_{10}, C_{11}).

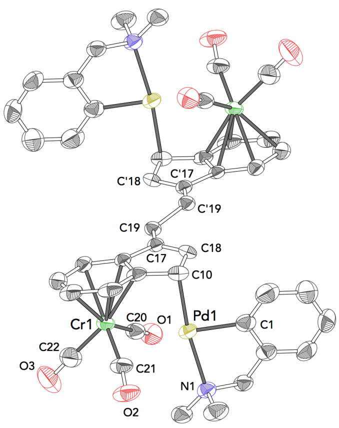

Compound **26a**
Space Group: **P -1**
R-Factor (%): **3.25**

N°	A	B	C	D	Lengths (Å)	Angles (°)
1	Cr_1	Pd_1	-	-	2.8929(4)	-
	Cr_1	C_{20}	-	-	1.853(2)	
2	Cr_1	C_{21}	-	-	1.837(3)	-
3	Cr_1	C_{22}	-	-	1.832(3)	-
4	C_{20}	O_1	-	-	1.151(3)	-
5	C_{21}	O_2	-	-	1.156(3)	-
6	C_{22}	O_3	-	-	1.155(4)	-
7	Pd_1	C_{10}	-	-	2.110(2)	-
8	Pd_1	C_1	-	-	2.020(3)	-
9	Pd_1	N_1	-	-	2.192(1)	-
10	Pd_1	C_{20}	-	-	2.647(3)	-
11	Pd_1	C_{21}	-	-	2.649(3)	-
12	C_{10}	C_{18}	-	-	1.471(3)	-
13	C_{18}	C_{17}	-	-	1.358(3)	-
14	C_{17}	C_{19}	-	-	1.493(3)	-
15	C_{19}	$C_{19'}$	-	-	1.521(3)	-
16	Cr_1	C_{20}	O_1	-	-	173.1(2)
17	Cr_1	C_{21}	O_2	-	-	171.2(2)
18	Cr_1	C_{22}	O_3	-	-	178.4(3)
19	C_{20}	Cr_1	C_{21}	-	-	98.1(1)

3 - Experimental methods of chapter IV compounds.

3.1 - Generalities.

All experiments were carried out under a dry atmosphere of argon using the standard Schlenk technique or in an argon-filled glove box when necessary. *n*-Butyllithium was purchased from Aldrich Chem. Co as a 1.6 M solution in hexane, hexacarbonylchromium was purchased from ABCR, 2-methyl-*1H*-indene (98 %) and Fluorene (98 %) were purchased from Aldrich Chem. Co., Celite 545 was purchased from VWR Prolabo. Precious metal chlorides were purchased from Pressure Chemical Co. Anhydrous tetrahydrofurane (abbr. THF) was distilled from purple solutions of Na/benzophenone under argon. All other solvents were distilled over sodium or CaH_2 under argon. Deuterated solvents were dried over sodium or CaH_2 and purified by trap-to-trap techniques, degassed by freeze-pump-thaw cycles and stored under argon. ^{1}H, ^{13}C NMR spectra were obtained on Bruker DPX 300, 400, Avance I 500 and Avance III 600 spectrometers. Chemical shifts (expressed in parts per million) were referenced against solvent peaks or external references. IR spectra were acquired with a FT-IR Bruker alpha spectrometer using an ATR solid-state sample cell.

3.2 - Computational details.

Computations were performed with methods of Density Functional Theory, *i.e.* the Tao-Perdew-Staroverov-Scuseria (*TPSS*) [1077] meta-GGA functional implemented in the Amsterdam Density Functional package (ADF2013 version)[1078] and augmented with Grimme's DFT-D3(BJ) implementation of Dispersion with a Becke-Johnson (BJ) damping function.[1079] Scalar relativistic computations with the *Zeroth Order Regular Approximation* were carried out using *ad hoc* all-electron (AE) basis sets: polarized triple-ζ (TZP) Slater type orbitals were used in this study for all elements. Natural Population analyses (NPA) were carried out on singlet ground state relaxed geometries.

[1077] [N°743] Tao, J.; Perdew, J. P.; Staroverov, V. N.; Scuseria, G. E. *Phys. Rev. Lett.* **2003**, *91*, 146401.

[1078] [N°861] In *Amsterdam Density Functional ADF2013*; SCM: Theoretical Chemistry, Vrije Universiteit, Amsterdam, The Netherlands.

[1079] [N°187] Grimme, S.; Ehrlich, S.; Goerigk, L. *J. Comput. Chem.* **2011**, *32*, 1456.

Geometry optimizations by energy gradient minimization were carried out in all cases with integration accuracy comprised between 6 and 7.5, an energy gradient convergence criterion of 10^{-3} au and tight to very tight SCF convergence criterion. Counterpoise correction for basis set superposition error (BSSE) was neglected throughout this study. ETS-NOCV analyses,[1080,1081] simulations of NMR spectra, as well as calculations of vibrational modes (analytical second derivative frequencies) were performed with optimized geometries using ADF2013 subroutines. Vibrational modes were computed in all cases to verify that the optimized geometries were related to energy minima. Natural atomic orbital (NAO) and natural bond orbital (NBO) analyses as well as Wiberg indice determination were performed with the GENNBO 5.0 module of ADF.[1082] AIM[1083] and NCI[1084, 1085] analyses were carried out using the modules embedded within ADF2013. Representations of molecular structures and orbitals were drawn using *ADFview* 2013

3.3 - X-ray diffraction analyses.

Reflections were collected with a Nonius KappaCCD and with an APEX diffractometer equipped with an Oxford Cryosystem liquid N_2 device, using Mo Kα radiation (λ = 0.71073 Å). The crystal detector distance was 38 mm. The cell parameters were determined (APEX2 software)[1086] from reflections taken from three sets of 12 frames, each at 10 s exposures. The structures were solved by direct methods using the program SHELXS-97.[1087] The refinement and all further calculations were carried out using SHELXL-97.[1088] The crystal structures acquired with the Nonius Kappa CCD were

1080 [N°750] Mitoraj, M. P.; Michalak, A.; Ziegler, T. *J. Chem. Theory Comput.* **2009**, *5*, 962.

1081 [N°751] Mitoraj, M. P.; Michalak, A.; Ziegler, T. *Organometallics* **2009**, *28*, 3727.

1082 [N°813] Weinhold, F.; Landis, C. R. *Valency and Bonding, a Natural Bond Orbital Donor-Acceptor Perspective*; University Press: Cambridge, UK, **2005**.

1083 [N°755] Bader, R. F. W. In *Atoms in Molecules: A Quantum Theory*; Clarendon: Oxford, **1990**.

1084 [N°629] Contreras-García, J.; Johnson, E. R.; Keinan, S.; Chaudret, R.; Piquemal, J.-P.; Beratan, D. N.; Yang, W. *J. Chem. Theory Comput.* **2011**, *7*, 625.

1085 [N°630] Johnson, E. R.; Keinan, S.; Mori-Sánchez, P.; Contreras-García, J.; Cohen, A. J.; Yang, W. *J. Am. Chem. Soc.* **2010**, *132*, 6498.

1086 [N°857] In *M86-E01078 APEX2 User Manual*: Bruker AXS Inc.: Madison, USA, **2006**.

1087 [N°858] Sheldrick, G. *Acta Cryst. Sect. A* **1990**, *46*, 467.

1088 [N°859] Sheldrick, G. M.; Universität Göttingen: Göttingen, Germany, **1998**.

solved using SIR-97[1089] and refined with SHELXL-97. The refinement and all further calculations were carried out using SHELXL-97. The H-atoms were included in calculated positions and treated as riding atoms using SHELXL default parameters. The non-H atoms were refined anisotropically, using weighted full-matrix least-squares on F^2. A semiempirical absorption correction was applied using SADABS in APEX2.

[1089][N°860] Altomare, A.; Burla, M. C.; Camalli, M.; Cascarano, G. L.; Giacovazzo, C.; Guagliardi, A., . . . Spagna, R. *J. Appl. Cryst.* **1999**, *32*, 115.

3.4 - Synthesis and characterizations.

3.4.1 - Compound *syn*-31a.

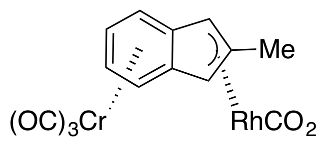

syn-**31a**

Synthesis:

A solution of **5a** (0.100 g, 0.38 mmol) in THF (5 mL) was treated with 1.1 equivalent of *n*-BuLi (0.26 mL, 0.41 mmol) at -40 °C. The solution of anion was transferred after 30 min at -40 °C via cannula transfer to a THF solution (5 mL) containing 0.51 equivalent of $[Rh(\mu\text{-}Cl)(CO)]_2$ (0.074 g, 0.19 mmol). After stirring for 2 h whilst temperature was slowly raised to -5 °C, the solvent was removed under reduced pressure and the residue extracted with diethyl ether. After filtration through Celite the solvent was pumped off and the residue was crystallized from a dichloromethane-pentane mixture to afford dark red crystals (0.061 g, 0.14 mmol, 38 %).

Characterizations:

Calcd for $C_{15}H_9CrO_5Rh$: C, 42.48; H, 2.14. Found: C, 42.23; H, 2.25. HRMS-ESI (*m/z*): $[M]^+$ calcd for $C_{15}H_9CrO_5Rh$, 423.8910; found, 423.8909. IR (cm^{-1}) ν(CO): 2043 (s), 1994 (s), 1934 (s), 1882 (s), 1850 (vs).

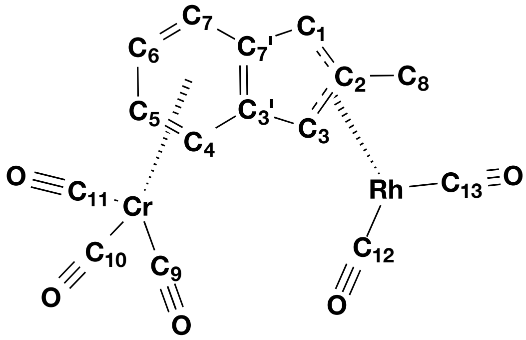

^{1}H NMR (500 MHz, 293 K, $CDCl_3$) δ 5.28 – 5.23 (m, 2H, H_7, H_4), 4.66 – 4.62 (m, 2H, H_5, H_6), 4.63 (s, 2H, H_1, H_3), 2.46 (s, 3H, H_8). ^{13}C NMR (126 MHz, 293 K, $CDCl_3$) δ 234.42 (C_{10}, C_9, C_{11}), 190.27 (d, J = 82.5 Hz, C_{12}, C_{13}), 116.14 (d, J = 6.6 Hz, C_2), 108.12 (d, J = 0.8 Hz, $C_{7'}$, $C_{3'}$), 89.74 (C_7, C_4), 76.12 (C_5, C_6), 64.04 (d, J = 3.9 Hz, C_1, C_3), 16.48 (C_8).

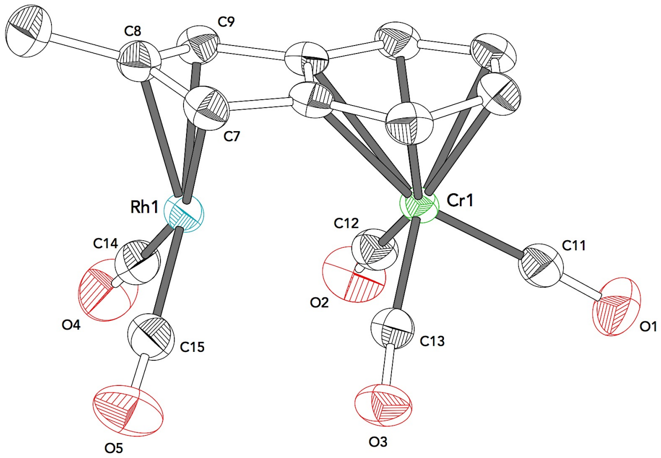

Compound *syn*-**31a**
Space Group: **P 2_1/c**
R-Factor (%): **1.89**

N°	*A*	*B*	*C*	*Lengths (Å)*	*Angles (°)*
1	Rh_1	Cr_1	-	3.0641(5)	
2	Rh_1	C_7	-	2.210(2)	-
3	Rh_1	C_8	-	2.191(2)	-
4	Rh_1	C_9	-	2.221(1)	-
5	Rh_1	C_{14}	-	1.882(2)	-
6	Rh_1	C_{15}	-	1.879(2)	-
7	Rh_1	C_{12}	-	3.130(2)	-
8	Rh_1	C_{13}	-	3.171(2)	-
9	C_{14}	O_4	-	1.132(3)	-
10	C_{15}	O_5	-	1.135(2)	-
11	Cr_1	C_{11}	-	1.821(2)	-
12	Cr_1	C_{12}	-	1.854(2)	-
13	Cr_1	C_{13}	-	1.853(1)	-
14	C_{11}	O_1	-	1.155(2)	-
15	C_{12}	O_2	-	1.156(2)	-
16	C_{13}	O_3	-	1.152(2)	-
17	Rh_1	C_{14}	O_4	-	178.2(2)
18	Rh_1	C_{15}	O_5	-	177.8(2)
19	Cr_1	C_{11}	O_1	-	178.0(1)
20	Cr_1	C_{12}	O_2	-	174.8(1)
21	Cr_1	C_{13}	O_3	-	175.0(1)
22	C_{12}	Cr_1	C_{13}	-	95.16(7)
23	C_{14}	Rh_1	C_{15}	-	92.42(8)

3.4.2 - Compound *syn*-31b.

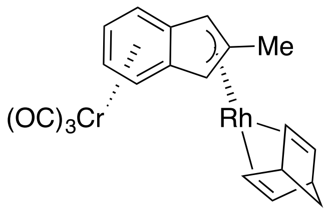

syn-**31b**

Synthesis:

A solution of **5a** (0.200 g, 0.75 mmol) in THF (10 mL) was treated with 1.1 equivalent of *n*-BuLi (0.52 mL, 0.83 mmol) at -40 °C. The solution of anion was transferred after 30 min at -40 °C via cannula to a THF solution (10 mL) containing 0.7 equivalent of [Rh(μ-Cl)(nbd)]$_2$ (0.242 g, 0.53 mmol). After stirring for 1 h whilst the temperature was slowly raised to -10 °C, the solvent was removed under reduced pressure and the residue extracted with cold cyclohexane. After filtration through celite the solvent was pumped off and the residue was crystallized from a dichloromethane-pentane mixture to afford red crystals (0.333 g, 0.72 mmol, 96 %).

Characterizations:

Calcd for $C_{20}H_{17}CrO_3Rh{\cdot}0.2CH_2Cl_2$: C, 50.84; H, 3.68. Found: C, 50.82; H, 3.89. HRMS-ESI (*m/z*): $[M+1Na]^+$ calcd for $C_{20}H_{17}CrO_3Rh$, 482.9530; found, 482.9503. IR (cm^{-1}) ν(CO): 1926 (s), 1858 (s), 1835 (vs).

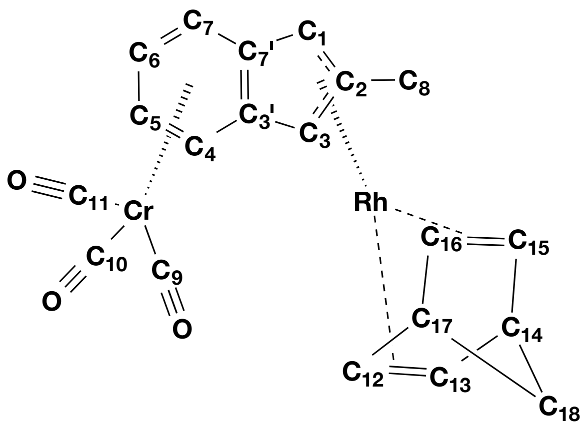

^{1}H NMR (500 MHz, 300 K, C_6D_6) δ 4.50 (dd, J = 5.0, 2.7 Hz, 2H, H_4, H_7), 3.85 (dd, J = 5.0, 2.7 Hz, 2H, H_5, H_6), 3.62 (q, J = 2.5 Hz, 4H, H_{12}, H_{13}, H_{15}, H_{16}), 3.44 (dq, J = 3.2, 1.7 Hz, 2H, H_{14}, H_{17}), 3.38 (s, 2H, H1, H_3), 2.38 (d, J = 1.1 Hz, 3H, H_8), 0.95 (t, J = 1.6 Hz, 2H, H_{18}). ^{13}C NMR (126 MHz, 300 K, C_6D_6) δ 236.18 (C_{10}, C_{11}, C_9), 105.94 (d, J = 6.6 Hz, C_2), 105.26 (d, J = 1.1 Hz, $C_{3'}$, $C_{7'}$), 87.68 (C_4, C_7), 74.38 (C_5, C_6), 61.97 (d, J = 4.6 Hz, C_1, C_3), 59.73 (d, J = 7.0 Hz, C_{18}), 47.69 (d, J = 2.6 Hz, C_{14}, C_{17}), 45.99 (d, J = 9.5 Hz, C_{12}, C_{13}, C_{15}, C_{16}), 15.38 (C_8).

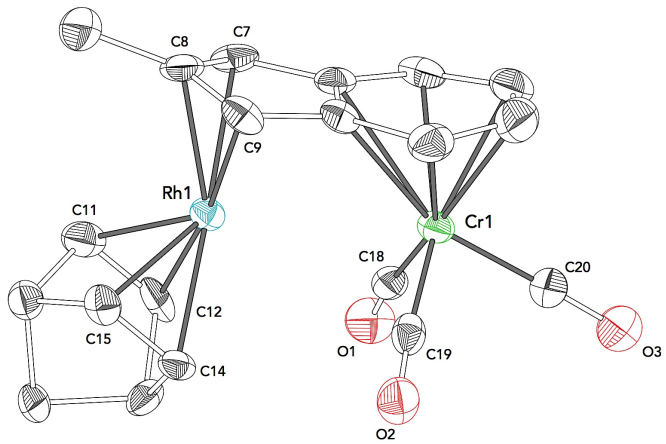

Compound *syn*-**31b**
Space Group: **C 2/c**
R-Factor (%): **4.82**

N°	*A*	*B*	*C*	*Lengths (Å)*	*Angles (°)*
1	Rh_1	Cr_1	-	3.156(1)	-
2	Rh_1	C_7	-	2.223(8)	-
3	Rh_1	C_8	-	2.190(8)	-
4	Rh_1	C_9	-	2.248(9)	-
5	Rh_1	C_{11}	-	2.104(7)	-
6	Rh_1	C_{12}	-	2.155(8)	-
7	Rh_1	C_{14}	-	2.173(7)	-
8	Rh_1	C_{15}	-	2.126(6)	-
9	Rh_1	C_{18}	-	3.196(7)	-
10	Rh_1	C_{19}	-	3.341(5)	-
11	Cr_1	C_{18}	-	1.855(7)	-
12	Cr_1	C_{19}	-	1.840(7)	-
13	Cr_1	C_{20}	-	1.820(6)	-
14	C_{18}	O_1	-	1.160(9)	-
17	C_{19}	O_2	-	1.158(8)	-
18	C_{20}	O_3	-	1.160(8)	-
19	Cr_1	C_{18}	O_1	-	173.5(6)
20	Cr_1	C_{19}	O_2	-	175.0(6)
21	Cr_1	C_{20}	O_3	-	178.5(6)
22	C_{18}	Cr_1	C_{19}	-	94.0(3)

3.4.3 - Compound *anti*-32a.

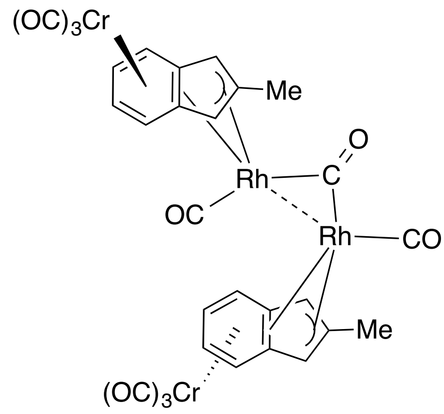

anti-**32a**

Synthesis:

A solution of **5a** (0.200 g, 0.75 mmol) in diethyl ether (5 mL) was treated with 1.1 equivalent of *n*-BuLi (0.52 mL, 0.83 mmol) at -40 °C. The solution of anion was transferred after 30 min at -40 °C via cannula transfer to a ether solution (5 mL) containing 0.51 equivalent of $[Rh(\mu\text{-}Cl)(CO)]_2$ (0.149 g, 0.38 mmol). After stirring for 2 h whilst temperature was slowly raised to -15 °C, the solvent was removed under reduced pressure and the residue extracted with cold cyclohexane. After filtration through Celite the solvent was pumped off and the residue was crystallized from a dichloromethane-pentane mixture to afford dark red crystals (0.167 g, 0.20 mmol, 27 %).

Characterizations:

Calcd for $C_{29}H_{18}Cr_2O_9Rh_2$: C, 42.46; H, 2.21. Found: C, 42.16; H, 2.51. HRMS-ESI (*m/z*): $[M+1H]^+$ calcd for $C_{29}H_{18}Cr_2O_9Rh_2$, 820.7944; found, 820.7869. IR (cm^{-1}) ν(CO): 2046 (s), 2000 (s), 1941 (s), 1892 (s), 1833 (vs), 1712 (s).

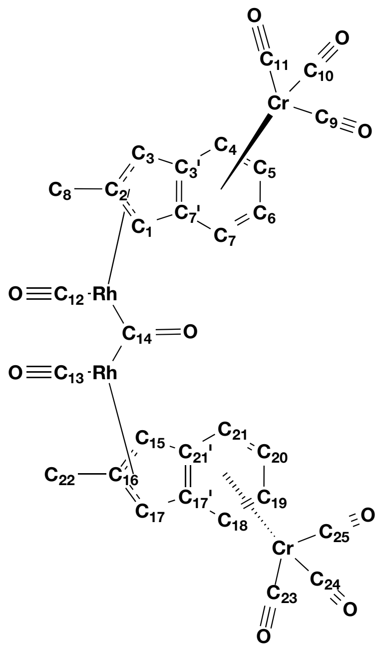

[1]H NMR (500 MHz, $CDCl_3$, 293 K) δ 5.70 (dd, J = 4.6, 2.7 Hz, 4H, H_{21}, H_{18}, H_4, H_7), 5.53 (s, 4H, H_{15}, H_{17}, H_3, H_1), 5.06 (dd, J = 4.8, 2.6 Hz, 4H, H_{19}, H_{20}, H_6, H_5), 2.20 (s, 3H, H_8), 2.20 (s, 3H, H_{22}). [13]C NMR (126 MHz, $CDCl_3$, 293 K) δ 233.73 (C_{10}, C_9, C_{11}, C_{24}, C_{23}, C_{25}), 211.63 (bs, C_{14}), 187.57 (d, J = 86.0 Hz, C_{12}, C_{13}), 129.70 (d, J = 6.6 Hz, C_{16}, C_2), 91.14 (bs, $C_{21'}$, $C_{17'}$, $C_{3'}$, $C_{7'}$), 90.12 (C_{19}, C_{20}, C_6, C_5), 83.77 (C_{21}, C_{18}, C_4, C_7), 74.52 (C_{15}, C_{17}, C_3, C_1), 17.28 (C_{22}, C_8).

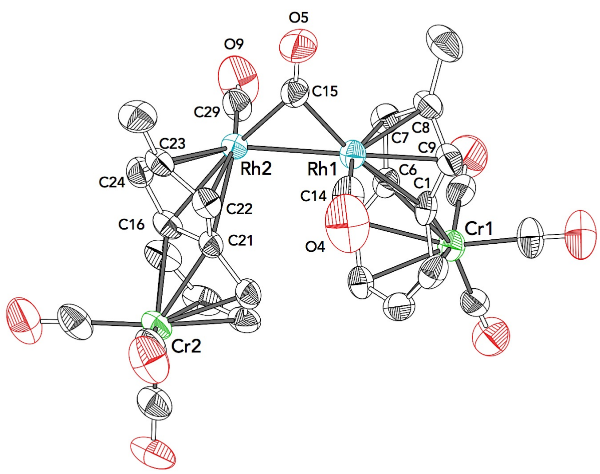

Compound *anti*-**32a**
Space Group: **P 2$_1$/c**
R-Factor (%): **5.73**

N°	*A*	*B*	*C*	*Lengths (Å)*	*Angles (°)*
1	Rh_1	Rh_2	-	2.6756(7)	-
2	Rh_1	C_1	-	2.372(6)	-
3	Rh_1	C_6	-	2.406(6)	-
4	Rh_1	C_7	-	2.243(6)	-
5	Rh_1	C_8	-	2.245(6)	-
6	Rh_1	C_9	-	2.219(6)	-
7	Rh_1	C_{14}	-	1.866(8)	-
8	Rh_1	C_{15}	-	1.991(7)	-
9	Rh_2	C_{16}	-	2.344(6)	-
10	Rh_2	C_{21}	-	2.356(6)	-
11	Rh_2	C_{22}	-	2.257(6)	-
12	Rh_2	C_{23}	-	2.288(5)	-
13	Rh_2	C_{24}	-	2.220(6)	-
14	Rh_2	C_{15}	-	1.971(7)	-
15	Rh_2	C_{29}	-	1.855(6)	-
16	C_{14}	O_4	-	1.133(9)	-
17	C_{15}	O_5	-	1.177(9)	-
18	C_{29}	O_9	-	1.140(8)	-
19	Rh_1	C_{15}	Rh_2	-	85.0(3)
20	Rh_1	C_{14}	O_4	-	176.8(7)
21	Rh_1	C_{15}	O_5	-	135.3(6)
22	Rh_2	C_{29}	O_9	-	178.2(6)
23	Rh_2	C_{15}	O_5	-	139.8(6)

3.4.4 - Compound *anti*-32c.

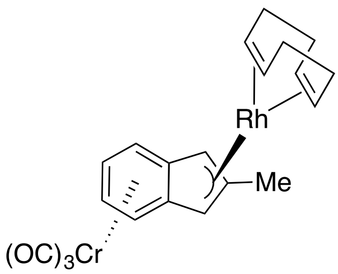

anti-**32c**

Synthesis:

A solution of **5a** (0.200 g, 0.75 mmol) in THF (15 mL) was treated with 1.1 equivalent of *n*-BuLi (0.52 mL, 0.83 mmol) at -40 °C. The resulting solution of anion was transfered after 30 min at -40 °C via a cannula to a THF solution (10 mL) containing 0.7 equivalent of $[Rh(\mu\text{-}Cl)(cod)]_2$ (0.259 g, 0.53 mmol). The resulting mixture was stirred for 1 h whilst temperature was slowly raised to -10 °C. The solvent was removed under reduced pressure and the residue extracted with cold cyclohexane. After filtration through celite the solvent was pumped off and the residue was recrystallized from a dichloromethane-pentane mixture to afford orange crystals (0.338 g, 0.71 mmol, 94 %).

Characterizations:

Calcd for $C_{21}H_{21}CrO_3Rh{\cdot}4/3CH_2Cl_2$: C, 45.52; H, 4.05. Found: C, 45.55; H, 4.04. HRMS-ESI (*m/z*): $[M]^+$ calcd for $C_{21}H_{21}CrO_3Rh$, 475.9951; found, 475.9985. IR (cm^{-1}) ν(CO): 1944 (s), 1866 (s),1829 (vs).

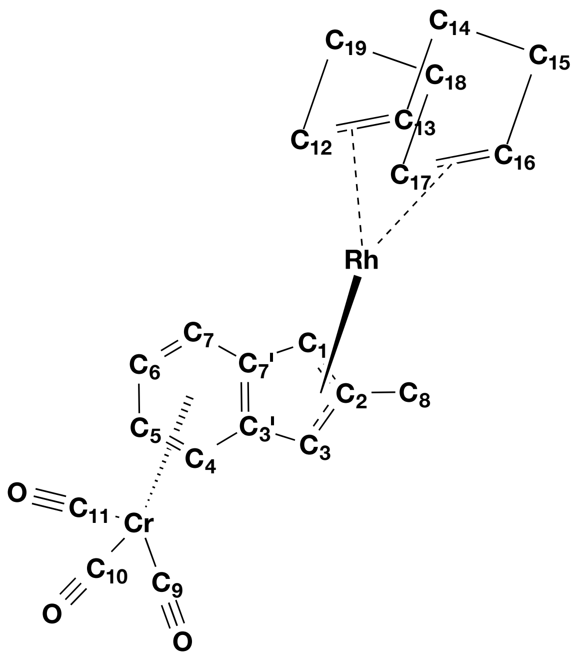

^{1}H NMR (500 MHz, 300 K, C_6D_6) δ 5.20 (dd, J = 4.9, 2.7 Hz, 2H, H_4, H_7), 4.53 (dd, J = 4.9, 2.7 Hz, 2H, H_5, H_6), 4.22 (s, 2H, H_1, H_3), 3.87 (s, 4H, H_{16}, H_{13}, H_{12}, H_{17}), 1.79 (d, J = 1.4 Hz, 3H, H_8), 1.73 – 1.47 (m, 8H, H_{14}, H_{15}, H_{19}, H_{18}). ^{13}C NMR (126 MHz, 300 K, C_6D_6) δ 234.95 (C_{10}, C_{11}, C_9), 120.46 (d, J = 5.5 Hz, C_2), 89.13 (C_5, C_6), 86.98 (d, J = 2.4 Hz, $C_{3'}$, $C_{7'}$), 84.22 (C_4, C_7), 76.17 (d, J = 4.2 Hz, C_1, C_3), 70.25 (d, J = 13.4 Hz, C_{16}, C_{13}, C_{12}, C_{17}), 31.34 (C_{14}, C_{15}, C_{19}, C_{18}), 15.31 (C_8).

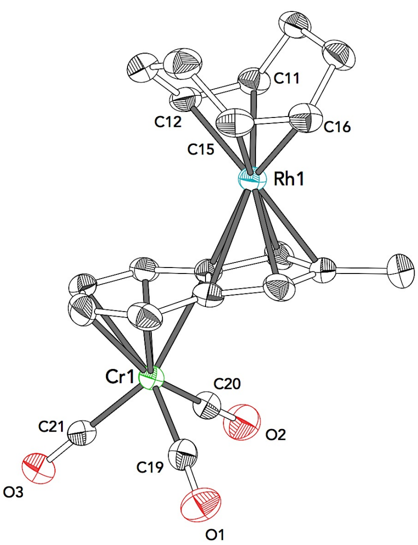

Compound *anti*-**32c**
Space Group: **P -1**
R-Factor (%): **3.99**

N°	*A*	*B*	*C*	*Lengths (Å)*	*Angles (°)*
1	Rh_1	C_{11}	-	2.170(3)	-
2	Rh_1	C_{12}	-	2.137(4)	-
3	Rh_1	C_{15}	-	2.140(3)	-
4	Rh_1	C_{16}	-	2.106(3)	-
5	Rh_1	C_1	-	2.377(4)	-
6	Rh_1	C_6	-	2.334(3)	-
7	Rh_1	C_7	-	2.248(3)	-
8	Rh_1	C_8	-	2.276(3)	-
9	Rh_1	C_9	-	2.223(4)	-
10	Cr_1	C_{19}	-	1.838(4)	-
11	Cr_1	C_{20}	-	1.841(3)	-
12	Cr_1	C_{21}	-	1.827(3)	-
13	C_{19}	O_1	-	1.152(5)	-
14	C_{20}	O_2	-	1.155(3)	-
15	C_{21}	O_3	-	1.159(4)	-
16	Cr_1	C_{19}	O_1	-	176.8(3)
17	Cr_1	C_{20}	O_2	-	179.6(3)
18	Cr_1	C_{21}	O_3	-	178.8(3)
19	C_{19}	Cr_1	C_{20}	-	87.3(1)

3.4.5 - Compound *syn*-33a.

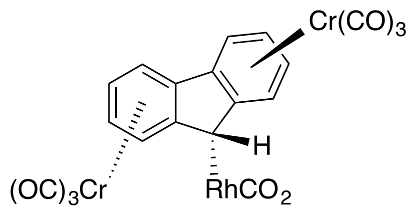

syn-**33a**

Synthesis:

A solution of **18a** (0.100 g, 0.23 mmol) in 5 mL THF was treated with 1 equivalent of *n*-BuLi (0.14 mL, 0.23 mmol) at -40 °C. The resulting solution of anion was transferred after 30 min at -40 °C via a cannula to a THF solution (5 mL) containing 0.8 equivalent of $[Rh(\mu\text{-}Cl)(CO)]_2$ (0.071 g, 0.18 mmol). The resulting mixture was stirred for 1 h during which the temperature was slowly raised to -5 °C and the solution stirred one more hour at room temperature. The solvent was then removed under reduced pressure and the residue extracted with diethyl ether. After filtration over celite the solvent was pumped off and the residue was recrystallized from a dichloromethane-pentane mixture to afford dark red crystals (0.041 g, 0.07 mmol, 30 %).

Characterizations:

Calcd for $C_{21}H_9Cr_2O_8Rh{\cdot}0.5CH_2Cl_2$: C, 40.43; H, 1.58. Found: C, 40.49; H, 1.62. HRMS-ESI (m/z): [M]+ calcd for $C_{21}H_9Cr_2O_8Rh$, 595.8163; found, 595.8069. IR (cm^{-1}) ν(CO): 2053 (s), 1990 (s),1941 (s), 1871 (s), 1848 (vs).

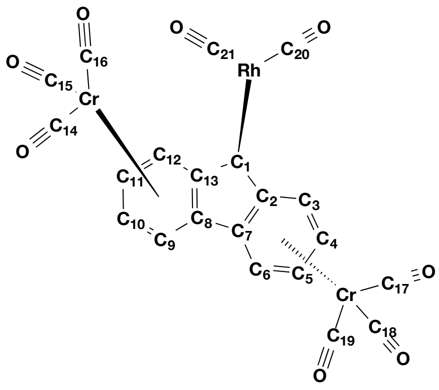

^{1}H NMR (600 MHz, 273 K, $CDCl_3$) δ 6.27 (d, J = 6.4 Hz, 1H, H_6), 6.22 (t, J = 6.3 Hz, 1H, H_5), 5.88 (d, J = 6.4 Hz, 1H, H_9), 5.72 (d, J = 6.9 Hz, 1H, H_{12}), 5.58 (t, J = 6.4 Hz, 1H, H_{11}), 5.37 (d, J = 6.5 Hz, 1H, H_3), 5.28 (t, J = 6.4 Hz, 1H, H_4), 5.14 (t, J = 6.5 Hz, 1H, H_{10}), 5.05 (d, J = 1.5 Hz, 1H, H_1).

Fast acquisition at room temperature in order to get the broad carbonyl signals which are not resolved at low temperature: ^{13}C NMR (126 MHz, 293 K, C_6D_6) δ 234.41 (bs, C_{16}), 233.68 (bs, C_{15}), 233.29 (C_{18}, C_{19}, C_{17}), 227.07 (bs, C_{14}), 191.64 (d, J = 69.2 Hz, C_{21}), 182.54 (bs, C_{20}).

^{13}C NMR (151 MHz, 279 K, $CDCl_3$) δ 232.85 (C_{18}, C_{19}, C_{17}), 190.67 (d, J = 71.0 Hz, C_{21}), 120.30 (C_{13}), 105.29 (C_2), 105.00 (C_7), 96.47 (C_8), 94.81 (C_{11}), 93.78 (C_5), 92.50 (C_4), 91.76 (C_3), 90.08 (C_6), 88.53 (C_9), 87.23 (C_{10}), 84.86 (C_{12}), 37.35 (bd, J = 6.9 Hz, C_1).

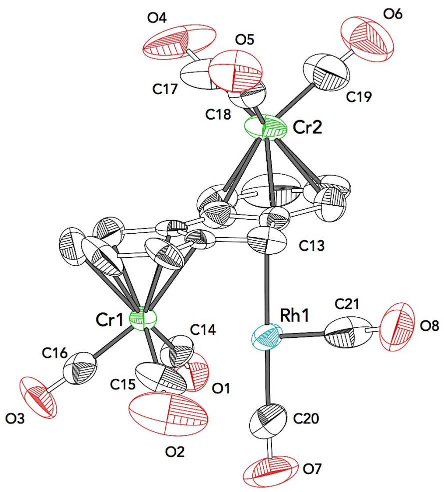

Compound *syn*-**33a**
Space Group: **P 2_1**
R-Factor (%): **9.97**

N°	A	B	C	Lengths (Å)	Angles (°)
1	Rh_1	Cr_1	-	2.802(3)	-
2	Rh_1	C_{13}	-	2.16(2)	-
3	Rh_1	C_{20}	-	1.88(3)	-
4	Rh_1	C_{21}	-	1.86(3)	-
5	Rh_1	C_{14}	-	2.64(2)	-
6	Rh_1	C_{15}	-	2.76(3)	-
7	C_{20}	O_7	-	1.13(5)	-
8	C_{21}	O_8	-	1.13(4)	-
9	Cr_1	C_{14}	-	1.82(2)	-
10	Cr_1	C_{15}	-	1.88(4)	-
11	Cr_1	C_{16}	-	1.83(2)	-
12	C_{14}	O_1	-	1.21(3)	-
13	C_{15}	O_2	-	1.15(5)	-
14	C_{16}	O_3	-	1.16(3)	-
15	Rh_1	C_{20}	O_7	-	177(3)
16	Rh_1	C_{21}	O_8	-	176(3)
17	Cr_1	C_{14}	O_1	-	170(2)
18	Cr_1	C_{15}	O_2	-	175(3)
19	Cr_1	C_{16}	O_3	-	177(2)
20	C_{14}	Cr_1	C_{15}	-	100(1)

3.4.6 - Compound *syn*-33b.

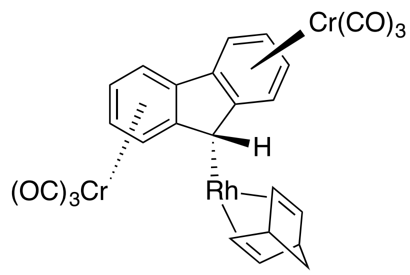

syn-**33b**

Synthesis:

A solution of **18a** (0.200 g, 0.46 mmol) in THF (8 mL) was treated with 1 equivalent of *n*-BuLi (0.29 mL, 0.46 mmol) at -40 °C. The solution of anion was transferred after 45 min at -40 °C via a cannula to a THF solution (5 mL) containing 1 equivalent of [Rh(μ-Cl)(nbd)]$_2$ (0.210 g, 0.46 mmol). The resulting mixture was stirred for 2 h, the temperature was slowly raised to -5 °C and the solution stirred one more hour at room temperature. The solvent was then removed under reduced pressure and the residue extracted with diethyl ether. After filtration through Celite the solvent was pumped off and the residue was crystallized from a dichloromethane-pentane mixture to afford dark red crystals (0.202 g, 0.32 mmol, 70 %).

Characterizations:

Calcd for $C_{26}H_{17}Cr_2O_6Rh$: C, 49.39; H, 2.71. Found: C, 49.00; H, 2.76. HRMS-ESI (*m/z*): $[M+1H]^+$ calcd for $C_{26}H_{17}Cr_2O_6Rh$, 632.8963; found, 632.8897. IR (cm^{-1}) ν(CO): 1938 (s), 1875 (s), 1843 (vs).

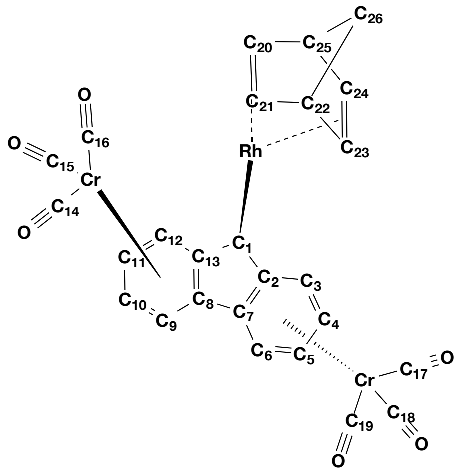

[1]H NMR (400 MHz, 233 K, Tol) δ 5.14 (d, J = 6.4 Hz, 1H, H_6), 4.89 (t, J = 6.5 Hz, 1H, H_{10}), 4.70 (t, J = 6.5 Hz, 1H, H_4), 4.50 (d, J = 6.6 Hz, 1H, H_9), 4.23 (dd, J = 6.7, 1.9 Hz, 2H, H_3, H_{12}), 4.16 – 4.07 (m, 3H, H_1, H_5, H_{23}), 4.05 (bs, 1H, H_{24}), 3.78 (t, J = 6.9 Hz, 1H, H_{11}), 3.47 (q, J = 4.0 Hz, 1H, H_{20}), 3.21 (bs, 1H, H_{25}), 2.92 (bs, 1H, H_{22}), 0.94 (d, J = 8.9 Hz, 1H, H_{26a}), 0.79 (d, J = 8.8 Hz, 1H, H_{26b}), 0.39 (t, J = 3.7 Hz, 1H, H_{21}). [13]C NMR (101 MHz, 233 K, Tol) δ 235.49 (bs, C_{16}), 233.68 (bs, C_{15}), 233.42 (C_{18}, C_{17}, C_{19}), 228.68 (bs, C_{14}), 127.63 (C_2), 107.12 (C_8), 101.20 (C_{13}), 96.40 (C_{12}), 96.16 (C_7), 93.57 (C_4), 93.15 (C_{10}), 89.62 (C_{11}), 89.33 (C_6), 86.38 (C_9), 86.30 (C_5), 82.42 (C_3), 66.38 (d, J = 5.1 Hz, C_{23}), 62.57 (bs, C_{26}), 62.29 (d, J = 5.5 Hz, C_{24}), 57.35 (d, J = 12.4 Hz, C_{20}), 49.47 (d, J = 2.6 Hz, C_{25}), 45.43 (d, J = 5.8 Hz, C_{21}), 44.59 (bs, C_{22}), 26.26 (d, J = 15.0 Hz, C_1).

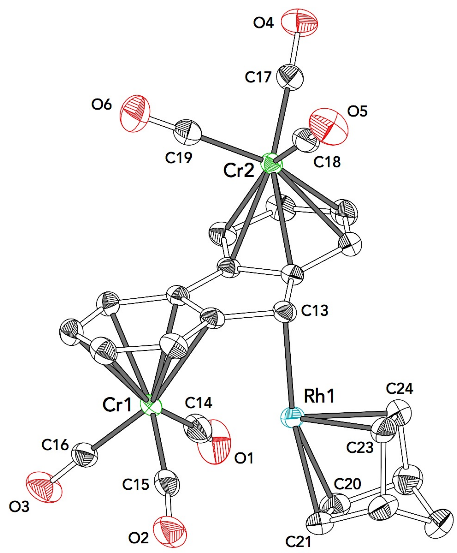

Compound *syn*-**33b**
Space Group: **P -1**
R-Factor (%): **2.06**

N°	A	B	C	Lengths (Å)	Angles (°)
1	Rh_1	Cr_1	-	2.8238(3)	-
2	Rh_1	C_{13}	-	2.172(1)	-
3	Rh_1	C_{14}	-	2.506(2)	-
4	Rh_1	C_{15}	-	2.954(2)	
5	Rh_1	C_{20}	-	2.198(1)	-
6	Rh_1	C_{21}	-	2.195(2)	-
7	Rh_1	C_{23}	-	2.113(2)	-
8	Rh_1	C_{24}	-	2.126(2)	-
9	Cr_1	C_{14}	-	1.871(1)	-
10	Cr_1	C_{15}	-	1.849(2)	-
11	Cr_1	C_{16}	-	1.838(2)	-
12	C_{14}	O_1	-	1.158(2)	-
16	C_{15}	O_2	-	1.155(2)	-
17	C_{16}	O_3	-	1.149(2)	-
21	Cr_1	C_{14}	O_1	-	166.1(1)
22	Cr_1	C_{15}	O_2	-	173.0(1)
23	Cr_1	C_{16}	O_3	-	178.3(1)
24	C_{14}	Cr_1	C_{15}	-	98.24(7)

VII

An excursion into non-covalence

Appendix

Chapter VII - Appendix

1 - Compound 2.

CDCl$_3$ – ^{1}H – 400 Mhz – 298.0 K.

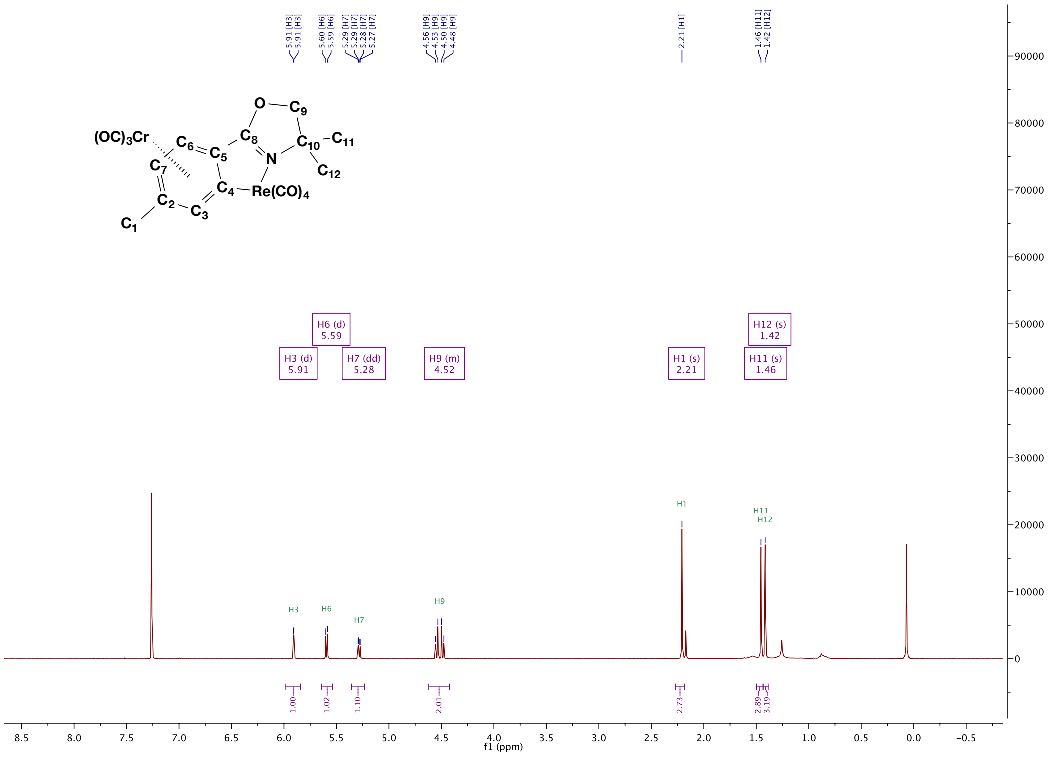

CDCl$_3$ – ^{13}C – 151 Mhz – 299 K.

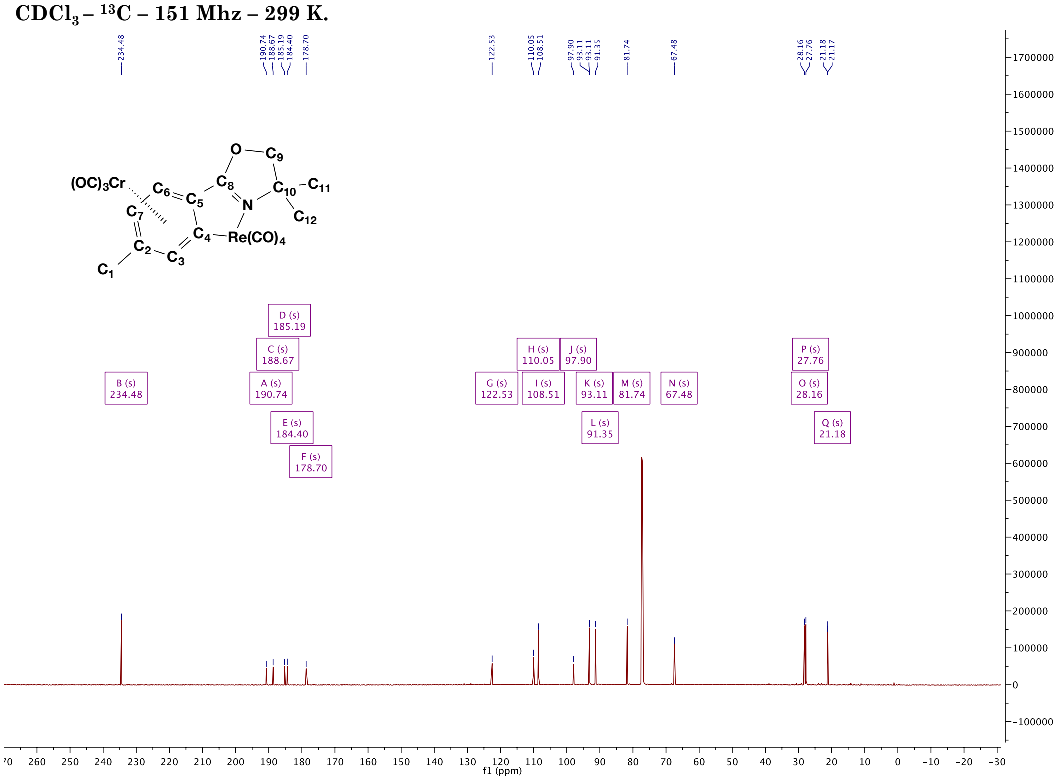

2 - Compound 3b.

Tol– ^{1}H – 500 Mhz – 227 K.

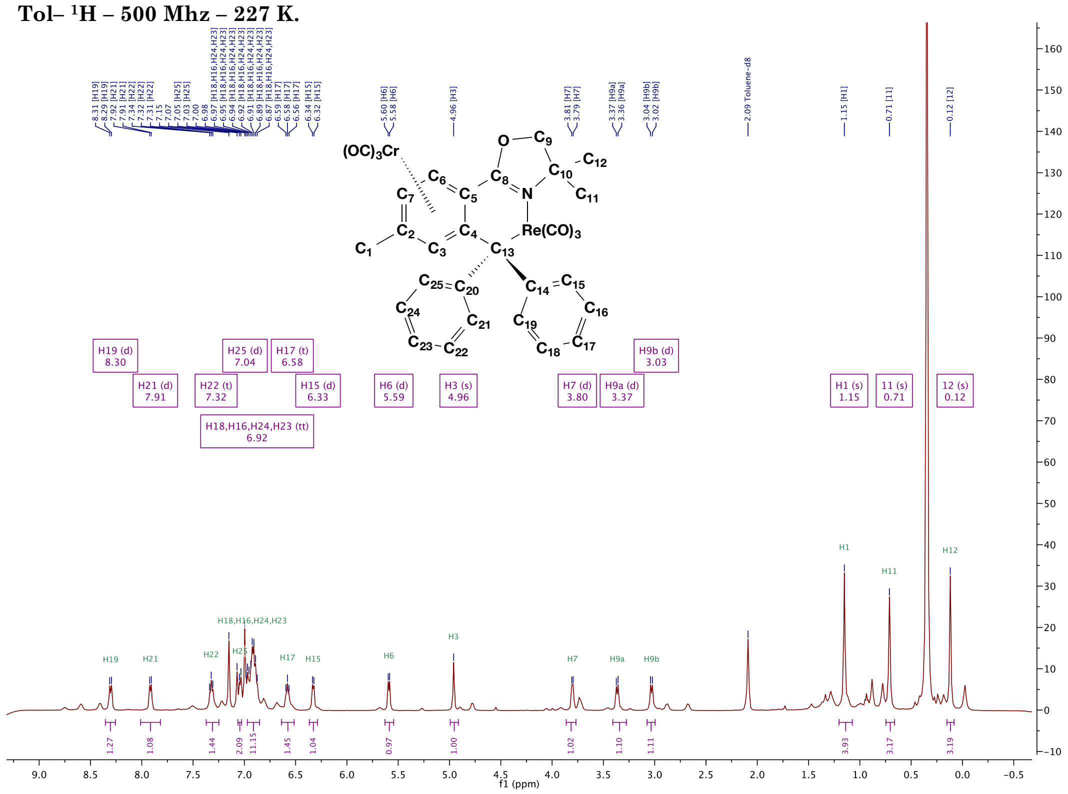

$CDCl_3$ – ^{13}C – 151 Mhz – 299 K.

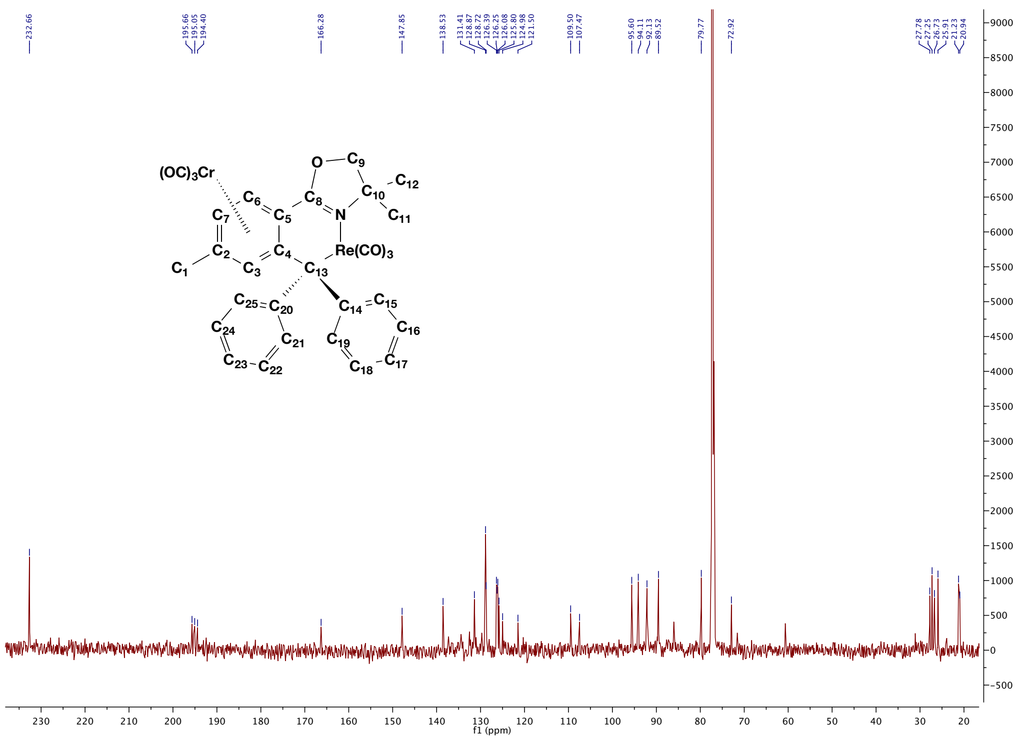

Tol – ^{1}H – 500 Mhz – Variable temperature.

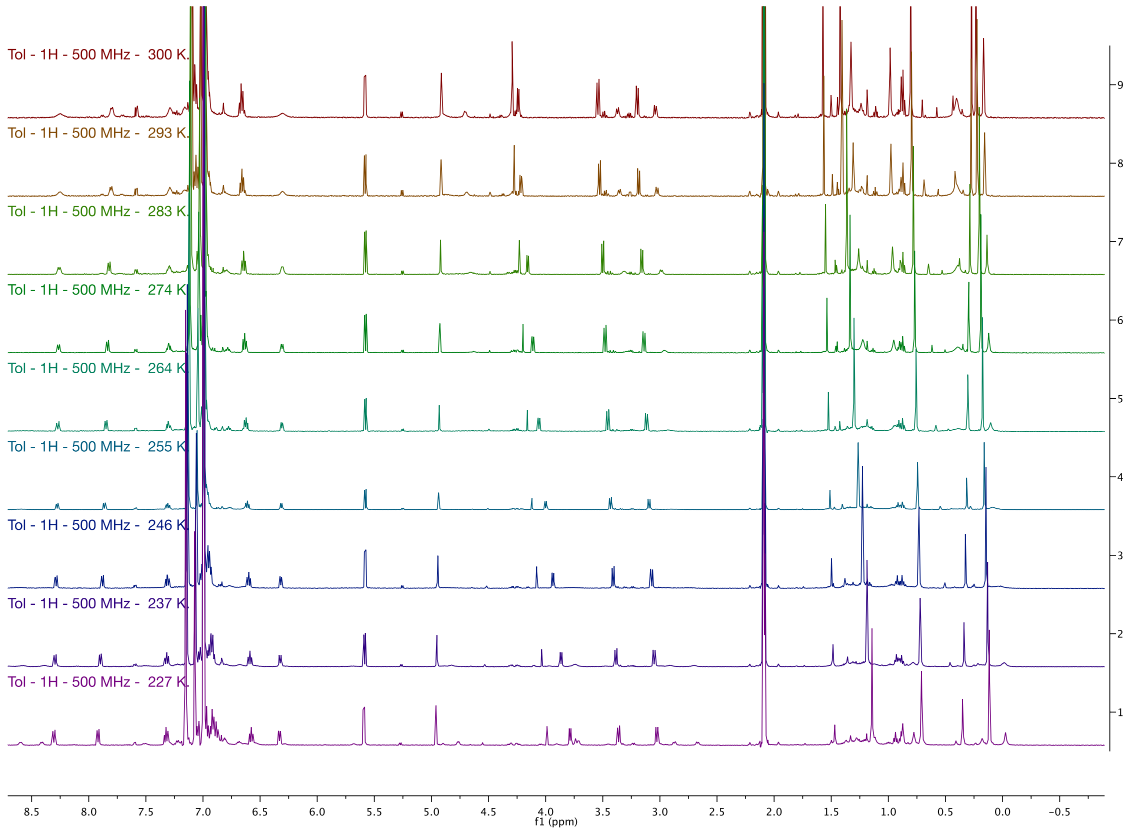

3 - Compound 4c.

$CDCl_3$ – ^{1}H – 500 Mhz – 300 K.

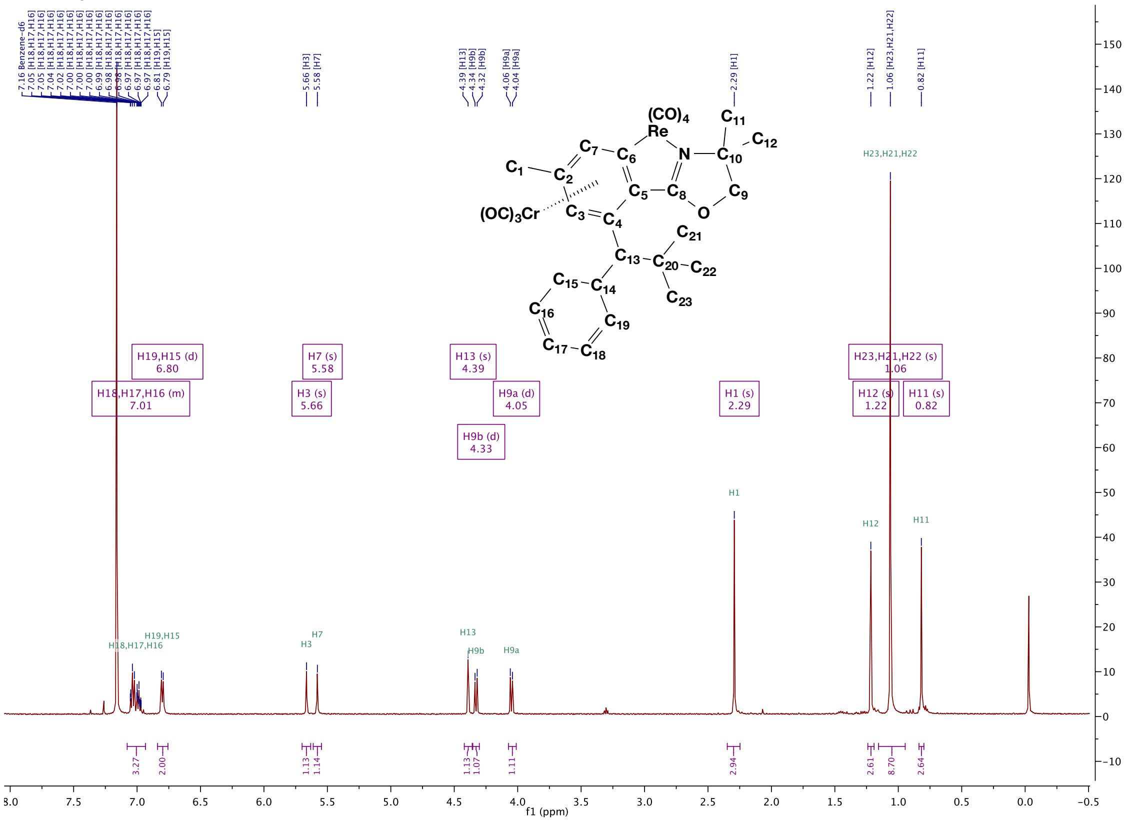

$CDCl_3$ – ^{13}C – 126 Mhz – 300.0 K.

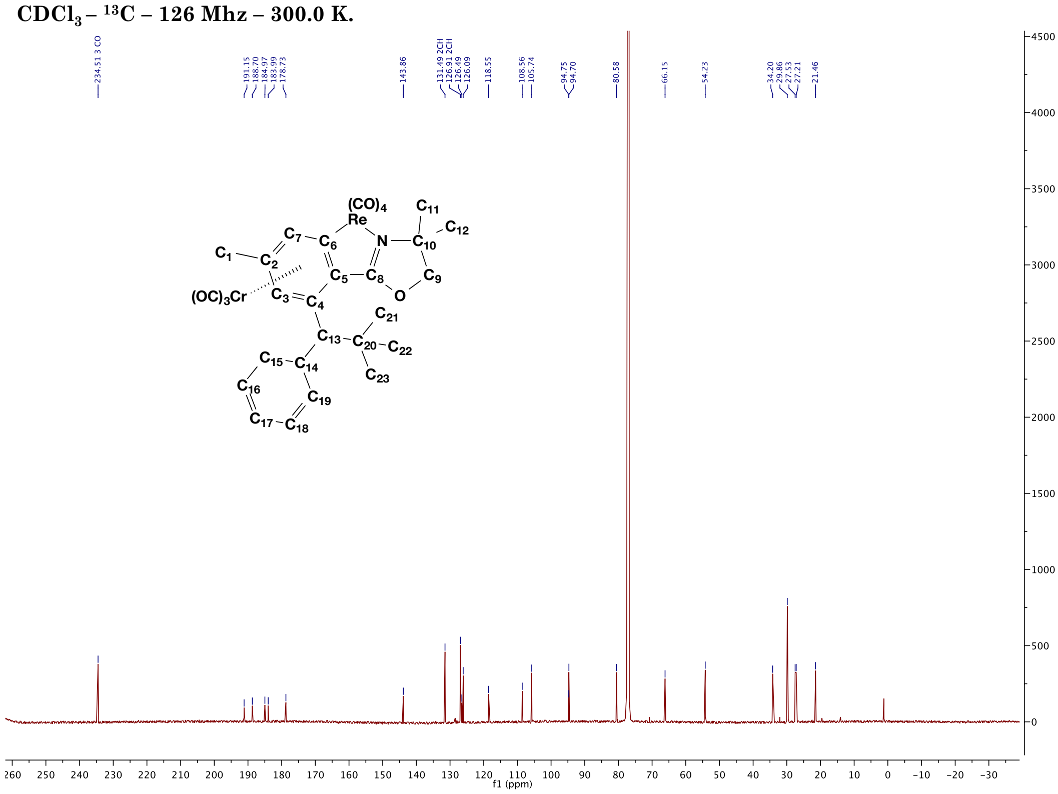

4 - Compound 5a.

C_6D_6 – ^1H – 500 Mhz – 300 K.

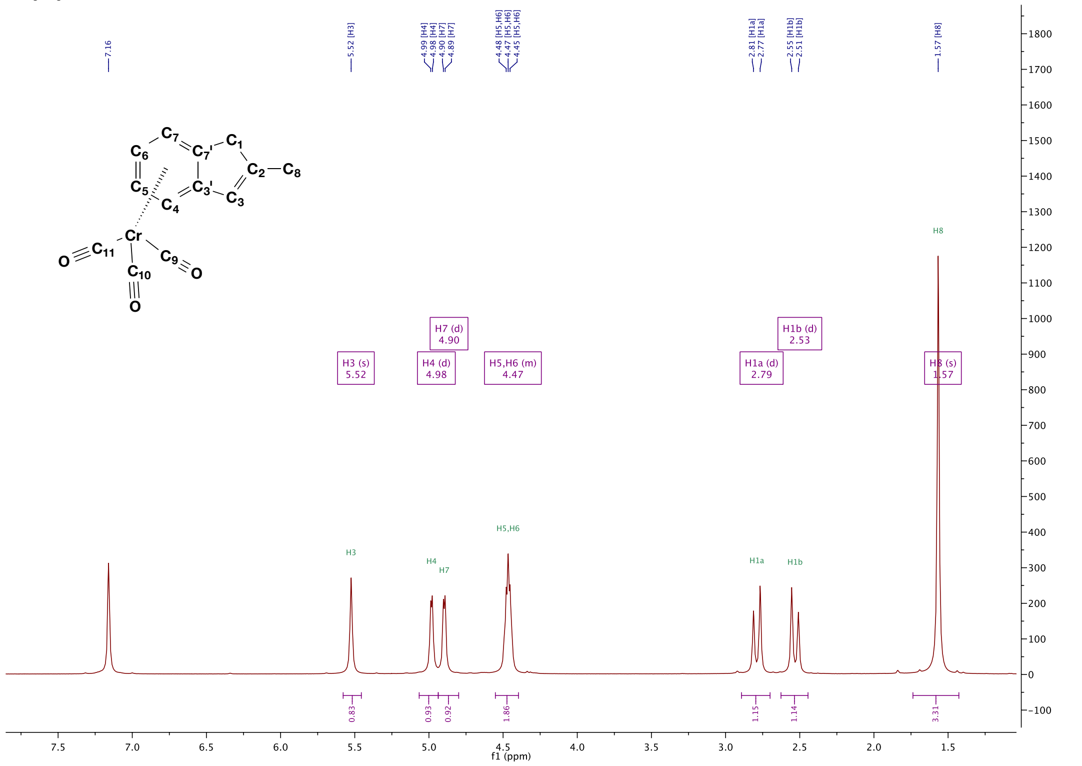

C_6D_6 – ^{13}C – 126 Mhz – 300 K.

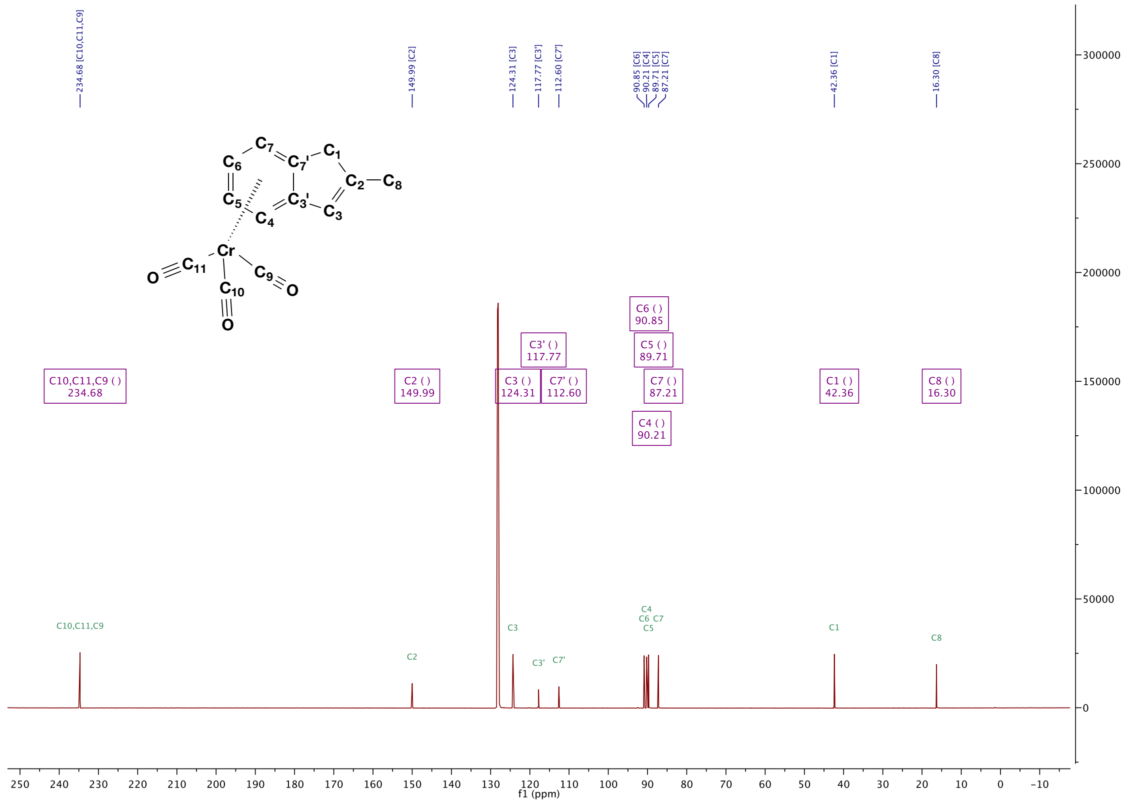

5 - Compound 7a.

C_6D_6 – ^1H – 500 Mhz – 300 K.

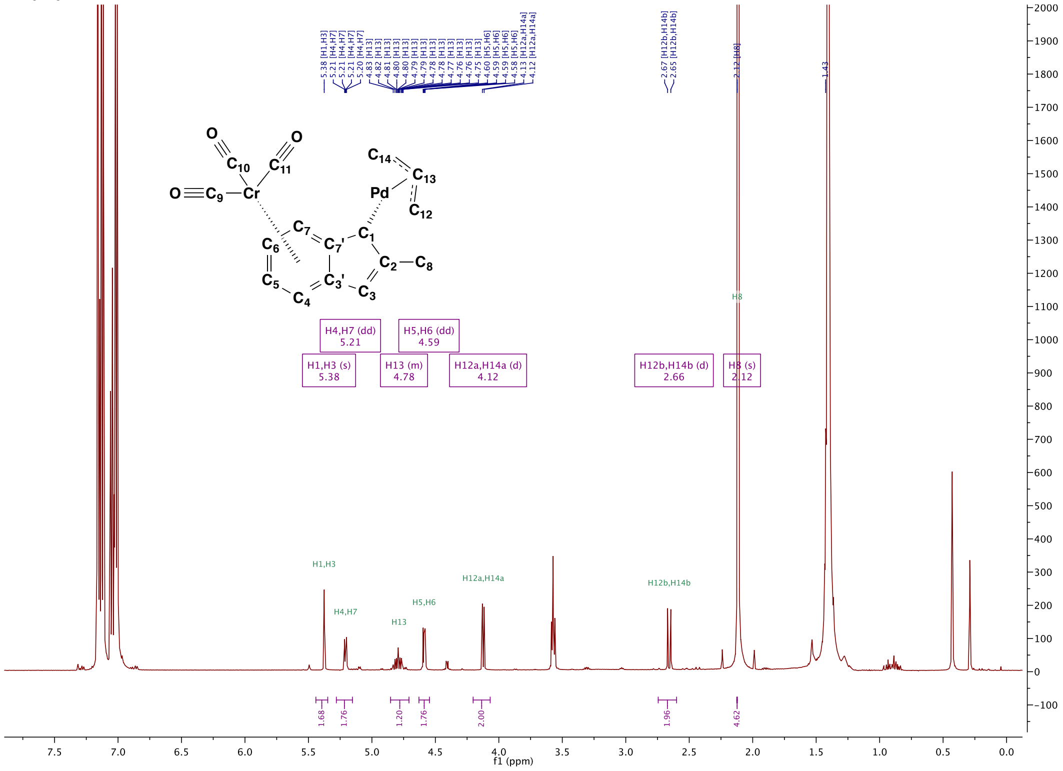

C_6D_6 – ^{13}C – 126 Mhz – 300 K.

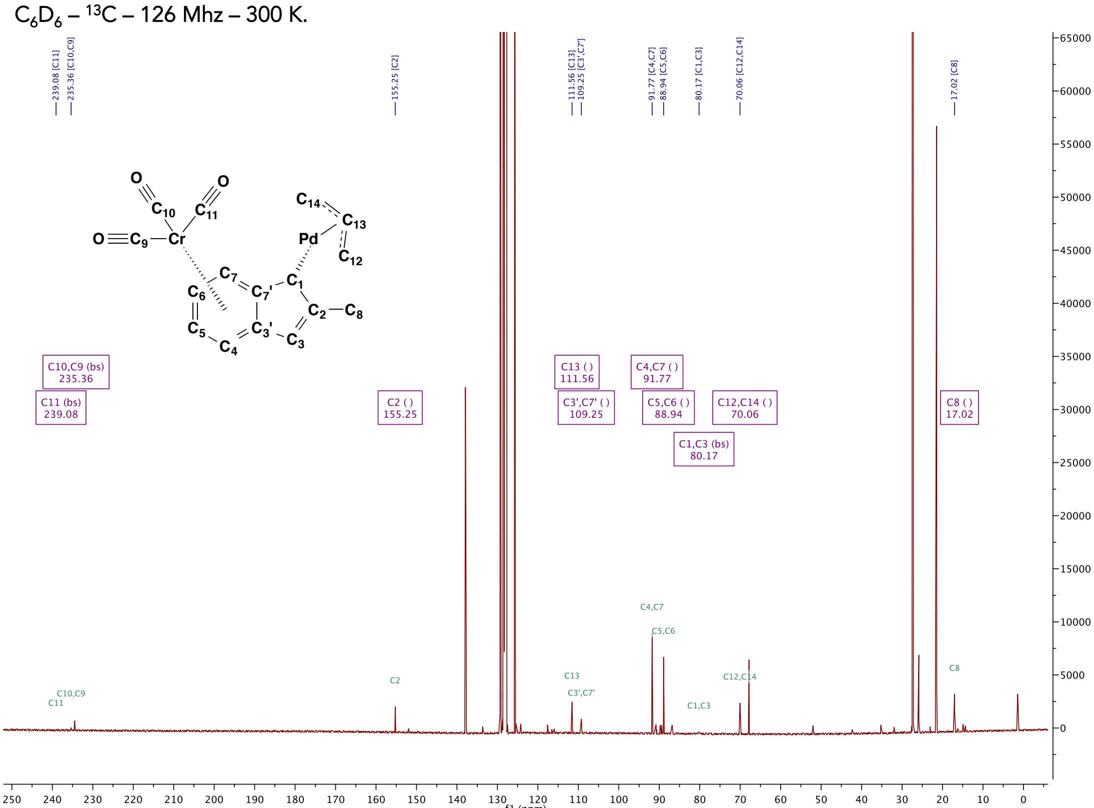

6 - Compound 7b.

C_6D_6 – ^1H – 500 Mhz – 298 K.

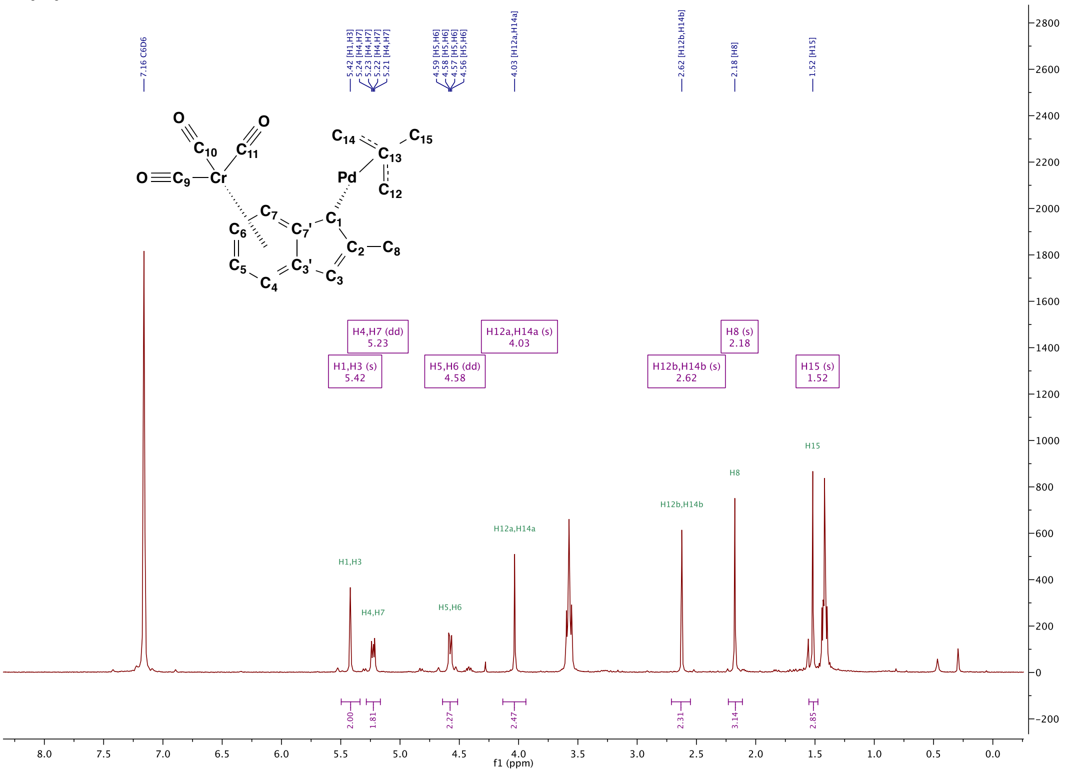

C_6D_6 – ^{13}C – 126 Mhz – 300 K.

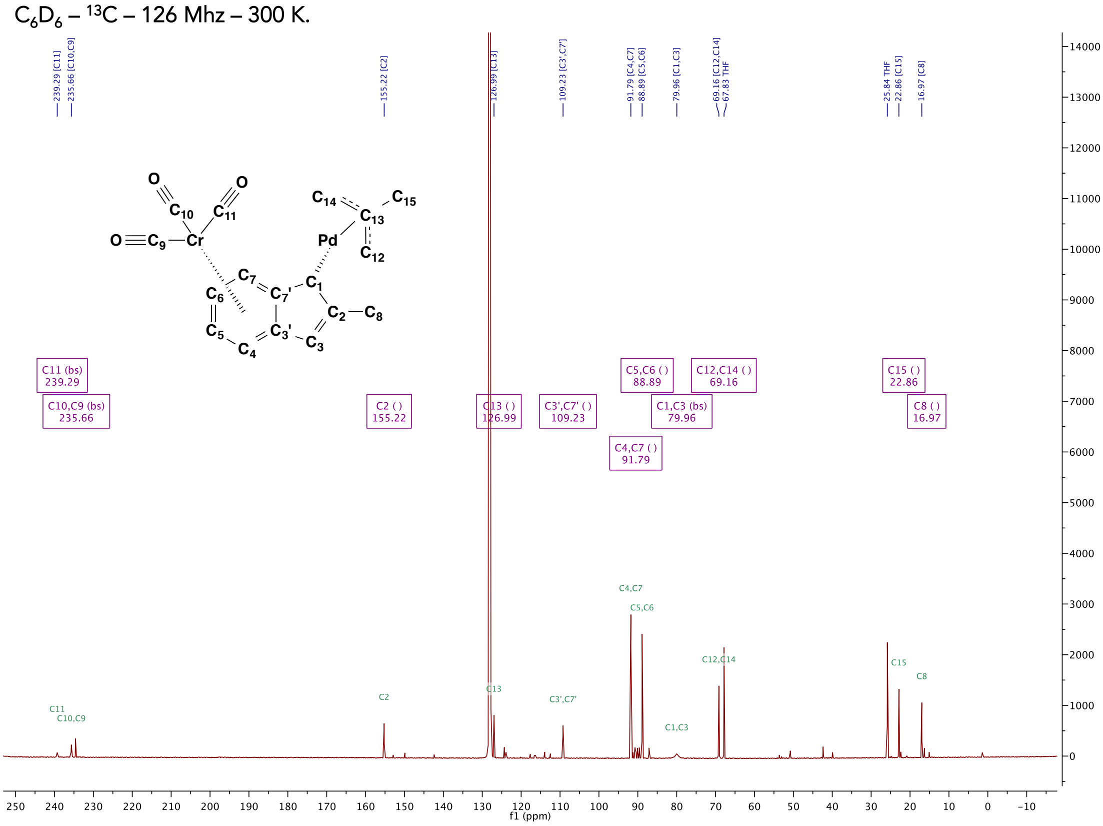

Tol – ^{1}H – 600 Mhz – Variable temperature.

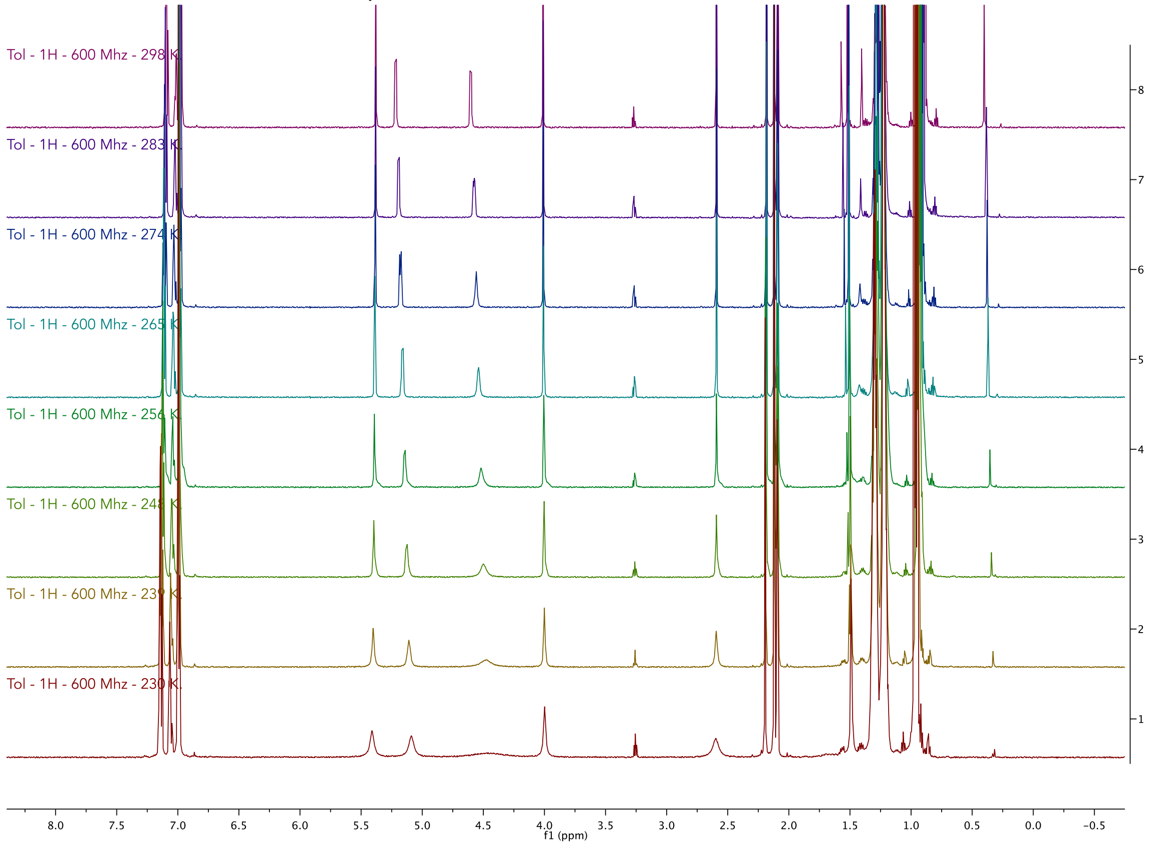

Tol – ^{13}C – 151 Mhz – Variable temperature.

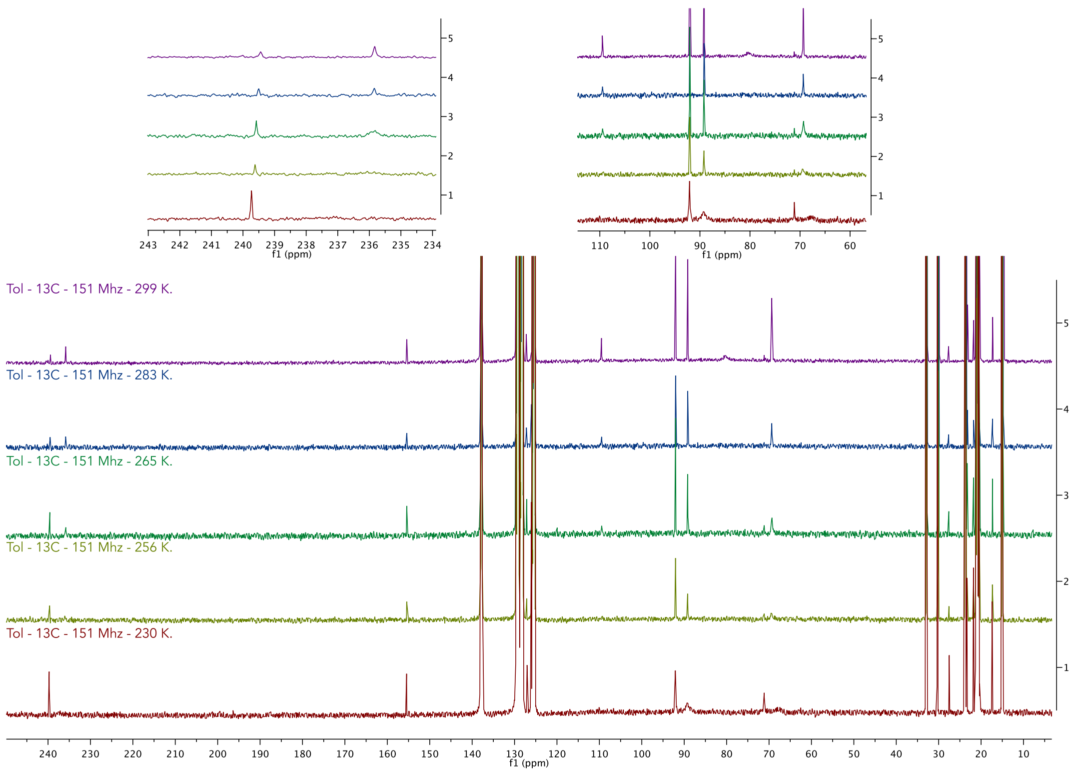

7 - Compound 7c.

$CDCl_3$ – ^1H – 500 Mhz - 300 K.

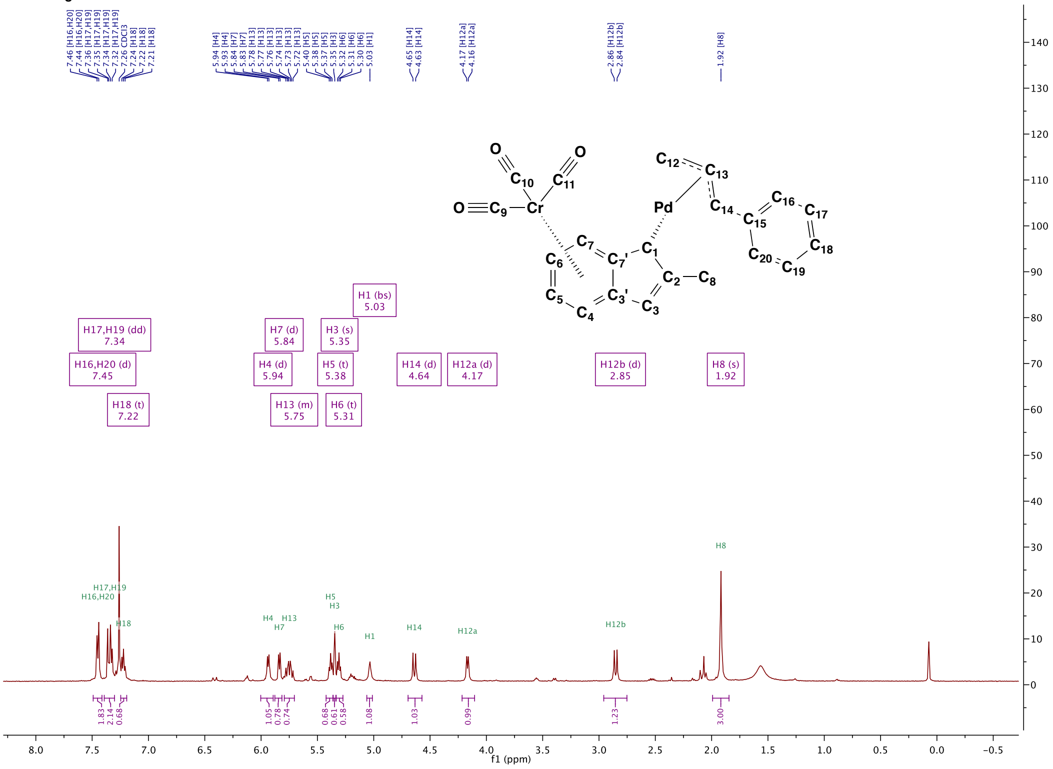

$CDCl_3$ – ^{13}C – 126 Mhz – 300 K.

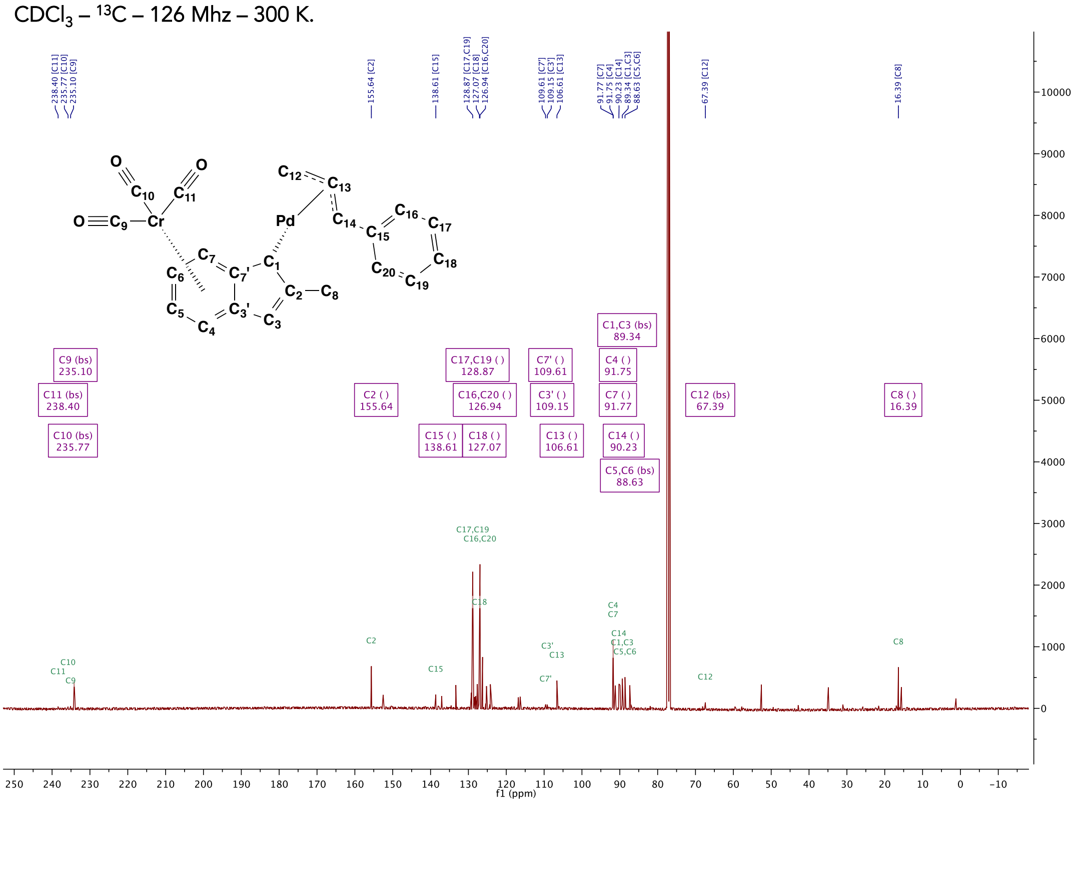

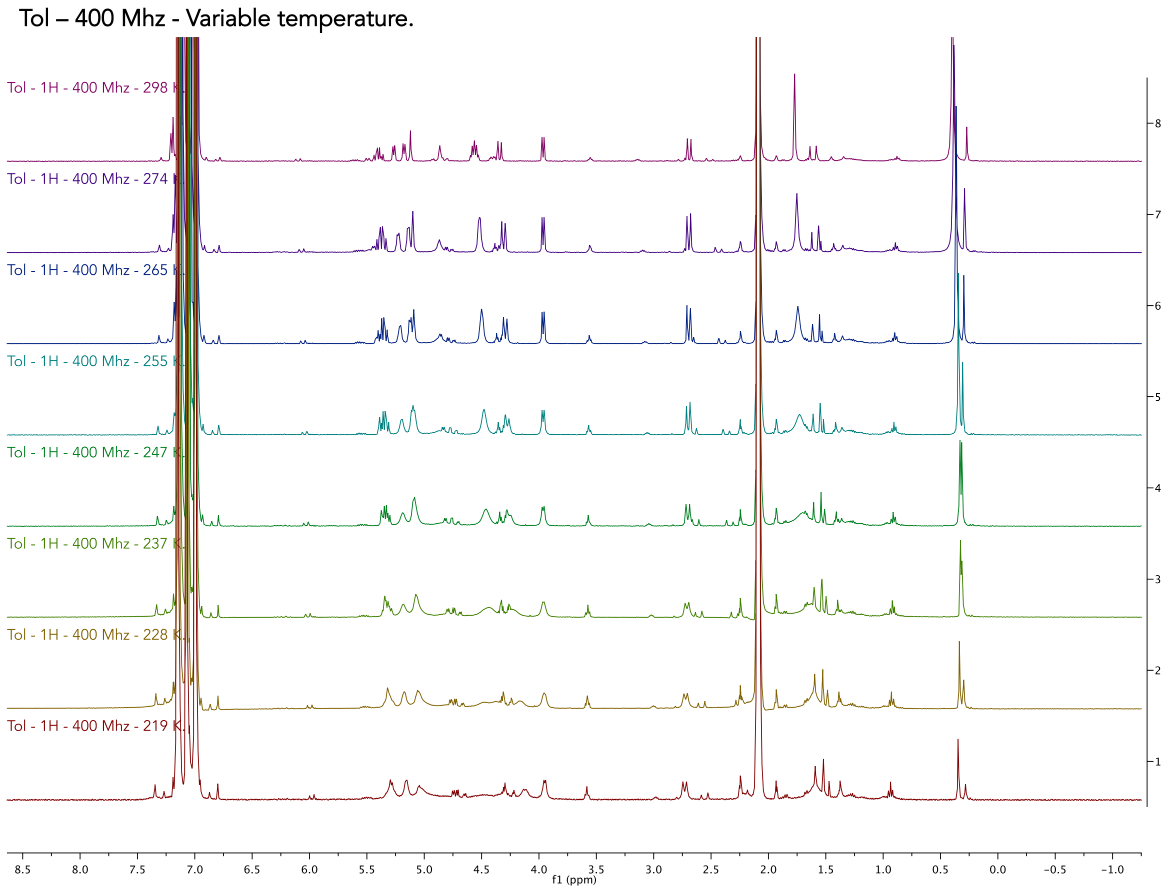
Tol – 400 Mhz - Variable temperature.
Tol - 1H - 400 Mhz - 298 K.
Tol - 1H - 400 Mhz - 274 K.
Tol - 1H - 400 Mhz - 265 K.
Tol - 1H - 400 Mhz - 255 K.
Tol - 1H - 400 Mhz - 247 K.
Tol - 1H - 400 Mhz - 237 K.
Tol - 1H - 400 Mhz - 228 K.
Tol - 1H - 400 Mhz - 219 K.
f1 (ppm)

8 - Compound 8a.

C_6D_6 – ^1H – 500 Mhz – 300 K.

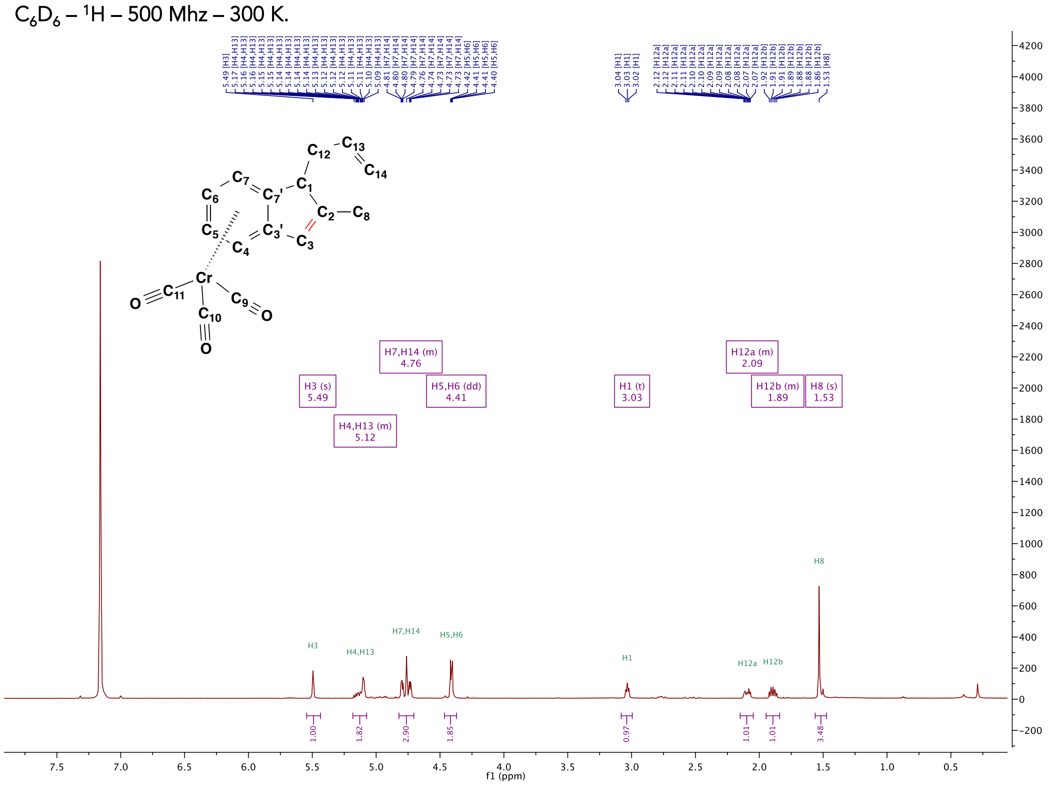

C_6D_6 – ^{13}C – 126 Mhz – 300 K.

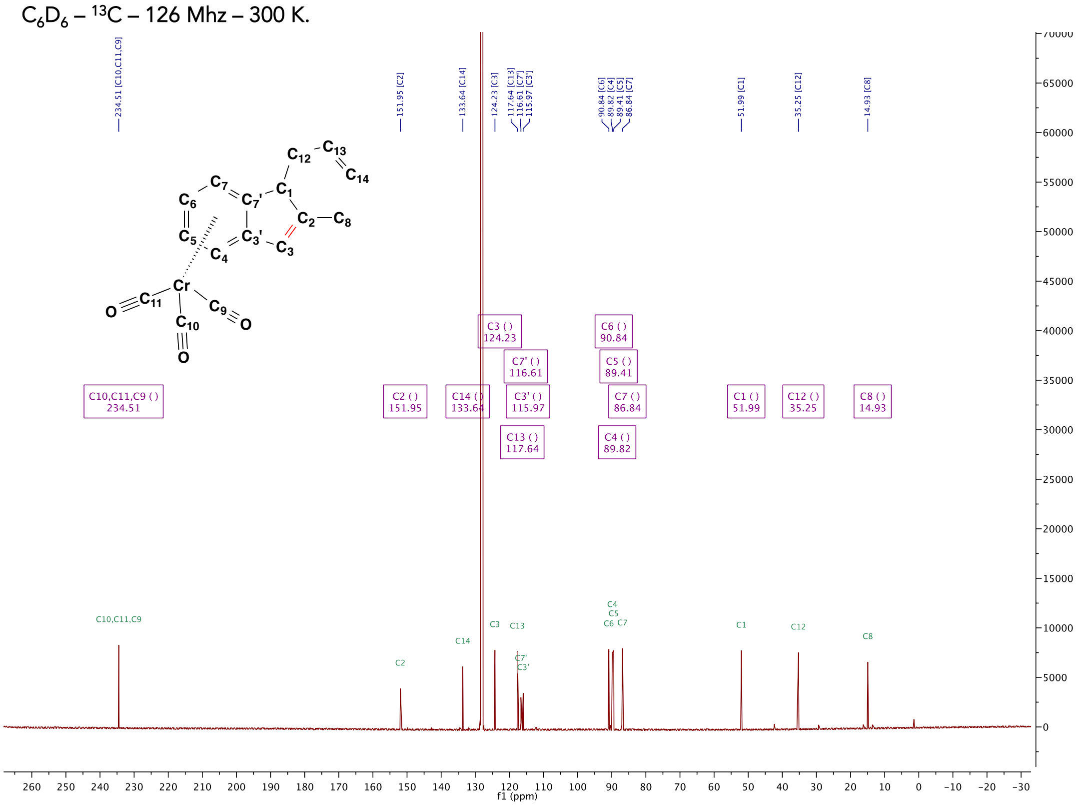

9 - Compound 8b.

C_6D_6 – ^1H – 500 Mhz – 300 K.

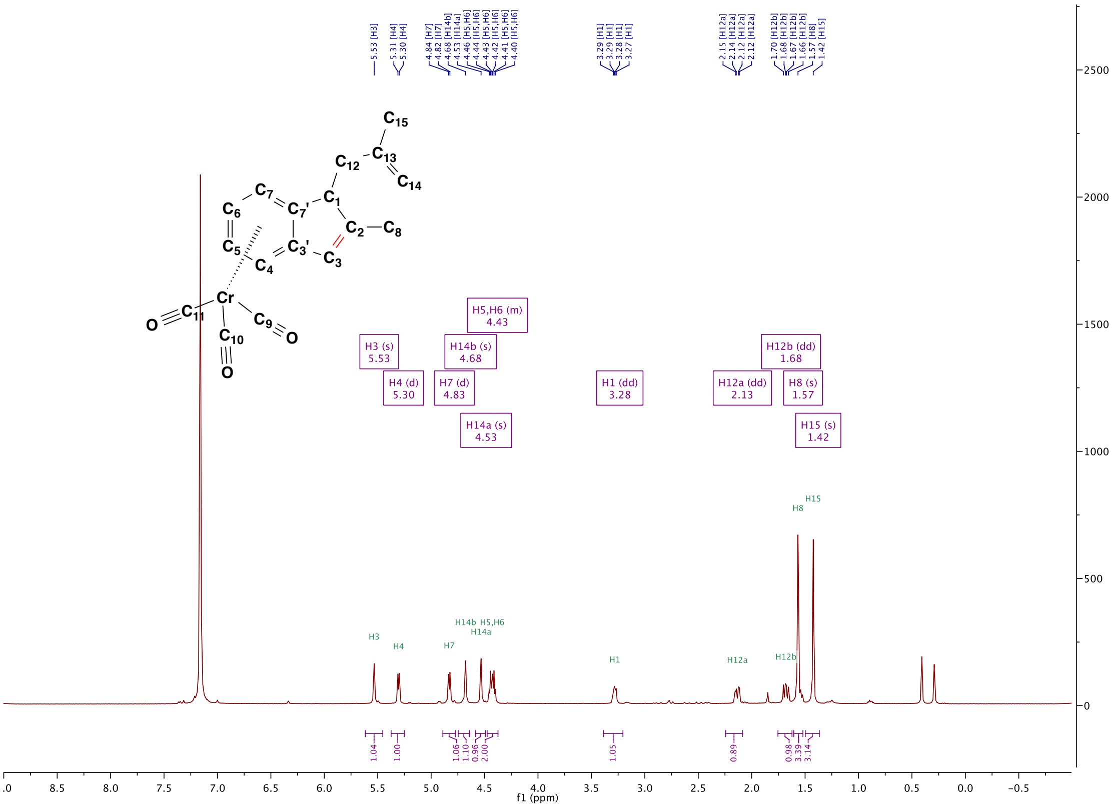

C_6D_6 – ^{13}C – 126 Mhz – 300 K.

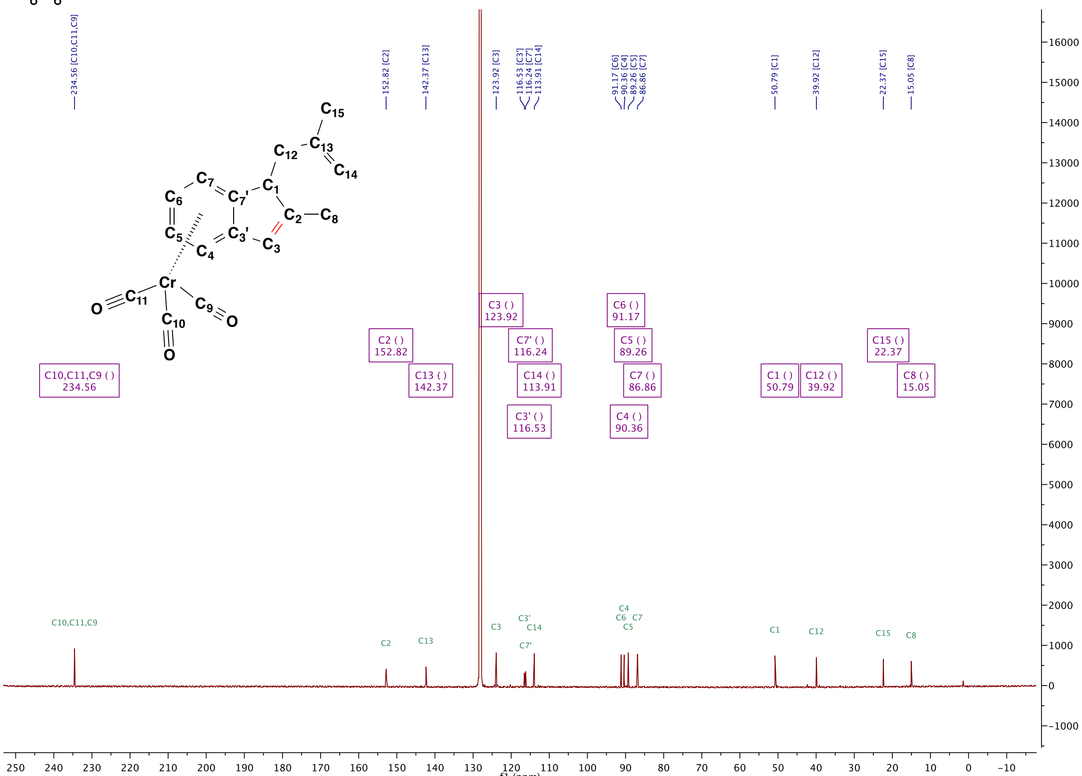

10 - Compound 8c.

CDCl$_3$ – ^{1}H – 400 Mhz – 298 K.

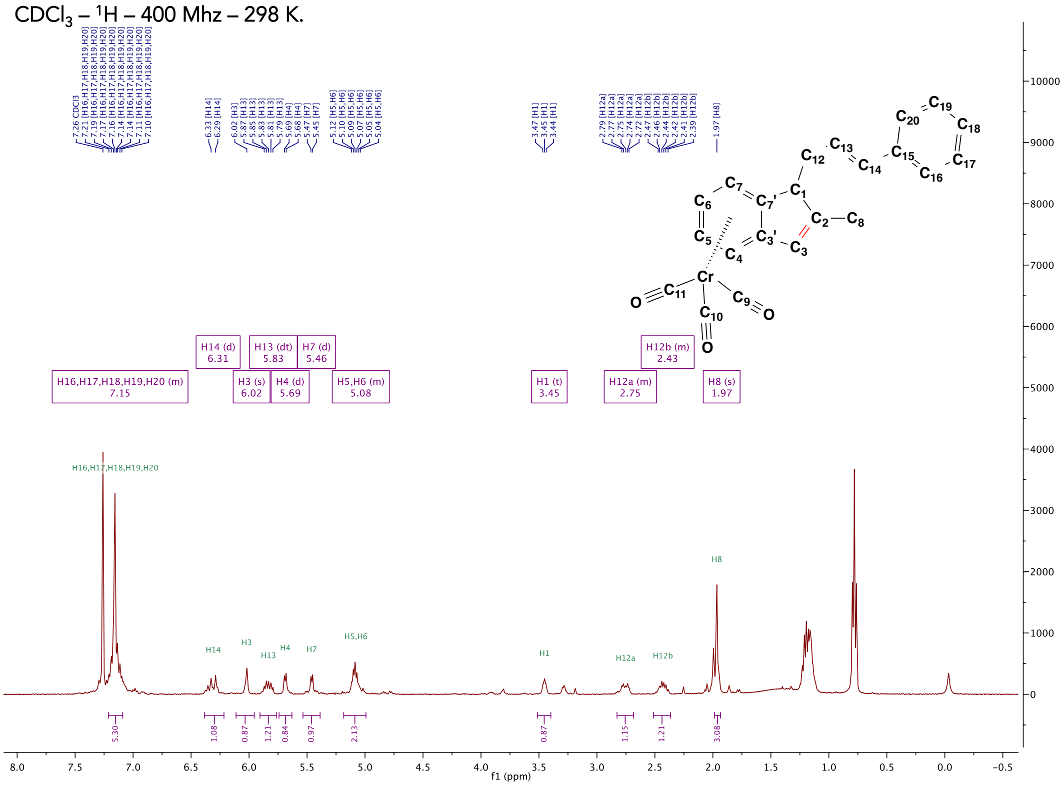

CDCl$_3$ – ^{13}C – 126 Mhz – 300 K.

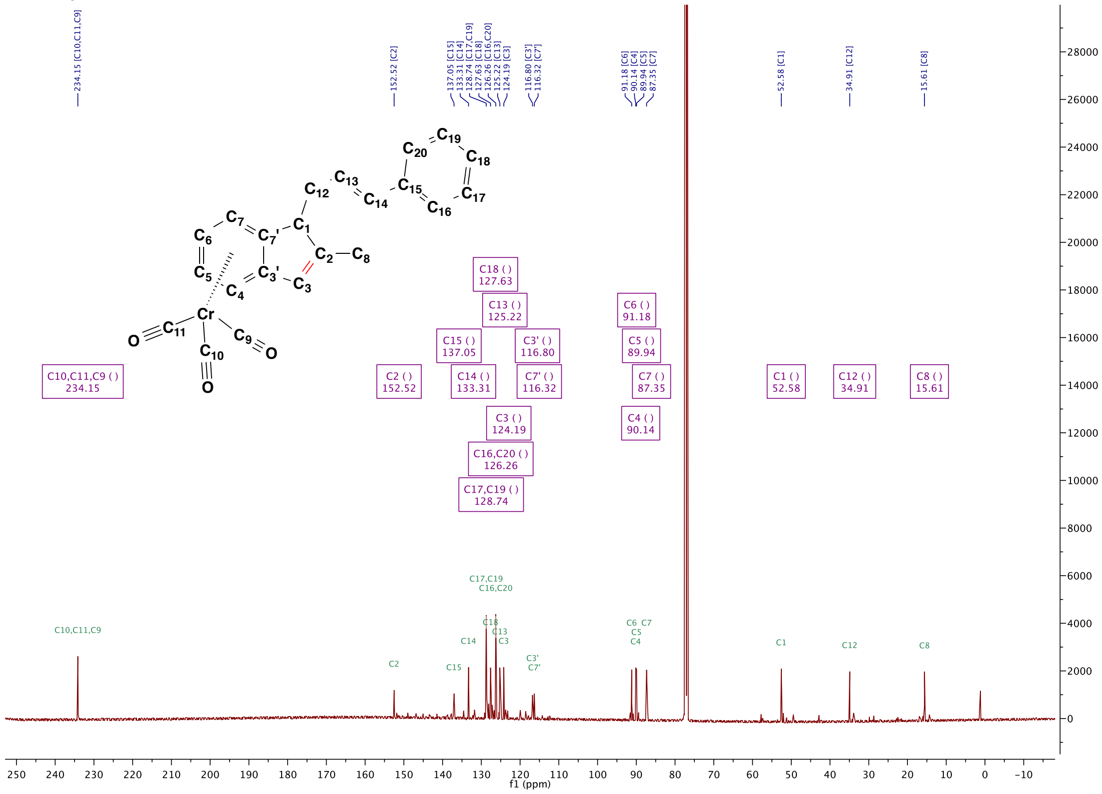

11 - Compound 8d.

C_6D_6 – ^1H – 600 Mhz - 298 K.

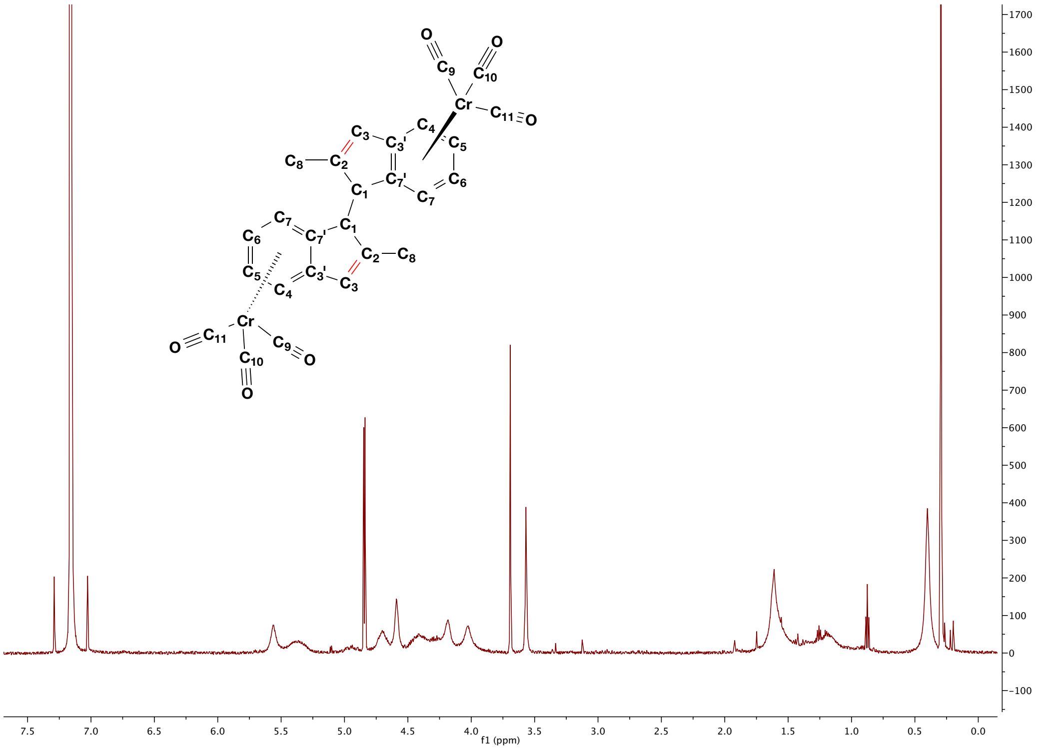

C_6D_6 – ^1H – 600 Mhz - 338 K.

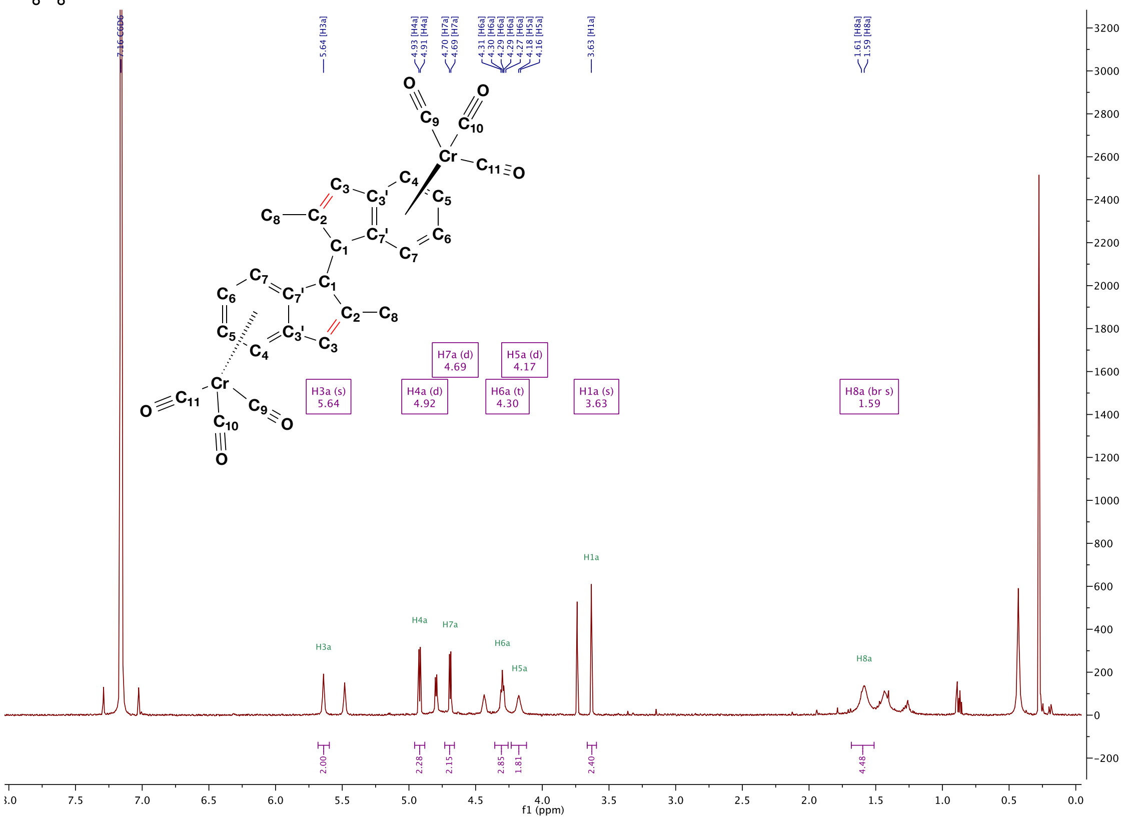

12 - Compound 9a.

C_6D_6 – ^1H – 500 Mhz – 300 K.

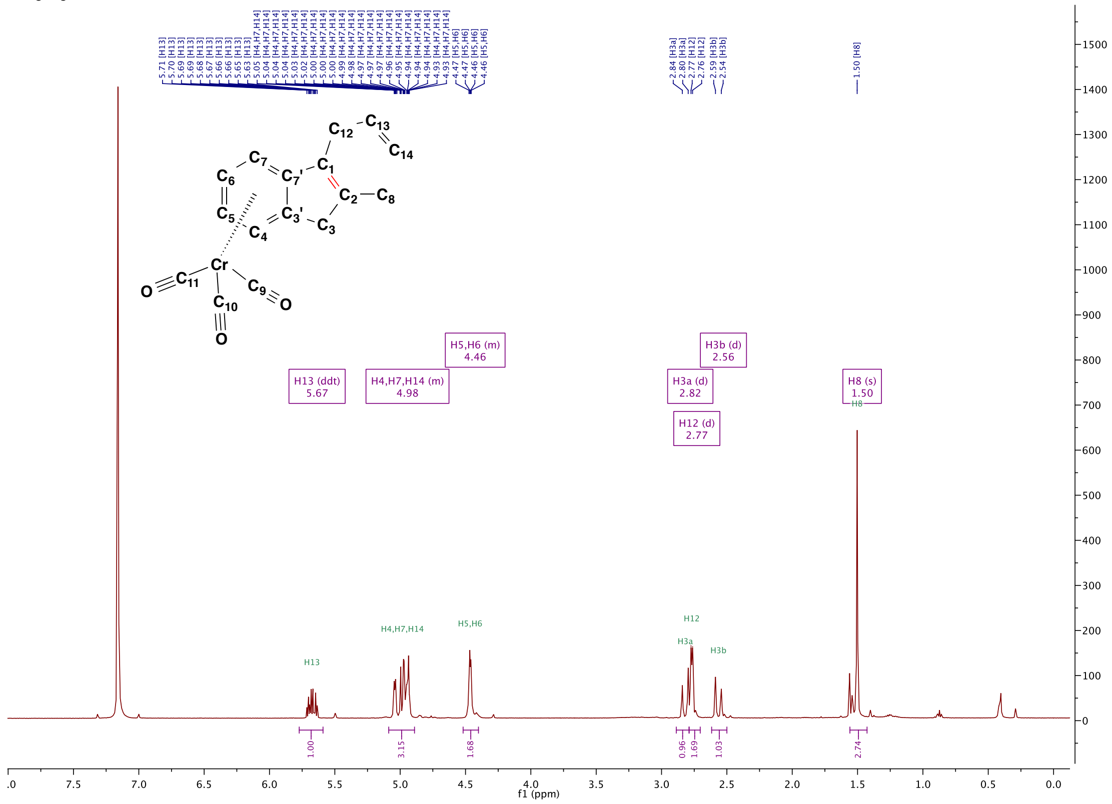

C_6D_6 – ^{13}C – 126 Mhz – 300 K.

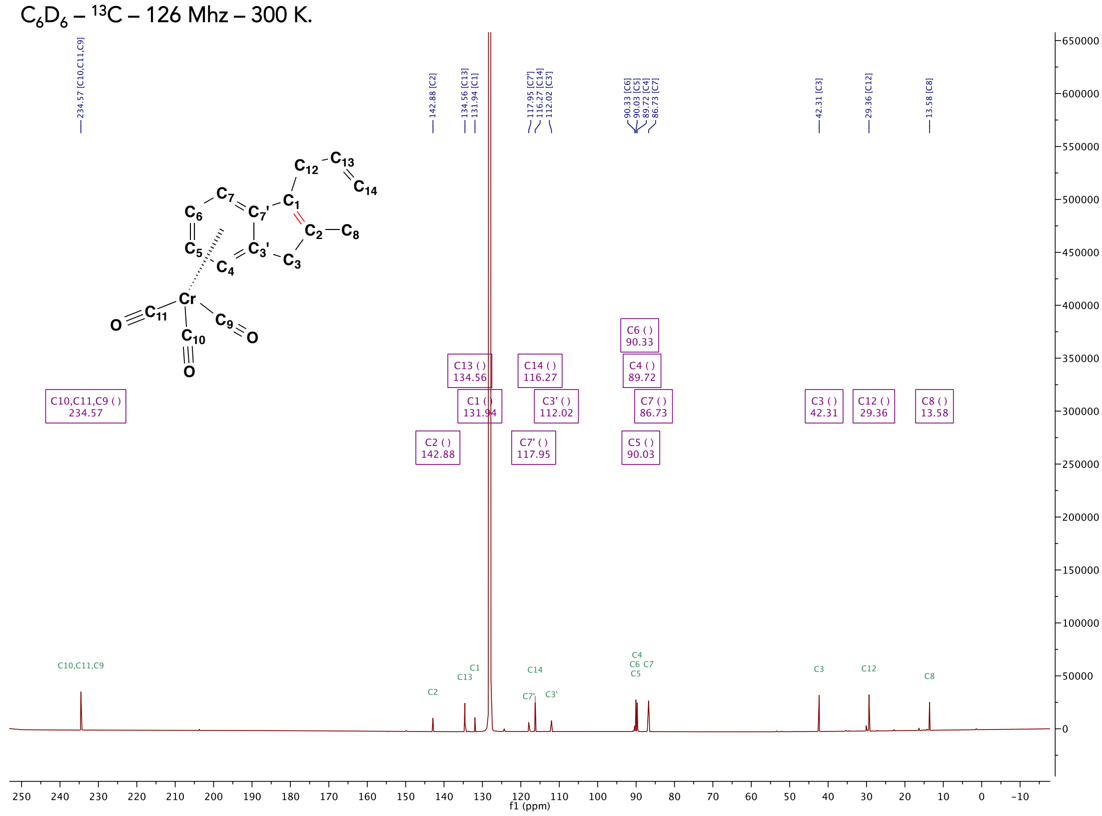

13 - Compound 9b.

C_6D_6 – ^1H – 500 Mhz – 300 K.

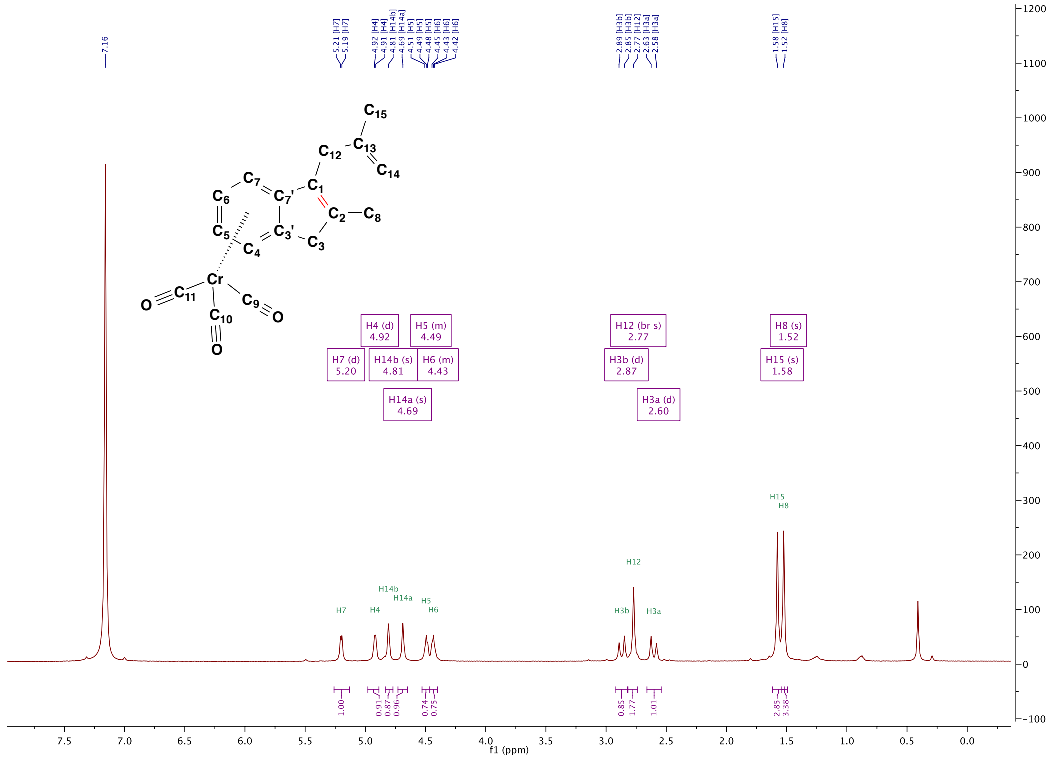

C_6D_6 – ^{13}C – 126 Mhz – 300 K.

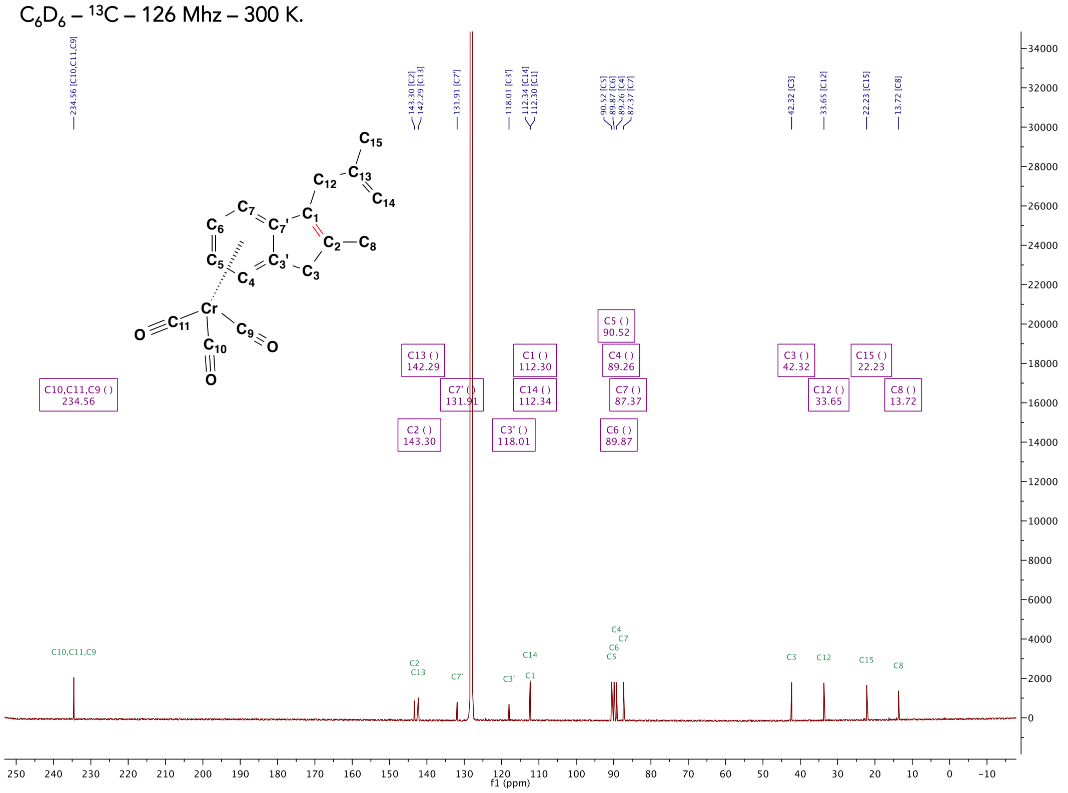

14 - Compound 9c.

CDCl$_3$ – ^{1}H – 600 Mhz – 298 K.

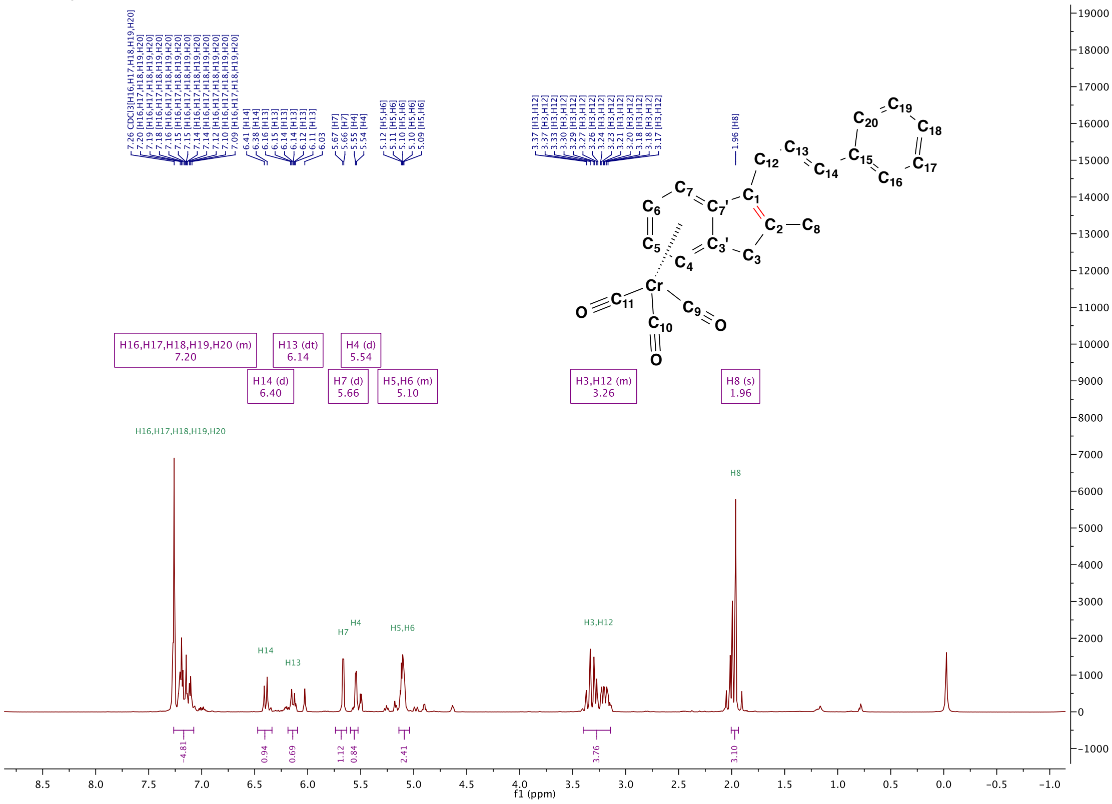

CDCl$_3$ – ^{13}C – 126 Mhz – 300 K.

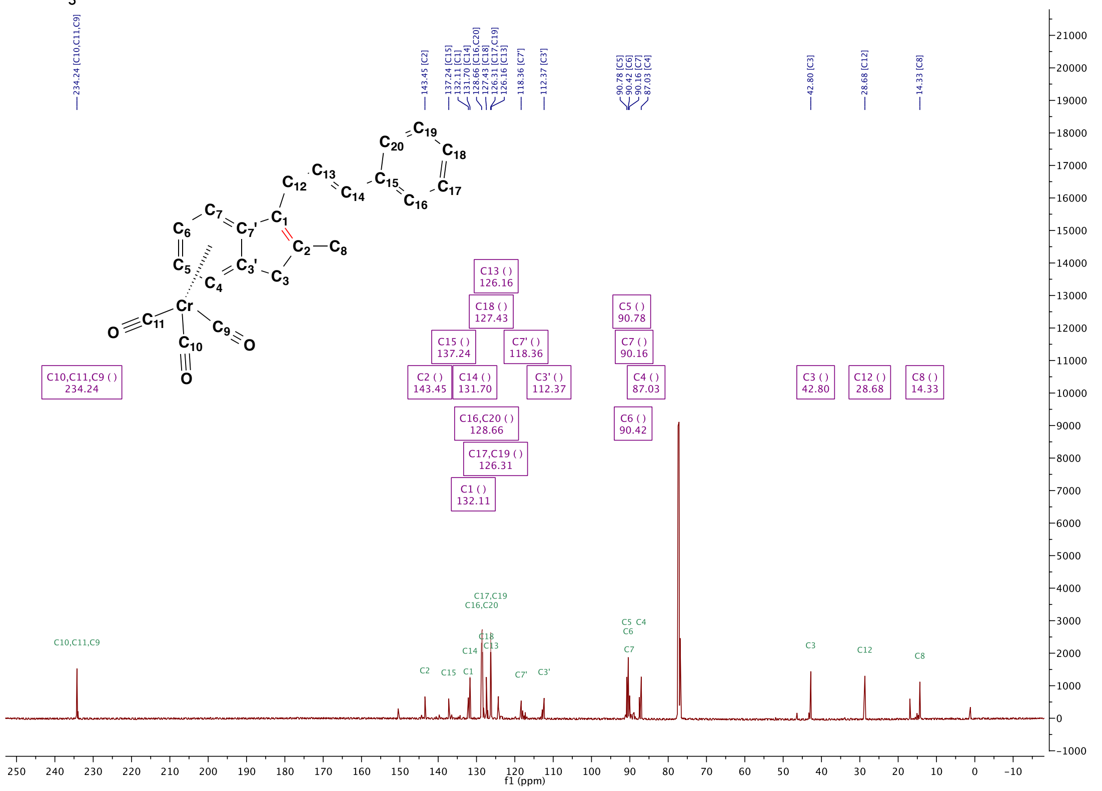

15 - Compound 9d.

C_6D_6 – ^1H – 500 Mhz - 300 K.

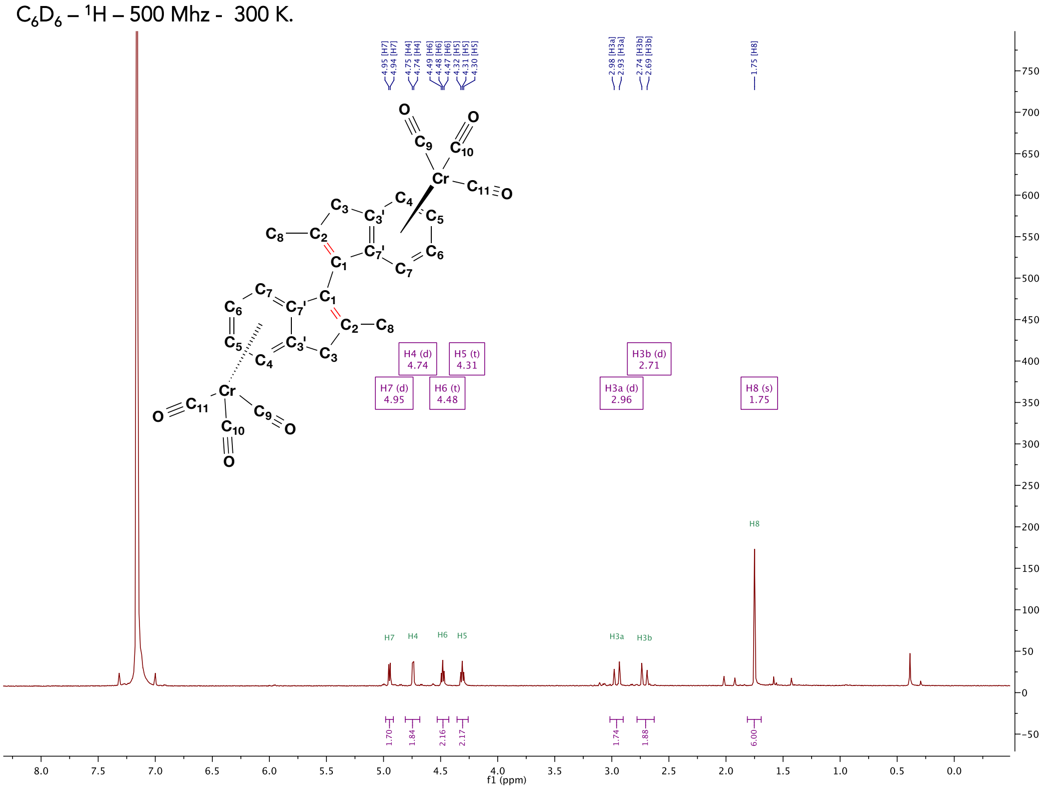

C_6D_6 – ^{13}C – 126 Mhz - 300 K.

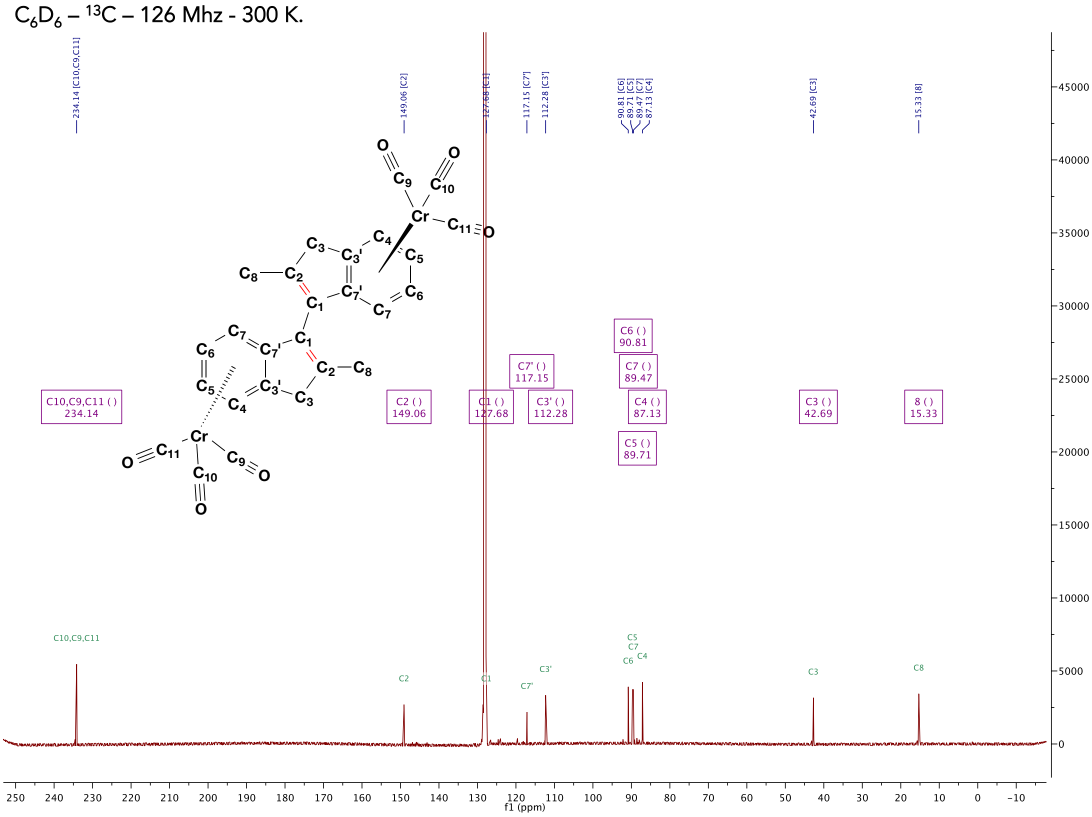

16 - Compound 10f.

C_6D_6 – ^1H – 500 Mhz – 293 K.

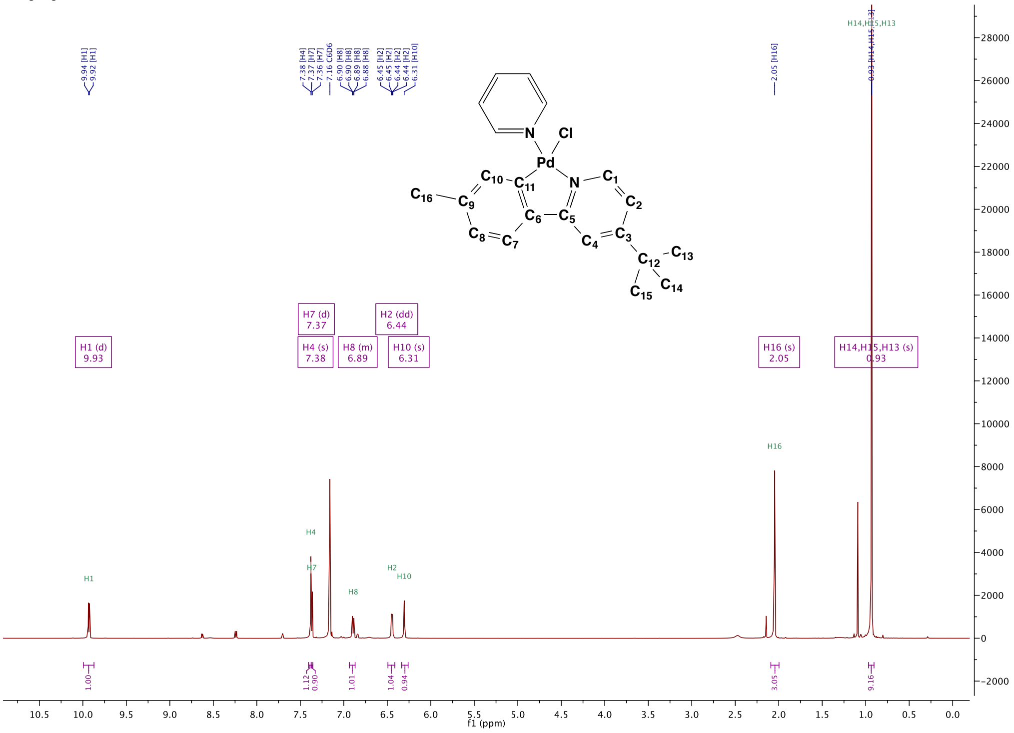

C_6D_6 – ^{13}C – 126 Mhz – 293 K.

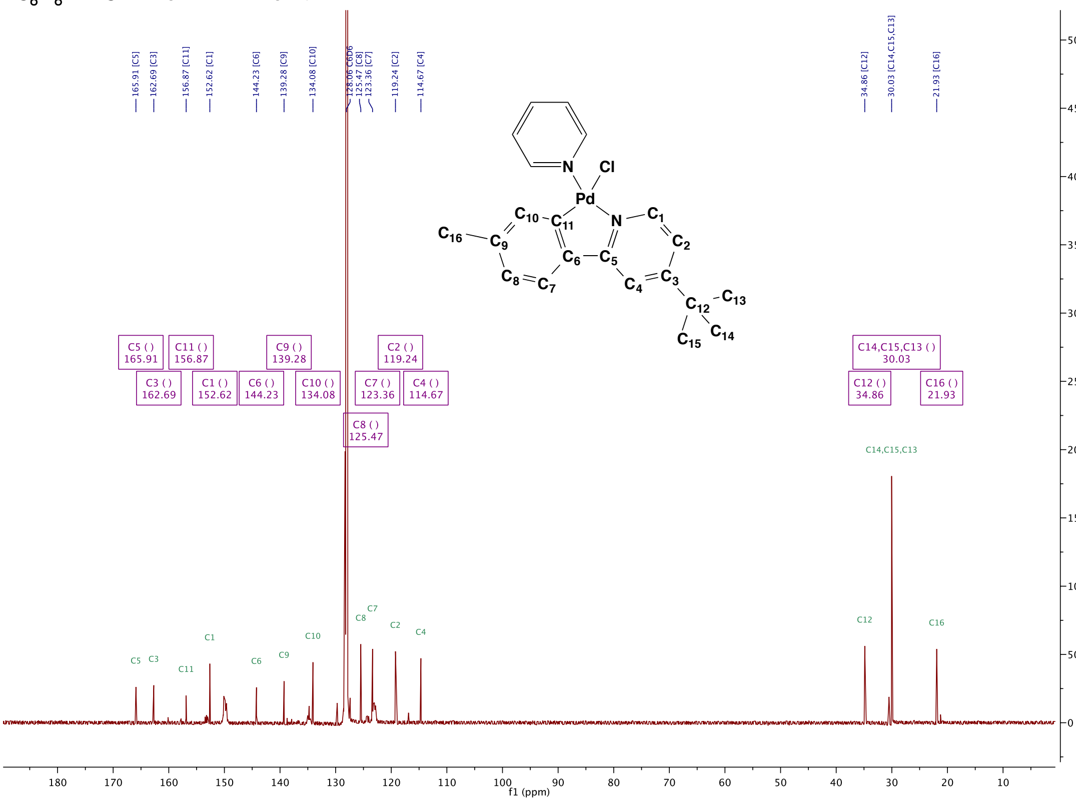

17 - Compound 10i.

C_6D_6 + Pyridine-d_5 – ^1H – 400 Mhz – 298 K.

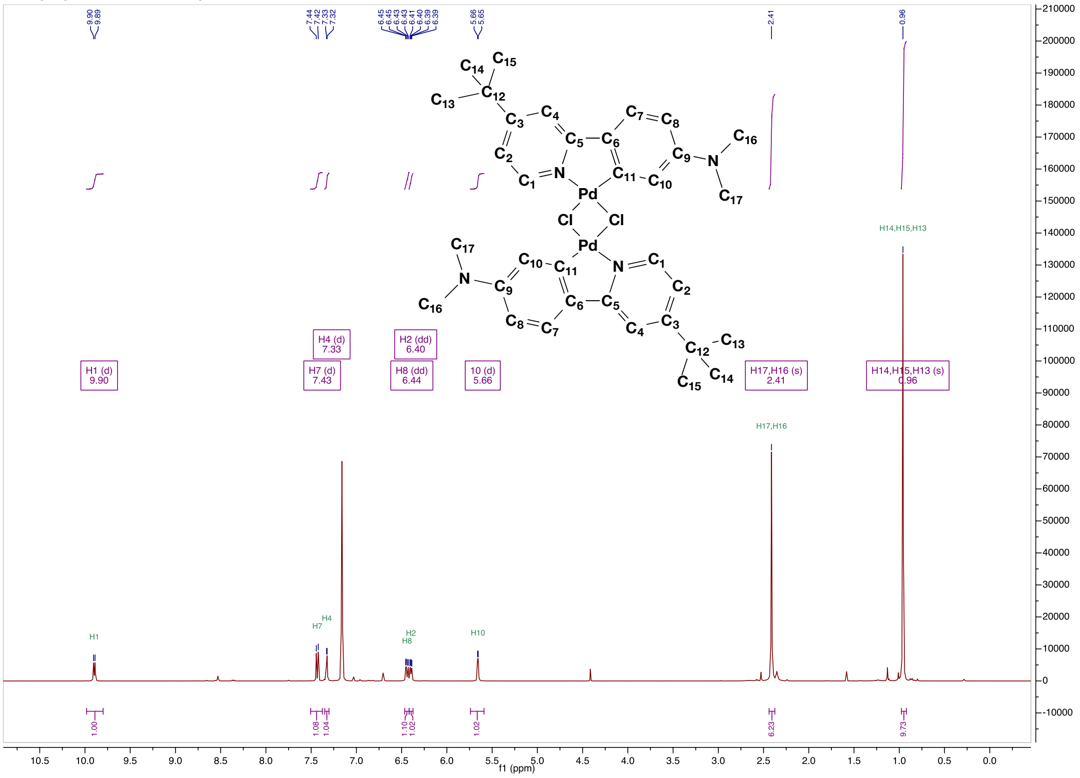

C_6D_6 + Pyridine-d_5 – ^{13}C – 101 Mhz – 298 K.

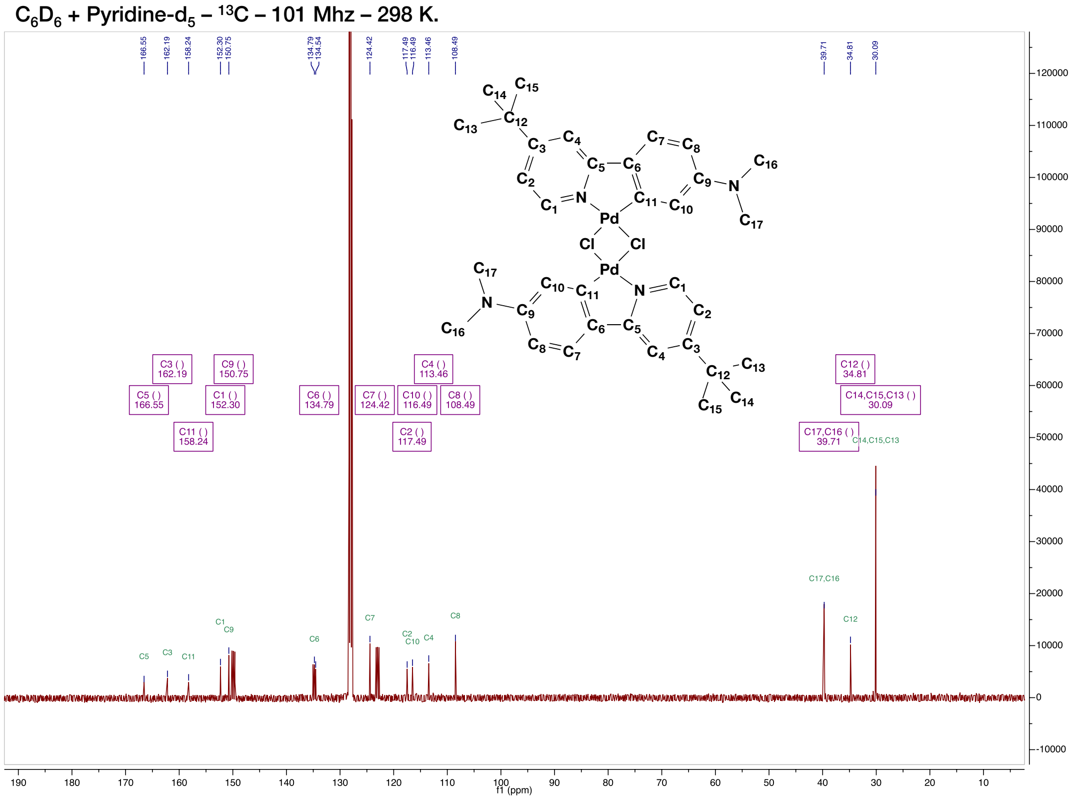

18 - Compound 12a.

C_6D_6 – ^{1}H – 500 Mhz – 293 K.

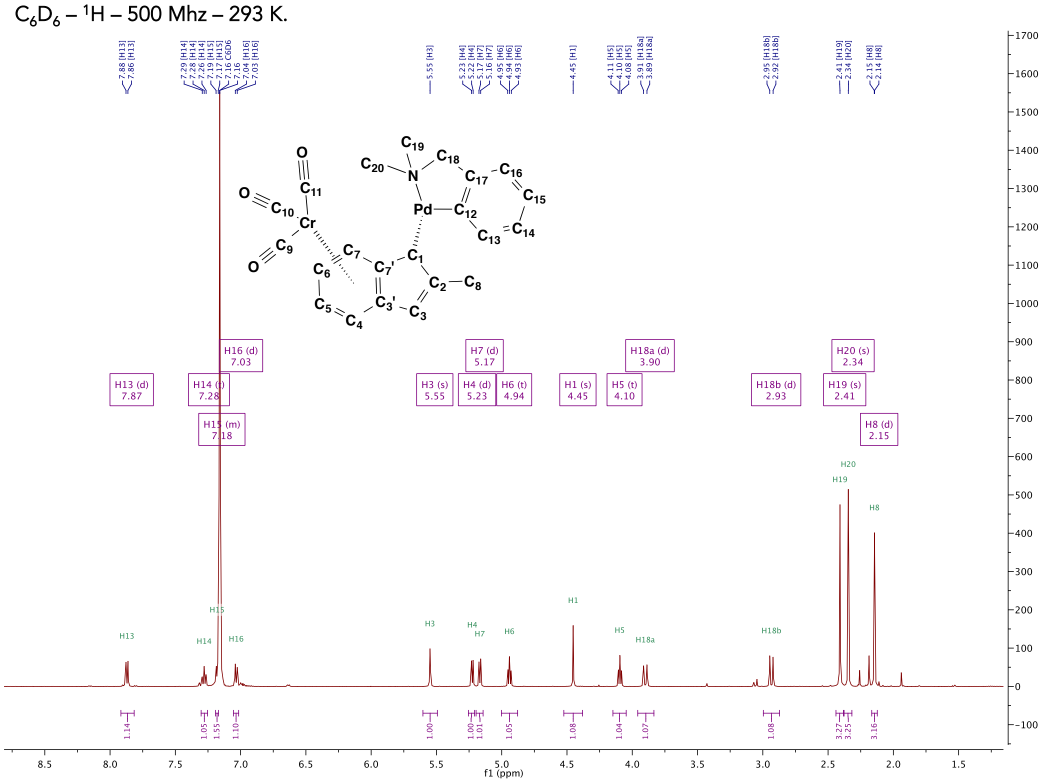

C_6D_6 – ^{13}C – 126 Mhz – 293 K.

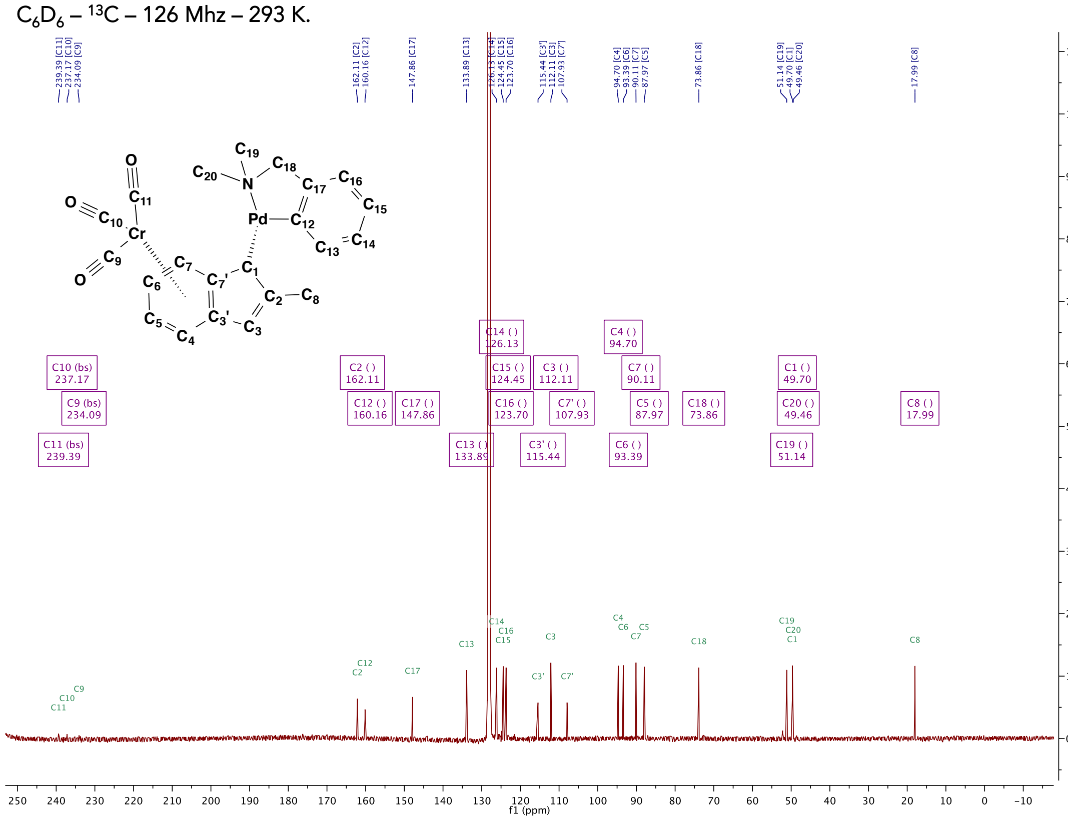

Tol– ^{1}H – 600 Mhz – variable temperature.

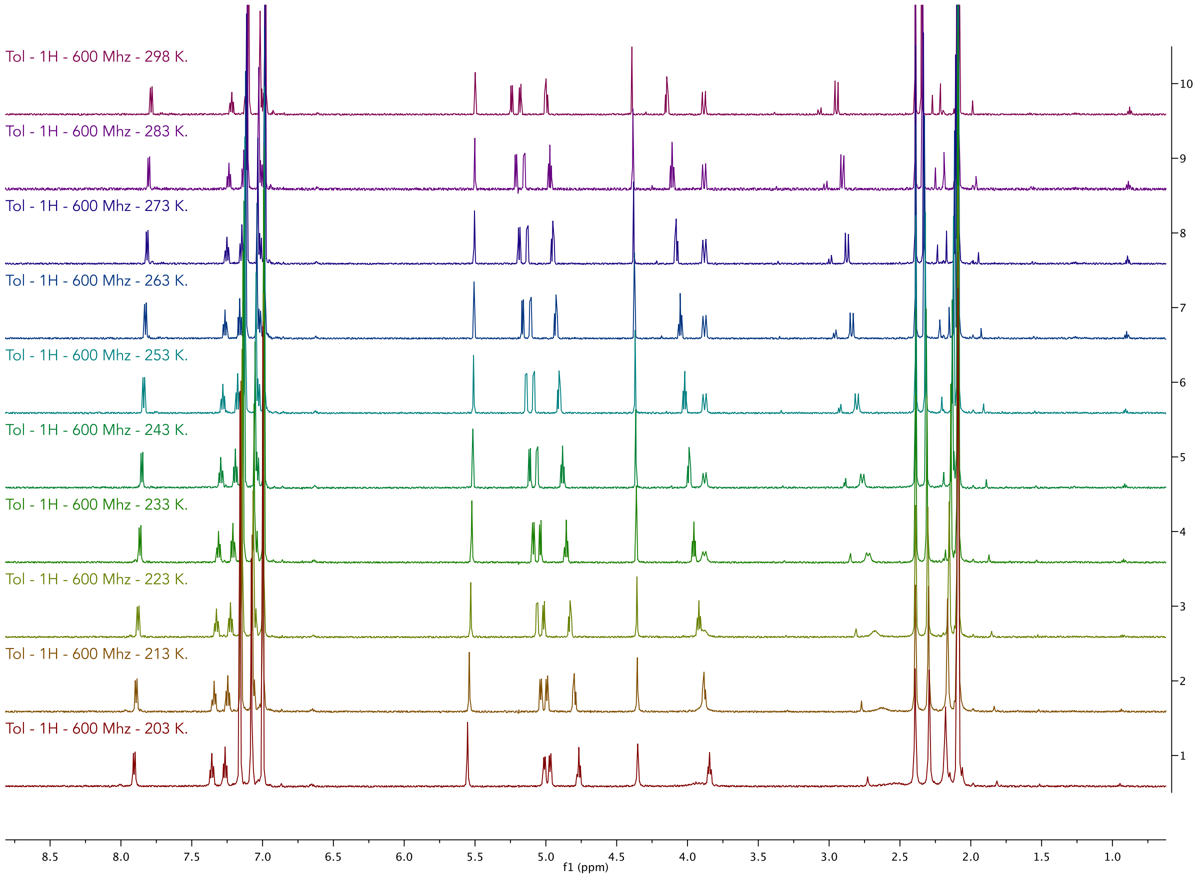

19 - Compound 12b.

C_6D_6 – ^1H – 500 Mhz – 293 K.

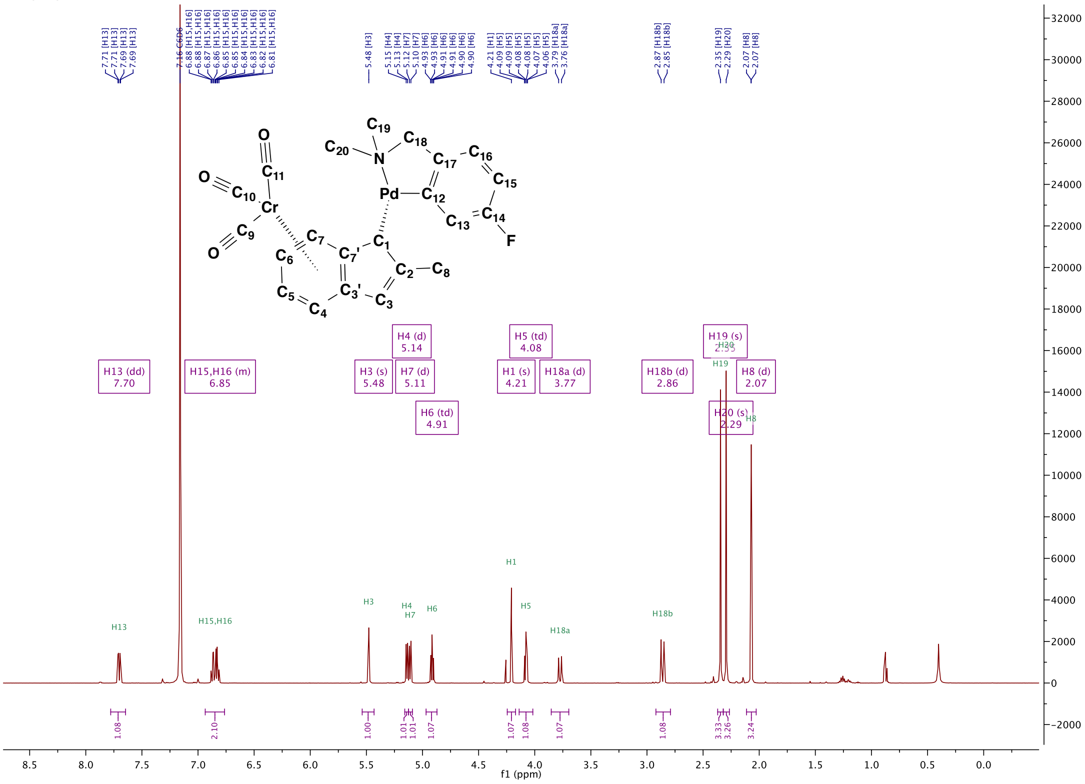

C_6D_6 – ^{13}C – 126 Mhz – 293.0 K.

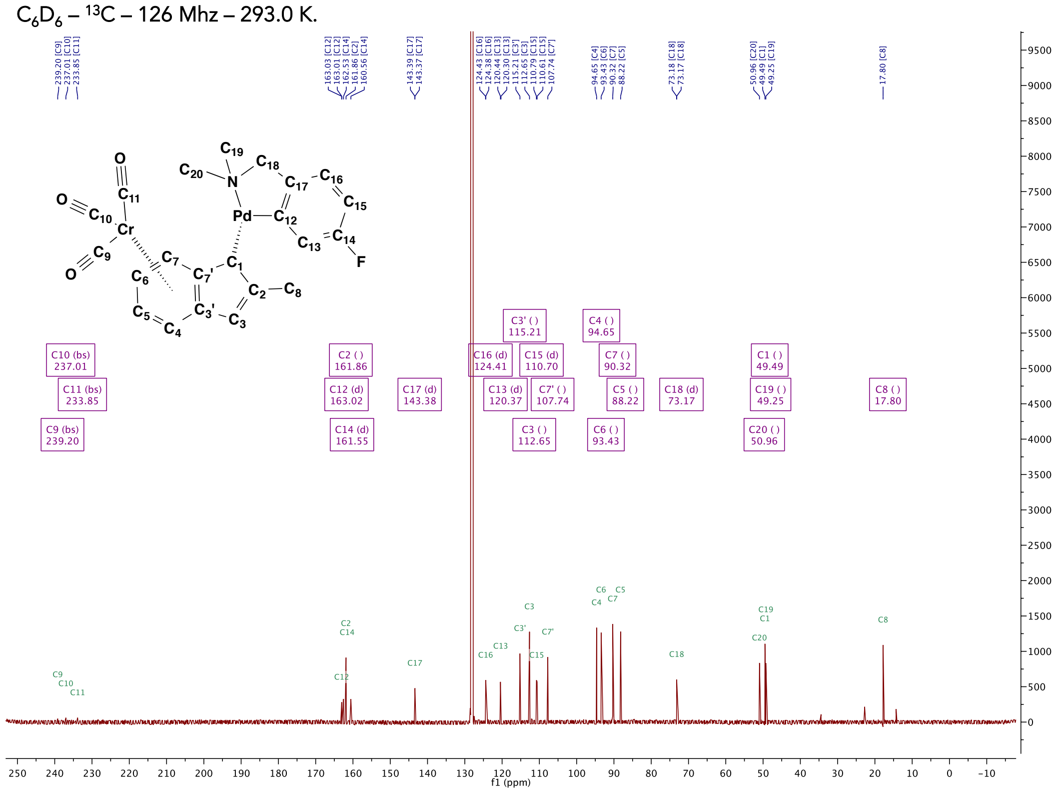

C_6D_6 – ^{19}F – 300 Mhz – 298 K.

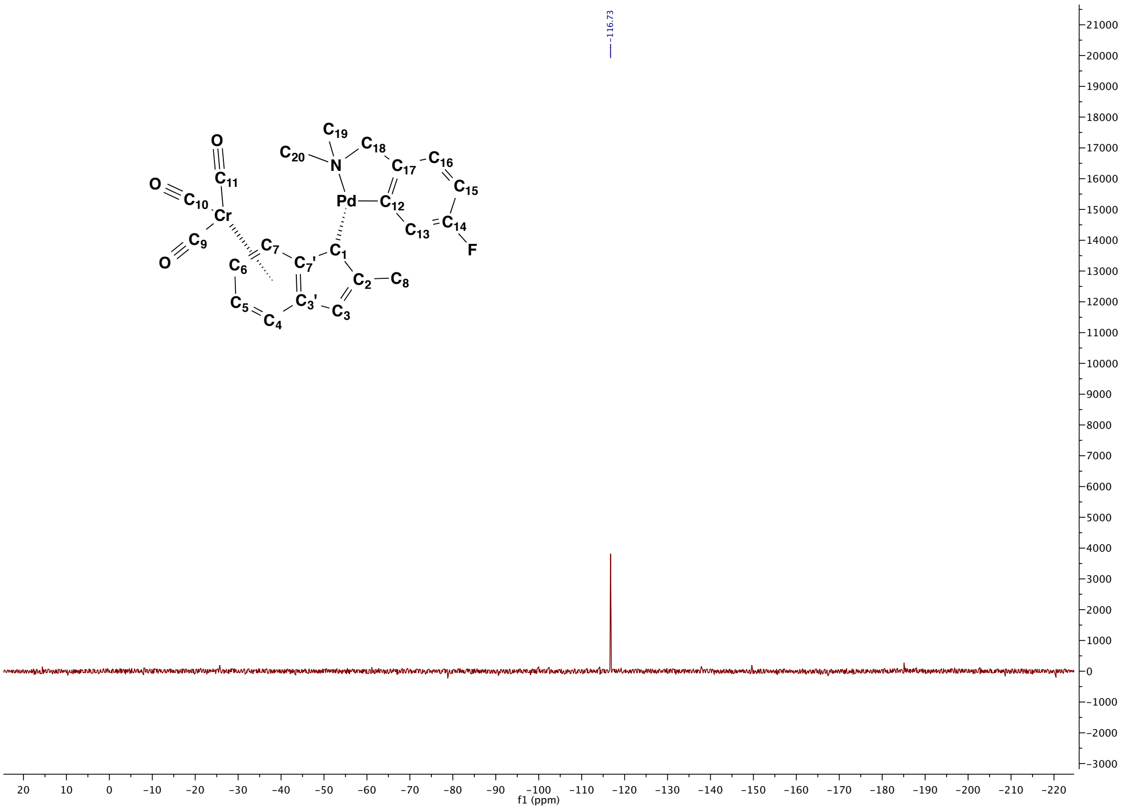

Tol – ^{1}H – 600 Mhz – variable temperature.

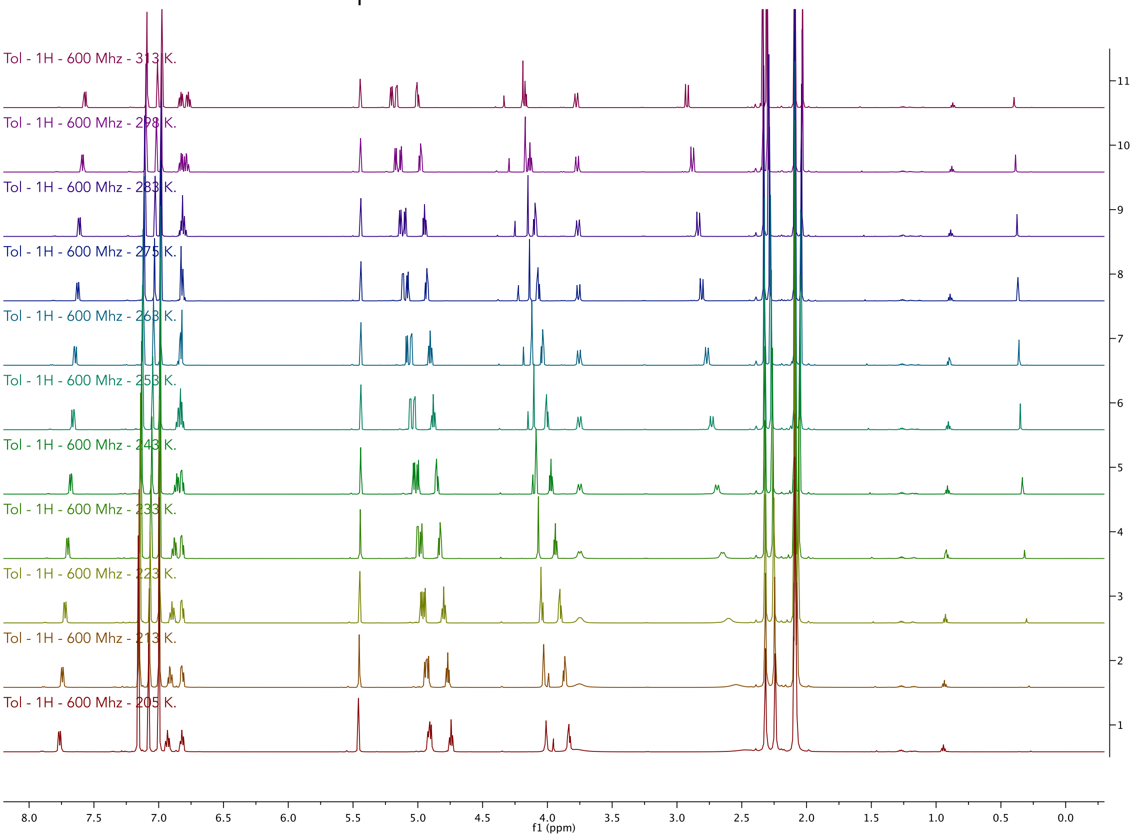

20 - Compound 12c.

C_6D_6 – ^1H – 500 Mhz – 300 K.

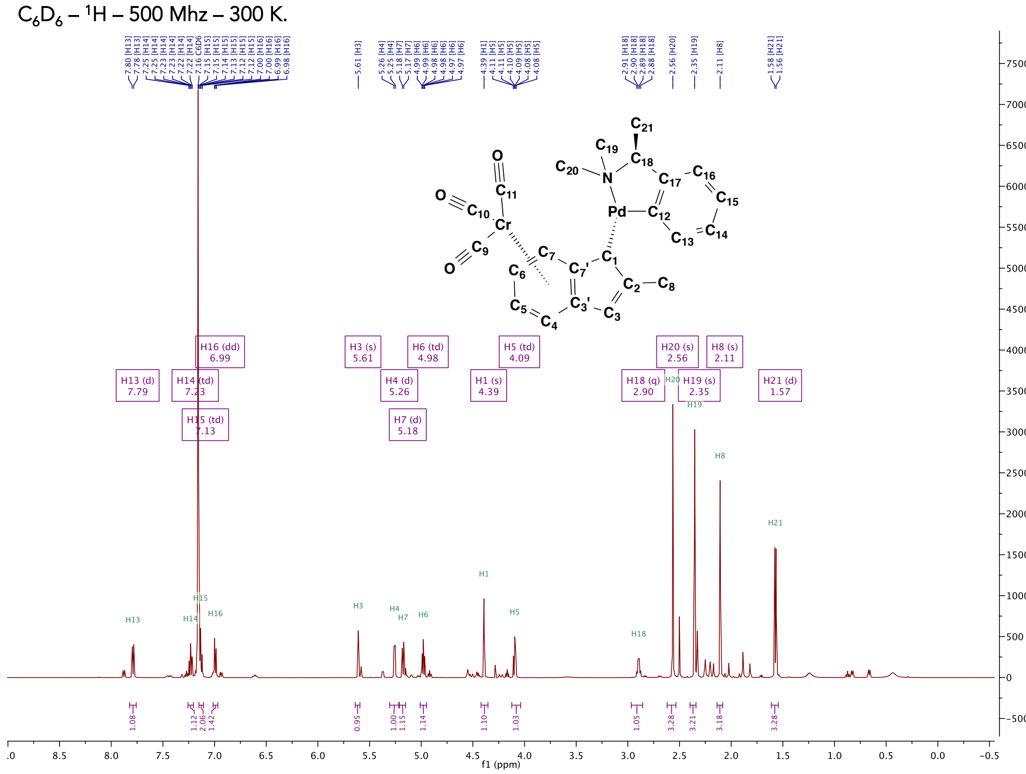

C_6D_6 – ^{13}C – 126 Mhz – 300 K.

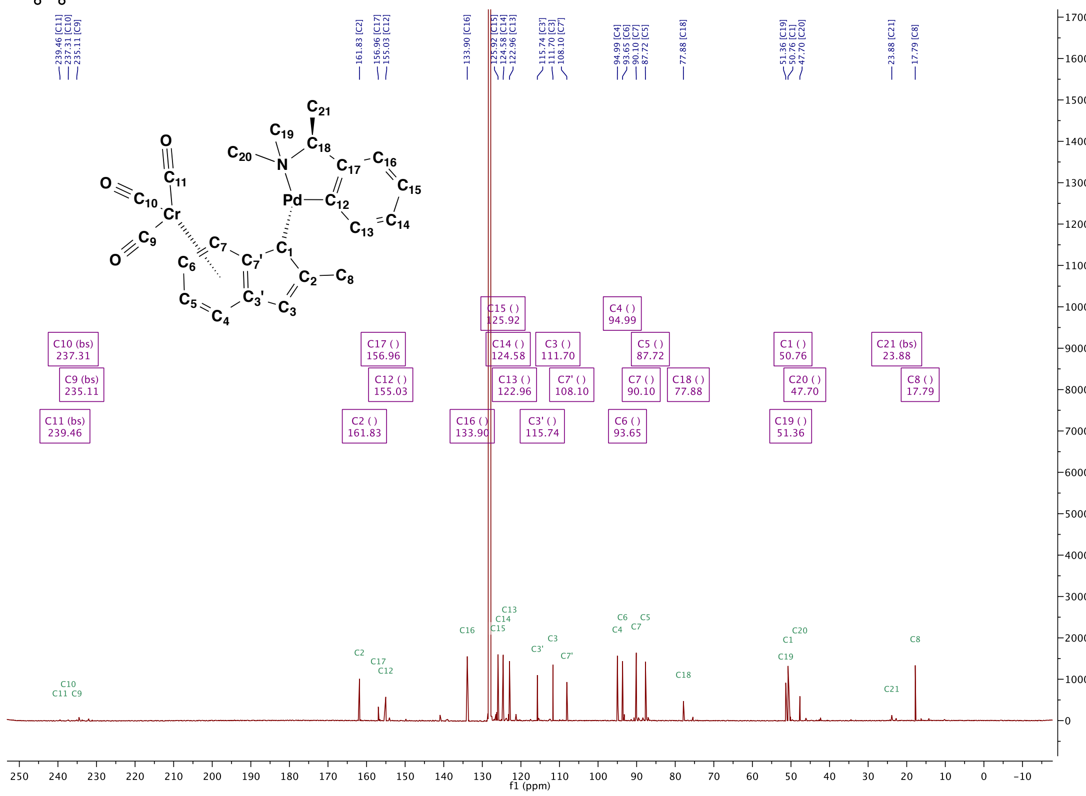

Tol– ^{1}H – 600 Mhz – variable temperature.

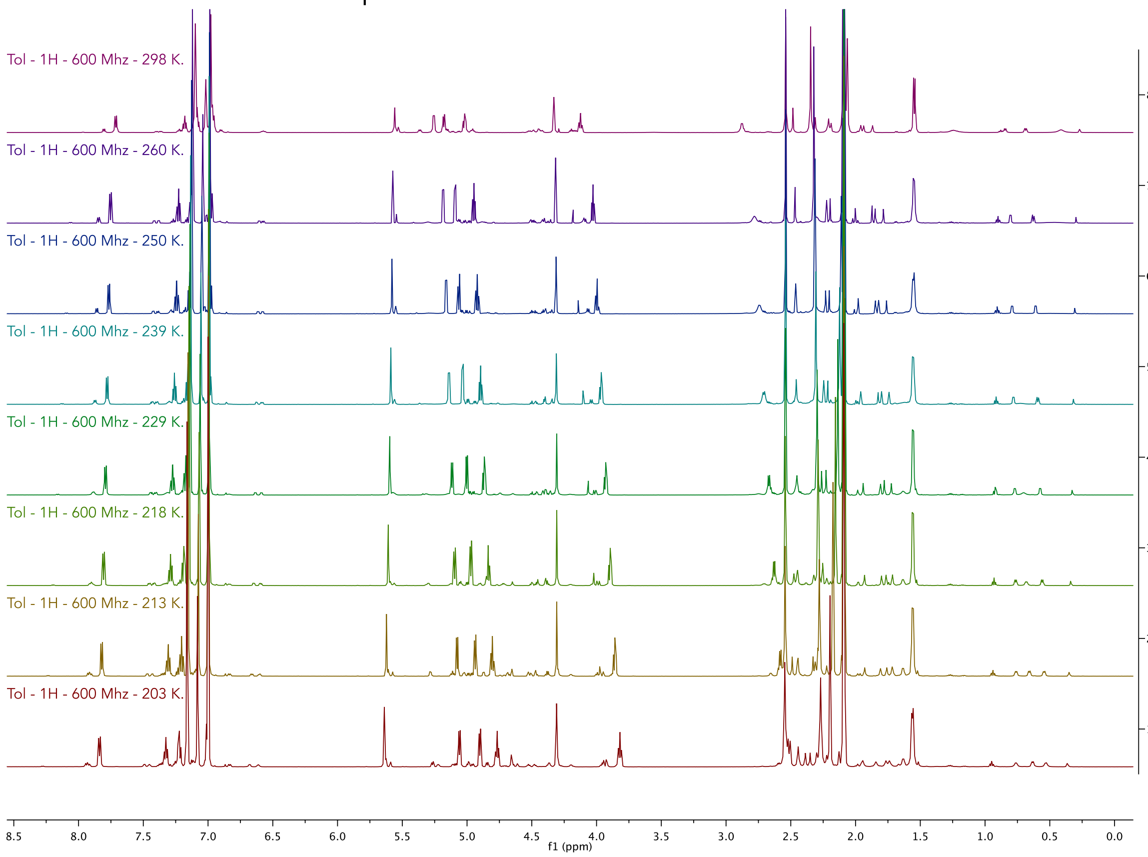

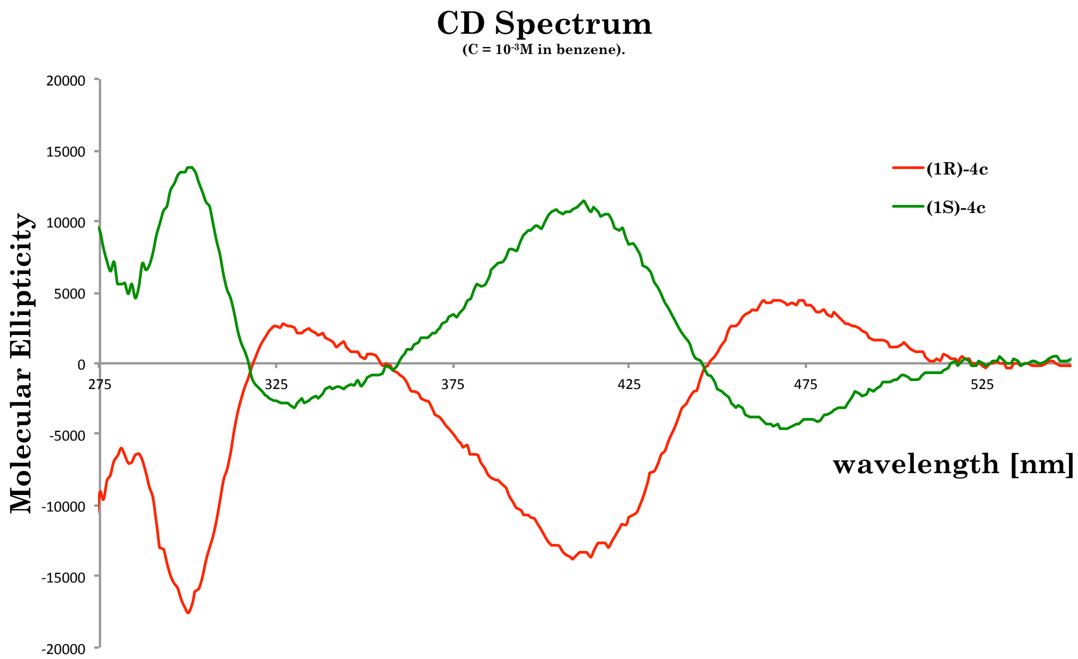

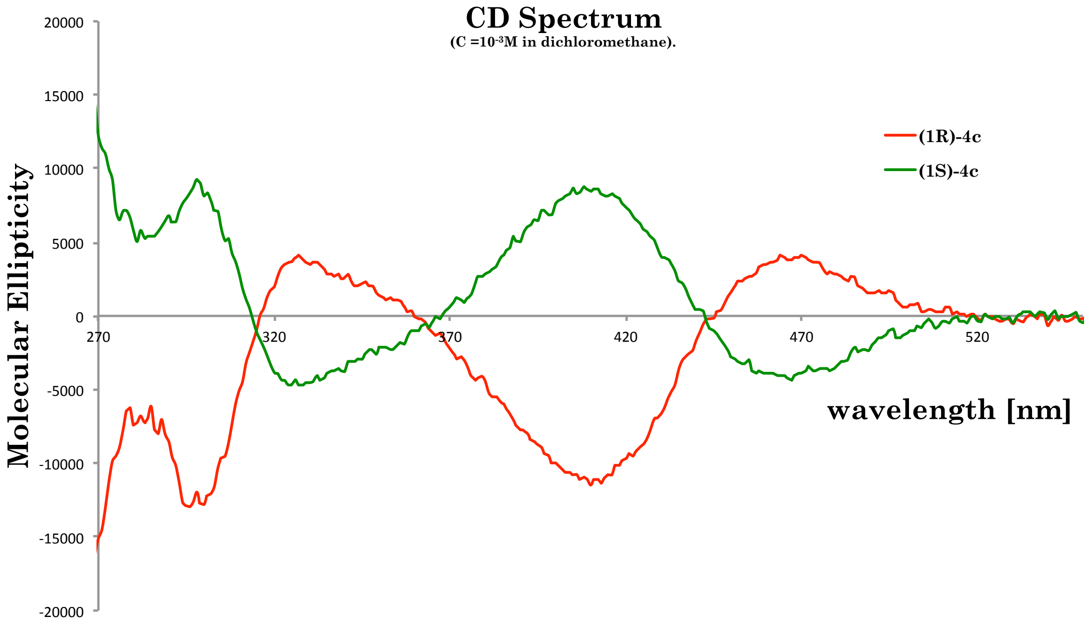
CD Spectrum
(C =10-3M in dichloromethane).
(1R)-4c
(1S)-4c
Molecular Ellipticity
wavelength [nm]
20000
15000
10000
5000
0
-5000
-10000
-15000
-20000
270
320
370
420
470
520

21 - Compound 12d.

C_6D_6 – ^1H – 500 Mhz – 293 K.

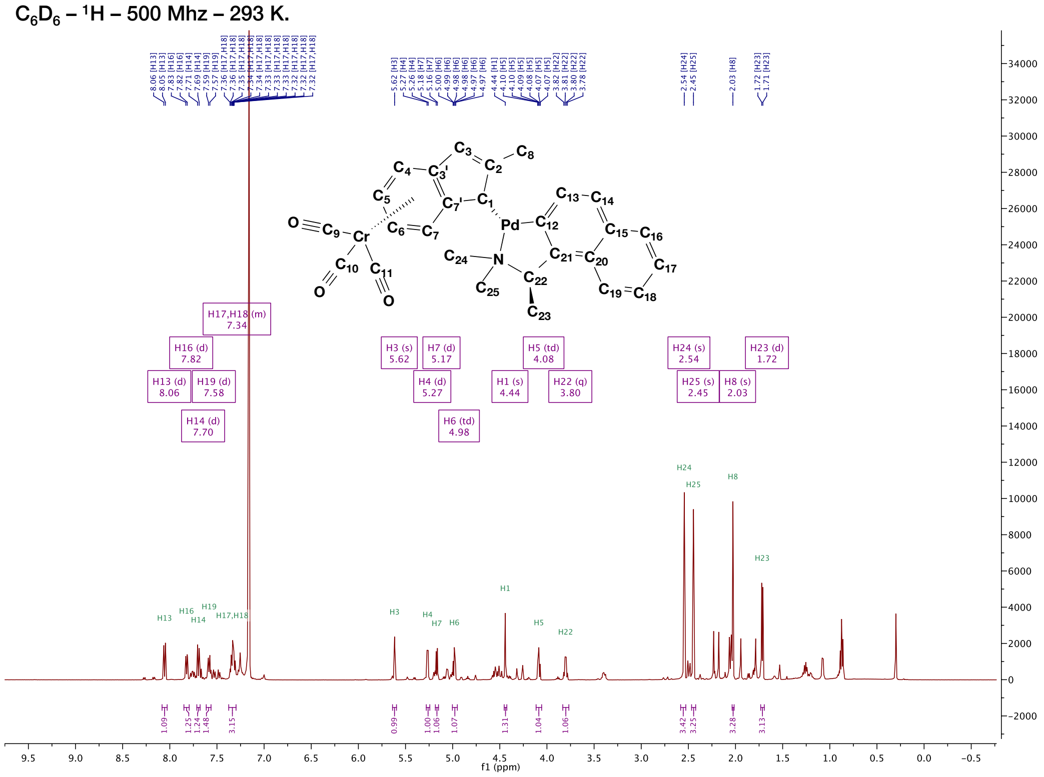

C_6D_6 – ^{13}C – 126 Mhz – 293 K.

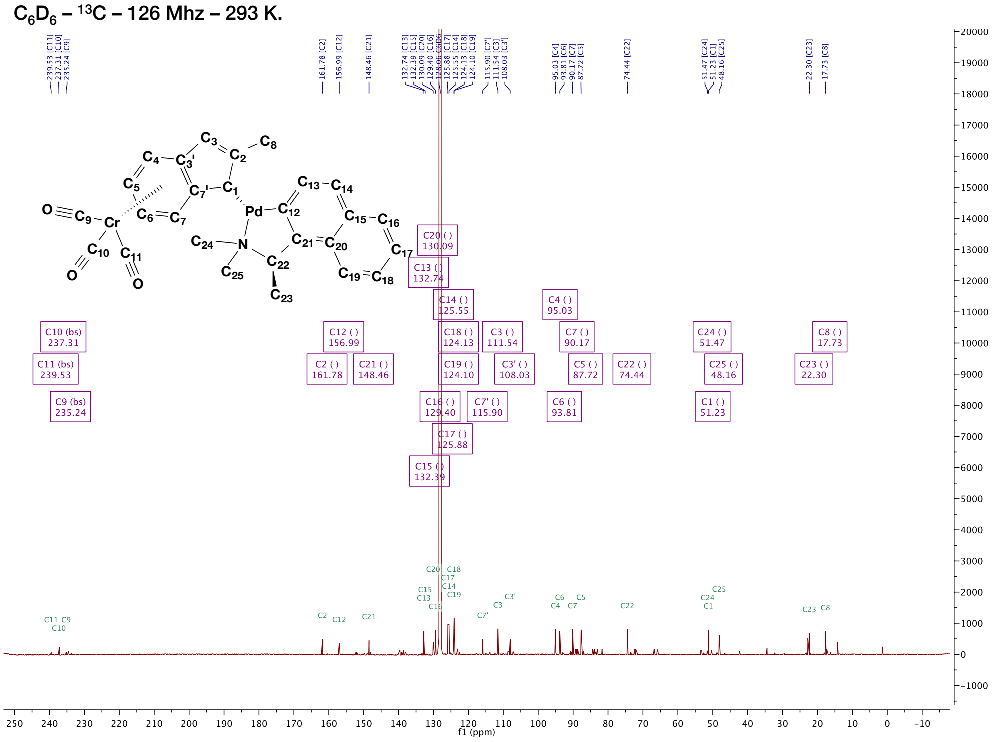

Tol – ^{1}H – 600 Mhz – Variable Temperature.

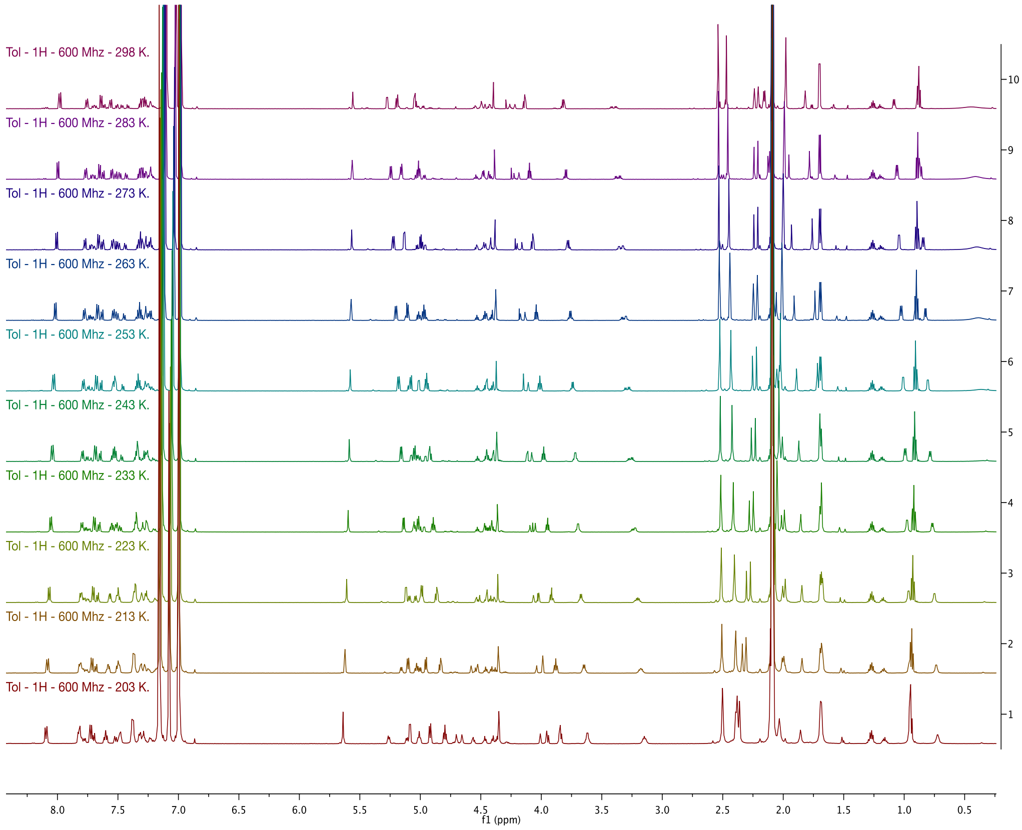

Circular dichroism (CD)

(C = 10^{-3}M in benzene).

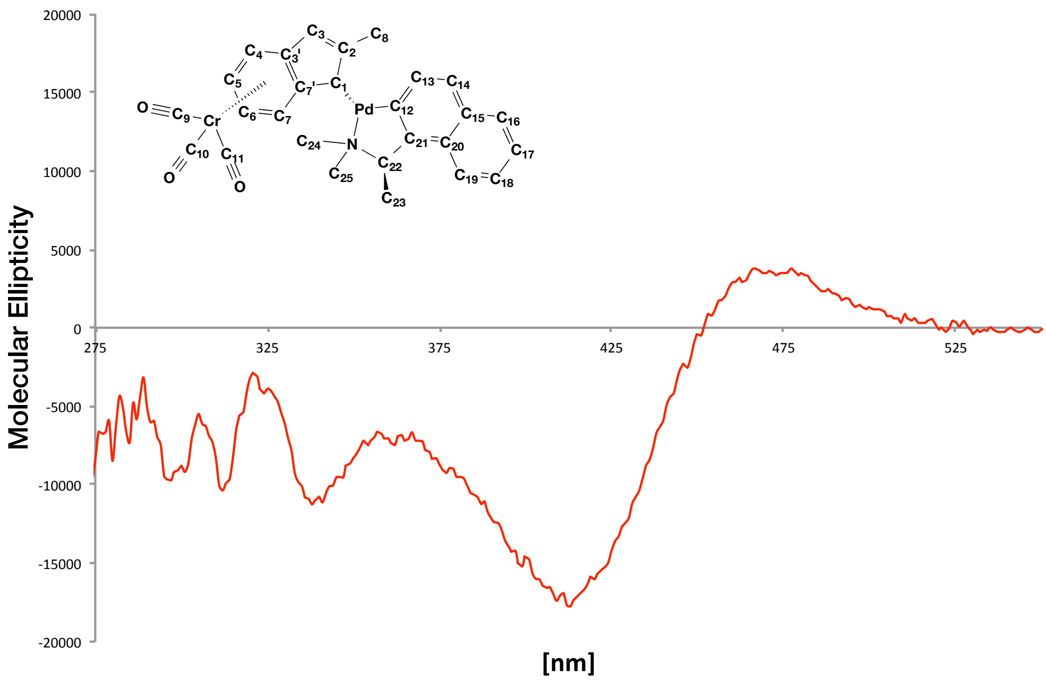

22 - Compound 12e.

C_6D_6 – ^1H – 500 Mhz – 300 K.

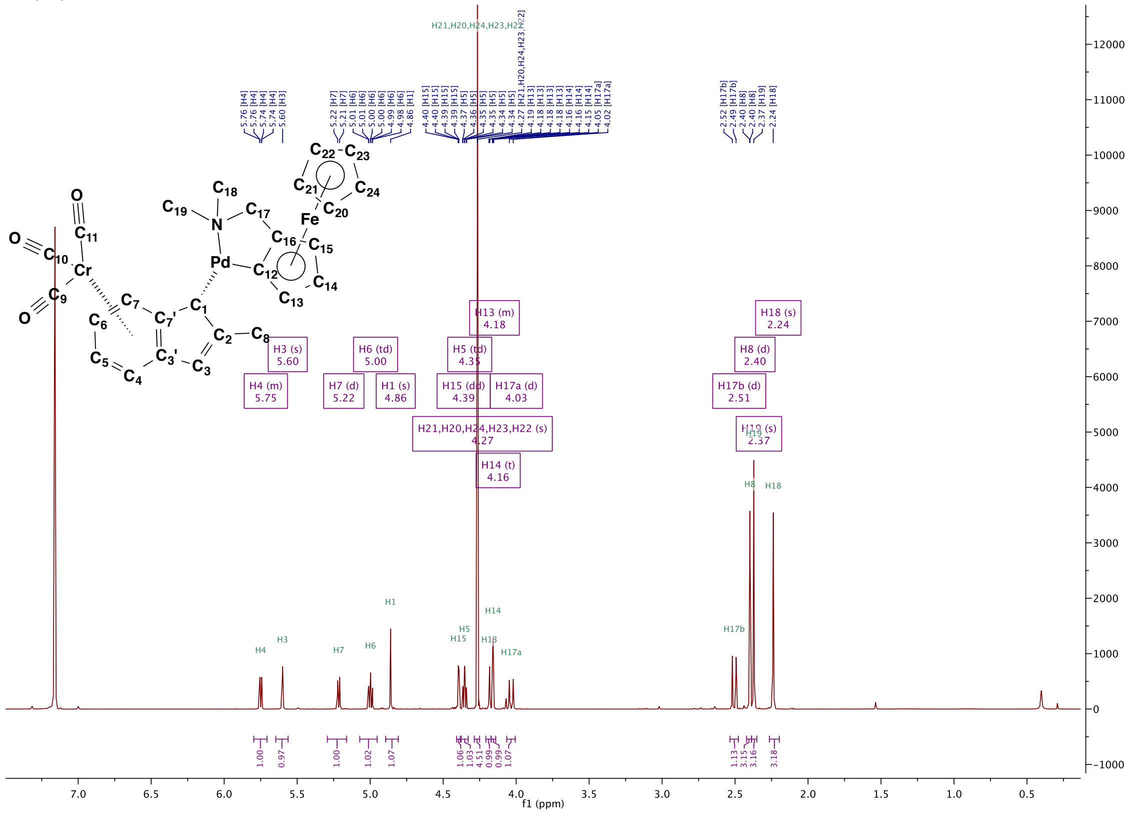

C_6D_6 – ^{13}C – 126 Mhz – 300 K.

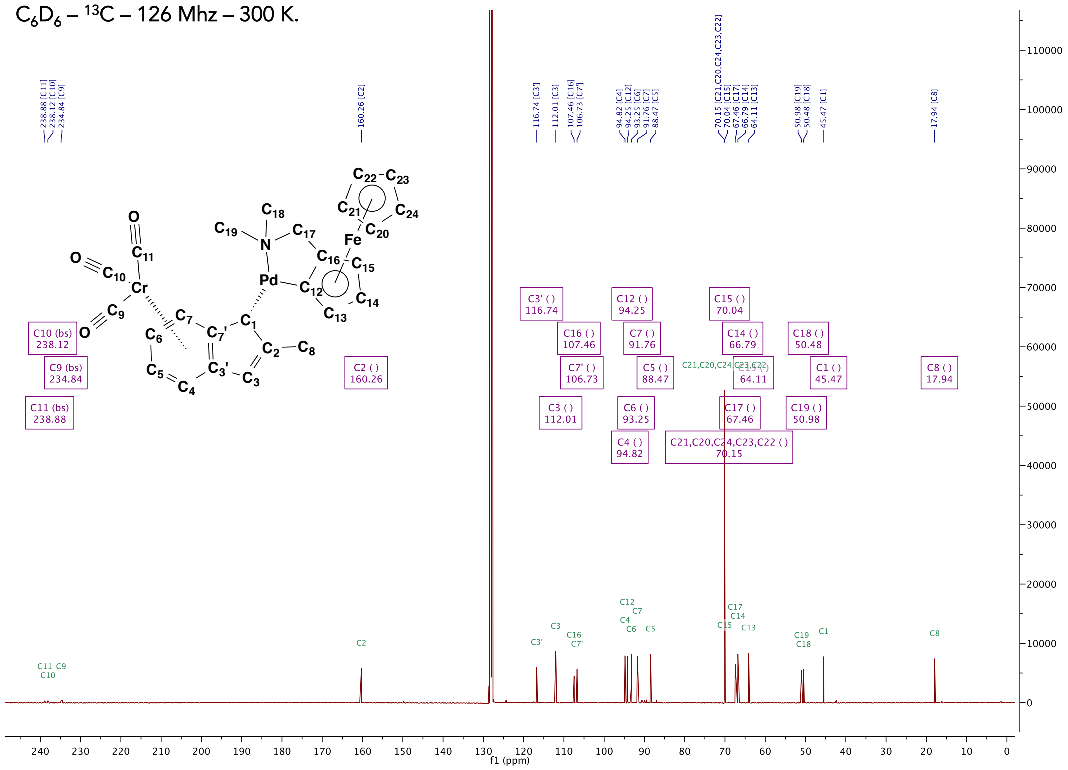

Tol– ^{1}H – 600 Mhz – variable temperature.

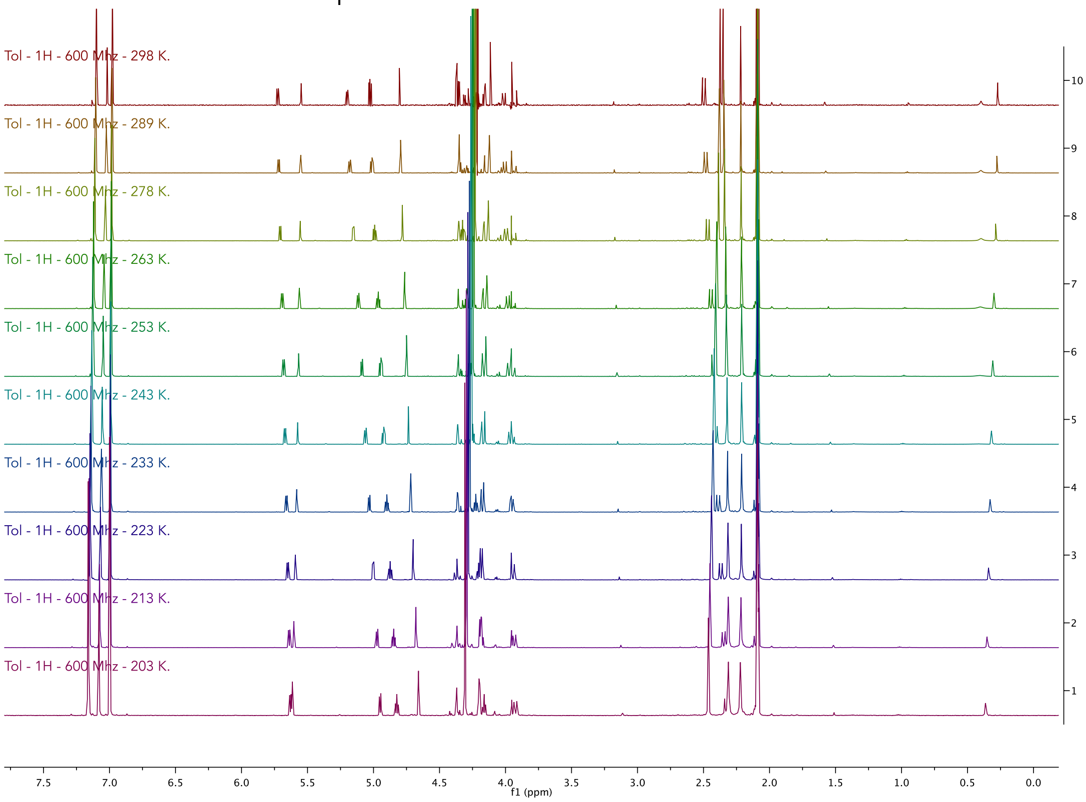

23 - Compound 12f.

CDCl$_3$ – ^{1}H – 500 Mhz – 300 K.

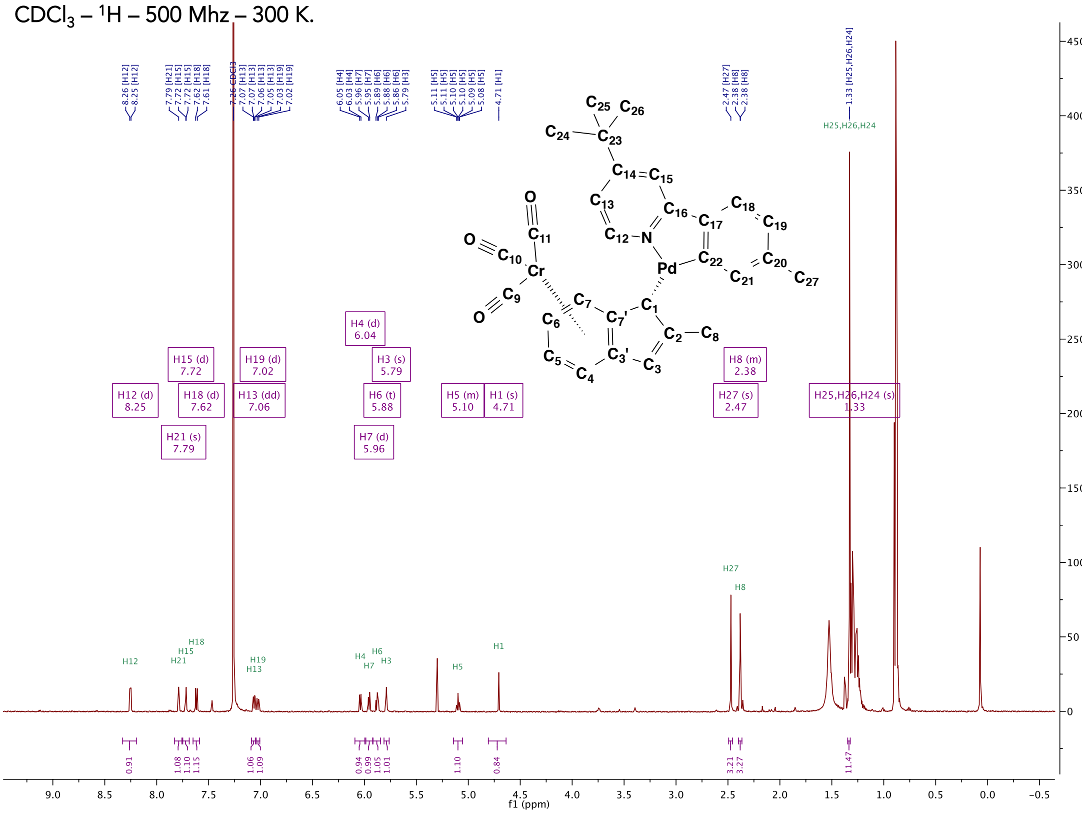

CDCl$_3$ – ^{13}C – 126 Mhz – 300 K.

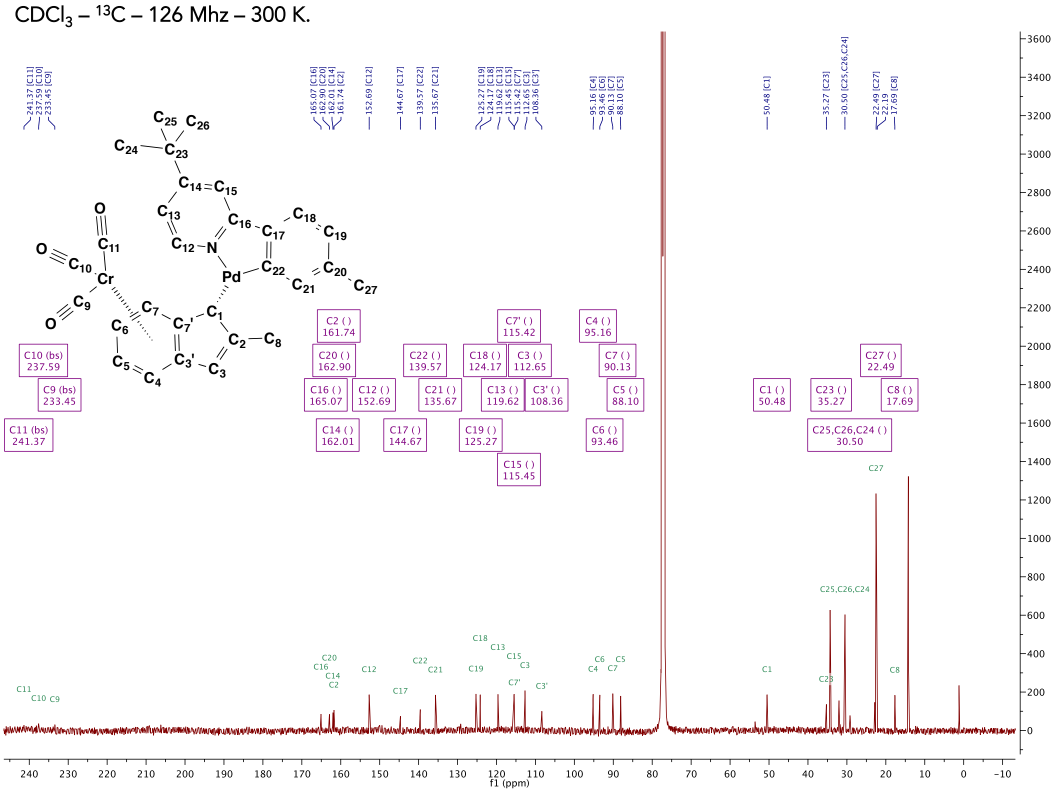

24 - Compound 12g.

C_6D_6 – ^1H – 500 Mhz – 293 K.

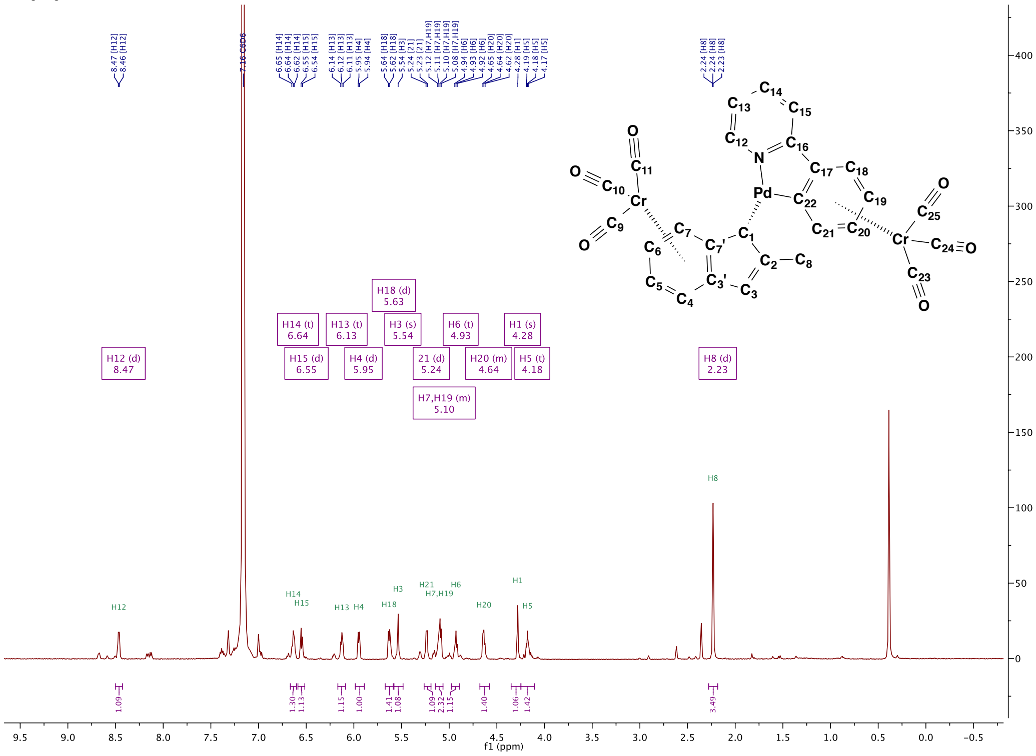

C_6D_6 – ^{13}C – 126 Mhz – 293 K.

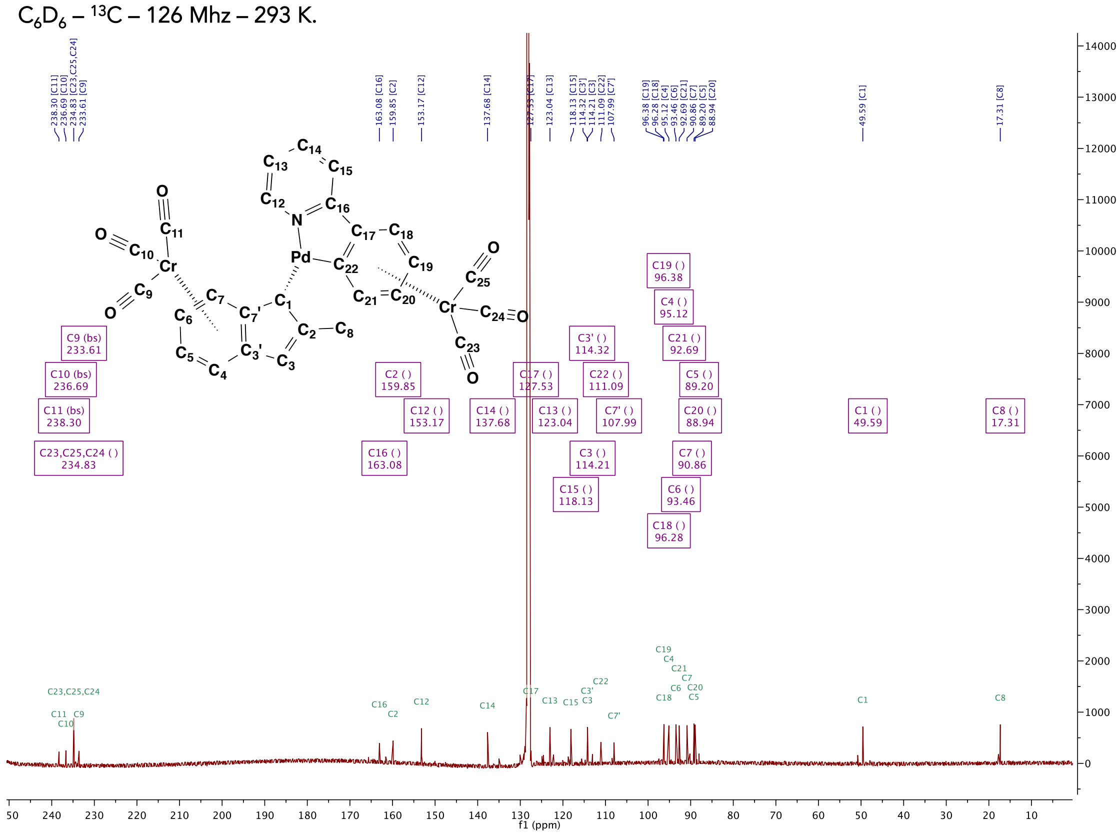

Tol– [1]H – 600 Mhz – variable temperature.

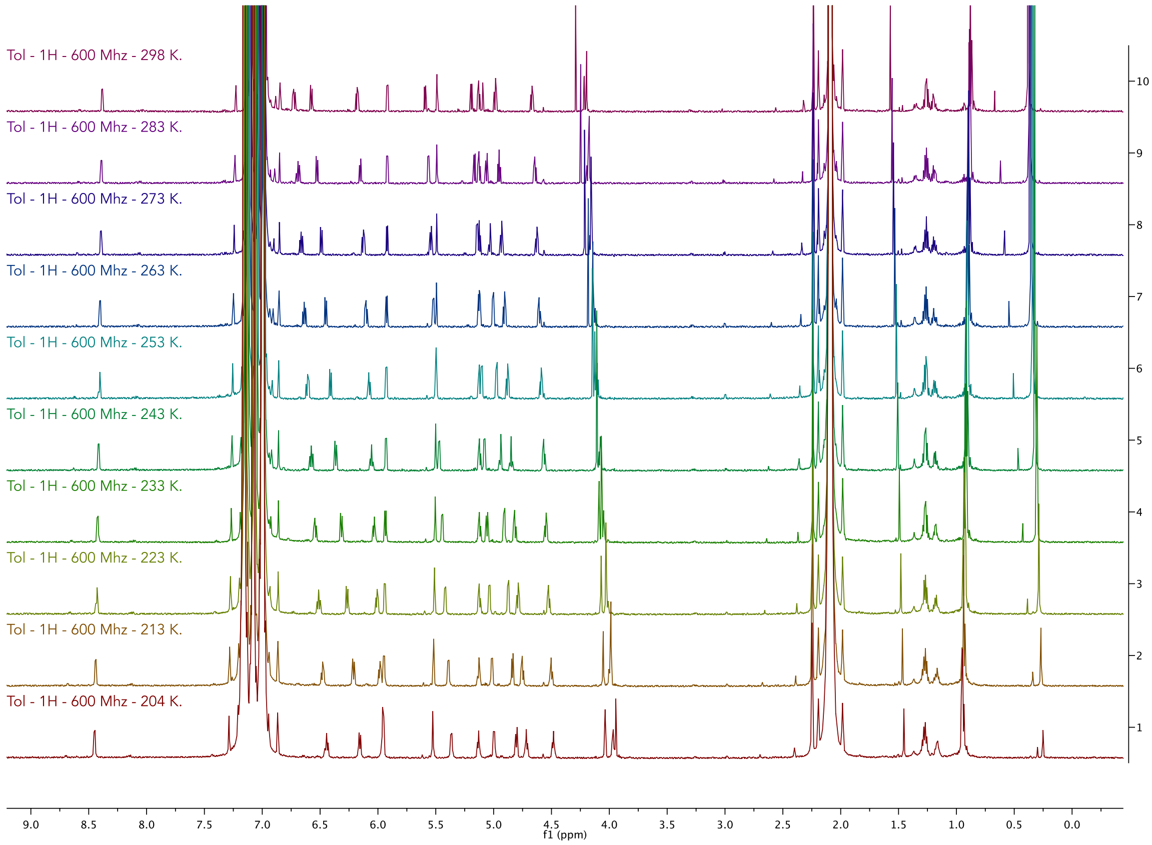

25 - Compound 13a.

C_6D_6 – ^1H – 600 Mhz – 298 K.

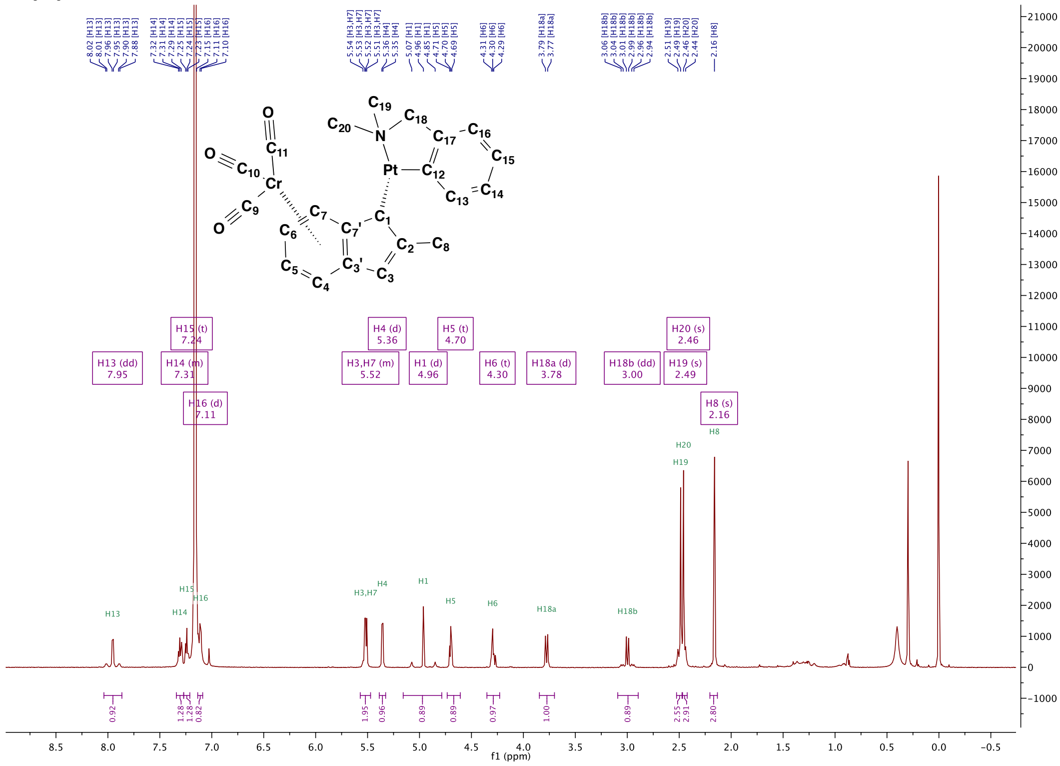

C_6D_6 – ^{13}C – 126 Mhz – 293 K.

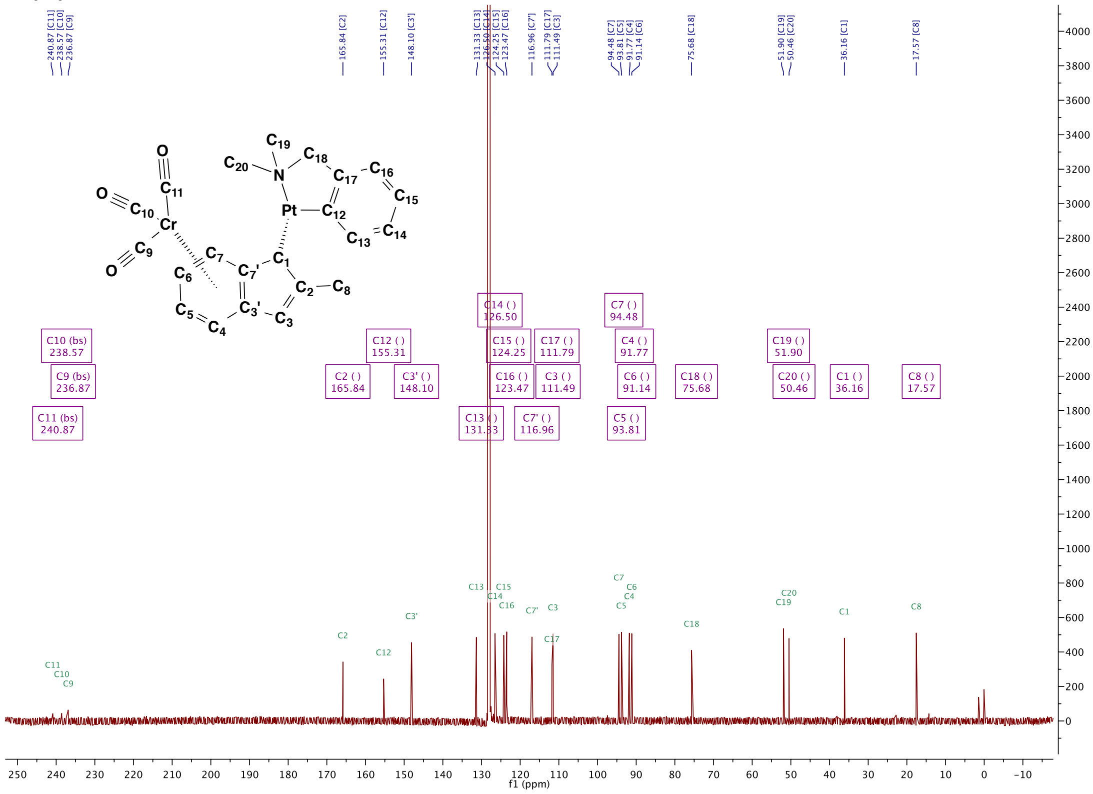

Tol – ^{195}Pt – 86 Mhz – 298 K.

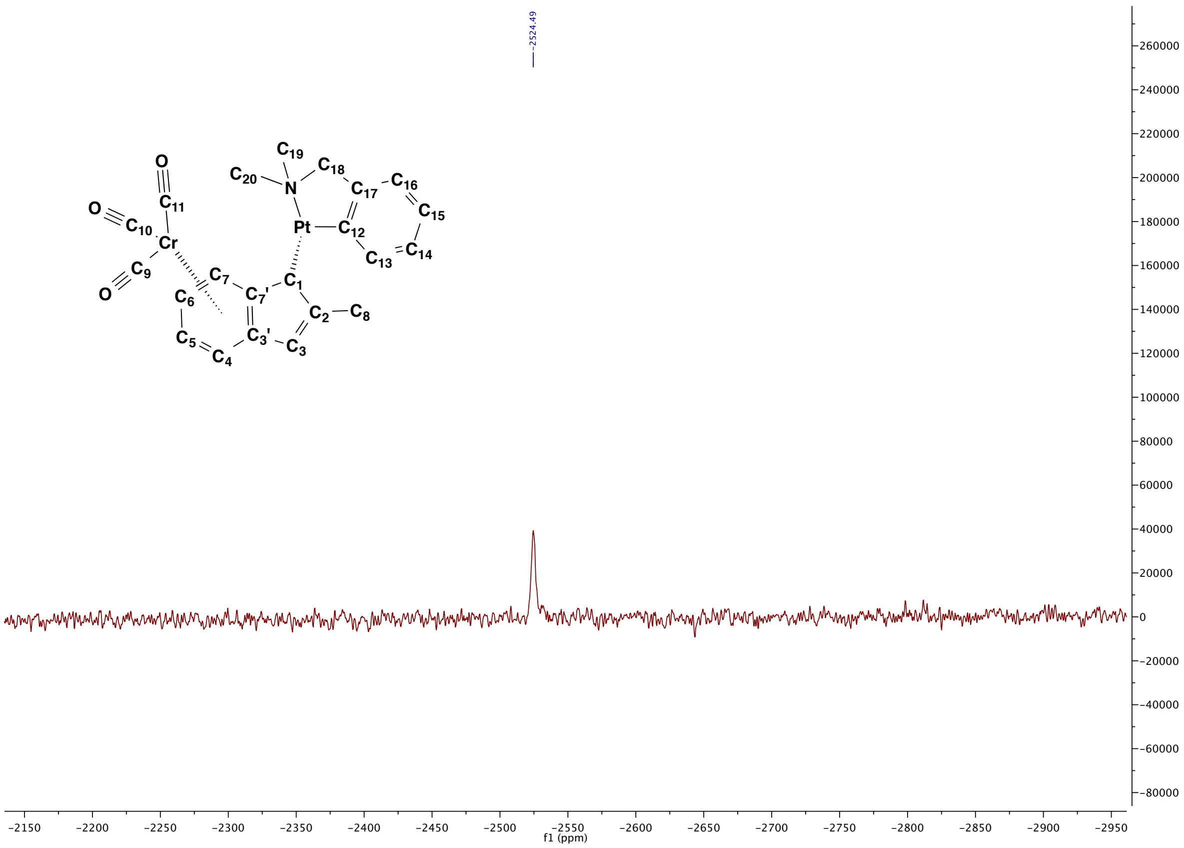

Tol – ^{1}H – 600 Mhz – variable temperature.

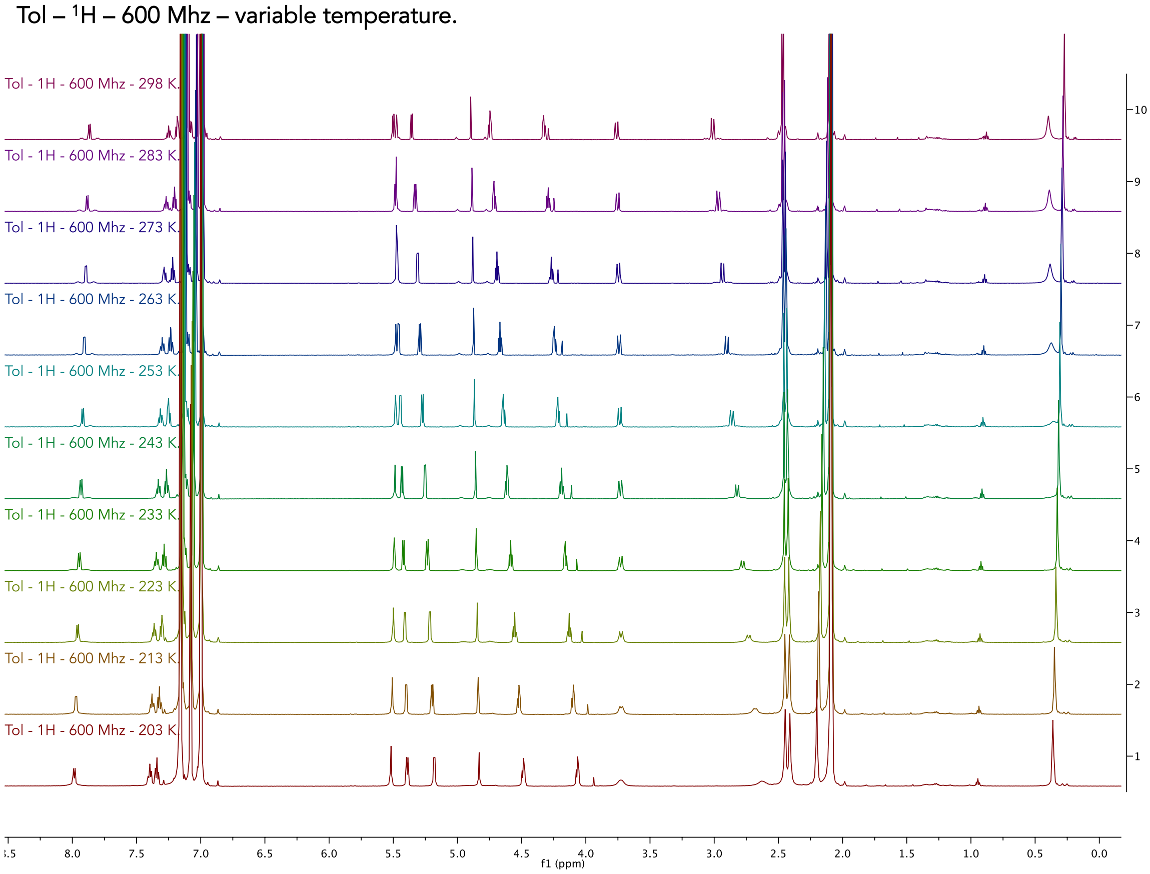

26 - Compound 14b.

C_6D_6 – ^{1}H – 500 Mhz – 293 K.

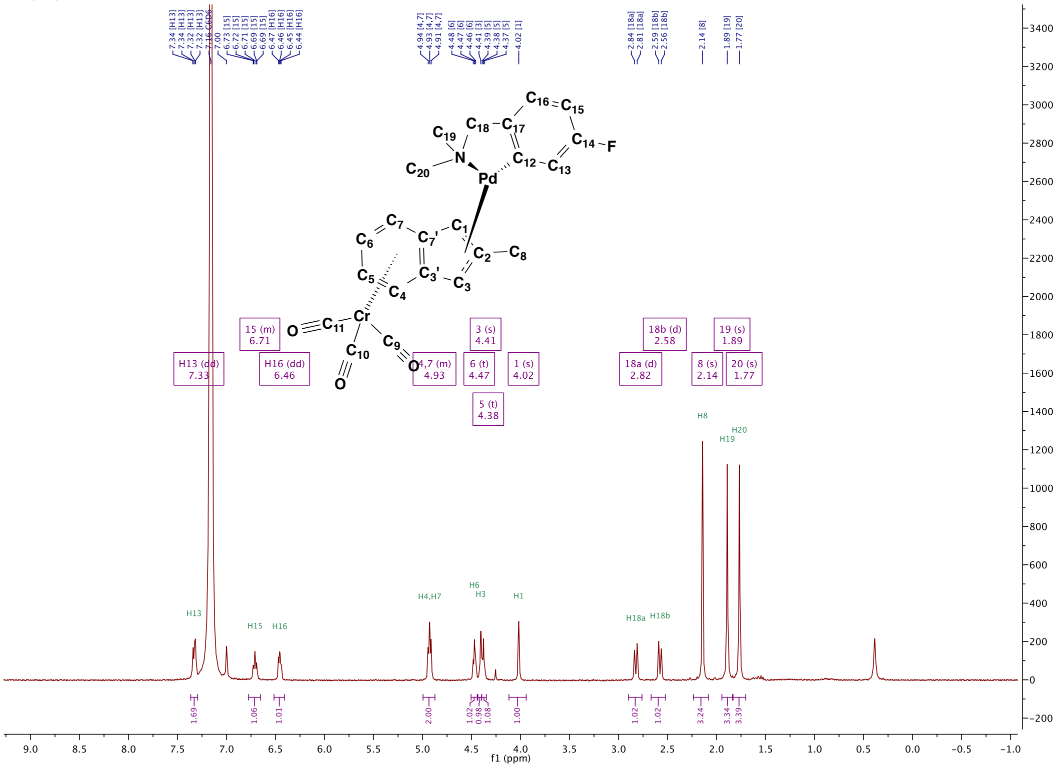

C_6D_6 – ^{13}C – 126 Mhz – 293 K.

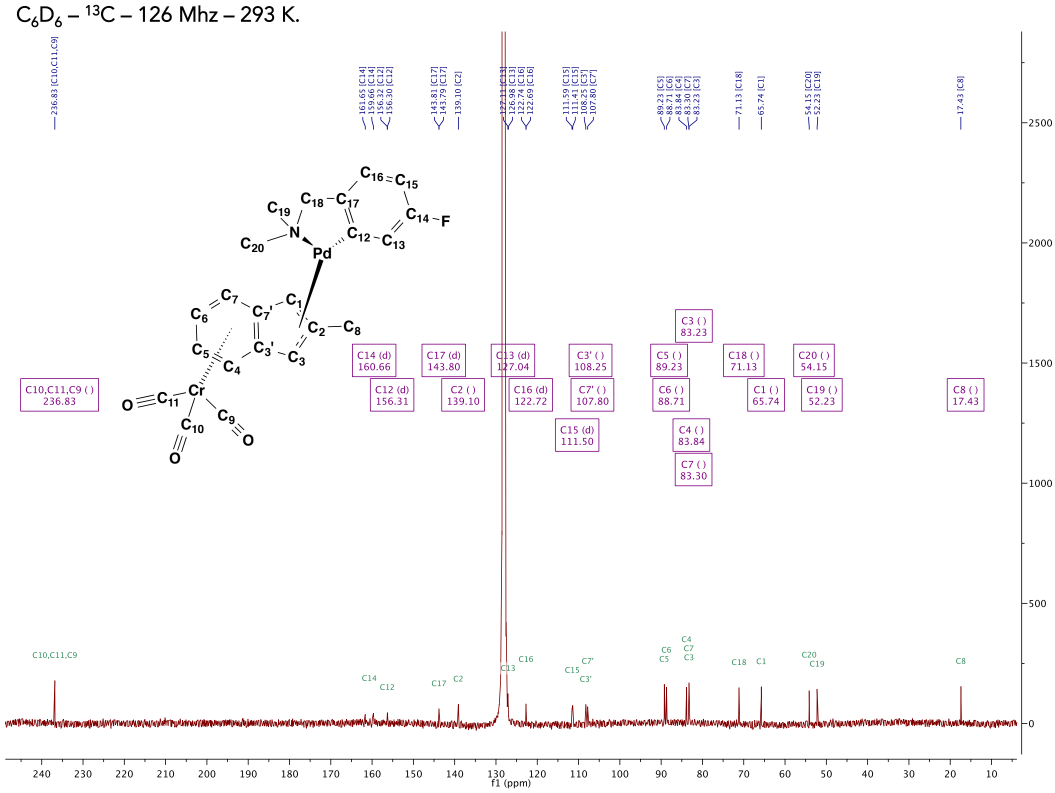

C_6D_6 – ^{19}F – 300 Mhz – 298 K.

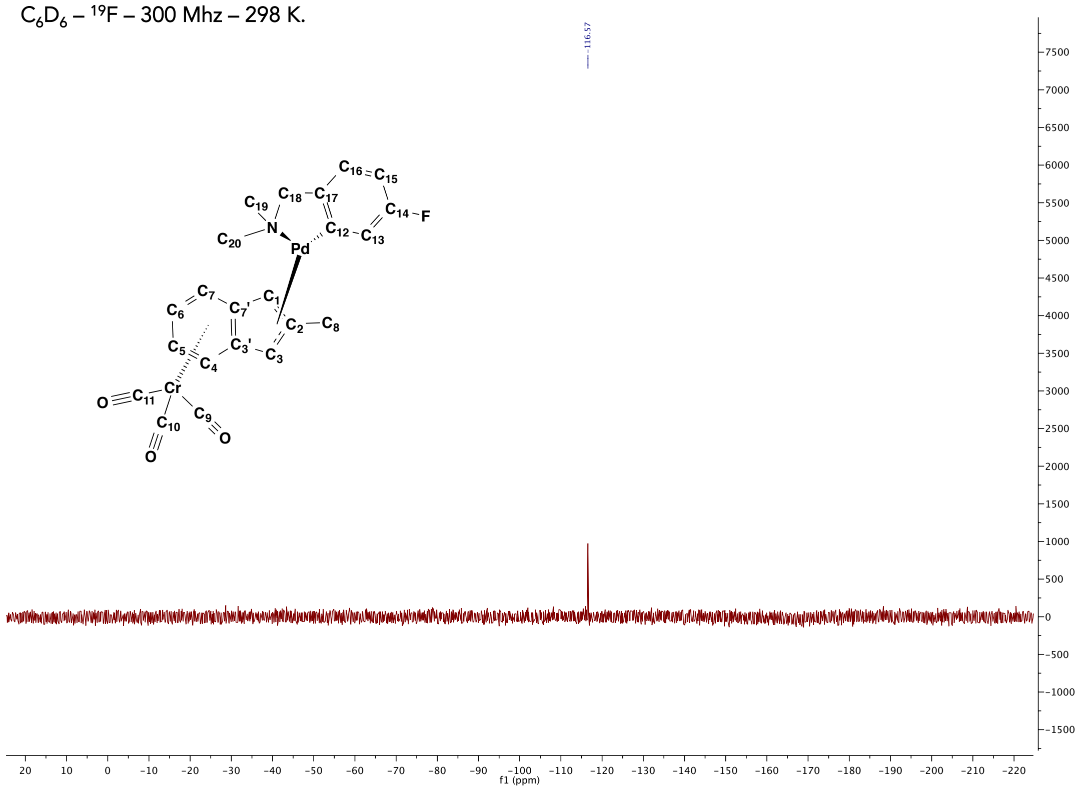

Tol– ^1H – 600 Mhz – variable temperature.

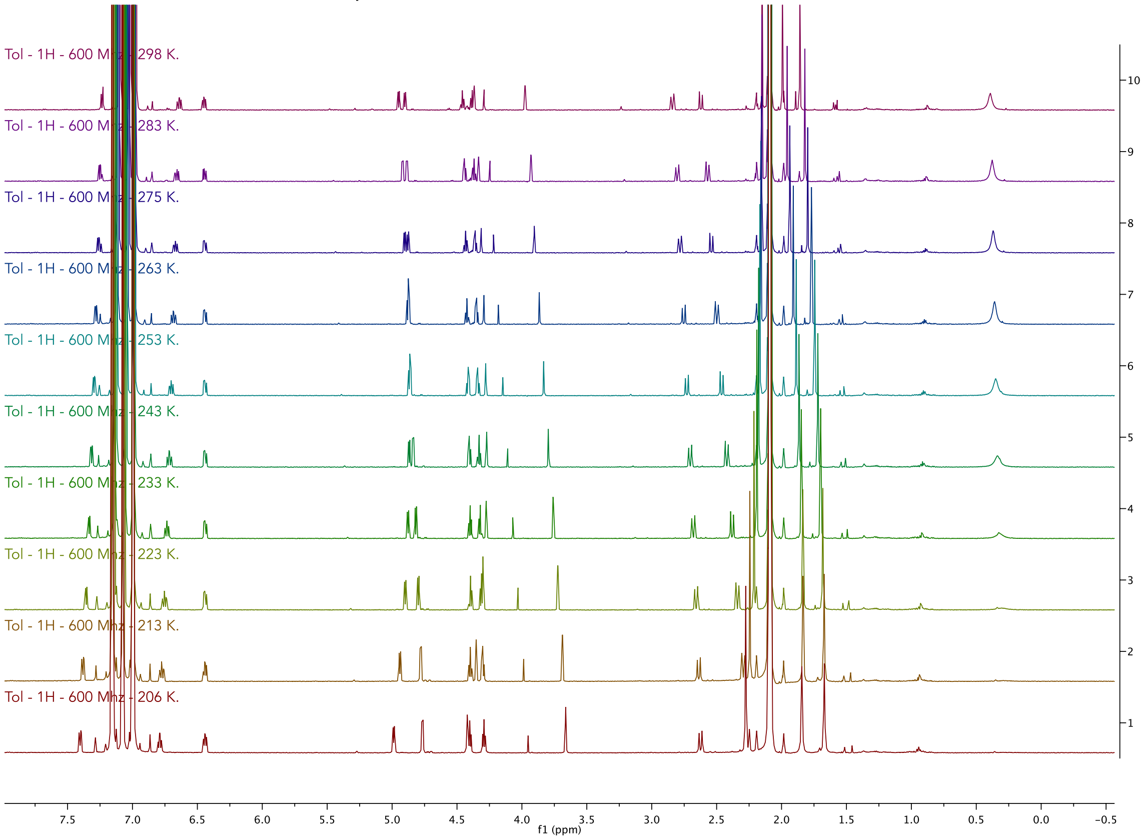

27 - Compound 14h.

C_6D_6 – ^1H – 600 Mhz – 298 K.

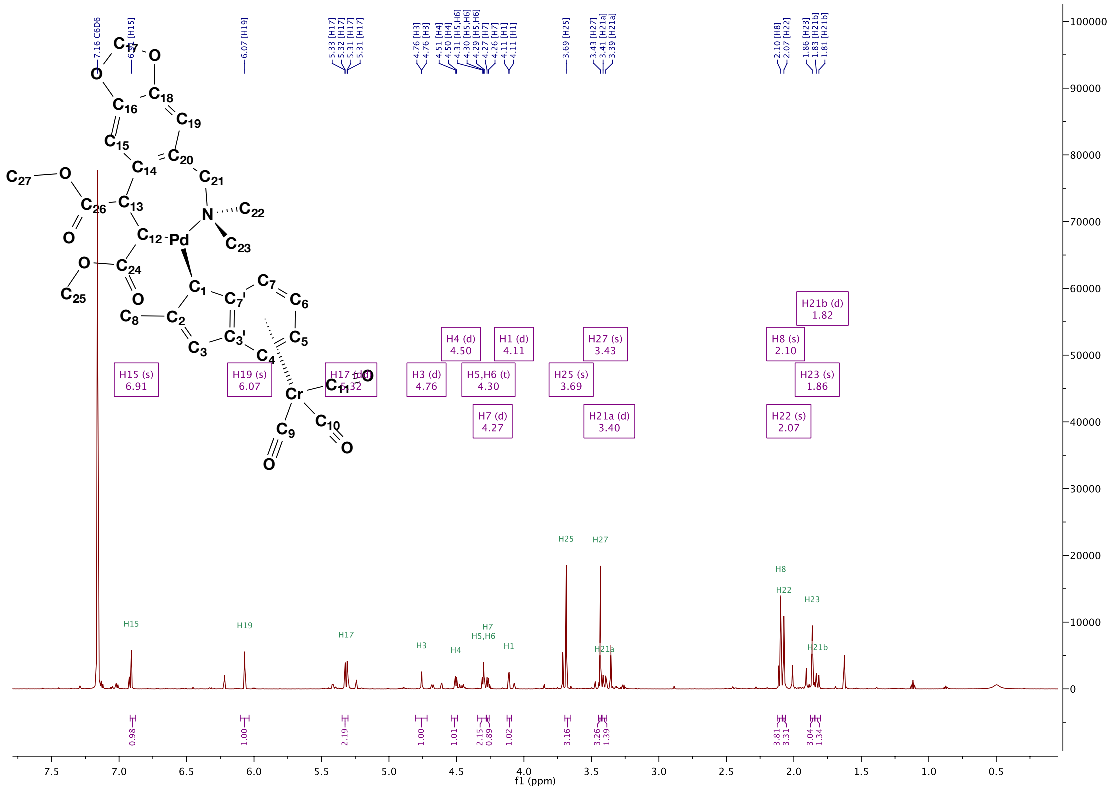

C_6D_6 – ^{13}C – 151 Mhz – 298 K.

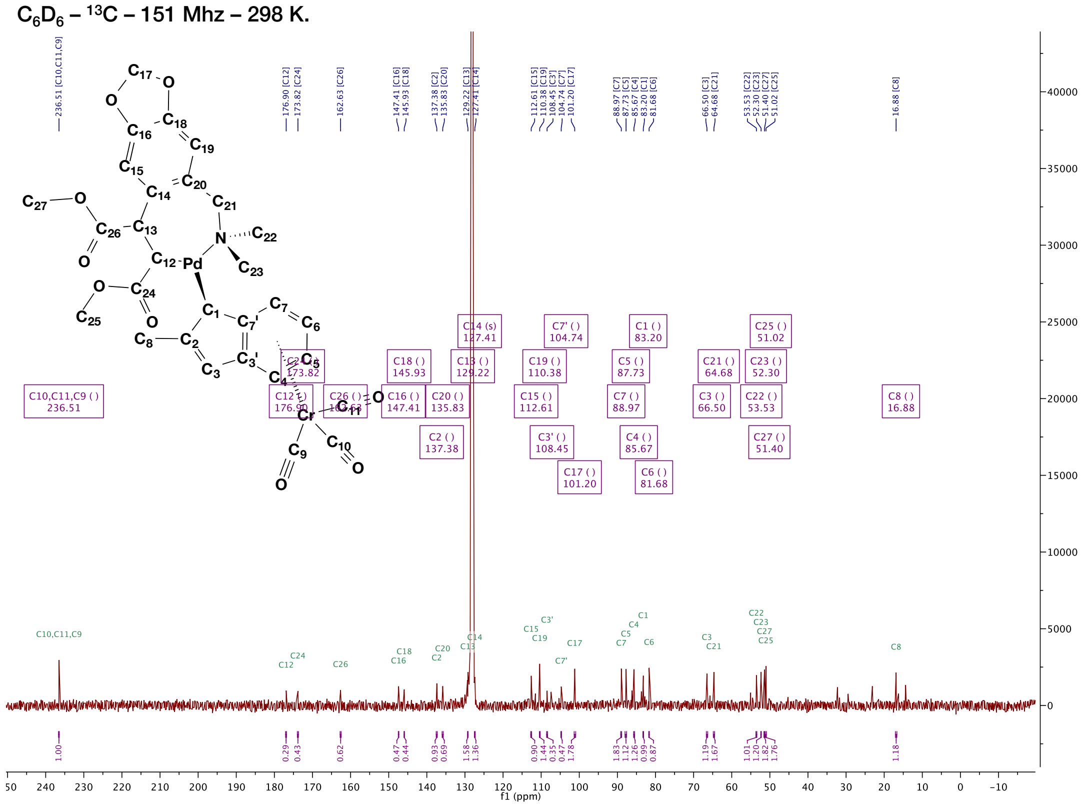

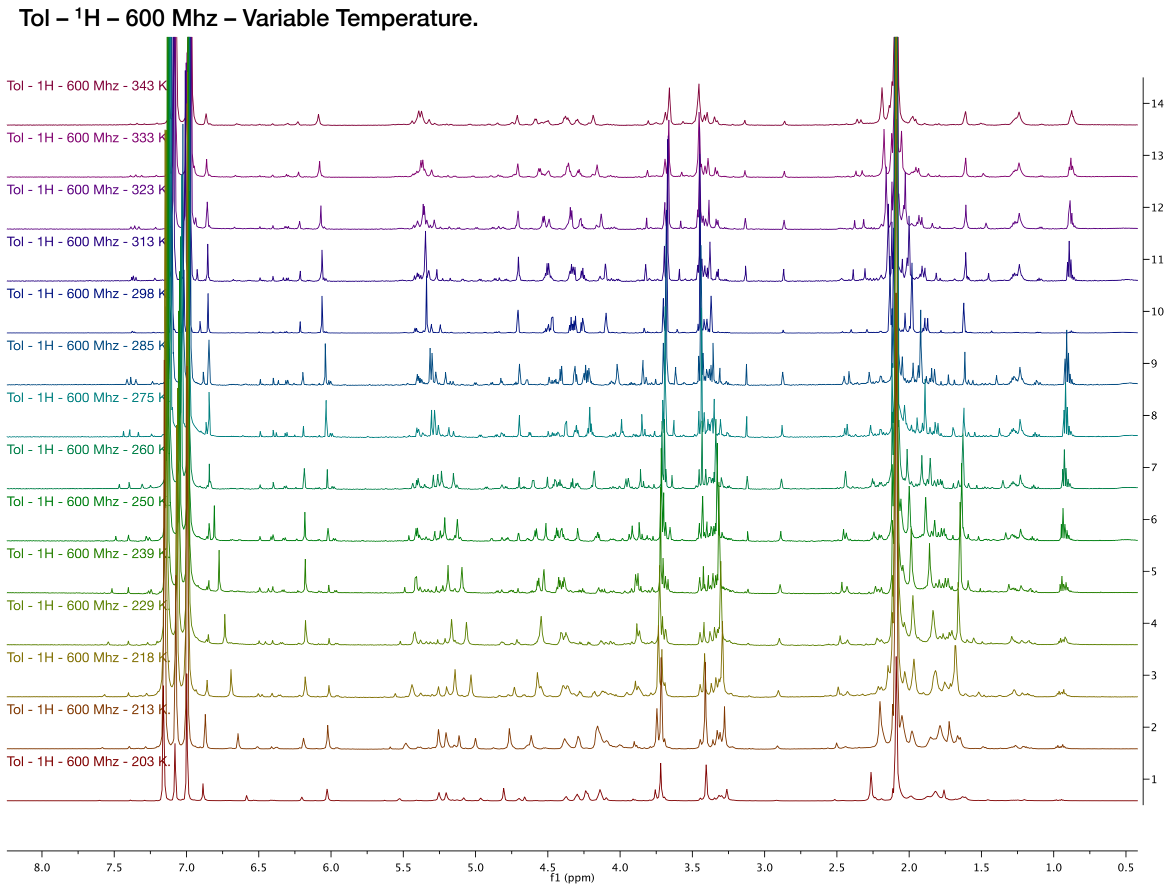
Tol – 1H – 600 Mhz – Variable Temperature.
Tol - 1H - 600 Mhz - 343 K
Tol - 1H - 600 Mhz - 333 K
Tol - 1H - 600 Mhz - 323 K
Tol - 1H - 600 Mhz - 313 K
Tol - 1H - 600 Mhz - 298 K
Tol - 1H - 600 Mhz - 285 K
Tol - 1H - 600 Mhz - 275 K
Tol - 1H - 600 Mhz - 260 K
Tol - 1H - 600 Mhz - 250 K
Tol - 1H - 600 Mhz - 239 K
Tol - 1H - 600 Mhz - 229 K
Tol - 1H - 600 Mhz - 218 K
Tol - 1H - 600 Mhz - 213 K
Tol - 1H - 600 Mhz - 203 K
f1 (ppm)

28 - Compound 15a.

C_6D_6 – ^1H – 300 Mhz – 298 K.

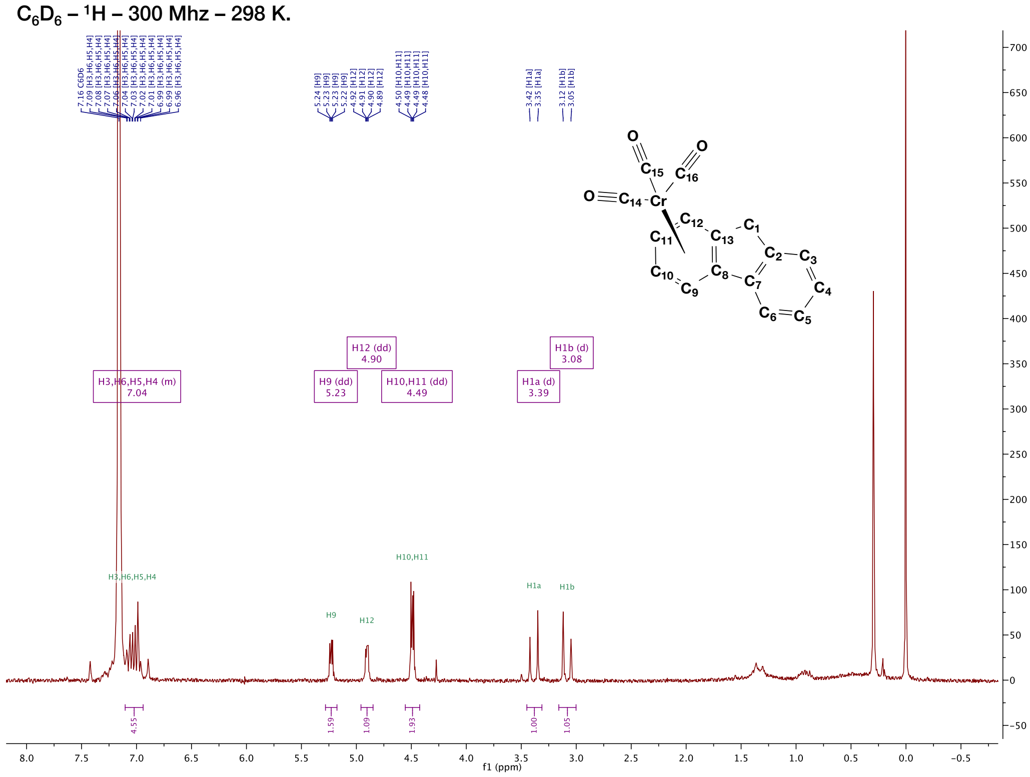

C_6D_6 – ^{13}C – 126 Mhz – 293 K.

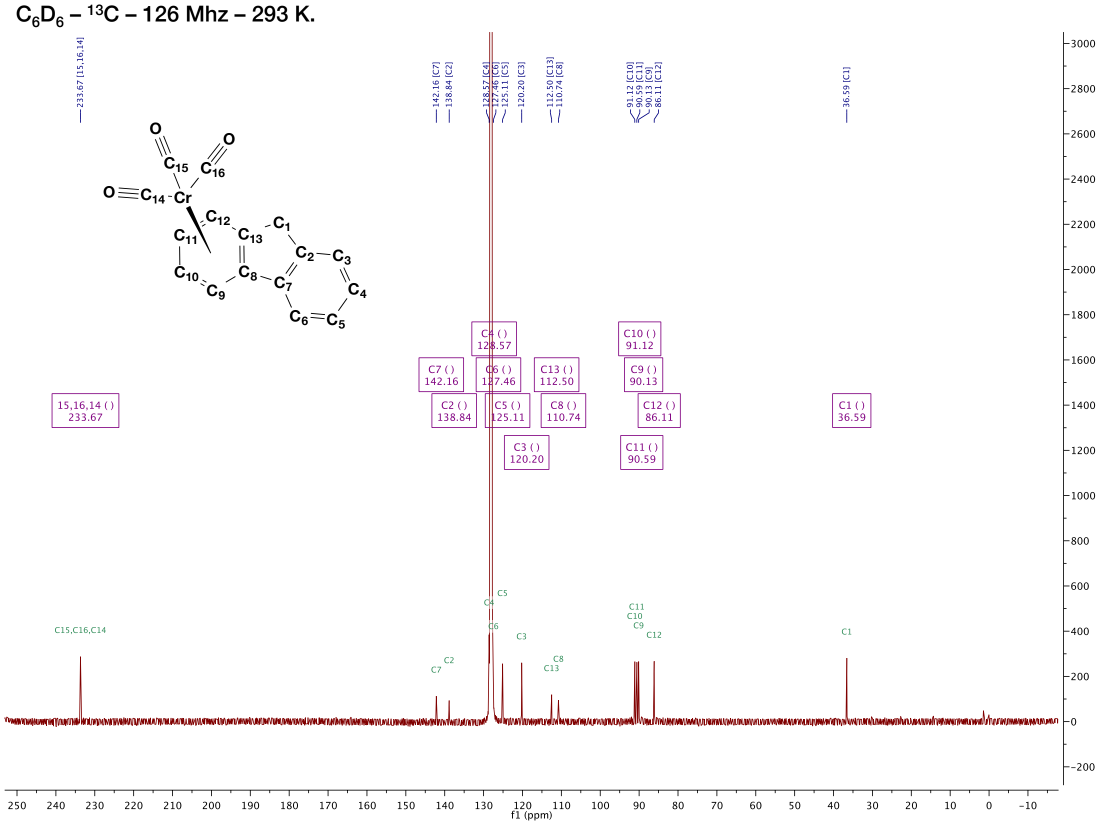

29 - Compound 16a.

Tol – ^{1}H – 600 Mhz – 223 K.

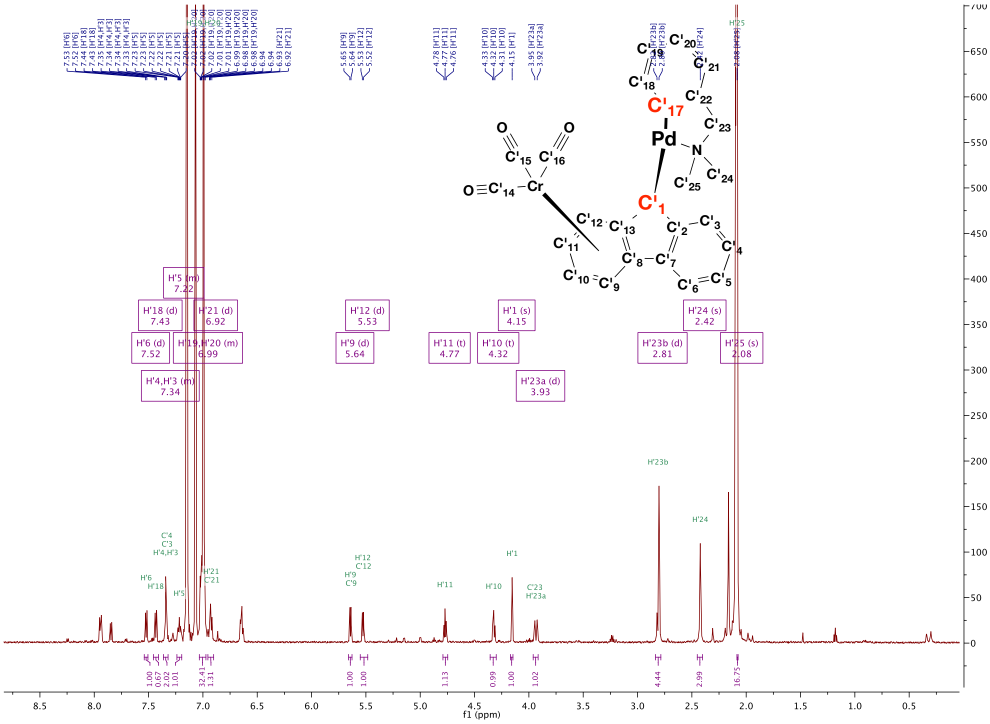

Tol – HSQC – (600 Mhz, 151 Mhz) – 223 K.

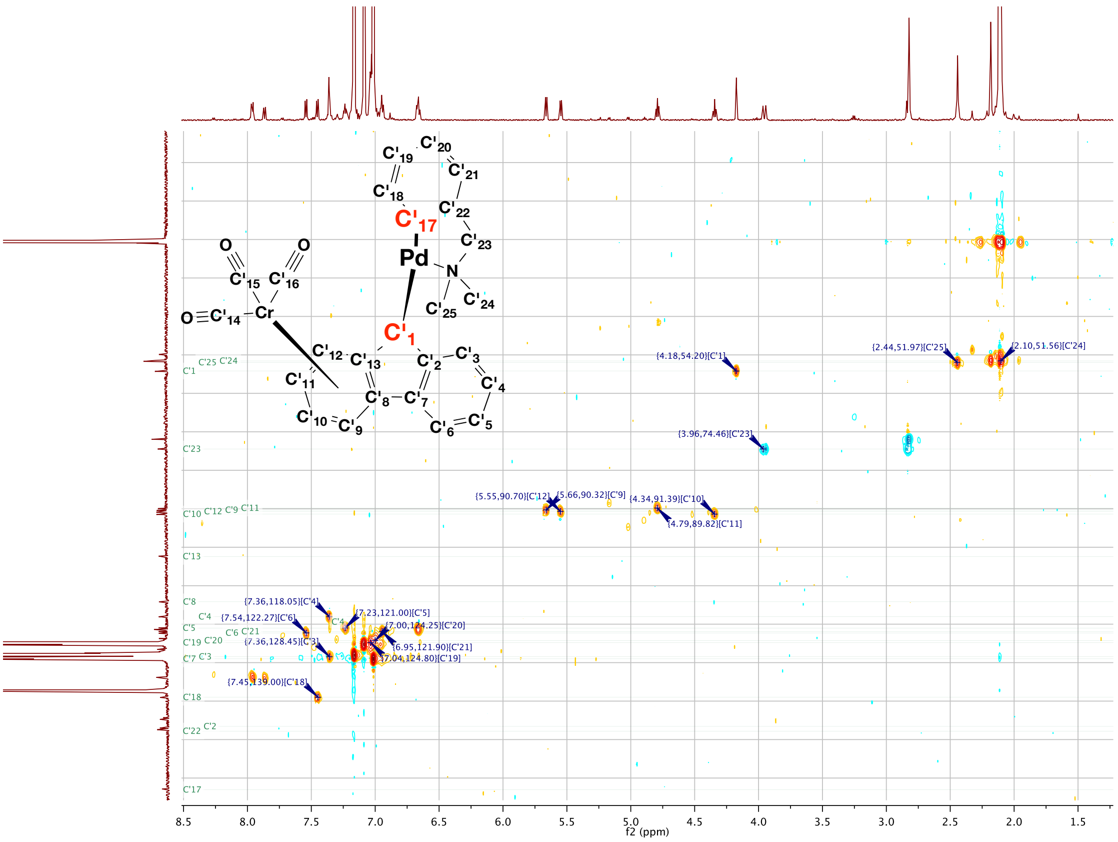

Tol – HMBC – (600 Mhz, 151 Mhz) – 223 K.

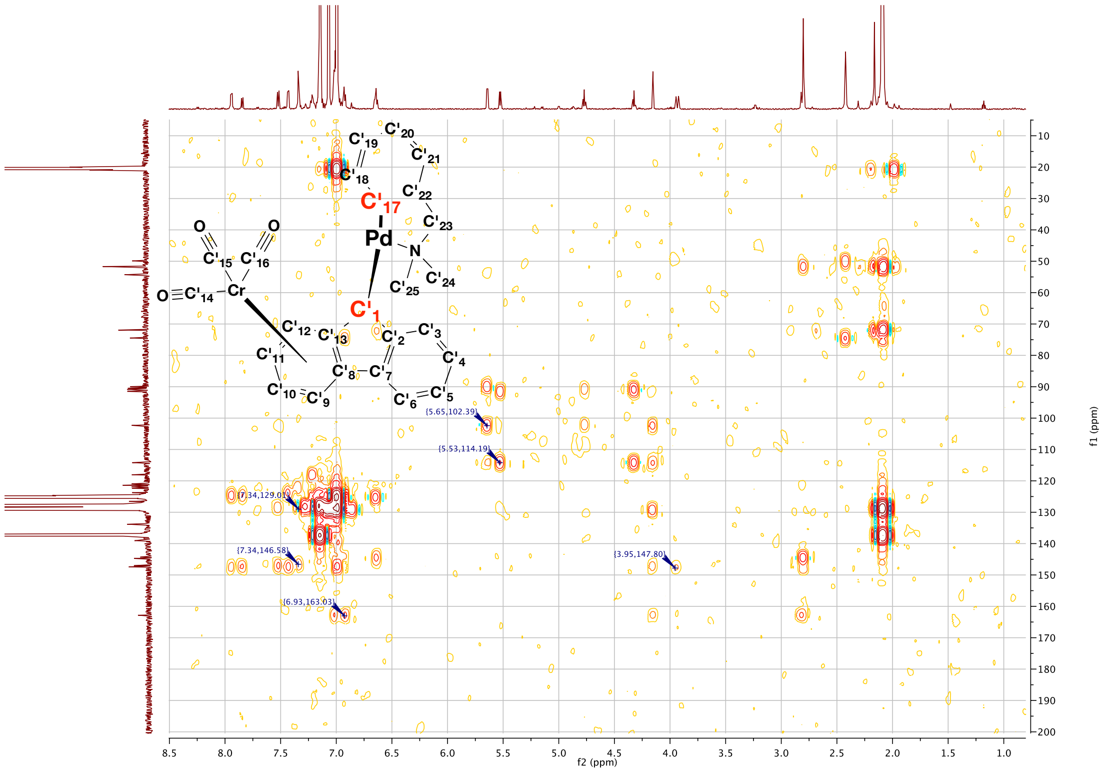

Tol – 13C – 126 Mhz – 223 K - Carbonyls.

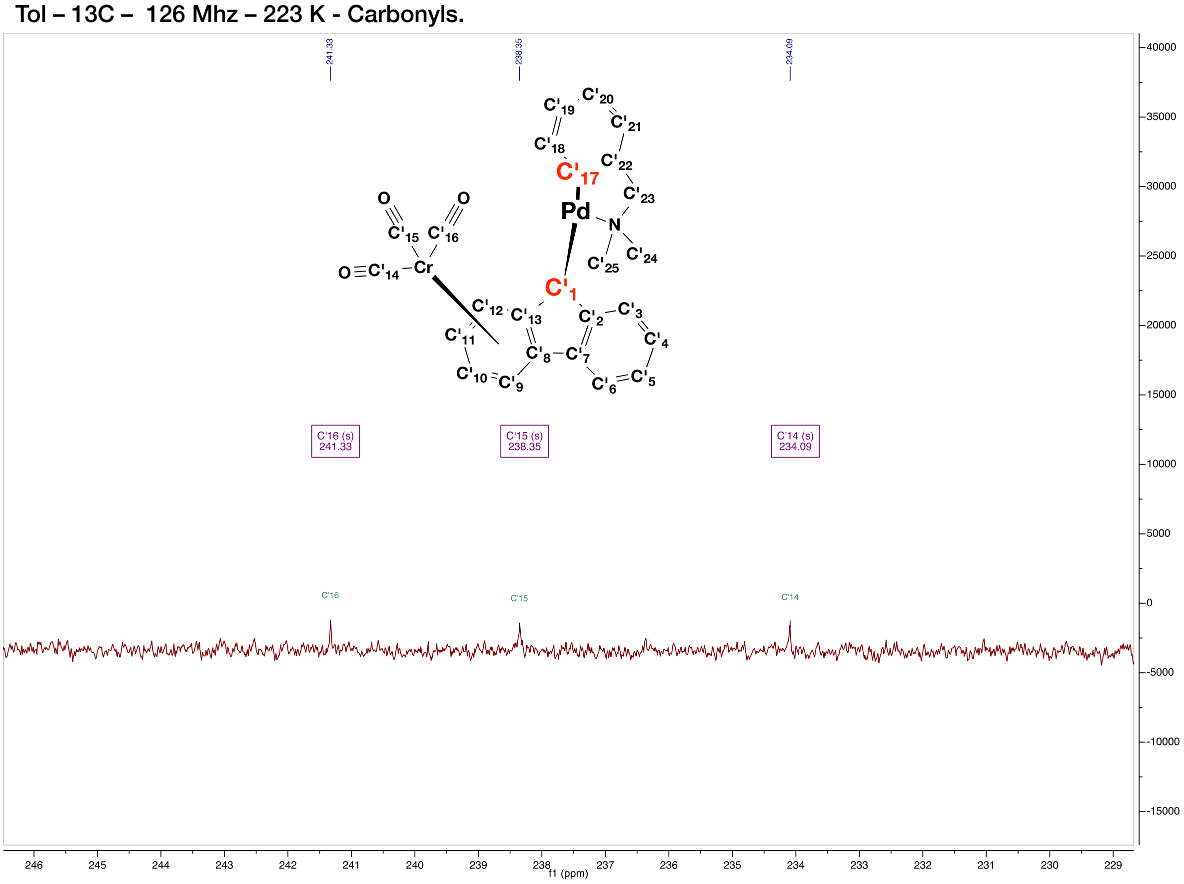

30 - Compound 17a.

C_6D_6 – ^1H – 600 Mhz – 298 K.

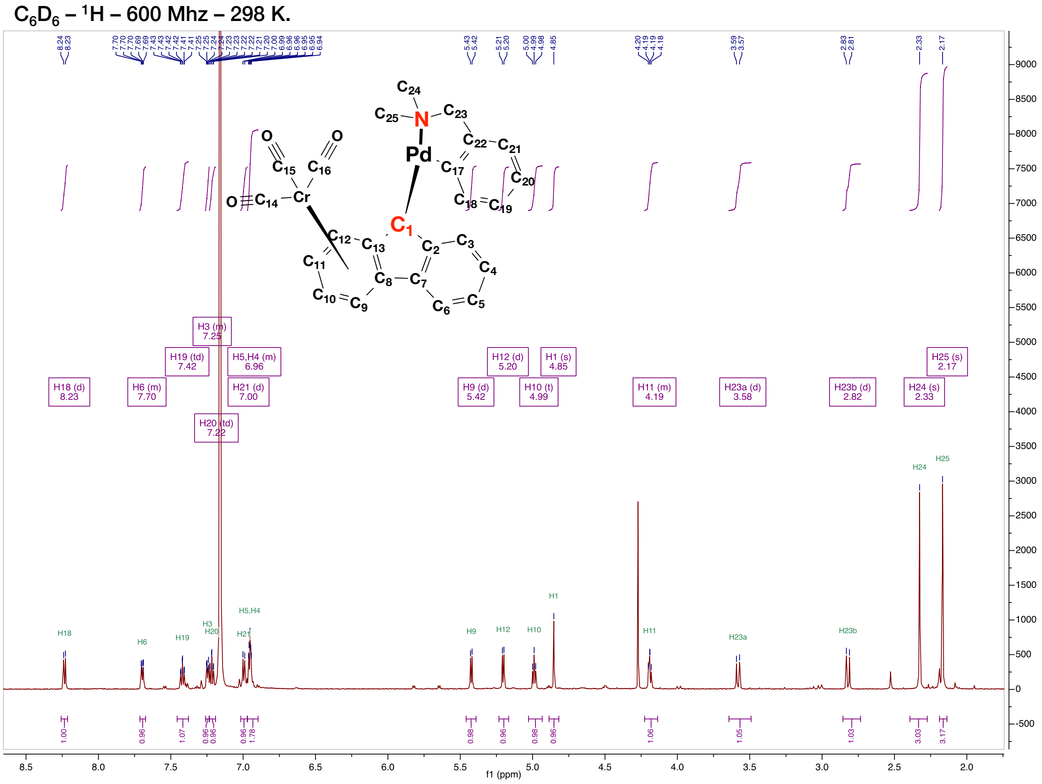

C_6D_6 – ^{13}C – 151 Mhz – 301 K.

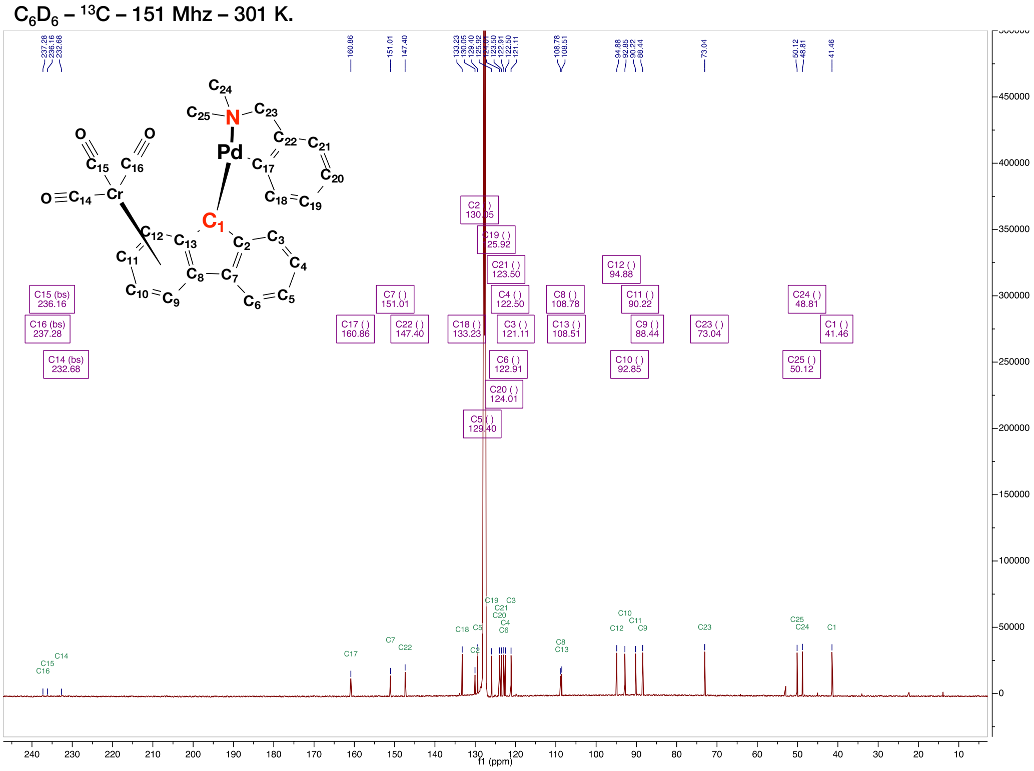

Tol – ^{1}H – 600 Mhz – Variable Temperature.

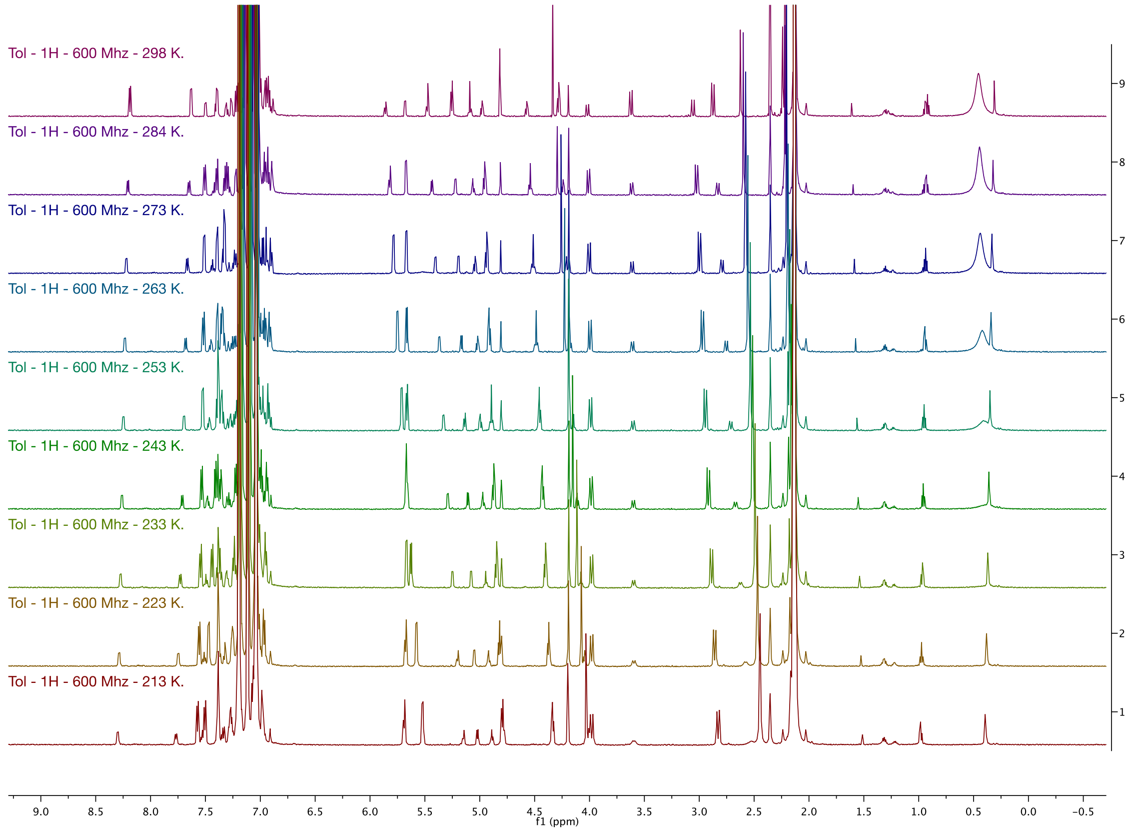

Tol – ^{1}H – 600 Mhz – Kinetic at 273 K – (C'_1-C'_{17})TRANS to CIS isomerization.

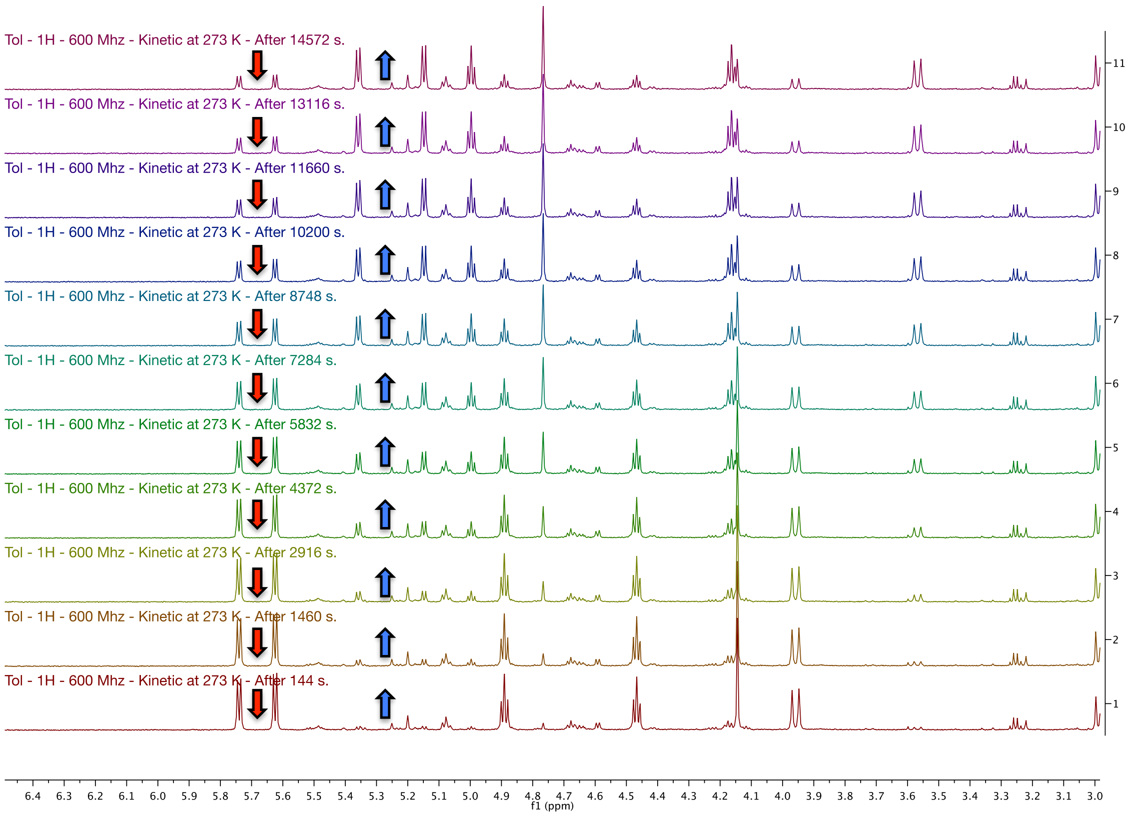

Tol – ^{1}H – 600 Mhz – Kinetic at 278 K – (C'$_{1}$-C'$_{17}$)TRANS to CIS isomerization.

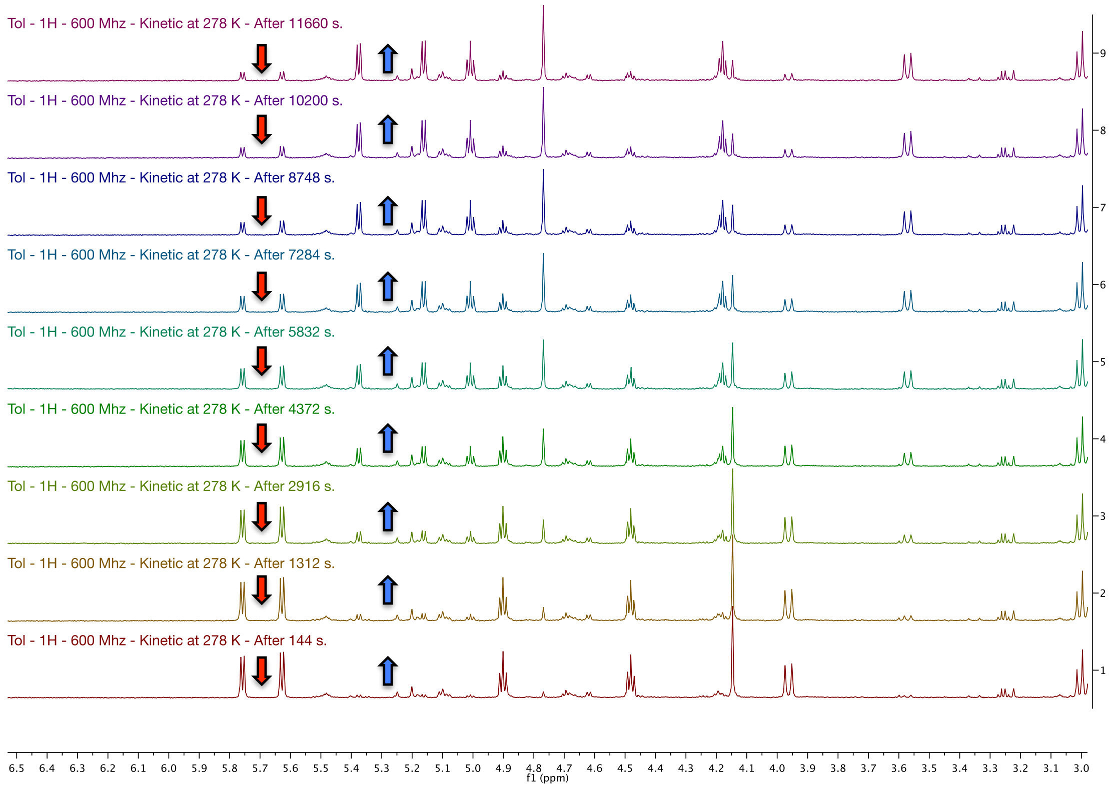

Tol – ^{1}H – 600 Mhz – Kinetic at 283 K – (C'$_{1}$-C'$_{17}$)TRANS to CIS isomerization.

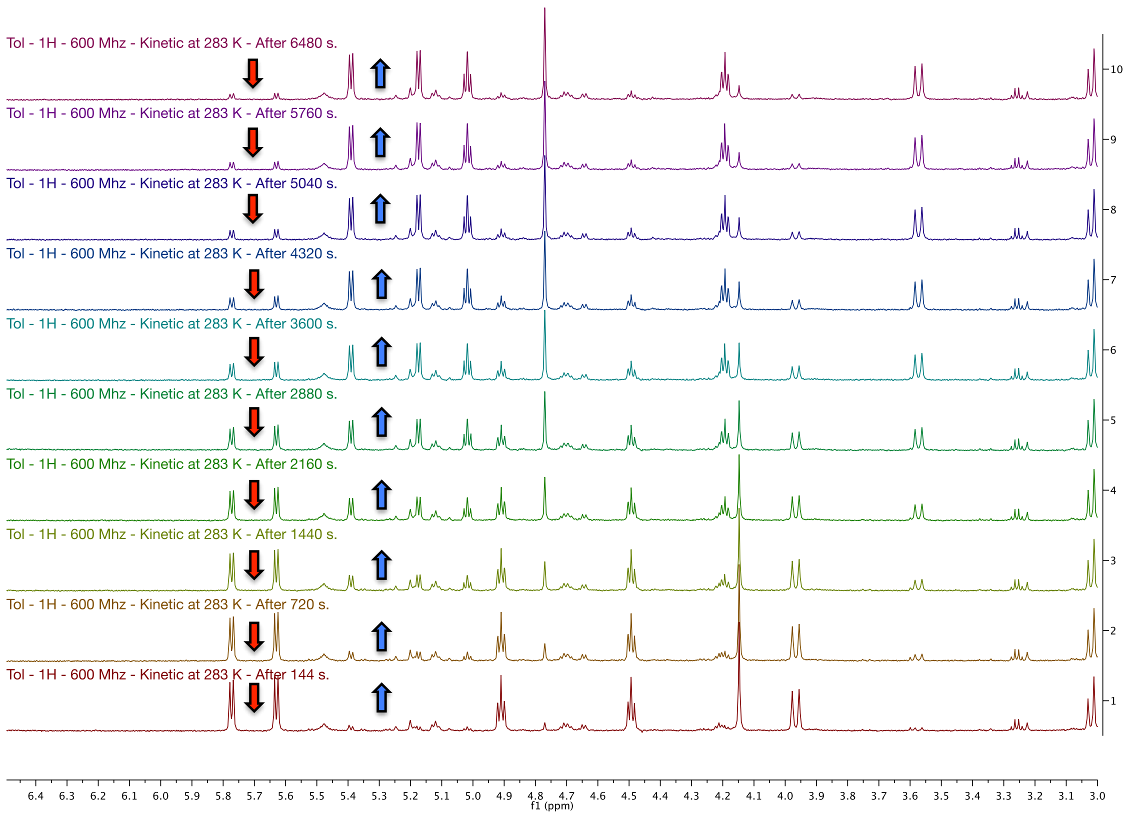

Tol – ^{1}H – 600 Mhz – Kinetic at 288 K – (C'$_1$-C'$_{17}$)TRANS to CIS isomerization.

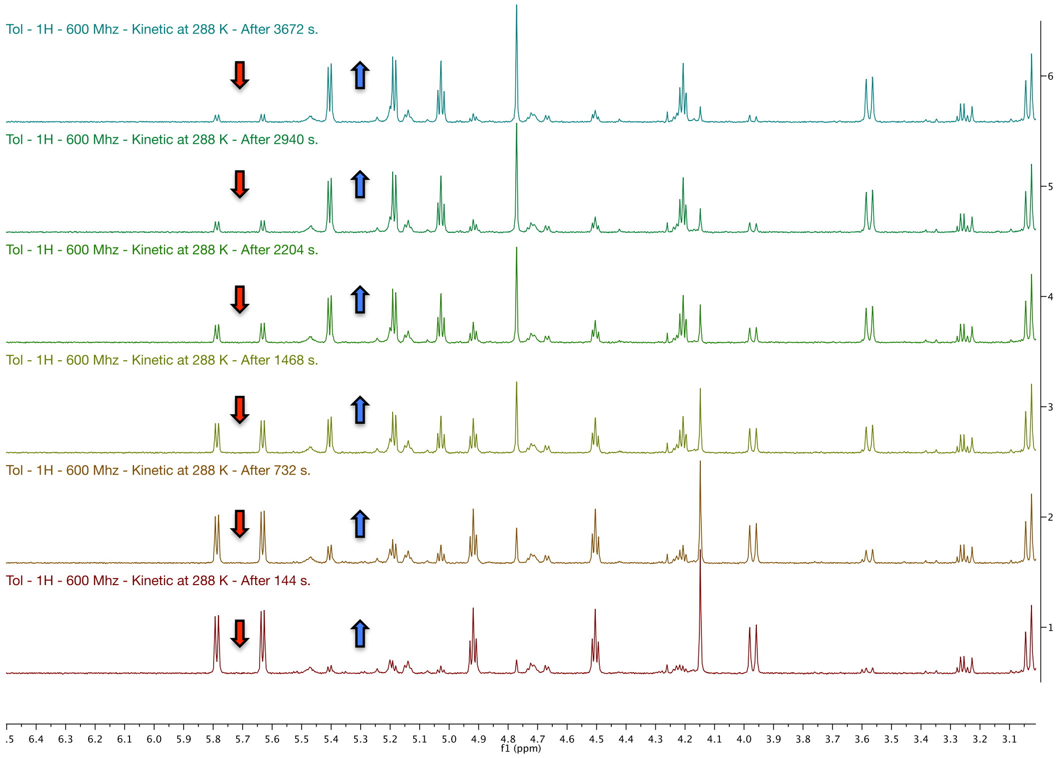

Tol – ^{1}H – 600 Mhz – Kinetic at 293 K – (C'$_1$-C'$_{17}$)TRANS to CIS isomerization.

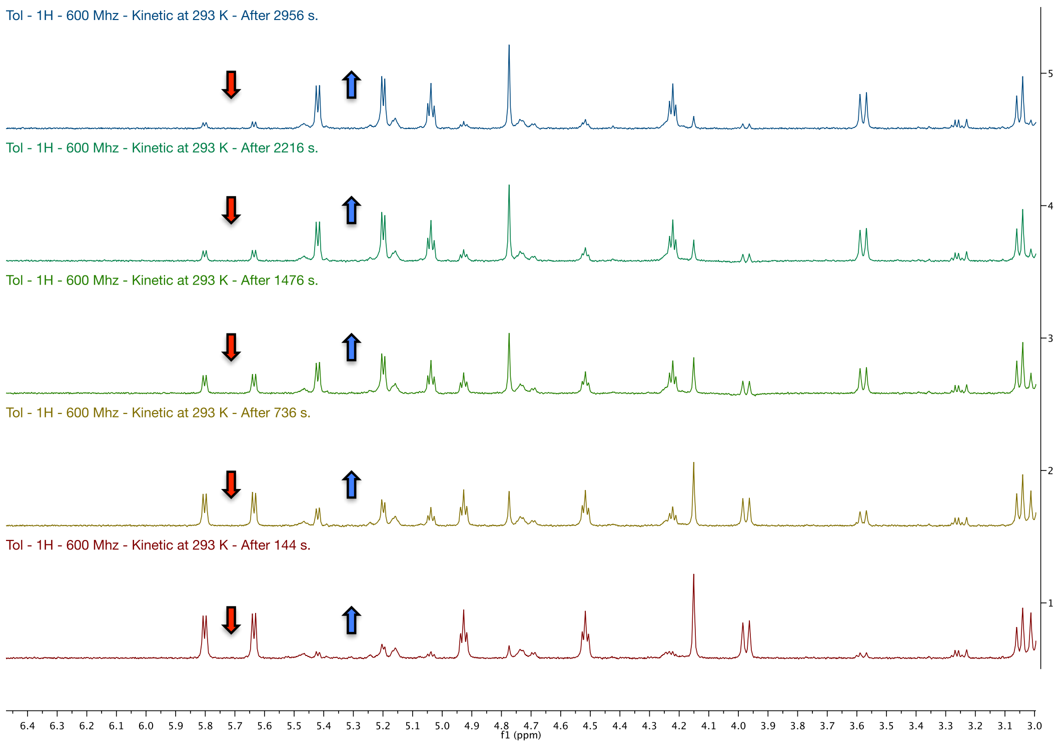

Tol – ^{1}H – 600 Mhz – Kinetic at 298 K – (C'$_1$-C'$_{17}$)TRANS to CIS isomerization.

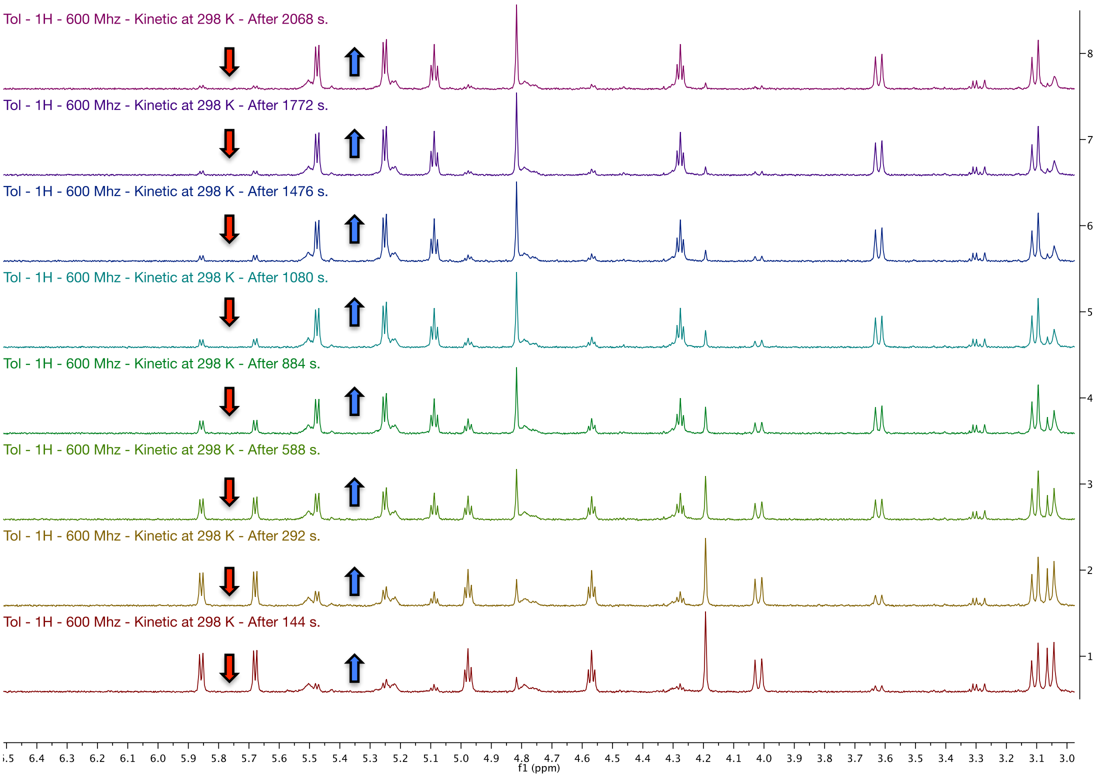

31 - Compound 16b.

Tol – ^{1}H – 600 Mhz – 223 K.

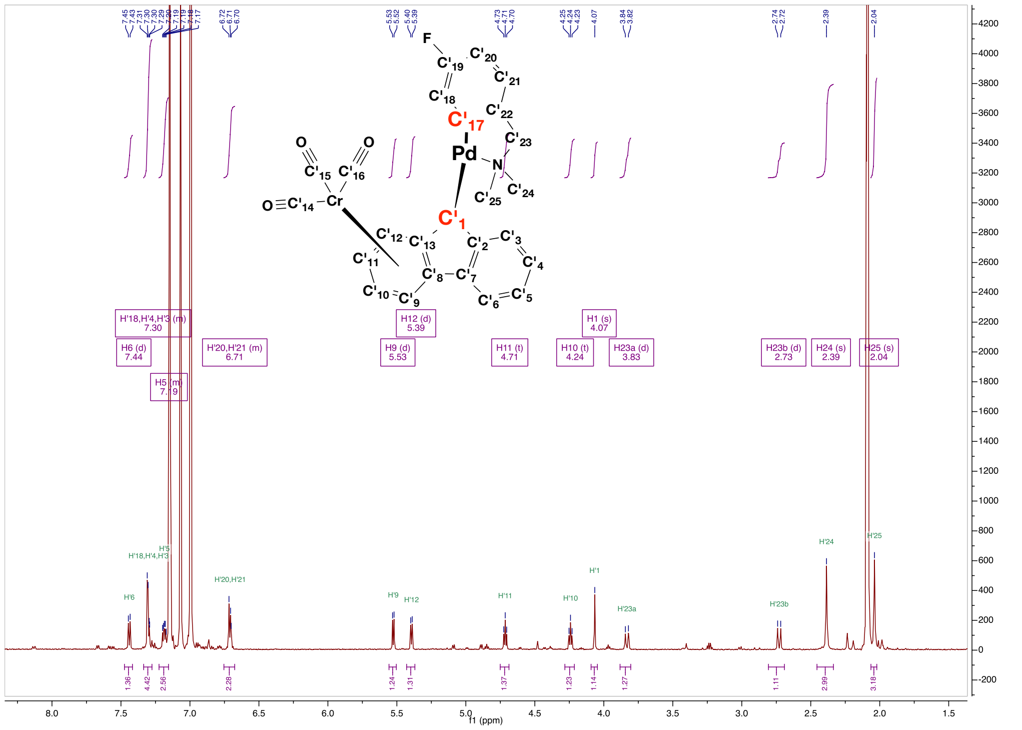

Tol – ^{13}C – 151 Mhz – 223 K.

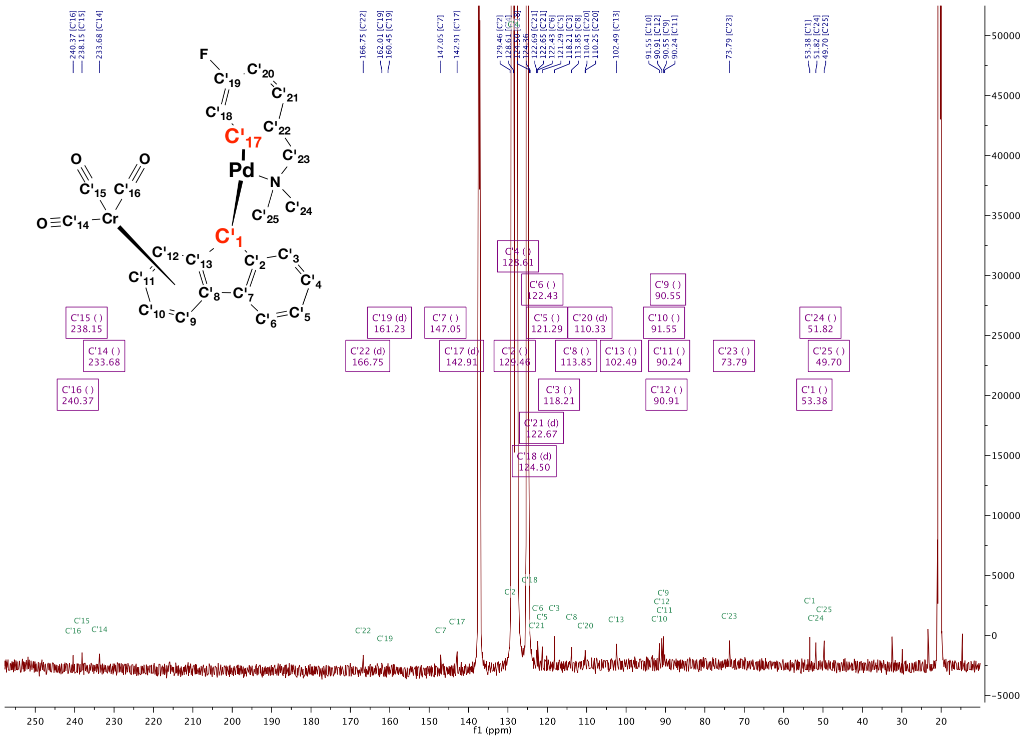

32 - Compound 17b.

C_6D_6 – ^1H – 500 Mhz – 293 K.

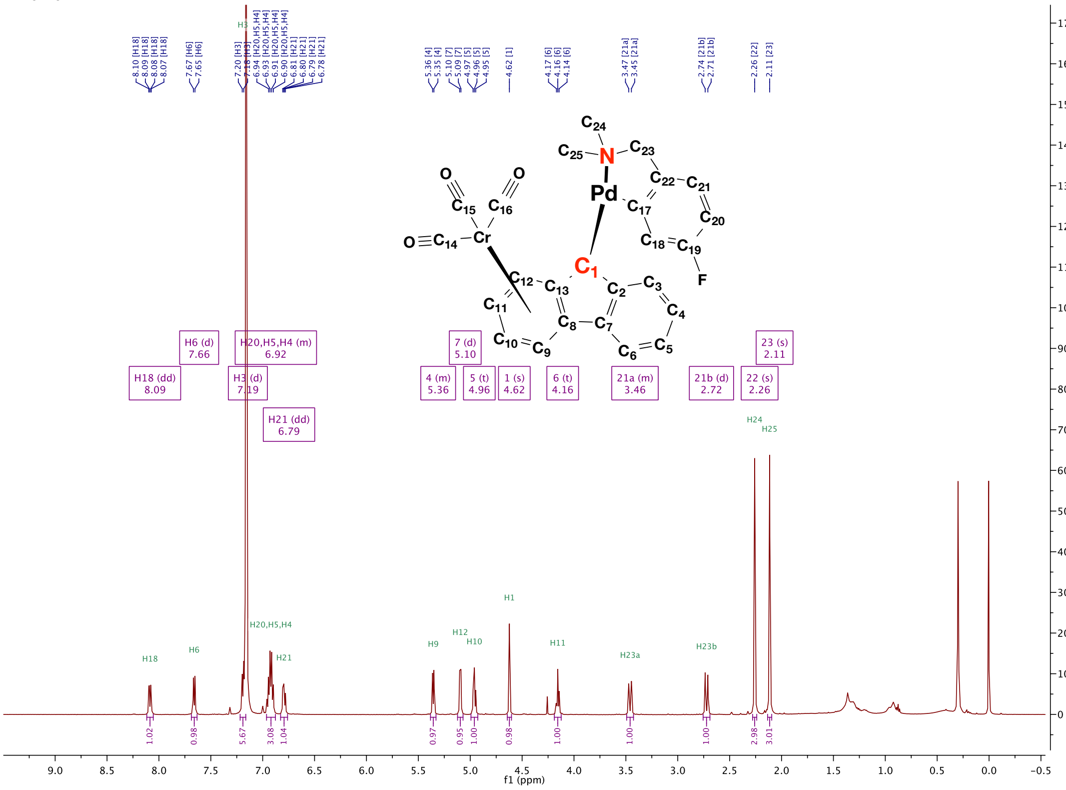

C_6D_6 – ^{13}C – 126 Mhz – 293 K.

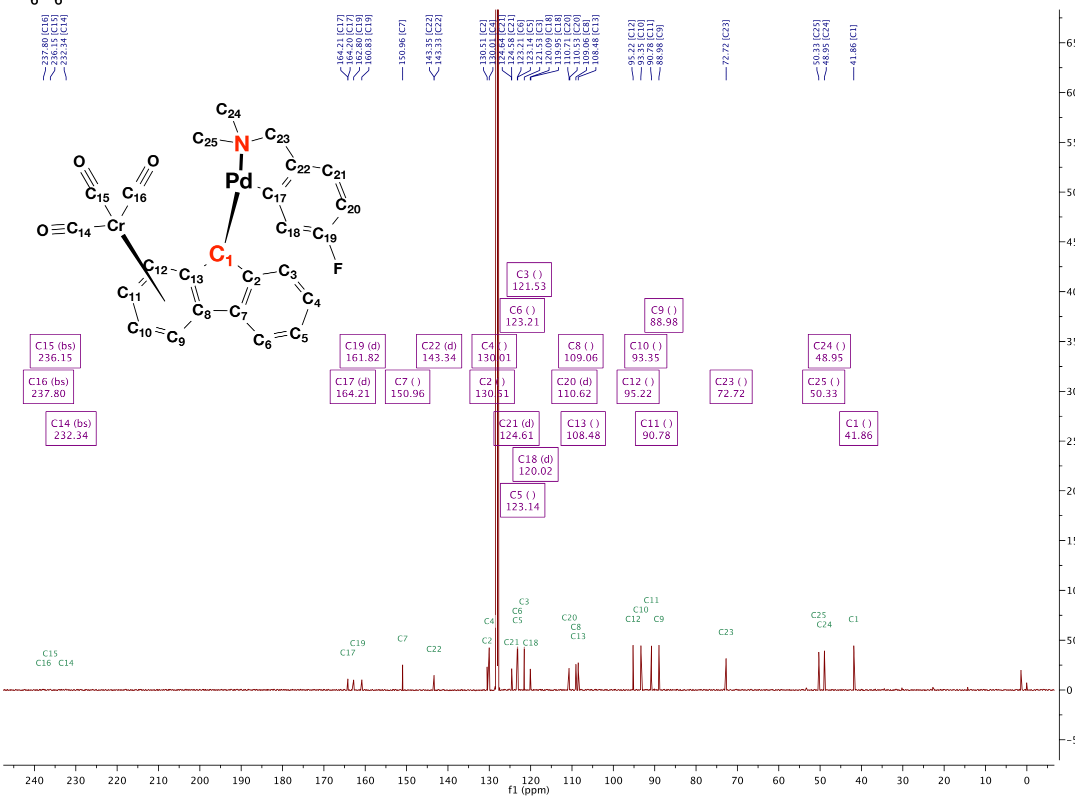

Tol – ^{1}H – 600 Mhz – Variable Temperature.

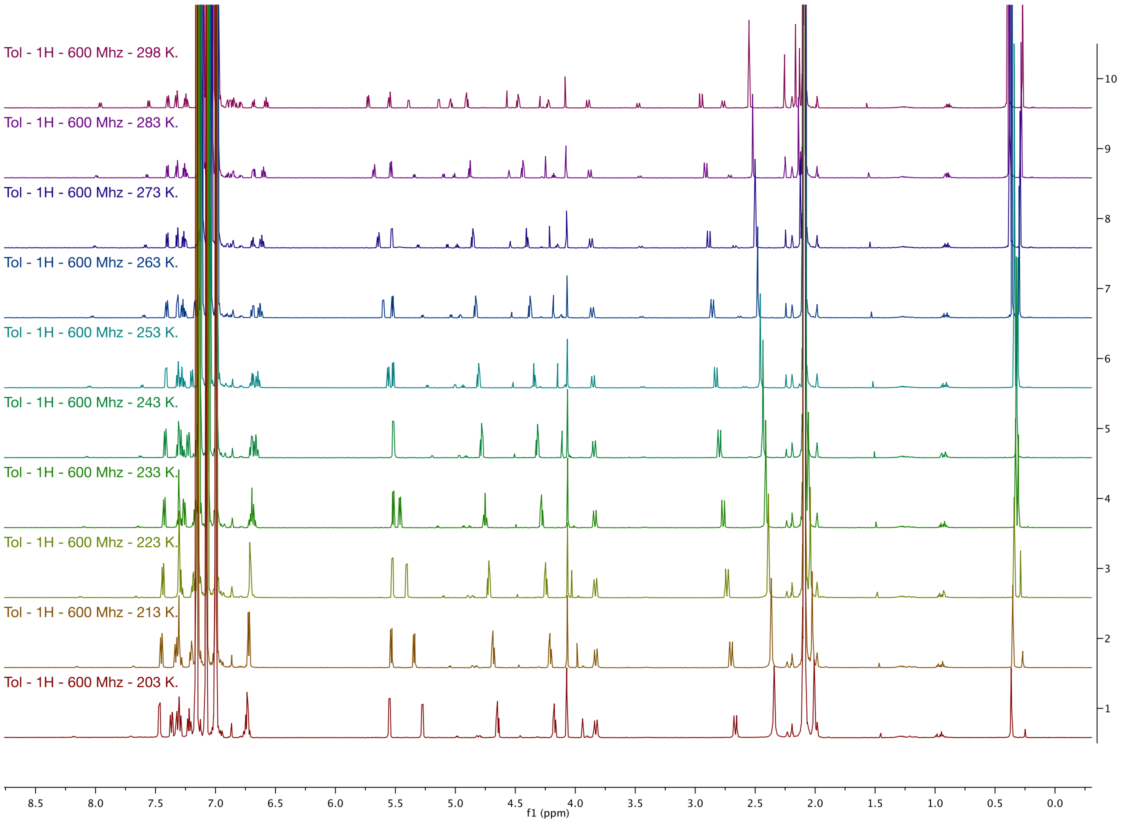

Tol – ^{1}H – 600 Mhz – Kinetic at 278 K – (C'$_{1}$-C'$_{17}$)TRANS to CIS isomerization.

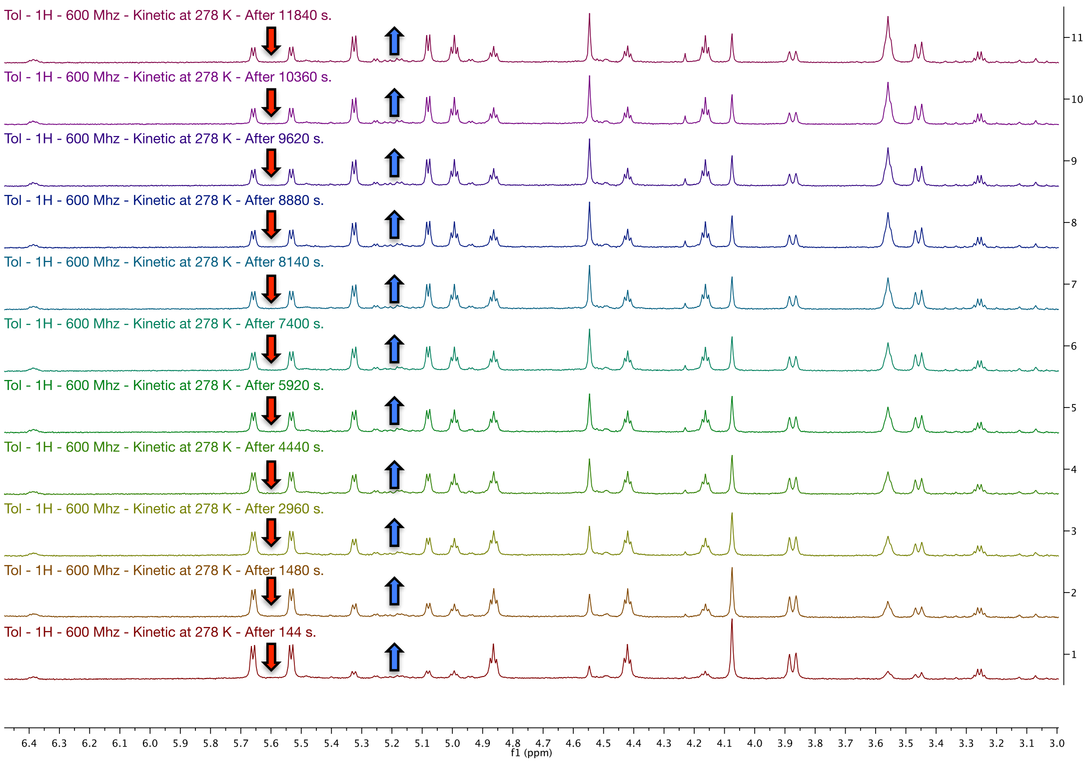

Tol – ^{1}H – 600 Mhz – Kinetic at 283 K – (C'$_1$-C'$_{17}$)TRANS to CIS isomerization.

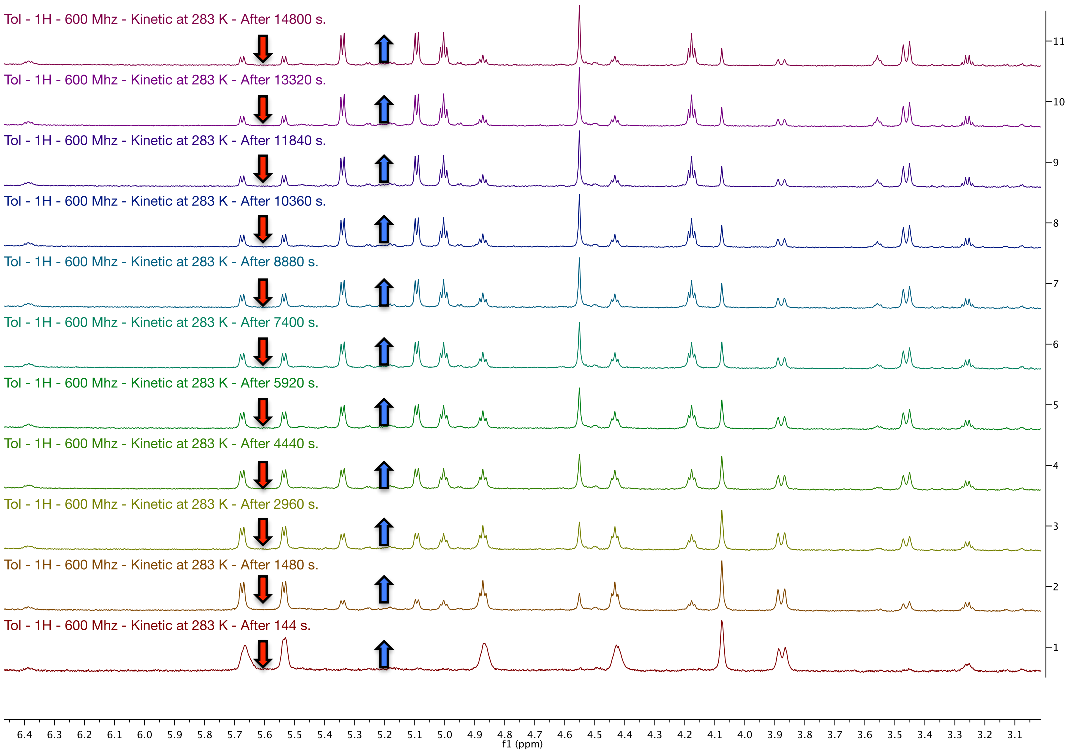

Tol – ^{1}H – 600 Mhz – Kinetic at 288 K – (C'$_1$-C'$_{17}$)TRANS to CIS isomerization.

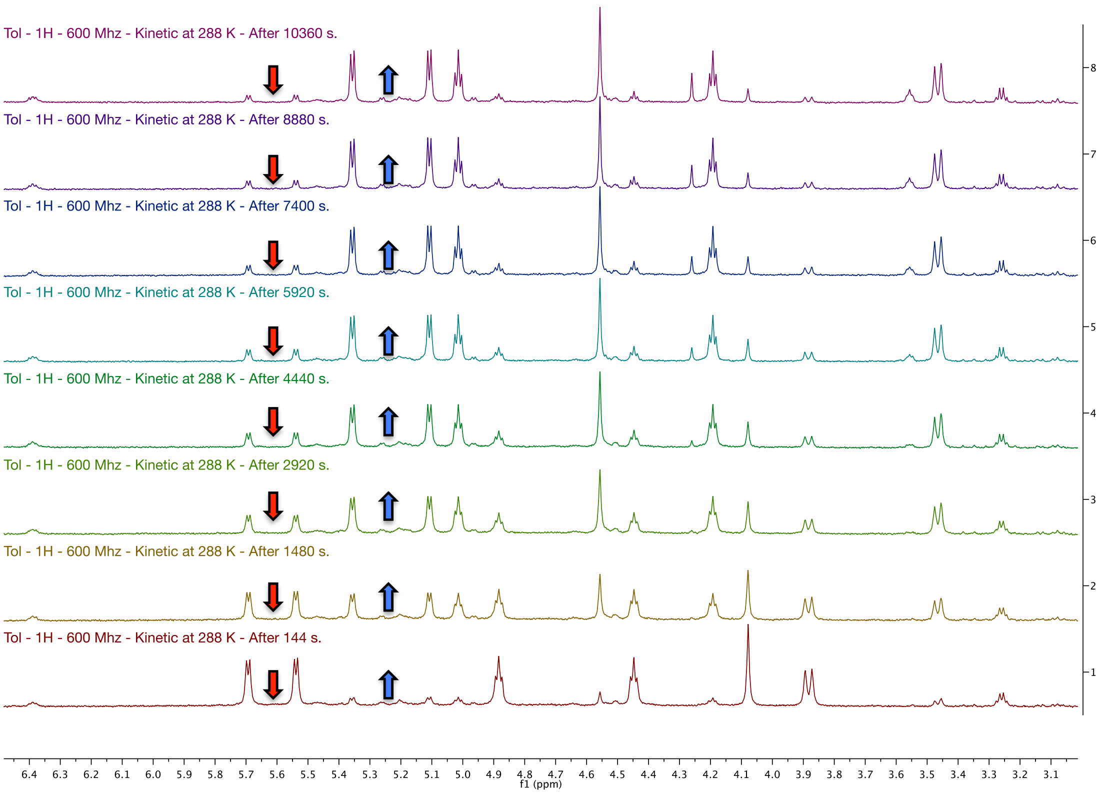

Tol – ^{1}H – 600 Mhz – Kinetic at 293 K – (C'$_1$-C'$_{17}$)TRANS to CIS isomerization.

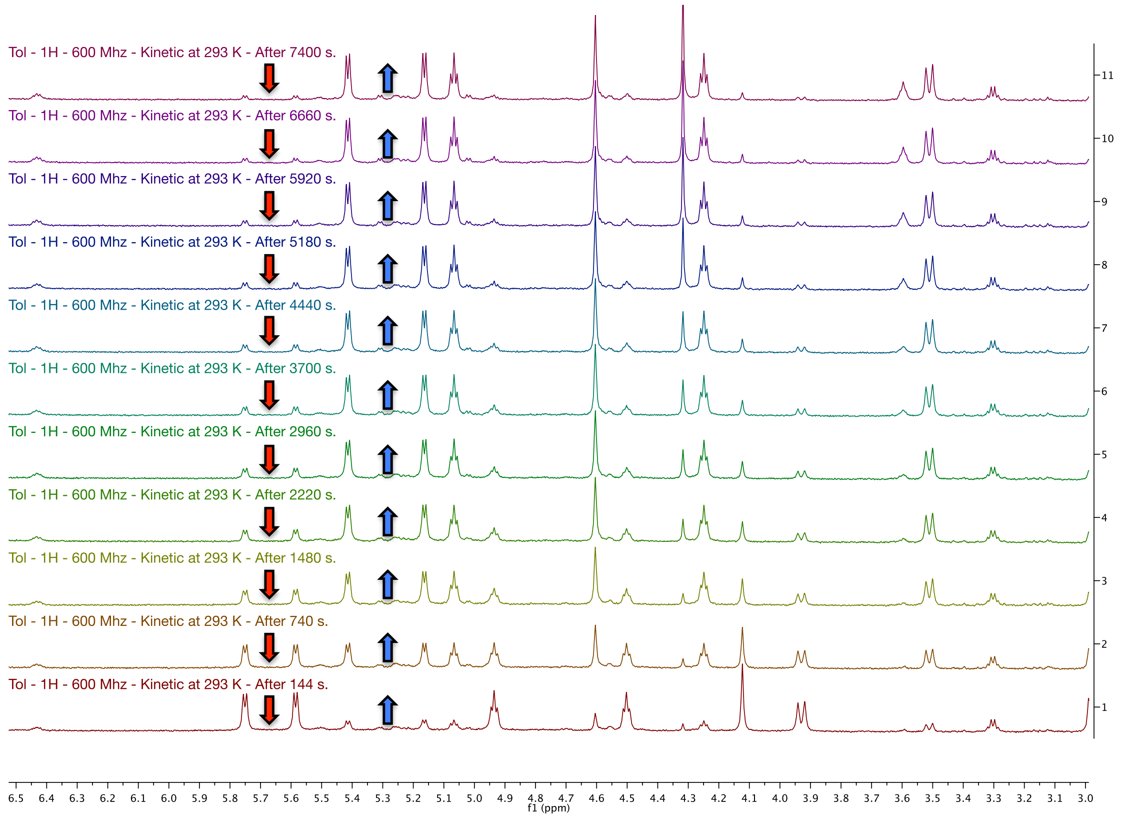

Tol – ^{1}H – 600 Mhz – Kinetic at 298 K – (C'$_1$-C'$_{17}$)TRANS to CIS isomerization.

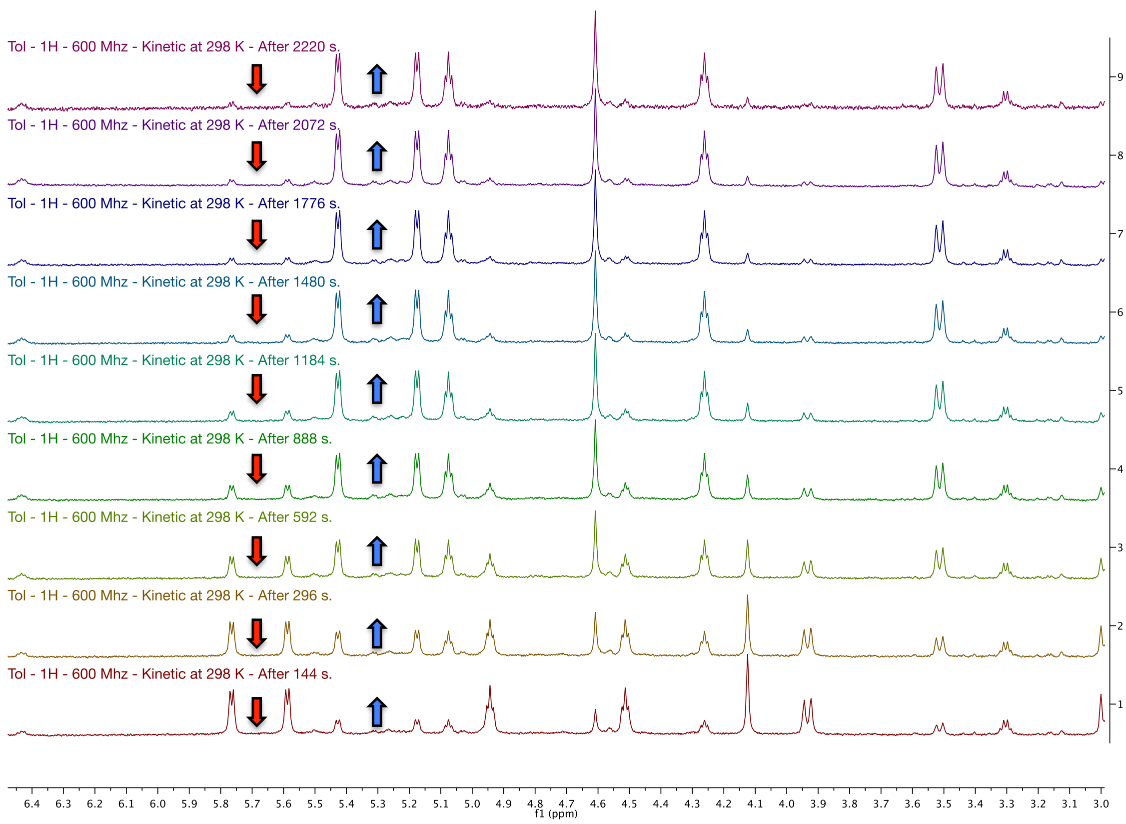

33 - Compound 16f.

Tol – ^{1}H – 600 Mhz – 223 K.

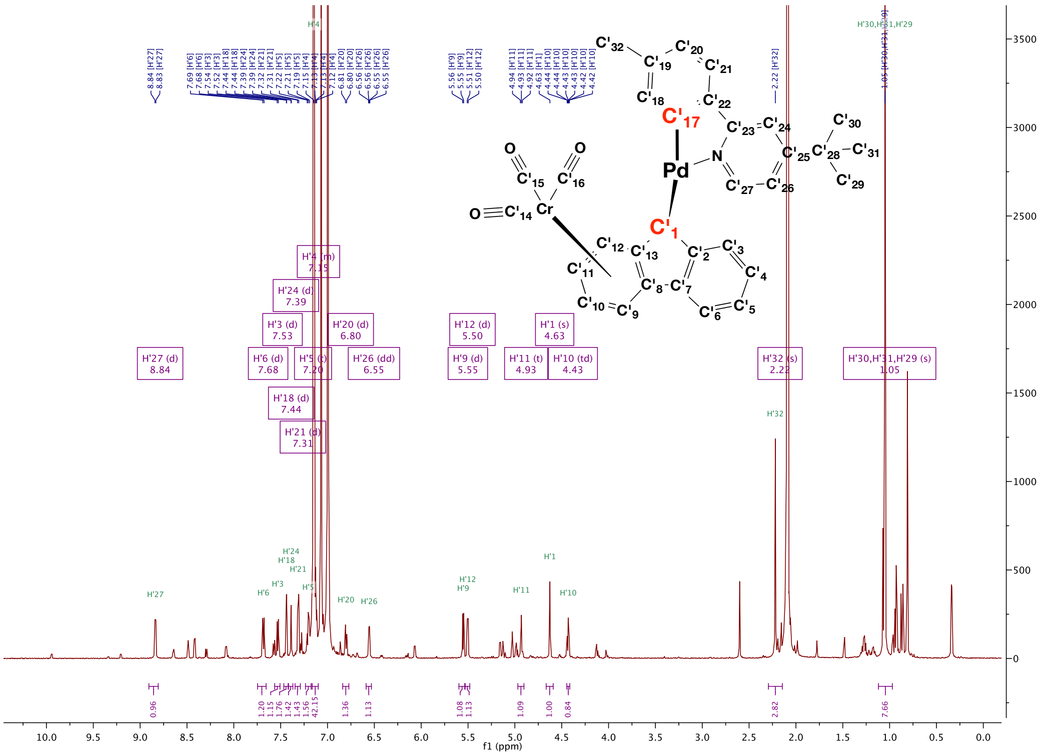

Tol – ^{13}C – 151 Mhz – 213 K.

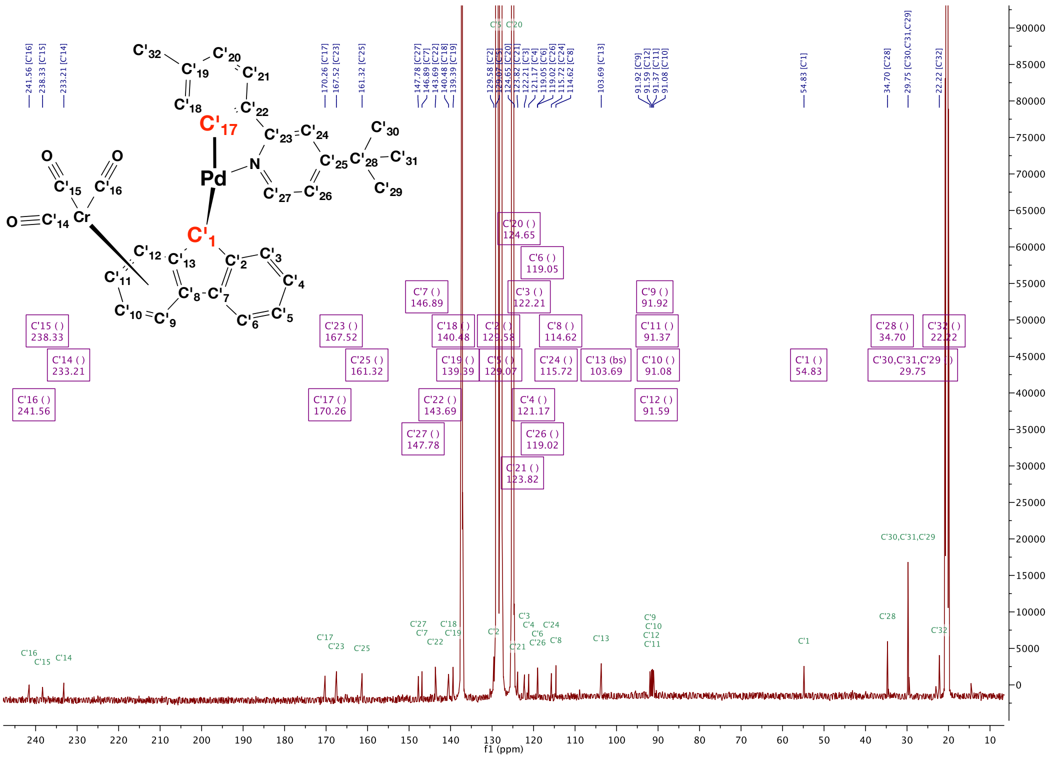

34 - Compound 17f.

C_6D_6 – ^1H – 500 Mhz – 293 K.

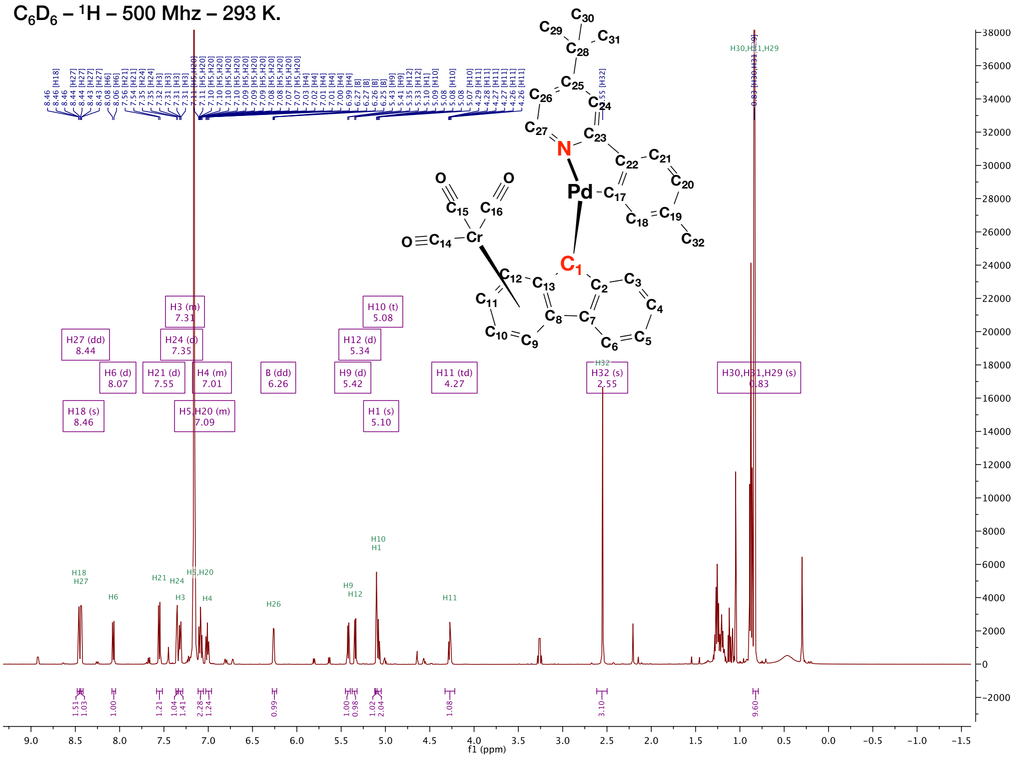

C_6D_6 – ^{13}C – 126 Mhz – 293 K.

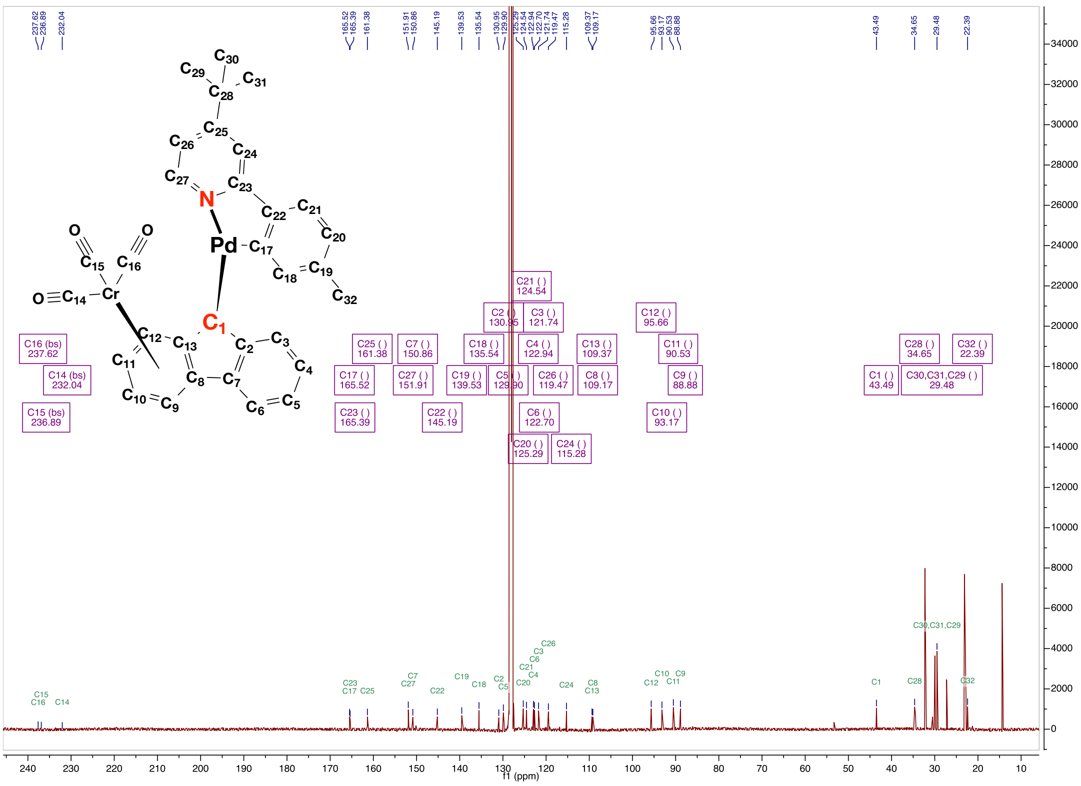

Tol – ¹H – 600 Mhz – Variable Temperature.

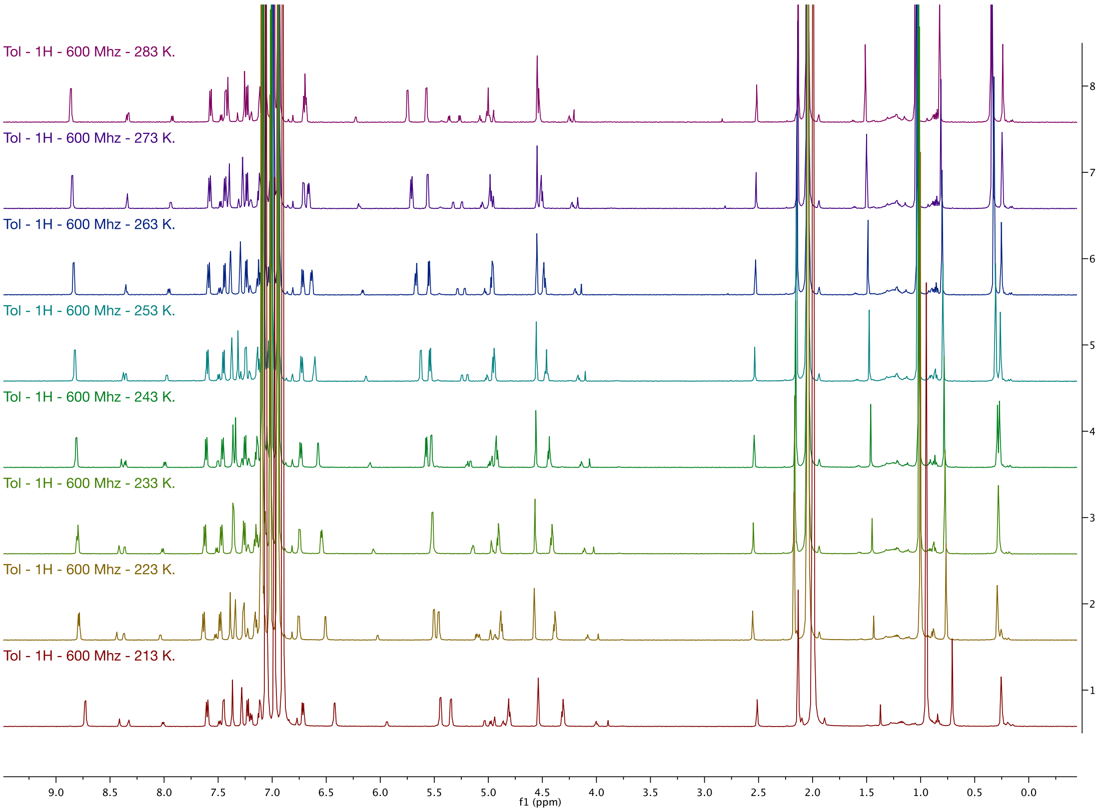

35 - Compound 16f.

Tol – ^{1}H – 600 Mhz – 223 K.

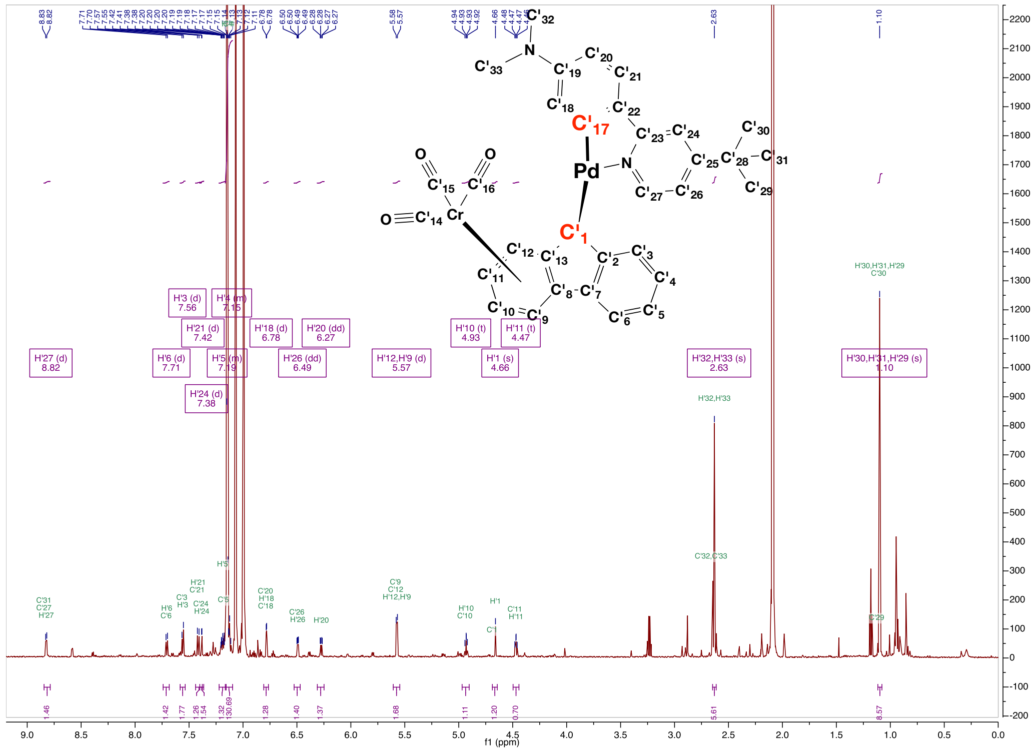

Tol – HSQC – (600 Mhz, 151 Mhz) – 223 K.

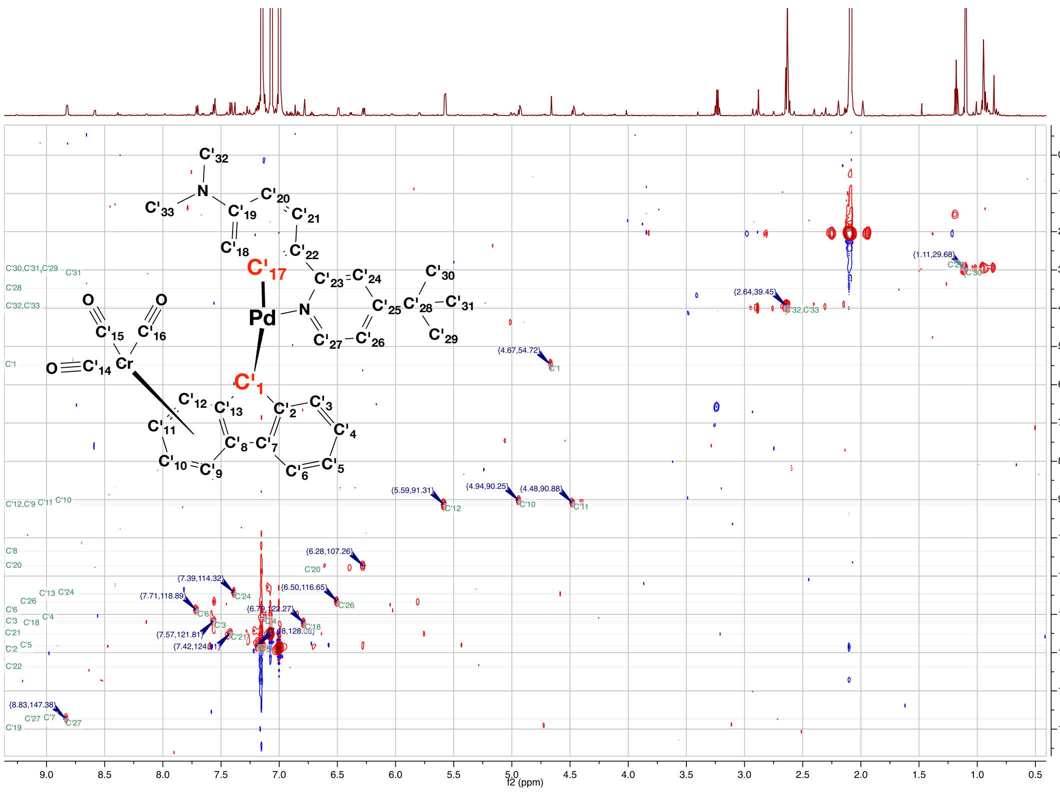

Tol – HMBC – (600 Mhz, 151 Mhz) – 223 K.

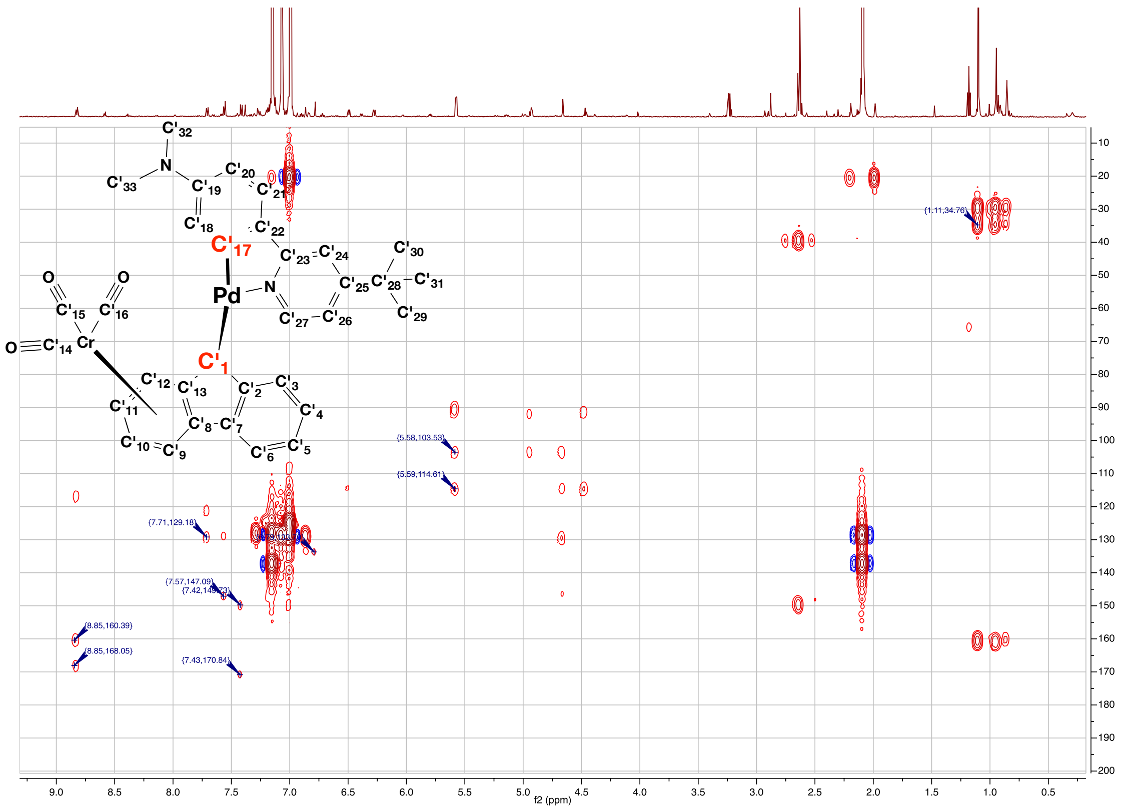

Tol – 13C – 126 Mhz – 293 K - Carbonyls.

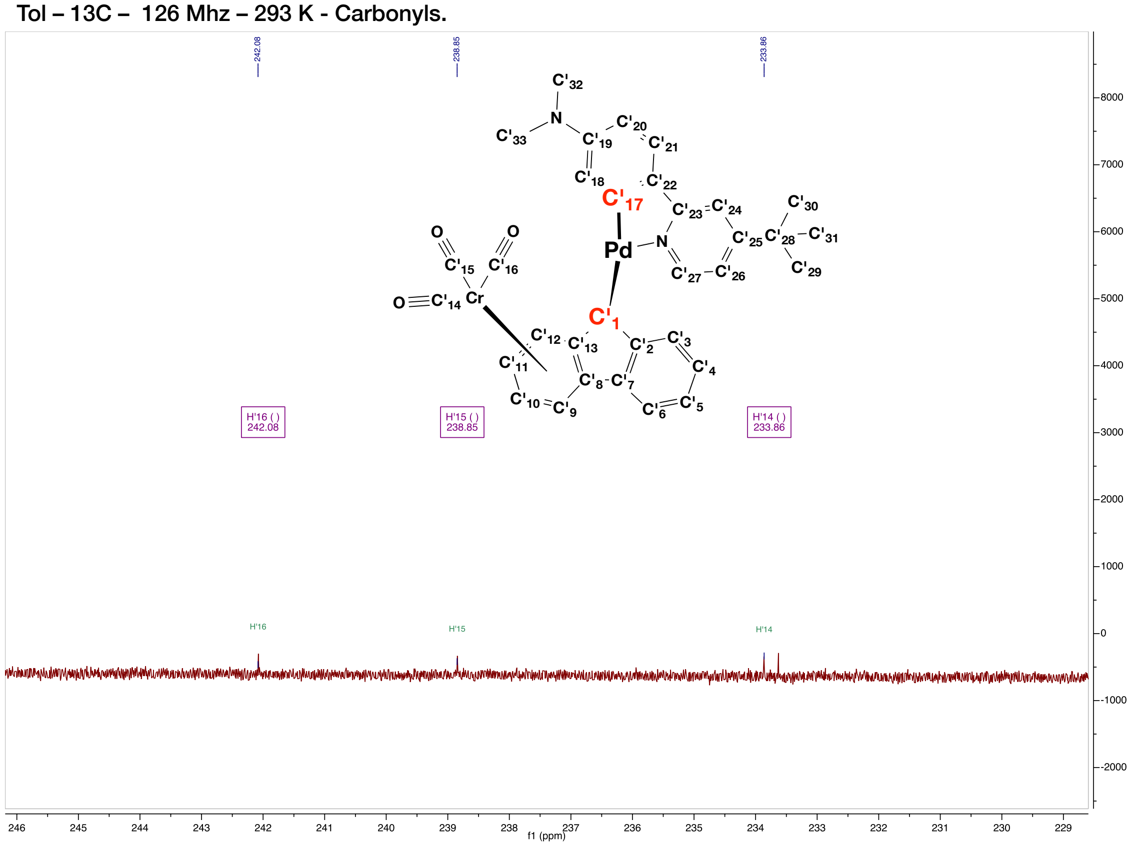

36 - Compound 17f.

C_6D_6 – ^1H – 500 Mhz – 293 K.

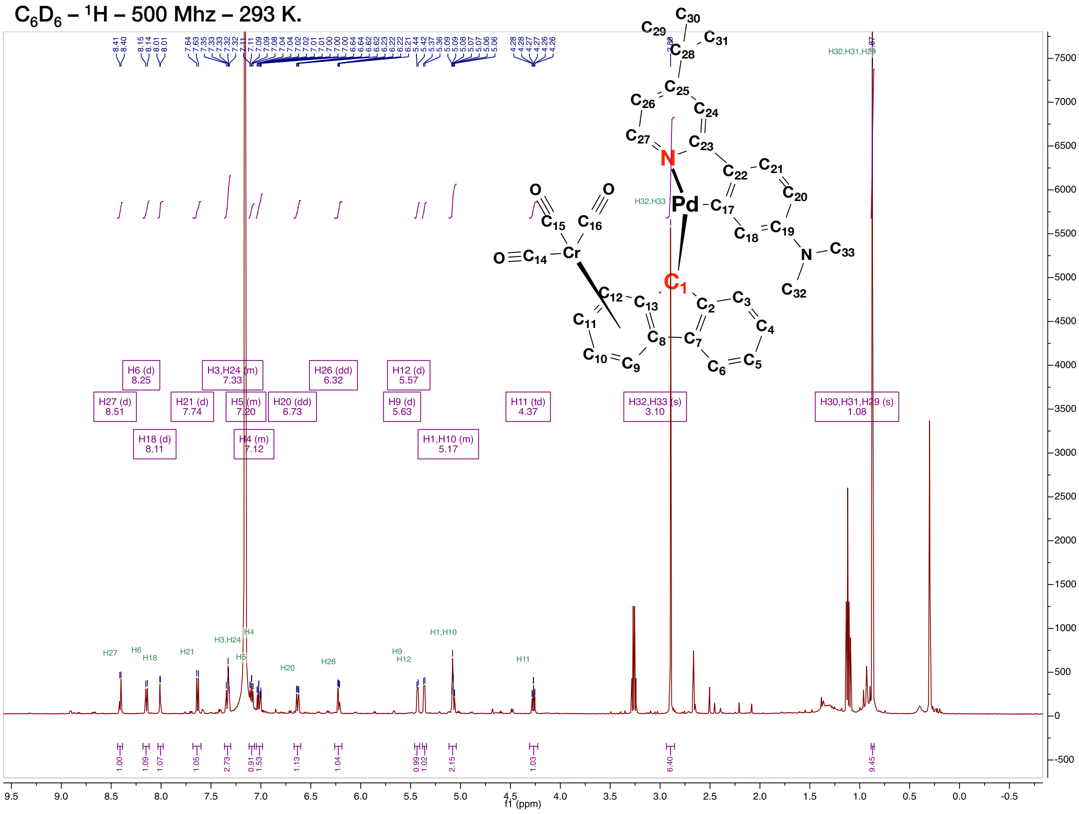

C_6D_6 – ^{13}C – 126 Mhz – 293 K.

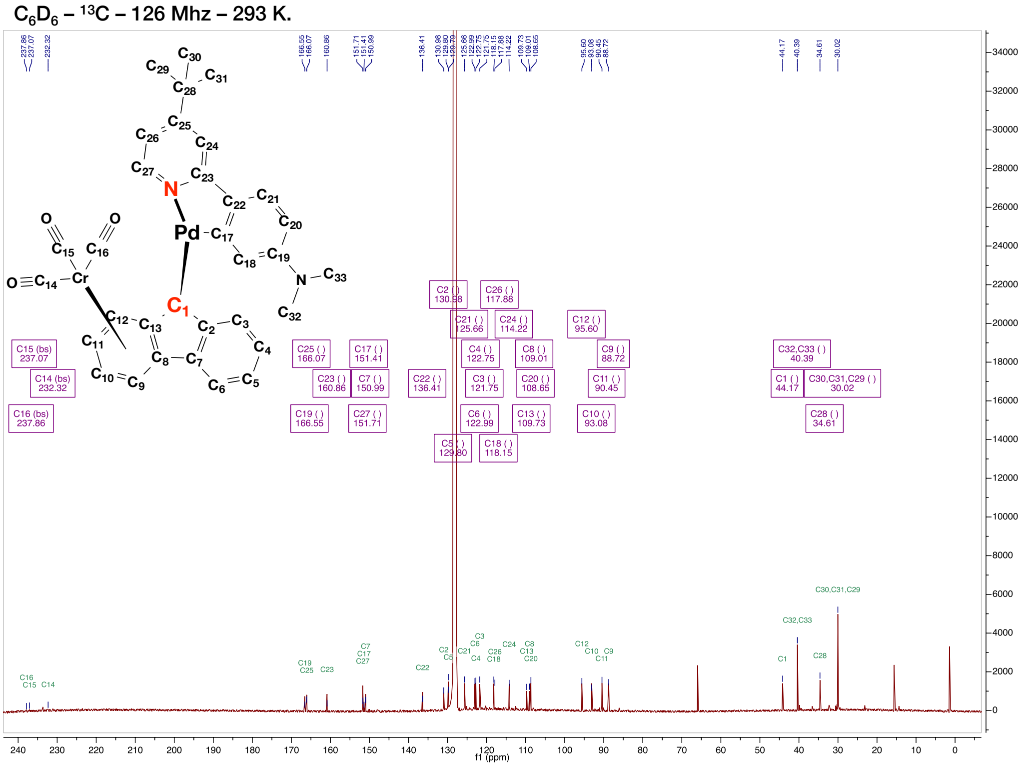

Tol – ^{1}H – 600 Mhz – Variable Temperature.

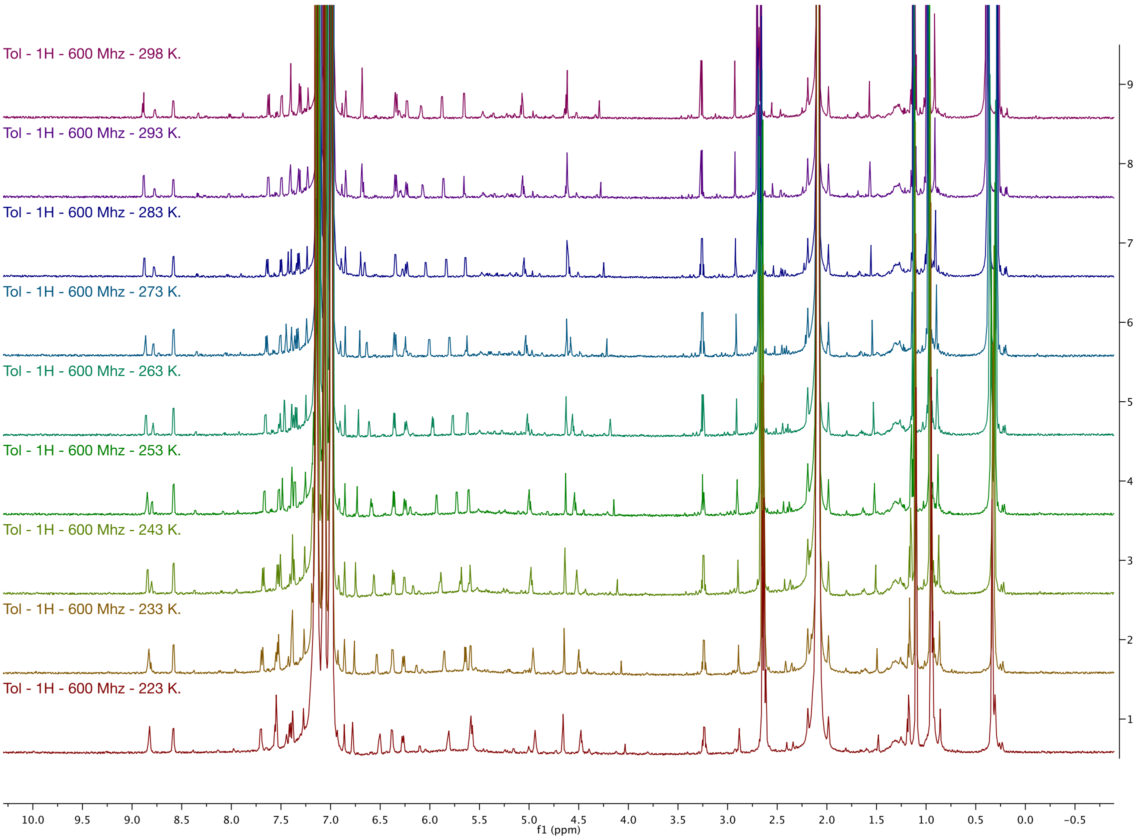

37 - Compound 17c.

Tol – ^{1}H – 600 Mhz – 223 K.

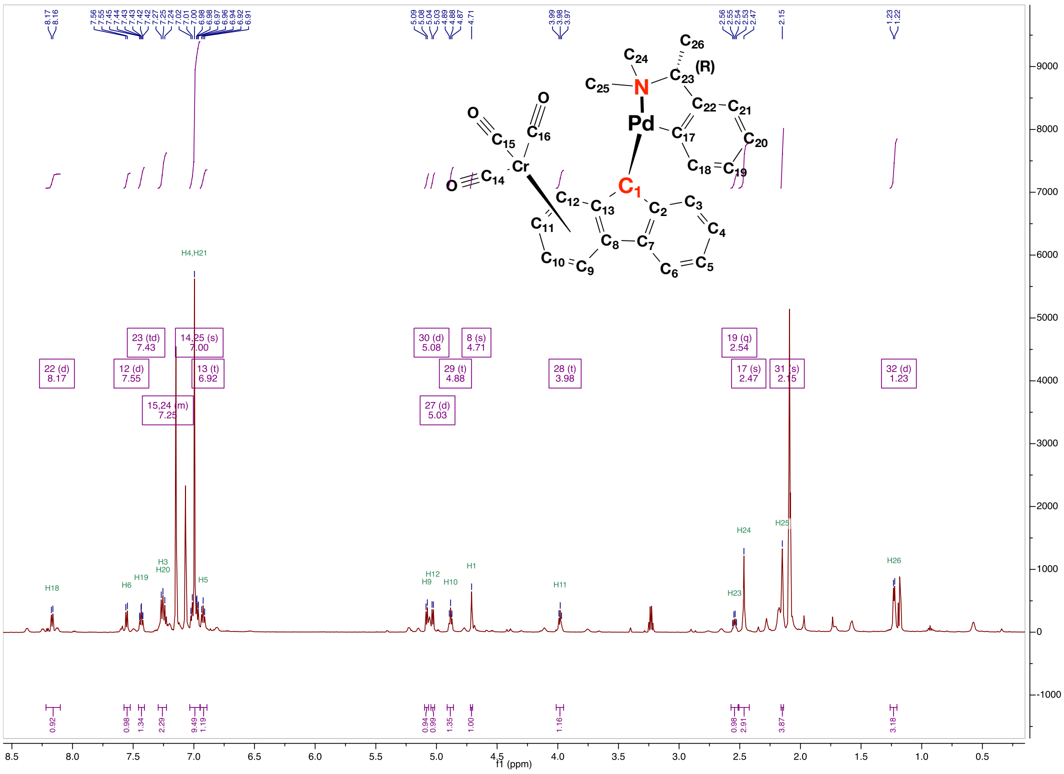

Tol – HSQC – (600 Mhz, 151 Mhz) – 223 K.

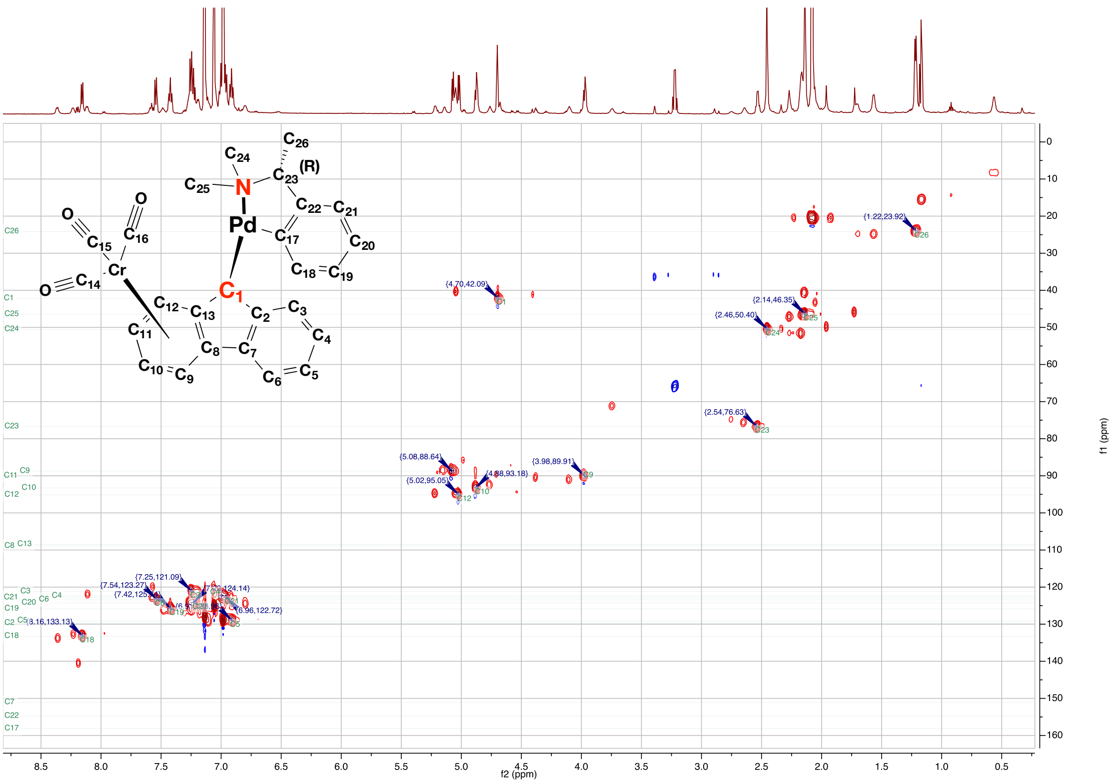

Tol – HMBC – (600 Mhz, 151 Mhz) – 223 K.

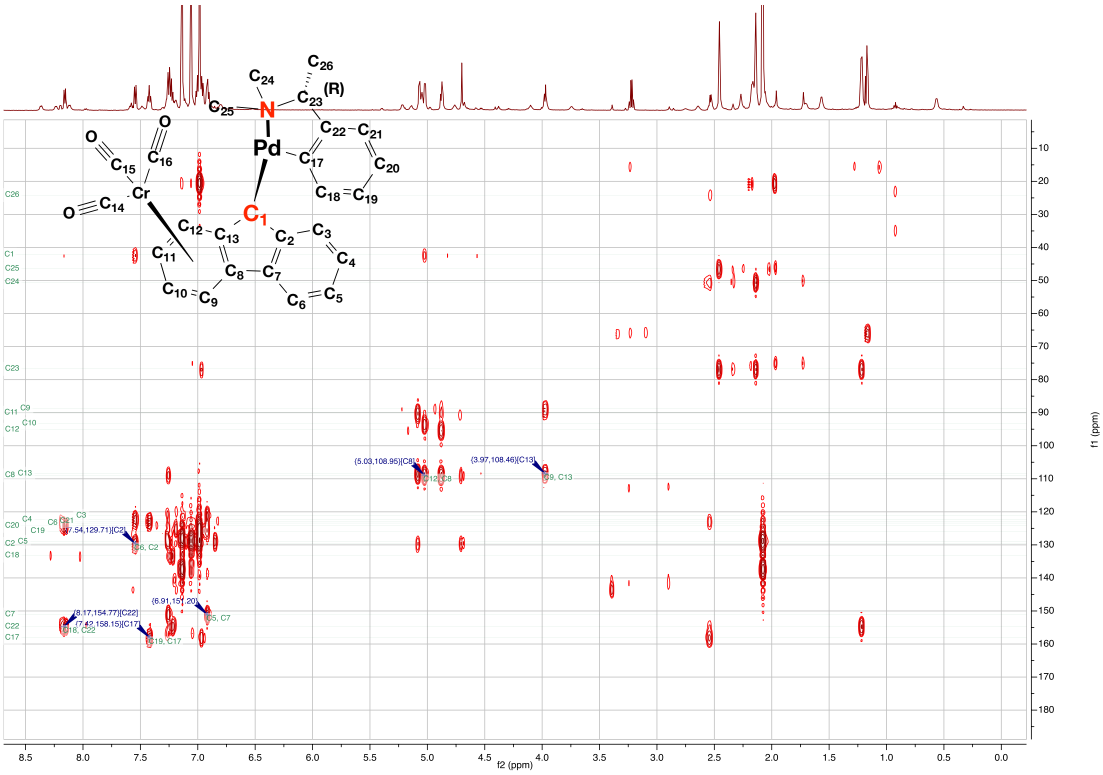

Tol – 13C – 151 Mhz – 223 K - Carbonyls.

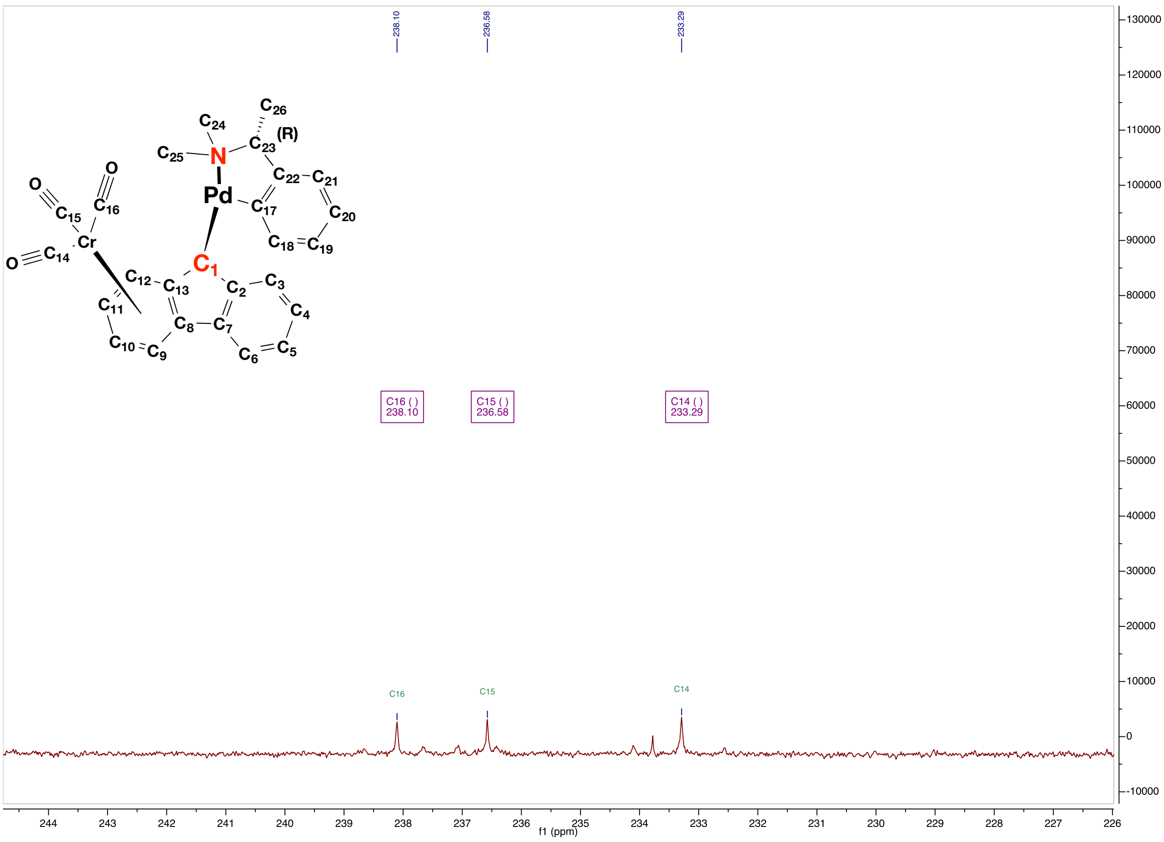

Tol – ^{1}H – 600 Mhz – Variable Temperature.

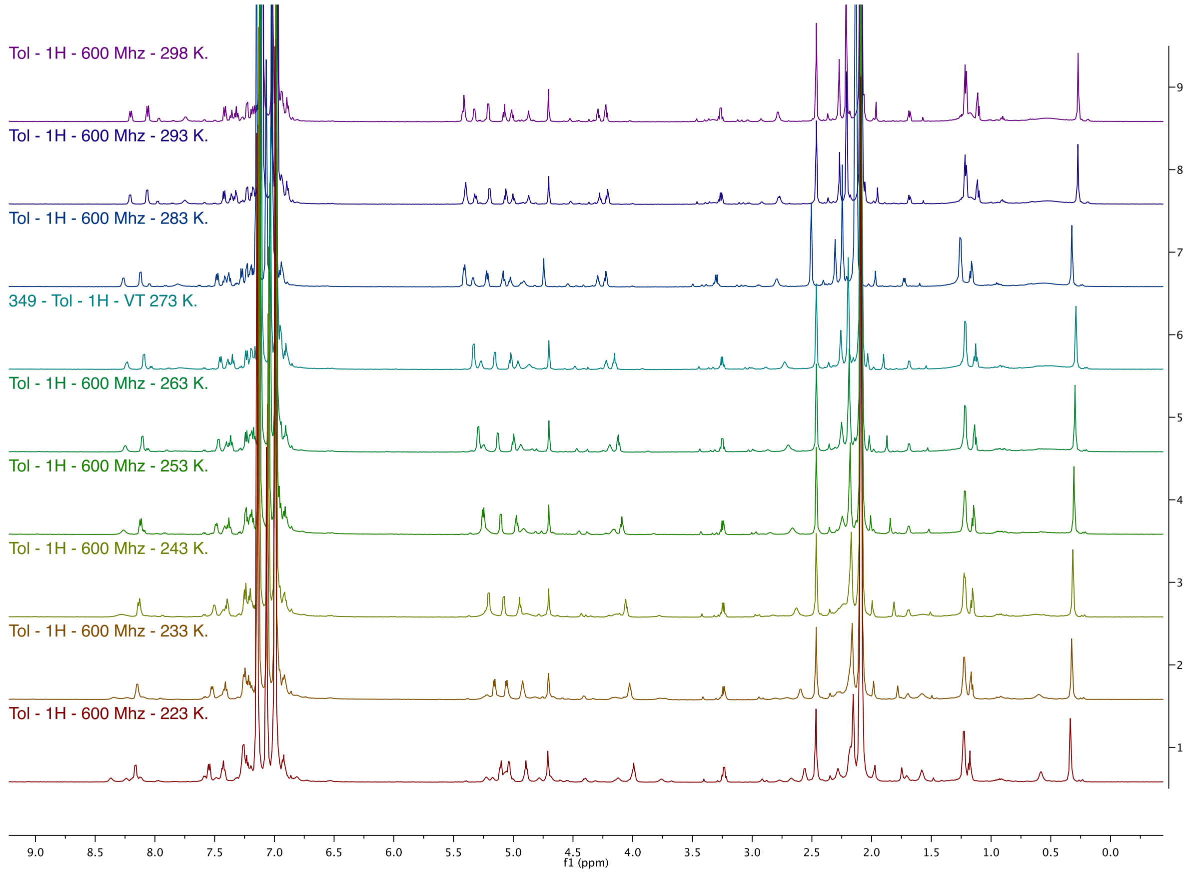

Circular dichroism (CD)

(C = 10⁻³M in benzene).

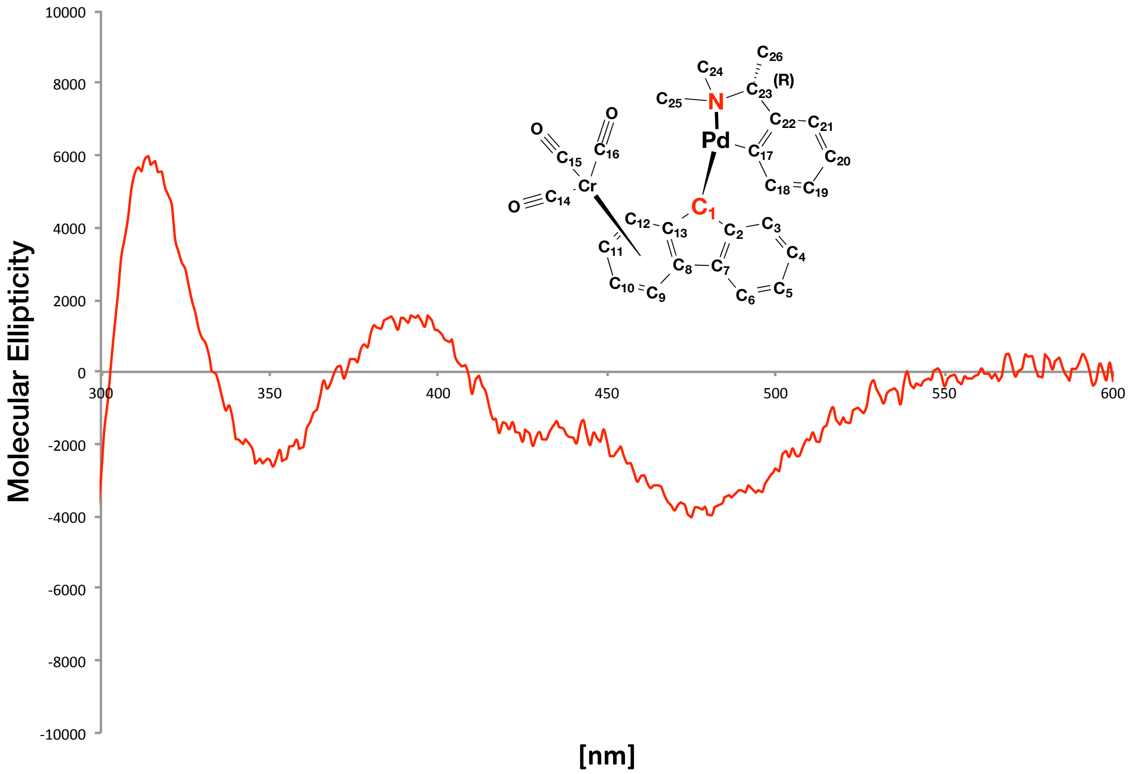

38 - Compound 17j.

C_6D_6 – ^1H – 600 Mhz – 298 K.

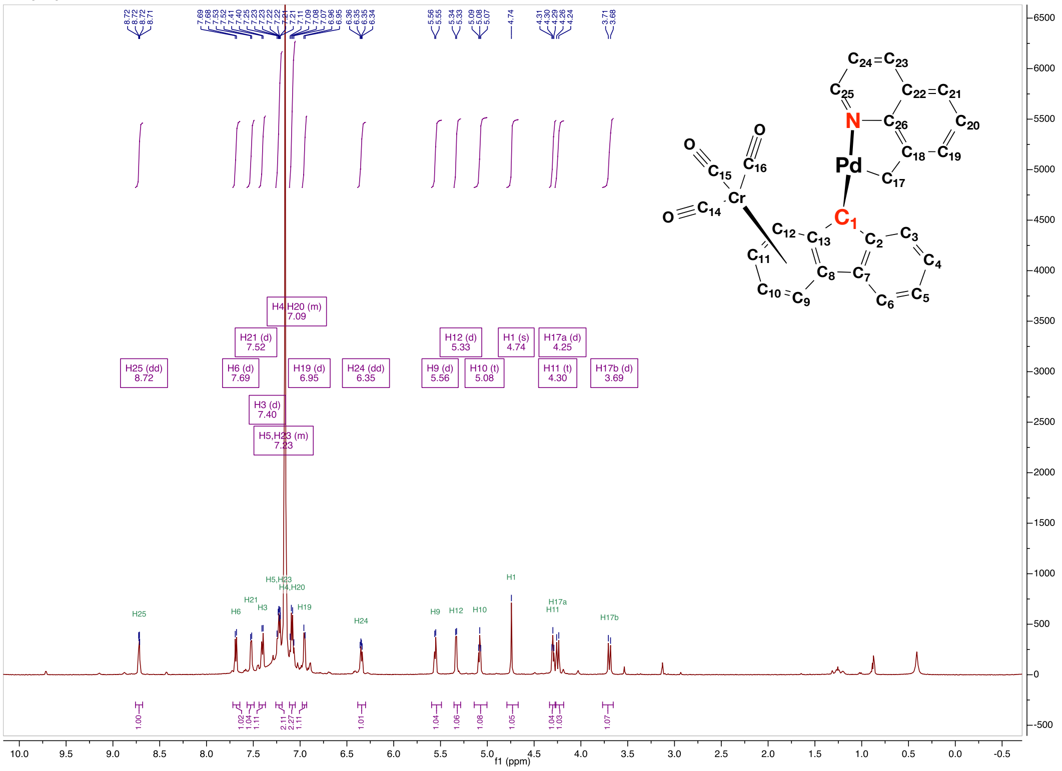

C_6D_6 – ^{13}C – 126 Mhz – 293 K.

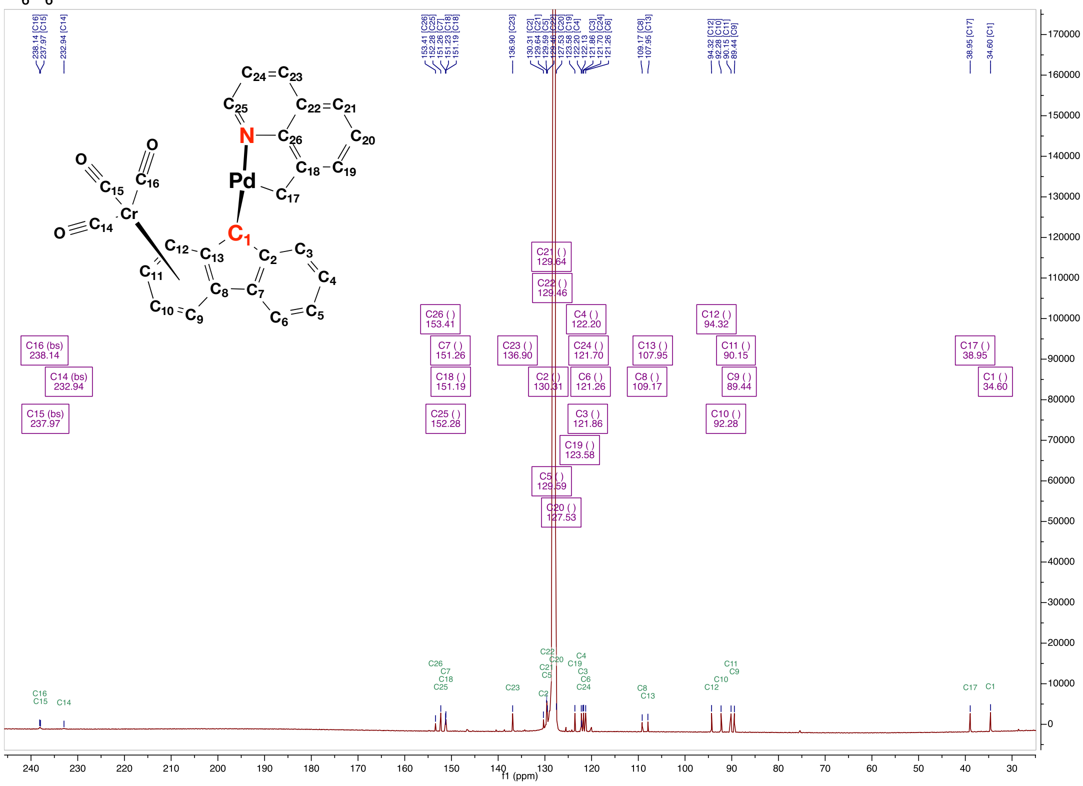

Tol – ^{1}H – 600 Mhz – Variable Temperature.

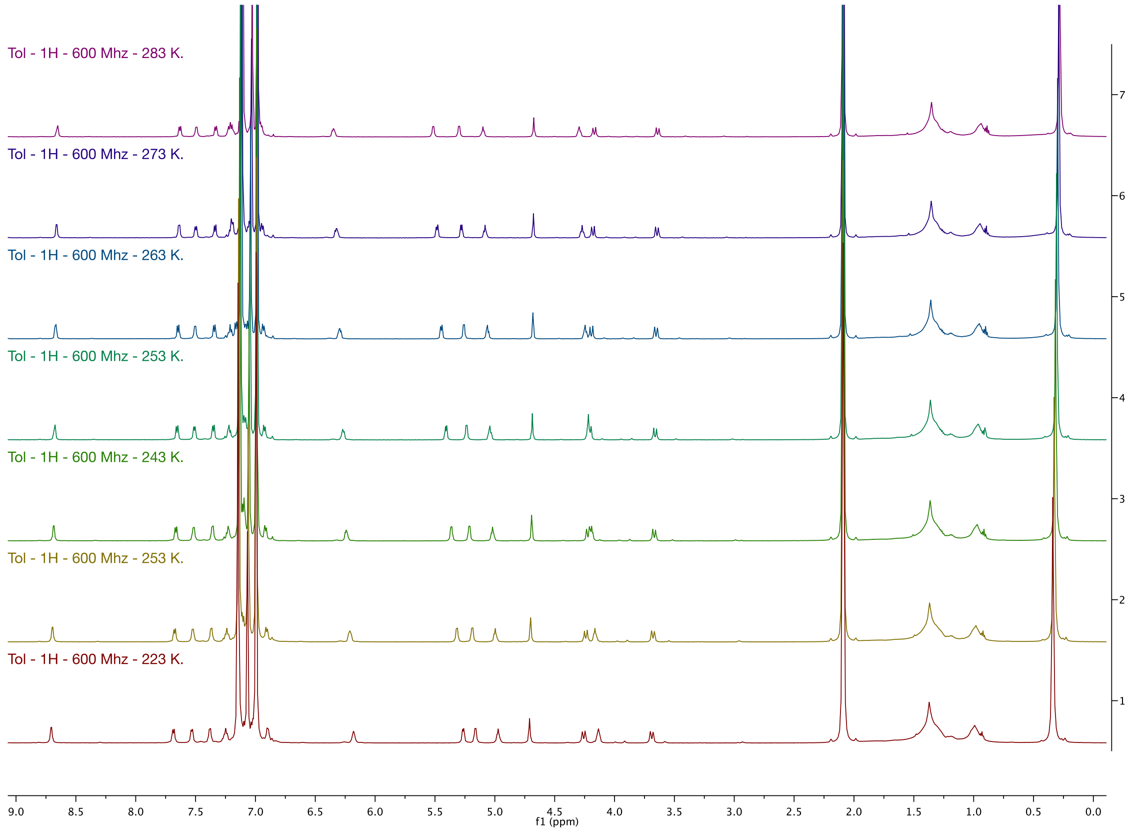

39 - Compound 18a.

C_6D_6 – ^1H – 600 Mhz – 298 K.

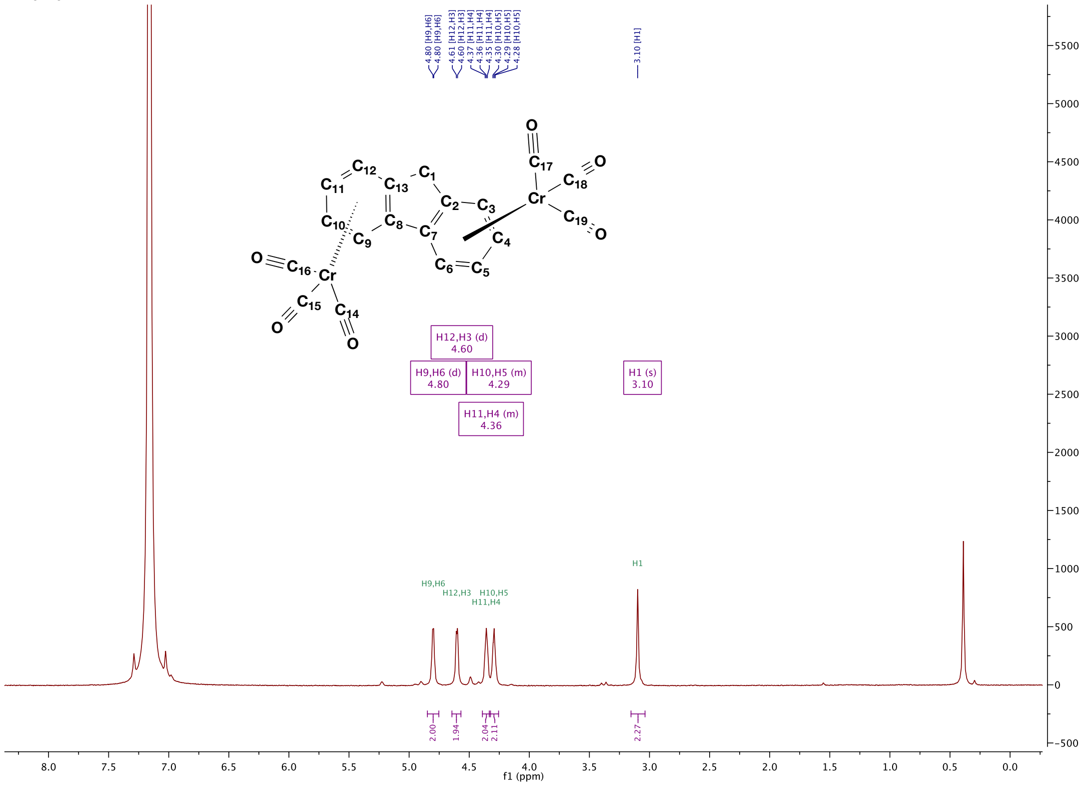

C_6D_6 – ^{13}C – 151 Mhz – 298 K.

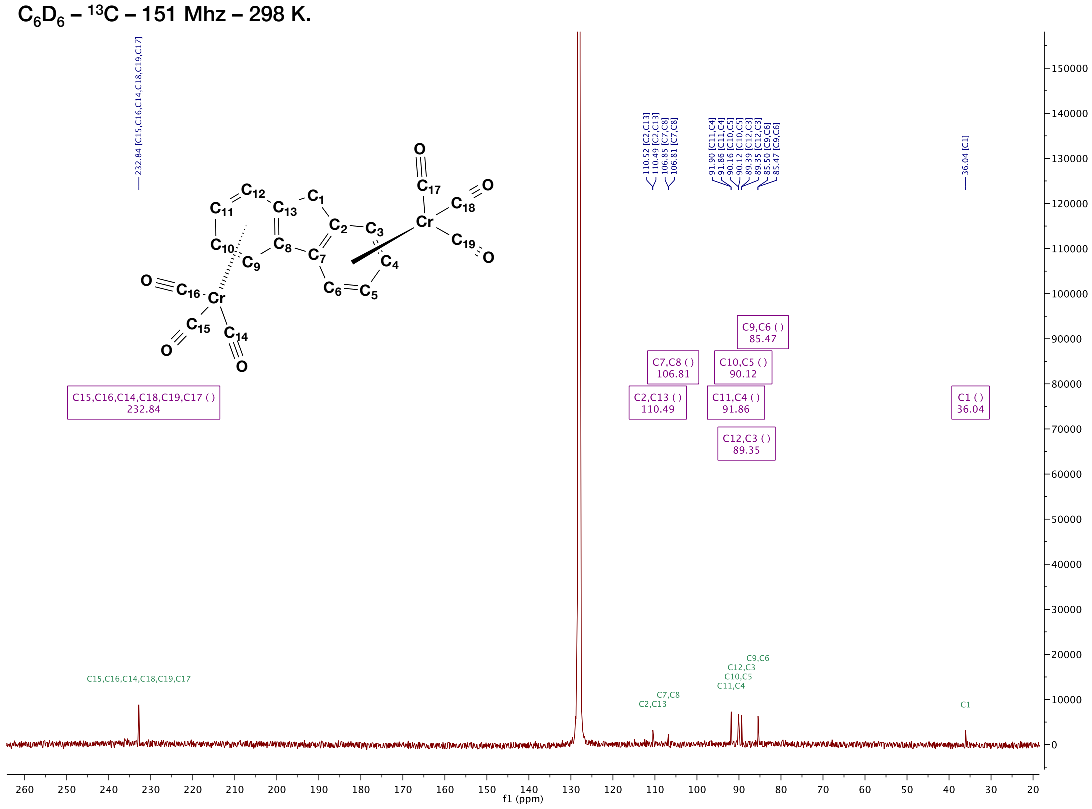

40 - Compound 19a.

C_6D_6 – ^1H – 600 Mhz – 298 K.

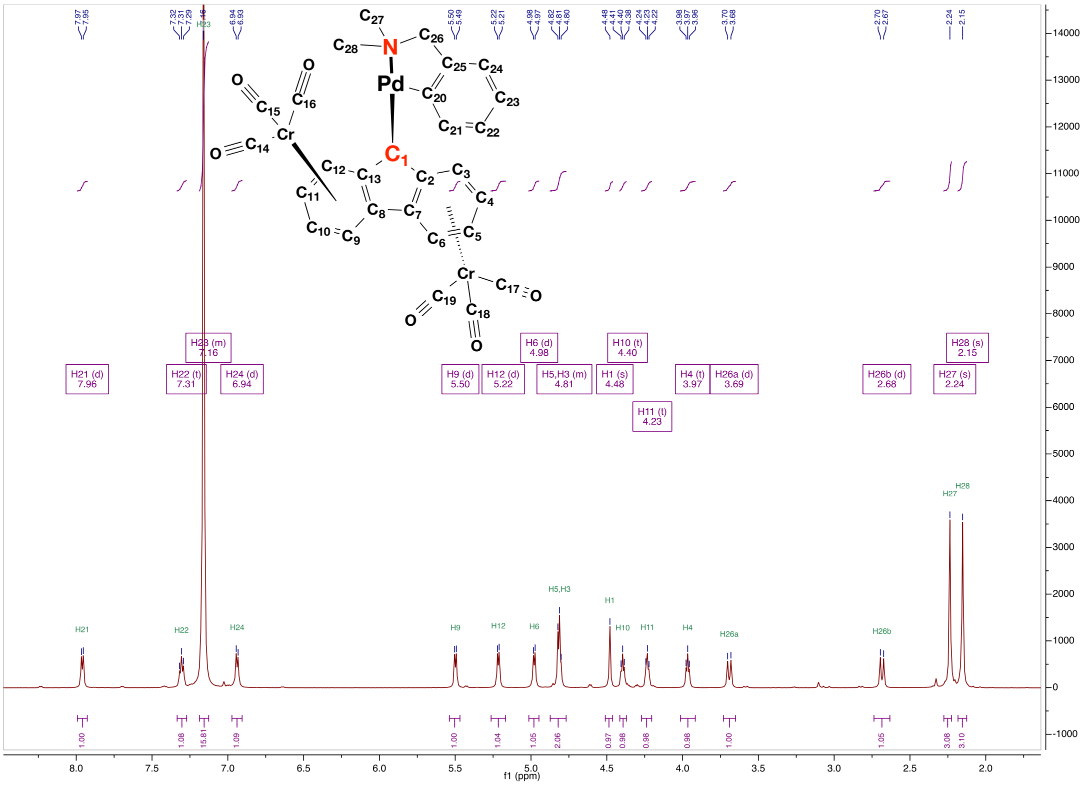

C_6D_6 – ^{13}C – 151 Mhz – 298 K.

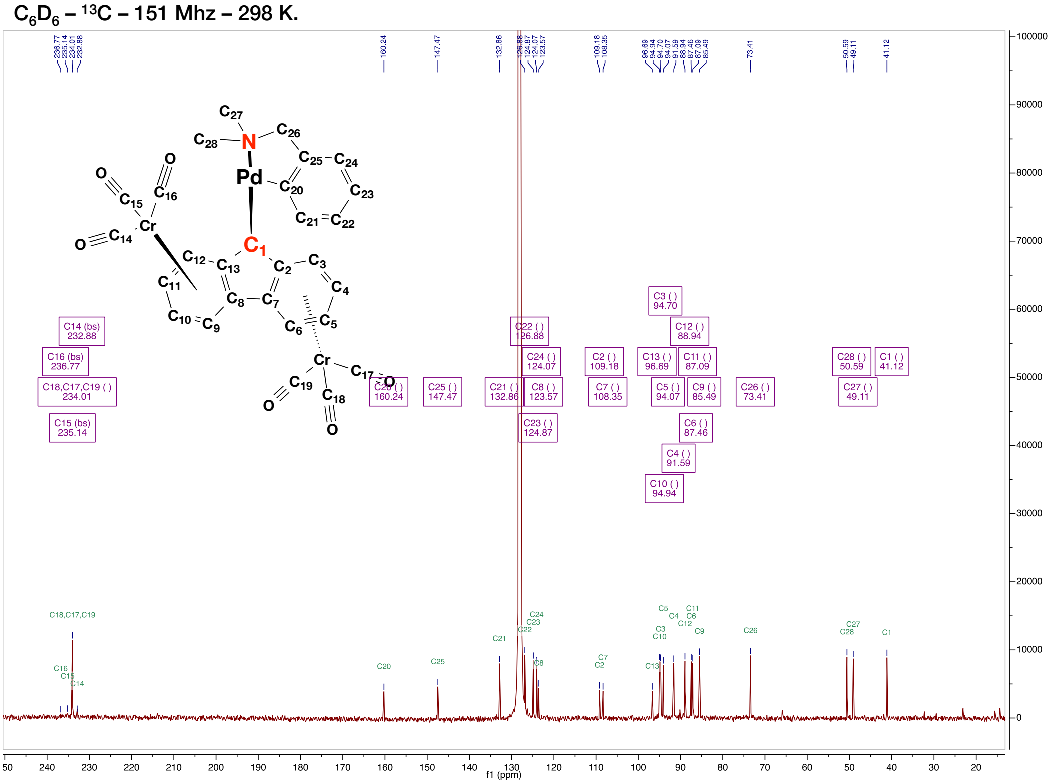

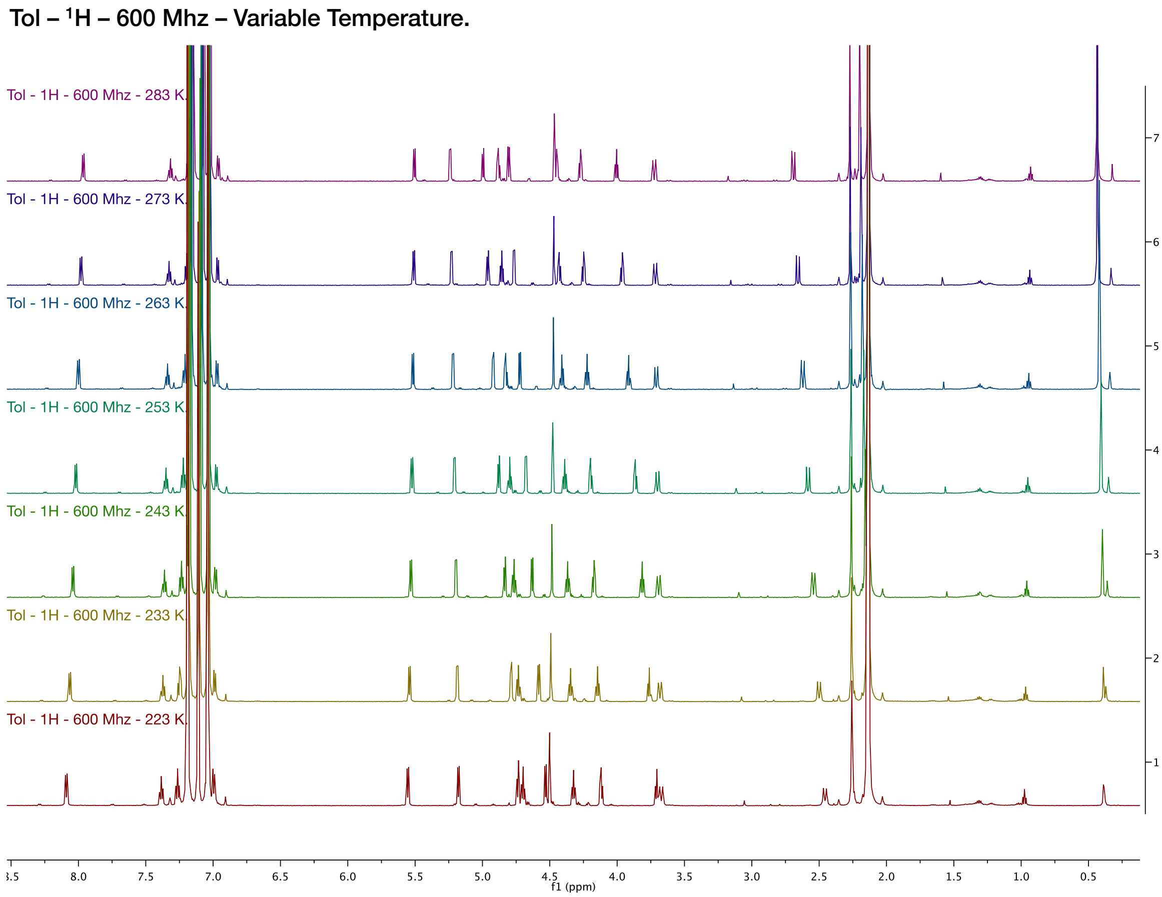
Tol – ¹H – 600 Mhz – Variable Temperature.
Tol - 1H - 600 Mhz - 283 K
Tol - 1H - 600 Mhz - 273 K
Tol - 1H - 600 Mhz - 263 K
Tol - 1H - 600 Mhz - 253 K
Tol - 1H - 600 Mhz - 243 K
Tol - 1H - 600 Mhz - 233 K
Tol - 1H - 600 Mhz - 223 K
f1 (ppm)

41 - Compound 19i.

C_6D_6 – ^1H – 500 Mhz – 293 K.

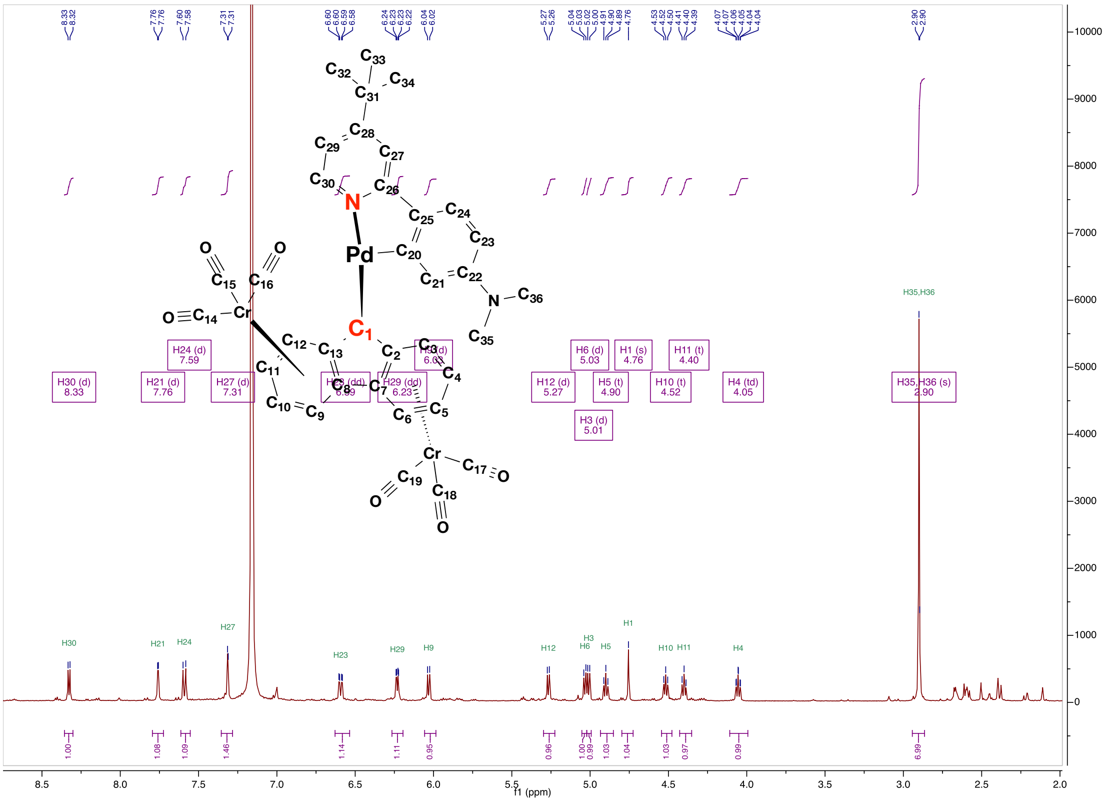

C_6D_6 – ^{13}C – 126 Mhz – 293 K.

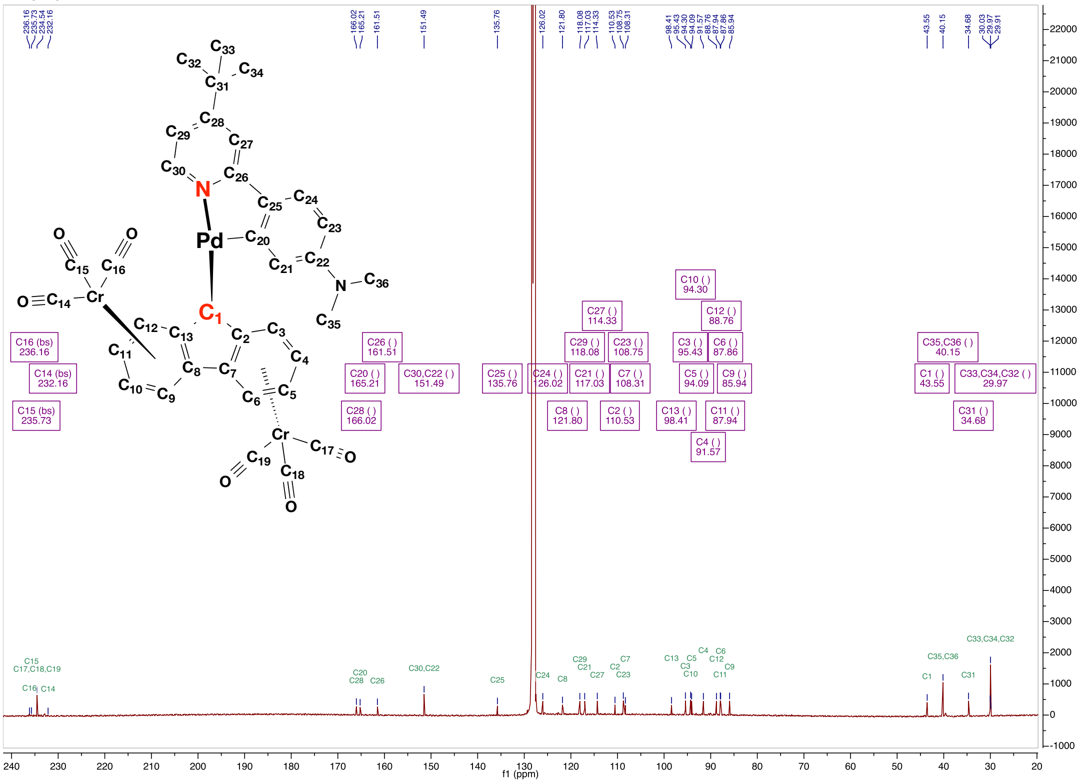

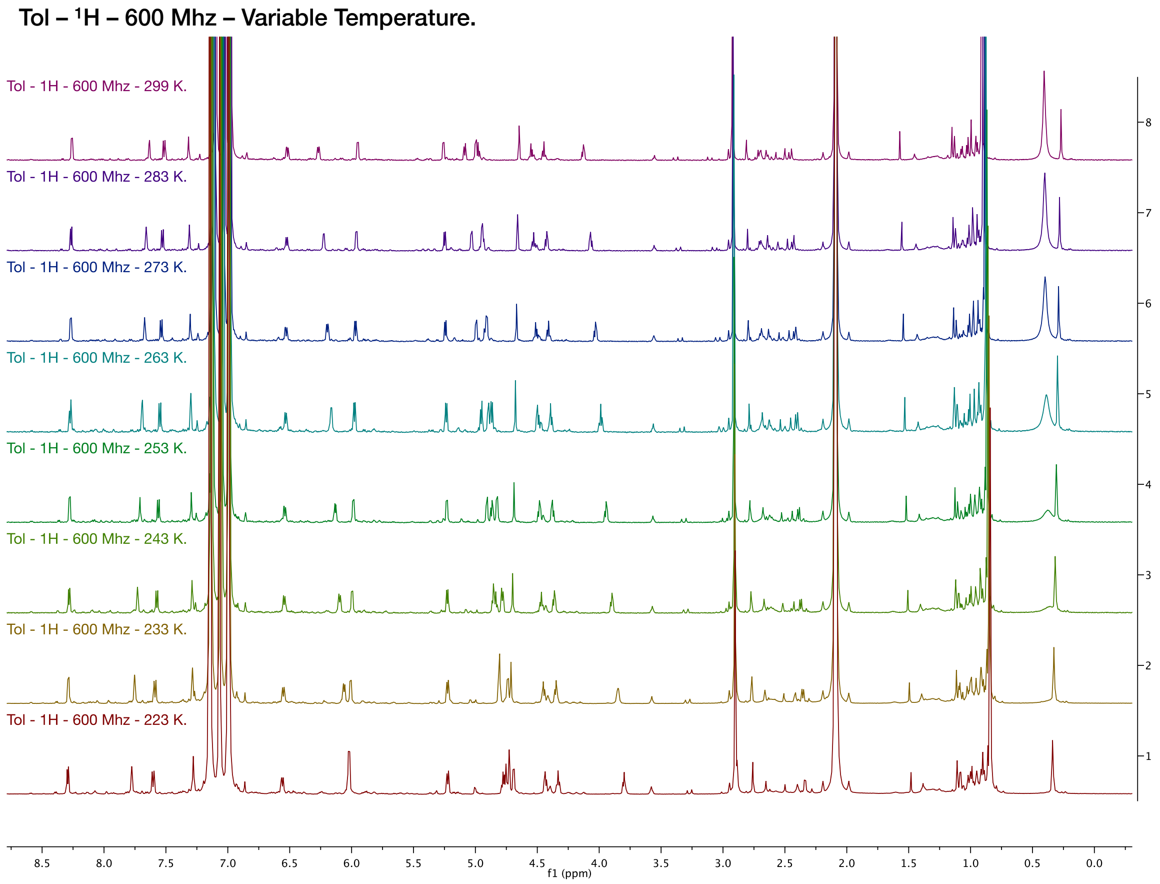
Tol – 1H – 600 Mhz – Variable Temperature.
Tol - 1H - 600 Mhz - 299 K.
Tol - 1H - 600 Mhz - 283 K.
Tol - 1H - 600 Mhz - 273 K.
Tol - 1H - 600 Mhz - 263 K.
Tol - 1H - 600 Mhz - 253 K.
Tol - 1H - 600 Mhz - 243 K.
Tol - 1H - 600 Mhz - 233 K.
Tol - 1H - 600 Mhz - 223 K.
8.5 8.0 7.5 7.0 6.5 6.0 5.5 5.0 4.5 4.0 3.5 3.0 2.5 2.0 1.5 1.0 0.5 0.0
f1 (ppm)
8 7 6 5 4 3 2 1

42 - Compound 20a.

C_6D_6 – ^1H – 300 Mhz – 298 K.

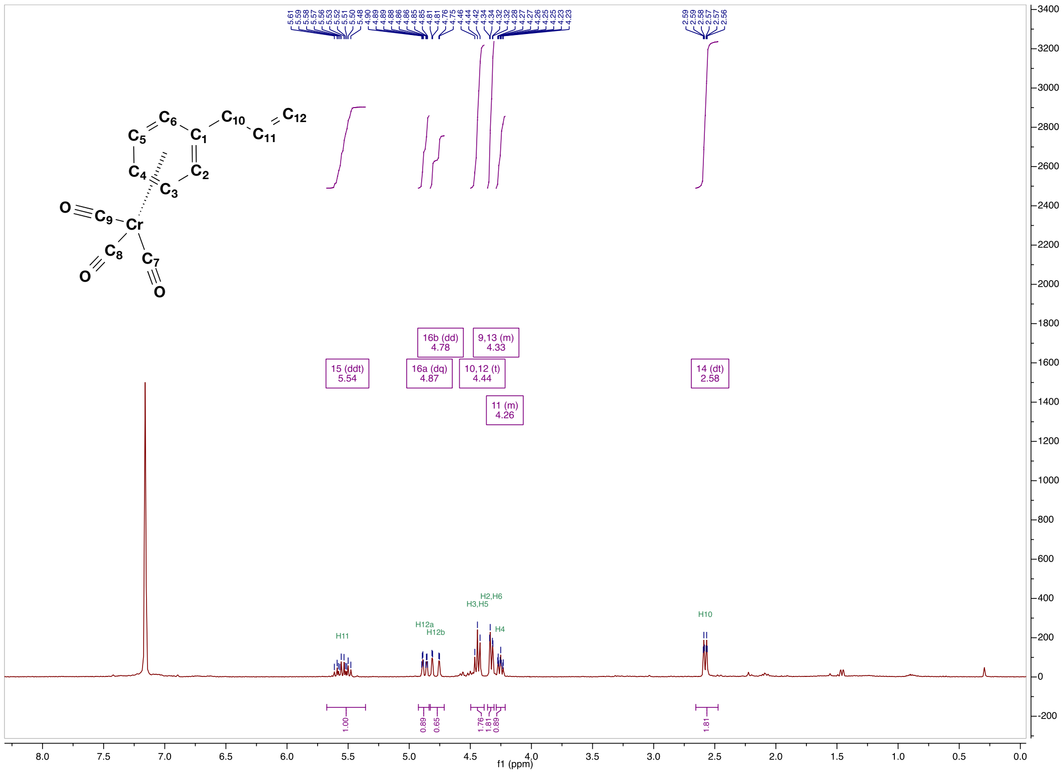

C_6D_6 – ^{13}C – 101 Mhz – 298 K.

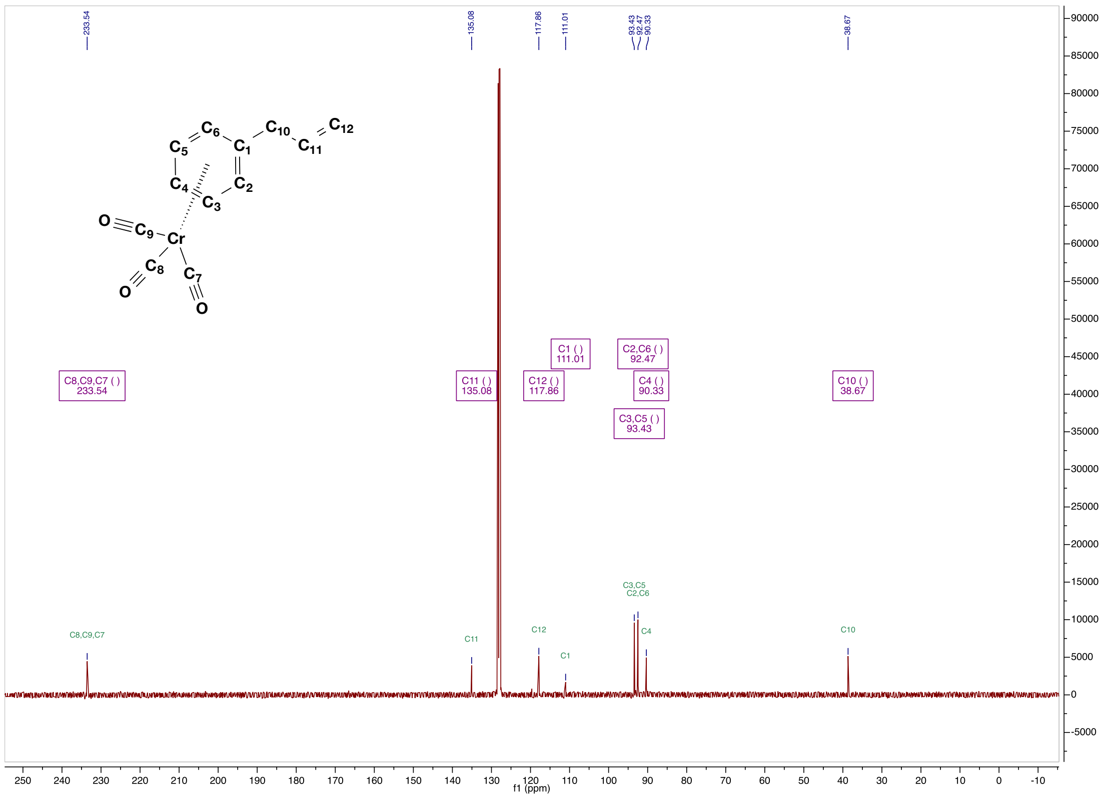

43 - Compound 21a.

Tol – ^{1}H – 600 Mhz – 223 K.

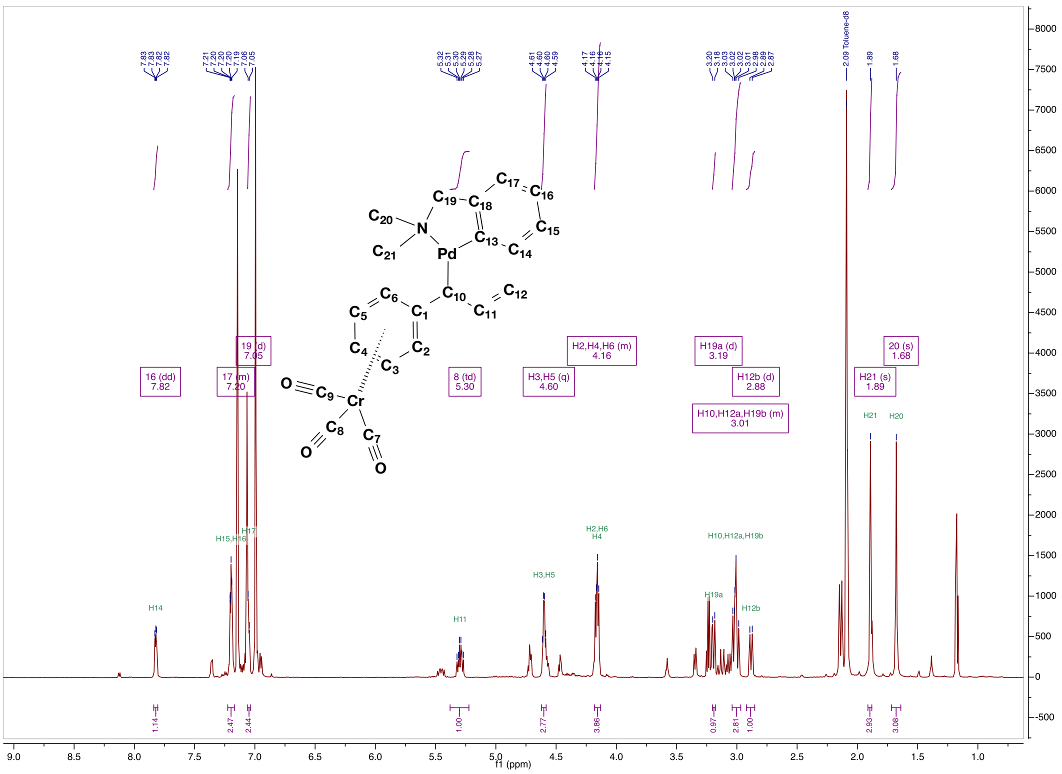

Tol – ^{13}C – 151 Mhz – 223 K.

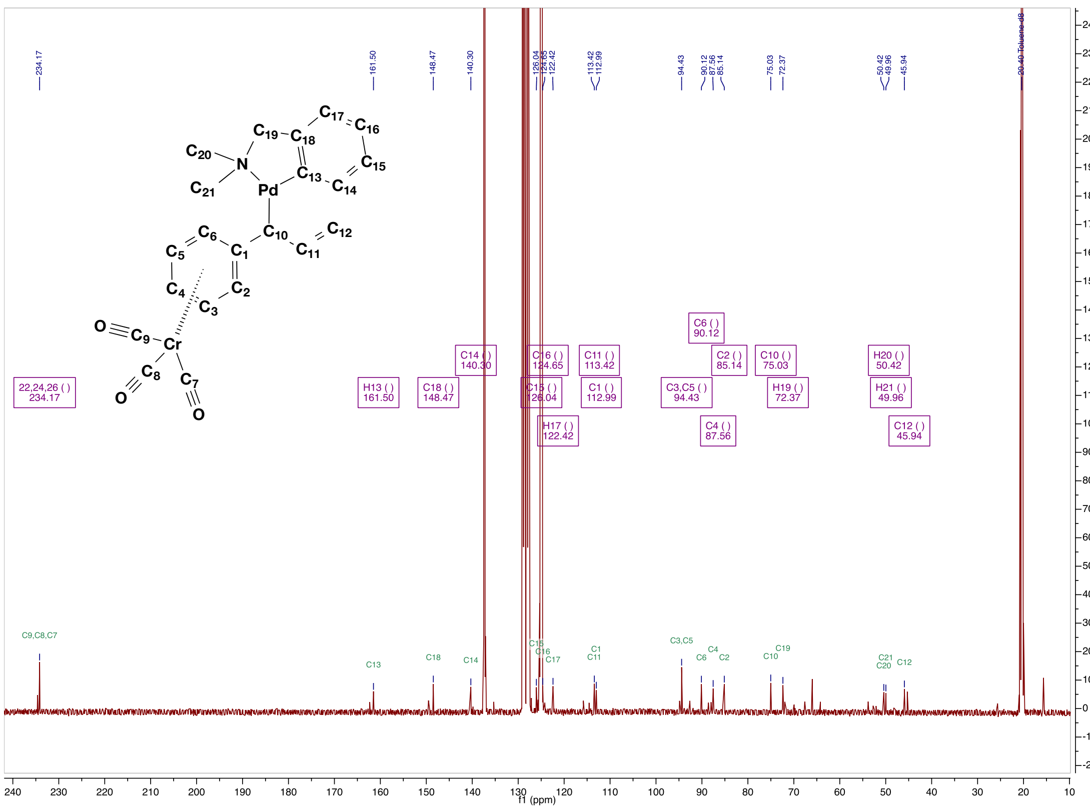

Tol – ^{1}H – 600 Mhz – Variable Temperature.

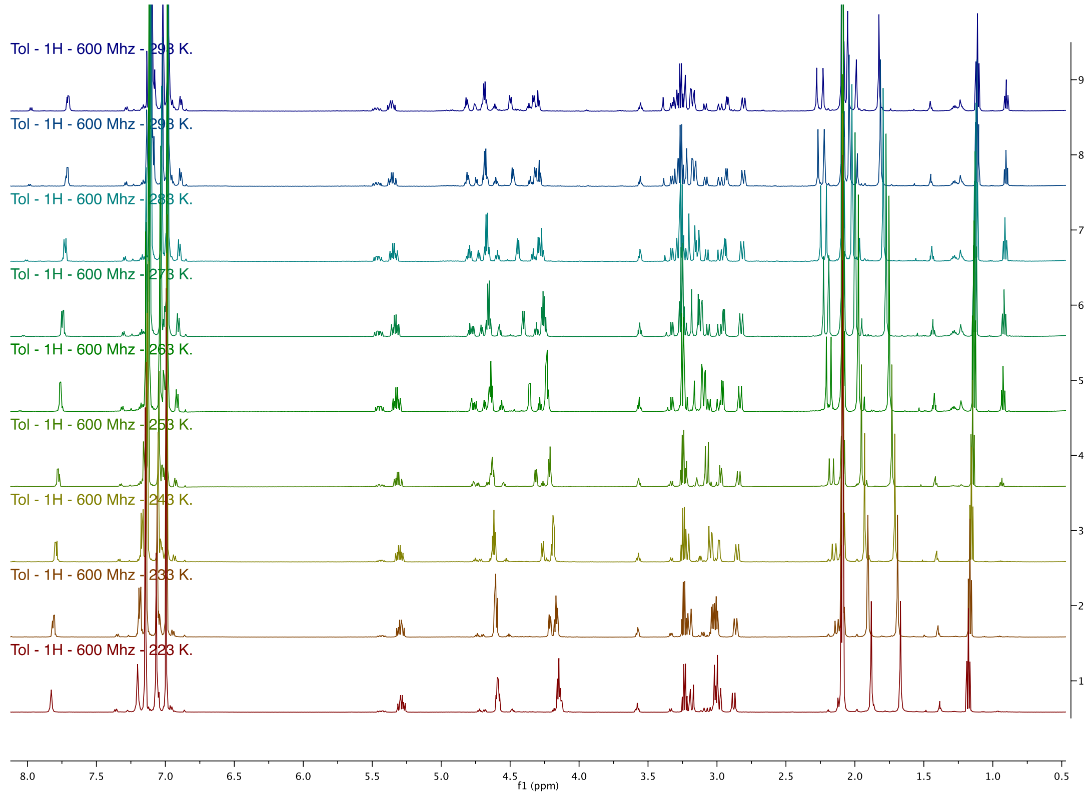

44 - Compound 21b.

Tol – ^{1}H – 600 Mhz – 233 K.

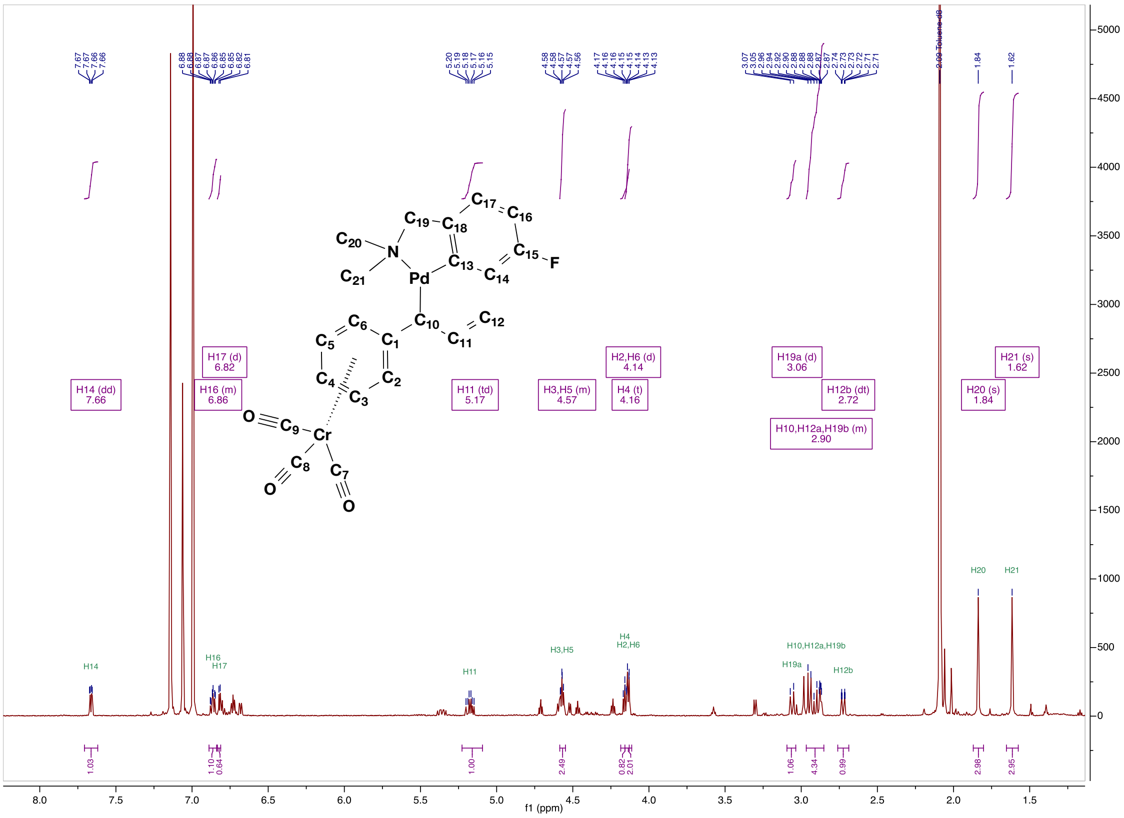

Tol – ^{13}C – 151 Mhz – 233 K.

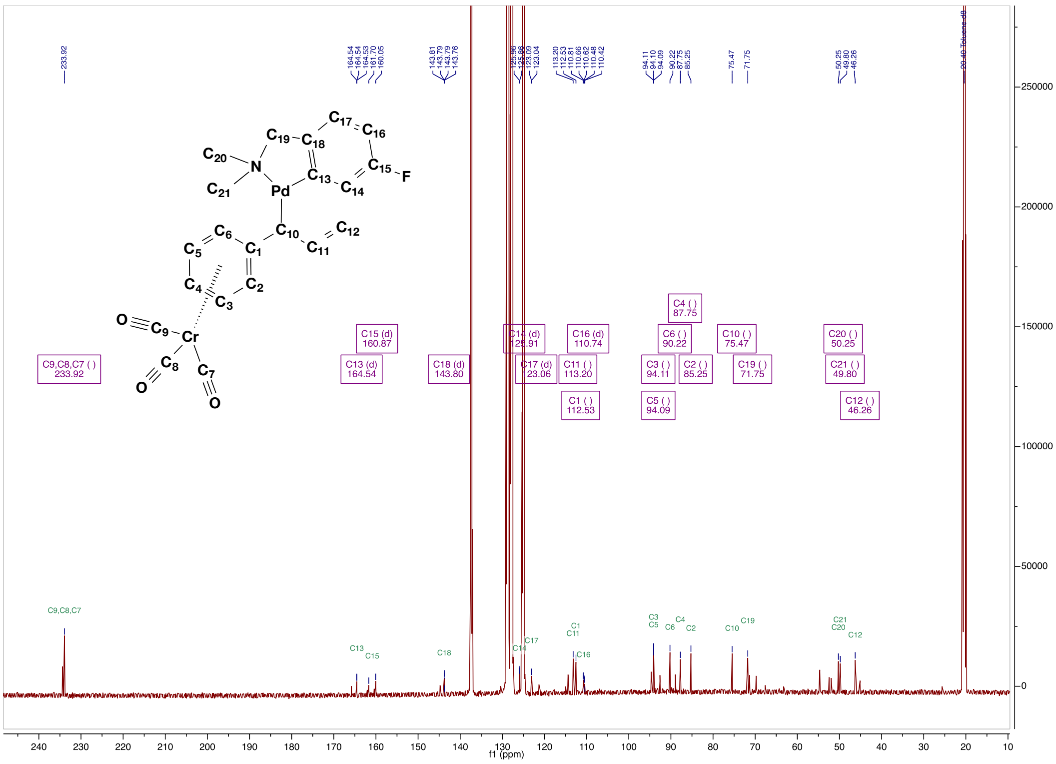

Tol – ¹H – 600 Mhz – Variable Temperature.

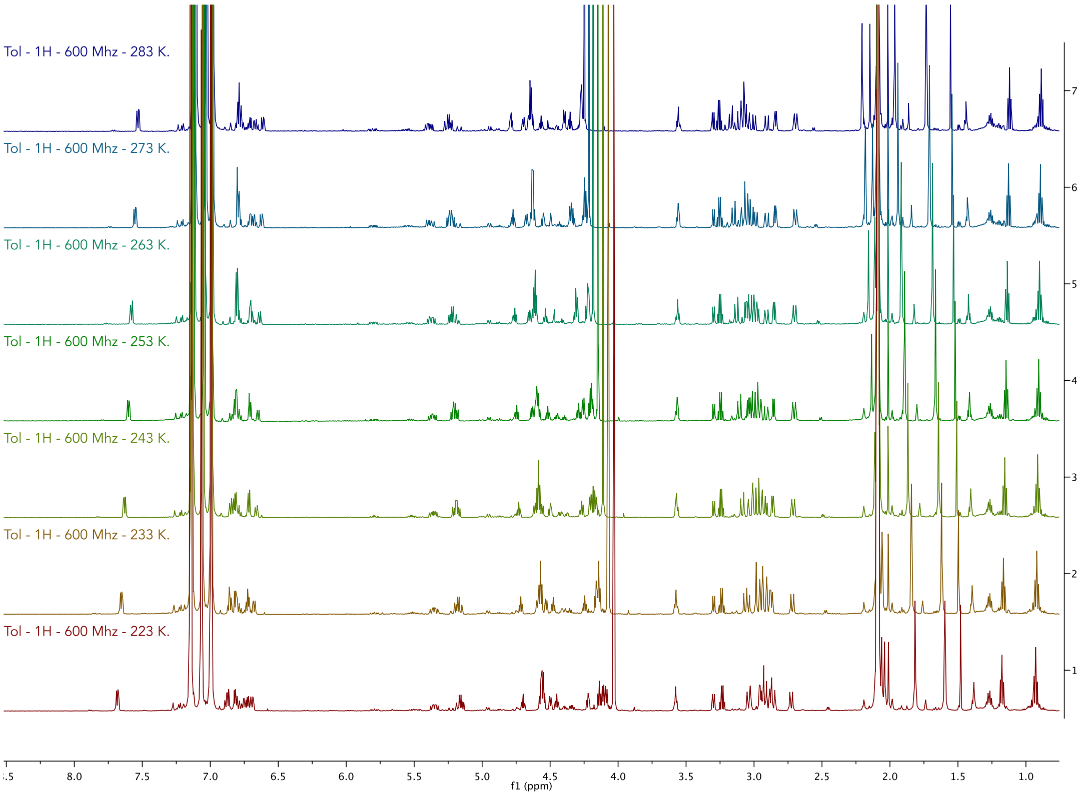

45 - Compound 21i.

Tol – ^{1}H – 600 Mhz – 233 K.

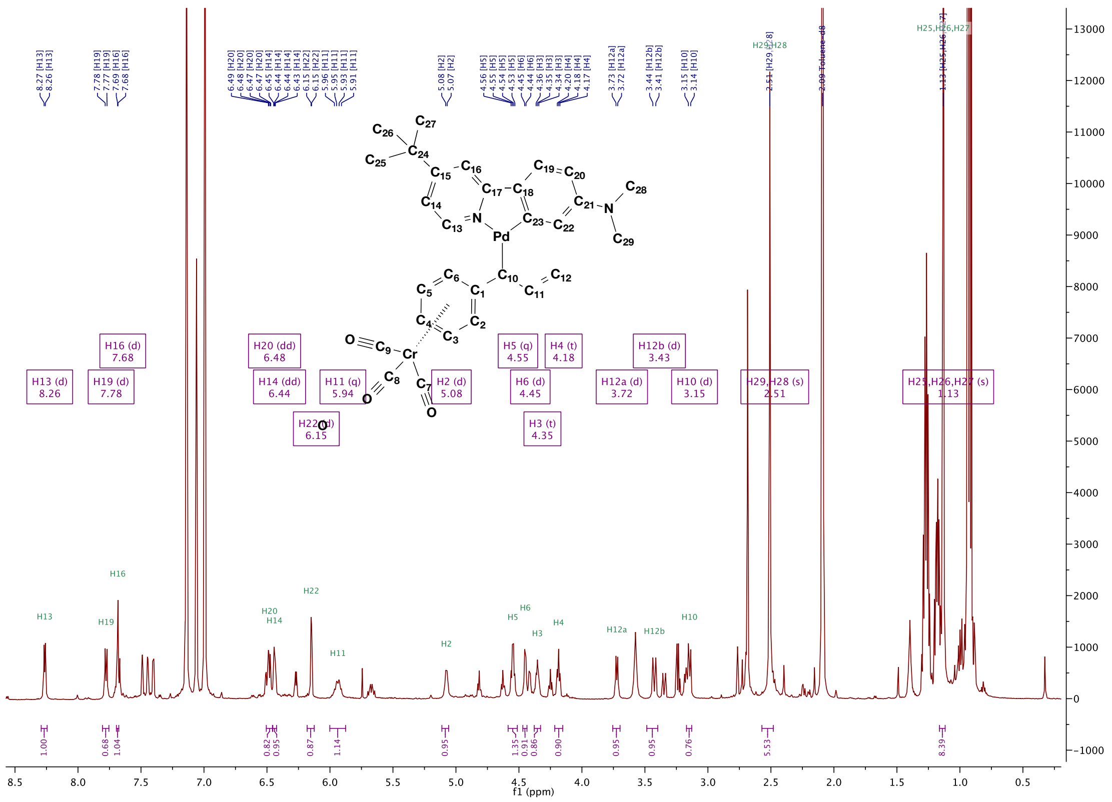

Tol – ^{13}C – 151 Mhz – 233 K.

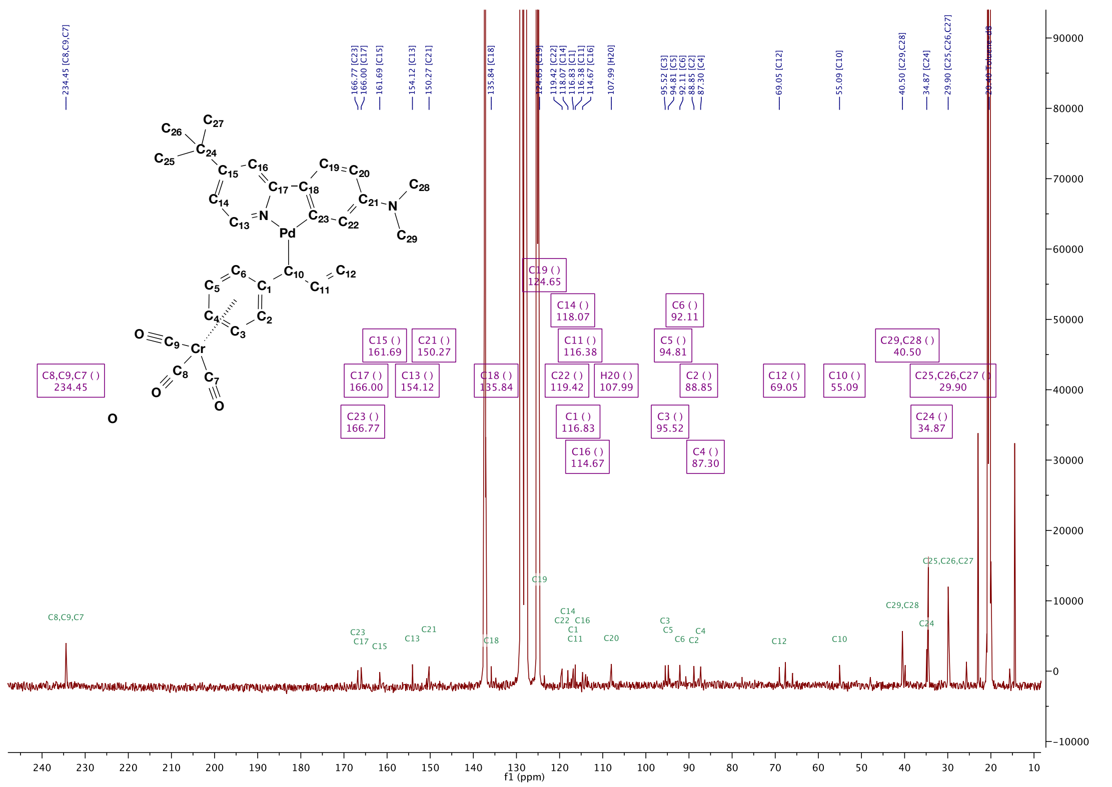

Tol – ^{1}H – 600 Mhz – Variable Temperature.

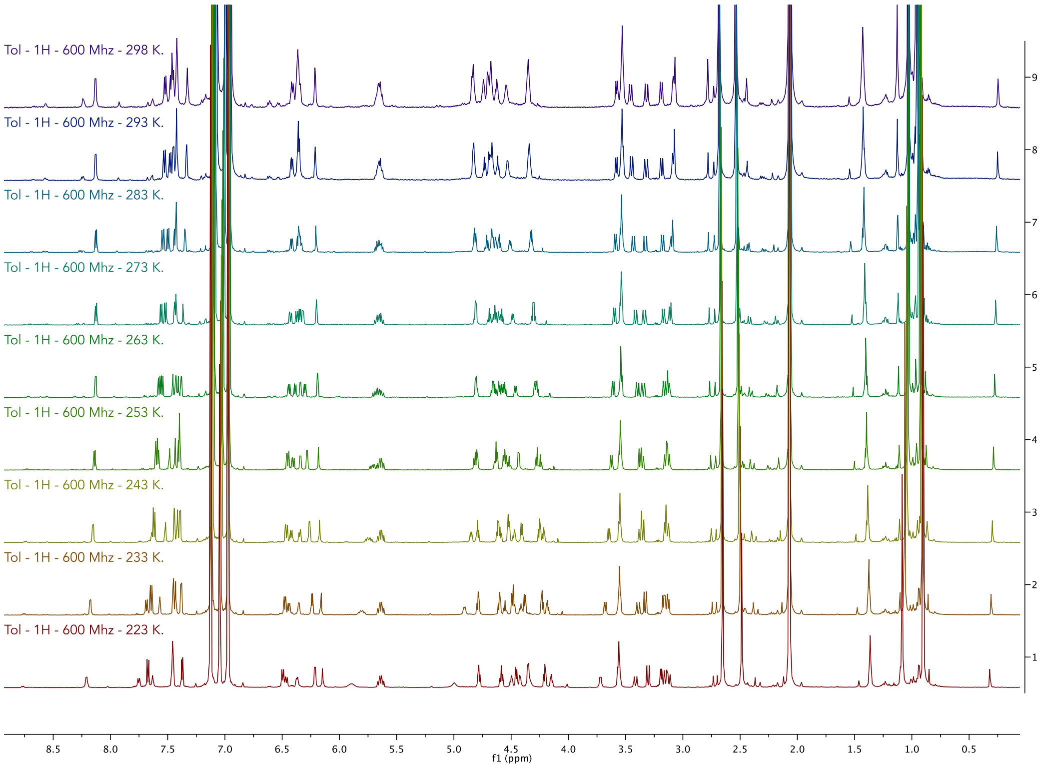

46 - Compound 23.

C_6D_6 – ^1H – 600 Mhz – 298 K.

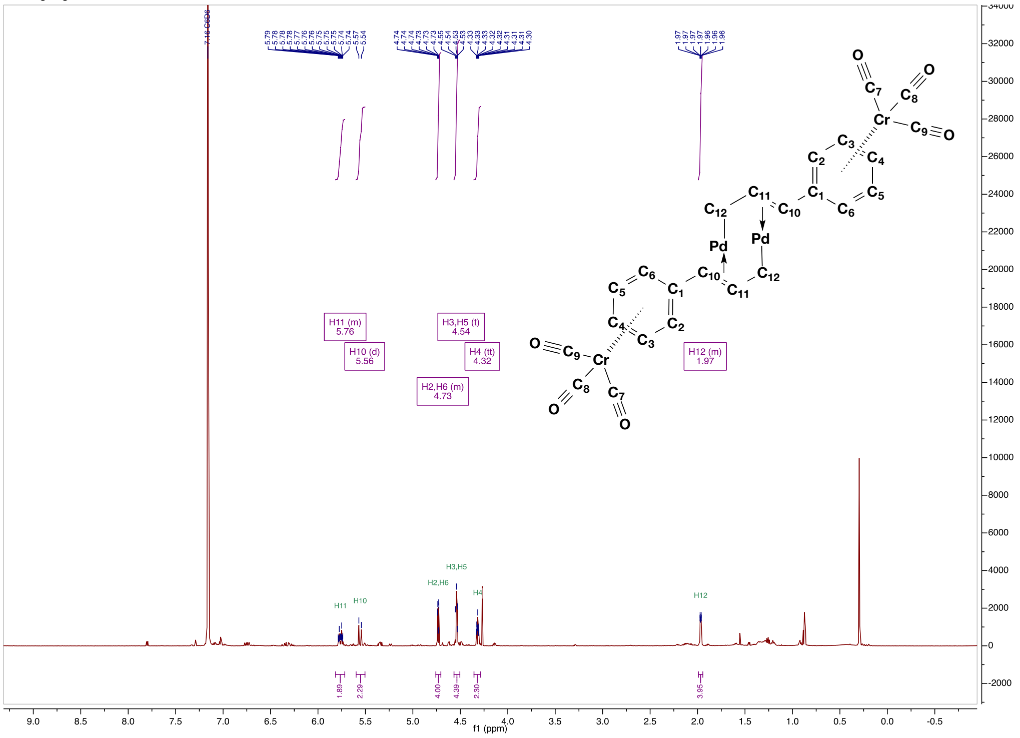

C_6D_6 – ^{13}C – 151 Mhz – 298 K.

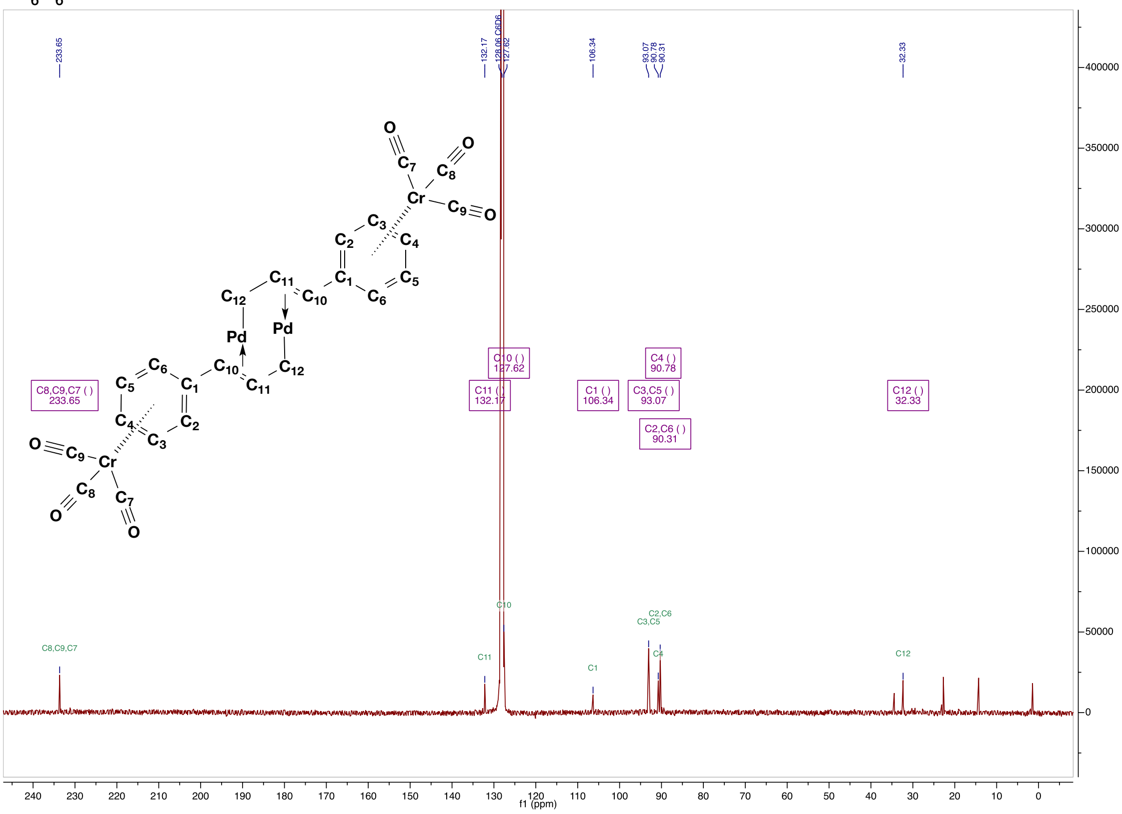

47 - Compound 25a.

C_6D_6 – ^1H – 500 Mhz – 293 K – isomer A.

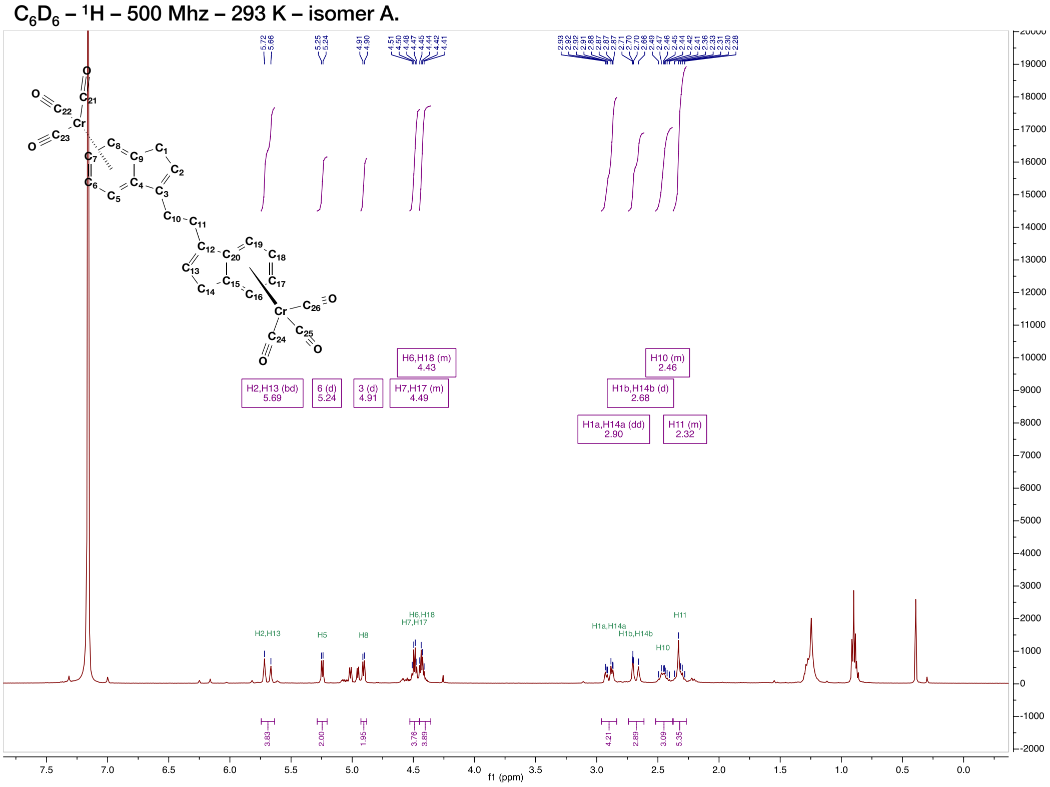

C_6D_6 – ^{13}C – 126 Mhz – 293 K – isomer A.

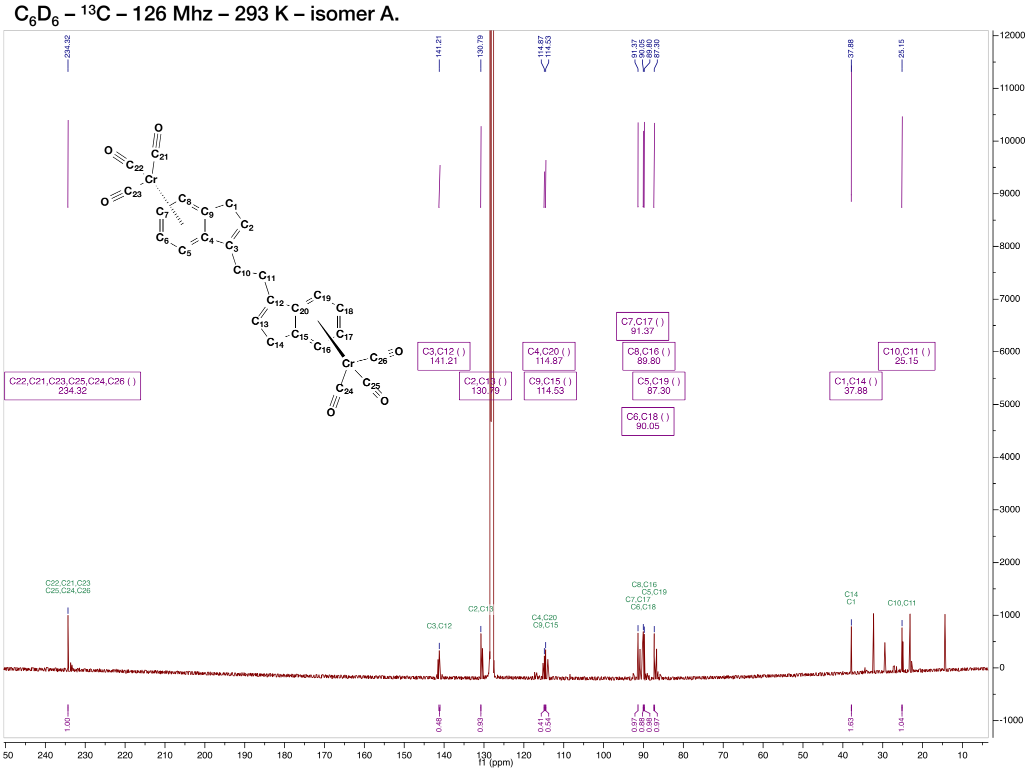

C_6D_6 – ^{1}H – 500 Mhz – 293 K – isomer B.

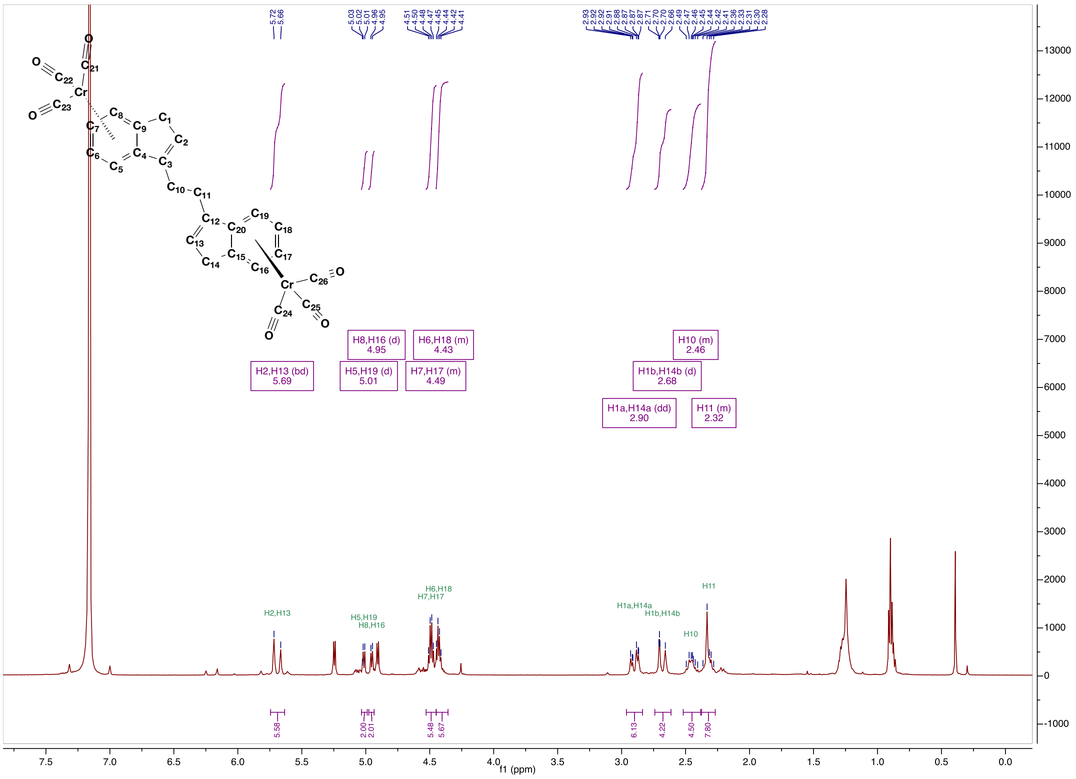

48 - Compound 26a.

C_6D_6 – ^{13}C – 126 Mhz – 293 K – isomer B.

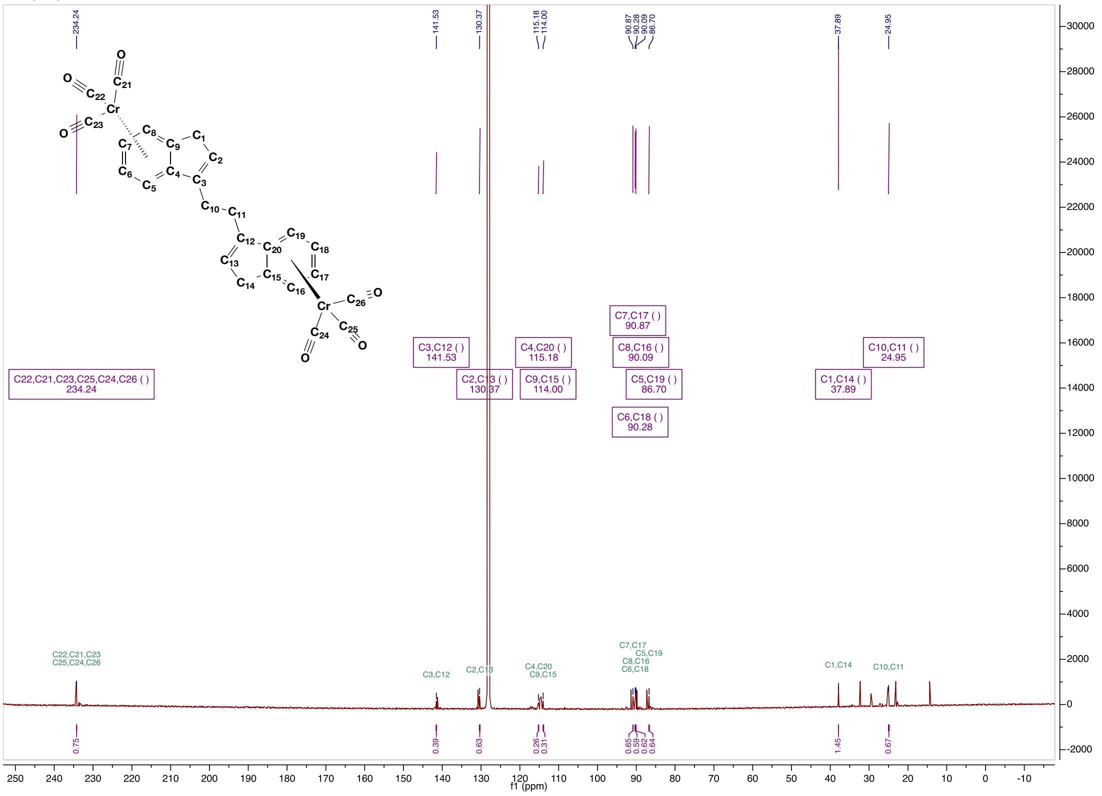

$CDCl_3$ – ^1H – 500 Mhz – 293 K.

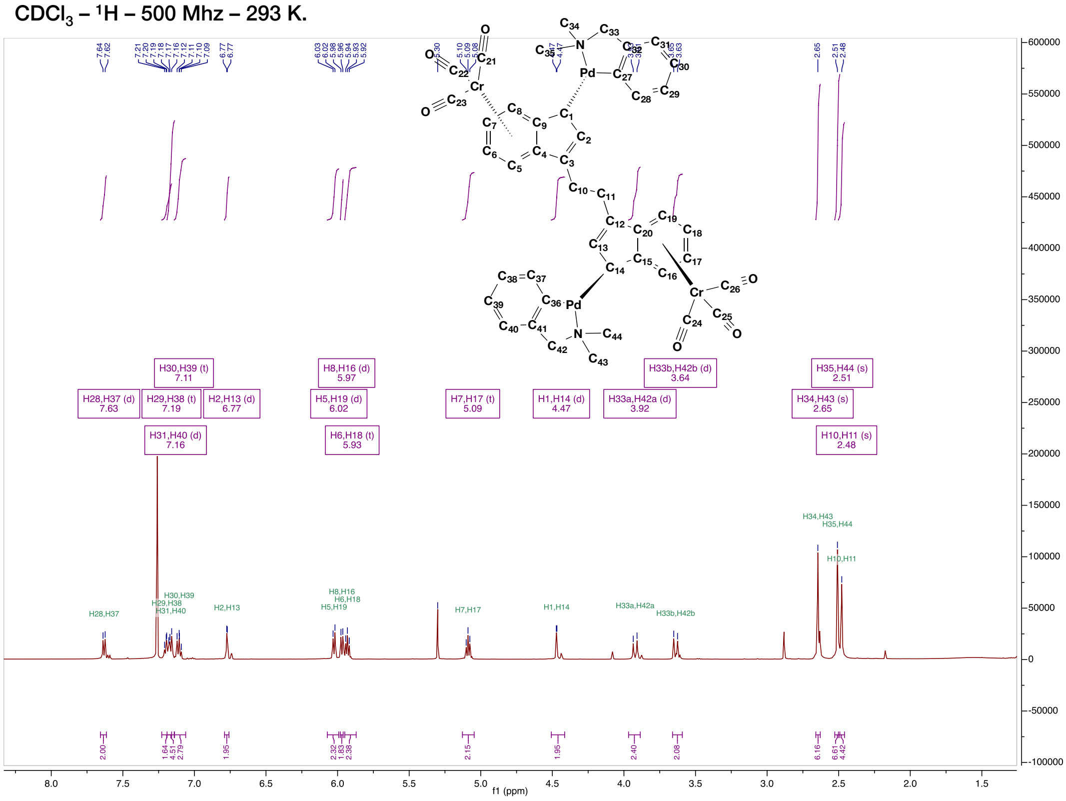

CDCl$_3$ – ^{13}C – 126 Mhz – 293 K.

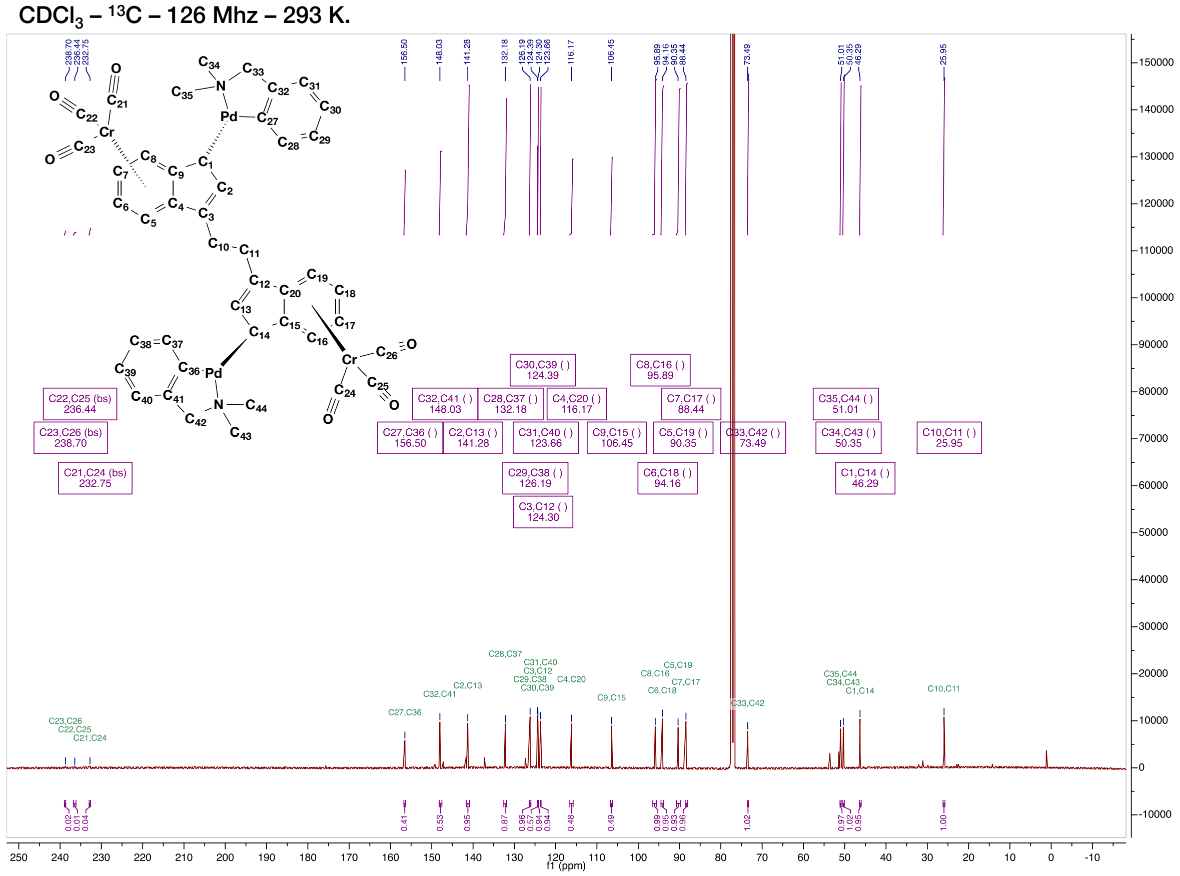

CDCl$_3$ – ^{1}H – 600 Mhz – Variable Temperature.

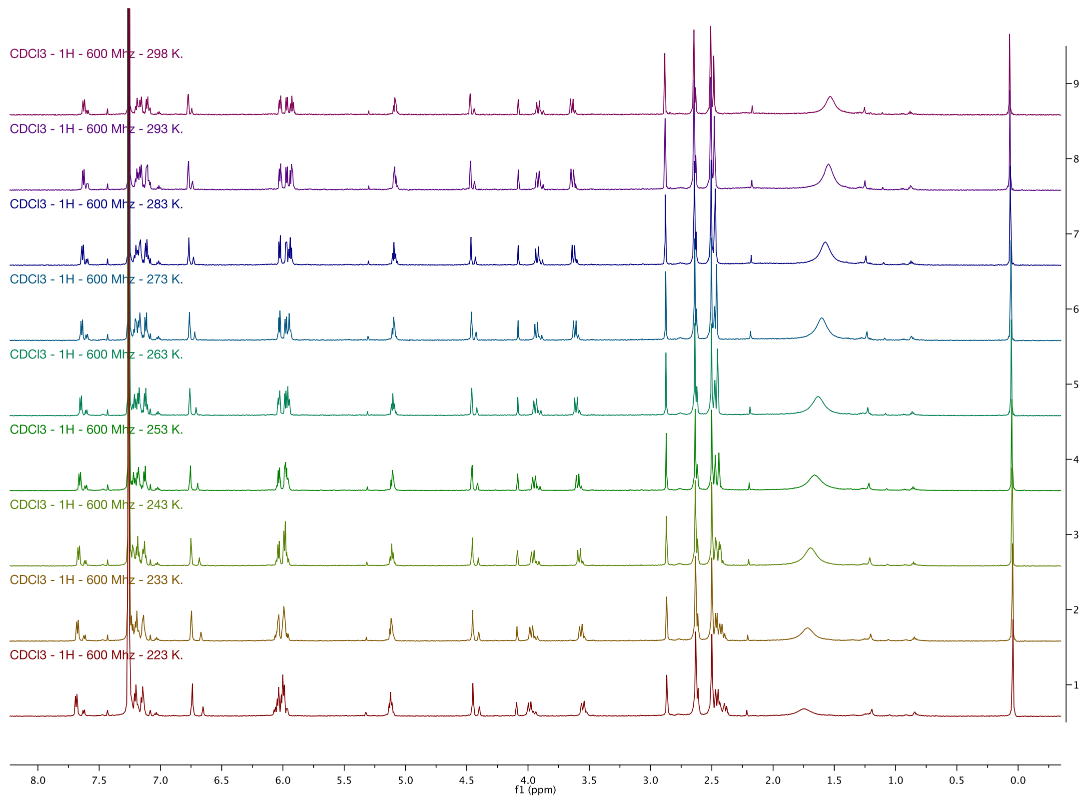

49 - Compound 31a.

CDCl$_3$ – ^{1}H – 500 Mhz – 293 K.

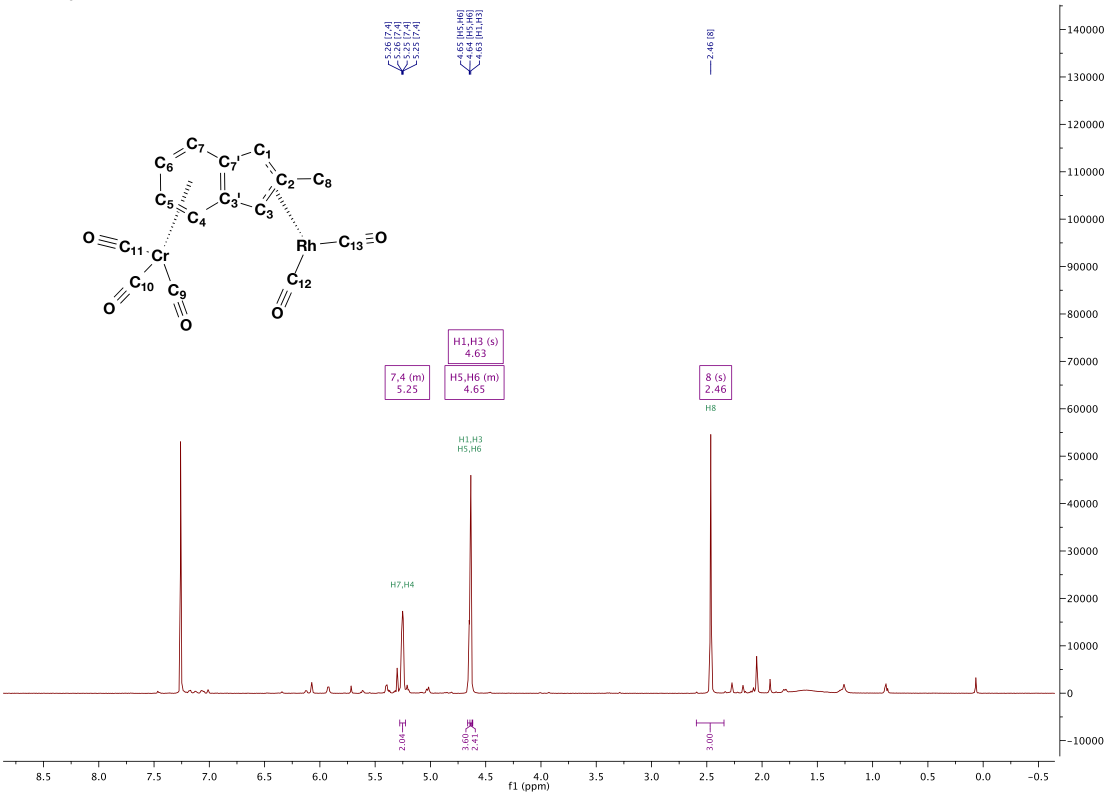

CDCl$_3$ – ^{13}C – 126 Mhz – 293 K.

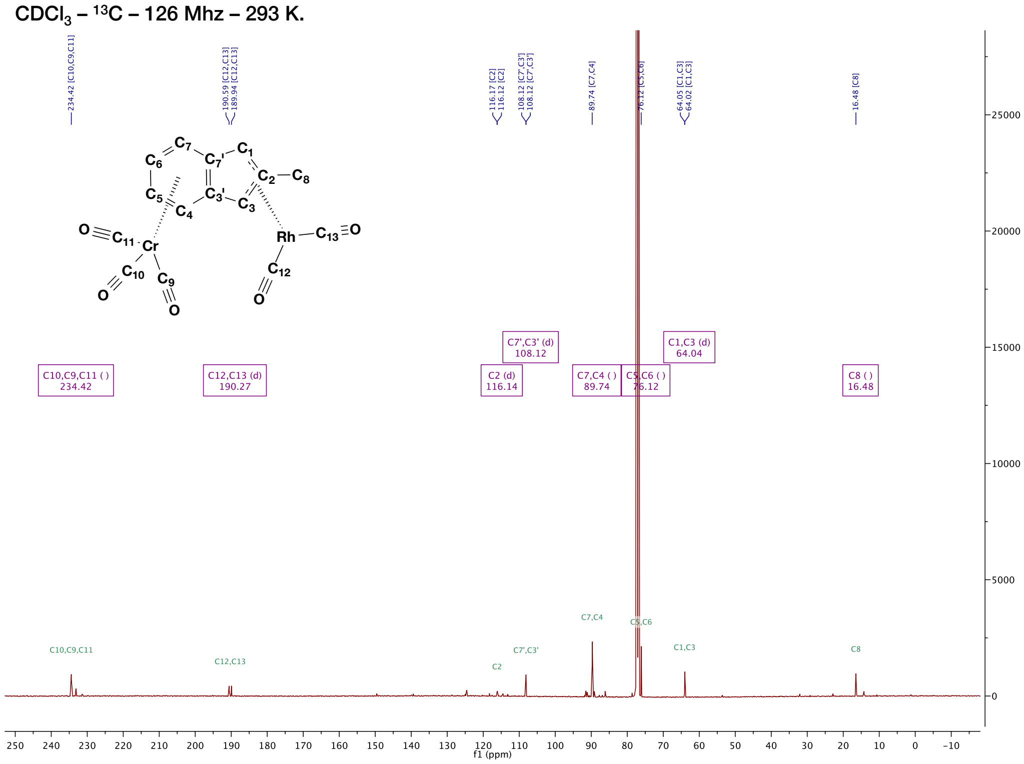

50 - Compound 31b.

C_6D_6 – ^1H – 500 Mhz – 300 K.

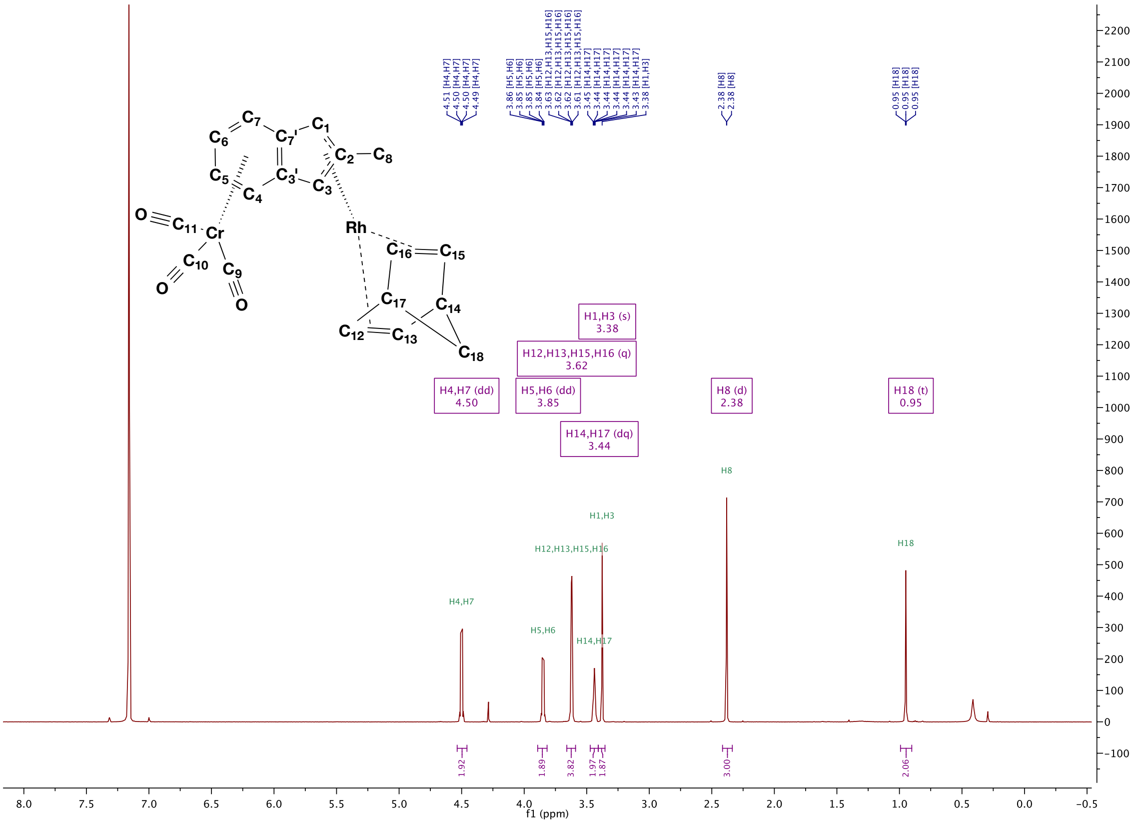

C_6D_6 – ^{13}C – 126 Mhz – 300 K.

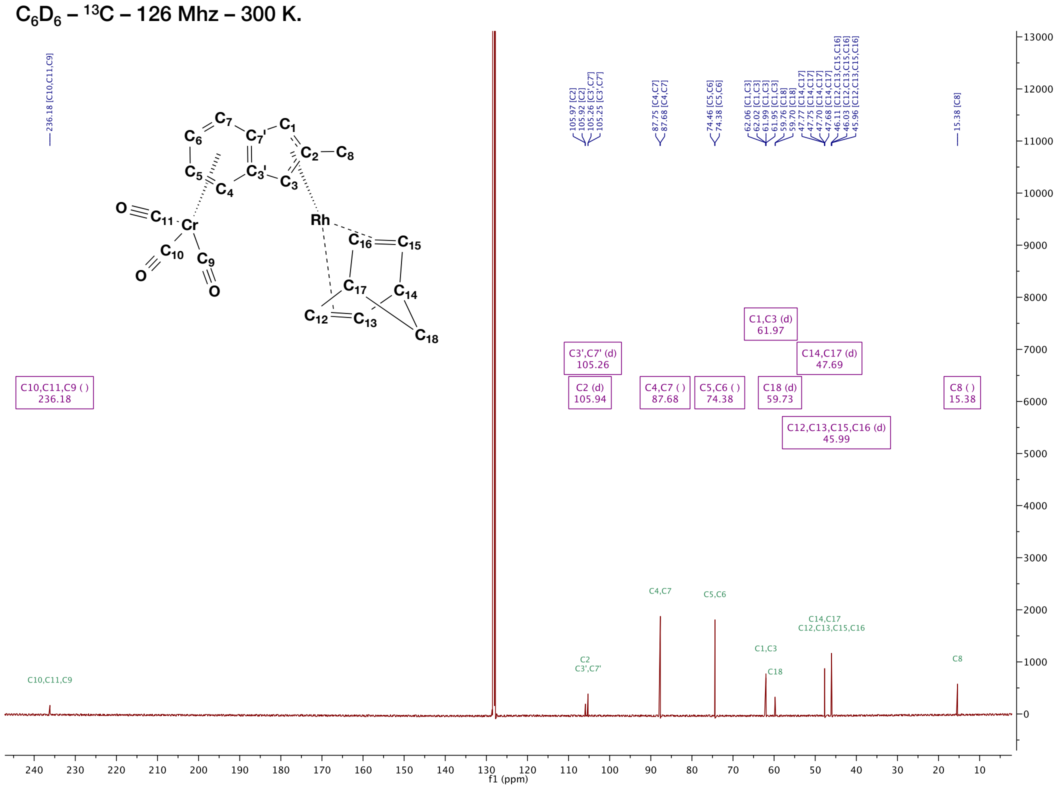

51 - Compound 32a.

CDCl$_3$ – ^{1}H – 500 Mhz – 293 K.

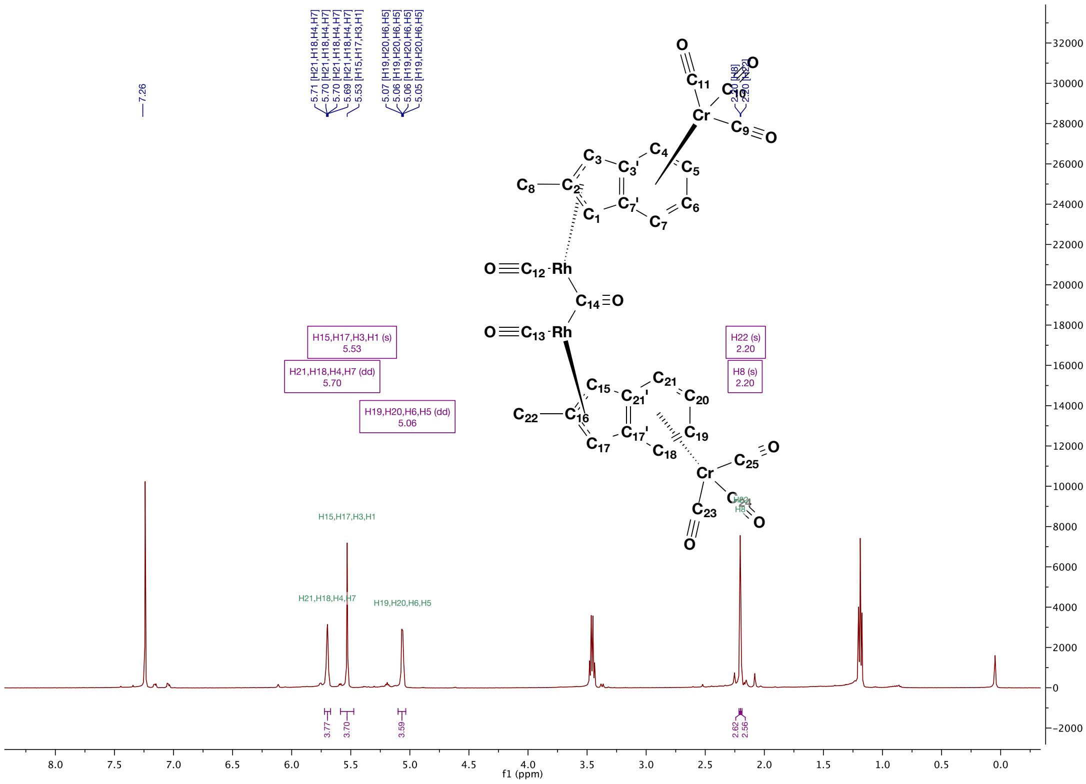

CDCl$_3$ – ^{13}C – 126 Mhz – 293 K.

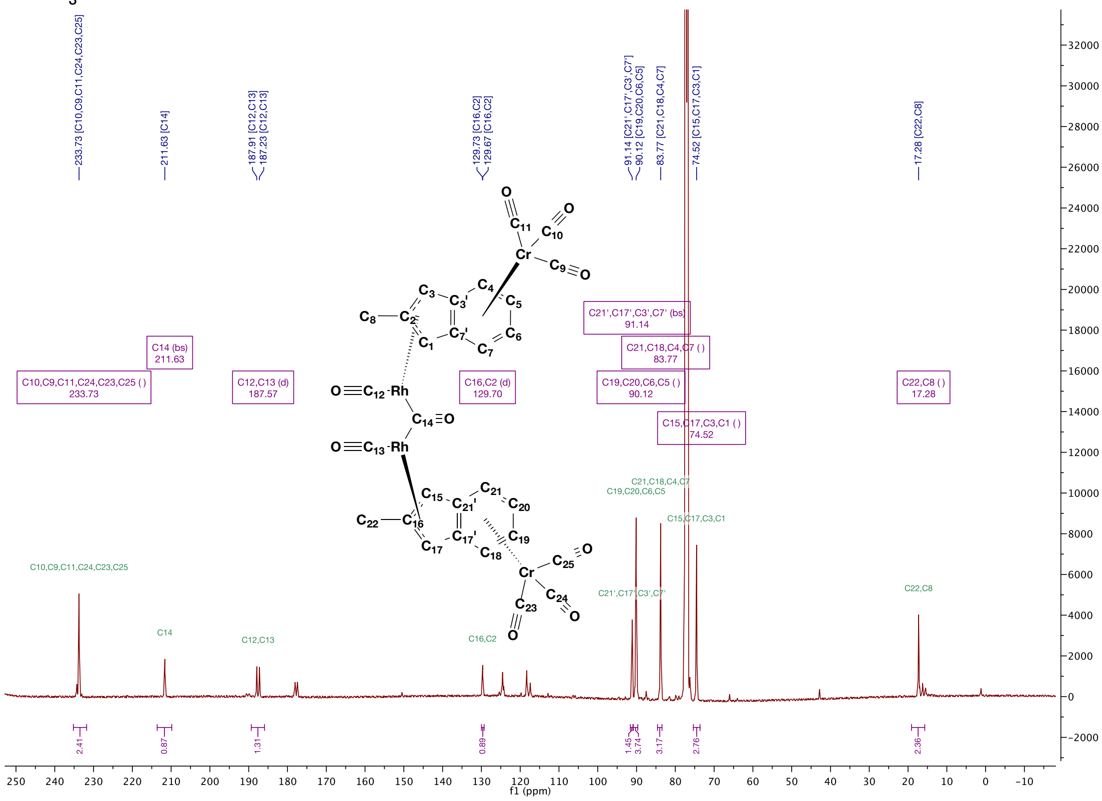

$CDCl_3$ – ¹H – 600 Mhz – Variable Temperature.

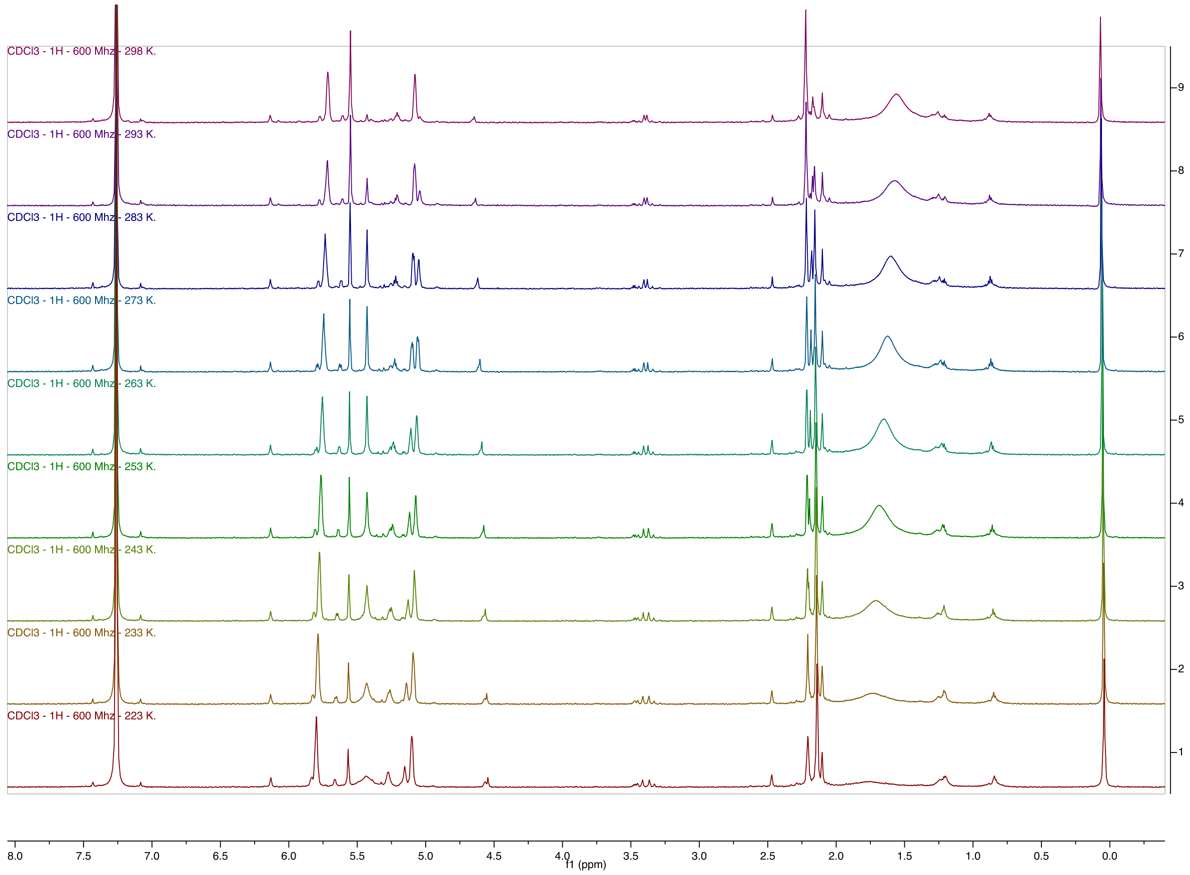

52 - Compound 32c.

C_6D_6 – ^1H – 500 Mhz – 300 K.

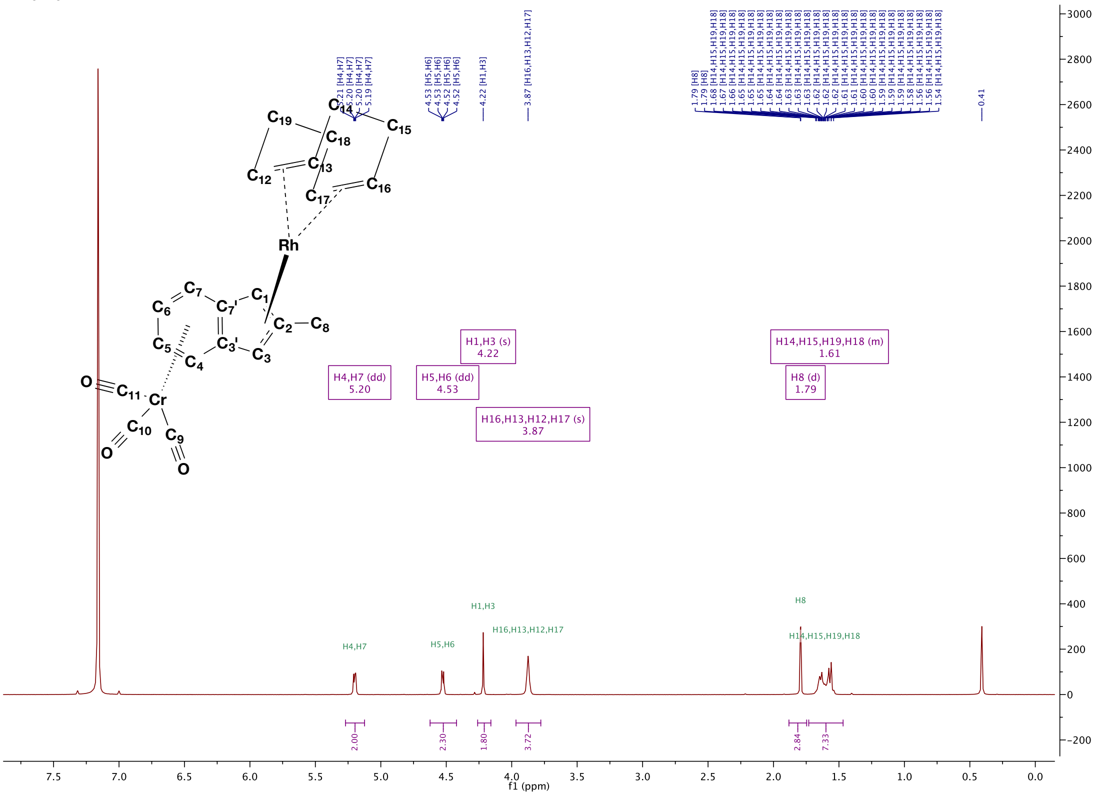

C_6D_6 – ^{13}C – 126 Mhz – 300 K.

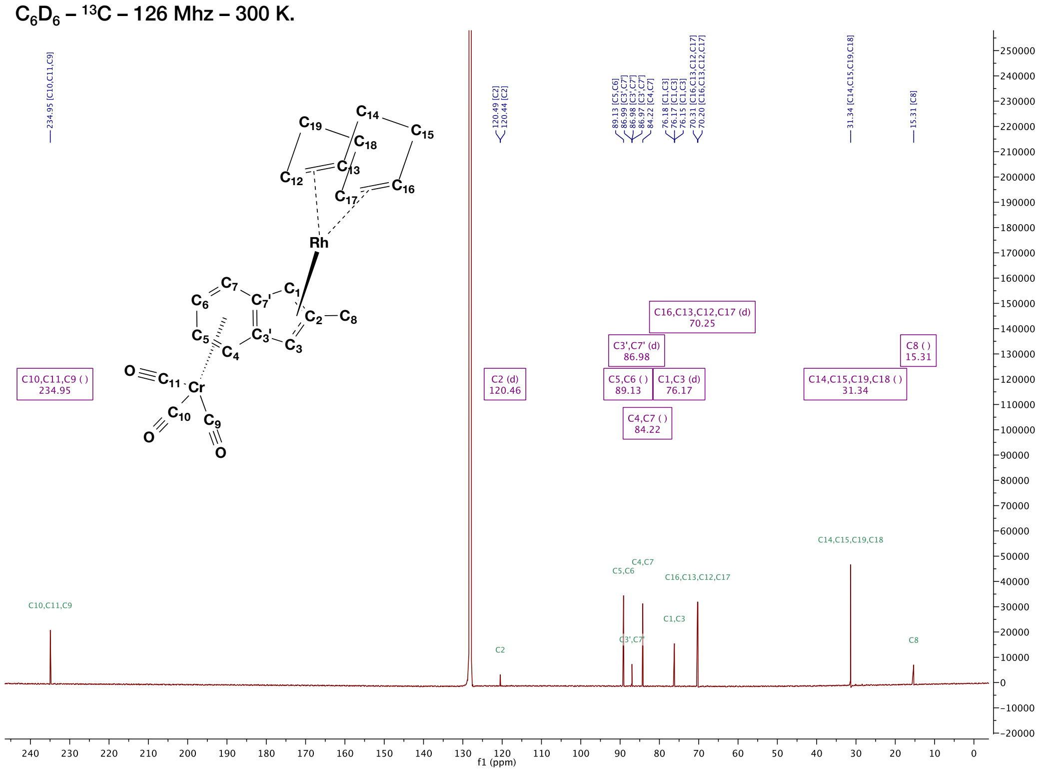

53 - Compound 33a.

CDCl$_3$ – ^{1}H – 600 Mhz – 273 K.

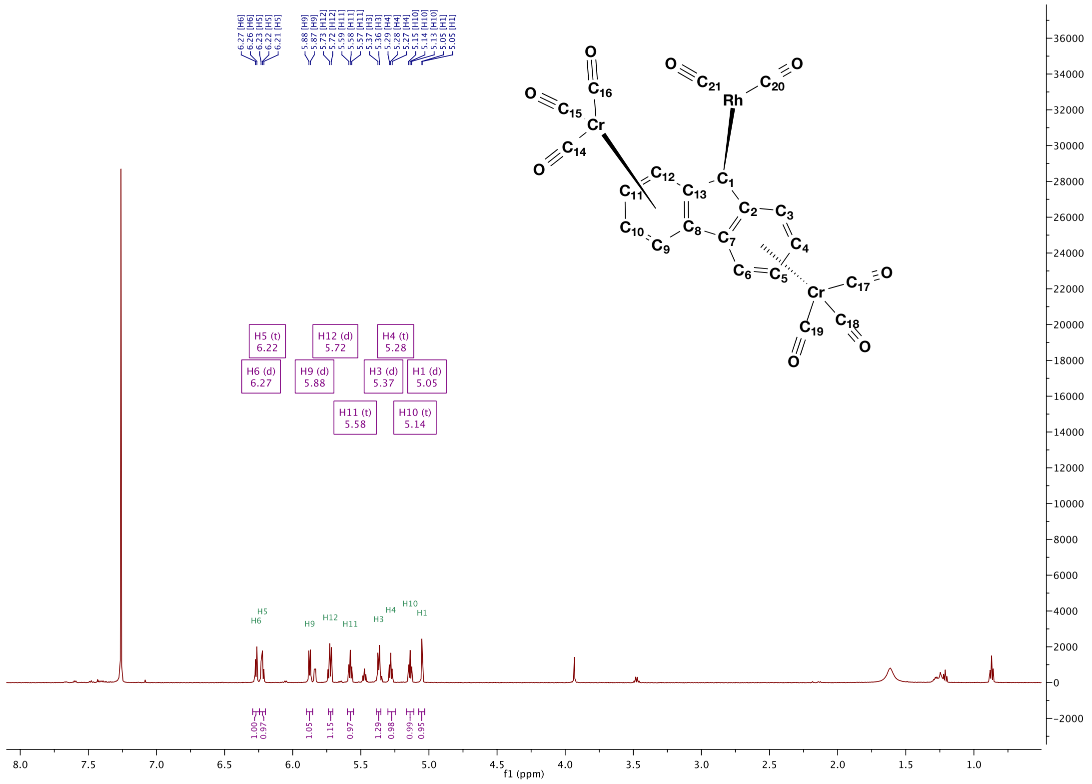

CDCl$_3$ – ^{13}C – 151 Mhz – 279 K.

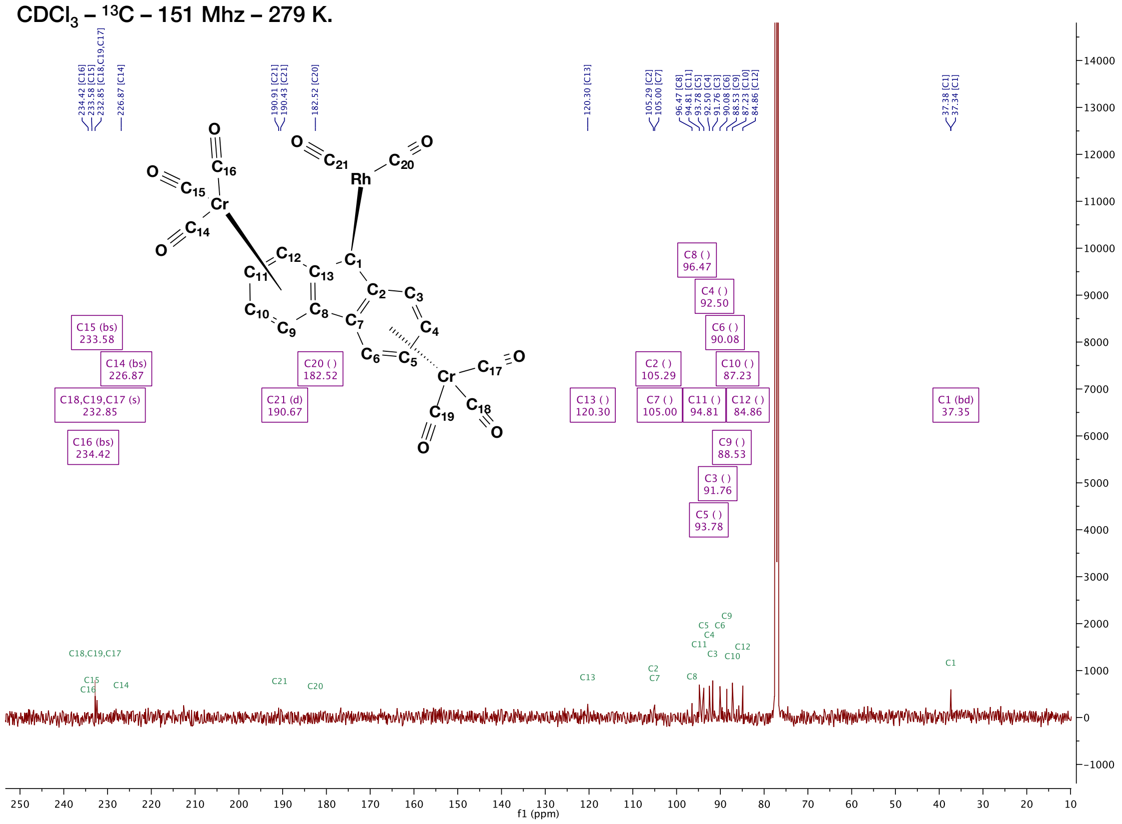

C_6D_6 – ^{13}C – 126 Mhz – 293 K.

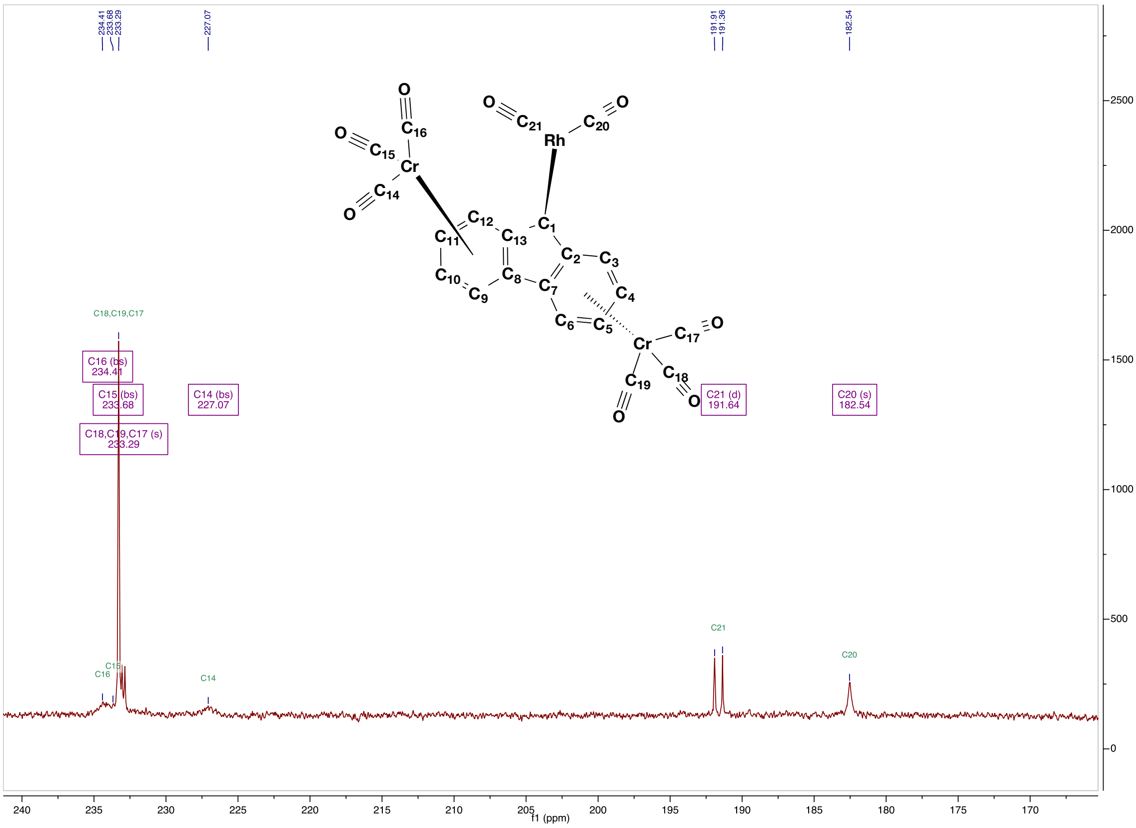

CDCl$_3$ – ^{1}H – 600 Mhz – Variable Temperature.

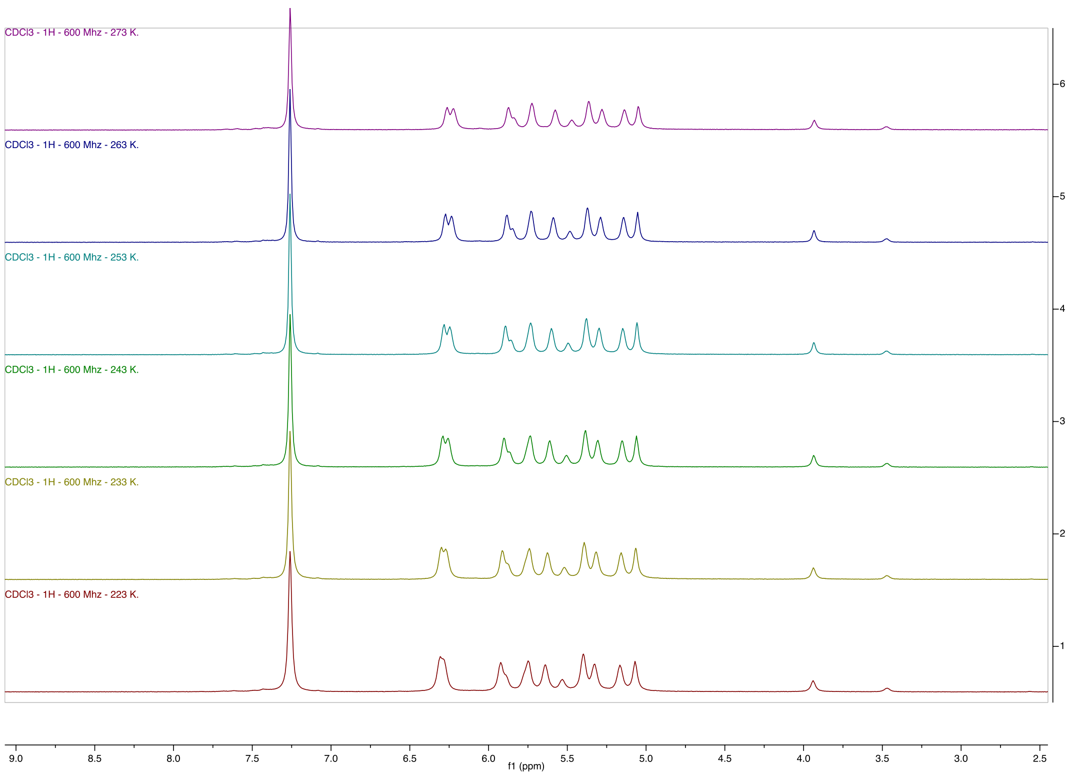

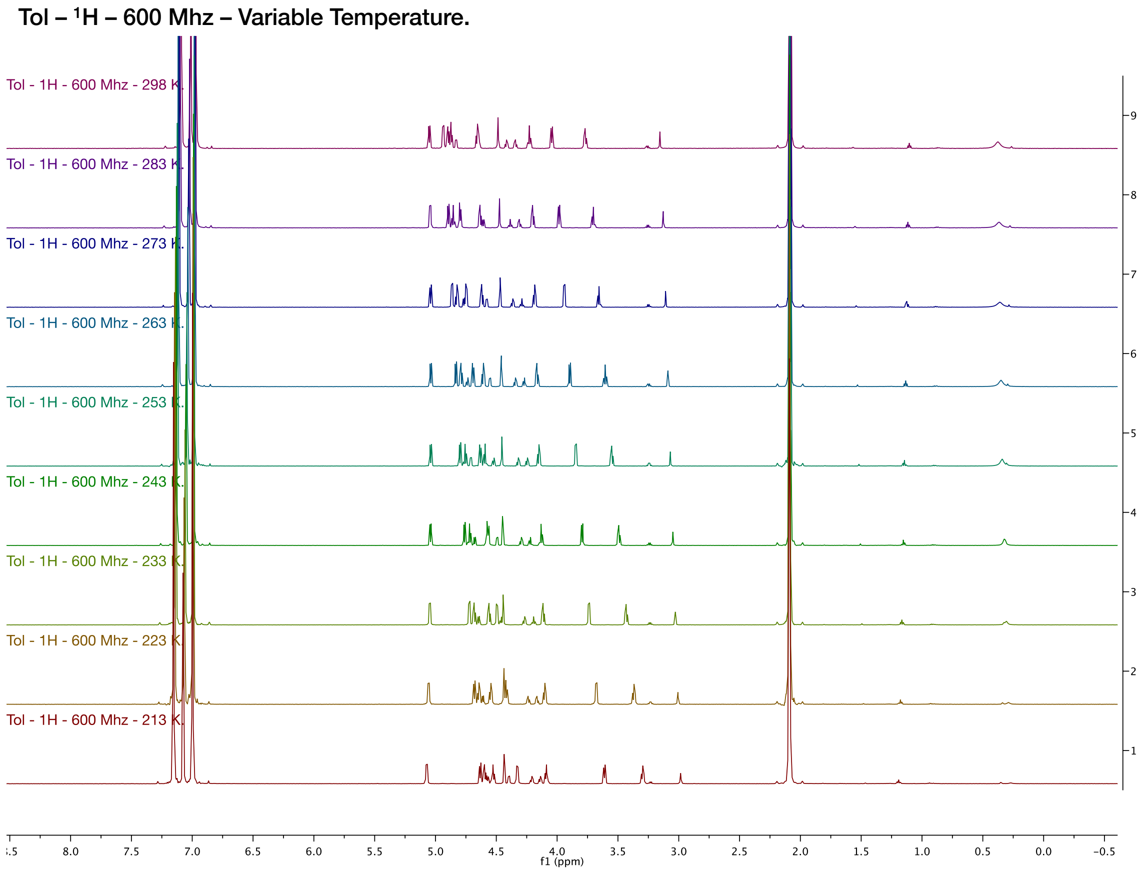
Tol – 1H – 600 Mhz – Variable Temperature.
Tol - 1H - 600 Mhz - 298 K.
Tol - 1H - 600 Mhz - 283 K.
Tol - 1H - 600 Mhz - 273 K.
Tol - 1H - 600 Mhz - 263 K.
Tol - 1H - 600 Mhz - 253 K.
Tol - 1H - 600 Mhz - 243 K.
Tol - 1H - 600 Mhz - 233 K.
Tol - 1H - 600 Mhz - 223 K.
Tol - 1H - 600 Mhz - 213 K.
f1 (ppm)

54 - Compound 33b.

Tol – ^{1}H – 400 Mhz – 233 K.

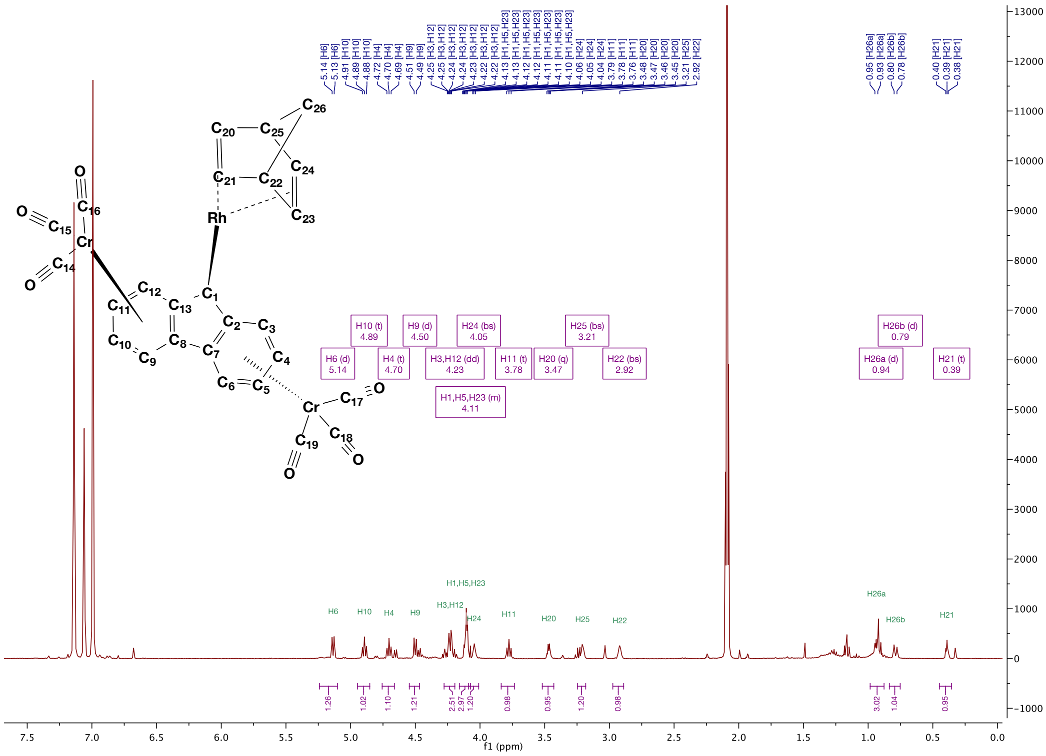

Tol – ^{13}C – 101 Mhz – 233 K.

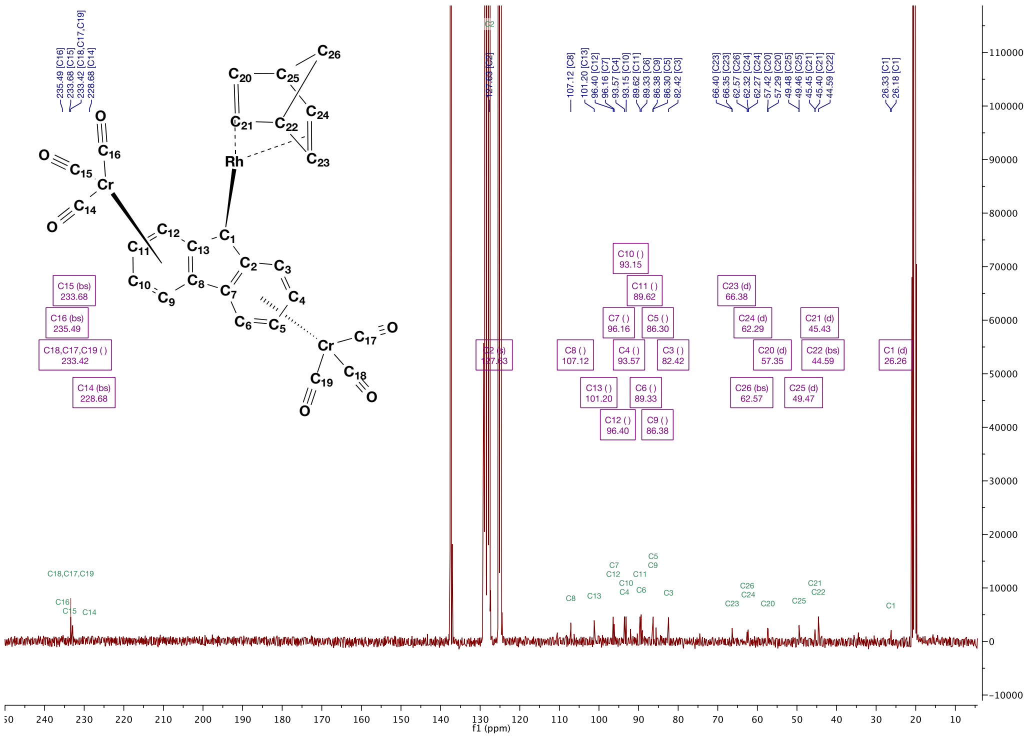

Tol – ^{1}H – 600 Mhz – Variable Temperature.

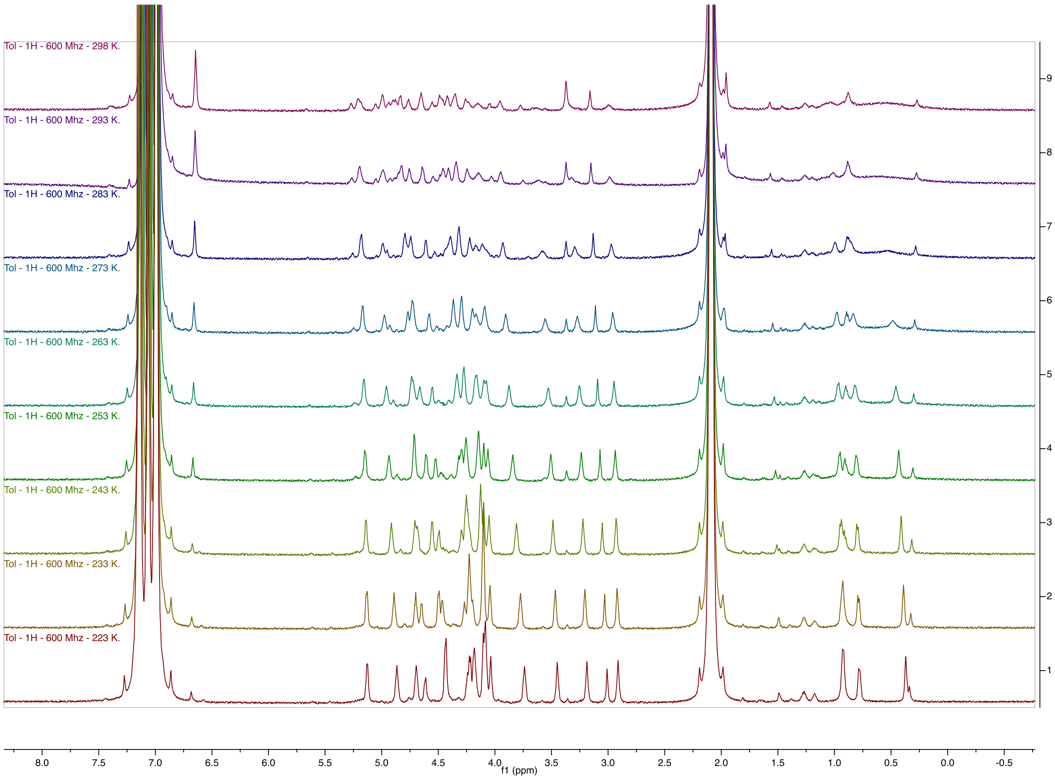

VIII

An excursion into non-covalence

Bibliography

This chapter contains all the literature references used in the context of this manuscript.

Chapter VIII - Bibliography.

Bibliographic references list

[N°1] Kuhn, T. S. *The structure of scientific revolutions*; Fourth edition, **2012**.
[N°2] *Fliegende Blätter* Universitätsbibliothek Heidelberg, **1892**; Vol. 2465, 147.
[N°3] van der Waals, J. D. In *Nobel Lecture: The Equation of State for Gases and Liquids*; Nobelprize.org, Nobel Media AB 2013: Web. 26 Jun 2014: nobelprize.org/nobel_prizes/physics/laureates/1910/waals-lecture.html, 1910.
[N°4] van der Waals, J. D. In *"Johannes Diderik van der Waals - Facts"*; Nobelprize.org, Nobel Media AB 2013: Web. 26 Jun 2014: nobelprize.org/nobel_prizes/physics/laureates/1910/waals-facts.html.
[N°5] Kamerlingh Onnes, H. *Proc. R. Netherlands Acad. Arts Sci. (KNAW) 11* **1909**, 168.
[N°6] Page, C. H. *Phys. Rev.* **1938**, *53*, 426.
[N°7] Kamerlingh Onnes, H. In *Nobel Lecture: Investigations into the Properties of Substances at Low Temperatures, which Have Led, amongst Other Things, to the Preparation of Liquid Helium*; Nobelprize.org, Nobel Media AB 2013: Web. 27 Jun 2014: nobelprize.org/nobel_prizes/physics/laureates/1913/onnes-lecture.html, 1913.
[N°8] London, F. *Trans. Faraday Soc.* **1937**, *33*, 8b.
[N°9] London, F. *Z. Physik* **1930**, *63*, 245.
[N°10] Eisenschitz, R.; London, F. *Z. Physik* **1930**, *60*, 491.
[N°11] Hellmann, H. *Acta Physicochim.* **1935**, 273.
[N°12] Hobza, P.; Zahradnik, R.; Muller-Dethlefs, K. *Collect Czech Chem C* **2006**, *71*, 443.
[N°13] Kaplan, I. G. *Intermolecular Interactions; Physical Picture, Computational Methods and Model Potentials*; Wiley, Chichester, **2006**.
[N°14] Stone, A. J. *The Theory of Intermolecular Forces,* ; Oxford University Press; Oxford, **2002**.
[N°15] Müller-Dethlefs, K.; Hobza, P. *Chem. Rev.* **2000**, *100*, 143.
[N°16] Hirschfelder, J. O.; Curtiss, C. F.; Bird, R. B. *Molecular Theory of Gases and Liquids*; Wiley, New York, **1954**.
[N°17] Lehn, J.-M. *Angew. Chem. Int. Ed. Engl.* **1988**, *27*, 89.
[N°18] Hobza, P.; Muller-Dethlefs, K. In *Non-Covalent Interactions: Theory and Experiment*; The Royal Society of Chemistry: **2009**.
[N°19] Ponder, J. W.; Case, D. A. *Advances in protein chemistry* **2003**, *66*, 27.
[N°20] Lewis, G. N. *J. Am. Chem. Soc.* **1916**, *38*, 762.
[N°21] Campargue, R. *J. Phys. Chem.* **1984**, *88*, 4466.
[N°22] Herzberg, G. *Molecular Spectra and Molecular Structure: Electronic Spectra and Electronic Structure of Polyatomic Molecules.*
[N°23] In *Molecular Symmetry and Spectroscopy*; Bunker, P. R., Ed.; Academic Press: **1979**.
[N°24] Pauling, L. *J. Am. Chem. Soc.* **1931**, *53*, 1367.
[N°25] Schrödinger, E. *Phys. Rev.* **1926**, *28*, 1049.
[N°26] Heisenberg, W. *Z. Physik* **1927**, *43*, 172.
[N°27] Than, J. Web. UC Davis Chemwiki an Open Access textbook environment.
[N°28] Atkins, P.; de Paula, J. *Physical Chemistry for the Life Sciences*; Oxford, UK: Oxford University Press. 2006. 95.
[N°29] Coulomb, C. A. *Premier mémoire sur l'électricité et le magnétisme*; Histoire de l'Académie Royale des Sciences, Imprimerie Royale, **1785**, 569–577.
[N°30] Coulomb, C. A. *Second mémoire sur l'électricité et le magnétisme*; Histoire de l'Académie Royale des Sciences, Imprimerie Royale, **1785**, 578–611.
[N°31] Jackson, J. D. *Classical Electrodynamics*; John Wiley & Sons Ltd., **1962**.
[N°32] Leachman, J. W.; Jacobsen, R. T.; Penoncello, S. G.; Lemmon, E. W. *J. Phys. Chem.* **2009**, *38*.
[N°33] Benmore, C. J.; Tomberli, B.; Egelstaff, P. A.; Neuefeind, J. *Mol. Phys.* **2001**, *99*, 787.
[N°34] Béguin, L.; Vernier, A.; Chicireanu, R.; Lahaye, T.; Browaeys, A. *Phys. Rev. Lett.* **2013**, *110*, 263201.
[N°35] Tadmor, R. *J. Phys. Condens. Mat.* **2001**, *13*, L195.
[N°36] de Boer, J. H. *Trans. Faraday Soc.* **1936**, *32*, 10.
[N°37] Bradley, R. S. *Phil. Mag. Ser. 7* **1932**, *13*, 853.
[N°38] Brdarski, S.; Karlström, G. *J. Phys. Chem. A* **1998**, *102*, 8182.
[N°39] Pavarini, E.; Koch, E.; Anders, F. In *Correlated electrons: From Models to Materials* **2012**.
[N°40] Weisskopf, V. F. *Science* **1975**, *187*, 605.
[N°41] Andersen, H. C.; Chandler, D.; Weeks, J. D. *J. Chem. Phys.* **1972**, *56*, 3812.
[N°42] Dirac, P. A. M. *Proc. royal. soc. Lond. S. A* **1926**, *112*, 661.
[N°43] Pauli, W. In *Nobel Lecture: Exclusion Principle and Quantum Mechanics*; Nobelprize.org, Nobel Media AB 2013: Web. 8 Jul 2014: nobelprize.org/nobel_prizes/physics/laureates/1945/pauli-lecture.html.
[N°44] In *IUPAC. Compendium of Chemical Terminology*; Version 2.3.3 - 2014-02-24 - the "Gold Book". ed. XML on-line corrected version: Web. 24 Jul 2014: goldbook.iupac.org.
[N°45] Nieckarz, R. J.; Oldridge, N.; Fridgen, T. D.; Li, G. P.; Hamilton, I. P.; McMahon, T. B. *J. Phys. Chem. A* **2009**, *113*, 644.
[N°46] Emsley, J.; Parker, R. J.; Overill, R. E. *J. Chem. Soc., Farad. T. 2* **1983**, *79*, 1347.
[N°47] Chandler, D. *Nature* **2005**, *437*, 640.
[N°48] Tanford, C. *Prot. Sci.* **1997**, *6*, 1358.
[N°49] Kauzmann, W. In *Advances in Protein Chemistry*; C.B. Anfinsen, M. L. A. K. B., John, T. E., Eds.; Academic Press: **1959**; Vol. Volume 14, p 1.
[N°50] Dyson, H. J.; Wright, P. E.; Scheraga, H. A. *Proc. Natl. Acad. Sci. USA* **2006**, *103*, 13057.
[N°51] Cerny, J.; Hobza, P. *Phys. Chem. Chem. Phys.* **2007**, *9*, 5291.
[N°52] Meyer, E. A.; Castellano, R. K.; Diederich, F. *Angew. Chem. Int. Ed. Engl.* **2003**, *42*, 1210.
[N°53] Kannan, N.; Vishveshwara, S. *Ptrotein Eng.* **2000**, *13*, 753.
[N°54] Kim, K. S.; Tarakeshwar, P.; Lee, J. Y. *Chem. Rev.* **2000**, *100*, 4145.
[N°55] Hobza, P.; Šponer, J. *Chem. Rev.* **1999**, *99*, 3247.
[N°56] Lehn, J.-M. In *Supramolecular Chemistry*; Wiley-VCH Verlag GmbH & Co. KGaA: **1995**.
[N°57] Djukic, J.-P.; Sortais, J.-B.; Barloy, L.; Pannetier, N.; Sirlin, C.; Pfeffer, M. *Organometallics* **2012**, *31*, 2821.
[N°58] Martinez, C. R.; Iverson, B. L. *Chem. Sci.* **2012**, *3*, 2191.

[N°59] Grimme, S. *Angew. Chem. Int. Ed. Engl.* **2008**, *47*, 3430.
[N°60] Swart, M.; van der Wijst, T.; Fonseca Guerra, C.; Bickelhaupt, F. M. *J. Mol. Model.* **2007**, *13*, 1245.
[N°61] Sinnokrot, M. O.; Sherrill, C. D. *J. Phys. Chem. A* **2006**, *110*, 10656.
[N°62] Grimme, S.; Mück-Lichtenfeld, C.; Antony, J. *J. Phys. Chem. C* **2007**, *111*, 11199.
[N°63] Rapacioli, M.; Calvo, F.; Spiegelman, F.; Joblin, C.; Wales, D. J. *J. Phys. Chem. A* **2005**, *109*, 2487.
[N°64] Podeszwa, R.; Bukowski, R.; Szalewicz, K. *J. Phys. Chem. A* **2006**, *110*, 10345.
[N°65] Grant Hill, J.; Platts, J. A.; Werner, H.-J. *Phys. Chem. Chem. Phys.* **2006**, *8*, 4072.
[N°66] Tsuzuki, S. In *Intermolecular Forces and Clusters I*; Wales, D. J., Ed.; Springer Berlin Heidelberg: **2005**; Vol. 115, p 149.
[N°67] Hunter, C. A.; Sanders, J. K. M. *J. Am. Chem. Soc.* **1990**, *112*, 5525.
[N°68] Cozzi, F.; Ponzini, F.; Annunziata, R.; Cinquini, M.; Siegel, J. S. *Angew. Chem. Int. Ed. Engl.* **1995**, *34*, 1019.
[N°69] Cubberley, M. S.; Iverson, B. L. *J. Am. Chem. Soc.* **2001**, *123*, 7560.
[N°70] Rashkin, M. J.; Waters, M. L. *J. Am. Chem. Soc.* **2002**, *124*, 1860.
[N°71] Wheeler, S. E. *J. Am. Chem. Soc.* **2011**, *133*, 10262.
[N°72] Wheeler, S. E.; Houk, K. N. *J. Am. Chem. Soc.* **2008**, *130*, 10854.
[N°73] Hobza, P.; Selzle, H. L.; Schlag, E. W. *Chem. Rev.* **1994**, *94*, 1767.
[N°74] Hobza, P.; Zahradnik, R. *Chem. Rev.* **1988**, *88*, 871.
[N°75] Riehn, C.; Lahmann, C.; Wassermann, B.; Brutschy, B. *Chem. Phys. Lett.* **1992**, *197*, 443.
[N°76] Tanner, C.; Henseler, D.; Leutwyler, S.; Connell, L. L.; Felker, P. M. *J. Chem. Phys.* **2003**, *118*, 9157.
[N°77] Lee, S.; Romascan, J.; Felker, P. M.; Pedersen, T. B.; Fernandez, B.; Koch, H. *J. Chem. Phys.* **2003**, *118*, 1230.
[N°78] Lee, S.; Chung, J. S.; Felker, P. M.; Cacheiro, J. L.; Fernandez, B.; Pedersen, T. B.; Koch, H. *J. Chem. Phys.* **2003**, *119*, 12956.
[N°79] Kim, W.; Schaeffer, M. W.; Lee, S.; Chung, J. S.; Felker, P. M. *J. Chem. Phys.* **1999**, *110*, 11264.
[N°80] Garrett, B. C.; Dixon, D. A.; Camaioni, D. M.; Chipman, D. M.; Johnson, M. A.; Jonah, C. D., . . . Zwier, T. S. *Chem. Rev.* **2005**, *105*, 355.
[N°81] Abou El-Nasr, A. B. E. H.; Fujii, A.; Ebata, T.; Mikami, N. *Mol. Phys.* **2005**, *103*, 1561.
[N°82] El-Hakam, E. A.; Ei-Nasr, A.; Fujii, A.; Yahagi, T.; Ebata, T.; Mikami, N. *J. Phys. Chem. A* **2005**, *109*, 2498.
[N°83] Imhof, P.; Krugler, D.; Brause, R.; Kleinermanns, K. *J. Chem. Phys.* **2004**, *121*, 2598.
[N°84] Wu, R. H.; Brutschy, B. *J. Phys. Chem. A* **2004**, *108*, 9715.
[N°85] Schmitt, M.; Ratzer, C.; Meerts, W. L. *J. Chem. Phys.* **2004**, *120*, 2752.
[N°86] Westphal, A.; Jacoby, C.; Ratzer, C.; Reichelt, A.; Schmitt, M. *Phys. Chem. Chem. Phys.* **2003**, *5*, 4114.
[N°87] Schmitt, M.; Jacoby, C.; Gerhards, M.; Unterberg, C.; Roth, W.; Kleinermanns, K. *J. Chem. Phys.* **2000**, *113*, 2995.
[N°88] Jacoby, C.; Roth, W.; Schmitt, M.; Janzen, C.; Spangenberg, D.; Kleinermanns, K. *J. Phys. Chem. A* **1998**, *102*, 4471.
[N°89] Roth, W.; Schmitt, M.; Jacoby, C.; Spangenberg, D.; Janzen, C.; Kleinermanns, K. *Chem. Phys.* **1998**, *239*, 1.
[N°90] Giuliano, B. M.; Ottaviani, P.; Caminati, W.; Schnell, M.; Banser, D.; Grabow, J. U. *Chem. Phys.* **2005**, *312*, 111.
[N°91] Sanchez, R.; Blanco, S.; Lesarri, A.; Lopez, J. C.; Alonso, J. L. *Chem. Phys. Lett.* **2005**, *401*, 259.
[N°92] Blanco, S.; Lopez, J. C.; Lesarri, A.; Caminati, W.; Alonso, J. L. *Mol. Phys.* **2005**, *103*, 1473.
[N°93] Giuliano, B. M.; Caminati, W. *Angew. Chem. Int. Ed. Engl.* **2005**, *44*, 603.
[N°94] Caminati, W.; Lopez, J. C.; Alonso, J. L.; Grabow, J. U. *Angew. Chem. Int. Ed. Engl.* **2005**, *44*, 3840.
[N°95] Lesarri, A.; Cocinero, E. J.; Lopez, J. C.; Alonso, J. L. *Angew. Chem. Int. Ed. Engl.* **2004**, *43*, 605.
[N°96] Alonso, J. L.; Antolinez, S.; Blanco, S.; Lesarri, A.; Lopez, J. C.; Caminati, W. *J. Am. Chem. Soc.* **2004**, *126*, 3244.
[N°97] Cole, G. C.; Legon, A. C. *J. Chem. Phys.* **2004**, *121*, 10467.
[N°98] Fowler, P. W.; Legon, A. C.; Thumwood, J. M. A.; Waclawik, E. R. *Coord. Chem. Rev.* **2000**, *197*, 231.
[N°99] Goldman, N.; Leforestier, C.; Saykally, R. J. *Philos. Trans. Roy .Soc. A* **2005**, *363*, 493.
[N°100] Keutsch, F. N.; Cruzan, J. D.; Saykally, R. J. *Chem. Rev.* **2003**, *103*, 2533.
[N°101] Cruzan, J. D.; Braly, L. B.; Liu, K.; Brown, M. G.; Loeser, J. G.; Saykally, R. J. *Science* **1996**, *271*, 59.
[N°102] Chervenkov, S.; Wang, P. Q.; Braun, J. E.; Georgiev, S.; Neusser, H. J.; Nandi, C. K.; Chakraborty, T. *J. Chem. Phys.* **2005**, *122*.
[N°103] Nguyen, T. V.; Korter, T. M.; Pratt, D. W. *Mol. Phys.* **2005**, *103*, 2453.
[N°104] Georgiev, S.; Neusser, H. J. *J. Electron Spect.* **2005**, *142*, 207.
[N°105] Kang, C.; Pratt, D. W. *Int. Rev. Phys. Chem.* **2005**, *24*, 1.
[N°106] Pratt, D. W. *Science* **2002**, *296*, 2347.
[N°107] Ford, M. S.; Muller-Dethlefs, K. *Phys. Chem. Chem. Phys.* **2004**, *6*, 23.
[N°108] Lee, Y. H.; Jung, J. W.; Kim, B.; Butz, P.; Snoek, L. C.; Kroemer, R. T.; Simons, J. P. *J. Phys. Chem. A* **2004**, *108*, 69.
[N°109] Tong, X.; Ford, M. S.; Dessent, C. E. H.; Muller-Dethlefs, K. *J. Chem. Phys.* **2003**, *119*, 12908.
[N°110] Ford, M. S.; Tong, X.; Dessent, C. E. H.; Muller-Dethlefs, K. *J. Chem. Phys.* **2003**, *119*, 12914.
[N°111] Dessent, C. E. H.; Muller-Dethlefs, K. *Chem. Rev.* **2000**, *100*, 3999.
[N°112] Muller-dethlefs, K. *J. Chem. Phys.* **1991**, *95*, 4821.
[N°113] Mullerdethlefs, K.; Sander, M.; Schlag, E. W. *Z. Naturforsch. A* **1984**, *39*, 1089.
[N°114] Mullerdethlefs, K.; Sander, M.; Schlag, E. W. *Chem. Phys. Lett.* **1984**, *112*, 291.
[N°115] Habenicht, W.; Reiser, G.; Mullerdethlefs, K. *J. Chem. Phys.* **1991**, *95*, 4809.
[N°116] Beattie, D. A.; Donovan, R. J. *Prog. React. Kinet. Mec.* **1998**, *23*, 281.
[N°117] Leutwyler, S.; Bosiger, J. *Chem. Rev.* **1990**, *90*, 489.
[N°118] Bernstein, R. B. *J. Phys. Chem.* **1982**, *86*, 1178.
[N°119] Krause, H.; Neusser, H. J. *J. Chem. Phys.* **1993**, *99*, 6278.
[N°120] Zhu, L.; Johnson, P. *J. Chem. Phys.* **1991**, *94*, 5769.
[N°121] Chapman, D. M.; Müller-Dethlefs, K.; Peel, J. B. *J. Chem. Phys.* **1999**, *111*, 1955.
[N°122] Dannenberg, J. J.; Rios, R. *J. Phys. Chem.* **1994**, *98*, 6714.
[N°123] vBuemi, G.; Gandolfo, C. *J. Chem. Soc., Faraday Trans. 2* **1989**, *85*, 215.
[N°124] Cao, J.; Ihee, H.; Zewail, A. H. *Proc. Natl. Acad. Sci. USA* **1999**, *96*, 338.
[N°125] Dantus, M.; Kim, S. B.; Williamson, J. C.; Zewail, A. H. *J. Phys. Chem.* **1994**, *98*, 2782.
[N°126] Srinivasan, R.; Feenstra, J. S.; Park, S. T.; Xu, S.; Zewail, A. H. *J. Am. Chem. Soc.* **2004**, *126*, 2266.
[N°127] Xu, S. J.; Park, S. T.; Feenstra, J. S.; Srinivasan, R.; Zewail, A. H. *J. Phys. Chem. A* **2004**, *108*, 6650.
[N°128] Caminati, W.; Grabow, J.-U. *J. Am. Chem. Soc.* **2005**, *128*, 854.
[N°129] Condon, E. *Phys. Rev.* **1926**, *28*, 1182.
[N°130] Froese Fischer, C. *Comp. Phys. Comm.* **1987**, *43*, 355.

[N°131] Jeziorski, B.; Moszynski, R.; Szalewicz, K. *Chem. Rev.* **1994**, *94*, 1887.
[N°132] Bukowski, R.; Jeziorski, B.; Szalewicz, K. *J. Chem. Phys.* **1996**, *104*, 3306.
[N°133] Moszynski, R.; Korona, T.; Wormer, P. E. S.; van der Avoird, A. *J. Chem. Phys.* **1995**, *103*, 321.
[N°134] Moszynski, R.; Wormer, P. E. S.; Jeziorski, B.; van der Avoird, A. *J. Chem. Phys.* **1994**, *101*, 2811.
[N°135] Lotrich, V. F.; Williams, H. L.; Szalewicz, K.; Jeziorski, B.; Moszynski, R.; Wormer, P. E. S.; van der Avoird, A. *J. Chem. Phys.* **1995**, *103*, 6076.
[N°136] Lotrich, V. F.; Jankowski, P.; Szalewicz, K. *J. Chem. Phys.* **1998**, *108*, 4725.
[N°137] Heijman, T. G. A.; Korona, T.; Moszynski, R.; Wormer, P. E. S.; vanderAvoird, A. *J. Chem. Phys.* **1997**, *107*, 902.
[N°138] Lotrich, V. F.; Szalewicz, K. *J. Chem. Phys.* **1997**, *106*, 9688.
[N°139] Mas, E. M.; Szalewicz, K.; Bukowski, R.; Jeziorski, B. *J. Chem. Phys.* **1997**, *107*, 4207.
[N°140] Mas, E. M.; Szalewicz, K. *J. Chem. Phys.* **1996**, *104*, 7606.
[N°141] Jankowski, P.; Szalewicz, K. *J. Chem. Phys.* **1998**, *108*, 3554.
[N°142] Bukowski, R.; Sadlej, J.; Jeziorski, B.; Jankowski, P.; Szalewicz, K.; Kucharski, S. A., . . . Rice, B. M. *J. Chem. Phys.* **1999**, *110*, 3785.
[N°143] Scheiner, S. *Hydrogen Bonding. A Theoretical Perspective;*; Oxford University Press: New York, **1997**.
[N°144] Bartlett, R. J.; Stanton, J. F. In *Reviews in Computational Chemistry*; John Wiley & Sons, Inc.: **2007**, p 65.
[N°145] Hobza, P. *Acc. Chem. Res.* **2012**, *45*, 663.
[N°146] Raghavachari, K.; Trucks, G. W.; Pople, J. A.; Head-Gordon, M. *Chem. Phys. Lett.* **1989**, *157*, 479.
[N°147] Bartlett, R. J. *An. Rev. Phys. Chem.* **1981**, *32*, 359.
[N°148] Saebo/, S.; Pulay, P. *J. Chem. Phys.* **1987**, *86*, 914.
[N°149] Kohn, W. In *Nobel Lecture: Electronic Structure of Matter Wave Functions and Density Functionals*; Nobelprize.org, Nobel Media AB 2013: Web. 11 Jul 2014: nobelprize.org/nobel_prizes/chemistry/laureates/1998/kohn-lecture.html, 1999.
[N°150] Hohenberg, P.; Kohn, W. *Phys. Rev.* **1964**, *136*, B864.
[N°151] Kohn, W.; Sham, L. J. *Phys. Rev.* **1965**, *140*, A1133.
[N°152] Schrödinger, E. *Annalen der Physik* **1926**, *79*, 361.
[N°153] Sirois, S.; Proynov, E. I.; Nguyen, D. T.; Salahub, D. R. *J. Chem. Phys.* **1997**, *107*, 6770.
[N°154] Sim, F.; St. Amant, A.; Papai, I.; Salahub, D. R. *J. Am. Chem. Soc.* **1992**, *114*, 4391.
[N°155] Liao, M. S.; Lu, Y.; Parker, V. D.; Scheiner, S. *J. Phys. Chem. A* **2003**, *107*, 8939.
[N°156] Desplanches, C.; Ruiz, E.; Rodríguez-Fortea, A.; Alvarez, S. *J. Am. Chem. Soc.* **2002**, *124*, 5197.
[N°157] Zaric, S. D. *Eur. J. Inorg. Chem.* **2003**, 2197.
[N°158] Hobza, P.; Sponer, J.; Reschel, T. *J. Comput. Chem.* **1995**, *16*, 1315.
[N°159] Kristyan, S.; Pulay, P. *Chem. Phys. Lett.* **1994**, *229*, 175.
[N°160] Zhang, Y. K.; Pan, W.; Yang, W. T. *J. Chem. Phys.* **1997**, *107*, 7921.
[N°161] Balabin, R. M. *J. Chem. Phys.* **2008**, *129*.
[N°162] Paizs, B.; Suhai, S. *J. Comput. Chem.* **1998**, *19*, 575.
[N°163] Jurecka, P.; Cerny, J.; Hobza, P.; Salahub, D. R. *J. Comput. Chem.* **2007**, *28*, 555.
[N°164] Civalleri, B.; Zicovich-Wilson, C. M.; Valenzano, L.; Ugliengo, P. *Crystengcomm* **2008**, *10*, 1693.
[N°165] Elstner, M.; Hobza, P.; Frauenheim, T.; Suhai, S.; Kaxiras, E. *J. Chem. Phys.* **2001**, *114*, 5149.
[N°166] Grimme, S. *J. Comput. Chem.* **2006**, *27*, 1787.
[N°167] Grimme, S. *J. Comput. Chem.* **2004**, *25*, 1463.
[N°168] Plumley, J. A.; Dannenberg, J. J. *J. Comput. Chem.* **2011**, *32*, 1519.
[N°169] Ceperley, D. M.; Alder, B. J. *Phys. Rev. Lett.* **1980**, *45*, 566.
[N°170] Perdew, J. P.; Burke, K.; Ernzerhof, M. *Phys. Rev. Lett.* **1996**, *77*, 3865.
[N°171] Thonhauser, T.; Cooper, V. R.; Li, S.; Puzder, A.; Hyldgaard, P.; Langreth, D. C. *Phys. Rev. B* **2007**, *76*, 125112.
[N°172] Björkman, T.; Gulans, A.; Krasheninnikov, A. V.; Nieminen, R. M. *J. Phys. Condens. Mat.* **2012**, *24*, 424218.
[N°173] Silvestrelli, P. L. *Phys. Rev. Lett.* **2008**, *100*, 053002.
[N°174] Yanai, T.; Tew, D. P.; Handy, N. C. *Chem. Phys. Lett.* **2004**, *393*, 51.
[N°175] Langreth, D. C.; Mehl, M. J. *Phys. Rev. B* **1983**, *28*, 1809.
[N°176] Wu, X.; Vargas, M. C.; Nayak, S.; Lotrich, V.; Scoles, G. *J. Chem. Phys.* **2001**, *115*, 8748.
[N°177] Lee, K.; Murray, É. D.; Kong, L.; Lundqvist, B. I.; Langreth, D. C. *Phys. Rev. B* **2010**, *82*, 081101.
[N°178] Dion, M.; Rydberg, H.; Schröder, E.; Langreth, D. C.; Lundqvist, B. I. *Phys. Rev. Lett.* **2004**, *92*, 246401.
[N°179] Tkatchenko, A.; Ambrosetti, A.; DiStasio, R. A. *J. Chem. Phys.* **2013**, *138*.
[N°180] Tkatchenko, A.; Scheffler, M. *Phys. Rev. Lett.* **2009**, *102*, 073005.
[N°181] Lüder, J.; Sanyal, B.; Eriksson, O.; Puglia, C.; Brena, B. *Phys. Rev. B* **2014**, *89*, 045416.
[N°182] DiLabio, G. A.; Johnson, E. R.; Otero-de-la-Roza, A. *Phys. Chem. Chem. Phys.* **2013**, *15*, 12821.
[N°183] Marom, N.; Tkatchenko, A.; Rossi, M.; Gobre, V. V.; Hod, O.; Scheffler, M.; Kronik, L. *J. Chem. Theory Comput.* **2011**, *7*, 3944.
[N°184] DiLabio, G.; Koleini, M.; Torres, E. *Theor. Chem. Acc.* **2013**, *132*, 1.
[N°185] Grimme, S. *WIREs: Comput. Mol. Sci.* **2011**, *1*, 211.
[N°186] Hujo, W.; Grimme, S. *Phys. Chem. Chem. Phys.* **2011**, *13*, 13942.
[N°187] Grimme, S.; Ehrlich, S.; Goerigk, L. *J. Comput. Chem.* **2011**, *32*, 1456.
[N°188] Grimme, S.; Steinmetz, M. *Phys. Chem. Chem. Phys.* **2013**, *15*, 16031.
[N°189] Grimme, S.; Huenerbein, R.; Ehrlich, S. *ChemPhysChem* **2011**, *12*, 1258.
[N°190] Rousseau, V. G. *Phys. Rev. E* **2008**, *77*, 056705.
[N°191] Mella, M.; Anderson, J. B. *J. Chem. Phys.* **2003**, *119*, 8225.
[N°192] Foulkes, W. M. C.; Mitas, L.; Needs, R. J.; Rajagopal, G. *Rev. mod. Phys.* **2001**, *73*, 33.
[N°193] Diedrich, C.; Luchow, A.; Grimme, S. *J. Chem. Phys.* **2005**, *123*, 184106.
[N°194] Lubman, D. M.; Rettner, C. T.; Zare, R. N. *J. Phys. Chem.* **1982**, *86*, 1129.
[N°195] Zhou, Y.; Pu, J. *J. Chem. Theory Comput.* **2014**.
[N°196] Manby, F. R. *Accurate Condensed-Phase Quantum Chemistry (Computation in Chemistry)*; CRC Press, **2010**.
[N°197] Knight, C.; Maupin, C. M.; Izvekov, S.; Voth, G. A. *J. Chem. Theory Comput.* **2010**, *6*, 3223.
[N°198] Glover, W. J.; Larsen, R. E.; Schwartz, B. J. *J. Chem. Phys.* **2010**, *132*.
[N°199] Politzer, P.; Murray, J. S.; Peralta-Inga, Z. *Int. J. Quantum Chem.* **2001**, *85*, 676.
[N°200] Knight, C.; Voth, G. A. *Acc. Chem. Res.* **2011**, *45*, 101.
[N°201] Haynes, W. M. *Handbook of Chemistry and Physics*; CRC Press, 95th ed., **2014**.

[N°202] Moilanen, D. E.; Fenn, E. E.; Lin, Y.-S.; Skinner, J. L.; Bagchi, B.; Fayer, M. D. *Proc. Natl. Acad. Sci. USA* **2008**, *105*, 5295.
[N°203] Smith, J. D.; Cappa, C. D.; Wilson, K. R.; Cohen, R. C.; Geissler, P. L.; Saykally, R. J. *Proc. Natl. Acad. Sci. USA* **2005**, *102*, 14171.
[N°204] Berg, J. M.; Tymoczko, J. L.; Stryer, L. *Biochemistry*; W.H.Freeman & Co Ltd; 5th Revised edition - Internationnal edition, **2002**.
[N°205] Sharp, K. A. In *eLS*; John Wiley & Sons, Ltd: **2001**.
[N°206] Eisenberg, D.; Kauzmann, W. *The Structure and Properties of Water*; Oxford University Press, New York, **1969**; Vol. 166.
[N°207] Owen, B. B.; Miller, R. C.; Milner, C. E.; Cogan, H. L. *J. Phys. Chem.* **1961**, *65*, 2065.
[N°208] Denniston, K.; Topping, J.; Woodrum, K.; Caret, R. *General, Organic and Biochemistry* **2013**.
[N°209] Karukstis, K. K.; Frazier, A. A.; Martula, D. S.; Whiles, J. A. *J. Phys. Chem.* **1996**, *100*, 11133.
[N°210] Pauling, L.; Corey, R. B.; Branson, H. R. *Proc. Natl. Acad. Sci. USA* **1951**, *37*, 205.
[N°211] Astbury, W. T. *Trans. Faraday Soc.* **1933**, *29*, 193.
[N°212] Strekowski, L.; Wilson, B. *Mut. Res.* **2007**, *623*, 3.
[N°213] Watson, J. D.; Crick, F. H. C. *Nature* **1953**, *171*, 737.
[N°214] Breiten, B.; Lockett, M. R.; Sherman, W.; Fujita, S.; Al-Sayah, M.; Lange, H., . . . Whitesides, G. M. *J. Am. Chem. Soc.* **2013**, *135*, 15579.
[N°215] Griffiths, A. J. F.; Miller, J. H.; Suzuki, D. T.; Lewontin, R. C.; Gelbart, W. M. *An Introduction to Genetic Analysis*; New York: W. H. Freeman, 7th edition, **2000**.
[N°216] Yurenko, Y. P.; Novotny, J.; Sklenar, V.; Marek, R. *Phys. Chem. Chem. Phys.* **2014**, *16*, 2072.
[N°217] Blanco, F.; Kelly, B.; Sánchez-Sanz, G.; Trujillo, C.; Alkorta, I.; Elguero, J.; Rozas, I. *J. Phys. Chem. B* **2013**, *117*, 11608.
[N°218] Kolar, M.; Hobza, P. *J. Phys. Chem. A* **2007**, *111*, 5851.
[N°219] Jurecka, P.; Hobza, P. *J. Am. Chem. Soc.* **2003**, *125*, 15608.
[N°220] Jurecka, P.; Hobza, P. *Chem. Phys. Lett.* **2002**, *365*, 89.
[N°221] Hobza, P.; Sponer, J. *J. Am. Chem. Soc.* **2002**, *124*, 11802.
[N°222] Hobza, P.; Riehn, C.; Weichert, A.; Brutschy, B. *Chem. Phys.* **2002**, *283*, 331.
[N°223] Baron, R.; McCammon, J. A. *An. Rev. Phys. Chem.* **2013**, *64*, 151.
[N°224] Bielawski, C.; Chen, Y.-S. *Chem. Commun.* **1998**, 1313.
[N°225] Grunenberg, J. *Phys. Chem. Chem. Phys.* **2011**, *13*, 10136.
[N°226] Cosic, I. *Biomed. Eng.* **1994**, *41*, 1101.
[N°227] Gellman, S. H. *Chem. Rev.* **1997**, *97*, 1231.
[N°228] Knox, J. R.; Pratt, R. F. *Antimicrob. Agents Chemother.* **1990**, *34*, 1342.
[N°229] Forbes, P. *The gecko's foot: How scientists are taking a leaf from nature's book*; Harper Perennial, **2006**.
[N°230] Russell, A. P. *J. Zool.* **1975**, *176*, 437.
[N°231] Maderson, P. F. A. *Nature* **1964**, *203*, 780.
[N°232] Aristotle In *Historia Animalium*; Clarendon, Oxford ed. WEB: classics.mit.edu/Aristotle/historypanim.html, 1918.
[N°233] Hu, S.; Lopez, S.; Niewiarowski, P. H.; Xia, Z. *J. Royal Soc. Inter.* **2012**.
[N°234] Kim, T. W.; Bhushan, B. *Journal of the Royal Society, Interface / the Royal Society* **2008**, *5*, 319.
[N°235] Persson, B. N. J. *MRS Bulletin* **2007**, *32*, 486.
[N°236] Autumn, K.; Sitti, M.; Liang, Y. A.; Peattie, A. M.; Hansen, W. R.; Sponberg, S., . . . Full, R. J. *Proc. Natl. Acad. Sci. USA* **2002**, *99*, 12252.
[N°237] Autumn, K.; Peattie, A. M. *Intergr. Comp. Biol.* **2002**, *42*, 1081.
[N°238] Autumn, K.; Liang, Y. A.; Hsieh, S. T.; Zesch, W.; Chan, W. P.; Kenny, T. W., . . . Full, R. J. *Nature* **2000**, *405*, 681.
[N°239] Autumn, K.; Hsieh, T.; Zesch, W.; Chan, W. P.; Fearing, R.; Full, R. J. *Am. Zool.* **1999**, *39*, 105A.
[N°240] Hiller, U. *Z. Morph. Tiere* **1968**, *62*, 307.
[N°241] WILLIAMS, E. E.; PETERSON, J. A. *Science* **1982**, *215*, 1509.
[N°242] Ruibal, R.; Ernst, V. *J. Morph.* **1965**, *117*, 271.
[N°243] Murphy, M. P.; Aksak, B.; Sitti, M. *Small* **2009**, *5*, 170.
[N°244] Jeong, H. E.; Lee, J.-K.; Kim, H. N.; Moon, S. H.; Suh, K. Y. *Proc. Natl. Acad. Sci. USA* **2009**, *106*, 5639.
[N°245] Qu, L.; Dai, L.; Stone, M.; Xia, Z.; Wang, Z. L. *Science* **2008**, *322*, 238.
[N°246] Autumn, K.; Gravish, N. *Phil. Trans. Royal Soc. A* **2008**, *366*, 1575.
[N°247] Northen, M. T.; Greiner, C.; Arzt, E.; Turner, K. L. *Adv. Mater.* **2008**, *20*, 3905.
[N°248] del Campo, A.; Greiner, C.; Álvarez, I.; Arzt, E. *Adv. Mater.* **2007**, *19*, 1973.
[N°249] Ge, L.; Sethi, S.; Ci, L.; Ajayan, P. M.; Dhinojwala, A. *Proc. Natl. Acad. Sci. USA* **2007**, *104*, 10792.
[N°250] Zhao, Y.; Tong, T.; Delzeit, L.; Kashani, A.; Meyyappan, M.; Majumdar, A. *J. Vac. Sci. Tech. B* **2006**, *24*, 331.
[N°251] Michael, T. N.; Kimberly, L. T. *Nanotech.* **2005**, *16*, 1159.
[N°252] Yurdumakan, B.; Raravikar, N. R.; Ajayan, P. M.; Dhinojwala, A. *Chem. Commun.* **2005**, 3799.
[N°253] Geim, A. K.; Dubonos, S. V.; Grigorieva, I. V.; Novoselov, K. S.; Zhukov, A. A.; Shapoval, S. Y. *Nat. Mater.* **2003**, *2*, 461.
[N°254] Pârvulescu, V. I.; Hardacre, C. *Chem. Rev.* **2007**, *107*, 2615.
[N°255] Scariot, M.; Silva, D. O.; Scholten, J. D.; Machado, G.; Teixeira, S. R.; Novak, M. A., . . . Dupont, J. *Angew. Chem. Int. Ed. Engl.* **2008**, *47*, 9075.
[N°256] Prechtl, M. H. G.; Scariot, M.; Scholten, J. D.; Machado, G.; Teixeira, S. R.; Dupont, J. *Inorg. Chem.* **2008**, *47*, 8995.
[N°257] Lu, A.-H.; Salabas, E. L.; Schüth, F. *Angew. Chem. Int. Ed. Engl.* **2007**, *46*, 1222.
[N°258] Migowski, P.; Dupont, J. *Chem. Eur. J.* **2007**, *13*, 32.
[N°259] Park, J.; Joo, J.; Kwon, S. G.; Jang, Y.; Hyeon, T. *Angew. Chem. Int. Ed. Engl.* **2007**, *46*, 4630.
[N°260] Mastai, Y.; Gedanken, A. *Chemistry of Nanomaterials*; ed. C. N. R. Rao, A. Müller and A. K. Cheetham, Wiley-VCH, Weinheim, **2004**.
[N°261] Gedanken, A. *Ultrasonics Sonochemistry* **2004**, *11*, 47.
[N°262] Braunstein, P.; Rosé, J. *Metal Clusters in Chemistry*; ed. Braunstein, P.; Oro; L. A. and Raithby, P. R. - Wiley-VCH, Weinheim, vol. 2, ch. 2, **2001**, 616–677.
[N°263] Redel, E.; Thomann, R.; Janiak, C. *Chem. Commun.* **2008**, 1789.
[N°264] Kramer, J.; Redel, E.; Thomann, R.; Janiak, C. *Organometallics* **2008**, *27*, 1976.
[N°265] Redel, E.; Kramer, J.; Thomann, R.; Janiak, C. *J. Organomet. Chem.* **2009**, *694*, 1069.
[N°266] Redel, E.; Thomann, R.; Janiak, C. *Inorg. Chem.* **2008**, *47*, 14.
[N°267] Redel, E.; Walter, M.; Thomann, R.; Vollmer, C.; Hussein, L.; Scherer, H., . . . Janiak, C. *Chem. Eur. J.* **2009**, *15*, 10047.
[N°268] Dupont, J. *J. Braz. Chem. Soc.* **2004**, *15*, 341.

[N°269] Kaper, H.; Endres, F.; Djerdj, I.; Antonietti, M.; Smarsly, B. M.; Maier, J.; Hu, Y. S. *Small* **2007**, *3*, 1753.
[N°270] Astruc, D.; Lu, F.; Aranzaes, J. R. *Angew. Chem. Int. Ed. Engl.* **2005**, *44*, 7852.
[N°271] Antonietti, M.; Kuang, D. B.; Smarsly, B.; Yong, Z. *Angew. Chem. Int. Ed. Engl.* **2004**, *43*, 4988.
[N°272] Taylor, R. *Crystengcomm* **2014**, *16*, 6852.
[N°273] O'Keeffe, M.; Yaghi, O. M. *Chem. Rev.* **2011**, *112*, 675.
[N°274] Lu, W.; Chan, M. C. W.; Zhu, N.; Che, C.-M.; He, Z.; Wong, K.-Y. *Chem. Eur. J.* **2003**, *9*, 6155.
[N°275] Moulton, B.; Zaworotko, M. J. *Chem. Rev.* **2001**, *101*, 1629.
[N°276] Ohba, S.; Hosomi, H.; Ito, Y. *J. Am. Chem. Soc.* **2001**, *123*, 6349.
[N°277] Xu, Z.; Lee, S.; Kiang, Y. H.; Mallik, A. B.; Tsomaia, N.; Mueller, K. T. *Adv. Mater.* **2001**, *13*, 637.
[N°278] Galan-Mascaros, J. R.; Dunbar, K. R. *Chem. Commun.* **2001**, 217.
[N°279] Noro, S.-i.; Kitagawa, S.; Kondo, M.; Seki, K. *Angew. Chem. Int. Ed. Engl.* **2000**, *39*, 2081.
[N°280] Tabares, L. C.; Navarro, J. A. R.; Salas, J. M. *J. Am. Chem. Soc.* **2000**, *123*, 383.
[N°281] Seo, J. S.; Whang, D.; Lee, H.; Jun, S. I.; Oh, J.; Jeon, Y. J.; Kim, K. *Nature* **2000**, *404*, 982.
[N°282] Miller, J. S. *Inorg. Chem.* **2000**, *39*, 4392.
[N°283] Eddaoudi, M.; Li, H.; Yaghi, O. M. *J. Am. Chem. Soc.* **2000**, *122*, 1391.
[N°284] R. Desiraju, G. *Chem. Commun.* **1997**, 1475.
[N°285] Li, H.; Eddaoudi, M.; O'Keeffe, M.; Yaghi, O. M. *Nature* **1999**, *402*, 276.
[N°286] Hollingsworth, M. D.; Werner-Zwanziger, U.; Brown, M. E.; Chaney, J. D.; Huffman, J. C.; Harris, K. D. M.; Smart, S. P. *J. Am. Chem. Soc.* **1999**, *121*, 9732.
[N°287] Shin, Dong M.; Lee, In S.; Chung, Young K. *Eur. J. Inorg. Chem.* **2003**, *2003*, 2311.
[N°288] Braga, D.; Maini, L.; Polito, M.; Scaccianoce, L.; Cojazzi, G.; Grepioni, F. *Coord. Chem. Rev.* **2001**, *216-217*, 225.
[N°289] Braga, D.; Maini, L.; Grepioni, F.; Elschenbroich, C.; Paganelli, F.; Schiemann, O. *Organometallics* **2001**, *20*, 1875.
[N°290] Aakeroy, C. B.; Beatty, A. M.; Leinen, D. S.; Lorimer, K. R. *Chem. Commun.* **2000**, 935.
[N°291] Atencio, R.; Domasevitch, K. V.; Zaworotko, M. J. *Crystal Eng.* **2000**, *3*, 63.
[N°292] Aakeröy, C. B.; Beatty, A. M.; Leinen, D. S. *Angew. Chem. Int. Ed. Engl.* **1999**, *38*, 1815.
[N°293] B. Aakeroy, C.; M. Beatty, A.; A. Helfrich, B. *J. Chem. Soc., Dalton Trans.* **1998**, 1943.
[N°294] Braga, D.; Maini, L.; Grepioni, F. *Angew. Chem. Int. Ed. Engl.* **1998**, *37*, 2240.
[N°295] Braga, D.; Grepioni, F.; Desiraju, G. R. *Chem. Soc. Rev.* **1998**, *98*, 1375.
[N°296] Chen, Z.-N.; Zhang, H.-X.; Yu, K.-B.; Zheng, K.-C.; Cai, H.; Kang, B.-S. *J. Chem. Soc., Dalton Trans.* **1998**, 1133.
[N°297] Aakeröy, C. B.; Beatty, A. M.; Leinen, D. S. *J. Am. Chem. Soc.* **1998**, *120*, 7383.
[N°298] Munakata, M.; Wu, L. P.; Kuroda-Sowa, T.; Maekawa, M.; Suenaga, Y.; Ning, G. L.; Kojima, T. *J. Am. Chem. Soc.* **1998**, *120*, 8610.
[N°299] Braga, D.; Grepioni, F. *Acc. Chem. Res.* **1997**, *30*, 81.
[N°300] Schauer, C. L.; Matwey, E.; Fowler, F. W.; Lauher, J. W. *J. Am. Chem. Soc.* **1997**, *119*, 10245.
[N°301] Braga, D.; Grepioni, F. *Chem. Commun.* **1996**, 571.
[N°302] Burrows, A. D.; Chan, C.-W.; Chowdhry, M. M.; McGrady, J. E.; Mingos, D. M. P. *Chem. Soc. Rev.* **1995**, *24*, 329.
[N°303] Feltham, H. L. C.; Brooker, S. *Coord. Chem. Rev.* **2014**, *276*, 1.
[N°304] Inglis, R.; Papaefstathiou, G. S.; Wernsdorfer, W.; Brechin, E. K. *Aust. J. Chem.* **2009**, 1108.
[N°305] Aromi, G.; Brechin, E. K. *Struct. Bond* **2006**, *122*, 1.
[N°306] Bircher, R.; Chaboussant, G.; Dobe, C.; Gudel, H. U.; Ochsenbein, S. T.; Sieber, A.; Waldmann, O. *Adv. Funct. Mater.* **2006**, *16*, 209.
[N°307] Christou, G.; Gatteschi, D.; Hendrickson, D. N.; Sessoli, R. *MRS Bulletin* **2000**, *25*, 66.
[N°308] Gatteschi, D.; Sessoli, R. *Angew. Chem. Int. Ed. Engl.* **2003**, *42*, 268.
[N°309] Bogani, L.; Sangregorio, C.; Sessoli, R.; Gatteschi, D. *Angew. Chem. Int. Ed. Engl.* **2005**, *44*, 5817.
[N°310] Bernot, K.; Bogani, L.; Caneschi, A.; Gatteschi, D.; Sessoli, R. *J. Am. Chem. Soc.* **2006**, *128*, 7947.
[N°311] Miyasaka, H.; Yamashita, M. *Dalton Trans.* **2007**, 399.
[N°312] Wittick, L. M.; Murray, K. S.; Moubaraki, B.; Batten, S. R.; Spiccia, L.; Berry, K. J. *Dalton Trans.* **2004**, 1003.
[N°313] Yoo, J.; Wernsdorfer, W.; Yang, E.-C.; Nakano, M.; Rheingold, A. L.; Hendrickson, D. N. *Inorg. Chem.* **2005**, *44*, 3377.
[N°314] Roubeau, O.; Clérac, R. *Eur. J. Inorg. Chem.* **2008**, *2008*, 4325.
[N°315] Hill, S.; Edwards, R. S.; Aliaga-Alcalde, N.; Christou, G. *Science* **2003**, *302*, 1015.
[N°316] Wernsdorfer, W.; Aliaga-Alcalde, N.; Hendrickson, D. N.; Christou, G. *Nature* **2002**, *416*, 406.
[N°317] Ferbinteanu, M.; Cimpoesu, F.; Kajiwara, T.; Yamashita, M. *Solid State Sci* **2009**, *11*, 760.
[N°318] Tanase, S.; Reedijk, J. *Coord. Chem. Rev.* **2006**, *250*, 2501.
[N°319] Ferbinteanu, M.; Zaharia, A.; Girtu, M. A.; Cimpoesu, F. *Cent. Eur. J. Chem.* **2010**, *8*, 519.
[N°320] Maretti, L.; Ferbinteanu, M.; Cimpoesu, F.; Islam, S. S.; Ohba, Y.; Kajiwara, T., . . . Yamauchi, S. *Inorg. Chem.* **2007**, *46*, 660.
[N°321] Pointillart, F.; Bernot, K.; Sessoli, R.; Gatteschi, D. *Chem. Eur. J.* **2007**, *13*, 1602.
[N°322] Mishra, A.; Wernsdorfer, W.; Abboud, K. A.; Christou, G. *J. Am. Chem. Soc.* **2004**, *126*, 15648.
[N°323] Zaleski, C. M.; Depperman, E. C.; Kampf, J. W.; Kirk, M. L.; Pecoraro, V. L. *Angew. Chem. Int. Ed. Engl.* **2004**, *43*, 3912.
[N°324] Costes, J.-P.; Dahan, F.; Donnadieu, B.; Fernandez-Garcia, M.-I.; Rodriguez-Douton, M.-J. *Dalton Trans.* **2003**, 3776.
[N°325] Ferbinteanu, M.; Kajiwara, T.; Choi, K. Y.; Nojiri, H.; Nakamoto, A.; Kojima, N., . . . Yamashita, M. *J. Am. Chem. Soc.* **2006**, *128*, 9008.
[N°326] Costes, J.-P.; Dahan, F.; Wernsdorfer, W. *Inorg. Chem.* **2005**, *45*, 5.
[N°327] Ishikawa, N.; Sugita, M.; Wernsdorfer, W. *Angew. Chem. Int. Ed. Engl.* **2005**, *44*, 2931.
[N°328] Ishikawa, N.; Sugita, M.; Wernsdorfer, W. *J. Am. Chem. Soc.* **2005**, *127*, 3650.
[N°329] Paulovič, J.; Cimpoesu, F.; Ferbinteanu, M.; Hirao, K. *J. Am. Chem. Soc.* **2004**, *126*, 3321.
[N°330] Świderek, K.; Paneth, P. *Chem. Rev.* **2013**, *113*, 7851.
[N°331] Wade, D. *Chem. Biol. Inter.* **1999**, *117*, 191.
[N°332] Kohen, A.; Limbach, H. H. *Isotope Effects in Chemistry and Biology*; Taylor & Francis -CRC Press.
[N°333] Liu, Y.; Warmuth, R. *Org. Lett. 9* **2007**, *9*, 2883.
[N°334] Zhao, Y.-L.; Houk, K. N.; Rechavi, D.; Scarso, A.; Rebek, J. *J. Am. Chem. Soc.* **2004**, *126*, 11428.
[N°335] Liu, M.; Girma, E.; Glicksman, M. A.; Stein, R. L. *Biochemistry* **2010**, *49*, 4921.
[N°336] Wiley, K. L.; Tormos, J. R.; Quinn, D. M. *Chem. Biol. Inter.* **2010**, *187*, 124.
[N°337] Gonzalez-James, O. M.; Singleton, D. A. *J. Am. Chem. Soc.* **2010**, *132*, 6896.
[N°338] Abe, T.; Miyazawa, A.; Konno, H.; Kawanishi, Y. *Chem. Phys. Lett.* **2010**, *491*, 199.

[N°339] Giagou, T.; Meyer, M. P. *Chem. Eur. J.* **2010**, *16*, 10616.
[N°340] Stojković, V.; Kohen, A. *Israel J. Chem.* **2009**, *49*, 163.
[N°341] de La Harpe, K.; Crespo-Hernández, C. E.; Kohler, B. *J. Am. Chem. Soc.* **2009**, *131*, 17557.
[N°342] Zhang, H.; Wang, S.; Sun, Q.; Smith, S. C. *Phys. Chem. Chem. Phys.* **2009**, *11*, 8422.
[N°343] Leung, D. H.; Bergman, R. G.; Raymond, K. N. *J. Am. Chem. Soc.* **2008**, *130*, 2798.
[N°344] Yoshizawa, M.; Klosterman, J. K.; Fujita, M. *Angew. Chem. Int. Ed. Engl.* **2009**, *48*, 3418.
[N°345] Saalfrank, R. W.; Maid, H.; Scheurer, A. *Angew. Chem. Int. Ed. Engl.* **2008**, *47*, 8794.
[N°346] Oshovsky, G. V.; Reinhoudt, D. N.; Verboom, W. *ChemInform.* **2007**, *38*, no.
[N°347] Stang, P. J.; Olenyuk, B. *Acc. Chem. Res.* **1997**, *30*, 502.
[N°348] Pluth, M. D.; Fiedler, D.; Mugridge, J. S.; Bergman, R. G.; Raymond, K. N. *Proc. Natl. Acad. Sci. USA* **2009**, *106*, 10438.
[N°349] Hastings, C. J.; Pluth, M. D.; Biros, S. M.; Bergman, R. G.; Raymond, K. N. *Tetrahedron* **2008**, *64*, 8362.
[N°350] Davis, A. V.; Fiedler, D.; Seeber, G.; Zahl, A.; van Eldik, R.; Raymond, K. N. *J. Am. Chem. Soc.* **2006**, *128*, 1324.
[N°351] Parac, T. N.; Scherer, M.; Raymond, K. N. *Angew. Chem. Int. Ed. Engl.* **2000**, *39*, 1239.
[N°352] Pluth, M. D.; Bergman, R. G.; Raymond, K. N. *Angew. Chem. Int. Ed. Engl.* **2007**, *46*, 8587.
[N°353] Leung, D. H.; Bergman, R. G.; Raymond, K. N. *J. Am. Chem. Soc.* **2006**, *128*, 9781.
[N°354] Leung, D. H.; Fiedler, D.; Bergman, R. G.; Raymond, K. N. *Angew. Chem. Int. Ed. Engl.* **2004**, *43*, 963.
[N°355] Felder, T.; Schalley, C. A. *Angew. Chem. Int. Ed. Engl.* **2003**, *42*, 2258.
[N°356] Mugridge, J. S.; Bergman, R. G.; Raymond, K. N. *J. Am. Chem. Soc.* **2011**, *134*, 2057.
[N°357] Mugridge, J. S.; Bergman, R. G.; Raymond, K. N. *J. Am. Chem. Soc.* **2010**, *132*, 1182.
[N°358] Haino, T.; Fukuta, K.; Iwamoto, H.; Iwata, S. *Chem. Eur. J.* **2009**, *15*, 13286.
[N°359] Tran, C. D.; Mejac, I.; Rebek, J.; Hooley, R. J. *Anal. Chem.* **2008**, *81*, 1244.
[N°360] Laughrey, Z. R.; Upton, T. G.; Gibb, B. C. *Chem. Commun.* **2006**, 970.
[N°361] Liu, Y.; Warmuth, R. *Angew. Chem. Int. Ed. Engl.* **2005**, *44*, 7107.
[N°362] Wang, A. S.; Matsui, Y. *Bull. Chem. Soc. Jpn.* **1994**, *67*, 2917.
[N°363] Fujimoto, T.; Yanagihara, R.; Kobayashi, K.; Aoyama, Y. *Bull. Chem. Soc. Jpn.* **1995**, *68*, 2113.
[N°364] Mal, P.; Breiner, B.; Rissanen, K.; Nitschke, J. R. *Science* **2009**, *324*, 1697.
[N°365] El Aroussi, B.; Guénée, L.; Pal, P.; Hamacek, J. *Inorg. Chem.* **2011**, *50*, 8588.
[N°366] Amo-Ochoa, P.; Zamora, F. *Coord. Chem. Rev.* **2014**, *276*, 34.
[N°367] Zhang, J.; Chen, Y. P.; Miller, K. P.; Ganewatta, M. S.; Bam, M.; Yan, Y., . . . Tang, C. *J. Am. Chem. Soc.* **2014**, *136*, 4873.
[N°368] Eloi, J.-C.; Chabanne, L.; Whittell, G. R.; Manners, I. *Materials Today* **2008**, *11*, 28.
[N°369] Abd-El-Aziz, A. S.; Manners, I. In *Frontiers in Transition Metal-Containing Polymers*; John Wiley & Sons, Inc.: **2007**, p i.
[N°370] Williams, K. A.; Boydston, A. J.; Bielawski, C. W. *Chem. Soc. Rev.* **2007**, *36*, 729.
[N°371] Whittell, G. R.; Manners, I. *Adv. Mater.* **2007**, *19*, 3439.
[N°372] Caseri, W. R.; Chanzy, H. D.; Feldman, K.; Fontana, M.; Smith, P.; Tervoort, T. A., . . . Stutzmann, N. *Adv. Mater.* **2003**, *15*, 125.
[N°373] Leininger, S.; Olenyuk, B.; Stang, P. J. *Chem. Rev.* **2000**, *100*, 853.
[N°374] Eddaoudi, M.; Moler, D. B.; Li, H.; Chen, B.; Reineke, T. M.; O'Keeffe, M.; Yaghi, O. M. *Acc. Chem. Res.* **2001**, *34*, 319.
[N°375] Caulder, D. L.; Raymond, K. N. *Acc. Chem. Res.* **1999**, *32*, 975.
[N°376] Do, L.; Smith, R. C.; Tennyson, A. G.; Lippard, S. J. *Inorg. Chem.* **2006**, *45*, 8998.
[N°377] Weder, C. *Chem. Commun.* **2005**, 5378.
[N°378] Holliday, B. J.; Swager, T. M. *Chem. Commun.* **2005**, 23.
[N°379] Cameron, C. G.; MacLean, B. J.; Pickup, P. G. *Macromol. Symp.* **2003**, *196*, 165.
[N°380] G. Pickup, P. *J. Mat. Chem.* **1999**, *9*, 1641.
[N°381] Chan, W. K.; Hui, C. S.; Man, K. Y. K.; Cheng, K. W.; Wong, H. L.; Zhu, N.; Djurišić, A. B. *Coord. Chem. Rev.* **2005**, *249*, 1351.
[N°382] Man, K. Y. K.; Wong, H. L.; Chan, W. K.; Kwong, C. Y.; Djurišić, A. B. *Chem. Mater.* **2004**, *16*, 365.
[N°383] Zhang, M.; Lu, P.; Wang, X.; He, L.; Xia, H.; Zhang, W., . . . Tamai, N. *J. Phys. Chem. B* **2004**, *108*, 13185.
[N°384] Pron, A.; Rannou, P. *Prog. Polym. Sci.* **2002**, *27*, 135.
[N°385] Ng, P. K.; Gong, X.; Chan, S. H.; Lam, L. S. M.; Chan, W. K. *Chem. Eur. J.* **2001**, *7*, 4358.
[N°386] Dahm, C. E.; Peters, D. G. *Anal. Chem.* **1994**, *66*, 3117.
[N°387] Kingsborough, R. P.; Swager, T. M. *Chem. Mater.* **2000**, *12*, 872.
[N°388] Chan, W. K. *Metal Coordination Polymers; Macromolecules Containing Metal and Metal-Like Elements*; Vol. 5; Abd-El-Aziz, A. S., Carraher, C. E., Jr., Pittman, C. U., Jr., Zeldin, M., Eds.; Wiley: New York, **2005**.
[N°389] Hayashida, N.; Yamamoto, T. *Bull. Chem. Soc. Jpn.* **1999**, *72*, 1153.
[N°390] Kokil, A.; Yao, P.; Weder, C. *Macromolecules* **2005**, *38*, 3800.
[N°391] Kokil, A.; Huber, C.; Caseri, W. R.; Weder, C. *Macromol. Chem. Phys.* **2003**, *204*, 40.
[N°392] Kokil, A.; Shiyanovskaya, I.; Singer, K. D.; Weder, C. *J. Am. Chem. Soc.* **2002**, *124*, 9978.
[N°393] Huber, C.; Bangerter, F.; Caseri, W. R.; Weder, C. *J. Am. Chem. Soc.* **2001**, *123*, 3857.
[N°394] Roncali, J. *J. Mat. Chem.* **1999**, *9*, 1875.
[N°395] Knapton, D.; Rowan, S. J.; Weder, C. *Macromolecules* **2005**, *39*, 651.
[N°396] Iyer, P. K.; Beck, J. B.; Weder, C.; Rowan, S. J. *Chem. Commun.* **2005**, 319.
[N°397] Serrano Ruiz, M.; Romerosa, A.; Sierra-Martin, B.; Fernandez-Barbero, A. *Angew. Chem. Int. Ed. Engl.* **2008**, *47*, 8665.
[N°398] Lidrissi, C.; Romerosa, A.; Saoud, M.; Serrano-Ruiz, M.; Gonsalvi, L.; Peruzzini, M. *Angew. Chem. Int. Ed. Engl.* **2005**, *117*, 2624.
[N°399] Wang, X.-S.; Winnik, M. A.; Manners, I. *Macromol. Rap. Comm.* **2002**, *23*, 210.
[N°400] Shioya, T.; Swager, T. M. *Chem. Commun.* **2002**, 1364.
[N°401] Smith, R. C.; Tennyson, A. G.; Lim, M. H.; Lippard, S. J. *Org. Lett.* **2005**, *7*, 3573.
[N°402] Crabtree, R. H.; Eisenstein, O.; Sini, G.; Peris, E. *J. Organomet. Chem.* **1998**, *567*, 7.
[N°403] Belkova, N. V.; Besora, M.; Baya, M.; Dub, P. A.; Epstein, L. M.; Lledos, A., . . . Shubina, E. S. *Chem. Eur. J.* **2008**, *14*, 9921.
[N°404] Belkova, N. V.; Gribanova, T. N.; Gutsul, E. I.; Minyaev, R. M.; Bianchini, C.; Peruzzini, M., . . . Epstein, L. M. *J. Mol. Struct.* **2007**, *844*, 115.
[N°405] Belkova, N. V.; Dub, P. A.; Baya, M.; Houghton, J. *Inorg Chim Acta*
Inorg Chim Acta **2007**, *360*, 149.
[N°406] Belkova, N. V.; Shubina, E. S.; Epstein, L. M. *Accounts of chemical research* **2005**, *38*, 624.
[N°407] Belkova, N. V.; Collange, E.; Dub, P.; Epstein, L. M.; Lemenovskii, D. A.; Lledos, A., . . . Vorontsov, E. V. *Chemistry* **2005**, *11*, 873.
[N°408] Shubina, E. S.; Belkova, N. V.; Epstein, L. M. *J. Organomet. Chem.* **1997**, *536*, 17.

[N°409] Epstein, L. M.; Shubina, E. S. *Coord. Chem. Rev.* **2002**, *231*, 165.
[N°410] Brammer, L. *Dalton Trans.* **2003**, 3145.
[N°411] Alkorta, I.; Elguero, J. *Chem. Soc. Rev.* **1998**, *27*, 163.
[N°412] Custelcean, R.; Jackson, J. E. *Chem. Rev.* **2001**, *101*, 1963.
[N°413] Kubas, G. J.; Ryan, R. R.; Swanson, B. I.; Vergamini, P. J.; Wasserman, H. J. *J. Am. Chem. Soc.* **1984**, *106*, 451.
[N°414] Kubas, G. J. *Metal Dihydrogen and σ-Bond Complexes*; Kluwer Academic/Plenum Press, New York, **2001**.
[N°415] Szymczak, N. K.; Tyler, D. R. *Coord. Chem. Rev.* **2008**, *252*, 212.
[N°416] Lau, C. P.; Ng, S. M.; Jia, G.; Lin, Z. *Coord. Chem. Rev.* **2007**, *251*, 2223.
[N°417] Esteruelas, M. A.; Oro, L. A. *Chem. Rev.* **1998**, *98*, 577.
[N°418] Besora, M.; Lledos, A.; Maseras, F. *Chem. Soc. Rev.* **2009**, *38*, 957.
[N°419] Algarra, A. G.; Basallote, M. G.; Feliz, M.; Fernández-Trujillo, M. J.; Llusar, R.; Safont, V. S. *Chem. Eur. J.* **2006**, *12*, 1413.
[N°420] Basallote, M. G.; Feliz, M.; Fernández-Trujillo, M. J.; Llusar, R.; Safont, V. S.; Uriel, S. *Chem. Eur. J.* **2004**, *10*, 1463.
[N°421] Belkova, N. V.; Besora, M.; Epstein, L. M.; Lledós, A.; Maseras, F.; Shubina, E. S. *J. Am. Chem. Soc.* **2003**, *125*, 7715.
[N°422] Gründemann, S.; Ulrich, S.; Limbach, H.-H.; Golubev, N. S.; Denisov, G. S.; Epstein, L. M., . . . Chaudret, B. *Inorg. Chem.* **1999**, *38*, 2550.
[N°423] Dub, P. A.; Belkova, N. V.; Filippov, O. A.; Daran, J.-C.; Epstein, L. M.; Lledós, A., . . . Poli, R. *Chem. Eur. J.* **2010**, *16*, 189.
[N°424] Baya, M.; Dub, P. A.; Houghton, J.; Daran, J.-C.; Belkova, N. V.; Shubina, E. S., . . . Poli, R. *Inorg. Chem.* **2008**, *48*, 209.
[N°425] Dub, P. A.; Baya, M.; Houghton, J.; Belkova, N. V.; Daran, J.-C.; Poli, R., . . . Shubina, E. S. *Eur. J. Inorg. Chem.* **2007**, *2007*, 2813.
[N°426] Brammer, L.; Minguez Espallargas, G.; Libri, S. *Crystengcomm* **2008**, *10*, 1712.
[N°427] Hassel, O. *Science* **1970**, *170*, 497.
[N°428] Legon, A. C. *Phys. Chem. Chem. Phys.* **2010**, *12*, 7736.
[N°429] Metrangolo, P.; Meyer, F.; Pilati, T.; Resnati, G.; Terraneo, G. *Angew. Chem. Int. Ed. Engl.* **2008**, *47*, 6114.
[N°430] Nguyen, H. L.; Horton, P. N.; Hursthouse, M. B.; Legon, A. C.; Bruce, D. W. *J. Am. Chem. Soc.* **2003**, *126*, 16.
[N°431] Metrangolo, P.; Resnati, G. *Chem. Eur. J.* **2001**, *7*, 2511.
[N°432] Corradi, E.; Meille, S. V.; Messina, M. T.; Metrangolo, P.; Resnati, G. *Angew. Chem. Int. Ed. Engl.* **2000**, *39*, 1782.
[N°433] Cavallo, G.; Metrangolo, P.; Pilati, T.; Resnati, G.; Sansotera, M.; Terraneo, G. *Chem. Soc. Rev.* **2010**, *39*, 3772.
[N°434] Metrangolo, P.; Neukirch, H.; Pilati, T.; Resnati, G. *Acc. Chem. Res.* **2005**, *38*, 386.
[N°435] Parisini, E.; Metrangolo, P.; Pilati, T.; Resnati, G.; Terraneo, G. *Chem. Soc. Rev.* **2011**, *40*, 2267.
[N°436] Lu, Y.; Wang, Y.; Zhu, W. *Phys. Chem. Chem. Phys.* **2010**, *12*, 4543.
[N°437] Lu, Y.; Shi, T.; Wang, Y.; Yang, H.; Yan, X.; Luo, X., . . . Zhu, W. *J. Med. Chem.* **2009**, *52*, 2854.
[N°438] Auffinger, P.; Hays, F. A.; Westhof, E.; Ho, P. S. *Proc. Natl. Acad. Sci. USA* **2004**, *101*, 16789.
[N°439] Politzer, P.; Murray, J. S.; Clark, T. *Phys. Chem. Chem. Phys.* **2010**, *12*, 7748.
[N°440] Clark, T.; Hennemann, M.; Murray, J.; Politzer, P. *J. Mol. Model.* **2007**, *13*, 291.
[N°441] Politzer, P.; Lane, P.; Concha, M.; Ma, Y.; Murray, J. *J. Mol. Model.* **2007**, *13*, 305.
[N°442] Politzer, P.; Riley, K. E.; Bulat, F. A.; Murray, J. S. *Comp. Theor. Chem.* **2012**, *998*, 2.
[N°443] Clemente-Juan, J. M.; Coronado, E.; Minguez Espallargas, G.; Adams, H.; Brammer, L. *Crystengcomm* **2010**, *12*, 2339.
[N°444] Mínguez Espallargas, G.; Zordan, F.; Arroyo Marín, L.; Adams, H.; Shankland, K.; van de Streek, J.; Brammer, L. *Chem. Eur. J.* **2009**, *15*, 7554.
[N°445] Mínguez Espallargas, G.; Brammer, L.; Allan, D. R.; Pulham, C. R.; Robertson, N.; Warren, J. E. *J. Am. Chem. Soc.* **2008**, *130*, 9058.
[N°446] Smart, P.; Espallargas, G. M.; Brammer, L. *Crystengcomm* **2008**, *10*, 1335.
[N°447] Zordan, F.; Espallargas, G. M.; Brammer, L. *Crystengcomm* **2006**, *8*, 425.
[N°448] Mínguez Espallargas, G.; Brammer, L.; Sherwood, P. *Angew. Chem. Int. Ed. Engl.* **2006**, *45*, 435.
[N°449] Brammer, L.; Minguez Espallargas, G.; Adams, H. *Crystengcomm* **2003**, *5*, 343.
[N°450] L. Brammer, F. Z., G. Mínguez Espallargas, S. L. Purver, L. Arroyo Marín, H. Adams *Trans. Am. Cryst. Assoc.* **2004**, *39*, 114.
[N°451] Zhao, Q.; Feng, D. *J. Mol. Model.* **2013**, *19*, 1267.
[N°452] Wu, W.; Lu, Y.; Liu, Y.; Peng, C.; Liu, H. *Comp. Theor. Chem.* **2014**, *1029*, 21.
[N°453] Wang, Y.; Wu, W.; Liu, Y.; Lu, Y. *Chem. Phys. Lett.* **2013**, *578*, 38.
[N°454] Xu, L.; Lv, J.; Sang, P.; Zou, J. W.; Yu, Q. S.; Xu, M. B. *Chem. Phys.* **2011**, *379*, 66.
[N°455] Cheng, N.; Liu, Y.; Zhang, C.; Liu, C. *J. Mol. Model.* **2013**, *19*, 3821.
[N°456] Ohno, K.; Sugaya, T.; Kato, M.; Matsumoto, N.; Fukano, R.; Ogino, Y., . . . Nagasawa, A. *Cryst. Growth Des.* **2014**.
[N°457] Caracelli, I.; Haiduc, I.; Zukerman-Schpector, J.; Tiekink, E. R. T. *Coord. Chem. Rev.* **2013**, *257*, 2863.
[N°458] Fiol, J. J.; Barceló-Oliver, M.; Tasada, A.; Frontera, A.; Terrón, À.; García-Raso, Á. *Coord. Chem. Rev.* **2013**, *257*, 2705.
[N°459] Singh, N. J.; Min, S. K.; Kim, D. Y.; Kim, K. S. *J. Chem. Theory Comput.* **2009**, *5*, 515.
[N°460] Schneider, H.-J. *Angew. Chem. Int. Ed. Engl.* **2009**, *48*, 3924.
[N°461] Nishio, M.; Umezawa, Y.; Honda, K.; Tsuboyama, S.; Suezawa, H. *Crystengcomm* **2009**, *11*, 1757.
[N°462] Gray, J. C.; Pagelot, A.; Collins, A.; Fabbiani, F. P. A.; Parsons, S.; Sadler, P. J. *Eur. J. Inorg. Chem.* **2009**, *2009*, 2673.
[N°463] Tiekink, E. R. T.; Zukerman-Schpector, J. *Crystengcomm* **2009**, *11*, 1176.
[N°464] Ringer, A. L.; Sherrill, C. D. *J. Am. Chem. Soc.* **2009**, *131*, 4574.
[N°465] Wheeler, S. E.; Houk, K. N. *Mol. Phys.* **2009**, *107*, 749.
[N°466] Yi, H.-B.; Lee, H. M.; Kim, K. S. *J. Chem. Theory Comput.* **2009**, *5*, 1709.
[N°467] Fernández-Botello, A.; Holý, A.; Moreno, V.; Operschall, B. P.; Sigel, H. *Inorg. Chim. Acta* **2009**, *362*, 799.
[N°468] Singh, M.; Butcher, R. J.; Singh, N. K. *Polyhedron* **2009**, *28*, 1197.
[N°469] Yanagisawa, S.; Crowley, P. B.; Firbank, S. J.; Lawler, A. T.; Hunter, D. M.; McFarlane, W., . . . Dennison, C. *J. Am. Chem. Soc.* **2008**, *130*, 15420.
[N°470] Cherrier, M. V.; Cavazza, C.; Bochot, C.; Lemaire, D.; Fontecilla-Camps, J. C. *Biochemistry* **2008**, *47*, 9937.
[N°471] Dinadayalane, T. C.; Afanasiev, D.; Leszczynski, J. *J. Phys. Chem. A* **2008**, *112*, 7916.
[N°472] Qu, X.; Wang, X.; Zhu, D. *Environ. Sci. Technol.* **2007**, *41*, 8321.
[N°473] Terrón, A.; Fiol, J. J.; García-Raso, A.; Barceló-Oliver, M.; Moreno, V. *Coord. Chem. Rev.* **2007**, *251*, 1973.
[N°474] Novokmet, S.; Heinemann, F. W.; Zahl, A.; Alsfasser, R. *Inorg. Chem.* **2005**, *44*, 4796.
[N°475] Burghardt, T. P.; Juranić, N.; Macura, S.; Ajtai, K. *Biopolymers* **2002**, *63*, 261.
[N°476] Steiner, T. *Angew. Chem. Int. Ed. Engl.* **2002**, *41*, 48.
[N°477] Pletneva, E. V.; Laederach, A. T.; Fulton, D. B.; Kostić, N. M. *J. Am. Chem. Soc.* **2001**, *123*, 6232.
[N°478] Malenov, D. P.; Ninković, D. B.; Sredojević, D. N.; Zarić, S. D. **2014**, n/a.

[N°479] Jurca, T.; Korobkov, I.; Gorelsky, S. I.; Richeson, D. S. *Inorg. Chem.* **2013**, *52*, 5749.
[N°480] Mosae Selvakumar, P.; Suresh, E.; Subramanian, P. S. *Polyhedron* **2009**, *28*, 245.
[N°481] Wang, X.-J.; Jian, H.-X.; Liu, Z.-P.; Ni, Q.-L.; Gui, L.-C.; Tang, L.-H. *Polyhedron* **2008**, *27*, 2634.
[N°482] Sredojevic, D.; Bogdanovic, G. A.; Tomic, Z. D.; Zaric, S. D. *Crystengcomm* **2007**, *9*, 793.
[N°483] Sredojević, D.; Tomić, Z.; Zarić, S. *Cent. Eur. J. Chem.* **2007**, *5*, 20.
[N°484] Tomic, Z. D.; Sredojevic, D.; Zaric, S. D. *Cryst. Growth Des.* **2006**, *6*, 29.
[N°485] Pucci, D.; Albertini, V.; Bloise, R.; Bellusci, A.; Cataldi, A.; Catapano, C. V., . . . Crispini, A. *J. Inorg. Chem.* **2006**, *100*, 1575.
[N°486] Tomic, Z. D.; Novakovic, S. B.; Zaric, S. D. *Eur. J. Inorg. Chem.* **2004**, 2215.
[N°487] Mukhopadhyay, U.; Choquesillo-Lazarte, D.; Niclos-Gutierrez, J.; Bernal, I. *Crystengcomm* **2004**, *6*, 627.
[N°488] Craven, E.; Zhang, C.; Janiak, C.; Rheinwald, G.; Lang, H. *Z. Anorg. Allg. Chem.* **2003**, *629*, 2282.
[N°489] Castiñeiras, A.; Sicilia-Zafra, A. G.; González-Pérez, J. M.; Choquesillo-Lazarte, D.; Niclós-Gutiérrez, J. *Inorg. Chem.* **2002**, *41*, 6956.
[N°490] Pitoňák, M.; Neogrády, P.; Řezáč, J.; Jurečka, P.; Urban, M.; Hobza, P. *J. Chem. Theory Comput.* **2008**, *4*, 1829.
[N°491] Lee, E. C.; Kim, D.; Jurečka, P.; Tarakeshwar, P.; Hobza, P.; Kim, K. S. *J. Phys. Chem. A* **2007**, *111*, 3446.
[N°492] Milcic, M. K.; Ostojic, B. D.; Zaric, S. D. *Inorg. Chem.* **2007**, *46*, 7109.
[N°493] Masui, H. *Coord. Chem. Rev.* **2001**, *219–221*, 957.
[N°494] Milčić, M. K.; Medaković, V. B.; Zarić, S. D. *Inorg. Chim. Acta* **2006**, *359*, 4427.
[N°495] Milcic, M. K.; Medakovic, V. B.; Sredojevic, D. N.; Juranic, N. O.; Zaric, S. D. *Inorg. Chem.* **2006**, *45*, 4755.
[N°496] Sredojević, D. a. N.; Tomić, Z. D.; Zarić, S. a. D. *Cryst. Growth Des.* **2010**, *10*, 3901.
[N°497] Raghavender, U. S.; Chatterjee, B.; Saha, I.; Rajagopal, A.; Shamala, N.; Balaram, P. *J. Phys. Chem. B* **2011**, *115*, 9236.
[N°498] Voloshina, E.; Usvyat, D.; Schutz, M.; Dedkov, Y.; Paulus, B. *Phys. Chem. Chem. Phys.* **2011**, *13*, 12041.
[N°499] Natarajan, R.; Charmant, J. P. H.; Orpen, A. G.; Davis, A. P. *Angew. Chem. Int. Ed. Engl.* **2010**, *49*, 5125.
[N°500] Kim, S.-J.; Seo, H.-I.; Boo, B. H. *Mol. Phys.* **2009**, *107*, 1261.
[N°501] Takaiwa, D.; Hatano, I.; Koga, K.; Tanaka, H. *Proc. Natl. Acad. Sci. USA* **2008**, *105*, 39.
[N°502] Agre, P. *Angew. Chem. Int. Ed. Engl.* **2004**, *43*, 4278.
[N°503] Kozono, D.; Yasui, M.; King, L. S.; Agre, P. *J. Clinical Invest.* **2002**, *109*, 1395.
[N°504] Hummer, G.; Rasaiah, J. C.; Noworyta, J. P. *Nature* **2001**, *414*, 188.
[N°505] Steiner, T.; Koellner, G. *J. Mol. Biol.* **2001**, *305*, 535.
[N°506] Zaric, S. D.; Popovic, D. M.; Knapp, E. W. *Chemistry* **2000**, *6*, 3935.
[N°507] Veljkovic, D. Z.; Janjic, G. V.; Zaric, S. D. *Crystengcomm* **2011**, *13*, 5005.
[N°508] Slipchenko, L. V.; Gordon, M. S. *J. Phys. Chem. A* **2008**, *113*, 2092.
[N°509] Tarakeshwar, P.; Choi, H. S.; Lee, S. J.; Lee, J. Y.; Kim, K. S.; Ha, T.-K., . . . Lee, H. *J. Chem. Phys.* **1999**, *111*, 5838.
[N°510] Feller, D. *J. Phys. Chem. A* **1999**, *103*, 7558.
[N°511] Courty, A.; Mons, M.; Dimicoli, I.; Piuzzi, F.; Gaigeot, M.-P.; Brenner, V., . . . Millié, P. *J. Phys. Chem. A* **1998**, *102*, 6590.
[N°512] F. Malone, J.; M. Murray, C.; H. Charlton, M.; Docherty, R.; J. Lavery, A. *J. Chem. Soc., Faraday Trans.* **1997**, *93*, 3429.
[N°513] Suzuki, S.; Green, P. G.; Bumgarner, R. E.; Dasgupta, S.; Goddard, W. A.; Blake, G. A. *Science* **1992**, *257*, 942.
[N°514] Gierszal, K. P.; Davis, J. G.; Hands, M. D.; Wilcox, D. S.; Slipchenko, L. V.; Ben-Amotz, D. *J. Phys. Chem. Lett.* **2011**, *2*, 2930.
[N°515] Wang, J.; White, T. A.; Arachchige, S. M.; Brewer, K. J. *Chem. Commun.* **2011**, *47*, 4451.
[N°516] Yamada, S.; Nojiri, Y. *Chem. Commun.* **2011**, *47*, 9143.
[N°517] Kleiner, C. M.; Schreiner, P. R. *Chem. Commun.* **2006**, 4315.
[N°518] Paschek, D.; Ludwig, R. *Angew. Chem. Int. Ed. Engl.* **2011**, *50*, 352.
[N°519] Vojislavljevic, D. Z.; Janjic, G. V.; Ninkovic, D. B.; Kapor, A.; Zaric, S. D. *Crystengcomm* **2013**, *15*, 2099.
[N°520] Coffey, C. E.; Lewis, J.; Nyholm, R. S. *J. Chem. Phys.* **1964**, 1741.
[N°521] Tiekink, E. R. T. *Coord. Chem. Rev.* **2014**, *275*, 130.
[N°522] Pyykko, P. *Chem. Rev.* **1997**, *97*, 597.
[N°523] Jansen, M. *Angew. Chem. Int. Ed. Engl.* **1987**, *26*, 1098.
[N°524] Xia, B.-H.; Zhang, H.-X.; Che, C.-M.; Leung, K.-H.; Phillips, D. L.; Zhu, N.; Zhou, Z.-Y. *J. Am. Chem. Soc.* **2003**, *125*, 10362.
[N°525] Crespo, O.; Laguna, A.; Fernández, E. J.; López-de-Luzuriaga, J. M.; Jones, P. G.; Teichert, M., . . . Werner, H.-J. *Inorg. Chem.* **2000**, *39*, 4786.
[N°526] Yoon, K.; Parkin, G. *Polyhedron* **1995**, *14*, 811.
[N°527] Rundle, R. E. *J. Am. Chem. Soc.* **1954**, *76*, 3101.
[N°528] Weber, M.; Klein, J. E. M. N.; Miehlich, B.; Frey, W.; Peters, R. *Organometallics* **2013**, *32*, 5810.
[N°529] Nebra, N.; Ladeira, S.; Maron, L.; Martin-Vaca, B.; Bourissou, D. *Chem. Eur. J.* **2012**, *18*, 8474.
[N°530] Luo, J.; Khusnutdinova, J. R.; Rath, N. P.; Mirica, L. M. *Chem. Commun.* **2012**, *48*, 1532.
[N°531] Smith, D. C.; Gray, H. B. *Coord. Chem. Rev.* **1990**, *100*, 169.
[N°532] Mathieson, T.; Schier, A.; Schmidbaur, H. *J. Chem. Soc., Dalton Trans.* **2000**, 3881.
[N°533] Grohmann, A.; Schmidbaur, H. In *Comprehensive Organometallic Chemistry II*; Abel, E. W., Stone, F. G. A., Wilkinson, G., Eds.; Elsevier: Oxford, **1995**, p 1.
[N°534] Schmidbaur, H. *Gold Bull.* **1990**, *23*, 11.
[N°535] Scherbaum, F.; Grohmann, A.; Huber, B.; Krüger, C.; Schmidbaur, H. *Angew. Chem. Int. Ed. Engl.* **1988**, *27*, 1544.
[N°536] Vicente, J.; Chicote, M. T.; Lagunas, M. C. *Inorg. Chem.* **1993**, *32*, 3748.
[N°537] Carvajal, M. A.; Alvarez, S.; Novoa, J. J. *Chem. Eur. J.* **2004**, *10*, 2117.
[N°538] Hayes, I. C.; Stone, A. J. *Mol. Phys.* **1984**, *53*, 83.
[N°539] Schuh, W.; Braunstein, P.; Benard, M.; Rohmer, M. M.; Welter, R. *J. Am. Chem. Soc.* **2005**, *127*, 10250.
[N°540] Schuh, W.; Braunstein, P.; Benard, M.; Rohmer, M. M.; Welter, R. *Angew. Chem. Int. Ed. Engl.* **2003**, *42*, 2161.
[N°541] Grimme, S.; Djukic, J.-P. *Inorg. Chem.* **2011**, *50*, 2619.
[N°542] Mandal, S.; Reber, A. C.; Qian, M.; Liu, R.; Saavedra, H. M.; Sen, S., . . . Sen, A. *Dalton Trans.* **2012**, *41*, 5454.
[N°543] Laurila, E.; Tatikonda, R.; Oresmaa, L.; Hirva, P.; Haukka, M. *Crystengcomm* **2012**, *14*, 8401.
[N°544] van der Eide, E. F.; Yang, P.; Walter, E. D.; Liu, T.; Bullock, R. M. *Angew. Chem. Int. Ed. Engl.* **2012**, *51*, 8361.
[N°545] Liddle, S. T.; Mills, D. P.; Gardner, B. M.; McMaster, J.; Jones, C.; Woodul, W. D. *Inorg. Chem.* **2009**, *48*, 3520.
[N°546] Niskanen, M.; Hirva, P.; Haukka, M. *J. Chem. Theory Comput.* **2009**, *5*, 1084.
[N°547] Liddle, S. T.; McMaster, J.; Mills, D. P.; Blake, A. J.; Jones, C.; Woodul, W. D. *Angew. Chem. Int. Ed. Engl.* **2009**, *48*, 1077.

[N°548] Hartl, F.; Renfrew, A. K.; Lafolet, F.; Mahabiersing, T.; Calhorda, M. J.; Chardon-Noblat, S., . . . Deronzier, A. *Inorg. Chem.* **2009**, *48*, 8233.
[N°549] Minasian, S. G.; Krinsky, J. L.; Williams, V. A.; Arnold, J. *J. Am. Chem. Soc.* **2008**, *130*, 10086.
[N°550] Katz, M. J.; Sakai, K.; Leznoff, D. B. *Chem. Soc. Rev.* **2008**, *37*, 1884.
[N°551] Hirva, P.; Haukka, M.; Jakonen, M.; Pakkanen, T. A. *Inorg. Chim. Acta* **2006**, *359*, 853.
[N°552] Villarroya, B. E.; Tejel, C.; Rohmer, M.-M.; Oro, L. A.; Ciriano, M. A.; Bénard, M. *Inorg. Chem.* **2005**, *44*, 6536.
[N°553] Angurell, I.; Martinez-Ruiz, I.; Rossell, O.; Seco, M.; Gomez-Sal, P.; Martin, A. *Chem. Commun.* **2004**, 1712.
[N°554] Fontana, M.; Chanzy, H.; Caseri, W. R.; Smith, P.; Schenning, A. P. H. J.; Meijer, E. W.; Gröhn, F. *Chem. Mater.* **2002**, *14*, 1730.
[N°555] Masciocchi, N.; Moret, M.; Cairati, P.; Ragaini, F.; Sironi, A. *J. Chem. Soc., Dalton Trans.* **1993**, 471.
[N°556] Porchia, M.; Casellato, U.; Ossola, F.; Rossetto, G.; Zanella, P.; Graziani, R. *J. Chem. Soc., Chem. Commun.* **1986**, 1034.
[N°557] Underhill, A. E.; Watkins, D. M. *Chem. Soc. Rev.* **1980**, *9*, 429.
[N°558] Arnold, P. L.; McMaster, J.; Liddle, S. T. *Chem. Commun.* **2009**, 818.
[N°559] Hyla-Kryspin, I.; Grimme, S.; Djukic, J. P. *Organometallics* **2009**, *28*, 1001.
[N°560] Bonifaci, C.; Ceccon, A.; Santi, S.; Mealli, C.; Zoellner, R. W. *Inorg Chim Acta* **1995**, *240*, 541.
[N°561] Pizzotti, M.; Ugo, R.; Dragonetti, C.; Annoni, E.; Demartin, F.; Mussini, P. *Organometallics* **2003**, *22*, 4001.
[N°562] Schwabe, T.; Grimme, S.; Djukic, J.-P. *J. Am. Chem. Soc.* **2009**, *131*, 14156.
[N°563] Lattanzi, A.; De Fusco, C.; Russo, A.; Poater, A.; Cavallo, L. *Chem. Commun.* **2012**, *48*, 1650.
[N°564] Grasso, G. I.; Bellia, F.; Arena, G.; Vecchio, G.; Rizzarelli, E. *Inorg. Chem.* **2011**, *50*, 4917.
[N°565] Shinisha, C. B.; Sunoj, R. B. *Org. Biomol. Chem.* **2008**, *6*, 3921.
[N°566] Sabo-Etienne, S.; Chaudret, B. In *Modern Coordination Chemistry: The Legacy of Joseph Chatt*; Leigh, G. J., Winterton, N., Eds.; The Royal Society of Chemistry: **2002**, p 45.
[N°567] Knowles, J. R. *Nature* **1991**, *350*, 121.
[N°568] Borghesani, G.; Pulidori, F.; Remelli, M.; Purrello, R.; Rizzarelli, E. *J. Chem. Soc., Dalton Trans.* **1990**, 2095.
[N°569] Okawa, H.; Tokunaga, H.; Katsuki, T.; Koikawa, M.; Kida, S. *Inorg. Chem.* **1988**, *27*, 4373.
[N°570] Ōkawa, H.; Nakamura, M.; Kida, S. *Inorg. Chim. Acta* **1986**, *120*, 185.
[N°571] Mantovani, L.; Ceccon, A.; Gambaro, A.; Santi, S.; Ganis, P.; Venzo, A. *Organometallics* **1997**, *16*, 2682.
[N°572] Bonifaci, C.; Carta, G.; Ceccon, A.; Gambaro, A.; Santi, S.; Venzo, A. *Organometallics* **1996**, *15*, 1630.
[N°573] Bonifaci, C.; Ceccon, A.; Gambaro, A.; Ganis, P.; Santi, S.; Venzo, A. *Organometallics* **1995**, *14*, 2430.
[N°574] Bonifaci, C.; Ceccon, A.; Gambaro, A.; Ganis, P.; Santi, S.; Valle, G.; Venzo, A. *Organometallics* **1993**, *12*, 4211.
[N°575] Ceccon, A.; Gambaro, A.; Santi, S.; Valle, G.; Venzo, A. *J. Chem. Soc., Chem. Commun.* **1989**, 51.
[N°576] Cecchetto, P.; Ceccon, A.; Gambaro, A.; Santi, S.; Ganis, P.; Gobetto, R., . . . Venzo, A. *Organometallics* **1998**, *17*, 752.
[N°577] Bonifaci, C.; Ceccon, A.; Gambaro, A.; Manoli, F.; Mantovani, L.; Ganis, P., . . . Venzo, A. *J. Organomet. Chem.* **1998**, *557*, 97.
[N°578] Sieffert, N.; Bühl, M. *Inorg. Chem.* **2009**, *48*, 4622.
[N°579] Grimme, S. *Angew. Chem. Int. Ed. Engl.* **2006**, *45*, 4460.
[N°580] Grimme, S. *Chem. Eur. J.* **2004**, *10*, 3423.
[N°581] Arndt, L. W.; Darensbourg, M. Y.; Delord, T.; Bancroft, B. T. *J. Am. Chem. Soc.* **1986**, *108*, 2617.
[N°582] Kalinin, V. N.; Cherepanov, i. y. A.; Moiseev, S. K.; Batsanov, A. S.; Struchkov, Y. T. *Mendeleev Commun.* **1991**, *1*, 77.
[N°583] Edelmann, F.; Töfke, S.; Behrens, U. *J. Organomet. Chem.* **1986**, *308*, 27.
[N°584] Hock, A. A.; Mills, O. S. *Acta Cryst.* **1961**, *14*, 139.
[N°585] Barr, R. D.; Green, M.; Marsden, K.; Stone, F. G. A.; Woodward, P. *J. Chem. Soc., Dalton Trans.* **1983**, 507.
[N°586] Einstein, F. W. B.; Pomeroy, R. K.; Rushman, P.; Willis, A. C. *Organometallics* **1985**, *4*, 250.
[N°587] Einstein, F. W. B.; Jones, T.; Pomeroy, R. K.; Rushman, P. *J. Am. Chem. Soc.* **1984**, *106*, 2707.
[N°588] Fleming, M. M.; Pomeroy, R. K.; Rushman, P. *J. Organomet. Chem.* **1984**, *273*, C33.
[N°589] Jiang, F.; Jenkins, H. A.; Biradha, K.; Davis, H. B.; Pomeroy, R. K.; Zaworotko, M. J. *Organometallics* **2000**, *19*, 5049.
[N°590] Jiang, F.; Biradha, K.; Leong, W. K.; Pomeroy, R. K.; Zaworotko, M. J. *Can. J. Chem.* **1999**, *77*, 1327.
[N°591] Poblet, J.-M.; Benard, M. *Chem. Commun.* **1998**, 1179.
[N°592] Jiang, F.; Male, J. L.; Biradha, K.; Leong, W. K.; Pomeroy, R. K.; Zaworotko, M. J. *Organometallics* **1998**, *17*, 5810.
[N°593] Shipley, J. A.; Batchelor, R. J.; Einstein, F. W. B.; Pomeroy, R. K. *Organometallics* **1991**, *10*, 3620.
[N°594] Batchelor, R. J.; Davis, H. B.; Einstein, F. W. B.; Pomeroy, R. K. *J. Am. Chem. Soc.* **1990**, *112*, 2036.
[N°595] Davis, H. B.; Einstein, F. W. B.; Glavina, P. G.; Jones, T.; Pomeroy, R. K.; Rushman, P. *Organometallics* **1989**, *8*, 1030.
[N°596] Einstein, F. W. B.; Jennings, M. C.; Krentz, R.; Pomeroy, R. K.; Rushman, P.; Willis, A. C. *Inorg. Chem.* **1987**, *26*, 1341.
[N°597] Einstein, F. W. B.; Martin, L. R.; Pomeroy, R. K.; Rushman, P. *J. Chem. Soc., Chem. Commun.* **1985**, 345.
[N°598] Martin, L. R.; Einstein, F. W. B.; Pomeroy, R. K. *Inorg. Chem.* **1985**, *24*, 2777.
[N°599] Grimme, S.; Djukic, J.-P. *Inorg. Chem.* **2010**, *49*, 2911.
[N°600] Nakatsuji, H.; Hada, M.; Kawashima, A. *Inorg. Chem.* **1992**, *31*, 1740.
[N°601] Cullen, W. R.; Rettig, S. J.; Zhang, H. *Organometallics* **1993**, *12*, 1964.
[N°602] Töfke, S.; Behrens, U. *J. Organomet. Chem.* **1980**, *338*, 29.
[N°603] Lindley, P. F.; Mills, O. S. *J. Chem. Soc. A* **1969**, 1286.
[N°604] Djukic, J. P.; Pfeffer, M.; Dotz, K. H. *C.R. Acad. Sci. Paris, Ser. IIc* **1999**, *2*, 403.
[N°605] Djukic, J. P.; Maisse, A.; Pfeffer, M.; Dotz, K. H.; Nieger, M. *Eur. J. Inorg. Chem.* **1998**, 1781.
[N°606] Djukic, J. P.; Maisse, A.; Pfeffer, M. *J. Organomet. Chem.* **1998**, *567*, 65.
[N°607] Djukic, J. P.; Dotz, K. H.; Pfeffer, M.; DeCian, A.; Fischer, J. *Organometallics* **1997**, *16*, 5171.
[N°608] Djukic, J. P.; Maisse-Francois, A.; Pfeffer, M.; Dotz, K. H.; De Cian, A.; Fischer, J. *Organometallics* **2000**, *19*, 5484.
[N°609] Djukic, J. P.; Michon, C.; Maisse-Francois, A.; Allagapen, R.; Pfeffer, M.; Dotz, K. H., . . . Fischer, J. *Chem. Eur. J.* **2000**, *6*, 1064.
[N°610] Djukic, J. P.; Michon, C.; Berger, A.; Pfeffer, M.; de Cian, A.; Kyritsakas-Gruber, N. *J. Organomet. Chem.* **2006**, *691*, 846.
[N°611] Djukic, J. P.; Maisse, A.; Pfeffer, M.; Dotz, K. H.; Nieger, M. *Organometallics* **1999**, *18*, 2786.
[N°612] Werlé, C.; Le Goff, X. F.; Djukic, J. P. *J. Organomet. Chem.* **2014**, *751*, 754.
[N°613] Cobar, E. A.; Khaliullin, R. Z.; Bergman, R. G.; Head-Gordon, M. *Proc. Natl. Acad. Sci. USA* **2007**, *104*, 6963.
[N°614] Lai, C. C.; Own, Z. Y.; Unruh, L. E.; Chou, M. W. *J. Chin. Chem. Soc.* **1991**, *38*, 207.
[N°615] Djukic, J. P.; Dotz, K. H.; Pfeffer, M.; De Cian, A.; Fischer, J. *Inorg. Chem.* **1998**, *37*, 3649.
[N°616] Schwab, P.; Grubbs, R. H.; Ziller, J. W. *J. Am. Chem. Soc.* **1996**, *118*, 100.
[N°617] Schwab, P.; Mahr, N.; Wolf, J.; Werner, H. *Angew. Chem. Int. Ed. Engl.* **1993**, *32*, 1480.
[N°618] Herrmann, W. A.; Weidenhammer, K.; Ziegler, M. L. *Z. Anorg. Allg. Chem.* **1980**, *460*, 200.

[N°619] Herrmann, W. A. *Angew. Chem. Int. Ed. Engl.* **1978**, *17*, 800.
[N°620] Herrmann, W. A. *Chem. Ber.* **1975**, *108*, 486.
[N°621] Doyle, M. P. *Chem. Rev.* **1986**, *86*, 919.
[N°622] Pfeiffer, J.; Nieger, M.; Dotz, K. H. *Eur. J. Org. Chem.* **1998**, 1011.
[N°623] Michon, C.; Djukic, J. P.; Ratkovic, Z.; Collin, J. P.; Pfeffer, M.; de Cian, A., . . . Nieger, M. *Organometallics* **2002**, *21*, 3519.
[N°624] Grigsby, W. J.; Main, L.; Nicholson, B. K. *Organometallics* **1993**, *12*, 397.
[N°625] Liebeskind, L. S.; Gasdaska, J. R.; Mccallum, J. S.; Tremont, S. J. *J. Org. Chem.* **1989**, *54*, 669.
[N°626] Cambie, R. C.; Metzler, M. R.; Rutledge, P. S.; Woodgate, P. D. *J. Organomet. Chem.* **1990**, *381*, C26.
[N°627] Cambie, R. C.; Metzler, M. R.; Rutledge, P. S.; Woodgate, P. D. *J. Organomet. Chem.* **1992**, *429*, 41.
[N°628] Michon, C.; Djukic, J. P.; Pfeffer, M.; Gruber-Kyritsakas, N.; de Cian, A. *J. Organomet. Chem.* **2007**, *692*, 1092.
[N°629] Contreras-García, J.; Johnson, E. R.; Keinan, S.; Chaudret, R.; Piquemal, J.-P.; Beratan, D. N.; Yang, W. *J. Chem. Theory Comput.* **2011**, *7*, 625.
[N°630] Johnson, E. R.; Keinan, S.; Mori-Sánchez, P.; Contreras-García, J.; Cohen, A. J.; Yang, W. *J. Am. Chem. Soc.* **2010**, *132*, 6498.
[N°631] Hart-Davis, A. J.; Mawby, R. J. *J. Chem. Soc. A* **1969**, 2403.
[N°632] Rerek, M. E.; Ji, L. N.; Basolo, F. *J. Chem. Soc., Chem. Commun.* **1983**, 1208.
[N°633] Rerek, M. E.; Basolo, F. *J. Am. Chem. Soc.* **1984**, *106*, 5908.
[N°634] Angelici, R. J.; Loewen, W. *Inorg. Chem.* **1967**, *6*, 682.
[N°635] Ji, L. N.; Rerek, M. E.; Basolo, F. *Organometallics* **1984**, *3*, 740.
[N°636] Veiros, L. F. *Organometallics* **2000**, *19*, 3127.
[N°637] Calhorda, M. J.; Veiros, L. s. F. *Coord. Chem. Rev.* **1999**, *185–186*, 37.
[N°638] Cadierno, V.; Díez, J. n.; Pilar Gamasa, M.; Gimeno, J.; Lastra, E. *Coord. Chem. Rev.* **1999**, *193–195*, 147.
[N°639] Calhorda, M. J.; Romao, C. C.; Veiros, L. F. *Chemistry* **2002**, *8*, 868.
[N°640] Veiros, L. F.; Calhorda, M. J. *Dalton Trans.* **2011**, *40*, 11138.
[N°641] Anderson, S.; Hill, A. F.; Nasir, B. A. *Organometallics* **1995**, *14*, 2987.
[N°642] Okuda, J.; König, P.; Rushkin, I. L.; Kang, H.-C.; Massa, W. *J. Organomet. Chem.* **1995**, *501*, 37.
[N°643] Bitterwolf, T. E.; Lukmanova, D.; Gallagher, S.; Rheingold, A. L.; Guzei, I. A.; Liable-Sands, L. *J. Organomet. Chem.* **2000**, *605*, 168.
[N°644] Groux, L. F.; Belanger-Gariepy, F.; Zargarian, D. *Can. J. Chem.* **2005**, *83*, 634.
[N°645] Glockner, A.; Arias, O.; Bannenberg, T.; Daniliuc, C. G.; Jones, P. G.; Tamm, M. *Dalton Trans.* **2011**, *40*, 11511.
[N°646] Glöckner, A.; Bannenberg, T.; Ibrom, K.; Daniliuc, C. G.; Freytag, M.; Jones, P. G., . . . Tamm, M. *Organometallics* **2012**, *31*, 4480.
[N°647] Pevear, K. A.; Holl, M. M. B.; Carpenter, G. B.; Rieger, A. L.; Rieger, P. H.; Sweigart, D. A. *Organometallics* **1995**, *14*, 512.
[N°648] Casey, C. P.; Vos, T. E.; Brady, J. T.; Hayashi, R. K. *Organometallics* **2003**, *22*, 1183.
[N°649] Garrett, C. E.; Fu, G. C. *J. Org. Chem.* **1998**, *63*, 1370.
[N°650] Schmid, M. A.; Alt, H. G.; Milius, W. *J. Organomet. Chem.* **1996**, *514*, 45.
[N°651] Llinas, G. H.; Day, R. O.; Rausch, M. D.; Chien, J. C. W. *Organometallics* **1993**, *12*, 1283.
[N°652] Foo, T.; Bergman, R. G. *Organometallics* **1992**, *11*, 1801.
[N°653] Marder, T. B.; Roe, D. C.; Milstein, D. *Organometallics* **1988**, *7*, 1451.
[N°654] Borrini, A.; Diviersi, P.; Ingrosso, G.; Lucherini, A.; Serra, G. *J. Mol. Catal.* **1985**, *30*, 181.
[N°655] Bönnemann, H. *Angew. Chem. Int. Ed. Engl.* **1985**, *24*, 248.
[N°656] Huber, T. A.; Bayrakdarian, M.; Dion, S.; Dubuc, I.; Bélanger-Gariépy, F.; Zargarian, D. *Organometallics* **1997**, *16*, 5811.
[N°657] Stradiotto, M.; McGlinchey, M. J. *Coord. Chem. Rev.* **2001**, *219-221*, 311.
[N°658] O'Hare, D. *Organometallics* **1987**, *6*, 1766.
[N°659] Alías, F. M.; Belderraín, T. R.; Paneque, M.; Poveda, M. L.; Carmona, E.; Valerga, P. *Organometallics* **1998**, *17*, 5620.
[N°660] Sui-Seng, C.; Enright, G. D.; Zargarian, D. *Organometallics* **2004**, *23*, 1236.
[N°661] Sui-Seng, C.; Enright, G. D.; Zargarian, D. *J. Am. Chem. Soc.* **2006**, *128*, 6508.
[N°662] Fischer, E. O.; Öfele, K. *Chem. Ber.* **1957**, *90*, 2532.
[N°663] Kündig, E. P.; Fabritius, C.-H.; Grossheimann, G.; Romanens, P.; Butenschön, H.; Wey, H. G. *Organometallics* **2004**, *23*, 3741.
[N°664] Auffrant, A.; Prim, D.; Rose-Munch, F.; Rose, E.; Schouteeten, S.; Vaissermann, J. *Organometallics* **2003**, *22*, 1898.
[N°665] Kamikawa, K.; Norimura, K.; Furusyo, M.; Uno, T.; Sato, Y.; Konoo, A., . . . Uemura, M. *Organometallics* **2003**, *22*, 1038.
[N°666] Kundig, E. P.; Fabritius, C. H.; Grossheimann, G.; Robvieux, F.; Romanens, P.; Bernardinelli, G. *Angew. Chem. Int. Ed. Engl.* **2002**, *41*, 4577.
[N°667] Abd-El-Aziz, A. S.; Bernardin, S. *Coord. Chem. Rev.* **2000**, *203*, 219.
[N°668] Mills, R. C.; Abboud, K. A.; Boncella, J. M. *Organometallics* **2000**, *19*, 2953.
[N°669] Harman, W. D. *Chem. Rev.* **1997**, *97*, 1953.
[N°670] Davies, S. G. *Organotransition Metal Chemistry: applications to Organic Synthesis*; Pergamon Press: Oxford, U.K., **1992**.
[N°671] Beller, M.; Bolm, C. *Transition Metals for Organic Synthesis*; Wiley-VCH: Weinheim, Germany, **1998**.
[N°672] Kündig, E. P. *Transition Metal Arene π-Complexes in Organic Synthesis and Catalysts; Topics in Organometallic Chemistry*, **2004**; Vol. 7.
[N°673] Rosillo, M.; Dominguez, G.; Perez-Castells, J. *Chem. Soc. Rev.* **2007**, *36*, 1589.
[N°674] Ziegler, T.; Heber, U. *Beilstein J. Org. Chem.* **2012**, *8*, 1059.
[N°675] Holmes, J. D.; Jones, D. A. K.; Pettit, R. *J. Organomet. Chem.* **1965**, *4*, 324.
[N°676] Solladié-Cavallo, A. *Polyhedron* **1985**, *4*, 901.
[N°677] Merlic, C. A.; Miller, M. M.; Hietbrink, B. N.; Houk, K. N. *J. Am. Chem. Soc.* **2001**, *123*, 4904.
[N°678] Pape, A. R.; Kaliappan, K. P.; Kündig, E. P. *Chem. Rev.* **2000**, *100*, 2917.
[N°679] Semmelhack, M. F.; Hall, H. T.; Farina, R.; Yoshifuji, M.; Clark, G.; Bargar, T., . . . Clardy, J. *J. Am. Chem. Soc.* **1979**, *101*, 3535.
[N°680] Semmelhack, M. F.; Clark, G. R.; Garcia, J. L.; Harrison, J. J.; Thebtaranonth, Y.; Wulff, W.; Yamashita, A. *Tetrahedron* **1981**, *37*, 3957.
[N°681] Vasen, D.; Salzer, A.; Gerhards, F.; Gais, H.-J.; Stürmer, R.; Bieler, N. H.; Togni, A. *Organometallics* **2000**, *19*, 539.
[N°682] Netz, A.; Polborn, K.; Nöth, H.; Müller, T. J. J. *Eur. J. Org. Chem.* **2005**, *2005*, 1823.
[N°683] Netz, A.; Drees, M.; Strassner, T.; Muller, T. J. J. *Eur. J. Org. Chem.* **2007**, 540.
[N°684] Koide, H.; Hata, T.; Uemura, M. *J. Org. Chem.* **2002**, *67*, 1929.
[N°685] Merlic, C. A.; Hietbrink, B. N.; Houk, K. N. *J. Org. Chem.* **2001**, *66*, 6738.
[N°686] Merlic, C. A.; Walsh, J. C. *J. Org. Chem.* **2001**, *66*, 2265.

[N°687] Merlic, C. A.; Walsh, J. C.; Tantillo, D. J.; Houk, K. N. *J. Am. Chem. Soc.* **1999**, *121*, 3596.
[N°688] Xie, L.; Jones, G. B. *Tetrahedron Lett.* **2005**, *46*, 3579.
[N°689] Gibson, S. E.; Ibrahim, H. *Chem. Commun.* **2002**, 2465.
[N°690] Rose-Munch, F.; Rose, E. *Eur. J. Inorg. Chem.* **2002**, *2002*, 1269.
[N°691] Kamikawa, K.; Watanabe, T.; Uemura, M. *J. Synth. Org. Chem. Jpn.* **2001**, *59*, 1078.
[N°692] Nelson, S. G.; Hilfiker, M. A. *Org. Lett. 9* **1999**, *1*, 1379.
[N°693] Bolm, C.; Muniz, K. *Chem. Soc. Rev.* **1999**, *28*, 51.
[N°694] Butenschon, H. *Synlett* **1999**, 680.
[N°695] Son, S. U.; Jang, H. Y.; Lee, I. S.; Chung, Y. K. *Organometallics* **1998**, *17*, 3236.
[N°696] Schlogl, K. *J. Organomet. Chem.* **1986**, *300*, 219.
[N°697] Schlögl, K. *Top. Stereochem.* **1967**, *1*, 39.
[N°698] Cahn, R. S.; Ingold, C.; Prelog, V. *Angew. Chem. Int. Ed. Engl.* **1966**, *5*, 385.
[N°699] Solladié-Cavallo, A. *Advances in Metal Organic Chemistry*; ed. L. S. Liebeskind, JAI, London, **1989**; Vol. 2, p. 99.
[N°700] Mahaffy, C. A. L.; Pauson, P. L. *Inorg. Synth.* **1990**, *28*, 136.
[N°701] Lee, Y. T.; Choi, S. Y.; Lee, S. I.; Chung, Y. K.; Kang, T. J. *Tetrahedron Lett.* **2006**, *47*, 6569.
[N°702] Kündig, E. P.; Perret, C.; Spichiger, S.; Bernardinelli, G. *J. Organomet. Chem.* **1985**, *286*, 183.
[N°703] Prim, D.; Andrioletti, B.; Rose-Munch, F.; Rose, E.; Couty, F. *Tetrahedron* **2004**, *60*, 3325.
[N°704] Berger, A.; Djukic, J. P.; Michon, C. *Coord. Chem. Rev.* **2002**, *225*, 215.
[N°705] Faza, R. Á. O. N.; de Lera, A. R.; Cárdenas, D. J. *Adv. Synth. Catal.* **2007**, *349*, 887.
[N°706] Sergeev, A. G.; Spannenberg, A.; Beller, M. *J. Am. Chem. Soc.* **2008**, *130*, 15549.
[N°707] Marrone, A.; Re, N.; Romeo, R. *Organometallics* **2008**, *27*, 2215.
[N°708] Jensen, W. B. *J. Chem. Educ.* **2005**, *82*, 28.
[N°709] Langmuir, I. *Science* **1921**, *54*, 59.
[N°710] Pyykkö, P. *J. Organomet. Chem.* **2006**, *691*, 4336.
[N°711] Urtel, H.; Meier, C.; Eisenträger, F.; Rominger, F.; Joschek, J. P.; Hofmann, P. *Angew. Chem. Int. Ed. Engl.* **2001**, *40*, 781.
[N°712] Walter, M. D.; White, P. S.; Brookhart, M. *New J. Chem.* **2013**, *37*, 1128.
[N°713] Rivada-Wheelaghan, O.; Ortuño, M. A.; Díez, J.; Lledós, A.; Conejero, S. *Angew. Chem. Int. Ed. Engl.* **2012**, *51*, 3936.
[N°714] Braunschweig, H.; Gruss, K.; Radacki, K. *Angew. Chem. Int. Ed. Engl.* **2007**, *46*, 7782.
[N°715] Crosby, S. H.; Clarkson, G. J.; Rourke, J. P. *J. Am. Chem. Soc.* **2009**, *131*, 14142.
[N°716] Baratta, W.; Stoccoro, S.; Doppiu, A.; Herdtweck, E.; Zucca, A.; Rigo, P. *Angew. Chem. Int. Ed. Engl.* **2003**, *42*, 105.
[N°717] Ara, I.; Forniés, J.; García, A.; Gómez, J.; Lalinde, E.; Moreno, M. T. *Chem. Eur. J.* **2002**, *8*, 3698.
[N°718] Gerber, R.; Blacque, O.; Frech, C. M. *Dalton Trans.* **2011**, *40*, 8996.
[N°719] Pérez-Rodríguez, M. n.; Braga, A. A. C.; de Lera, A. R.; Maseras, F.; Álvarez, R.; Espinet, P. *Organometallics* **2010**, *29*, 4983.
[N°720] Yandulov, D. V.; Tran, N. T. *J. Am. Chem. Soc.* **2007**, *129*, 1342.
[N°721] Stambuli, J. P.; Weng, Z.; Incarvito, C. D.; Hartwig, J. F. *Angew. Chem. Int. Ed. Engl.* **2007**, *46*, 7674.
[N°722] Stambuli, J. P.; Incarvito, C. D.; Bühl, M.; Hartwig, J. F. *J. Am. Chem. Soc.* **2004**, *126*, 1184.
[N°723] Kefalidis, C. E.; Tsipis, C. A. *J. Comput. Chem.* **2012**, *33*, 1689.
[N°724] Braunschweig, H.; Radacki, K.; Rais, D.; Scheschkewitz, D. *Angew. Chem. Int. Ed. Engl.* **2005**, *44*, 5651.
[N°725] Ingleson, M. J.; Mahon, M. F.; Weller, A. S. *Chem. Commun.* **2004**, 2398.
[N°726] Clegg, W.; Eastham, G. R.; Elsegood, M. R. J.; Heaton, B. T.; Iggo, J. A.; Tooze, R. P., . . . Zacchini, S. *Organometallics* **2002**, *21*, 1832.
[N°727] Lewis, R. A.; George, S. P.; Chapovetsky, A.; Wu, G.; Figueroa, J. S.; Hayton, T. W. *Chem. Commun.* **2013**, *49*, 2888.
[N°728] Emerich, B. M.; Moore, C. E.; Fox, B. J.; Rheingold, A. L.; Figueroa, J. S. *Organometallics* **2011**, *30*, 2598.
[N°729] Margulieux, G. W.; Weidemann, N.; Lacy, D. C.; Moore, C. E.; Rheingold, A. L.; Figueroa, J. S. *J. Am. Chem. Soc.* **2010**, *132*, 5033.
[N°730] Labios, L. A.; Millard, M. D.; Rheingold, A. L.; Figueroa, J. S. *J. Am. Chem. Soc.* **2009**, *131*, 11318.
[N°731] Fox, B. J.; Sun, Q. Y.; DiPasquale, A. G.; Fox, A. R.; Rheingold, A. L.; Figueroa, J. S. *Inorg. Chem.* **2008**, *47*, 9010.
[N°732] Werlé, C.; Bailly, C.; Karmazin-Brelot, L.; Le Goff, X. F.; Ricard, L.; Djukic, J. P. *J. Am. Chem. Soc.* **2013**, *135*, 17839.
[N°733] Werlé, C.; Hamdaoui, M.; Bailly, C.; Le Goff, X. F.; Brelot, L.; Djukic, J. P. *J. Am. Chem. Soc.* **2013**, *135*, 1715.
[N°734] Moiseev, S. K.; Cherepanov, I. A.; Petrovskii, P. V.; Ezernitskaya, M. G.; Butenschön, H.; Strotmann, M.; Kalinin, V. N. *Inorg. Chim. Acta* **1998**, *280*, 71.
[N°735] Kalinin, V. N.; Cherepanov, I. A.; Moiseev, S. K.; Dolgushin, F. M.; Yanovsky, A. I.; Struchkov, Y. T. *Acta Cryst. Sect. C* **1993**, *49*, 805.
[N°736] van Meurs, F.; Baas, J. M. A.; van Bekkum, H. *J. Organomet. Chem.* **1977**, *129*, 347.
[N°737] van Meurs, F.; Baas, J. M. A.; van Bekkum, H. *J. Organomet. Chem.* **1976**, *113*, 353.
[N°738] Grimme, S.; Antony, J.; Ehrlich, S.; Krieg, H. *J. Chem. Phys.* **2010**, *132*, 154104.
[N°739] Steinmann, S. N.; Piemontesi, C.; Delachat, A.; Corminboeuf, C. *J. Chem. Theory Comput.* **2012**, *8*, 1629.
[N°740] Steinmann, S. N.; Corminboeuf, C. *J. Chem. Theory Comput.* **2011**, *7*, 3567.
[N°741] Zhao, Y.; Truhlar, D. *Theor. Chem. Acc.* **2008**, *120*, 215.
[N°742] Zhao, Y.; Truhlar, D. G. *J. Chem. Phys.* **2006**, *125*.
[N°743] Tao, J.; Perdew, J. P.; Staroverov, V. N.; Scuseria, G. E. *Phys. Rev. Lett.* **2003**, *91*, 146401.
[N°744] Ernzerhof, M.; Scuseria, G. E. *J. Chem. Phys.* **1999**, *110*, 5029.
[N°745] Adamo, C.; Barone, V. *J. Chem. Phys.* **1999**, *110*, 6158.
[N°746] Stephens, P. J.; Devlin, F. J.; Chabalowski, C. F.; Frisch, M. J. *J. Phys. Chem.* **1994**, *98*, 11623.
[N°747] van Lenthe, E.; van Leeuwen, R.; Baerends, E. J.; Snijders, J. G. *Int. J. Quantum Chem.* **1996**, *57*, 281.
[N°748] Nakasuji, K.; Yamaguchi, M.; Murata, I.; Tatsumi, K.; Nakamura, A. *Organometallics* **1984**, *3*, 1257.
[N°749] Ziegler, T.; Rauk, A. *Inorg. Chem.* **1979**, *18*, 1755.
[N°750] Mitoraj, M. P.; Michalak, A.; Ziegler, T. *J. Chem. Theory Comput.* **2009**, *5*, 962.
[N°751] Mitoraj, M. P.; Michalak, A.; Ziegler, T. *Organometallics* **2009**, *28*, 3727.
[N°752] Savin, A.; Jepsen, O.; Flad, J.; Andersen, O. K.; Preuss, H.; von Schnering, H. G. *Angew. Chem. Int. Ed. Engl.* **1992**, *31*, 187.
[N°753] Becke, A. D.; Edgecombe, K. E. *J. Chem. Phys.* **1990**, *92*, 5397.
[N°754] Popelier, P. *Atoms in Molecules, An Introduction*; Prentice Hall, Harlow, England, **2000**.
[N°755] Bader, R. F. W. In *Atoms in Molecules: A Quantum Theory*; Clarendon: Oxford, **1990**.
[N°756] Sandstrom, J. *Dynamic NMR Spectroscopy*; Academic Press: New York, **1982**.

[N°757] Cotton, F. A.; Marks, T. J. *J. Am. Chem. Soc.* **1969**, *91*, 3178.
[N°758] Klamt, A.; Schuurmann, G. *J. Chem. Soc., Perkin Trans. 2* **1993**, 799.
[N°759] Gritsenko, O. V.; Schipper, P. R. T.; Baerends, E. J. *Chem. Phys. Lett.* **1999**, *302*, 199.
[N°760] Binsch, G.; Kleier, D. A. *QCPE No. 165*; Indiana University, **1970**.
[N°761] Solin, N.; Szabó, K. J. *Organometallics* **2001**, *20*, 5464.
[N°762] Morales-Morales, D. In *Palladacycles*; Wiley-VCH Verlag GmbH & Co. KGaA: **2008**.
[N°763] Dupont, J.; Consorti, C. S.; Spencer, J. *Chem. Rev.* **2005**, *105*, 2527.
[N°764] Dehand, J.; Pfeffer, M. *Coord. Chem. Rev.* **1976**, *18*, 327.
[N°765] Schwarz, J.; Herdtweck, E.; Herrmann, W. A.; Gardiner, M. G. *Organometallics* **2000**, *19*, 3154.
[N°766] Braunstein, P.; Dehand, J.; Pfeffer, M. *J. Inorg. Nucl. Chem.* **1974**, *10*, 581.
[N°767] Kleiman, J. P.; Dubeck, M. *J. Am. Chem. Soc.* **1963**, *85*, 1544.
[N°768] Cope, A. C.; Siekman, R. W. *J. Am. Chem. Soc.* **1965**, *87*, 3272.
[N°769] Cope, A. C.; Friedrich, E. C. *J. Am. Chem. Soc.* **1968**, *90*, 909.
[N°770] Herrmann, W. A.; Brossmer, C.; Ofele, K.; Reisinger, C. P.; Priermeier, T.; Beller, M.; Fischer, H. *Angew. Chem. Int. Ed. Engl.* **1995**, *34*, 1844.
[N°771] Szabó, K. J. *Synlett* **2006**, *2006*, 811.
[N°772] Dunina, V. V.; Gorunova, O. N. *Rus. Chem. Rev.* **2005**, *74*, 871.
[N°773] Dunina, V. V.; Gorunova, O. N. *Rus. Chem. Rev.* **2004**, *73*, 309.
[N°774] Beletskaya, I. P.; Cheprakov, A. V. *J. Organomet. Chem.* **2004**, *689*, 4055.
[N°775] Omae, I. *Coord. Chem. Rev.* **2004**, *248*, 995.
[N°776] Singleton, J. T. *Tetrahedron* **2003**, *59*, 1837.
[N°777] van der Boom, M. E.; Milstein, D. *Chem. Rev.* **2003**, *103*, 1759.
[N°778] Bedford, R. B. *Chem. Commun.* **2003**, 1787.
[N°779] Dupont, J.; Pfeffer, M.; Spencer, J. *Eur. J. Inorg. Chem.* **2001**, *2001*, 1917.
[N°780] Albrecht, M.; van Koten, G. *Angew. Chem. Int. Ed. Engl.* **2001**, *40*, 3750.
[N°781] Steenwinkel, P.; Gossage, R. A.; van Koten, G. *Chem. Eur. J.* **1998**, *4*, 759.
[N°782] Pfeffer, M. *Pure Appl. Chem.* **1992**, *64*, 335.
[N°783] Ryabov, A. D. *Chem. Rev.* **1990**, *90*, 403.
[N°784] Newkome, G. R.; Puckett, W. E.; Gupta, V. K.; Kiefer, G. E. *Chem. Rev.* **1986**, *86*, 451.
[N°785] Rothwell, I. P. *Polyhedron* **1985**, *4*, 177.
[N°786] Ryabov, A. D. *Synthesis* **1985**, 233.
[N°787] Constable, E. C. *Polyhedron* **1984**, *3*, 1037.
[N°788] Omae, I. *Coord. Chem. Rev.* **1982**, *42*, 245.
[N°789] Omae, I. *Coord. Chem. Rev.* **1980**, *32*, 235.
[N°790] Omae, I. *Coord. Chem. Rev.* **1979**, *28*, 97.
[N°791] Bruce, M. I. *Angew. Chem. Int. Ed. Engl.* **1977**, *16*, 73.
[N°792] Catellani, M. *Synlett* **2003**, 298.
[N°793] Dyker, G. *Chem. Ber.* **1997**, *130*, 1567.
[N°794] Dyker, G.; Korning, J.; Nerenz, F.; Siemsen, P.; Sostmann, S.; Wiegand, A., . . . Bubenitschek, P. *Pure Appl. Chem.* **1996**, *68*, 323.
[N°795] Alacid, E.; Alonso, D. A.; Botella, L.; Najera, C.; Pacheco, M. C. *Chem. Rec.* **2006**, *6*, 117.
[N°796] Bellina, F.; Carpita, A.; Rossi, R. *Synthesis* **2004**, 2419.
[N°797] Bedford, R. B.; Cazin, C. S. J.; Holder, D. *Coord. Chem. Rev.* **2004**, *248*, 2283.
[N°798] Herrmann, W. A.; Ofele, K.; Von Preysing, D.; Schneider, S. K. *J. Organomet. Chem.* **2003**, *687*, 229.
[N°799] Herrmann, W. A.; Bohm, V. P. W.; Reisinger, C. P. *J. Organomet. Chem.* **1999**, *576*, 23.
[N°800] Berger, A.; de Cian, A.; Djukic, J.-P.; Fischer, J.; Pfeffer, M. *Organometallics* **2001**, *20*, 3230.
[N°801] Ryabov, A. D.; Van Eldik, R.; Le Borgne, G.; Pfeffer, M. *Organometallics* **1993**, *12*, 1386.
[N°802] Gaunt, J. C.; Shaw, B. L. *J. Organomet. Chem.* **1975**, *102*, 511.
[N°803] Otsuka, S.; Nakamura, A.; Kano, T.; Tani, K. *J. Am. Chem. Soc.* **1971**, *93*, 4301.
[N°804] Schmulling, M.; Ryabov, A. D.; van Eldik, R. *J. Chem. Soc., Chem. Commun.* **1992**, 1609.
[N°805] Thomas, S. W.; Venkatesan, K.; Müller, P.; Swager, T. M. *J. Am. Chem. Soc.* **2006**, *128*, 16641.
[N°806] Slater, J. C. *J. Chem. Phys.* **1964**, *41*, 3199.
[N°807] W. Neuse, E. *J. Organomet. Chem.* **1975**, *99*, 287.
[N°808] Adams, D. M.; Squire, A. *J. Chem. Soc., Dalton Trans.* **1974**, 558.
[N°809] Deverell, C.; Morgan, R. E.; Strange, J. H. *Mol. Phys.* **1970**, *18*, 553.
[N°810] Van Lenthe, E.; Baerends, E. J. *J. Comput. Chem.* **2003**, *24*, 1142.
[N°811] Staroverov, V. N.; Scuseria, G. E.; Tao, J.; Perdew, J. P. *J. Chem. Phys.* **2003**, *119*, 12129.
[N°812] Weinhold, F. In *Encyclopedia of Computational Chemistry*; Schleyer, P. v. R., Allinger, N. L., Clark, T., Gasteiger, J., Kollman, P. A., III, H. F. S., Schreiner, P. R., Eds.; John Wiley & Sons, Chichester, UK: **1998**; Vol. 3, p 1792.
[N°813] Weinhold, F.; Landis, C. R. *Valency and Bonding, a Natural Bond Orbital Donor-Acceptor Perspective*; University Press: Cambridge, UK, **2005**.
[N°814] Macchi, P.; Garlaschelli, L.; Martinengo, S.; Sironi, A. *J. Am. Chem. Soc.* **1999**, *121*, 10428.
[N°815] Bo, C.; Sarasa, J. P.; Poblet, J. M. *J. Phys. Chem.* **1993**, *97*, 6362.
[N°816] Bo, C.; Costas, M.; Poblet, J. M.; Rohmer, M.-M.; Benard, M. *Inorg. Chem.* **1996**, *35*, 3298.
[N°817] Johansson, M. P.; Swart, M. *Phys. Chem. Chem. Phys.* **2013**, *15*, 11543.
[N°818] Bielinski, E. A.; Dai, W.; Guard, L. M.; Hazari, N.; Takase, M. K. *Organometallics* **2013**, *32*, 4025.
[N°819] Chalkley, M. J.; Guard, L. M.; Hazari, N.; Hofmann, P.; Hruszkewycz, D. P.; Schmeier, T. J.; Takase, M. K. *Organometallics* **2013**, *32*, 4223.
[N°820] Bickelhaupt, F. M.; Baerends, E. J.; Lipkowitz, K. B.; Boyd, D. B.; Eds.; Wiley: New-York, **2000**, pp 1-86.
[N°821] te Velde, G.; Bickelhaupt, F. M.; Baerends, E. J.; Fonseca Guerra, C.; van Gisbergen, S. J. A.; Snijders, J. G.; Ziegler, T. *J. Comp. Chem.* **2001**, *22*, 931.
[N°822] Djukic, J.-P.; Hijazi, A.; Flack, H. D.; Bernardinelli, G. *Chem. Soc. Rev.* **2008**, *37*, 406.
[N°823] Flack, H. D.; Bernardinelli, G. *Acta Cryst. Sect. A* **1999**, *55*, 908.
[N°824] Pescitelli, G.; Kurtan, T.; Florke, U.; Krohn, K. *Chirality* **2009**, *21*, E181.

[N°825] Lacour, J. *C.R. Chimie* **2010**, *13*, 985.
[N°826] Favarger, F.; Goujon-Ginglinger, C.; Monchaud, D.; Lacour, J. *J. Org. Chem.* **2004**, *69*, 8521.
[N°827] Lacour, J. *Chimia* **2002**, *56*, 672.
[N°828] Lokshin, B. V.; Rusach, E. B.; Kolobova, N. E.; Makarov, Y. V.; Ustynyuk, N. A.; Zdanovich, V. I., . . . Setkina, V. N. *J. Organomet. Chem.* **1976**, *108*, 353.
[N°829] Magomedov, G. K. I.; Syrkin, V. G.; Frenkel, A. S.; Zakharchenko, O. A. *Zh. Obshch. Khim.* **1975**, *45*, 2530.
[N°830] Edgar, K.; Johnson, B. F. G.; Lewis, J.; Wild, S. B. *J. Chem. Soc. A* **1968**, 2851.
[N°831] Morgan, G. T.; Drew, H. D. K. *J. Chem. Soc., Trans.* **1920**, *117*, 1456.
[N°832] Farrugia, L. J.; Senn, H. M. *J. Phys. Chem. A* **2010**, *114*, 13418.
[N°833] Farrugia, L. J. *Chem. Phys. Lett.* **2005**, *414*, 122.
[N°834] Gervasio, G.; Bianchi, R.; Marabello, D. *Chem. Phys. Lett.* **2005**, *407*, 18.
[N°835] Overgaard, J.; Clausen, H. F.; Platts, J. A.; Iversen, B. B. *J. Am. Chem. Soc.* **2008**, *130*, 3834.
[N°836] Bader, R. F. W.; Gatti, C. *Chem. Phys. Lett.* **1998**, *287*, 233.
[N°837] Kohout, M. *Int. J. Quantum Chem.* **2004**, *97*, 651.
[N°838] Fradera, X.; Austen, M. A.; Bader, R. F. W. *J. Phys. Chem. A* **1999**, *103*, 304.
[N°839] Gatti, C. In *Zeitschrift für Kristallographie* 2005; Vol. 220, p 399.
[N°840] Burmeister, J. L.; DeStefano, N. J. *J. Chem. Soc., Chem. Commun.* **1970**, 1698.
[N°841] Jennings, M. A.; Wojcicki, A. *J. Organomet. Chem.* **1968**, *14*, 231.
[N°842] Giordano, G.; Crabtree, R. H. *Inorg. Synth.* **1990**, *28*, 88.
[N°843] Abel, E. W.; Bennett, M. A.; Wilkinson, G. *J. Chem. Soc. A* **1959**, 3178.
[N°844] Hanh Nguyen, D.; Lassauque, N.; Vendier, L.; Mallet-Ladeira, S.; Le Berre, C.; Serp, P.; Kalck, P. *Eur. J. Inorg. Chem.* **2014**, *2014*, 326.
[N°845] Bonifaci, C.; Ceccon, A.; Gambaro, A.; Ganis, P.; Santi, S.; Valle, G.; Venzo, A. *J. Organomet. Chem.* **1995**, *492*, 35.
[N°846] Ceccon, A.; Elsevier, C. J.; Ernsting, J. M.; Gambaro, A.; Santi, S.; Venzo, A. *Inorg. Chim. Acta* **1993**, *204*, 15.
[N°847] Werlé, C.; Bailly, C.; Karmazin-Brelot, L.; Le Goff, X.-F.; Pfeffer, M.; Djukic, J.-P. *Angew. Chem. Int. Ed. Engl.* **2014**, *53*, 9827.
[N°848] Ceccon, A.; Gambaro, A.; Venzo, A.; Lucchini, V.; Bitterwolf, T. E.; Shade, J. *J. Organomet. Chem.* **1988**, *349*, 315.
[N°849] Bondi, A. *J. Phys. Chem.* **1964**, *68*, 441.
[N°850] Wiberg, K. B. *Tetrahedron Lett.* **1968**, *24*, 1083.
[N°851] Javed, M. I.; Brewer, M. *Org. Lett. 9* **2007**, *9*, 1789.
[N°852] Ishiguro, K.; Ikeda, M.; Sawaki, Y. *J. Org. Chem.* **1992**, *57*, 3057.
[N°853] Djukic, J.-P.; Parkhomenko, K.; Hijazi, A.; Chemmi, A.; Allouche, L.; Brelot, L., . . . Le Goff, X.-F. *Dalton Trans.* **2009**, 2695.
[N°854] In *Amsterdam Density Functional ADF2012*; SCM: Theoretical Chemistry, Vrije Universiteit, Amsterdam, The Netherlands.
[N°855] Brown, D. A.; Fitzpatrick, N. J.; Glass, W. K.; Ahmed, H. A.; Cunningham, D.; McArdle, P. *J. Organomet. Chem.* **1993**, *455*, 157.
[N°856] Perdew, J. P.; Wang, Y. *Phys. Rev. B* **1992**, *45*, 13244.
[N°857] In *M86-E01078 APEX2 User Manual*: Bruker AXS Inc.: Madison, USA, **2006**.
[N°858] Sheldrick, G. *Acta Cryst. Sect. A* **1990**, *46*, 467.
[N°859] Sheldrick, G. M.; Universität Göttingen: Göttingen, Germany, **1998**.
[N°860] Altomare, A.; Burla, M. C.; Camalli, M.; Cascarano, G. L.; Giacovazzo, C.; Guagliardi, A., . . . Spagna, R. *J. Appl. Cryst.* **1999**, *32*, 115.
[N°861] In *Amsterdam Density Functional ADF2013*; SCM: Theoretical Chemistry, Vrije Universiteit, Amsterdam, The Netherlands.

Christophe WERLÉ

Experimental and theoretical study of non-covalent interactions in organometallic chemistry: The concept of Hemichelation

Résumé

Ce manuscrit présente une méthodologie rationnelle de synthèse, caractérisation, détermination de la structure électronique et du comportement dynamique d'espèces bimétalliques électroniquement insaturées de type Cr(0)-M (avec M = Pd(II), Pt(II) ou Rh(I)). Ces nouvelles espèces constituent de rares exemples d'entités électro-insaturées à 14 électrons ayant la spécificité d'être persistantes en solution. Leur cohésion structurale provient essentiellement de la compensation d'un faible caractère de type donneur/accepteur entre les deux métaux par des interactions non-covalentes Coulombiennes. Nous montrons ainsi qu'en tirant profit du caractère ambiphile d'un ligand hétéroditopique capable de chélater un centre métallique par l'établissement d'une liaison covalente et d'une interaction non-covalente, de nouvelles espèces coordinativement insaturées peuvent être obtenues. Nous proposons d'appeler ce nouveau mode de chelation : « Hemichelation ».

Mots-clés : Hemichelation, interactions non-covalentes, organométallique, théorie de la fonctionnelle de la densité, modes de coordination, espèce bimétallique, électro-insaturé.

Résumé en anglais

The present manuscript will present a rational method of synthesis, characterization, determination of the electronic structure and dynamic behaviour of solution-persistent, and formally unsaturated binuclear Cr(0)-M complexes (with M= Pd(II), Pt(II) or Rh(I)). This new class of complexes constitutes rare examples of persistent coordinatively unsaturated 14-electrons complexes, whose cohesion stems essentially from a compensation of insufficient donor/acceptor Cr-M bonding by non-covalent interactions of preponderant attractive Coulombic nature. By taking advantage of the ambiphilic character of a heteroditopic ligand capable of chelating a metal centre through covalent and noncovalent bonds, truly coordination-unsaturated complexes can be synthesized in a manageable form. We propose to name "Hemichelation" the half-covalent/half noncovalent bonding-relationship between the ambiphilic heteroditopic ligand and the electron-unsaturated metallic centre.

Keywords : Hemichelation, non-covalent interactions, organometallic, density functionnal theory, coordination modes, bimetallic complex, electron-unsaturated.